## REMARKS

Reconsideration and allowance are respectfully requested.

Claims 1-25 and 40-42 are pending. Claims 10 and 19-23 were withdrawn from consideration by the Examiner as directed to non-elected inventions. Rejoinder of the withdrawn claims is requested.

Claims 1-9, 11-19, 24-25 and 40-42 were objected to as allegedly informal. They are the subject of the concurrently filed Petition under 37 CFR §§ 1.144 and 1.181 to review the Examiner's final restriction requirement. Favorable reconsideration and withdrawal of this objection are requested.

### *35 U.S.C. 101 –Utility*

Claims 1-9, 11-19, 24-25 and 40-42 were rejected under Section 101 because the invention allegedly "is not supported by either a credible, specific and substantial asserted utility or a well established utility." Applicants traverse.

The Utility Examination Guidelines (66 FR 1092) of January 5, 2001 states:

> [A] patent is required to disclose one practical utility. If a well-established utility is readily apparent, the disclosure is deemed to be implicit. If an application fails to disclose one specific, substantial, and credible utility, and the examiner discerns no well-established utility, the examiner will reject the claim under section 101. The rejection shifts the burden to the applicant to show that the examiner erred, or that a well-established utility would have been readily apparent to one of skill in the art. The applicant cannot rebut the rejection by relying on a utility that would not have been readily apparent at the time the application was filed.

Applicants' invention is directed, in one respect, to an animal model for human disease. Like other research tools, transgenic animals having altered melusin expression are useful in studying the physiology of cardiovascular disease (e.g., hypertension, cardiac hypertrophy, cardiac dilation, heart failure, and other cardiomyopathies) as well as determining whether a drug is effective in treating disease. These applications of the claimed invention are taught by Applicants in their specification at pages

Non-human transgenic animal models have played important roles in the understanding of the pathophysiology and treatment of congestive heart failure. See Hasenfuss (1998), Jaenisch (1988) and Doetschman (1999). Transgenic mice with mutations affecting specific genes and developing heart pathologies are key tools in identifying new molecular targets of therapeutic interest, as well as for testing and optimizing new therapies before they are implemented on human patients (i.e., at a preclinical stage). Other than administration of new drugs, such new therapies include heart transplantation, left ventricular assist devices, artificial hearts and cardiac bioassist techniques.

Several mouse model carrying specific genetic mutations and/or transgenes have been generated and shown to be a reliable model for human cardiac pathologies including mice lacking expression of the sarcomeric protein MLP (Knoll, 2002), mice carrying a mutation in the myosin light chain-2 (Welikson, 1999), mice overexpressing tropomodulin (Sussman, 1998), mice expressing a truncated troponin allele analogous to one found in familial hypertrophic cardiomyopathy patients (Tardiff, 1998), mice expressing varying amounts of a mutated MyBP-C (Yang, 1998). In addition, a number of these mice have proven to be effective models for testing the therapeutic action of new drugs. In calstabin-2-deficient mice, which display diastolic sarcoplasmic reticulum $Ca^{2+}$ leak, the 1,4-benzothiazepine JTV519 inhibited that leak and resultant arrhythmias (Lehnart, 2006). Similarly, three different transgenic mouse models of hypertrophic cardiomyopathy with aberrant expression of tropomodulin, myosin light chain-2 or fetal beta-tropomyosin in the heart were used to show the in vivo therapeutic efficacy of calcineurin inhibitors (i.e., cyclosporin and FK506) to prevent disease (Sussman, 1998).

The validity of animal models is further supported by the representative examples of patents/applications listed below:

- **WO-A-2005/104833**

*Method of constructing animal model suffering from left ventricular diastolic disorder for examining heart failure and method of examining remedy for heart failure caused by left ventricular diastolic failure with the use of the animal model*

An animal model is provided which can be used for testing efficacy of a drug on left ventricular myocardial diastolic dysfunction, for example heart failure due to left ventricular diastolic failure. The present invention resides in a method for preparing an animal model with left ventricular diastolic dysfunction for testing a therapeutic agent for heart failure, the method comprising: intravenously injecting an aqueous solution of a water-soluble calcium salt into an anesthetized experimental small animal; and intravenously injecting an aqueous catecholamine solution into the animal, while continuing the intravenous injection of the aqueous solution of the water-soluble calcium salt, to raise left ventricular end-diastolic pressure of the heart of the animal to a level higher than normal left ventricular end-diastolic pressure, and it also resides in a method for preparing an animal model with left ventricular diastolic dysfunction for testing a therapeutic agent for heart failure due to left ventricular diastolic failure, the method comprising: intravenously injecting an aqueous norepinepfrine solution into the animal model prepared by the former method; measuring left ventricular end-diastolic pressure; and comparing the measured left ventricular end-diastolic pressure with normal left ventricular end-diastolic pressure of before the injection of the aqueous norepinephrine solution.

- **US-A-2005/066381**

*Regulation of cardiac contractility and heart failure propensity*

The methods and compositions of the present invention find use in altering expression of PKCalpha in transgenic animals. The compositions of the invention include isolated transgenic animal cells, transgenic tissue, transgenic animals, and transgenic mice. The transgenic animals of the invention exhibit altered PKCalpha activity. The methods allow generation of transgenic animals with altered expression of

PKCalpha. The invention allows modulation of cardiac contractility. In particular, the invention provides a method for altering the susceptibility of a transgenic animal to cardiomyopathy. A transgenic animal of the invention finds use in identifying anti-cardiomyopathic compounds.

- **US-B-6,201,165; US-B-6,657,104; US-B-6,673,768**

*Transgenic animal models for cardiac hypertrophy and methods of use thereof (screening)*

Transgene constructs for generating transgenic animals, wherein the transgene encodes a gene product which modulates transcription of a hypertrophy-sensitive gene, are provided. Further provided are recombinant vectors comprising the transgenes of the invention. Further provided are transgenic animals generated using the transgene constructs. Further provided are enzyme-based, cell-based, and whole-animal-based assays for detecting substances having therapeutic activity toward cardiac hypertrophy. Further provided are compositions comprising substances which modulate levels of active product of a hypertrophy-sensitive gene. Further provided are methods of treating cardiac hypertrophy.

- **WO-A-2005/063007**

*Non-human mammal comprising a modified serca2 gene and methods, cells, genes, and vectors thereof*

The present invention relates to a non-human vertebrate, more particularly a non-human mammal, in which all cells contain genetic modifications in a $Ca^{2+}$ handling Serca ATPase gene, more particularly the Serca2 ATPase. Defective $Ca^{2+}$ handling is induced in live animals by introducing genetic elements which direct the timing and specificity of the gene inactivation to the organ or tissue of interest; e.g. cardiac muscle cells. The primary application is to provide a standardized and reproducible animal model for heart failure or other human diseases, in which the defective $Ca^{2+}$ handling

function by the Serca gene can be manipulated in live animals. This is the only existing animal to date with such genetic modifications for this class of $Ca^{2+}$ handling proteins.

- **US-A-2004/0152088**

*Methods for diagnosing and treating heart disease*

The invention provides methods of diagnosing heart disease, such as heart failure, methods for identifying compounds that can be used to treat or to prevent heart disease, and methods of using these compounds to treat or to prevent heart disease. Also provided in the invention are animal model systems that can be used in screening methods.

- **US-B-7,169,612**

*Use of EDG2 receptor in an animal model of heart failure*

Mammals and myocardial mammal cells transformed with G protein coupled receptor EDG2 are presented for use in an animal model for heart failure.

- **WO-A-03/09680**

*Heparin-binding epidermal growth factor-like growth factor gene-modified animal, screening method, embryonic stem cells and preventive and/or remediy for heart failure*

A nonhuman animal having a DNA sequence of a heparin-binding epidermal growth factor-like growth factor gene into which a mutation of modifying the function of the heparin-binding epidermal growth factor-like growth factor gene has been transferred and a method of constructing the same; nonhuman embryonic stem cells having a DNA sequence of a heparin-binding epidermal growth factor-like growth factor gene into which a mutation of modifying the function of the heparin-binding epidermal growth factor-like growth factor gene has been transferred; a method of screening a preventive and/or a remedy for heart failure; and a preventive and/or a remedy for heart failure.

- **US-B-7,166,762**

*Method of constructing heart failure model animal*

A non-human mammal which is usefully and effectively applicable to the screening of a substance to be employed for preventing and treating heart failure. This animal is an animal model of heart failure prepared by starting both coronary stenosis and the stenosis of arteries other than the coronary artery and the abdominal artery of a non-human mammal within the same period of time.

- **US-A-2003/213002**

*Extensive myocardial infarction model animal, method for preparation there of, and application for drug screening and regenerative medicine*

The prior art has problems such as high mortality of model animals due to complication of heart failure, necessity of taking into consideration the effects from other organs for investigation of the mechanism of the disease, being unable to prepare an extensive myocardial infarction model, and others. The invention allows exclusion of the state of heart failure and provides an extensive myocardial infarction model animal which permits to prepare a model of the pathology of extensive myocardial infarction. The invention is an extensive myocardial infarction model animal, the method for preparation thereof, and the method for screening of drugs and/or genes using the model animal, wherein the heart of a normal animal is extirpated, the left main trunk of the extirpated heart is ligated, the heart after the ligation is heterotopically grafted to the abdomen of another normal animal, and the animal given the heterotopic graft is used as the extensive myocardial infarction model animal. Three weeks after the graft, the model of extensive myocardial infarction pathology is established.

- **US-B-6,194,632**

*Mouse model for congestive heart failure*

The present invention relates to transgenic mice which express CREB. These transgenic mice provide a genetic model of dilated cardiomyopathy.

**In view of the foregoing, one of skill in the art would conclude that the use of a non-human transgenic animal for studying heart pathology and the treatment of cardiovascular disease represents a credible, specific and substantial utility and a well established utility.**

In addition to animal models described in the scientific literature (and accepted through the peer-review process) and in patents/patent applications, the animal model described by Applicants represents a novel and particularly suitable animal model to test new therapeutic agents for treatment of heart failure. Melusin null mice, in fact, do not display structural and functional cardiac defects in basal conditions and are perfectly healthy throughout their entire life span. But they develop cardiac dilation and then heart failure when subjected to chronic conditions of high blood pressure as exemplified by surgical banding of the transverse aorta. Under these conditions and in the absence of melusin, the heart rapidly undergoes dilation and congestive heart failure.

This pathology and phenotype of the animal model closely mimic the clinical histories of human patients with hypertension, who frequently develop cardiac dilation and congestive heart failure. The fact that the melusin null mouse model is highly relevant for human pathology is also demonstrated by a study of human patients who have developed heart failure as a consequence of aortic stenosis (Brokat, 2007). In these patients, in fact, reduction in melusin expression parallels the functional cardiac impairment. These data strongly indicate that reduced expression of melusin in the heart corresponds to increased susceptibility to develop heart dysfunction and, on the other hand, indicates that therapeutic strategies aimed at sustaining melusin function will represent a highly promising new treatment for humans.

The importance of melusin in the hypertrophic response of the heart is further supported by recent studies in a dog animal model (Donker, 2007). Studying myocardial

remodelling during atrioventricular block, the authors found that upregulation of melusin coincides with a phase of strong compensated hypertrophy and concomitant upregulation of P-Akt, P-GSK3 and MLP. An important aspect of the melusin null model resides in the fact that melusin is a protein expressed selectively in skeletal muscle and heart. Thus representing an ideal target for therapeutic intervention. Its absence from other tissues in the human body will, in fact, minimize possible undesired side effect of drugs specifically targeting melusin.

Another important fact establishing melusin null mice as a valuable animal model to investigate cardiovascular disease is that melusin is a new protein whose function in heart hypertrophy has been recently disclosed by the results Applicants teach in their specification. This aspect opens a new important therapeutic perspective on controlling and/or treating heart failure.

The validity of the melusin null animal model is further documented by the fact that it has been selected as the best animal model suitable for identifying the molecular mechanism involved in protection from left ventricle dilation and heart failure by a consortium of 20 different laboratories and three SMI Biotech companies within Europe that are collaborating within an integrated research project (EUGeneHeart) founded by the European Community (http://www.eugeneheart.com/).

Applicants completely disagree with the allegation on page 10 of the Action that there is a lack of correlation between the inactivation of melusin expression and the cardiac phenotype observed in melusin null mice. As taught in Example 1 by Applicants (see page 12 of the specification), the mouse genome was selectively mutated by deletion of the first four exons of the melusin gene using homologous recombination. This technology allows the selective targeting of specific sequences within the genome (i.e., the first four exons of the melusin gene), and excludes the possibility of introducing undesired or unknown mutations in genetic loci other than the selected melusin gene. This differs from the conventional technology used to generate transgenic mouse mutations in which a (trans)gene is introduced randomly within the mouse genome with the

possible risk of insertional mutagenesis: i.e., random disruption of an endogenous gene with the consequence of an unpredictable genetic mutation. The selective elimination of the melusin gene product is also demonstrated in Figure 4 by Applicants where it was shown that both skeletal muscle and heart of melusin null mice lack melusin expression by Western blot analysis. They show unaltered expression of α7b and β1D integrins, the membrane receptors interacting with melusin in muscle cells, as a control.

The relationship between cardiac phenotype and mutation in the melusin gene is clearly documented by comparison of the phenotypes of melusin null and wildtype mice. After four weeks of pressure overload induced by aortic banding, wildtype mice showed a compensated hypertrophy, while mice lacking melusin expression disclosed features of cardiac dilation. Since the only difference between these two strains of mice is the inactivation of the melusin gene, one of skill in the art would conclude that the lack of melusin is the cause of the heart dilation in melusin null mice. The causative role of melusin in generating the cardiac phenotype is thus a direct consequence of melusin gene ablation. The role of melusin in controlling the hypertrophic response in cardiomyocytes subjected to pressure overload is further demonstrated by the analysis of the cardiac phenotype in transgenic mice overexpressing melusin selectively in the heart (De Acetis, 2005). This animal model represents a gain of function and showed that increasing melusin expression in the heart leads to a phenotype exactly opposite to that of melusin null (i.e., loss of function) animal. Transgenic mice overexpressing melusin, in fact, showed compensatory cardiac hypertrophy, and were protected from dilation and failure of the left ventricle when subjected to long standing pressure overload. The results of the analysis of the melusin null phenotype have been published in Nature Medicine immediately after submission of Applicants' PCT application (Brancaccio, 2003). None of the three reviewers of the paper raised the issue that there is a lack of correlation between the melusin gene inactivation and the phenotype described (see enclosed Annex 1). The paper would not have been published if there were any doubts by the peer reviewers on this aspect of the invention.

The fact that the phenotype of the melusin null mice was not predictable on the basis of the information available from the protein sequence and expression data (Brancaccio, 1999) is not surprising since the melusin gene was not previously described and its function at the cellular level was completely unknown. But this situation was radically changed by later results that are taught by Applicants in their specification. The cardiac phenotype as described in Applicants' specification (see Example 2) represents a novel finding of strong industrial interest (e.g., EUGeneHeart) and is thus the basis of their patent application.

Withdrawal of the Section 101 rejection is requested because Applicants have taught that the claimed invention is useful.

*35 U.S.C. 112 – Enablement*

The Patent Office has the initial burden to question the enablement provided for the claimed invention. M.P.E.P. § 2164.04, and the cases cited therein. It is incumbent upon the Patent Office, whenever a rejection on this basis is made, to explain why it doubts the truth or accuracy of any statement in a supporting disclosure and to back up assertions of its own with acceptable evidence or reasoning which is inconsistent with the contested statement. *In re Marzocchi*, 169 USPQ 367, 370 (C.C.P.A. 1971). Specific technical reasons are always required. See M.P.E.P. § 2164.04.

Claims 1-9, 11-19, 24-25 and 40-42 were rejected under Section 112, first paragraph, because they allegedly fail to comply with the enablement requirement. It was further alleged that they contain "subject matter which was not described in the specification in such a way as to enable one skilled in the art to which it pertains, or with which it is most nearly connected, to make and/or use the invention." Applicants traverse.

On page 12 of the Action, Doetschman (1999) was cited for the comment that "knock out mice are not useful because they frequently do not yield the expected phenoltype, or they don't seem to have any phenotype." Therein, several examples are mentioned in which genes considered well characterized in vitro produced unexpected

phenotypes or indiscernible or no phenotypes in transgenic or knockout mice. Doetschman, however, concludes as follows at page 137, left column, first paragraph:

> The conclusion will be that the knock out phenotype do in fact provide accurate information concerning gene function that we should let the unexpected phenotypes lead us to the specific cell, tissue, organ, culture, and whole animal experiments that are relevant to the function of the gene in question, and that the absence of phenotype indicate that we have not discovered where or how to look for a phenotype.

Thus the conclusion reached by Doetschman is exactly the opposite of what was quoted on page 12 of the Action. He stresses that the analysis of gene function can only be based on the analysis of knock out mice phenotypes rather than in vitro studies. The importance and relevance of in vivo studies on transgenic animal models is further established in another paper Jaenisch (1988), which was cited in the Action, at page 1468, left column, first paragraph:

> The information gained from the use of the transgenic technology is relevant to almost any aspect of modern biology including developmental gene regulation, the action of oncogenes, the immune system, and mammalian development. Because specific mutations can be introduced into transgenic mice, it becomes feasible to generate precise animal models for human genetic diseases and to begin a systematic genetic dissection of the mammalian genome.

On page 12 of the Action, Moens (1993) was cited for the statement that "two mutations produced by homologous recombination in two different locations of the N-myc gene produce two different phenotypes in mouse embryonic stem cells." In this particular case, the two mutations differentially affect the expression of the N-myc gene. In fact, while the first mutation leads to complete gene inactivation and abrogation of protein expression (as is true for the melusin null mutation shown in Figure 4 of Applicants' specification), the second mutation obtained by Moens is a leaky mutation that allows expression albeit at low level (25%). These two mutations would of course lead to different phenotypes because, in the first case, the mutation leads to the abrogation of protein expression while, in the second case, the mutation allows expression of the

protein at low level. One of skill in the art knows that is absolutely necessary to demonstrate the absence of protein expression to prove the efficacy of the mutation introduced by homologous recombination, as Applicants demonstrated in Figure 4 of their specification. Null mutations do not require undue experimentation to select; they can be made in a straightforward manner by deleting at least a portion of the gene's coding region, as was done by deleting the first four exons of the mouse melusin gene. Therefore, the argument made in the Action is not applicable to the claimed invention when practiced by the skilled artisan.

On page 12 of the Action, two other papers were cited in which mutation of the retinoblastoma or HPRT gene in mice led to a different phenotype from that caused by the same mutations in humans (Jacks, 1992; Kuehn, 1987). In a limited number of situations, the same monogenic mutation can lead to different phenotypes in different animal species or even strains of the same species. This however does not apply to the melusin gene since the results obtained with melusin null mice closely mimic the situation observed in human patients. Mice that do not express melusin in the heart when subjected to surgical aortic banding (see Figure 6 of Applicants' specification), which mimics aortic stenosis in human patients, undergo rapid and dramatic left ventricle dilation (Figure 8 of Applicants' specification).

Applicants have recently shown that in human patients developing dilated cardiomyopathy as a consequence of aortic stenosis, lower melusin levels in the left ventricle are associated with higher degrees of left ventricle dilation and reduced cardiac function (Brokat, 2007). This closely parallels the mouse phenotype in which absence of melusin causes left ventricle dilation and is strong confirmation that melusin null mice represent a reliable animal model to study human heart failure.

On page 13 of the Action, it was alleged that at the time this application was filed, mouse was the only non-human animal in which embryonic stem (ES) cells can be obtained and then used to generate chimeras extending to the germ line. Applicants disagree with these allegations as Wheeler (2001) reports at page 1351 that pluripotent

stem cells have been obtained from several different non-human animal species other than mouse: e.g., hamster (Doetschman, 1988); rat (Iannaccone, 1994); rabbit (Giles, 1993; Graves, 1993; Schoonjans, 1996); mink (Sukoyan, 1992; Sukoyan, 1993); pig (Notarianni, 1990; Piedrahita, 1990; Notarianni, 1991); cow (Talbot, 1995; van Stekelenburg-Hamers, 1995; Stice, 1996); sheep (Campbell, 1996; Piedrahita, 1990; Talbot, 1993; Wilmut, 1997); and primate (Thomson, 1995; Thomson, 1996).

ES cells isolated from several different non-human animal species other than mouse are also able to generate chimeric animals (Schoonjans, 1996; Wheeler, 1994; Shim, 1997) and to contribute to the germ line (Prelle, 2002). Pain (1996) described the ability of chicken stem cells to colonize the germ line. Other techniques beside ES cell chimerism are also available to generate germ line chimeras. As taught by Prelle at page 176, right column, second paragraph:

> Transgenesis and targeted mutagenesis via nuclear transfer circumvents the need for generating chimeric animals, reduces costs and saves time, especially in larger animals, and obviously has several additional advantages: (a) sex selection is possible (e.g. female transgenic cell lines could be used for the production of valuable proteins in the milk); (b) integration and eventually expression of the transferred construct can be detected in cultured cells before nuclear transfer; (c) cell lines can be cryopreserved; (d) all cells within a cloned offspring contain the introduced gene, eliminating mosaicism and ensuring germ line transmission; (e) the number of animals required reduced since all animals generated are transgenic.

Generation of transgenic animals by nuclear transfer is based on the transfer of the nucleus from a somatic cell containing a diploid genome into an enucleated oocyte as illustrated on the next page.

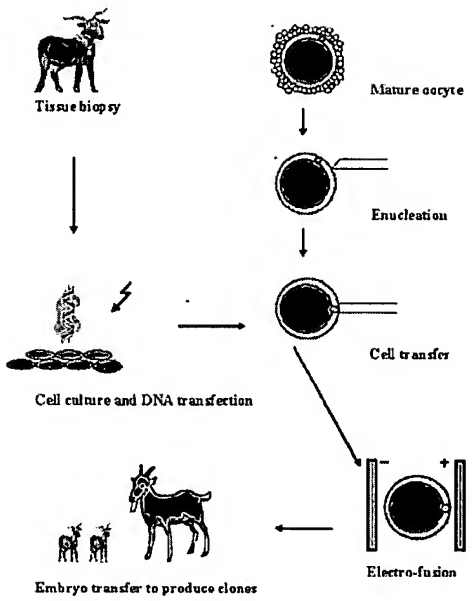


Procedure of producing gene-targeted animals (goats) by cloning: Reprodutive Biology and Endocrinology 1:103, 2003 doi: 10.1186/1477-7827-1-103. © 2003 by Wang and Zhou.

Nuclear transfer technology is widely used by numerous laboratories to produce animals from the somatic cells of animal fetuses and adults. These nuclear transfer procedures have been successfully applied to various mammalian species and have resulted in live births of sheep (Campbell, 1996; Wells, 1997); mice (Wakayama, 1998); cattle (Kato, 1998); goats (Baguisi, 1999; Keefer, 2001); pigs (Polejaeva, 2000); rabbits (Chesne, 2002) and cats (Shin, 2002).

The generation of transgenic animals with nuclear transfer technology is based on the ability to introduce targeted gene mutations in somatic cells used for the nuclear transfer. In fact, homologous recombination can be obtained not only in ES cells but also in other somatic cells such as fetal fibroblasts from different animal species. Gene-targeted animal clones have been successfully produced in sheep (McCreath, 2000;

Denning, 2001) and pigs (Lai, 2002; Dai, 2002) by homologous recombination in fetal fibroblast cells and subsequent nuclear transfer.

As discussed above, the phenotype of melusin null mice closely mimics the clinical history of human hypertensive patients who frequently develop cardiac dilation and congestive heart failure. The fact that the melusin null mouse model is highly relevant for the human pathology is also demonstrated by a study in human patients that have developed heart failure as a consequence of aortic stenosis (Brokat, 2007). In these patients, in fact, reduction in melusin expression parallels the functional cardiac impairment. These data strongly indicate that reduced level of melusin in the heart corresponds to increased susceptibility to develop heart dysfunction and, on the other hand, indicates that therapeutic strategies aimed at sustaining melusin function will represent a highly promising new treatment for humans.

The importance of melusin in the heart's hypertrophic response in animal models other than mice are confirmed by Donker (2007) in which the effects of increased load on myocardial remodelling during atrioventricular block was investigated using a dog model of heart hypertrophy. In this model system, upregulation of melusin coincides with a phase of strong compensated hypertrophy and concomitant upregulation of P-Akt, P-GSK3 and MLP.

Applicants have clearly demonstrated by the results in their specification that the pathological phenotype of melusin null mice is left ventricle dilation and heart failure upon exposure to hemodynamic pressure overload (see Example 2). Therefore, they do not understand the concerns raised on pages 15-16 of the Action of the alleged unpredictability of the melusin null mouse phenotype since, as stated above, the pathology and cardiac phenotype of these melusin null mice have been experimentally determined and the results presented in their specification. Moreover, the relationship between the phenotype of the animal model and the pathology of human patients is also convincingly demonstrated by the results discussed above in humans affected by aortic stenosis in

whom lower level of melusin expression correspond to worst cardiac function (Brokat, 2007).

For the reasons stated above, Applicants submit that their claimed non-human transgenic animals are useful to investigate and validate both novel and known drugs pharmacologically active in prevention and treatment of cardiac dilation and heart failure in human patients.

Withdrawal of the enablement rejection made under Section 112, first paragraph, is requested because it would not require undue experimentation for a person of skill in the art to make and use the claimed invention.

*Conclusion*

Having fully responded to all of the pending objections and rejections contained in this Office Action, Applicants submit that the claims are in condition for allowance and earnestly solicit an early Notice to that effect. The Examiner is invited to contact the undersigned if any further information is required.

Respectfully submitted,

**NIXON & VANDERHYE P.C.**

By: _____

Gary R. Tanigawa
Reg. No. 43,180

901 North Glebe Road, 11th Floor
Arlington, VA 22203-1808
Telephone: (703) 816-4000
Facsimile: (703) 816-4100


ANNEX 1

Subject:
NM14259
Date:
Tue, 23 Jul 2002 15:46:01 -0400
From:
Medicine <MEDICINE@NATURENY.com>
To:
"'guido.tarone@unito.it" <guido.tarone@unito.it>

Dr. Guido Tarone
Universita di Torino
Dept of Genetics, Biology & Biochemistry
Via Santena, 5bis
10126 TURIN,
Italy
FAX: 39 011 6706547
guido.tarone@unito.it

July 23, 2002

Dear Dr. Tarone

We have now received three reports from referees of your manuscript (NM14259) entitled "Melusin, a muscle specific b1 integrin interacting protein, required to prevent cardiac failure in response to chronic pressure overload". As you will see, although the referees feel this report is interesting, they have raised a number of serious concerns that need to be addressed. In light of these comments, we cannot accept the manuscript for publication at this time, but would be willing to consider a revised version that addresses all of the referees' concerns.

While all three referees found your report interesting, they require further mechanistic investigation, in particular as mentioned specifically by Ref 1, as pertains GSK3b phosphorylation status over a longer period of examination. Also, several methodological concerns about strain- and sex-specificity must be clarified.

We hope you will find the referees comments useful as you decide how to proceed. If you wish to present a significantly revised manuscript, please bear in mind that we will be reluctant to approach the referees again in the absence of major revisions.

If you decide to resubmit, we will need four copies of the revised

manuscript, a new diskette version, and a detailed, point-by-point account of how you have responded to each of the referees' comments. In the event that these revisions are not received within 6 weeks of this letter, the manuscript will be assigned a new "manuscript received" date to reflect the changes.

We are looking forward to seeing the revised manuscript and thank you for the opportunity to review your work.

Sincerely,

Ushma Savla, Ph.D.
Assistant Editor

REF ONE
This very interesting paper demonstrates a role for melusin in the cardiac hypertrophic response to mechanical pressure overload. In a series of elegant studies the authors demonstrate that melusin-null mice have a blunted hypertrophic response to pressure overload, but retain a normal response to suppressor dose Gq coupled receptor agonists. The authors further show attenuation of GSK3b phosphorylation after short-term mechanical overload in melusin-null mice. While these findings are novel and very interesting, a few critical issues need to be addressed.

1) The 7-day TAC data (Figure 2), and the data showing a preserved hypertrophic response to angiotensin and phenylephrine (Figure 4) are elegant. However, there are concerns with regard to the longer-term TAC experiments (Figure 3 and Table 1). Since data regarding the pressure gradients in individual mice at four weeks are not presented, it is unknown whether the difference in chamber size and cardiac function between the groups of mice is related more to differences in loading conditions then to genotype. This is important because recent studies by others have shown a similar decrement in cardiac function in aortic-banded wild type mice after four weeks of pressure overload.

2) No information is provided as to the genetic background, gender, or age of the mice undergoing TAC, which are all potential contributors to the observed difference in the echocardiographic phenotype. Indeed, it is known that B6 mice are more susceptible to pressure overload compared to 129 mice. Littermates from a F1 or F2 129/B6 backcross are sufficiently genetically disparate that it could account for observed phenotypic difference independent of the melusin genotype. Wild type littermates of null mice backcrossed at least seven generations into either B6 or another appropriate inbreed strain would be needed to rule out this concern. It would also be important to follow pressure overloaded mice for a longer period of time.

3) A number of recent studies have suggested that hypertrophy may not be compensatory and that the suppression of the hypertrophic response may in fact be protective to preserve long-term cardiac function. The authors should discuss this relevant literature in the context of their data.

4) It is somewhat curious that the sample size for the seven-day TAC (Figure 2) and the long-term TAC (Table 1) are identical. Since the seven-day TAC animals were a terminal experiment, and separate mice must have been used for long-term TAC, it is surprising that by chance alone the number of animals in each group would be identical. The authors should confirm that there was no selection bias.

5) The data regarding signaling pathways (Figure 5) is intriguing and important since the authors have identified a protein that is potentially involved in mechanical stress induced hypertrophy. However, additional experiments need to be performed to make a convincing argument. Given that the key finding in the melusin-null mice is the attenuation of cardiac hypertrophy after seven-days of pressure overload, it would be important to interrogate the GSK pathway at that time point. Both GSK3b activity and phosphorylation status should be determined in melusin-null mice seven-days post TAC compared to pressure overloaded wild type mice. vAkt and MAPK kinase pathways should also be examined in seven-day TAC mice.

Since GSK3b is a negative regulator of cardiac hypertrophy, it is quite possible that in response to pressure overload the integrin-associated protein melusin promotes signals leading to the inactivation of GSK3b and the enhancement of hypertrophic pathways. Additional experiments that demonstrate greater phosphorylation and inactivation of downstream GSK3b substrates such as GATA4, eIF2Be and/or NF-AT in seven-day pressure overloaded null mice compared to wild type would bolster that claim and make a more convincing argument.

Additional Comments

1. Figure 2C. It appears the magnification of the histological sections is not the same between the sham and TAC examples. A magnification scale should be present on the figure.

2. There are a number of grammatical errors and paragraphs with poor sentence structure that would benefit from careful proofreading.

==========

REF TWO

The authors have studied the muscle-specific beta-1 integrin interacting

protein melusin by gene targeting in mice, and show that mechanical load induces a dilated cardiomyopathy (whereas the absence of melusin was well-tolerated during development and in normal adult physiology).

Interesting data, beyond just this important and provocative genetic demonstration, include the lack of dependence on melusin in agonist-induced cardiac hypertrophy (one of the nicest examples for an effect exclusive to the mechanical signaling pathway) and the specific inability of mechanical stress to cause phosphorylation of GSK3beta. Because inactivation of this kinase by phosphorylation is well implicated in hypertrophy, failure to inactivate the kinase provides an attractive and plausible explanation for the observed phenotype.

Overall, the paper is well written and persuasive. Minor additional data are recommended with respect to figures1 and 5.

Specific comments

Page 2. For Gq cite the knockout, not the dominant-inhibitor. I'd suggest citing recent reviews by Olson, Dorn. More surprising are omissions of directly relevant work on mechanical signaling in cardiac muscle by Ross and colleagues, including interference with integrin signaling, and, more recently, the conditional knockout of beta-1 integrin.

Page 4. "impairs hypertrophic remodeling" is jargon: indicate what is meant, for readers not familiar with the field. (Work by Sadoshima & Izumo indicates that growth and fetal gene reprogramming are separable, pharmacologically.)

Page 5. transverse, not transversal

Page 6. What was the reproducibility of blinded echocardiographic assessment using the 10 MHz transducer?

Page 7. Olympus, not Olimpus X

Page 9. Indicate in the text which integrin was examined. Fig. 1 would benefit from immunostaining for melusin plus beta-1-D integrin in the wild-type and knockout mice. Put Fig. 2cd before fig. 2ab, and cite the new Fig. 2a instead of 'not shown' for the normal histology.

Page 10. Conclusions about differentiation and sarcomere assembly are tempting but unfounded, since neither was examined. As rationale for the loading studies, cite the available precedents of genes that impede growth induced by hypertrophic signals but not cardiac muscle in physiological conditions. I'd recommend including the apoptosis data, including whatever

positive and negative controls were used and representative raw results, since the absence of apoptosis here is the one major difference from the floxed gp130 story.

Page 11. How was the difference in mortality tested for significance?

Page 12. Minor additional data. (1) For completeness, what about JNK? (2) Because the conclusions regarding GSK3beta are so important to the paper, corroboration by an immune complex kinase assay would be valuable. (3) Because the phenotype induced by mechanical stress in melusin -/- mice so closely resembles the conditional knockout of gp130 and germline mutation of CD95/Fas, it is disappointing that the authors do not show whether the absence of melusin prevents normal levels of these proteins' expression. (4) It would be unreasonable to require the authors in this study to prove, genetically, that GSK3beta is responsible for the observed phenotype. On the other hand, it is logical to test, if Akt signaling is defective here, as an explanation for the defective phosphorylation of GSK3 beta.

REF THREE

I think this is a very interesting paper with remarkable but not unreasonable results. It appears that melusin is part of a signal transduction pathway from the cardiac cytoskeleton to select intracellular hypertrophic pathways that would appear to involve the gsk3b but not p38 or erk pathways. I do, however, have some criticisms that can be addressed.

1) Of course, the sex of the animals has not been disclosed. This may be an important point given the propensity for males to have eccentric remodeling and females to have concentric remodeling.

2) The HR of the animals during the echos and Millar BPs should be mentioned. This is important since the HR may influence the BP generated as well as the FS.

3) In the results the description of the LV chamber dimensions is confusing and should be reworded.

4) There is no reference to the absolute body weights of each group. Since skeletal muscle mass is a substantial portion of body weight and these muscles are also without melusin it is important to note the BW in addition to the histopathology.

5) I disagree with this model being important for studying human HTN CMP. The mechanism behind the dilation in this model is more likely to be dissimilar than similar to the process in the presence of this protein. In addition, it would be interesting to know if this protein has been noted in

human myocardium. I think this model is much more relevant to evaluation the signaling pathways between the cytoskeletal and the intracellular pathways as I mentioned above. It would be more interesting if the authors had any potential mechanisms in mind.

6) In addition, there are numerous grammatical and spelling errors that I suspect are due to English not being their first language.

ANNEX 2

Dev Biol. 1988 May;127(1):224-7.



## Establishment of hamster blastocyst-derived embryonic stem (ES) cells.

Doetschman T, Williams P, Maeda N.

Medical Genetics Department, University of Wisconsin, Madison 53706.

The establishment of four ES cell lines from the Syrian "golden" hamster (Mesocricetus auratus) is described. The cells can be maintained in the undifferentiated state when grown on primary mouse embryonic fibroblast feeder layers. In suspension culture they spontaneously differentiate into embryoid bodies of increasing complexity which contain a variety of tissues including embryonic ectoderm and myocardium. All four lines--one female and three male--are karyotypically normal with 44 chromosomes. Hamster is the second species from which ES cells have been established. As in mouse, the cells should be useful for developmental and transgenic studies.

Dev Biol. 1994 May;163(1):288-92.

## Pluripotent embryonic stem cells from the rat are capable of producing chimeras.

Iannaccone PM, Taborn GU, Garton RL, Caplice MD, Brenin DR.

Markey Program in Developmental Biology, Northwestern University Medical School, Chicago, Illinois 60611.

Embryonic stem cells have been enormously important in the production of targeted mutations in mice used in the study of gene function and biological aspects of disease states. The use of these cells for mouse studies is now wide-spread but the production of animals from similar cell lines derived from other species has not been previously reported. We demonstrate here the derivation of diploid rat embryonic stem cells (RESC-01). RESC-01 cells are SSEA-1 and alkaline phosphatase positive, grow best on primary rat embryonic fibroblasts, and can differentiate extensively in vivo. RESC-01 cells form cystic embryoid bodies capable of rhythmic contractions. Rat blastocysts injected with RESC-01 cells form chimeras. The results indicate that the successful in vitro propagation and chimera production with embryonic stem cells is not limited to the mouse. The long-term culture of rat ES cells will provide an important resource for the study of normal physiology and disease models where rat is the species of choice.

Mol Reprod Dev. 1993 Oct;36(2):130-8.

## Pluripotency of cultured rabbit inner cell mass cells detected by isozyme analysis and eye pigmentation of fetuses following injection into blastocysts or morulae.

**Giles JR**, **Yang X**, **Mark W**, **Foote RH**.

Department of Animal Science, Cornell University, Ithaca, New York 14853.

Pluripotency of isolated rabbit inner cell masses (ICMs) and cultured (3 days) inner cell mass (ICM) cells was tested by injecting these donor cells into day 3.5 blastocysts (experiment 1) or day 3 morulae (experiment 2) to produce chimeric embryos. Injected (n = 107) and noninjected (n = 103) embryos were transferred to the opposite uterine horns of the same recipient females. Chimerism was determined by adenosine deaminase (ADA) isozyme analysis on fetal tissue and by eye pigmentation at midgestation. In experiment 1, 53% and 64%, respectively, of blastocysts injected with ICMs or cultured ICM cells developed to midgestation, compared with 52% and 48% for controls. Of these fetuses, four (31%) and one (6%), respectively, had ADA chimerism. In experiment 2, 38% and 62%, respectively, of the morulae injected with ICMs or cultured ICM cells developed to midgestation, compared with 46% and 56% for control morulae. Six (43%) chimeric fetuses from morulae injected with ICMs were detected by ADA analysis, but 12 (86%) chimeric fetuses were detected by eye pigmentation, indicating that eye pigmentation was a more sensitive marker for chimerism than our ADA assay. None of the 14 fetuses recovered after injecting morulae with cultured ICM cells were chimeric with either marker. No chimeras developed from control embryos. These studies demonstrate 1) that pregnancy rates are not compromised by injection of blastocysts or morulae with ICMs or cultured ICM cells, 2) that chimeric rabbit fetuses can be produced by injecting ICMs into either blastocysts or morulae, and 3) that cultured ICM cells can contribute to embryonic development when injected into blastocysts.

Mol Reprod Dev. 1993 Dec;36(4):424-33.

## Derivation and characterization of putative pluripotential embryonic stem cells from preimplantation rabbit embryos.

**Graves KH**, **Moreadith RW**.

Department of Internal Medicine, University of Texas Southwestern Medical Center, Dallas 75235-8573.

We have derived putative embryonic stem (ES) cell lines from preimplantation rabbit embryos and report here their initial characterization. Two principal cell types emerged

following serial passage of explanted embryos, and each has subsequently given rise to immortalized cell lines. One cell type has morphology identical to primary outgrowths of trophectoderm, is strictly feeder-cell dependent, and spontaneously forms trophectodermal vesicles at high cell density. The second type appears to represent pluripotent ES cells derived from the inner cell mass as evidenced by 1) ability to grow in an undifferentiated state on feeder layers, 2) maintenance of a predominantly normal karyotype through serial passage (over 1 year), and 3) ability to form embryoid bodies, which form terminally differentiated cell types representative of ectoderm, mesoderm, and endoderm. These ES cells may ultimately be suitable for introduction of germline mutations (via homologous recombination). The rabbit's size, reproductive capability, and well-characterized physiology make it suitable for a wide range of investigations, particularly for development of large animal models of human disease.

Mol Reprod Dev. 1996 Dec;45(4):439-43.

## Pluripotential rabbit embryonic stem (ES) cells are capable of forming overt coat color chimeras following injection into blastocysts.

**Schoonjans L**, **Albright GM**, **Li JL**, **Collen D**, **Moreadith RW**.

Center for Transgene Technology and Gene Therapy, Flanders Interuniversity Institute for Biotechnology, KULeuven, Belgium.

The isolation of pluripotent embryonic stem (ES) cell lines from preimplantation rabbit embryos and their in vitro properties have been previously described. In the present investigation, these ES cell lines were further characterized and their capacity to contribute to formation of adult, fertile animals upon injection into recipient New Zealand White blastocysts demonstrated. The efficiency of chimera formation was low (5% of live born), but the degree of chimerism, as assessed by coat color contribution from the Dutch belted strain, was high (10-50%). Thus a significant step is taken toward the development of gene-targeting technology in the rabbit, an animal whose physiology and size lend itself to unique applications in biomedical research.

Mol Reprod Dev. 1992 Dec;33(4):418-31.

## Isolation and cultivation of blastocyst-derived stem cell lines from American mink (Mustela vison).

**Sukoyan MA**, **Golubitsa AN**, **Zhelezova AI**, **Shilov AG**, **Vatolin SY**, **Maximovsky LP**, **Andreeva LE**, **McWhir J**, **Pack SD**, **Bayborodin SI**, **et al**.

Institute of Cytology and Genetics, Academy of Sciences of Russia, Siberian Department, Novosibirsk.

Ten embryonic stem (ES) cell lines from mink blastocysts were isolated and characterized. All the lines had a normal diploid karyotype; of the ten lines studied, five

had the XX and five had the XY constitution. Testing of the pluripotency of the ES-like cells demonstrated that 1) among four lines of genotype XX, and X was late-replicating in three; both Xs were active in about one-third of cells of line MES8, and analysis of glucose-6-phosphate dehydrogenase revealed no dosage compensation for the X-linked gene; 2) when cultured in suspension, the majority of lines were capable of forming "simple" embryoid bodies (EB), and two only showed the capacity for forming "cystic" multilayer EBs. However, formation of ectoderm or foci of yolk sac hematopoiesis, a feature of mouse ES cells, was not observed in the "cystic" EB; 3) when cultured as a monolayer without feeder, the ES cells differentiated into either vimentin-positive fibroblast-like cells or cytokeratin-positive epithelial-like cells (less frequently); neural cells appeared in two lines; 4) when injected into athymic mice, only one of the four tested lines gave rise to tumors. These were fibrosarcomas composed of fibroblast-like cells, with an admixture of smooth muscular elements and stray islets of epithelial tissue; (5) when the ES cells of line MES1 were injected into 102 blastocyst cavities and subsequently transplanted into foster mothers, we obtained 30 offspring. Analysis of the biochemical markers and coat color did not demonstrate the presence of chimaeras among offspring. Thus the cell lines derived from mink blastocysts are true ES cells. However, their pluripotential capacities are restricted.

Mol Reprod Dev. 1993 Oct;36(2):148-58.

## Embryonic stem cells derived from morulae, inner cell mass, and blastocysts of mink: comparisons of their pluripotencies.

Sukoyan MA, Vatolin SY, Golubitsa AN, Zhelezova AI, Semenova LA, Serov OL.

Academy of Sciences of Russia, Siberian Department, Novosibirsk.

A characterization of cell lines that we derived from morulae (three lines), blastocysts (two lines), and the inner cell mass (ICM) is given. The karyotype of all the lines was normal; the genotype of four lines was XX, and four lines were genotypically XY. The pluripotencies and commitment status of the derived lines were estimated. First, there were not less than two-thirds of cells in the populations of the lines derived from morulae and the ICM with both Xs active; 70-100% of cells of the blastocyst-derived lines had one of the Xs in an inactive state. The activity of glucose-6-phosphate dehydrogenase (G6PD) in the lines (genotype XX) derived from morulae and ICM was found to be twofold higher than in lines with genotype XY, and G6PD activity was the same in the blastocyst-derived XX lines and XY lines. Second, when injected intraperitoneally into athymic mice, morulae- and ICM-derived cells gave rise to simple and complex embryoid bodies (EB) resembling to typical "cystic" mouse EBs. Third, when injected subcutaneously to athymic mice, the ICM- or morula-derived cells gave rise to typical teratomas containing derivatives of the three germ layers and components of organogenesis. Comparisons of cell lines of different derivations demonstrated that the pluripotencies of the ES cells derived from morulae or the ICM are higher than those of blastocyst derivation.

J Reprod Fertil Suppl. 1990;41:51-6.

## Maintenance and differentiation in culture of pluripotential embryonic cell lines from pig blastocysts.

**Notarianni E**, **Laurie S**, **Moor RM**, **Evans MJ**.

Department of Genetics, University of Cambridge, UK.

Cell lines were established from explanted blastocysts of domestic pigs; the cells could be maintained indefinitely when grown on mouse fibroblast feeder cell layers. They differentiate spontaneously at high densities, or when allowed to form aggregates when cultured on a non-adhesive substratum. Their appearance and differentiative behaviour resembles that of mouse embryonic stem cell lines. We are currently attempting to establish whether these cultures represent primary ectodermal lineages which would be of particular relevance to developmental and transgenic studies.

Theriogenology. 1990 Nov;34(5):865-77.

## Influence of feeder layer type on the efficiency of isolation of porcine embryo-derived cell lines.

**Piedrahita JA**, **Anderson GB**, **Bondurant RH**.

Department of Animal Science, School of Veterinary Medicine, University of California, Davis, USA.

Experiments were conducted to determine the effects of feeder layers composed of different cell types on the efficiency of isolation and the behavior of porcine embryo-derived cell lines. Inner cell masses (ICM) isolated from 7- to 8-d-old embryos were plated on feeder layers composed of Buffalo rat liver cells (BRL), a continuous cell line of murine embryonic fibroblasts (STO), STO combined with BRL at a 9:1 and 1:1 ratio, STO with BRL-conditioned medium (STO + CM), porcine embryonic fibroblasts (PEF), PEF combined with BRL at a 9:1 and 1:1 ratio, porcine uterine epithelial cells (PUE), murine embryonic fibroblasts (MEF), or an epithelial-like porcine embryo-derived cell line (PH3A). It was found that embryo-derived cell lines could be isolated only from the STO and the STO with BRL-conditioned medium treatments. The isolated cell lines were of epithelial-like and embryonic stem cell-like (ES-like) morphology. The feeders tested had an effect on the behavior of plated ICM. Some feeders, represented by PUE, BRL, STO:BRL (1:1), PEF:BRL (1:1), and PH3A, did not promote attachment of the ICM to the feeder layer; others, represented by STO and MEF, allowed attachment, differentiation and proliferation. On PEF feeders the ICM spread onto the feeder layer

after attachment without apparent signs of proliferation or differentiation. None of the feeders tested increased the efficiency of isolation or the growth characteristics of embryo-derived (both ES-like and epithelial-like) cell lines over that of STO feeders.

J Reprod Fertil Suppl. 1991;43:255-60.

## Derivation of pluripotent, embryonic cell lines from the pig and sheep.

**Notarianni E, Galli C, Laurie S, Moor RM, Evans MJ.**

Department of Genetics, University of Cambridge, UK.

As previously described for the establishment of stable, pluripotent cell lines from pig blastocysts, an analogous cell line was isolated from a sheep blastocyst. There are common features in the morphologies and growth characteristics of the pig and sheep cells in culture; in particular, pig and sheep cells display large nuclei and relatively sparse cytoplasm, as is observed in mouse embryonic stem cells. Furthermore, the morphology of the sheep cells closely resembles that of cells in primary cultures of inner cell masses isolated immunosurgically from sheep blastocysts. This suggests that the sheep cell line represents a primary ectodermal lineage.

Mol Reprod Dev. 1995 Sep;42(1):35-52.

## In vitro pluripotency of epiblasts derived from bovine blastocysts.

**Talbot NC, Powell AM, Rexroad CE.**

U.S. Department of Agriculture, Agricultural Research Service, Beltsville Agricultural Research Center, MD 20705, USA.

Two experiments were conducted to compare the utility of in vitro- and in vivo-derived bovine blastocysts for the isolation of pluripotent epiblasts. In experiment 1, the inner cell masses (ICMs) of in vivo-collected blastocysts yielded a higher proportion of epiblasts after culture on STO feeder cells than ICMs from in vitro-produced blastocysts ($P = .0157$). In experiment 2, ICMs of in vivo-collected blastocysts that hatched on day 8 yielded a greater proportion of epiblasts after culture on STO feeder cells than ICMs from in vitro-produced blastocysts that hatched on day 8. The difference was reversed but smaller for blastocysts that hatched on day 9 (Interaction, $P = .0125$). Epiblasts from blastocysts that hatched on day 8 regardless of their source generated more differentiated cell lines in extended culture than did blastocysts that hatched on day 9. Extended epiblast culture yielded cells identifiable as products of the three embryonic germ layers

that included epithelial cells, fibroblasts, neuronal cells, hepatocyte-like cells, and macrophage-like cells. Alkaline phosphatase activity combined with cell morphology identified the bovine epiblast cells and distinguished them from trophectoderm and endoderm that frequently contaminated epiblast cell cultures. In vivo-derived blastocysts, especially from early-hatching blastocysts, were a superior source of pluripotent epiblasts. Epiblast cells in this study all differentiated or senesced indicating that standard conditions for mouse embryonic stem cell culture do not maintain bovine epiblast cells in an undifferentiated state.

Mol Reprod Dev. 1995 Apr;40(4):444-54.

## Isolation and characterization of permanent cell lines from inner cell mass cells of bovine blastocysts.

**Van Stekelenburg-Hamers AE, Van Achterberg TA, Rebel HG, Fléchon JE, Campbell KH, Weima SM, Mummery CL.**

Hubrecht Laboratory, Netherlands Institute for Developmental Biology, Utrecht.

Inner cell masses (ICM) from in vitro produced day 8 or 9 bovine blastocysts were isolated by immunosurgery and cultured under different conditions in order to establish which of two feeder cell types and culture media were most efficient in supporting attachment and outgrowth of the bovine ICM cells. The efficiency of attachment and outgrowth of the ICM cells could be markedly improved when STO feeder cells were used instead of bovine uterus epithelial cells, and by using charcoal-stripped serum instead of normal serum to supplement the culture medium. More than 20 stable cell lines were obtained. Some of these lines were examined by immunofluorescence for developmentally regulated markers. From these results we conclude that the cell lines resemble epithelial cells, rather than pluripotent ICM cells. The developmental potential of cells of one of the lines was tested in the nuclear transfer assay. The cell line could support the initial development of enucleated oocytes, but none of the reconstructed embryos passed the eight-cell block.

Nature. 1996 Mar 7;380(6569):64-6.

## Sheep cloned by nuclear transfer from a cultured cell line.

**Campbell KH, McWhir J, Ritchie WA, Wilmut I.**

Roslin Institute (Edinburgh), UK.

Nuclear transfer has been used in mammals as both a valuable tool in embryological studies and as a method for the multiplication of 'elite' embryos. Offspring have only been reported when early embryos, or embryo-derived cells during primary culture, were used as nuclear donors. Here we provide the first report, to our knowledge, of live mammalian offspring following nuclear transfer from an established cell line. Lambs

were born after cells derived from sheep embryos, which had been cultured for 6 to 13 passages, were induced to quiesce by serum starvation before transfer of their nuclei into enucleated oocytes. Induction of quiescence in the donor cells may modify the donor chromatin structure to help nuclear reprogramming and allow development. This approach will provide the same powerful opportunities for analysis and modification of gene function in livestock species that are available in the mouse through the use of embryonic stem cells.

Theriogenology. 1990 Nov;34(5):879-901.

## On the isolation of embryonic stem cells: Comparative behavior of murine, porcine and ovine embryos.

**Piedrahita JA**, **Anderson GB**, **Bondurant RH**.

Department of Animal Science, School of Veterinary Medicine, University of California, Davis, USA.

The efficiency of isolation and the characteristics of embryo-derived cell lines from murine, porcine, and ovine embryos cultured on STO feeders or homologous embryonic fibroblasts (HEF) feeders were compared. While murine isolated ICM or intact embryos plated on STO or HEF feeders gave rise to cell lines with embryonic stem cell-like (ES-like) morphology, ovine embryos did not. Cell lines with ES-like morphology were isolated from porcine intact embryos and isolated ICM when plated on STO feeders but not when plated on HEF. Neither murine nor porcine ES-like cell lines expressed cytokeratin 18 or vimentin. Unlike murine ES-like cell lines, porcine ES-like cells did not undergo observable differentiation in vitro or in vivo. Cell lines with epithelial-like morphology were isolated from porcine and ovine embryos. Both porcine and ovine epithelial-like cell kines expressed cytokeratin 18. When induced to differentiate in vitro, porcine and ovine epithelial-like cell lines formed vesicular structures. Electron microscopy revealed that the porcine vesicles were composed of polarized epithelial cells, each with a basally-located nucleus and an apical border containing numerous microvilli with a well organized microfilament core. The results of this study show that conditions which allow isolation of ES cells from murine embryos allow the isolation of porcine embryo-derived cell lines sharing some, but not all, the characteristics of murine ES cells.

Mol Reprod Dev. 1993 Oct;36(2):139-47.

## Alkaline phosphatase staining of pig and sheep epiblast cells in culture.

**Talbot NC**, **Rexroad CE**, **Pursel VG**, **Powell AM**.

U.S. Department of Agriculture, Beltsville Agricultural Research Center, MD 20705.

To define better the characteristics of pig and sheep epiblast cells in culture, the cells were tested for the presence of alkaline phosphatase (AP), a biochemical marker characteristic of mouse embryonic stem cells. Pig and sheep epiblast cells were positive for AP staining both at isolation from the blastocyst and after primary in vitro culture. The innermost portion of the attendant endoderm surrounding the epiblast was also positive for AP staining during primary culture. AP staining was lost upon differentiation or senescence of the epiblast cells. Also, all differentiated epiblast-derived cell cultures were negative for AP staining, with the exception of neuron-like cultures. Epiblast-like cells were cultured from day 10 (pig) and day 13 (sheep) embryonic discs, and these cells were also AP positive until they differentiated. Trophectoderm-endoderm-like cells from embryonic discs were AP negative or weakly positive. AP is a convenient marker for undifferentiated pig and sheep epiblast cells in culture when used in conjunction with cell morphology analysis.

Reprod Fertil Dev. 1994;6(5):563-8.

## Development and validation of swine embryonic stem cells: a review.

**Wheeler MB**.

Department of Animal Sciences, University of Illinois, Urbana 61801, USA.

The establishment of embryonic cell lines from swine should be useful for studies of cell differentiation, developmental gene regulation and the production of transgenics. This paper summarizes the establishment of porcine (Sus scrofa) embryonic stem (ES) cell lines from preimplantation blastocysts and their ability to develop into normal chimaeras. ES cells can spontaneously differentiate into cystic embryoid bodies with ectodermal, endodermal, and mesodermal cell types. Further, culture of ES cells to confluence or induction of differentiation with retinoic acid or dimethylsulfoxide results in morphological differentiation into fibroblasts, adipocytes, and epithelial, neuronal, and muscle cells. These ES cells have a normal diploid complement of 38 chromosomes. Scanning electron microscopy of the ES cells reveals a rounded or polygonal, epithelial-like cell with numerous microvilli. The differentiation of these embryonic cell lines into several cell types indicates a pluripotent cell. Furthermore, chimaeric swine have been successfully produced using such ES cells.

RESEARCH

# Production of goats by somatic cell nuclear transfer

Alexander Baguisi[2,3†], Esmail Behboodi[1†], David T. Melican[1], Julie S. Pollock[4], Margaret M. Destrempes[1], Christine Cammuso[1], Jennifer L. Williams[1], Scott D. Nims[1], Catherine A. Porter[1], Patricia Midura[1], Monica J. Palacios[2,3], Sandra L. Ayres[3], Richard S. Denniston[5], Michael L. Hayes[4], Carol A. Ziomek[1], Harry M. Meade[1], Robert A. Godke[5], William G. Gavin[1], Eric W. Overström[2,3*], and Yann Echelard[1*]

[1]Genzyme Transgenics Corporation, Framingham MA, 01701-9322. [2]Nuclear Transfer Laboratory and [3]Department of Biomedical Sciences, Tufts University School of Veterinary Medicine, North Grafton, MA 01356. [4]Cell and Protein Therapeutic Department, Genzyme Corporation, Framingham, MA 01701-9322. [5]Department of Animal Science, Lousiana State University, Baton Rouge, LA 70803.
[†]These authors contributed equally to this work. *Corresponding authors (e-mail: eoverstrom@infonet.tufts.edu; yechelard@genzyme.com).

Received 22 February 1999; accepted 24 March 1999

**In this study, we demonstrate the production of transgenic goats by nuclear transfer of fetal somatic cells. Donor karyoplasts were obtained from a primary fetal somatic cell line derived from a 40-day transgenic female fetus produced by artificial insemination of a nontransgenic adult female with semen from a transgenic male. Live offspring were produced with two nuclear transfer procedures. In one protocol, oocytes at the arrested metaphase II stage were enucleated, electrofused with donor somatic cells, and simultaneously activated. In the second protocol, activated in vivo oocytes were enucleated at the telophase II stage, electrofused with donor somatic cells, and simultaneously activated a second time to induce genome reactivation. Three healthy identical female offspring were born. Genotypic analyses confirmed that all cloned offspring were derived from the donor cell line. Analysis of the milk of one of the transgenic cloned animals showed high-level production of human antithrombin III, similar to the parental transgenic line.**

Keywords: nuclear transfer, oocyte, transgenic, antithrombin III, goat



The production of human recombinant pharmaceuticals in the milk of transgenic farm animals[1,2] solves many of the problems associated with microbial bioreactors (lack of post-translational modifications, improper folding, high purification costs) or animal cell bioreactors (high capital costs, expensive culture media, low yields). Dairy goats are ideal for transgenic production of therapeutic recombinant proteins. At concentrations of recombinant protein of 1–5 g/L that have been reproducibly achieved with various animal models by this and other groups[1–3], herds of transgenic goats of manageable size could easily yield 1–300 kg of purified product per year. Moreover, the much lower incidence of scrapie in goats (only seven cases reported by the US Department of Agriculture through 1998) relative to sheep (1,117 US cases through 1992[4]) adds to the goats' attractiveness for recombinant protein production.

To date, the only reliable method available to produce transgenic goats has been pronuclear microinjection. While successful, this approach has had limited efficiency. Transgene integration into the genome of founder animals is low, with only 0.5–3% of the microinjected embryos producing transgenic offspring[5]. Moreover, the frequent generation of mosaic founder animals resulting from pronuclear microinjection[6–8] complicates the expansion of transgenic herds.

The application of nuclear transfer technology using blastomeres of early caprine embryos has been reported[9]. This approach is limited by the small numbers of available embryonic blastomeres and by the inefficiency of introducing foreign genetic material into such cells. In contrast, the discoveries that differentiated embryonic[10–12], fetal[11,13–15], or adult somatic cells[10,15–17] can function as karyoplast donors for nuclear transfer have provided a wide range of possibilities for germline modification. The use of recombinant somatic cell lines for nuclear transfer allows the introduction of transgenes by traditional transfection methods, increases the efficiency of transgenic animal production to 100%, and overcomes the problem of founder mosaicism.

In this report, we describe the application of somatic cell nuclear transfer to the propagation of transgenic goats. Three transgenic female goats carrying a transgene targeting the expression of recombinant human antithrombin III (rhAT) to the mammary gland were generated following two activation protocols. Southern blotting, fluorescence in situ hybridization (FISH) and polymerase chain reaction–restriction fragment length polymorphism (PCR-RFLP) analyses verified that these animals were clones of the female hAT cell line. One of the resulting transgenic females was hormonally induced to lactate, and rhAT expression in its milk was consistent with rhAT expression detected in the milk of other transgenic does from the same line obtained by natural breeding[3].

## Results

Caprine fetal somatic cells. Six fetal somatic cell lines were generated from four 35-day and two 40-day fetuses resulting from the mating of a founder BC6 (goat β-casein–hAT cDNA transgene[3]) transgenic buck with two nontransgenic does. The BC6 transgenic line was chosen for these experiments because it provides a well-characterized genetic marker to the somatic cell lines (BC6 transgene), and it targets high-level expression of a complex glycosylated protein (hAT) in the milk of lactating transgenic does. Following PCR analysis of the six primary cultures, two male and four female lines were identified. One transgenic female cell line (CFF6, derived from a 40-day fetus) was used in all nuclear transfer experiments described in this study. In CFF6 cell cultures, as well as in the other primary caprine fetal somatic cell lines, two morphologically distinct cell types were noted. Larger "fibroblast-like" cells (Fig. 1A, center) and smaller

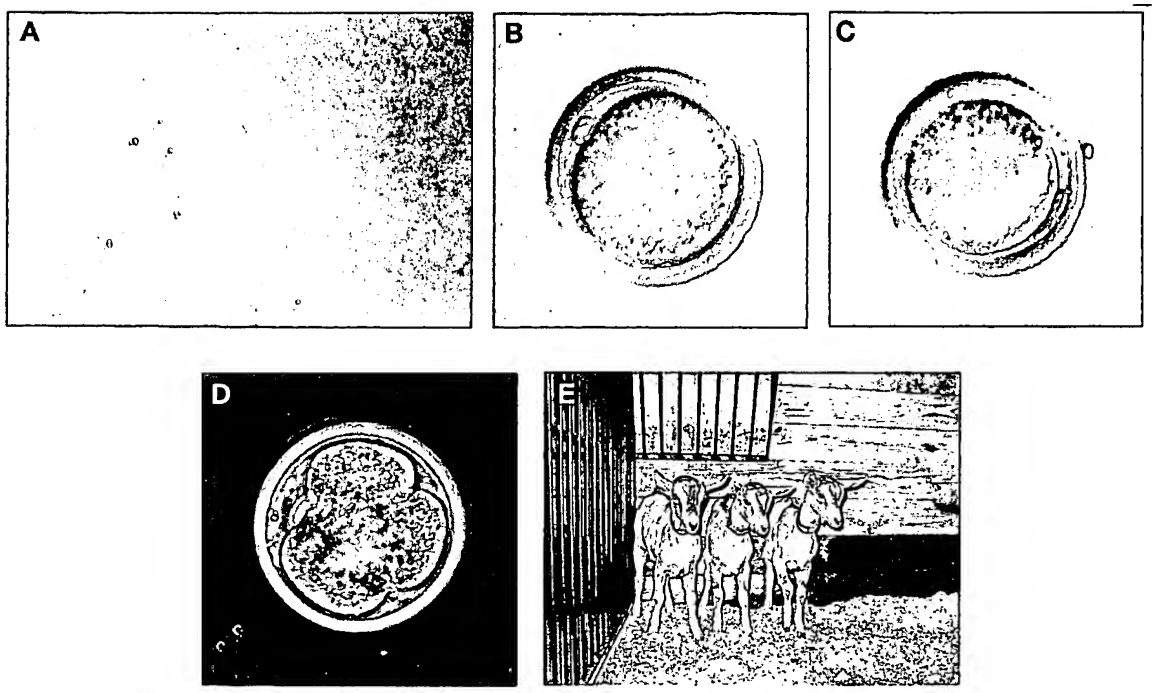


**Figure 1. (A) In vitro-cultured caprine fetal somatic cells at Passage 6, magnification ×200. (B) In vivo-matured Metaphase-II stage caprine oocyte, magnification ×400. (C) In vivo-matured, activated Telophase-II stage caprine oocyte, magnification × 400. (D) A reconstructed 4-cell stage caprine embryo 48 h after fusion of a CFF6 cell to an in vivo-matured, activated Telophase II stage enucleated cytoplast, magnification ×400. This reconstructed embryo was transferred to recipient 1169 (along with one 2-cell stage and another 4-cell stage reconstructed embryo) that delivered the nuclear transfer offspring CFF6-2 and CFF6-3. (E) Three cloned goats at 8 weeks (CFF6-1) and 5 weeks (CFF6-2 and CFF6-3) that were produced by nuclear transfer with fetal somatic cells from the CFF6 transgenic cell line. From left to right, CFF6-1, CFF6-2 and CFF6-**



"epithelial-like" cells (Fig. 1A, bottom left and right sides) coexisted in primary cultures. At first, larger cells dominated (>80%), but with increasing number of passages the proportion of epithelial-like cells increased to >50% of the total cell population.

Production of nuclear transfer embryos. Donor fetal somatic cells were synchronized by seven days of serum deprivation, followed by exposure to medium containing 10% fetal bovine serum (FBS) for 1–3 h before the nuclear transfer procedure. A total of 14 rounds of oocyte collection and embryo transfer procedures were performed. In an effort to optimize the use of oocytes collected, three enucleation/activation protocols were employed: arrested metaphase II oocytes (Fig. 1B), calcium-activated telophase II oocytes (Telophase-II-Ca; Fig. 1C), or ethanol-induced calcium-activated telophase II oocytes (Telophase-II-EtOH). Following fusion/activation, reconstituted embryos were cocultured with primary goat oviduct cells for 48 h, until 2- to 16-cell stage embryos had developed. The majority of embryos were transferred to progestin-synchronized recipient does, at chronologically correct two- and four-cell stages (Fig. 1D). Rates of development were slightly greater when using cytoplasts from Telophase-II-Ca (45%) and Telophase-II-EtOH (56%) oocytes when compared with arrested metaphase II (35%) oocytes (Table 1).

Pregnancy and cloned transgenic offspring. Recipient does were examined by ultrasonography starting at 25 days after embryo transfer. For all three oocyte enucleation/activation protocols, a high proportion of does (55–78%) exhibited vesicle formation very similar to that seen in does at 30 days of gestation (Table 1). In most cases, fetal heartbeats could not be detected at this early stage. The echogenic patterns suggested the presence of trophoblastic vesicles, in the absence of normal embryonic structures. Weekly examinations, between day 25 and day 40 post-transfer, failed to reveal normal embryonic development. By days 55–70, vesicular structures had been resorbed, and the recipient does had returned to estrus.

**Table 1. Development of caprine embryos reconstructed by nuclear transfer using CFF6 transgenic fetal somatic cells.**

| Nuclear transfer protocols | Metaphase-II | Telophase-II-Ca | Telophase-II-EtOH |
|---|---|---|---|
| Oocytes reconstructed | 138 | 92 | 55 |
| Oocyte lysis (%) | 67 (48.5) | 38 (41.3) | 23 (41.8) |
| Embryo cleavage (%) | 48 (34.8) | 41 (44.6) | 31 (56.4) |
| Embryos transferred (%) | 47 (34) | 38 (41.3) | 27 (49.1) |
| Recipients | 15 | 14 | 9 |
| **Ultrasound positive (%)** | | | |
| 30 days | 9 (60) | 11 (78.6) | 5 (55.5) |
| 40 days | 1 (6.7) | 1 (7.1) | 0 |
| 60 days | 1 (6.7) | 1 (7.1) | 0 |
| Term pregnancy (%) | 1 (6.7) | 1 (7.1) | 0 |
| Offspring | 1 | 2 | 0 |
| % of embryos transferred | 2.1 | 5.2 | 0 |
| % of embryos reconstructed | 0.7 | 2.2 | 0 |

Three enucleation protocols were used (see text for details): Metaphase-II (Metaphase-II arrested), Telophase-II-Ca (calcium-activated Telophase-II oocytes), Telophase-II-EtOH (ethanol-induced calcium-activated Telophase-II oocytes). In all cases, simultaneous electrical fusion and activation were induced.

In two recipients, fetal heartbeats were confirmed by day 40 post-transfer. In both of these cases, ultrasound examination between day 25 and day 40 also revealed the development of recognizable fetal structures. One of these two pregnancies resulted from the transfer of embryos (four four-cell stage) that were produced using the arrested metaphase II nuclear transfer protocol. Karyoplasts were from passage 6 of the CFF6 cell line. A healthy transgenic female kid, CFF6-1 (Fig. 1E, left), was delivered on day 154 of gestation after induction of parturition on day 152. The

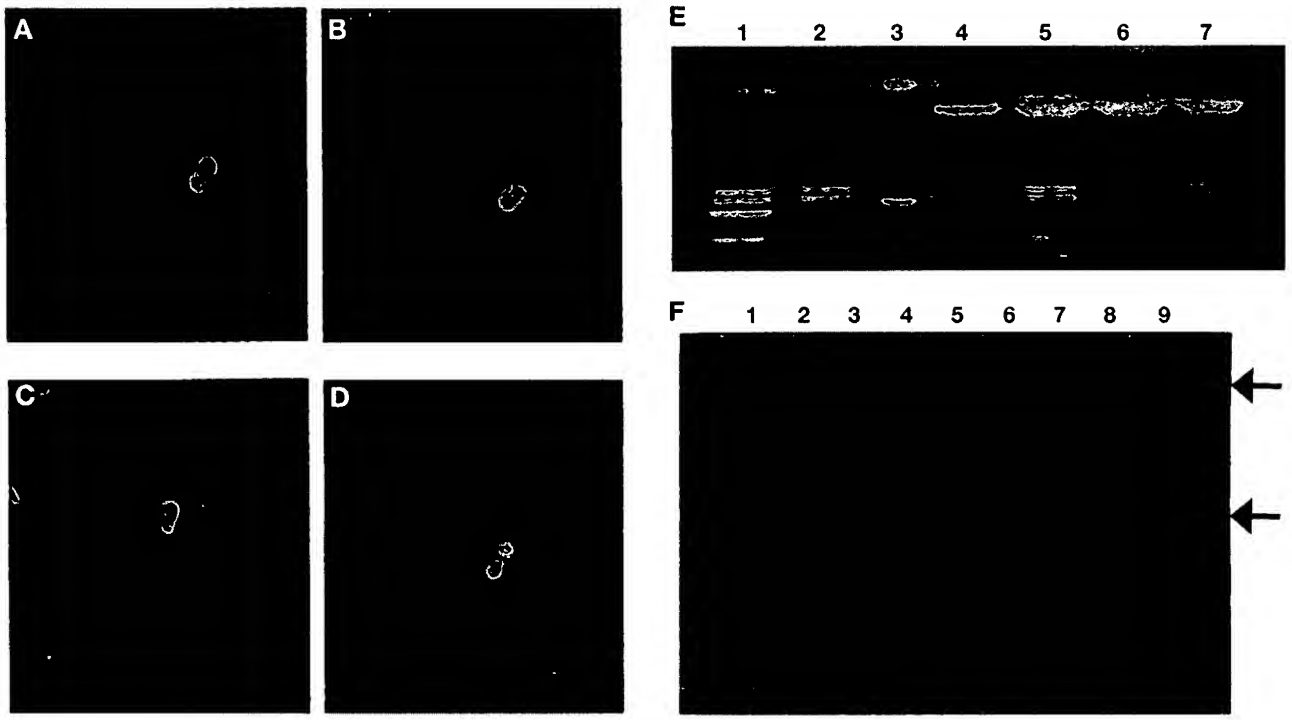


**Figure 2. Genotypic analysis of nuclear transfer goats. FISH analysis of BC6 transgene integration for (A) the CFF-6 cell line, (B) the CFF6-1, (C) the CFF6-2 and (D) the CFF6-3 kid. The BC6 integration (green dots) is located close to the telomere of caprine chromosome 5 (C 5q). (E) *Rsa* I PCR-RFLP analysis of the second exon of the caprine MHC class II DRB gene. Lane 1: recipient 1034, lane 2: recipient 1169, lane 3: molecular weight marker (Gibco BRL 100 bp ladder, 100b and 200 bp fragments are visible), lane 4: CFF6 cell line, lane 5: CFF6-1, lane 6: CFF6-2, lane 7: CFF6-3. (F) Southern blot analysis of *Eco*RI restriction digests of genomic DNAs. Lane 1: CFF6-1, lane 2: CFF6-2, lane 3: CFF6-3, lane 4: CFF6, lane 5: recipient 1034, lane 6: recipient 1169, lane 7: molecular weight marker (λ phage DNA digested with *Bst* EII restriction enzyme), lane 8: negative goat, lane 9: BC6 transgenic control. The top arrow shows the hybridization signal (14 kb band) of the hAT cDNA probe to the endogenous caprine AT locus and serves as an internal loading control. The bottom arrow shows the hybridization signal (4.1 kb band) of the hAT cDNA probe to the BC6 transgene.**



weight at birth was 2.35 kg, which is within the normal range for newborns of this breed. The second pregnancy (twins) resulted from the transfer of embryos produced by the activated Telophase-II-Ca nuclear transfer protocol with karyoplasts originating from passage 5 of the CFF6 cell line. In this case, three nuclear transfer embryos (one two-cell stage and two four-cell stage) were transferred to a recipient doe. Two healthy female kids, CFF6-2 and CFF6-3 (both 3.5 kg at birth, Fig. 1E center and right), were born following a natural delivery (151-day gestation). The coat color was similar in all three kids and reflected the phenotype of the BC6 transgenic buck.

All pregnancies that reached 60 days were carried to term, and no postpartum morbidity was noted. No term pregnancy was produced in this study with embryos generated from oocytes activated with ethanol.

**Genotyping of cloned offspring.** Genomic DNA was isolated from blood and ear tissue of the cloned animals and compared with genomic DNA samples isolated from the recipient does (1034 and 1169) and from the transgenic CFF6 donor somatic cell line. Southern blot analysis (Fig. 2F) demonstrated the presence and integrity of the BC6 transgene. Hybridization to a diagnostic 4.1 kb *Eco*RI fragment was detected for all three cloned animals, the CFF6 cell line, and a transgenic positive control (BC6 buck), but not for the two recipient does. As expected, cross-hybridization of the hAT cDNA probe to the endogenous goat AT locus caused a 14 kb band to be detected in all samples.

Analysis of blood cultures from each transgenic kid with FISH probes for the BC6 transgene showed that all three carry a chromosome 5 (C5) transgene integration identical to that found in metaphase spreads derived from the CFF6 cell line (Fig. 2A–D). Moreover, analysis of more than 75 metaphase spreads for each cloned offspring confirmed that they are not mosaic for the C5 transgenic integration.

**Table 2. rhAT expression in CFF6-1 goat milk from an induced lactation.**

| CFF6-1 induced lactation day | hAT concentration (g/liter) | h AT activity (U/ml) |
|---|---|---|
| Day 3 | 4.7 | N/D |
| Day 5 | 5.8 | 20.5 |
| Day 6 | 5.0 | 18.3 |
| Day 7 | 4.7 | 15.6 |
| Day 8 | 4.1 | 14.4 |
| Day 9 | 3.7 | 14.6 |

N/D: not determined.

As final confirmation that all three kids are derived from the transgenic CFF6 cell line, PCR-RFLP analysis for the very polymorphic[18] major histocompatibility complex (MHC) class II *DRB* gene was undertaken (Fig. 2E). As illustrated by the *Rsa*I digests of the *DRB* gene second exon, the three cloned females are identical to each other and identical to the CFF6 donor cell line, whereas the recipient does carry different alleles.

**Expression of rhAT.** At two months-of-age, the first cloned goat CFF6-1 was subjected to a two-week hormonal lactation-induction

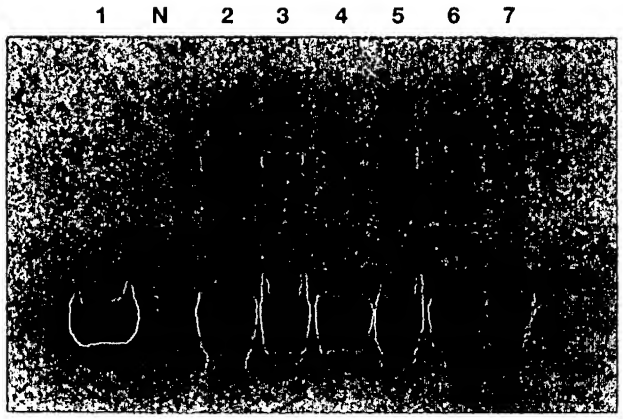


**Figure 3. Western blot of rhAT expressed in the milk of the cloned transgenic doe CFF6-1. Five micrograms of protein were applied to the standard hAT lane. The Western blot was developed with a sheep anti-hAT HRP conjugated antibody (SeroTEC) and color development was performed using the ECL system (Amersham). Lane 1: purified hAT standard (5 µg), Lane N: negative goat milk (10 µl), Lanes 2 to 7: samples (9–13 µl) from lactation day 3, 5, 6, 7, 8 and 9, respectively.**



protocol. At the end of treatment, milk samples (0.5–10 ml) were collected daily for 33 days. The volumes had increased to 10 ml/day by the time lactation was stopped, with a total of 159 ml produced over the 33 days of milking. The concentration and activity of hAT in representative samples was evaluated (Table 2). As had been noted[3] with does from this specific BC6 transgenic line, high-level expression of the rhAT was detected by western blot analysis (Fig. 3). The concentration of rhAT in the milk of the CFF6-1 animal (Table 2) was 5.8 g/L (20.5 U/ml) at day 5, and 3.7 g/L (14.6 U/ml) by day 9.

## Discussion

Three cloned transgenic goats were generated by nuclear transfer of fetal caprine somatic cells to in vivo-derived caprine oocytes. All cloned offspring born in this study were healthy with birthweights within the normal range for their breed. This contrasts with the perinatal morbidity/mortality observed with other demonstrations of cultured cell nuclear transfers in ovine[10–13] and bovine[14,15,17] systems. It is not clear whether this is due to a lesser susceptibility of caprine embryos to as yet ill-defined perturbations caused by the nuclear transfer process, in vivo sourcing of mature oocytes, or a reflection of the relatively low number of clones produced in the caprine nuclear transfer system. It is also noteworthy that, in this program, embryos were transferred to the oviduct of recipient does at the two- or four-cell stage, with minimal in vitro culture.

In this study, nonviable early pregnancies were found in two-thirds of the embryo transfers performed irrespective of the nuclear transfer protocol that was used. Vesicle-like structures were detected by ultrasonography at 25 days post-transfer, and these "embryonic" structures had been resorbed by 55 days post-transfer. It is possible that the vesicular structures were a result of aberrant placental development and were of trophoblast origin. This may reflect the failure of blastocyst differentiation and inner cell mass development as a consequence of faulty genome activation. Alternatively, some of the vesicular structures may have resulted from the transfer of parthenogenetic, aneuploid, or polyploid embryos, an artifact of incomplete enucleation of recipient oocytes.

Nuclear transfer was performed on oocytes that were enucleated either at the arrested metaphase II stage or the activated telophase II stage. Subsequent studies of the cell cycle status of fetal caprine somatic cells has suggested that the starved cells were likely at the G0/G1 transition following restoration of 10% serum. Immunofluorescence screening revealed that after seven days of serum starvation, fetal somatic cells were negative for G1-stage cyclins D1, D2, D3, and proliferating cell nuclear antigen (PCNA).

Previous successful efforts to produce cloned animals by somatic cell nuclear transfer have used either quiescent (G0) donor karyoplasts[11–13,16,17] or actively dividing (G1) donor karyoplast cells[14,15] with arrested metaphase II oocyte-derived cytoplasts. The use of an activated telophase II cytoplast may have several practical and biological advantages. Enucleation of telophase II oocytes is technically easier and removes considerably fewer cytoplasmic factors and organelles. Moreover, telophase II enucleation provides a synchronous population of activated recipient cytoplasts that, when used for embryo reconstruction, show a higher rate of embryonic development in vitro (ref. 19 and the present study).

The ability to use preactivated oocytes could be important in the context of a commercial operation involved in the generation of transgenic animals for the production of therapeutic proteins. Regulatory guidelines recommend the use of closed herds of well-characterized scrapie-free goats as embryo donors and recipients. This then requires an efficient use of such limited valuable animals as donors and recipients. It should not be overlooked that gonadotropin-treated donors most frequently yield heterogeneous populations of in vivo-matured oocytes. The option of using both metaphase II and telophase II-stage oocytes for nuclear transfer will permit a more efficient use of donor goat herds.

Oocytes that were activated by ethanol treatment did not give rise to term pregnancies, in spite of a good cleavage rate (56%) following reconstruction. It could be that these oocytes were developmentally compromised from the beginning, that the ethanol treatment was too harsh and caused irreversible damage to the embryo, or merely that a low number of transfers was performed using the Telophase-II-EtOH protocol.

Our data suggest that nuclear transfer of transgenic somatic cells is at least as efficient as microinjection for generating transgenic animals. Overall, 2.6% of the nuclear transfer embryos transferred to recipients (3.5% if one does not consider the ethanol activation protocol) gave rise to nonmosaic transgenic offspring. This is in comparison with 0.5–3% of the embryos transferred in a typical caprine microinjection program[5] (data not shown). However, in a founder production program, nontransgenic fetal somatic cell lines would need to be transfected with appropriate transgenes and clonal selection applied. Although it is obvious that caprine fetal somatic cell cultures have a finite life span, it has been possible to transfect and select these cells before the onset of senescence (data not shown). Work is ongoing to verify that transfected caprine cell lines can efficiently serve as karyoplast donors for nuclear transfer. Previous work has demonstrated that transfected bovine and ovine primary fibroblasts are capable of producing cloned transgenic animals[13,14].

The generation of transgenic animals that have completely identical genetic backgrounds enhances the possibility of studying the expression and secretion characteristics of recombinant proteins by the mammary gland. For example, the availability of several completely identical transgenic females producing rhAT will help determine the extent of variation in the carbohydrate structure of this protein, as it is produced by the mammary gland. Thus, it may be feasible either to improve the characteristics of the recombinant proteins produced in the transgenic animal system by varying environmental factors such as nutrition, or to increase the milk yield from lactation-induction protocols to diminish further the time necessary to obtain adequate amounts of recombinant protein for preclinical or clinical programs.

The high-level expression of rhAT detected in the milk of the CFF6-1 cloned goat illustrates one of the most important aspects of

this technology. By combining nuclear transfer with lactation-induction in prepubertal goats, it may be possible to characterize transgenic animals and the proteins they secrete in eight to nine months from the time of cell line transfection to milk expression. The amount of milk collected in an induced lactation is not only sufficient to evaluate the recombinant protein yield, but when expression levels in milligrams per milliliter are obtained, is adequate for such qualitative analyses as glycosylation, preliminary pharmacokinetics, and biological and pharmacological activities. The continued availability of the transfected donor cell line also insures that genetically identical animals can be quickly produced, in order to generate a ready supply of therapeutic proteins (with predictable characteristics) for clinical trials.

## Experimental protocol

Goats. The herds of pure- and mixed-breed, scrapie-free, Alpine, Saanen, and Toggenburg dairy goats used for this study were maintained under Good Agricultural Practice (GAP) guidelines at the Genzyme Transgenics Farm in Massachusetts.

Isolation of caprine fetal somatic cell lines. Six primary caprine fetal fibroblast cell lines to be used as karyoplast donors were derived from 35- and 40-day fetuses produced by artificially inseminating two nontransgenic does with fresh-collected semen from the transgenic BC6 founder buck[3]. Fetuses were surgically removed and placed in equilibrated phosphate-buffered saline (PBS, $Ca^{2+}$/$Mg^{2+}$-free). Single-cell suspensions were prepared by mincing fetal tissue exposed to 0.025% trypsin, 0.5 mM EDTA at 38 °C for 10 min. Cells were washed with fetal cell medium (equilibrated Medium 199 [M199]; Gibco, Gaithersburg, MD) with 10% FBS supplemented with nucleosides, 0.1 mM 2-mercaptoethanol, 2 mM L-glutamine, and 1% penicillin/streptomycin (10,000 IU/ml each), and were cultured in 25 $cm^2$ flasks. A confluent monolayer of primary fetal cells was harvested by trypsinization after four days of incubation and then maintained in culture or cryopreserved.

Sexing and genotyping of donor cell lines. Genomic DNA was isolated from fetal tissue[20] and analyzed by PCR for the presence of hAT sequences, as well as, for sequences useful for sexing. The hAT sequence was detected by amplification of a 367-bp sequence with oligonucleotides GTC 11 and GTC 12. Sexing was performed[21] using a zfX/zfY primer pair and *Sac*I restriction enzyme digest of the amplified fragments. Oligonucleotide sequences are, for GTC 11, 5′-CTCCATCAGTTGCTGGAGGGTGTCATTA-3′; for GTC 12, 5′-GAAGGTTTATCTTTTGTCCTTGCTGCTCA-3′; for zfX, 5′-ATAATCA-CATGGAGAGCCACAAGC-3′; for zfY, 5′-GCACTTCTTTGGTATCTGA-GAAAG-3′.

Preparation of donor cells for embryo reconstruction. The transgenic female line (CFF6) was used for all nuclear transfer procedures. Fetal somatic cells were seeded in four-well plates with fetal cell medium and maintained in culture (5% $CO_2$, 39°C). After 48 h, the medium was replaced with fresh low-serum (0.5% FBS) fetal cell medium. The culture medium was replaced with low-serum fetal cell medium every 48–72 h over the next seven days. On the seventh day following the first addition of low-serum medium, somatic cells (to be used as karyoplast donors) were harvested by trypsinization. The cells were resuspended in equilibrated M199 with 10% FBS supplemented with 2 mM L-glutamine, 1% penicillin/streptomycin (10,000 IU/ml each) 1–3 h before fusion to the enucleated oocytes.

Oocyte collection. Oocyte donor does were synchronized and superovulated as described[22] and were mated to vasectomized males over a 48 h interval. After collection, oocytes were cultured in equilibrated M199 with 10% FBS supplemented with 2 mM L-glutamine and 1% penicillin/streptomycin (10,000 IU/ml each).

Cytoplast preparation and enucleation. Oocytes with attached cumulus cells were discarded. Cumulus-free oocytes were divided into two groups: arrested metaphase II (one polar body) and telophase II protocols (no clearly visible polar body or presence of a partially extruding second polar body). The oocytes in the arrested metaphase II protocol were enucleated first. The oocytes allocated to the activated telophase II protocols were prepared by culturing for 2–4 h in M199/10% FBS. After this period, all activated oocytes (criterion: presence of a partially extruded second polar body) were grouped as culture-induced, calcium-activated telophase II oocytes (Telophase-II-Ca) and enucleated. Oocytes that had not activated during the culture period were subsequently incubated 5 min in M199, 10% FBS containing 7% ethanol to induce activation[19], and then cultured in M199 with 10% FBS for an additional 3 h to reach telophase II (Telophase-II-EtOH protocol). All oocytes were treated with cytochalasin-B (5 µg/ml in M199 with 10% FBS; Sigma, St. Louis, MO) 15–30 min before enucleation. Metaphase II-stage oocytes were enucleated with a 25–30 µm glass pipette by aspirating the first polar body and adjacent cytoplasm surrounding the polar body (~30% of the cytoplasm) to remove the metaphase plate. Telophase-II-Ca and Telophase-II-EtOH oocytes were enucleated by removing the first polar body and the surrounding cytoplasm (10–30% of cytoplasm) containing the partially extruding second polar body. After enucleation, all oocytes were immediately reconstructed.

Nuclear transfer. Donor cell injection was conducted in the same medium used for oocyte enucleation. One donor cell was placed between the zona pellucida and the ooplasmic membrane using a glass pipette. The cell-oocyte couplets were incubated in M199 for 30–60 min before electrofusion and activation procedures. Reconstructed oocytes were equilibrated in fusion medium (300 mM mannitol, 0.05 mM $CaCl_2$, 0.1 mM $MgSO_4$, 1 mM $K_2HPO_4$, 0.1 mM glutathione, and 0.1 mg/ml bovine serum albumin) for 2 min. Electrofusion and activation were conducted at room temperature in a fusion chamber with two stainless-steel electrodes (500 µm gap; BTX-Genetronics, San Diego, CA) filled with fusion medium. Fusion and activation were simultaneously induced with an initial alignment/holding pulse of 5–10 V a.c. for 7 s, followed by a fusion pulse of 1.4–1.8 kV/cm d.c. for 70 µs using an Electrocell Manipulator 200 (BTX-Genetronics). Reconstructed embryos were washed in fusion medium for 3 min, then incubated at 39°C in M199 containing 5 µg/ml cytochalasin-B and 10% FBS for 1 h before culture.

Nuclear transfer embryo culture and transfer to recipients. All nuclear transfer embryos were cocultured on monolayers of primary goat oviduct epithelial cells in 50 µl droplets of M199 with 10% FBS overlaid with mineral oil. Embryo cultures were maintained in a humidified 39°C incubator with 5% $CO_2$ for 48 h before transfer of the embryos to recipient does. Recipient embryo transfer was performed as described[22].

Pregnancy and perinatal care. Pregnancy was determined by ultrasonography starting on day 25 after the first day of standing estrus. Does were evaluated weekly until day 75 of gestation, and once a month thereafter to assess fetal viability. For the pregnancy that continued beyond 152 days, parturition was induced with 5 mg of prostaglandin-$F_{2\alpha}$ ($PGF_{2\alpha}$) (Lutalyse; Pharmacia & Upjohn, London). Parturition occurred within 24 h after treatment. Kids were removed from the dam immediately after birth, and received heat-treated colostrum within 1 h after delivery.

Genotyping of cloned animals. Shortly after birth, blood samples and ear skin biopsy specimens were obtained from the cloned female goats and the surrogate dams for genomic DNA isolation[20]. Each sample was first analyzed by PCR using hAT-specific primers, and then subjected to Southern blot analysis using the hAT cDNA[3]. For each sample, 5 µg of genomic DNA were digested with *Eco*RI (New England Biolabs, Beverly, MA), electrophoresed in 0.7% agarose gels (SeaKem; FMC BioProducts, Rockland, ME), and immobilized on nylon membranes (MagnaGraph; MSI, Westboro, MA) by capillary transfer following standard procedures[23]. Membranes were probed with the 1.5 kb *Xho*I to *Sal*I hAT cDNA fragment labeled with $\alpha$-$^{32}$P-dCTP using the Prime-It kit (Stratagene, La Jolla, CA). Hybridization[24] was executed at 65°C overnight. The blot was washed with 0.2× SSC , 0.1% SDS, and exposed to X-OMAT AR (Kodak, Rochester, NY) film for 48 h.

PCR-RFLP typing. Typing for the second exon of the caprine MHC class II *DRB* gene was performed as described[25]. A 15 µl aliquot of nested PCR product was digested with 20 units of *Rsa*I (New England Biolabs, Beverly, MA). Following digestion, restriction fragments were separated at room temperature in a 4–20% nondenaturing polyacrylamide gel (MVP precast gel; Stratagene) in the presence of ethidium bromide.

FISH analysis. For typing of the cloned goats, whole blood was cultured for lymphocytes harvest[26]. Fibroblast cells and lymphocytes were pretreated[27] and hybridized[28], as described. A digoxygenin-labeled probe containing the entire 14.7-kb BC6 transgene was used in this procedure. The TSA-Direct system (NEN Life Science Products, Boston, MA) was used to amplify the signal. R-bands were visualized using DAPI counterstain and identified as in ref. 29. A Zeiss Axioskop microscope mounted with a Hamamatsu digital camera was used with Image-Pro Plus software (Media Cybernetics, Silver Spring, MD) to capture and process images.

Milk protein analyses. Hormonal induction of lactation[30] for the CFF6-1 female was performed at two months-of-age. The CFF6-1 kid was hand-milked once daily to collect milk samples for hAT expression analyses. Western blot and rhAT activity analyses were performed, as described[3].

## Acknowledgments

*This work was supported, in part, by a grant from the NIH (Small Business Innovation Research Program, R43 HD35395-01) to Genzyme Transgenics Corporation, and by Genzyme Transgenics Corporation. The authors gratefully acknowledge the help of M. Schofield, D.V.M., A. O'Coin, S. Bombard, N. Hawkins, S. Blash, R. Burns, and B. Kuehholzer. We wish to thank Gary Anderson for critical reading of the manuscript and helpful comments.*

1. Meade, H.M. et al. in *Gene expression systems: using nature for the art of expression*, (eds Fernandez, J.M. & Hoeffler, J.P.) 399–427 (Academic Press, San Diego; 1998).
2. Clark, A.J. The mammary gland as a bioreactor: expression, processing, and production of recombinant proteins. *J. Mammary Gland Biol. Neoplasia* **3**, 337–350 (1998).
3. Edmunds, T. et al. Transgenically produced human antithrombin—structural and functional comparison to human plasma-derived antithrombin. *Blood* 91, 4561–4571 (1998).
4. Wineland, N.E., Detwiler, L.A. & Salman, M.D. Epidemiologic analysis of reported scrapie in sheep in the United States: 1,117 cases (1947–1992). *J. Am. Vet. Med. Assoc.* **212**, 713–718 (1998).
5. Ebert, K.M. & Schindler, J.E.S. Transgenic farm animals: Progress report. *Theriogenology* **39**, 121–135 (1993).
6. Wilkie, T.M., Brinster, R.L. & Palmiter, R.D. Germline and somatic mosaicism in transgenic mice. *Dev. Biol.* **118**, 9–18 (1986).
7. Burdon, T.G. & Wall, R.J. Fate of microinjected genes in preimplantation mouse embryos. *Mol. Reprod. Dev.* **33**, 436–442 (1992).
8. Whitelaw, C.B.A., Springbett, A.J., Webster, J. & Clark, A.J. The majority of $G_0$ transgenic mice are derived from mosaic embryos. *Transgenic Res.* **2**, 29–32 (1992).
9. Yong, Z. & Yuqiang, L. Nuclear-cytoplasmic interaction and development of goat embryos reconstructed by nuclear transplantation: production of goats by serially cloning embryos. *Biol. Reprod.* **58**, 266–269 (1998).
10. Campbell, K.H.S., McWhir, J., Ritchie, W.A. & Wilmut, I. Sheep cloned by nuclear transfer from a cultured cell line. *Nature* **380**, 64–66, (1996).
11. Wilmut, I., Schnieke, A.E., McWhir, J., Kind, A.J. & Campbell, K.H.S. Viable offspring derived from fetal and adult mammalian cells. *Nature* **385**, 810–813 (1997).
12. Wells, D.N., Misica, P.M., Day, T.A. & Tervit, H.R. Production of cloned lambs from an established embryonic cell line: a comparison between in vivo- and in vitro-matured cytoplasts. *Biol. Reprod* **57**, 385–393 (1997).
13. Schnieke, A.E. et al. Human Factor IX transgenic sheep produced by transfer of nuclei from transfected fetal fibroblasts. *Science* **278**, 2130–2133 (1997).
14. Cibelli, J.B. et al. Cloned transgenic calves produced from nonquiescent fetal fibroblasts. *Science* **280**, 1256–1258 (1998).
15. Vignon, X. et al. Developmental potential of bovine embryos reconstructed from enucleated matured oocytes fused with cultured somatic cells. *C.R. Acad. Sci.* **321**, 735–745 (1998).
16. Wakayama, T., Perry, A.C.F., Zuccotti, M., Johnson, K.R., & Yanagimachi, R. Full-term development of mice from enucleated oocytes injected with cumulus cells nuclei. *Nature* **394**, 369–374 (1998).
17. Kato, Y. et al. Eight calves cloned form somatic cells of a single adult. *Science* **282**, 2095–2098 (1998).
18. Amills, M., Francino, O. & Sànchez, A. Nested PCR allows the characterization of *TaqI* and *PstI* RFLPs in the second exon of the caprine MHC class II *DRB* gene. *Vet. Immunol. Immunopathol.* **48**, 313–321 (1996).
19. Bordignon, V. & Smith, L.C. Telophase enucleation: an improved method to prepare recipient cytoplasts for use in bovine nuclear transfer. *Mol. Reprod. Dev.* **49**, 29–36 (1998).
20. Laird, P.W. et al. Simplified mammalian DNA isolation procedure. *Nucleic Acids Res.* **19**, 4293 (1991).
21. Aasen, E. & Medrano, J.F. Amplification of the *ZFY* and *ZFX* genes for sex identification in humans, cattle, sheep and goats. *Bio/Technology* **8**, 1279–1281 (1990).
22. Gavin, W.G. in *Transgenic animals—generation and use* (ed. Houdebine, L.M.) 19–21 (Harwood Academic Publishers, Amsterdam, 1996).
23. Maniatis, T., Fritsch, E.F. & Sambrook, J. *Molecular cloning, a laboratory manual.* (Cold Spring Harbor Press, Cold Spring Harbor, NY, 1982).
24. Church, G.M. & Gilbert, W. Genomic sequencing. *Proc. Natl. Acad. Sci. USA* **81**, 1991–1995 (1984).
25. Amills, M., Francino, O. & Sànchez, A. A PCR-RFLP typing method for the caprine *Mhc* class II *DRB* gene. *Vet. Immunol. Immunopathol.* **55**, 255–260 (1996).
26. Ponce de Leon, F.A., Li, Y. & Weng, Z. Early and late replicative chromosomal banding patterns of *Gallus domesticus*. *J. Hered.* **83**, 36–42 (1992).
27. van de Corput, M.P.C., Dirks, R.W., van Gijlswijk, R.P.M., van de Rijke, F.M. & Raap, A.K. Fluorescence in situ hybridization using horseradish peroxidase-labeled oligodeoxynucleotides and tyramide signal amplification for sensitive DNA and mRNA detection. *Histochem Cell Biol.* **110**, 431–437 (1998).
28. Klinger, K. et al. Rapid detection of chromosome aneuploidies in uncultured amniocytes by using fluorescence in situ hybridization (FISH). *Am. J. Hum. Genet.* **51**, 55–65 (1992).
29. Di Berardino, D. et al. R-banding pattern of the prometaphase chromosomes of the goat. *J. Hered.* **78**, 225–230 (1987).
30. Ryot, K.D., Vadnere S.V. & Prakash P. Hormonal induction of lactation and histomorphology of mammary glands in prepubertal goats. *Indian J. Anim. Res.* **10**, 49–51 (1989).

THE JOURNAL OF BIOLOGICAL CHEMISTRY
Vol. 274, No. 41, Issue of October 8, pp. 29282–29288, 1999
Printed in U.S.A.


# Melusin Is a New Muscle-specific Interactor for $\beta_1$ Integrin Cytoplasmic Domain*

(Received for publication, April 22, 1999, and in revised form, July 12, 1999)

**Mara Brancaccio‡§, Simona Guazzone‡, Nadia Menini‡, Elena Sibona‡, Emilio Hirsch‡, Marco De Andrea¶, Mariano Rocchi‖, Fiorella Altruda‡, Guido Tarone‡, and Lorenzo Silengo‡**

*From the ‡Department of Genetics, Biology and Biochemistry, University of Torino, Torino 10126, Italy, the ¶Immunogenetic and Experimental Oncology Center, CNR, Torino 10126, Italy, and the ‖Institute of Genetics, University of Bari, Bari 70122, Italy*

**Here we describe the isolation and partial characterization of a new muscle-specific protein (Melusin) which interacts with the integrin cytoplasmic domain. The cDNA encoding Melusin was isolated in a two-hybrid screening of a rat neonatal heart library using $\beta_1$A and $\beta_1$D integrin cytoplasmic regions as baits. Melusin is a cysteine-rich cytoplasmic protein of 38 kDa, with a stretch of acidic amino acid residues at the extreme carboxyl-terminal end. In addition, putative binding sites for SH3 and SH2 domains are present in the amino-terminal half of the molecule. Chromosomic analysis showed that *melusin* gene maps at Xq12.1/13 in man and in the synthenic region X band D in mouse. Melusin is expressed in skeletal and cardiac muscles but not in smooth muscles or other tissues. Immunofluorescence analysis showed that Melusin is present in a costamere-like pattern consisting of two rows flanking α-actinin at Z line. Its expression is up-regulated during *in vitro* differentiation of the C2C12 murine myogenic cell line, and it is regulated during *in vivo* skeletal muscle development. A fragment corresponding to the tail region of Melusin interacted strongly and specifically with $\beta_1$ integrin cytoplasmic domain in a two-hybrid test, but the full-length protein did not. Because the tail region of Melusin contains an acidic amino acid stretch resembling high capacity and low affinity calcium binding domains, we tested the possibility that $Ca^{2+}$ regulates Melusin-integrin association. *In vitro* binding experiments demonstrated that interaction of full-length Melusin with detergent-solubilized integrin heterodimers occurred only in absence of cations, suggesting that it can be regulated by intracellular signals affecting $Ca^{2+}$ concentration.**

Integrins are heterodimeric αβ membrane receptors that link extracellular matrix proteins to cytoskeletal elements controlling adhesive and motile behavior of cells. They are also crucial in transferring signals that affect cell proliferation and differentiation. Both the ability to interact with cytoskeletal proteins and to generate intracellular signals depends on the integrin cytoplasmic domain that consists of short amino acid sequences, devoid of enzymatic activity. Mutational analyses have shown that the $\beta_1$ subunit cytoplasmic domain is responsible for the localization of the integrin heterodimer in focal adhesions, the sites where actin filaments are connected to the plasma membrane (1, 2). $\beta_1$ cytoplasmic domain interacts with several cytoskeletal and signaling molecules such as talin, filamin, α-actinin, paxillin, and $p125^{FAK}$ as shown by *in vitro* binding assays (3, 4). All these proteins are selectively concentrated at focal adhesions, and their association with integrins *in vivo* is likely to require the organization of supramolecular complexes. Using the two-hybrid system, new proteins such as the serine-threonine kinase ILK (Integrin Linked Kinase) (5), ICAP (Integrin Cytoplasmic Domain Associated Protein) (6, 7), and RACK1 (Receptor for Activated Protein Kinase C) (8) were shown to bind directly to the $\beta_1$ integrin cytoplasmic domain. Analysis of the integrin cytoplasmic domain indicated the existence of four different splicing variants referred as $\beta_1$A, -B, -C, and -D (9). Whereas $\beta_1$B and $\beta_1$C are rare isoforms expressed at low level only in human species, the $\beta_1$A is the most widely expressed isoform and $\beta_1$D is selectively expressed in striated muscle tissues where it represents the only $\beta_1$ integrin splice variant (10). We have previously shown that $\beta_1$D cytoplasmic domain endows this isoform with higher binding affinity for both cytoskeletal and extracellular matrix proteins, indicative of the ability of $\beta_1$D to form stable cytoskeleton/matrix connections (11).

In muscle tissue, the membrane-actin cytoskeleton interaction occurs at myotendinous junctions and costamers, two highly specialized junctional complexes. At myotendinous junctions, actomyosin filaments are anchored end-on to the plasma membrane, whereas at costamers they are joined laterally. Integrins are selectively enriched both in myotendinous junctions and costamers (10, 12, 13), suggesting an important role of these receptors in connecting the cytoskeleton to the extracellular matrix in muscles. Direct evidence of the role of integrins in muscle function and in actin organization also comes from gene knockout experiments. In *Drosophila*, lack of integrin β subunit expression causes muscle detachment from its attachment points when the first contraction occurs (14). Gene knockout experiments in mice indicated that $\beta_1$ is not essential for myoblast fusion during *in vitro* myogenic differentiation (15), but an impaired sarcomere cytoarchitecture is observed in $\beta_1$-null cardiomyocytes derived by *in vitro* differentiated embryonic stem cells (16). Moreover, mice lacking expression of α7, the major muscle integrin α subunit, develop muscular dystrophy postnatally and display major alterations in the muscle-tendon junction (17).

* This work was supported by Grants 851 (to G. T.) and E.672 (to M. R.) from Theleton, from the Ministry of University and Scientific Research (to F. A.), from the National Research Council (P. F. Biotecnologie) (to F. A.) and from ASI (Italian Space Agency Grant 98-112). The costs of publication of this article were defrayed in part by the payment of page charges. This article must therefore be hereby marked "*advertisement*" in accordance with 18 U.S.C. Section 1734 solely to indicate this fact.

*The nucleotide sequence(s) reported in this paper has been submitted to the GenBank™/EBI Data Bank with accession number(s) AF140690 and AF140691.*

§ To whom correspondence should be addressed: Dept. of Genetics, Biology and Biochemistry, Via Santena 5 bis, 10126 Torino, Italy. Tel.: 39-011-6706680; Fax: 39-011-6706547; E-mail: brancacc@molinette.unito.it.

Experiments directed to investigate whether integrins are involved in the formation of the sarcomeres or in their stabilization after formation indicate that localization of integrins to actin-membrane junctions occurs once the organization of actin in sarcomeres has already occurred (18, 19). These data strongly suggest that the localization of integrins at myotendinous junctions and costamers is driven by the organization of actin inside the cells. Their presence at these sites is crucial for the mechanical stabilization of these junctions as indicated by the gene knockout experiments (16, 17).

To better understand the mechanisms of integrin-cytoskeletal interactions, we searched for muscle proteins capable of interacting with the $\beta_1$ integrin cytoplasmic domain. Using a two-hybrid screening, we isolated a new muscle-specific interactor capable of binding both $\beta_1$A and $\beta_1$D isoforms, but not other integrin $\beta$ subunits.

## MATERIALS AND METHODS

*Interaction Trap*—Screening for proteins that interact with cytoplasmic tails of $\beta_1$A and $\beta_1$D was performed as described (20). To construct bait plasmids, sequences encoding amino acids 752–798 of $\beta_1$A and amino acids 752–801 of $\beta_1$D were amplified by PCR[1] using primers containing *Eco*RI and *Bam*HI site on either ends ($\beta_1$A, 5′-GGAATTCAAGCTTTTAATGATAATT-3′and 5′-CGGGATCCTCATTTTCCCTCATACTT-3′; $\beta_1$D, 5′-GGAATTCAAGCTTTTAATGATAATT-3′and 5′-CGGGATCCTCAGAGACCAGCTTTACG-3′) and cloned in pEG202 vector in frame with LexA coding sequence. Both plasmids were unable to activate transcription when cotransformed in EGY48 yeast strain with pSH18–34 reporter plasmid (data not shown). We confirmed the expression of these fusion proteins in yeast total protein extracts by Western blot analysis using an anti-LexA antibody (a gift from A. Zervos). A cDNA library from heart neonatal rat fused to a galactose-inducible activation domain (a gift from A. Zervos) was transformed in yeast strain EGY48 that already contained pSH18–34 reporter plasmid and pEG202-$\beta_1$A or -$\beta_1$D using a LiAc high efficiency transformation protocol (21). Primary transformants ($2 \times 10^6$) were screened by plating 10 million colonies on selectable medium lacking Ura, His, Trp, and Leu. Several positive clones for $\beta_1$A and $\beta_1$D were isolated, and their specific binding to integrins was tested by assaying the interaction with control baits such as bicoid, bFGF, a ciclyn A, and c-Myc (a gift from A. Zervos).

Other baits were produced to test the ability of Melusin to interact with other integrin cytoplasmic tails: sequences encoding amino acids 724–769 of $\beta_2$ (5′-CATGCCATGGAAGGCTCTGATCCACCTG-3′ and 5′CCGCTCGAGCTAACTCTCAGCAAACTT-3′), 716–762 of human $\beta_3$ (5′-GCATGCCATGGAAACTCCTCATCACCATC-3′ and 5′-CCGCTCGAGTTAAGTGCCCCGGTACGT-3′), 752–789 of $\beta_1$B (5′-GGAATTCAAGCTTTTAATGATAATT-3 and 5′-CGGGATCCTTATAAGCCACTTTGCTT-3′), 752–777 of $\beta_1$ common region (5′-GGAATTCAAGCTTTTAATGATAATT-3 and 5′-GGATCCTCACGTGTCCCATTTGGC-3′), and 1022–1049 of $\alpha_5$ (5′-GGAATTCAAGCTTGGATTCTTCAAA-3′ and 5′-CGGGATCCTCAGGCATCAGAGGTGGC-3′) were amplified by PCR and cloned in frame with LexA coding sequence in pEG202.

To map the integrin binding site in Melusin, an additional construct was created. The Melusin cDNA fragment coding for amino acids 211–320 (D3–2Δ) was amplified by PCR (5′-CGGAATTCTGGGCAAAGCAGCTGCCA-3′ and 5′-CCCTCGAGTTATAGTAAAACCCCTGCCCT-3′) and cloned in frame with the B42 transactivation domain in pJG4–5.

*Sequencing and cDNA Cloning*—Positive clones were sequenced using ABI PRISM Big Dye Terminator Cycle Sequencing Ready Reaction Kit (Perkin-Elmer). D3–2 and D7–2 cDNA fragments containing overlapping sequences of Melusin were used to isolate the full-length cDNA from a human skeletal muscle library in λgt10 (CLONTECH) and a mouse skeletal muscle library in λgt11 (CLONTECH). Positive human and mouse clones were subcloned in pBluescript II SK$^-$ and sequenced. Sequences were analyzed with the BLAST (22) server at the National Center for Biotechnology Information. Our cDNA contains the complete Melusin coding sequence as indicated by the fact that mouse cDNA transfected COS cells show a band which co-migrates with the endogenous Melusin present in differentiated C2C12 myogenic cells. The first atg of the sequence was considered the putative start codon. Analysis of mouse genomic DNA sequences showed that two stop codons are present 18 and 30 nt upstream of this putative atg. This genomic region just upstream of the start codon is not an intronic sequence because it is present in dbEST (23) data base that contains randomly expressed sequences.

*Northern Blot*—RNA from C2C12 cells and from mouse embryo and neonatal skeletal muscle was extracted using RNeasy Mini kit (QIAGEN Inc.). Adult skeletal muscle RNA was extracted according to Chomczynsky and Sacchi (24). 20 μg of total RNA from each sample was run on 0.8% agarose-formaldehyde gels and transferred to N$^+$ nylon membranes (Amersham Pharmacia Biotech). Poly(A)$^+$ RNA isolated from human and mouse tissues and immobilized onto nitrocellulose filters after electrophoretic separation was obtained from CLONTECH (Multiple Tissue Northern blot). Filters were probed at 65 °C with D3–2 insert labeled with $^{32}$P using a random prime labeling system (Rediprime II, Amersham Pharmacia Biotech) and were washed twice with 2× SSC, 1% SDS and twice with 0.4% SSC, 1% SDS at 65 °C, and exposed to x-ray film.

*In Situ Hybridization*—Human metaphase spreads were obtained from PHA-stimulated peripheral lymphocytes of a normal donor by standard procedures. Mouse spreads were prepared from a mouse cell line containing multiple well characterized Robertsonian translocations allowing an easy identification of the mouse chromosomes (25). The cell line was a generous gift from Dr. H. Hameister (Ulm, Germany). Full-length human Melusin cDNA and 14.8-kilobase mouse genomic DNA fragment spanning the atg-containing exon and the three following ones were used as probes. Chromosome preparations were hybridized *in situ* with probes labeled with biotin nick translation, essentially as described by Lichter *et al.* (26), with minor modifications. Briefly, 500 ng of labeled probe were used for the FISH experiments; hybridization was performed at 37 °C in 2× SSC, 50% (v/v) formamide, 10% (w/v) dextran sulfate, 5 μg COT1 DNA (Roche Molecular Biochemicals), and 3 μg of sonicated salmon sperm DNA in a volume of 10 μl. Post-hybridization washing was performed at 42 °C in 2× SSC, 50% formamide (×3) followed by three washes in 0.1× SSC at 60 °C. Biotin-labeled DNA was detected with Cy3-conjugated avidin (Amersham Pharmacia Biotech). Chromosome identification was obtained by simultaneous DAPI staining, that produces a Q-banding pattern.

*Antibody Preparation*—GST-Melusin fusion protein was produced by expressing the entire sequence of the human Melusin cloned in pGEX 4T2 (Amersham Pharmacia Biotech) in *Escherichia coli* BL21 bacterial strain. GST-Melusin was purified on glutathione-Sepharose 4B (Amersham Pharmacia Biotech), and elution was performed following the recommendations of the manufacturer. Rabbits were immunized by repeated intramuscular injections of the purified fusion protein (500 μg) suspended in Complete Freund Adjuvant. Specificity of the antiserum was demonstrated in Western blots on protein extracts from wild type and Melusin cDNA-transfected COS cells. To affinity purify antibodies from rabbit serum, Melusin was fused to maltose-binding protein (MBP) by cloning the cDNA into the pMALp2 vector (New England Biolabs). The MBP-Melusin fusion protein was purified on an amylose column according to the instructions of the manufacturer and coupled to Sepharose. Antibodies were adsorbed on the MBP-Melusin-Sepharose column and eluted with pH 3 glycin-HCl buffer.

*Cell Culture and Western Blot*—C2C12 mouse skeletal muscle cell line was maintained in Dulbecco's modified Eagle's medium with 10% fetal calf serum. Cells were induced to differentiate into myotubes by switching to culture medium with 2% horse serum.

Western blots on cell and tissue extracts were performed as follows. Cells were washed twice with PBS and lysed in Tris-buffered saline (TBS) (containing 0.5% Triton X-100 and the following protease inhibitors: 10 μg/ml leupeptin, 4 μg/ml pepstatin, and 0.1 TIU/ml aprotinin) for 10 min at 4 °C. Extracts were centrifuged at 14,000 rpm for 10 min to remove insoluble material. Tissues were frozen and triturated in liquid nitrogen and extracted in lysis buffer containing 150 mM NaCl, 50 mM Tris-HCl, pH 8, 5 mM EDTA, 1% Nonidet P-40, 10 μg/ml leupeptin, 4 μg/ml pepstatin, and 0.1 TIU/ml aprotinin. Tissue extracts were sonicated three times for 10 s and centrifuged at 14,000 rpm for 10 min to remove insoluble material. Protein concentration was determined using Bio-Rad Assay. 60 μg of every protein extract were separated on polyacrylamide gel in presence of SDS and subsequently blotted to nitrocellulose membranes. Membranes were saturated with TBS, 5% BSA and incubated in TBS, 1% BSA containing primary antibody overnight at 4 °C. After washing, the filters were incubated with peroxidase-conjugated secondary antibody for 2 h at room temperature,

[1] The abbreviations used are: PCR, polymerase chain reaction; dbEST, data base of expressed sequence tags; GST, glutathione *S*-transferase; MBP, maltose binding protein; bFGF, bovine fibroblast growth factor; nt, nucleotide(s); DAPI, 4,6-diamidino-2-phenylindole; PBS, phosphate-buffered saline; TBS, Tris-buffered saline; TIU, trypsin inhibitory units; BSA, bovine serum albumin; Cterm, carboxyl-terminal.

and detection was performed with chemiluminescent substrate ECL (Amersham Pharmacia Biotech).

*Muscle Regeneration*—Adult CBA male mice were anesthetized with Avertin (17 μl of 2.5% Avertin per gram of body weight). Tibialis anterior muscles were exposed, and degeneration was induced by deep freezing with liquid nitrogen-cooled steel rod according to Toyota *et al.* (27). Muscles were surgically removed 3, 6, 9, and 12 days after freezing, and protein extracts were obtained as described above. 100 μg of every total extract were separated on polyacrylamide gel, and equal loading was verified by Ponceau red staining. Untreated tibialis anterior muscle was used as control.

*Immunofluorescence*—1-week old mouse limb muscles and soleus muscle from 6-months old mice were collected and fixed in PBS, 4% paraformaldehyde for 2 h at room temperature. After washing in PBS and PBS, 15% sucrose for cryoprotection, muscle fragments were frozen in liquid nitrogen in Embedding Medium Compound (Bio-Optica S.p.a.). 10-μm cryosections were collected on polylysine-subbed slides. Sections were saturated with goat serum 1:100 in PBS, 1% BSA and incubated overnight at room temperature with primary antibody in PBS, 1% BSA, followed by 2-h incubation with fluorochrome-conjugated secondary antibody. The following primary antibodies were used: 5 μg/ml affinity purified rabbit anti-Melusin and 5 μg/ml monoclonal antibody EA-53 to sarcomeric α-actinin (Sigma). Secondary antibodies specific for rat or mouse IgG were labeled with fluorescein, while antibodies specific for rabbit IgG were labeled with Texas red (Molecular Probes). The specie specificity of the secondary antibodies was cross-tested. Non-immune rabbit and mouse IgG were used as controls and resulted in negative staining. Samples were observed under Olympus fluorescence microscope, and pictures were taken with an Olympus DP10 digital photomicrography system. Confocal images were obtained with Olympus 1X70 inverted confocal laser scanning microscope equipped with a krypton-argon ion laser (488/568 nm).

*Melusin-Integrin in Vitro Binding Assay*—GST fusion proteins were prepared by cloning the full-length human Melusin cDNA and a cDNA fragment coding for amino acid residues 149–350 (Cterm) in pGEX vectors (Amersham Pharmacia Biotech). GST and GST fusion proteins were expressed in *E. coli* BL21 bacterial strain and purified on glutathione-Sepharose 4B. COS cells, used as source of $\beta_1$ integrin heterodimers, were washed twice with cold PBS and lysed in TBS (25 mM Tris-HCl, pH 7.6, 150 mM NaCl, 1 mM $NaVO_4$, 10 mM NaF, 10 μg/ml leupeptin, 4 μg/ml pepstatin and 0.1 TIU/ml aprotinin) 0.5% Nonidet P-40 + 1 mM $Ca^{2+}$, or with TBS, 0.5% Nonidet P-40 + 5 mM EDTA. Cell extracts were precleared for 1 h at 4 °C with 10 μg of GST-Sepharose. 2 mg of every protein extract were incubated overnight at 4 °C with 10 μg of GST-Melusin, GST-Cterm and GST alone (as control). Sepharose beads were then washed, boiled in Laemmli buffer and proteins were separated on 6% polyacrylamide gel in nonreducing conditions. The gel was blotted to a nitrocellulose filter that was then saturated with TBS, 5% BSA and incubated over night at 4 °C in TBS 1% BSA containing 10 μg/ml TS2/16 monoclonal antibody to $\beta_1$ integrin. After washing, the filter was incubated with peroxidase conjugated anti-mouse antibody for 2 h at room temperature and detection was performed with chemiluminescent substrate ECL (Amersham).

## RESULTS

*Isolation of $\beta_1$ Integrin Cytoplasmic Domain Interactors*—To identify muscle proteins able to interact with the $\beta_1$ integrin subunit cytoplasmic domain, we carried out an interaction trap approach (20). We screened a heart neonatal rat library using the entire cytoplasmic region of $\beta_1$A, the ubiquitously expressed isoform, and $\beta_1$D, the muscle-specific isoform, as baits. We obtained 3 different specific interactors for $\beta_1$A and $\beta_1$D. One of the $\beta_1$A interactors was identified as the rat homologues of ICAP-1α (Integrin Cytoplasmic Domain-Associated Protein), also called bodenin, and recently described as a $\beta_1$ interacting protein (6, 7). Another protein that we found to weakly interact with $\beta_1$D was RACK-1 (Receptor for Activated Protein Kinase C), a molecule recently described as interactor for $\beta_1$, β2 and β5 integrin cytoplasmic domains (8, 7).

The most abundantly retrieved cDNA corresponded to an unknown sequence and was isolated once in the $\beta_1$A and 8 times in the $\beta_1$D screening, where it was obtained as two different overlapping cDNA fragments with an open reading frame of 423 nt (D3–2) and 561 nt (D7–2). To verify the specificity of this interaction we tested the ability of the proteins coded by the D3–2 and D7–2 cDNA fragments to bind $\beta_1$A, $\beta_1$D and other unrelated baits (cyclin A, bFGF, c-Myc and bicoid) in a yeast interaction test. Our results showed that D3–2 and D7–2 protein fragments bind specifically and strongly to $\beta_1$A and $\beta_1$D cytoplasmic domains and not to the unrelated baits. We consequently focused our study on this new interactor that we called Melusin.

*Isolation of Melusin Full-length cDNA*—Using D3–2 cDNA fragment as probe we isolated human and mouse full-length Melusin cDNAs from human and mouse skeletal muscle libraries. The human clone is 1235 nt in length and conceptual translation of this sequence revealed the presence of an open reading frame of 347 amino acids (GenBank™ AF140690). The mouse cDNA was 1420 nt in length, with an open reading frame coding for 350 amino acids (GenBank™ AF140691), with 92% identity with the human amino acidic sequence. The D3–2 and D7–2 cDNA fragments isolated by the two-hybrid screening were found to code for amino acid residues 211–350 and 164–350 respectively.

Sequence analysis by BLAST homology search (22) revealed no evident homology with any other known protein. Inspection of the sequence indicated the presence at the extreme carboxyl-terminal portion of the molecule of a region highly enriched in aspartic and glutamic acid residues. Analysis by FTHOM domain homology search (22, 28, 29) indicated that this acidic sequence of Melusin closely resembles calreticulin and calsequestrin C-domain, known to bind calcium at high capacity and low affinity (30, 31). At the amino-terminal end, Melusin contains two cysteine rich repeats spaced by an intervening sequence of approximately 90 amino acid residues. The cysteine residues contained in the cysteine repeats are characteristically spaced with a pattern that was not found in other proteins (Fig. 1*B*). Moreover, four distinct P*XXP* motifs, representing the minimal consensus sequence recognized by SH3 domains (32, 33) and two Y*XXI/P* sequences, putative binding sites for SH2 domains (34), are scattered in the amino-terminal half of the molecule.

The chromosomal localization of the Melusin gene was also investigated, both in man and in mouse. Fish analysis clearly showed that the gene is localized on the X chromosome in both species, respectively at Xq12.1–13 and at X band D.

*Regulation of Melusin Expression during Myogenic Differentiation*—To investigate the expression of this new gene, poly(A)$^+$ RNA from human and mouse tissues was analyzed by Northern blotting with a Melusin probe. A single transcript of 1.4 kilobases was detected in human skeletal and cardiac muscles, whereas no hybridization occurred in all other tested tissues (Fig. 2*A*). Identical expression pattern was detected in mouse tissues (not shown). Analysis of the Melusin protein by Western blotting with polyclonal antibodies raised against a GST-Melusin fusion protein confirmed the specific expression in striated muscles (Fig. 2*B*).

To evaluate if Melusin expression was regulated during muscle differentiation, we analyzed the C2C12 myogenic cell line that can be induced to differentiate to form myotubes by serum starvation. Melusin expression was tested both by Western and Northern blotting. As shown in Fig. 3*A*, Melusin was absent in undifferentiated myoblasts, and its expression was turned on in differentiated myotubes after 6 days of serum starvation.

Melusin expression was also examined during mouse embryonic development *in vivo*. Melusin protein and mRNA became detectable in embryo limbs at day 15 (*E15*), reached a maximum in newborn mice, and declined in adult limb muscles (Fig. 3*B*). In adult muscles a doublet of protein bands was detected by Western blotting, suggesting possible posttranslational

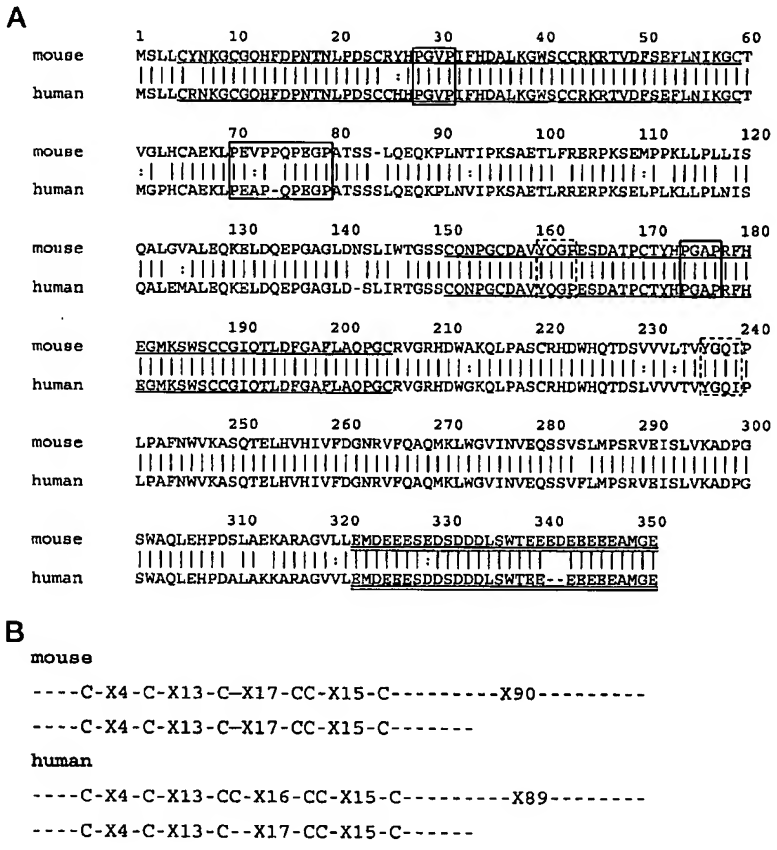


FIG. 1. **Amino acid sequence of Melusin.** *A*, the amino acid sequence was deduced from the full-length human and mouse cDNAs. Identical residues are indicated by *vertical bars* and conservative substitutions by *double dots*. The two cysteine-rich domains are *underlined*, and the acidic amino acid stretch at the extreme carboxyl-terminal is *double underlined*. *PXXP* sequences, putative SH3 domain binding motifs, are *boxed*. *YXXI/P* sequences, putative SH2 binding sites are shown in *dashed line boxes*. *B*, the spacing of cysteine residues in the two cysteine-rich motifs in mouse and human Melusin are indicated.

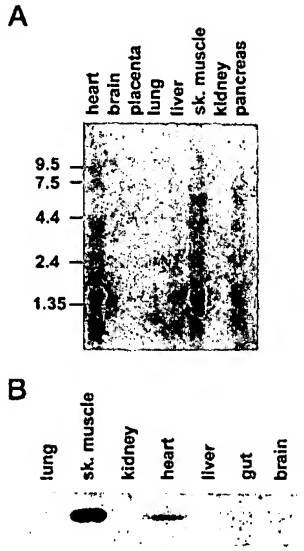


FIG. 2. **Expression of Melusin is restricted to striated muscle tissue.** *A*, poly(A)$^+$ RNA from different human tissues was hybridized with D3–2 rat probe isolated with the two-hybrid screening as described under "Materials and Methods." A single band of approximately 1.4 kilobases was present only in heart and skeletal muscles. *B*, protein extracts from newborn mouse tissues were separated by SDS-polyacrylamide gel electrophoresis and transferred to nitrocellulose filter. The filter was probed with polyclonal antibody raised against a GST-Melusin fusion protein as described under "Materials and Methods." A band of 38 kDa was detected in skeletal muscle and heart.

modifications. During heart development, on the other hand, Melusin level remains steady with no major changes in expression from embryonic day 15 to adult stage.

To investigate if Melusin expression is regulated in regenerating adult muscle, we induced regeneration of mouse tibialis anterior following freeze injury. 3, 6, 9, and 12 days after freeze trauma, muscles were collected and Melusin expression was investigated by Western blot analysis on total protein extracts using normal muscle as control. As shown in Fig. 3*C*, Melusin is up-regulated from day 6 on during muscle regeneration, consistent with a role of this molecule in myogenetic processes.

*Subcellular Localization of Melusin by Immunofluorescence*—Using affinity purified Melusin antibody, we performed immunofluorescence analysis on newborn and adult mouse muscle cryosections. Fluorescence was localized only on skeletal muscle and not in the surrounding tissues, confirming the muscle-specific expression. Longitudinal sections of posterior leg muscles from 1-week old mice clearly revealed a striated pattern of two Melusin rows flanking the $\alpha$-actinin band in the Z disc (Fig. 4). In adult soleus muscle, the striated localization of Melusin was still detectable although to a lower intensity compared with newborn muscles (Fig. 4).

*Mapping of the $\beta_1$ Integrin-Melusin Interaction Sites with the Two-hybrid Test*—The integrin $\beta$ subunit cytoplasmic domains are highly homologous to each other (3). Using the two-hybrid test, we analyzed whether Melusin was capable of interacting with $\beta$ subunits other than $\beta_1$. Using the protein fragment coded by plasmid D3–2, corresponding to the carboxyl-terminal of Melusin (tail domain) as a bait, interaction occurred with $\beta_1$ but not with $\beta_2$ and $\beta_3$ cytoplasmic domains (Table I). Moreover, no interaction occurred with the integrin $\alpha_5$ cytoplasmic domain used as control (Table I). The $\beta_1$ cytoplasmic domain consists of a 26-amino acid long membrane proximal subdomain common to all known isoforms and of variable carboxyl-terminal subdomains specific for each splicing variant (35). As shown in Table I, the interaction occurred with all three tested isoforms ($\beta_1$A, $\beta_1$B, and $\beta_1$D) suggesting that the interaction involved the common subdomain. To further test this hypoth-

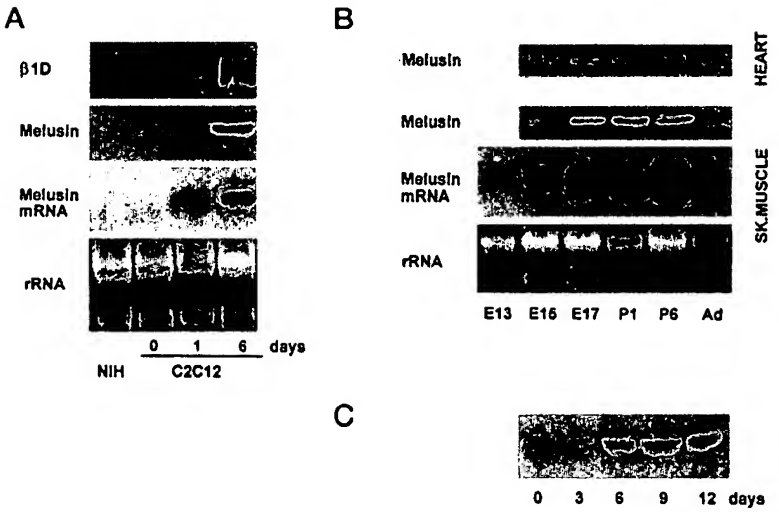


FIG. 3. **Melusin expression is regulated during *in vitro* and *in vivo* myogenesis and during muscle regeneration.** *A*, C2C12 mouse myoblasts (*0*) were allowed to differentiate in serum-free medium for 1 or 6 days. NIH 3T3 fibroblasts were used as negative control. Protein extracts were analyzed by Western blotting with antibodies to Melusin and to $\beta_1$D integrin as marker for differentiation (two *upper panels*). Total RNA was also extracted and hybridized with the Melusin probe, or stained with ethidium bromide as gel loading control (two *lower panels*). *B*, protein extracts (two *upper panels*) from heart and limb muscles of mouse embryos at 15 (*E15*) and 17 (*E17*) days of fetal life, newborn mice (*P1*), 1-week old (*P6*), and adult (*Ad*) mice were analyzed by Western blotting with Melusin polyclonal antibodies. Total RNA was also extracted from limb muscles at different stages of development and analyzed by Northern blotting with Melusin probe. Total RNA stained with ethidium bromide (*lower panel*) is shown as gel loading control. *C*, degeneration of tibialis anterior muscle of adult mice was induced by liquid nitrogen freezing, and regeneration was allowed to proceed for 3, 6, 9, and 12 days. The muscles were excised and protein extracts were analyzed by Western blotting for the expression of Melusin with specific polyclonal antibodies. Day 0 (*0*) is untreated tibialis anterior muscle.

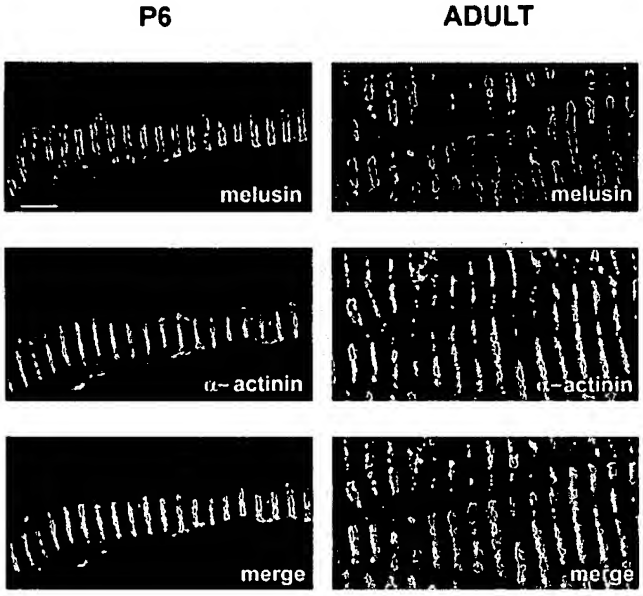


FIG. 4. **Melusin is enriched at costameres.** *Panels* in *left column* show longitudinal cryosections of 1-week old (*P6*) mouse limb co-stained with affinity purified Melusin polyclonal antibody and α-actinin monoclonal antibody. The two images are superimposed in the *lower panel* (*merge*). Soleus muscle from 6-month old mouse was also stained and is shown in panels of *right column*. Note the striated localization of Melusin and the reduced staining intensity in adult muscle. *Scale bar*, 10 μm.

esis, we used a truncated bait consisting only of the common subdomain. As shown in Table I, the common $\beta_1$ subdomain interacted with the tail region of Melusin with an intensity comparable with the one observed for the entire cytoplasmic regions.

Different Melusin constructs were also tested for their ability to interact with the $\beta_1$ integrin cytoplasmic domain. As mentioned above, the interaction occurred with preys consisting of the tail domain plus a large fragment of the second cysteine-rich repeat (D7–2) or the tail domain alone (D3–2) (Table II). Further deletion of the acidic amino acid stretch did not affect the interaction, allowing mapping the binding site for the $\beta_1$ integrin in a restricted portion of the Melusin tail domain from amino acid residues 211 to 320 (Table II). Interestingly the full-length Melusin construct showed no interaction (Tables I and II), suggesting that the tail domain is unavailable for binding to $\beta_1$ in the full-length protein.

*Binding of Melusin to $\beta_1$ Integrins in Vitro*—To further test the interaction of Melusin with integrin cytoplasmic domains, we performed *in vitro* binding assays. Either the full-length or a fragment (Cterm), consisting of the second cysteine-rich repeat and the tail domain, were fused to GST and bound to Sepharose beads (see "Materials and Methods" and Table II). When detergent extract of COS cells in $Ca^{2+}$-containing buffer was incubated with the Sepharose beads, $\beta_1$ integrins bound strongly to the Cterm Melusin fragment but not to the full-length protein. Because Melusin contains a putative $Ca^{2+}$ binding domain, we investigated whether $Ca^{2+}$ ions are inhibiting the interaction of the full-length Melusin with $\beta_1$ integrin. As shown in Fig. 5, $Ca^{2+}$ chelator (EDTA) strongly enhanced binding of Melusin to $\beta_1$ integrin. Interestingly, $Ca^{2+}$ concentration did not affect binding of the Cterm portion of Melusin to $\beta_1$ integrin (Fig. 5).

## DISCUSSION

In this work we describe a new muscle-specific protein, Melusin, interacting with the cytoplasmic domain of the $\beta_1$ integrin subunit. Melusin is expressed in striated skeletal and cardiac muscles, both at mRNA and protein level, but it is undetectable in all other tested tissues including gut smooth muscle, brain, placenta, lung, liver, kidney, and pancreas. Its expression appears to be regulated during myogenesis both *in vitro* and *in vivo*. In fact, Melusin was undetectable in cultured proliferating myoblasts, but it is highly expressed in differentiated myotubes. During *in vivo* skeletal muscle myogenesis, Melusin starts to be detectable in 15-day old embryos, and its level peaks in newborn mice. In adult skeletal muscle tissue

TABLE I

*Binding of integrin subunit cytoplasmic domains to melusin and its tail domain*

Baits consisting of different $\beta$ integrin cytoplasmic domains were used in the two-hybrid system to measure interaction with the D3–2 melusin fragment (coding for the tail domain, amino acid residues 211–350) and the full-length melusin protein. $\beta_1$A, $\beta_1$B and $\beta_1$D are different splicing variant of $\beta_1$ integrin. $\beta_1$Com is a mutant containing the cytoplasmic subdomain common to all splicing variants (35). $\alpha_6$ integrin subunit cytoplasmic domain was used as control.

| Baits | Cytoplasmic domain sequences | D3–2 | Melusin |
|---|---|---|---|
| $\beta_1$A | KLLMIIHDRREFAKFEKEKMNAKWDTGENPIYKSAVTTVVNPKYEGK | +++ | – |
| $\beta_1$B | KLLMIIHDRREFAKFEKEKMNAKWDTVSYKTSKKQSGL | +++ | – |
| $\beta_1$D | KLLMIIHDRREFAKFEKEKMNAKWDTQENPIYKSPINNFKNPNYGRKAGL | +++ | – |
| $\beta_1$Com | KLLMIIHDRREFAKFEKEKMNAKWDT | +++ | – |
| $\beta_2$ | KALIHLSDLREYRRFEKEKLKSQWNNDNPLFKSATTTVMNPKFAES | – | – |
| $\beta_3$ | KLLITIHDRKEFAKFEEERARAKWDTANNPLYKEATSTFTNITYRGT | – | – |
| $\alpha_6$ | KLGFFKRSLPYGTAMEKAQLKPPATSDA | – | – |

TABLE II

*Interaction of different melusin constructs with $\beta_1$ integrin*

Different melusin constructs used are schematized. The ability of the constructs to bind the $\beta_1$ integrin cytoplasmic domain in the two-hybrid test or the intact integrin complexes from COS cell extracts are indicated. nt, not tested.

| | CONSTRUCTS | RESIDUES | TWO HYBRID | IN VITRO BINDING | |
|---|---|---|---|---|---|
| | | | | $Ca^{2+}$ | EDTA |
| | Melusin full-length | 1-350 | - | - | + |
| | Cterm | 149-350 | nt | + | + |
| | D7-2 | 164-350 | + | nt | nt |
| | D3-2 | 211-350 | + | nt | nt |
| | D3-2Δ | 211-320 | + | nt | nt |

Cysteine-rich domain; Intervening sequence; Tail domain containing the acidic amino acid stretch (D).

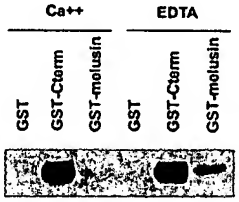


FIG. 5. **Interaction of Melusin with integrins is $Ca^{2+}$ dependent.** GST fusion proteins containing either the Cterm portion or the full-length Melusin protein (see "Materials and Methods" section and Table II) were bound to glutathione-Sepharose. GST protein alone was used as control. COS cells were detergent-extracted in buffer containing 1 mM $CaCl_2$ or 5 mM EDTA. Cell extracts were incubated with GST fusion protein-Sepharose, and $\beta_1$ integrin binding was determined by Western blot analysis of eluted material. While $\beta_1$ integrin binds to the Cterm region of Melusin both in the presence or absence of $Ca^{2+}$ ions, binding to the intact Melusin occurred only in the absence of divalent cations.

the level of expression slightly declines, and in Western blotting a doublet of bands becomes visible, suggesting that the molecule undergoes post-translational modifications. The doublet of bands could also be indicative of alternatively spliced isoforms of the protein, but reverse transcription PCR analysis of adult and neonatal muscle with primers covering the entire length of the molecule did not reveal the existence of alternatively spliced forms. This conclusion is also supported by the presence of a single band in Northern blot analysis from both newborn and adult mice (see Fig. 3*B*). The highest expression level of Melusin in skeletal muscle coincides with secondary myogenesis, a process in which a distinct myoblast population line up using primary myotubes as scaffold and fuse to each other forming secondary myotubes that will give rise to the muscle fibers of adult tissue. High level of Melusin expression was also observed in regenerating adult tibialis anterior muscle, further suggesting that Melusin might play a crucial role during maturation and/or organization of muscle cells. A possible role in myoblast fusion seems unlikely because Melusin is also expressed in heart where cardiomyocytes do not undergo cell fusion. The two-hybrid test showed that the tail domain of Melusin binds equally well to the cytoplasmic domain of both $\beta_1$A and $\beta_1$D integrin isoforms. These two isoforms are differentially expressed during muscle development (36). $\beta_1$A is expressed in muscles during embryonic development and is down-regulated after birth. On the other hand, the $\beta_1$D isoform starts to appear in skeletal muscle in 17-day embryos and becomes the only $\beta_1$ isoform in adult muscles. The ability to bind $\beta_1$A and $\beta_1$D integrin isoforms allows Melusin to interact with integrins both in developing and in adult muscles. Immunofluorescence analysis showed that Melusin is localized in rows flanking the Z line containing $\alpha$-actinin. Similar pattern has been described for vinculin (37) and $\beta_1$ integrin (12, 13, 10) and is thought to correspond to sites of lateral interaction of actin with the plasma membrane known as costameres (37, 38). This pattern of localization suggests that Melusin is a component of the actin-integrin junctional complex in muscle.

The amino acid sequence of Melusin revealed four domains. The protein consists of 347 and 350 amino acid residues in man and mouse, respectively, with a 92% identity (96% considering conservative substitutions). A 55-amino acid long domain, containing a unique cysteine-rich motif, is repeated twice in the molecule. These repeats share 42% identity among each other, while the cysteine pattern is conserved. Interestingly, in human Melusin, the first repeat contains an extra cysteine residue immediately adjacent to cysteine 3. This is not a sequence polymorphism or a mutation in our clones because codons coding these double cysteine residues were found in human Melusin cDNA fragments present in the dbEST data base. An intervening sequence of 89–90 amino acid residues is present between the two cysteine-rich regions. The carboxyl-terminal portion of the molecule consists of a tail domain of 143/145

residues and contains a stretch of 18/20 negatively charged amino acids at the extreme carboxyl-terminal. Similar acidic carboxyl-terminal sequences are present in calsequestrin (31) and calreticulin and are shown to bind $Ca^{2+}$ ions with high capacity and low affinity (30). As detected in the two-hybrid screening, the tail domain was sufficient to bind $\beta_1$ cytoplasmic region, and deletion experiments allowed to exclude a role of the acidic amino acid stretch in this process (see Table II). Interestingly, the full-length Melusin protein was unable to interact with $\beta_1$ cytoplasmic domain in the two-hybrid system (Tables I and II). *In vitro* binding experiments showed that the interaction of Melusin with integrins is regulated by divalent cations, and it occurs only in the absence of $Ca^{2+}$ (Table II). It is possible that $Ca^{2+}$ directly competes for binding to integrins. This, however, is not the case, in fact, the presence of $Ca^{2+}$ ions did not prevent binding of the truncated Melusin Cterm fragment (see Table II). In addition, the acidic amino acid stretch of Melusin, that it is likely to bind $Ca^{2+}$ ions, is not required for integrin binding (see Table II). Thus the most likely explanation is that $Ca^{2+}$ modulates the conformation of Melusin exposing the integrin binding site located in the tail domain. In this model the amino-terminal region of Melusin masks the integrin binding site present in the tail domain of the molecule, and removal of $Ca^{2+}$ releases this inhibition. These data suggest that Melusin-integrin interaction depends on $Ca^{2+}$ concentration and can thus be regulated by intracellular alteration of $Ca^{2+}$ level in response to extracellular stimuli.

Whereas Melusin tail domain is responsible for the interaction with $\beta_1$ integrin, the amino-terminal portion of the molecule can possibly bind to SH3- and SH2-containing proteins, as suggested by the presence of multiple proline-rich motifs and tyrosine phosphorylation sites. These properties suggest that Melusin could be an important molecular link between integrin receptors and cytoskeletal or transducing proteins in muscle cells.

*Acknowledgments*—We are grateful to Dr. G. P. Dotto for the generous hospitality in his laboratory in the initial phase of this work and to Drs. A. Zervos and C. Fusco for teaching the technique and all crucial laboratory tips of the two-hybrid screening. We are also indebted to Drs. A. Zervos and R. Brent for sharing a number of important reagents. We thank Dr. F. Di Cunto, Dr. E. Calautti, and Dr. G. Topley for stimulating discussion during the work. The technical help of P. Caudana, M. Isabello, I. Carfora, and L. Cavarretta is gratefully acknowledged.

REFERENCES

1. Reszka, A. A., Hayashi, Y., and Horwitz, A. F. (1992) *J. Cell Biol.* **117,** 1321–1330
2. Marcantonio, E. E., Guan, J. L., Trevithick, J. E., and Hynes, R. O. (1990) *Cell Regul.* **1,** 597–604
3. Sastry, S. K., and Horwitz, A. F. (1993) *Curr. Opin. Cell Biol.* **5,** 819–831
4. Hemler, M. E. (1998) *Curr. Opin. Cell Biol.* **10,** 578–585
5. Hannigan, G. E., Leung-Hagesteijn, C., Fitz-Gibbon, L., Coppolino, M. G., Radeva, G., Filmus, J., Bell, J. C., and Dedhar, S.(1996) *Nature* **379,** 91–96
6. Chang, D. D., Wong, C., Smith, H., and Liu, J. (1997) *J. Cell Biol.* **138,** 1149–1157
7. Zhang, X. A., and Hemler, M. E. (1999) *J. Biol. Chem.* **274,** 11–19
8. Lilental, J., and Chang, D. D. (1998) *J. Biol. Chem.* **273,** 2379–2383
9. Fornaro, M., and Languino, L. R.(1997) *Matrix Biol.* **16,** 185–193
10. Belkin, A. M., Zhidkova, N. I., Balzac, F., Altruda, F., Tomatis, D., Maier, A., Tarone, G., Koteliansky, V. E., and Burridge, K. (1996) *J. Cell Biol.* **132,** 211–226
11. Belkin, A. M., Retta, S. F., Pletjushkina, O. Y., Balzac, F., Silengo, L., Fassler, R., Koteliansky, V. E., Burridge, K., and Tarone, G. (1997) *J. Cell Biol.* **139,** 1583–1595
12. Bozyczko, D., Decker, C., Muschler, J., and Horwitz, A. F. (1989) *Exp. Cell Res.* **183,** 72–91
13. Swasdison, S., and Mayne, R.(1989) *Cell Tissue Res.* **257,** 537–543
14. Volk, T., Fessler, L. I., Fessler, J. H. (1990) *Cell* **63,** 525–536
15. Hirsch, E., Lohikangas, L., Gullberg, D., Hohansson, S., and Fassler, R. (1998) *J. Cell Sci.* **111,** 2397–2409
16. Fassler, R., Rohwedel, J., Maltsev, V., Bloch, W., Lentini, S., Guan, K., Gullberg, D., Hescheler, J., Addicks, K., and Wobus, A. M. (1996) *J. Cell Sci.* **109,** 2989–2999
17. Mayer, U., Saher, G., Fassler, R., Bornemann, A., Echtermeyer, F., von der Mark, H., Miosge, N., Poschl, E., and von der Mark, K. (1997) *Nat. Genet.* **17,** 318–323
18. McDonald, K. A., Lakonishok, M., and Horwitz, A. F. (1995) *J. Cell Sci.* **108,** 2573–2581
19. Martin-Bermudo, M. D., Brown, N. H. (1996) *J. Cell Biol.* **134,** 217–226
20. Gyuris, J., Golemis, E., Chertkov, H., and Brent, R. (1993) *Cell* **75,** 791–803
21. Gietz, D., St Jean, A., Woods, R. A., and Schiestl, R. H. (1992) *Nucleic Acids Res.* **20,** 1425
22. Altschul, S. F., Gish, W., Miller, W., Myers, E. W., and Lipman, D. J. (1990) *J. Mol. Biol.* **215,** 403–410
23. Boguski, M. S., Lowe, T. M., and Tolstoshev, C. M. (1993) *Nat. Genet.* **4,** 332–333
24. Chomczynski, P., and Sacchi, N. (1987) *Anal. Biochem.* **162,** 156–159
25. Zornig, M., Klett, C., Lovec, H., Hameister, H., Winking, H., Adolph, S., and Moroy, T. (1995) *Cytogenet. Cell Genet.* **71,** 37–40
26. Lichter, P., Tang Chang, C. J., Call, K., Hermanson, G., Evans, G. A., Housman, D., and Ward, D. C. (1990) *Science* **247,** 64–69
27. Toyota, N., and Shimada, Y. (1984) *Cell Tissue Res.* **236,** 549–554
28. Hegyi, H., and Pongor, S. (1993) *Comput. Appl. Biosci.* **9,** 371–372
29. Bairoch, A., and Boeckmann, B. (1993) *Nucleic Acids Res.* **21,** 3093–3096
30. Baksh, S., and Michalak, M. (1991) *J. Biol. Chem.* **266,** 21458–21465
31. Fliegel, L., Ohnishi, M., Carpenter, M. R., Khanna, V. K., Reithmeier, R. A., and MacLennan, D. H. (1987) *Proc. Natl. Acad. Sci. U. S. A.* **84,** 1167–1171
32. Rickles, R. J., Botfield, M. C., Weng, Z., Taylor, J. A., Green, O. M., Brugge, J. S., and Zoller, M. J. (1994) *EMBO J.* **13,** 5598–5604
33. Yu, H., Chen, J. K., Feng, S., Dalgarno, D. C., Brauer, A. W., and Schreiber, S. L. (1994) *Cell* **76,** 933–945
34. Songyang, Z., Shoelson, S. E., Chaudhuri, M., Gish, G., Pawson, T., Haser, W. G., King, F., Roberts, T., Ratnofsky, S., Lechleider, R. J., *et al.* (1993) *Cell* **72,** 767–778
35. Retta, S. F., Balzac, F., Ferraris, P., Belkin, A. M., Fassler, R., Humphries, M. J., De Leo, G., Silengo, L., and Tarone, G. (1998) *Mol. Biol. Cell* **4,** 715–731
36. Brancaccio, M., Cabodi, S., Belkin, A. M., Collo, G., Koteliansky, V. E., Tomatis, D., Altruda, F., Silengo, L., and Tarone, G. (1998) *Cell Adhes. Commun.* **5,** 193–205
37. Pardo, J. V., Siliciano, J. D., and Craig, S. W. (1983) *Proc. Natl. Acad. Sci. U. S. A.* **80,** 1008–1012
38. Koteliansky, V. E., and Gneushev, G. N (1983) *FEBS Lett.* **159,** 158–160

# Melusin, a muscle-specific integrin $\beta_1$–interacting protein, is required to prevent cardiac failure in response to chronic pressure overload

MARA BRANCACCIO[1], LUIGI FRATTA[2], ANTONELLA NOTTE[2], EMILIO HIRSCH[1,3], ROBERTA POULET[2], SIMONA GUAZZONE[1], MARIKA DE ACETIS[1], CARMINE VECCHIONE[2], GENNARO MARINO[2], FIORELLA ALTRUDA[1,3], LORENZO SILENGO[1,3], GUIDO TARONE[1,3] & GIUSEPPE LEMBO[2,4]

[1]*Department of Genetics, Biology, and Biochemistry, Turin University, 10126 Turin, Italy*
[2]*Department of Angiocardioneurology, IRCCS 'Neuromed', 86077 Pozzilli (IS), Italy*
[3]*Experimental Medicine Research Center, San Giovanni Battista Hospital, 10126 Turin, Italy*
[4]*Department of Experimental Medicine and Pathology, University of Rome 'La Sapienza' Rome, Italy*
*M.B. and L.F. contributed equally to this work.*
*Correspondence should be addressed to G.T. (e-mail: guido.tarone@unito.it) or G.L. (email: lembo@neuromed.it)*

Published online 23 December 2002, doi:10.1038/nm805

**Cardiac hypertrophy is an adaptive response to a variety of mechanical and hormonal stimuli, and represents an early event in the clinical course leading to heart failure. By gene inactivation, we demonstrate here a crucial role of melusin, a muscle-specific protein that interacts with the integrin $\beta_1$ cytoplasmic domain, in the hypertrophic response to mechanical overload. Melusin-null mice showed normal cardiac structure and function in physiological conditions, but when subjected to pressure overload—a condition that induces a hypertrophic response in wild-type controls—they developed an abnormal cardiac remodeling that evolved into dilated cardiomyopathy and contractile dysfunction. In contrast, the hypertrophic response was identical in wild-type and melusin-null mice after chronic administration of angiotensin II or phenylephrine at doses that do not increase blood pressure—that is, in the absence of cardiac biomechanical stress. Analysis of intracellular signaling events induced by pressure overload indicated that phosphorylation of glycogen synthase kinase-3β (GSK-3β) was specifically blunted in melusin-null hearts. Thus, melusin prevents cardiac dilation during chronic pressure overload by specifically sensing mechanical stress.**



Arterial hypertension imposes a biomechanical stress on the left ventricle, requiring the heart to work harder than under normal circumstances. Under these conditions, the heart undergoes hypertrophy resulting from increased synthesis and assembly of the contractile proteins of the actomyosin fibrils. Cardiac hypertrophy is considered beneficial because it allows the generation of greater contractile force, but it may also result in activation of pathways that reduce the efficiency of structural adaptation, promoting the transition toward cardiac dilation and failure[1]. Identifying the molecular mechanisms involved in cardiac hypertrophy and the transition toward dilation and dysfunction is thus an important challenge of cardiovascular biology and medicine[2].

Cardiac hypertrophic remodeling is triggered by a combined action of mechanical stretching of cardiac walls and activation of neurohumoral growth factors[1,3,4]. Mechanical stress is considered the primary trigger to induce the growth response in the overloaded myocardium. Indeed, cardiomyocytes possess an intrinsic mechanosensing mechanism, as indicated by the ability of cultured cardiomyocytes to undergo hypertrophy when subjected to mechanical stretching *in vitro*[5]. Stretching is thought to activate the release of a cascade of autocrine and paracrine humoral factors, such as angiotensin II, endothelin 1, insulin like growth factor (IGF-1), transforming growth factor-β (TGF-β), fibroblast growth factor (FGF) and cardiotrophin-1 (CT-1) (refs. 3,6–8), that in turn promote cardiomyocyte growth and heart tissue remodeling. The intracellular signaling pathways triggered by mechanical stress and by humoral trophic factors are probably temporally and mechanistically distinct; however, whether these pathways can act independently is still under debate. *In vitro* and *in vivo* studies have identified several signaling molecules and pathways involved in cardiac hypertrophy, including the αGq subunit of the heterotrimeric G protein coupled to the β-adrenergic receptors[9–11]; the phospholipase Cβ and protein kinase C, acting downstream of the G proteins[12]; the phosphoinositide 3-kinase; the calcineurin/NF-AT3 pathway; the Ras cascade, including Raf-1 and ERK1/2 MAP kinases; the stress kinases Jnk and p38; and the Jak-STAT pathway[13,14]. Although most of these molecules are activated by both biomechanical and humoral factors, some are specifically involved in cardiac hypertrophy induced by humoral factors. In fact, inactivation of the genes encoding angiotensin II type 1 (AT-1) and the $\alpha_{1b}$ adrenergic receptor ($\alpha_{1b}$-AR) abrogates cardiac hypertrophy induced by sub-pressor doses of angiotensin II or phenylephrine in the absence of mechanical stress, but does not affect the hypertrophic response to mechanical overload imposed by aortic coarcta-

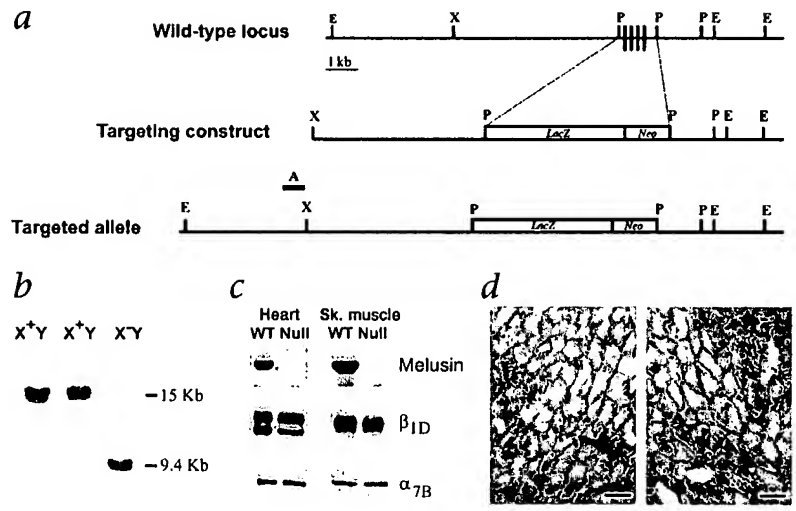


**Fig. 1** Targeted disruption of the mouse melusin gene. ***a***, Restriction map of the wild-type melusin (*Itgb1bp2*) locus, the targeting construct and the targeted locus. A *PstI* fragment containing exons 1–4 was replaced with a cassette containing IRES sequences linked to the *lacZ* gene followed by the neomycin-resistance gene driven by a *PGK* promoter. ***b***, Southern blot analysis: when analyzed using the probe shown in *a*, the targeted locus contains a 9.5 kb *Eco*RV fragment, whereas the intact allele generates a 15 kb band. Because the melusin gene maps to the X chromosome[21], one homologous recombination event was sufficient to target the single allele in male ES R1 cells. ***c***, Western blot analysis: protein extracts from heart and skeletal muscle of wild-type (WT) and melusin-null (null) male mice were separated by SDS-PAGE and probed with an affinity-purified polyclonal antibody against melusin (top row), $\beta_{1D}$ and integrin $\alpha_{7B}$ subunits (middle and bottom rows). ***d***, Immunohistochemical analysis of $\beta_{1D}$ integrin expression. Frozen sections of left ventricle from wild-type (left) and melusin-null (right) hearts were stained with affinity-purified polyclonal antibodies to $\beta_{1D}$ integrin followed by peroxidase-labeled secondary antibody. Scale bars, 40 μm.

tion[15,16]. This indicates the existence of a pathway triggered by angiotensin II or norepinephrine via AT-1 and an $\alpha_{1b}$-AR receptors, independently of mechanical stress.

In contrast, it is not known which molecules are required to couple mechanical stress to the induction of intracellular signals responsible for the hypertrophic response. Integrins and the associated signaling machinery are likely candidates, because of their role in linking the force-generating actin cytoskeleton inside the cell to the extracellular matrix[17]. Integrins are crucial to heart development and function, as indicated both by *in vitro* and *in vivo* studies. Both chimeric mice and embryoid bodies constructed from integrin $\beta_1$–null cells show delayed development and differentiation of $\beta_1$-deficient cells along the cardiac lineage, as well as abnormal sarcomerogenesis[18]. In addition, dominant-negative disruption of integrin $\beta_1$ function[19] as well as selective cardiac excision of the integrin $\beta_1$ gene[20] result in myocardial fibrosis and cardiac failure.

We recently identified melusin, a protein binding to the integrin $\beta_1$ cytoplasmic domain and specifically expressed in striated muscle tissue, where it localizes at costameres in proximity of the Z line along with integrins and vinculin[21]. By inactivating the gene encoding melusin, we show here that the absence of melusin does not affect cardiac development or basal function, but leads to a reduced left ventricular hypertrophy and favors the transition toward dilated cardiomyopathy and contractile dysfunction in response to chronic pressure overload. Yet the absence of melusin does not influence the development of cardiac hypertrophy to humoral factors such as angiotensin II or phenylephrine in the absence of biomechanical stress. Thus, melusin is most likely a specific mechanosensor transducing signal that acts in preventing the transition to heart failure in conditions of biomechanical stress.

### Generation of melusin-null mice

We generated a targeting construct to replace exons 1–4 of the melusin gene, with a cassette containing *LacZ* and neomycin-resistance genes (see Methods and Fig. 1*a*). In mice derived from two different recombinant clones, the mutant allele was inherited according to normal segregation ratios for an X-linked gene (Fig. 1*b*). Hemizygote males and homozygote mutant females developed normally, were fertile and appeared healthy up to 18 month of age. The body weights of wild-type and null mice were

**Table 1** Echocardiographic analysis after TAC

| | Wild type ($n = 13$) | | | | Melusin null ($n = 15$) | | | |
|---|---|---|---|---|---|---|---|---|
| | Basal | 1 wk TAC | 2 wk TAC | 4 wk TAC | Basal | 1 wk TAC | 2 wk TAC | 4 wk TAC |
| LVEDD (mm) | 3.74 ± .05 | 3.42 ± .1§ | 3.3 ± .1§ | 3.41 ± .1§ | 3.65 ± .05 | 3.8 ± .05§ | 4.1 ± .1*§ | 4.92 ± .2*§ |
| LVESD (mm) | 2.02 ± .05 | 1.62 ± .08§ | 1.64 ± .1§ | 1.71 ± .1§ | 1.92 ± .3 | 2.12 ± .2§ | 2.43 ± .1*§ | 3.37 ± .2*§ |
| IVSTd (mm) | 0.69 ± .01 | 1.13 ± .03§ | 1.24 ± .05§ | 1.22 ± .05§ | 0.64 ± .01 | 0.72 ± .03* | 0.8 ± .06*§ | 0.6 ± .04* |
| IVSTs (mm) | 1.31 ± .03 | 2.15 ± .04§ | 2.23 ± .01§ | 2.22 ± .08§ | 1.39 ± .05 | 1.27 ± .04 | 1.31 ± .08* | 0.89 ± .03*§ |
| PWTd (mm) | 0.64 ± .01 | 1.07 ± .04§ | 1.24 ± .05§ | 1.21 ± .05§ | 0.61 ± .01 | 0.70 ± .05* | 0.75 ± .05*§ | 0.54 ± .04* |
| PWTs (mm) | 1.28 ± .03 | 1.99 ± .05§ | 2.08 ± .04§ | 2.08 ± .03§ | 1.27 ± .03 | 1.18 ± .04 | 1.26 ± .08* | 0.81 ± .04*§ |
| RWT | 0.36 ± .01 | 0.65 ± .04§ | 0.76 ± .05§ | 0.72 ± .04§ | 0.34 ± .02 | 0.36 ± .01* | 0.38 ± .03* | 0.23 ± .02*§ |
| %FS | 46 ± 3 | 51 ± 3 | 51 ± 2 | 50 ± 2 | 48 ± 3 | 45 ± 2 | 41 ± 3# | 32 ± 3*§ |
| HR (bpm) | 505 ± 7 | 512 ± 8 | 509 ± 7 | 518 ± 9 | 515 ± 7 | 503 ± 8 | 520 ± 9 | 22 ± 9 |
| SPG (mmHg) | | | | 49 ± 3 | | | | 51 ± 3 |
| BW (g) | 28.3 ± .6 | | | 30.1 ± .9 | 26.8 ± .6 | | | 27.8 ± .8 |

§, $P < 0.01$ versus basal; *, $P < 0.01$ versus wild type; #, $P < 0.05$ versus wild type. LVEDD, left ventricular end-diastolic diameter; LVESD, left ventricular end-systolic diameter; IVSTd, interventricular septum thickness in end diastole; IVSTs, interventricular septum thickness in end systole; PWTd, posterior wall thickness in end diastole; PWTs, posterior wall thickness in end systole; RWT, relative wall thickness; %FS, percent fractional shortening; HR, heart rate; SPG, systolic pressure gradient; BW, body weight.

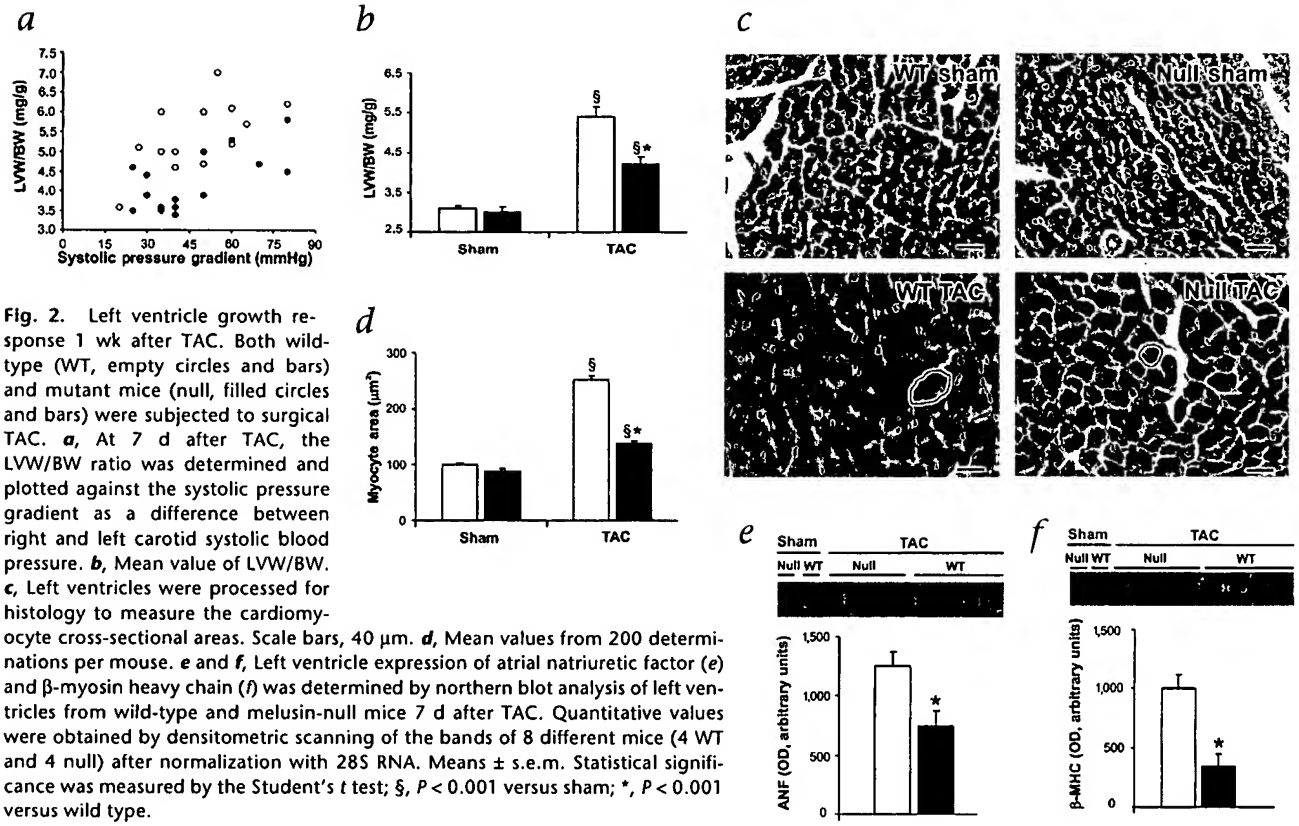


**Fig. 2.** Left ventricle growth response 1 wk after TAC. Both wild-type (WT, empty circles and bars) and mutant mice (null, filled circles and bars) were subjected to surgical TAC. ***a***, At 7 d after TAC, the LVW/BW ratio was determined and plotted against the systolic pressure gradient as a difference between right and left carotid systolic blood pressure. ***b***, Mean value of LVW/BW. ***c***, Left ventricles were processed for histology to measure the cardiomyocyte cross-sectional areas. Scale bars, 40 μm. ***d***, Mean values from 200 determinations per mouse. ***e*** and ***f***, Left ventricle expression of atrial natriuretic factor (***e***) and β-myosin heavy chain (***f***) was determined by northern blot analysis of left ventricles from wild-type and melusin-null mice 7 d after TAC. Quantitative values were obtained by densitometric scanning of the bands of 8 different mice (4 WT and 4 null) after normalization with 28S RNA. Means ± s.e.m. Statistical significance was measured by the Student's *t* test; §, $P < 0.001$ versus sham; *, $P < 0.001$ versus wild type.

comparable (Table 1). Western blot analysis with polyclonal antibodies against melusin (Fig. 1*c*) showed that the protein was absent from skeletal and cardiac muscles of mutant mice, whereas integrin $\alpha_{7B}\beta_{1D}$ was normally expressed (Fig. 1*c*) and localized to the plasma membrane (Fig. 1*d*).

### Absence of melusin does not affect basal cardiac function

Both male and female melusin-null mice had normal lifespans and no evidence of morphogenic defects in cardiac or skeletal muscle. Histological analysis of mutant cardiac and skeletal muscles derived from mice up to 1 year old showed no evidence of necrosis, fibrosis or myofibrillar disarray (data not shown).

We examined basal cardiac dimensions and function in male mice 10–16 weeks old and found them to be unaffected by the absence of melusin. In particular, left ventricular diameters, wall thickness and contractile function, as evaluated by echocardiography, were similar in melusin-null mice and their wild-type littermates (Table 1). Left ventricular contractility and diastolic function, assessed by left ventricle dP/dt, were similar in melusin-null and wild-type mice (left ventricular dP/dt max, 9,610 ± 750 versus 9,700 ± 600 mmHg/sec, n.s.; left ventricular dP/dt min, −9,930 ± 700 versus −10,530 ± 850 mmHg/sec, n.s.) and increased to a similar extent in response to an acute pressure overload evoked by transversal aortic coarctation (left ventricular dP/dt max, 15,860 ± 890 versus 15,535 ± 920 mmHg/sec, n.s.), indicating that the absence of melusin does not affect basal inotropic function and its reserve. During left ventricular hemodynamic evaluations, the basal heart rate (HR) was similar in melusin-null mice and wild-type controls (HR, 475 ± 8 versus 491 ± 10 b.p.m., n.s.) and during acute transversal aortic coarctation (TAC) (HR, 513 ± 10 versus 521 ± 9 b.p.m., n.s.). Finally, melusin-null mice did not show hypertrophy or heart failure up to 18 months of age. Thus, under physiological conditions melusin is not required for the development and organization of heart tissue or for basal cardiac function.

### Absence of melusin leads to heart dilation after TAC

Genetic mutations have been reported that do not affect basal cardiac function but cause heart failure under conditions of high blood pressure[22,23]. Therefore, we assessed the effects of exposing melusin-null mice to chronic pressure overload induced by transversal aortic coarctation (TAC). These and subsequent studies described here were carried out using 10–16-week-old male SV129 mice. Seven days after TAC, wild-type mice developed left ventricular hypertrophy as identified by left ventricular weight/body weight ratio (LVW/BW) (Fig. 2*a* and *b*). In contrast, the left ventricular hypertrophic response to TAC was markedly impaired in melusin-null mice (Fig. 2*a* and *b*), though they were exposed to a similar degree of biomechanical stress, as estimated from the systolic pressure gradient across the surgical aortic stenosis (mean values, 50 ± 4 mmHg in melusin-null versus 46 ± 4 mmHg in wild-type, n.s.; Fig. 2*a*).

Histological analysis showed that increase of the cardiomyocyte cross-sectional area was substantially lower in melusin-null mice subjected to TAC (Fig. 2*c* and *d*), whereas no differences were detectable between both genotypes in fibrosis (data not shown) and apoptosis (0.8 ± 0.2 and 0.75% ± 0.3 apoptotic cardiomyocytes in wild-type and melusin-null mice, respectively). In addition, induction of ANF and β-MHC expression, markers of left ventricular hypertrophy, was significantly lower in melusin-null mice (Fig. 2*e* and *f*).

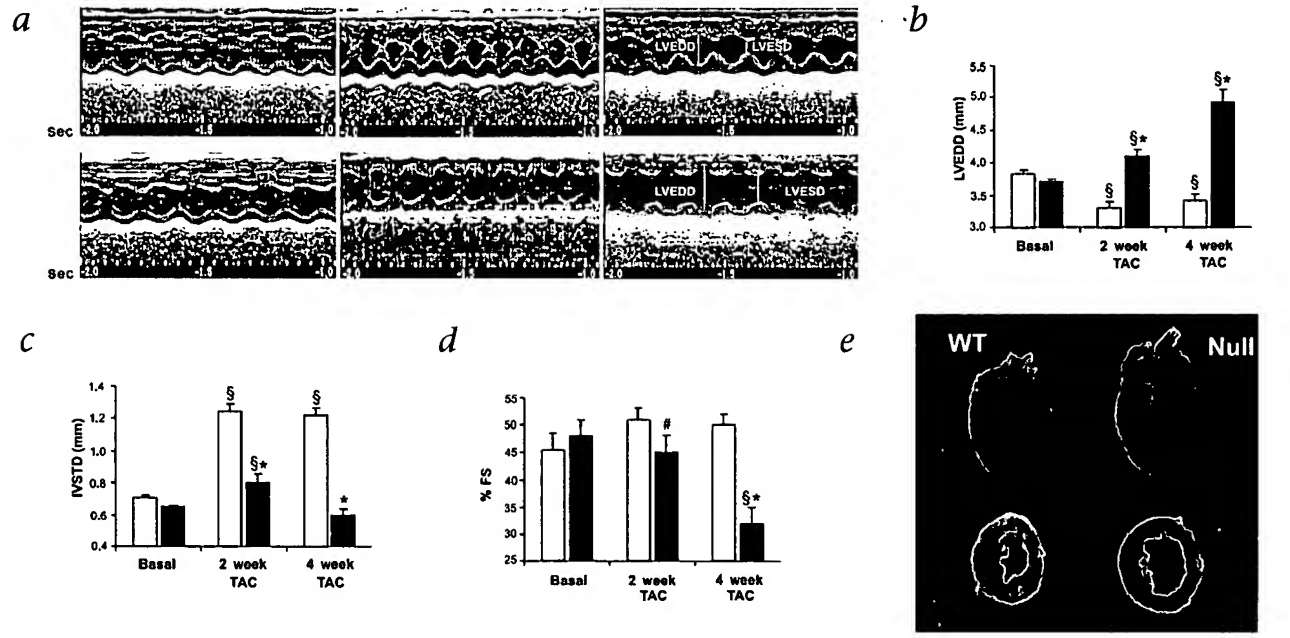


Fig. 3 Left ventricle remodeling and function 2 and 4 wk after TAC. Both wild-type (WT, empty bars) and mutant mice (Null, filled bars) were subjected to TAC. Cardiac structure and function were evaluated non-invasively by transthoracic echocardiography in basal condition and at 2 and 4 wk after TAC. All measurements were determined in a short-axis view at the level of papillary muscles. ***a***, Representative M-mode left ventricular echocardiographic recording of wild-type (top) and melusin-null mice (bottom) in the basal state (left), or 2 wk (middle) or 4 wk (right) after TAC. ***b***, Left ventricular end-diastolic diameter (LVEDD). ***c***, Interventricular septum thickness in end-diastole (IVSTD). ***d***, Percent fractional shortening (%FS) as parameter of left ventricle contractile function. ***e***, Representative gross morphology of whole hearts (upper rows) and transversal sections at base level of the left ventricles of wild-type (left) and melusin-null (right) mice after 4 wk after TAC. §, $P < 0.01$ versus basal; *, $P < 0.01$ versus wild type; #, $P < 0.05$ versus wild type.

To evaluate the geometric remodeling that occurred in response to chronic pressure overload, we subjected mice to TAC for 4 weeks, during which we examined them by serial echocardiographic analysis (Table 1). As expected, wild-type mice showed increased interventricular septum and posterior wall thickness and reduced end-systolic and end-diastolic left ventricular diameters, with a consequent increase in left ventricular relative wall thickness (Table 1 and Fig. 3). Such remodeling represents a typical pattern of concentric hypertrophy, an adaptive compensatory mechanism that occurs in response to sustained hypertensive conditions. In contrast, 7 days after TAC, melusin-null mice developed only modest thickening of ventricular walls and a substantial chamber enlargement without change in relative wall thickness. This represents a typical pattern of eccentric hypertrophic remodeling (Table 1), an unfavorable geometric adaptation to sustained hypertensive conditions. At 2 weeks after TAC, melusin-null mice showed a further enlargement of left ventricular chamber as compared to that in wild-type mice (Table 1 and Fig. 3). After 4 weeks, left ventricular dilation was even more evident and was associated with a marked deterioration of contractile function, as detected by fractional shortening (Table 1 and Fig. 3). Finally, lethality rates at 4 weeks after TAC were

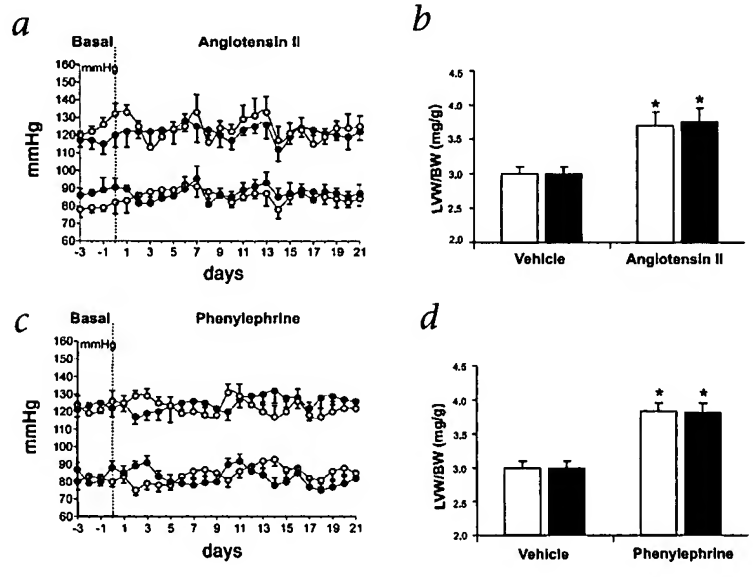


Fig. 4 Left ventricle hypertrophic growth response to sub-pressor doses of angiotensin II or phenylephrine. ***a-d***, Wild-type (empty circles and bars) and melusin-null (filled circles and bars) mice were infused subcutaneously, using osmotic minipumps, with angiotensin II (0.15 mg/kg/d) or phenylephrine (100 μg/kg/d) over a period of 21 d. Conscious systolic (upper) and diastolic (lower) blood pressure and heart rate (not shown) were measured in unrestrained conditions by a radiotelemetric system during angiotensin II (*a*) and phenylephrine (*c*) administration. LVW/BW was assessed after 21 d of treatment with angiotensin II (*b*) and phenylephrine (*d*) in wild-type and melusin-null mice.

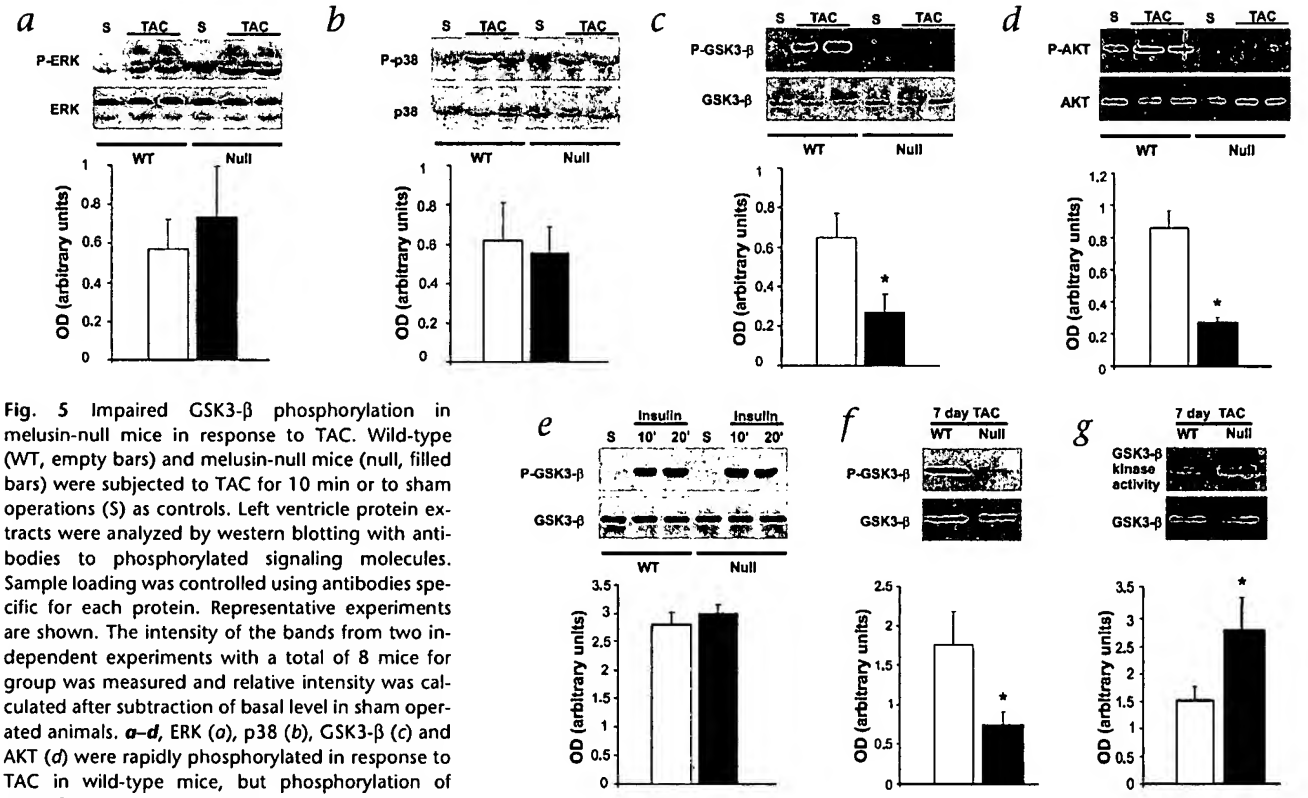


**Fig. 5** Impaired GSK3-β phosphorylation in melusin-null mice in response to TAC. Wild-type (WT, empty bars) and melusin-null mice (null, filled bars) were subjected to TAC for 10 min or to sham operations (S) as controls. Left ventricle protein extracts were analyzed by western blotting with antibodies to phosphorylated signaling molecules. Sample loading was controlled using antibodies specific for each protein. Representative experiments are shown. The intensity of the bands from two independent experiments with a total of 8 mice for group was measured and relative intensity was calculated after subtraction of basal level in sham operated animals. ***a–d***, ERK (*a*), p38 (*b*), GSK3-β (*c*) and AKT (*d*) were rapidly phosphorylated in response to TAC in wild-type mice, but phosphorylation of GSK3-β and AKT was strongly impaired in melusin-null mice. ***e***, GSK3-β was phosphorylated to a comparable level in both wild-type and melusin-null mice 10 and 20 min after IP injection of 2 IU of insulin. ***f*** and ***g***, Mice were subjected to TAC for 7 d and left ventricle protein extracts were analyzed by western blotting with antibodies to phoserine9-GSK3-β (*f*) or subjected to immunoprecipitation with GSK3-β antibodies and processed for kinase assay (*g*). The intensity of the bands from a total of 3 mice per group was measured and relative intensity was calculated. *, $P < 0.05$ versus wild-type.

greater in mutant than in wild-type mice (53.3% versus 30.7%). Thus, whereas wild-type mice developed a typical concentric compensatory hypertrophy in response to prolonged pressure overload, in the absence of melusin the pressure overload resulted in eccentric cardiac remodeling, which accelerates the transition toward heart failure.

### Normal hypertrophy in the absence of mechanical stress

Angiotensin II and norepinephrine induce heart hypertrophy by exerting a direct trophic action on cardiomyocytes via G protein–coupled seven-transmembrane-domain receptors[24]. To explore the role of melusin in cardiac hypertrophy caused by these trophic factors in the absence of biomechanical stress, mice were exposed chronically (for 21 days) to doses of angiotensin II or phenylephrine which did not affect arterial blood pressure. Systolic and diastolic blood pressure (Fig. 4*a* and *c*) and heart rate (data not shown), evaluated by radiotelemetry during the infusion period, were not affected by either treatment. After 21 days of infusion, left ventricular mass, as measured by LVW/BW, increased at similar extent in wild-type and melusin-null mice in response to both angiotensin II and phenylephrine (Fig. 4*b* and *d*). These data indicate that melusin is not required for cardiac hypertrophy induced by humoral stimulation that does not involve a biomechanical stress.

### Absence of melusin impairs GSK3-β signaling after TAC

To investigate the effect of melusin on cardiac intracellular signaling, we analyzed the phosphorylation of p38, ERK 1/2 and GSK3-β, proteins reported to be involved in cardiac hypertrophy[14,25–27]. In wild-type mice, all three molecules were strongly phosphorylated 10 minutes after TAC (Fig.5*a–c*) and were appreciably phosphorylated even at 5 minutes after TAC (data not shown). This is consistent with the hypothesis that these molecules respond to a mechanical event. In melusin-null mice, however, the degree of GSK3-β serine 9 phosphorylation was much lower (Fig. 5*c*). Notably, no significant differences were observed between wild-type and melusin-null mice in p38 and ERK1/2 phosphorylation in response to TAC (Fig. 5*a* and *b*). As a comparison, we analyzed the phosphorylation state of the kinase AKT, which regulates phosphorylation of serine 9 of GSK3-β. AKT is rapidly phosphorylated in response to TAC in wild-type mice, but this response is much weaker in melusin-null mice (Fig. 5*d*).

Because GSK3-β is well known to be a target of insulin receptor signaling[28], we also tested whether the absence of melusin affects GSK3-β phosphorylation in response to insulin. Western blot analysis of heart extracts from mice treated with insulin for 10 and 20 min showed that GSK3-β was phosphorylated to a comparable extent in both mouse genotypes (Fig. 5*e*).

Attenuation of cardiac hypertrophy in melusin-null mice was seen 7 days after TAC; we therefore tested GSK3-β signaling at this time point. Phosphorylation of GSK3-β serine 9 occurred to a lesser extent, however, in melusin-null mice than in wild-type mice 7 days after TAC (Fig. 5*f*). In addition, kinase activity was

greater in melusin-null mice, as would be predicted given the inhibitory effect of serine 9 phosphorylation (Fig. 5*g*). Thus altered GSK3-β signaling persists in melusin-null mice exposed to the effects of TAC for 7 days. Together, these data indicate that the absence of melusin selectively impairs left ventricular GSK3-β phosphorylation in response to biomechanical stress.

## Discussion

We previously identified melusin as a protein that binds to the integrin $\beta_1$ cytoplasmic domain and specifically expressed in striated muscle[21]. The phenotype of melusin-null mice reported here demonstrates that melusin, though dispensable for cardiac muscle development and for cardiac function under physiological conditions, is required to sustain compensatory left ventricle hypertrophy in response to pressure overload. Notably, the absence of melusin does not influence the cardiac hypertrophy evoked by trophic stimuli such as angiotensin II or phenylephrine at sub-pressor doses that do not impose a mechanical overload. As melusin interacts with integrin $\beta_1$ cytoplasmic domain and localizes at costameres[21], where contractile filaments are anchored laterally to the sarcolemma, we suggest that melusin senses high threshold levels of mechanical stress and consequently activates signaling pathways required to support cardiomyocyte hypertrophy.

Our analysis of the signaling events occurring in response to mechanical stress indicated that phosphorylation of p38 and ERK1/2 MAP kinases, as well as GSK3-β, is strongly stimulated within 5 minutes of induction of the stress in wild-type mice. These molecules are phosphorylated in response to integrin stimulation by matrix ligands *in vitro*[17,29,30], supporting the hypothesis that integrin stimulation could be responsible for their phosphorylation in heart after mechanical stress. The absence of melusin expression specifically reduced phosphorylation of GSK3-β serine 9, but did not substantially affect phosphorylation of p38 and ERK 1/2. In addition, phosphorylation of AKT was greatly impaired in aortic-banded heart of melusin-null mice. As AKT is the principal kinase that phosphorylates the inhibitory site of GSK3-β, this result points to an important role of melusin in regulating this pathway. GSK3-β is also phosphorylated in response to hormonal stimuli not involving mechanical stress, such as insulin[28]; this pathway, however, was unaffected in the melusin-null background. This observation, together with the very rapid kinetics of GSK3-β phosphorylation in response to aortic coarctaction, supports the hypothesis that melusin selectively senses the biomechanical stimuli. In contrast to other kinases, GSK3-β is highly active in unstimulated cells and becomes inactivated by phosphorylation of serine 9 in response to several stimuli[28]. Recent studies have shown that this inactivation is required for cardiac hypertrophy. In cardiomyocytes, active GSK3-β phosphorylates the transcription factors NF-AT and GATA4, inducing their translocation from the nucleus to the cytoplasm and thus inhibiting their transcriptional activity[25-27]. In addition, active GSK3-β also induces inhibition of eIF2B, a principal initiation factor regulating protein synthesis. Thus, the phosphorylation of serine 9 seen during aortic coarctation may allow the activation of both protein synthesis and transcriptional events required for the hypertrophic response. Indeed, expression of a constitutively active form of GSK3-β in transgenic mice causes an impaired cardiac hypertrophy in response to pressure overload[27]. It is thus likely that the reduced GSK3-β phosphorylation in response to pressure overload that we observed in melusin-null hearts can account, at least partially, for the defective hypertrophic response in these mice.

The impaired left ventricle remodeling of melusin-null mice in response to mechanical overload shows the typical pattern of eccentric left ventricular hypertrophy, characterized by an enlargement of the left ventricular chamber and an impaired wall thickening. This is an unfavorable geometric adaptation to hypertensive conditions that markedly accelerates the evolution toward heart failure[31]. Indeed, in contrast to the compensatory hypertrophy developed by control animals, melusin-null mice undergo a progressive left ventricle dilation followed by the onset of cardiac failure over a period of 4 weeks after TAC, and this is associated with an increased mortality rate. We conclude that the absence of melusin causes a deleterious left ventricular remodeling in conditions of sustained biomechanical stress, such as eccentric hypertrophy, thus accelerating the transition toward heart failure. In contrast, other studies[32] have reported that a reduced left ventricular hypertrophy is protective from the onset of cardiac dilation and dysfunction in two strains of genetically modified mice defective either for Gq signaling (Gq-transgenic) or for norepinephrine synthesis (Dbh null). A possible explanation for this conflicting evidence could be the difference in genetic background between the mice used in the two laboratories: we used inbred SV129, whereas the other researchers probably used different strains. Another possible explanation is that in both Gq-transgenic and Dbh-null mice, the genetic mutations affect G protein–coupled receptor (GPCR) signaling that is unaltered in melusin-null mice, as judged from the normal hypertrophy response to angiotensin II or phenylephrine. It is therefore likely that the differences in cardiac remodeling in response to long-standing pressure overload between melusin-null and Gq-transgenic or Dbh-null mice are attributable to the perturbation of two independent pathways that have opposing effects on heart remodeling. Whereas the GPCR pathway, when active, favors left ventricle dilation, the integrin-linked melusin pathway supports concentric compensatory hypertrophy.

Several genetically modified mouse models of dilated cardiomyopathy have been described, and have enabled different structural and signaling proteins involved in this process to be identified[1,33-35]. In most cases, however, altered expression of these molecules causes basal alteration in cardiac structure and function, with spontaneous development of dilated cardiomyopathy. Fewer examples have been reported in which abrogation of protein function by gene inactivation does not affect basal cardiac physiology, but causes dilated cardiomyopathy and failure in response to mechanical overload. The proteins involved in these cases include the gp130 cytokine receptor[22] and CD95/Fas receptor[23]. Mice in which gp130 is specifically inactivated in the heart have normal cardiac structure and function, but develop rapid-onset dilated cardiomyopathy, resulting from massive myocyte apoptosis, within 7 days after aortic pressure overload. The mechanism underlying cardiac dilation in these mice is distinct from that seen in melusin-null mice, as the latter do not develop cardiomyocyte apoptosis after pressure overload. The CD95/Fas receptor is a well-studied molecule that controls apoptosis in several cell types. In cardiomyocytes, however, Fas induces the pro-hypertrophic transcription factor AP-1 rather than inducing apoptosis[36]. Mice without a functional Fas receptor develop rapid-onset left ventricular dilation and failure in response to aortic coarctation, but no apoptotic mechanism is involved[23]. The possibility that the absence of melusin expression prevents normal of gp130 and/or CD95/Fas expression was excluded by western blot analysis of mutant and wild-type hearts (M.B., unpublished observations). Notably, the

absence of compensatory hypertrophy in CD95/Fas mutant mice is accompanied by impaired GSK3-β phosphorylation, indicating that the pathway controlled by melusin and Fas receptor converges on GSK3-β. Because integrins can cooperate with several growth-factor and cytokine receptors[37], it is tempting to speculate that melusin may be involved in integrin–Fas receptor cross-talk.

Finally, whereas mice with mutant gp130 or Fas receptors show cardiac dilation and dysfunction after 1 week of biomechanical stress[22,23], melusin-null mice showed cardiac dilation and then dysfunction only 4 weeks after aortic banding. The time-course in melusin-null mice is thus closer to that of the slowly developing process of dilated cardiomyopathy. Therefore, melusin-null mice may be a powerful model to clarify the molecular mechanisms linking the cytoskeleton to intracellular signaling pathways and their role in cardiac remodeling as a response to biomechanical stress.

## Methods

**Generation of melusin-null mice.** Using the murine cDNA probe[21], we isolated a genomic fragment of 14.8 kb encompassing the first exon, which contains the ATG start codon, and three other exons. A *PstI* fragment containing exons 1–4 was replaced with a cassette containing IRES sequences linked to the *LacZ* gene followed by the neomycin-resistance gene driven by a *PGK* promoter. We identified by Southern blot analysis three different ES R1 cell clones in which homologous recombination had occurred. Two generated chimeras that produced germline transmission. All studies presented in this work were performed using 10–16-wk-old male SV129 mice and were confirmed in female mice. The use of animals was in compliance with the guidelines of the European Community and was approved by the Animal Care and Use Committee of the University of Torino.

**Left ventricle hemodynamics.** Mice were anesthetized, as previously described[16], with an intraperitoneal injection of tribromoethanol (Avertin, 350 mg/kg), and inotropic and lusitropic function was evaluated by measuring the maximum rate of left ventricular pressure developed (dP/dt max) and left ventricular pressure decay (dP/dt min) with a micromanometer catheter (Millar 1.4 F, SPR 671, Millar Instruments, Houston, Texas) positioned in the left ventricle via right common carotid artery cannulation. To evaluate inotropic cardiac reserve, left ventricular dP/dt max was measured after an acute increase (60 mmHg) of cardiac afterload induced by temporary aortic coarctation, as described below.

***In vivo* biomechanical stress.** Mechanical stress was imposed on the left ventricle through transverse aortic coarctation (TAC) between the *truncus anonimus* and left carotid artery, as previously described[38]. A separate group of mice underwent the same surgical procedures but without aortic stenosis (sham procedure). To evaluate the degree of biomechanical stress imposed on the left ventricle, the systolic pressure gradient (SPG) was measured by selective cannulation of left and right carotid arteries[38]. After hemodynamic evaluation, the mice were weighed, then the hearts were excised and the ratio of left ventricular weight to body weight (LVW/BW) was calculated.

**Transthoracic echocardiography.** Echocardiographic analysis was performed using a commercially available echocardiograph (System Five Performance, General Electric Vingmed, Waukesha, Wisconsin) equipped with a 10 MHz imaging transducer. After good quality two-dimensional short-axis images of left ventricle were obtained, M-mode freeze frames were printed on common echocardiographic paper. End-diastolic and end-systolic interventricular septum (IVSTd, IVSTs), posterior wall thickness (PWTd, PWTs) and left ventricular internal diameters (LVEDD, LVESD) were measured using a computed NIH Image analysis system (National Institutes of Health, Bethesda, Maryland). Percent fractional shortening (%FS) and relative wall thickness (RWT) were calculated using standard formulas:

$$\%FS = [(LVEDD - LVESD)/LVEDD] \times 100$$
$$RWT = [(IVSd + PWd)/2]/(LVEDD/2)$$

Reproducibility, calculated as the difference between two determinations divided by the mean of the two determinations and expressed as percentage of error, was 3.7 ± 0.6 for left ventricular diameters and 7.2 ± 0.9 for wall thickness.

**Chronic infusions of angiotensin II or phenylephrine at sub-pressor doses.** Conscious blood pressure and heart rate were measured under unrestrained conditions by a radiotelemetric device (TA11PA-C20, Data Sciences International, St. Paul, Minnesota) whose sensing catheter was inserted into the femoral artery, as previously described[16]. After implantation, mice were housed in a single cage and allowed 10 d of recovery from surgical procedures. Blood pressure and heart rate were continuously recorded for 4 h daily (from 8:00 AM to 12:00 AM), in basal conditions (4 d) and during 21 d of active treatment with sub-pressor doses of angiotensin II (0.15 mg/kg/d) or phenylephrine (100 μg/kg/d), infused subcutaneously with osmotic minipumps. Telemetered pressure signals were stored and analyzed by a dedicated computed data acquisition system (Dataquest Acquisition and Analysis System, DQ ART 1.1 Gold, Data Sciences International) that calculated the mean value during the acquisition time.

**Antibodies.** Polyclonal antibodies against melusin α7B and against β1D were obtained as described[21,39,40]. Rabbit polyclonal antibodies against phospho-Ser9-GSK3-β, phospho-Ser473-AKT, AKT and phospho-ERK1/2 were from New England BioLabs (Beverly, Massachusetts); those against GSK3-β, ERK1 (C16) and FAS (M-20) were from Santa Cruz Biotechnology (Santa Cruz, California); those against p38 and phospho-p38 were from Calbiochem (Damstadt, Germany); and those against gp130 were from Upstate Biotechnology (Lake Placid, New York). Mouse monoclonal antibodies against GSK-3 were from BD Biosciences (Heidelberg, Germany).

**Histological analysis and immunohistochemistry.** Paraffin-embedded hearts were cut into 5 μm slices, which were stained with H&E for morphological analysis or with Picrosirius red (Fluka, Buchs, Switzerland) for detection of fibrosis. To measure myocyte area, suitable cross-sections were defined as those having nearly circular capillary profiles and nuclei. Detection of apoptotic cells and immunohistochemistry were performed as previously described[40,41].

**Analysis of signaling pathways and hypertrophic markers.** Mice were anesthetized with sodium pentobarbital (30 mg/kg injected intraperitoneally) and subjected to TAC as described above. After anesthesia was induced, the animals were maintained under controlled temperature and ventilation. A customized adjustable clamp was placed around the transverse aorta, after which the thoracic cavity was closed. After stabilization (20 min), pressure overload was initiated with adjustments of the aortic clamping while blood pressure signals from above and below the constriction were monitored. The experimental protocol included sustained increase (60 mmHg for 10 min) of systolic pressure gradient across the aortic coarctation. The ventricles were then rapidly removed, frozen and triturated in liquid nitrogen, and then extracted by sonication and boiling in a solution containing 60 mM Tris-Cl, pH 6.8, 1% SDS, 1 mM $Na_3VO_4$, 10 mM NaF, 10 μg/ml leupeptin, 0.4 μg/ml pepstatin and 0.1 TIU/ml aprotinin. Proteins were than analyzed by SDS-PAGE and western blotting using standard procedures.

To evaluate kinase activity, total GSK-3β was immunoprecipitated from ventricular protein extracts (in 1% Nonidet P-40, 150 mM NaCl, 50 mM Tris-Cl, pH 8, 1 mM $Na_3VO_4$, 10 mM NaF, 10 μg/ml leupeptin, 0.4 mg/ml pepstatin, 0.1 TIU/ml aprotinin) using the monoclonal antibody mentioned above. The immunocomplexes were then incubated in kinase assay buffer[42] with 1 μg protein phosphatase inhibitor-2 (Sigma), as substrate, 100 nM nonradioactive ATP (Sigma) and 5 μCi [$\gamma$-$^{32}$P]ATP (6,000 Ci/mM) for 10 min at 30 °C. Reactions were analyzed by 15% SDS-PAGE and autoradiography.

Left ventricular ANF and β-MHC expressions were evaluated in sham-operated and 7-d post-TAC mice, as previously described[38]. The optical density (OD) of ANF and β-MHC bands were normalized with 28S RNA.

**Statistical analysis.** Data, expressed as mean ± s.e.m., were analyzed with two-way ANOVA and Bonferroni's correction for multiple comparisons (SYSTAT).

*Acknowledgments*

*We thank O. Azzolino, I. Carfora and G. Russo for technical assistance; D.*

*Bongioanni, B. Canepa, R. Ferretti and M. Sbroggiò for help with several experiments; V. Poli and S. Cabodi for suggestions and critical reading of the manuscript; and A. Fubini for great enthusiasm and support in the initial analysis of the mouse phenotype. This work was supported by grants from Telethon to G.T., the Ministry of University and Research to G.T. and G.L., the Italian National Research Council to F.A. and E.H., and the Italian Ministry of Health to G.L.*

*Competing interests statement*

*The authors declare that they have no competing financial interests.*

RECEIVED 19 SEPTEMBER; ACCEPTED 22 NOVEMBER 2002

1. Chien, K.R. Stress pathways and heart failure. *Cell* **98**, 555–558 (1999).
2. Chien, K.R. & Olson, E.N. Converging pathways and principles in heart development and disease: CV@CSH. *Cell* **110**, 153–162 (2002).
3. Sadoshima, J. & Izumo, S. The cellular and molecular response of cardiac myocytes to mechanical stress. *Annu. Rev. Physiol.* **59**, 551–571 (1997).
4. Ruwhof, C. & van der Laarse, A. Mechanical stress-induced cardiac hypertrophy: mechanisms and signal transduction pathways. *Cardiovasc. Res.* **47**, 23–37 (2000).
5. Sadoshima, J. & Izumo, S. Mechanical stretch rapidly activates multiple signal transduction pathways in cardiac myocytes: potential involvement of an autocrine/paracrine mechanism. *EMBO J.* **12**, 1681–1692 (1993).
6. Schultz Jel, J. *et al.* TGF-β1 mediates the hypertrophic cardiomyocyte growth induced by angiotensin II. *J. Clin. Invest.* **109**, 787–796 (2002).
7. MacLellan, W.R. & Schneider, M.D. Genetic dissection of cardiac growth control pathways. *Annu. Rev. Physiol.* **62**, 289–319 (2000).
8. Yamazaki, T. *et al.* Endothelin-1 is involved in mechanical stress-induced cardiomyocyte hypertrophy. *J. Biol. Chem.* **271**, 3221–3228 (1996).
9. Wettschureck, N. *et al.* Absence of pressure overload induced myocardial hypertrophy after conditional inactivation of Gαq/Gα11 in cardiomyocytes. *Nat. Med.* **7**, 1236–1240 (2001).
10. Akhter, S.A. *et al.* Targeting the receptor-Gq interface to inhibit *in vivo* pressure overload myocardial hypertrophy. *Science* **280**, 574–577 (1998).
11. Dorn, G.W. 2nd & Brown, J H. Gq signaling in cardiac adaptation and maladaptation. *Trends Cardiovasc. Med.* **9**, 26–34 (1999).
12. Wakasaki, H. *et al.* Targeted overexpression of protein kinase C β2 isoform in myocardium causes cardiomyopathy. *Proc. Natl. Acad. Sci. USA* **94**, 9320–9325 (1997).
13. Sugden, P.H. & Clerk, A. Cellular mechanisms of cardiac hypertrophy. *J. Mol. Med.* **76**, 725–746 (1998).
14. Hunter, J.J. & Chien, K.R. Signaling pathways for cardiac hypertrophy and failure. *N. Engl. J. Med.* **341**, 1276–1283 (1999).
15. Harada, K. *et al.* Pressure overload induces cardiac hypertrophy in angiotensin II type 1A receptor knockout mice. *Circulation* **97**, 1952–1959 (1998).
16. Vecchione, C. *et al.* Cardiovascular influences of α1b-adrenergic receptor defect in mice. *Circulation* **105**, 1700–1707 (2002).
17. Schwartz, M.A., Schaller, M.D. & Ginsberg, M.H. Integrins: emerging paradigms of signal transduction. *Annu. Rev. Cell Dev. Biol.* **11**, 549–599 (1995).
18. Fassler, R. *et al.* Differentiation and integrity of cardiac muscle cells are impaired in the absence of β1 integrin. *J. Cell Sci.* **109**, 2989–2899 (1996).
19. Keller, R.S. *et al.* Disruption of integrin function in the murine myocardium leads to perinatal lethality, fibrosis, and abnormal cardiac performance. *Am. J. Pathol.* **158**, 1079–1090 (2001).
20. Shai, S.Y. *et al.* Cardiac myocyte-specific excision of the β1 integrin gene results in myocardial fibrosis and cardiac failure. *Circ. Res.* **90**, 458–464 (2002).
21. Brancaccio, M. *et al.* Melusin is a new muscle-specific interactor for β1 integrin cytoplasmic domain. *J. Biol. Chem.* **274**, 29282–29288 (1999).
22. Hirota, H. *et al.* Loss of a gp130 cardiac muscle cell survival pathway is a critical event in the onset of heart failure during biomechanical stress. *Cell* **97**, 189–198 (1999).
23. Badorff, C. *et al.* Fas receptor signaling inhibits glycogen synthase kinase 3β and induces cardiac hypertrophy following pressure overload. *J. Clin. Invest.* **109**, 373–381 (2002).
24. Rockman, H.A., Koch, W.J. & Lefkowitz, R.J. Seven-transmembrane-spanning receptors and heart function. *Nature* **415**, 206–212 (2002).
25. Haq, S. *et al.* Glycogen synthase kinase-3β is a negative regulator of cardiomyocyte hypertrophy. *J. Cell Biol.* **151**, 117–130 (2000).
26. Morisco, C. *et al.* Glycogen synthase kinase 3β regulates GATA4 in cardiac myocytes. *J. Biol. Chem.* **276**, 28586–28597 (2001).
27. Antos, C.L. *et al.* Activated glycogen synthase-3β suppresses cardiac hypertrophy *in vivo*. *Proc. Natl. Acad. Sci. USA* **99**, 907–912 (2002).
28. Cohen, P. & Frame, S. The renaissance of GSK3. *Nat. Rev. Mol. Cell Biol.* **2**, 769–776 (2001).
29. Persad, S. *et al.* Regulation of protein kinase B/Akt-serine 473 phosphorylation by integrin-linked kinase: critical roles for kinase activity and amino acids arginine 211 and serine 343. *J. Biol. Chem.* **276**, 27462–27469 (2001).
30. Ivaska, J. *et al.* Integrin α2β1 mediates isoform-specific activation of p38 and upregulation of collagen gene transcription by a mechanism involving the α2 cytoplasmic tail. *J. Cell Biol.* **147**, 401–416 (1999).
31. Norton, G.R. *et al.* Heart failure in pressure overload hypertrophy. The relative roles of ventricular remodeling and myocardial dysfunction. *J. Am. Coll. Cardiol.* **39**, 664–671 (2002).
32. Esposito, G. *et al.* Genetic alterations that inhibit *in vivo* pressure-overload hypertrophy prevent cardiac dysfunction despite increased wall stress. *Circulation* **105**, 85–92 (2002).
33. Wang, Y. Signal transduction in cardiac hypertrophy—dissecting compensatory versus pathological pathways utilizing a transgenic approach. *Curr. Opin. Pharmacol.* **1**, 134–140 (2001).
34. MacLellan, W.R. Advances in the molecular mechanisms of heart failure. *Curr. Opin. Cardiol.* **15**, 128–135 (2000).
35. Nicol, R.L. *et al.* Activated MEK5 induces serial assembly of sarcomeres and eccentric cardiac hypertrophy. *EMBO J.* **20**, 2757–2767 (2001).
36. Wollert, K.C. *et al.* The cardiac Fas (APO-1/CD95) Receptor/Fas ligand system relation to diastolic wall stress in volume-overload hypertrophy *in vivo* and activation of the transcription factor AP-1 in cardiac myocytes. *Circulation* **101**, 1172–1178 (2000).
37. Schwartz, M.A. & Ginsberg, M.H. Networks and crosstalk: integrin signalling spreads. *Nat. Cell Biol.* **4**, E65–E658 (2002).
38. Lembo, G. *et al.* Elevated blood pressure and enhanced myocardial contractility in mice with severe IGF-1 deficiency. *J. Clin. Invest.* **98**, 2648–2655 (1996).
39. Belkin, A.M. *et al.* Muscle β1D integrin reinforces the cytoskeleton-matrix link: modulation of integrin adhesive function by alternative splicing. *J. Cell Biol.* **139**, 1583–1595 (1997).
40. Brancaccio, M. *et al.* Differential onset of expression of α7 and β1D integrins during mouse heart and skeletal muscle development. *Cell Adhes. Commun.* **5**, 193–205 (1998).
41. Condorelli, G. *et al.* Increased cardiomyocyte apoptosis and changes in proapoptotic and antiapoptotic genes bax and bcl-2 during left ventricular adaptations to chronic pressure overload in the rat. *Circulation* **99**, 3071–3078 (1999).
42. Cabodi, S. *et al.* A PKC-β/Fyn-dependent pathway leading to keratinocyte growth arrest and differentiation. *Mol. Cell* **6**, 1121–1129 (2000).

ELSEVIER
European Journal of Heart Failure xx (2007) xxx–xxx
The European Journal of Heart Failure
www.elsevier.com/locate/ejheart

# Altered melusin expression in the hearts of aortic stenosis patients

Sebastian Brokat [a], Jenny Thomas [a], Lars R. Herda [a], Christoph Knosalla [b], Reinhard Pregla [b], Mara Brancaccio [c], Federica Accornero [c], Guido Tarone [c], Roland Hetzer [b], Vera Regitz-Zagrosek [a,b,*]

[a] *Center for Gender in Medicine and Cardiovascular Research Center (CCR), Charité Berlin, Germany*
[b] *German Heart Institute (DHZB), Berlin, Germany*
[c] *Department of Genetics, Biology and Biochemistry, University of Turin, Italy*

Received 10 July 2006; received in revised form 20 December 2006; accepted 22 February 2007

**Abstract**

*Background:* The role of melusin, a necessary component in pressure-induced left-ventricular hypertrophy (LVH) in mice, has not yet been determined in human cardiac hypertrophy. We analyzed for the first time the expression and regional distribution of melusin in human LVH due to aortic stenosis (AS) and determined AKT phosphorylation as a potential downstream effector of melusin signalling.
*Methods:* Regional distribution of melusin was evaluated in four normal hearts. Melusin staining, gene expression and protein content were assessed in biopsies from normal and diseased hearts and melusin gene expression was correlated with LV functional changes. The pAKT/AKT ratio was determined in parallel and correlated with melusin protein content.
*Results:* In normal hearts, melusin was found in the myocytes with a uniform regional distribution. Melusin staining, mRNA and protein were significantly decreased in human AS hearts. The reduction in melusin mRNA was significantly correlated with LVEF, LVEDD and LVESD. pAKT/AKT ratio was significantly decreased in human AS and was correlated with melusin content.
*Conclusion:* Reduction in melusin expression parallels the functional cardiac impairment in human AS. The simultaneous decrease of melusin and AKT phosphorylation suggests a connection between the loss of melusin and the decrease in systolic function.


*Keywords:* Melusin; Aortic stenosis; Hypertrophy; Gene expression; Proteinkinase B/AKT

## 1. Introduction

In human cardiovascular pathophysiology, different forms of hypertrophy are observed. Adaptive hypertrophy such as in trained athletes is not associated with an unfavourable prognosis [1]. It is characterized by increased ventricular wall thickness and cardiomyocyte size, lack of fibrosis, maintained systolic function and is fully reversible. Pressure overload — induced concentric hypertrophy, primarily increases wall thickness, reduces wall stress and is associated with maintained cardiac function in the early stages of pressure overload. In the later stages of chronic pressure load, the hypertrophic phenotype turns into thinning of ventricular walls, ventricular dilatation, fibrosis and systolic function decreases. Molecular markers to distinguish these different stages of hypertrophy and mechanisms leading to the development of dilatation and cardiac failure are currently being actively investigated [2].

Melusin, a cytosolic protein, whose expression pattern is restricted to cardiac and skeletal muscle, is thought to play a key role in cardiac hypertrophy. Melusin physically interacts with the integrin β1 cytoplasmic domain and localizes at costameres and is thus part of the molecular machinery connecting the sarcomeric structure to the sarcolemma and to

* Corresponding author. Center for Gender in Medicine and Center for Cardiovascular Research (CCR), in Cooperation with DHZB, Charité — Universitätsmedizin Berlin, Hessische Straße 3-4, D-10115 Berlin, Germany. Tel.: +49 30 450 525 172; fax: +49 30 450 525 972.
*E-mail addresses:* vera.regitz-zagrosek@charite.de, vrz@dhzb.de (V. Regitz-Zagrosek).

1388-9842/$ - see front matter © 2007 European Society of Cardiology. Published by Elsevier B.V. All rights reserved.
doi:10.1016/j.ejheart.2007.02.009

the extracellular matrix [3,4]. Gene inactivation experiments in mice suggest that melusin is not required for heart development, sarcomere organization or cardiac function in basal conditions [3]. Melusin ablation, however, strongly impairs the left ventricular hypertrophic response to pressure overload as induced by transverse aortic banding, and dramatically accelerates the transition to cardiac dilation [3,5]. At the same time, when melusin is over-expressed in the heart of transgenic mice, the left ventricle retains its compensatory concentric hypertrophy with full contractile function when hearts are subjected to long standing pressure overload [6]. These functional properties are accompanied by protection from cardiomyocyte apoptosis and lack of stromal tissue deposition, hallmarks of beneficial heart remodelling. Interestingly, endogenous melusin levels are upregulated during the initial phase of compensatory hypertrophy in mice subjected to aortic banding, but return to basal levels in hearts that have undergone the transition towards dilation. Melusin signalling includes the phosphorylation of AKT and GSK3β as well as phosphorylation of ERK1/2 [3]. These signalling kinases are known to regulate nuclear translocation of different transcription factors, including GATA 4 and NFAT, which are involved in cardiomyocyte hypertrophy [7,8].

Based on these findings, we investigated whether melusin expression is altered in human chronic aortic diseases and whether it correlates with changes in LV function. We also investigated whether regulation of melusin is accompanied by alterations in the phosphorylation of proteinkinase B/AKT in the human heart.

## 2. Material and methods

### 2.1. Patients

Left ventricular myocardial samples from 17 patients with aortic valve stenosis and 16 control (donor) subjects were analyzed for melusin mRNA or protein content as well as pAKT/AKT ratios, indicating AKT phosphorylation, depending on the amount of tissue available. Consecutive patients with isolated aortic stenosis, without aortic regurgitation or other valve disease exceeding grade I, after exclusion of significant coronary artery disease were included. Clinical data are summarized in Table 1. In patients with AS, biopsies were obtained from the left ventricular septum during elective aortic valve replacement surgery from an area underneath the surgical aortic valve and frozen at −80 °C. The control group was composed of donor hearts that were rejected for transplantation due to logistic reasons. All controls had normal systolic function and no history of cardiac disease. Post-mortem histology evaluated was normal in all cases, as described previously [9,10]. Four of the control donor hearts were also used to study the regional distribution of melusin within the left ventricle. All samples were obtained after written informed consent. The study was performed in accordance with the Declaration of Helsinki.

Table 1
Patient characteristics

| *N* | AS 17 | Controls * 16 |
|---|---|---|
| Age (years) | 70.5±6.8 | 56±6 |
| Sex (% male) | 76 | 50 |
| Hypertension (%) | 76 | – |
| Diabetes (%) | 47 | – |
| Diuretics (%) | 76 | – |
| ACEI (%) | 41 | – |
| β-blocker (%) | 41 | – |
| Digitalis (%) | 24 | – |
| LVEF (%) | 46.0±18.2 | 67±8* |
| *P* mean (mm Hg) | 45.1±18.6 | <2* |
| LV-FS (%) | 27±11 | 39±5* |
| LVEDD (mm) | 54.1±8.8 | 46±9* |
| LVESD (mm) | 40.9±11.7 | 34±5* |
| IVS (mm) | 14.4±2.7 | 12±2* |

AS: Aortic stenosis, ACEI: ACE inhibitors, IVS: thickness of interventricular septum, LVEDD, left ventricular end-diastolic diameter, LVESD, left ventricular end-systolic diameter, LV-FS, left ventricular fractional shortening, LVEF, left ventricular ejection fraction, *P* mean: pressure gradient over the aortic valve.

* Normal values for echo according to [13].

### 2.2. Quantification of mRNA by real time PCR

Total RNA preparation, deoxyribonuclease (DNase) digestion and reverse transcription were performed as described previously [9–11]. A "hot start" real time PCR procedure with SYBR Green, that was validated for reproducibility and linearity within the measuring range, was performed in duplicate with a TaqMan™ 7000 (ABI). Primers are available on request. To correct for potential variance between samples in mRNA extraction or in RT-efficiency, the mRNA content of the target genes was normalized to the expression of the stably expressed reference genes GAPDH or PDH in the same sample.

### 2.3. Protein extraction and immunoblotting

Myocardial samples were homogenized and blotted onto nitrocellulose membranes. Rabbit polyclonal affinity purified melusin antibodies were generated as previously described [4]. Purified antibodies were used in western blotting at a final dilution of 2 μg/ml. Antibodies to phospho-Ser473-AKT and to AKT (Santa Cruz) were used as described [4]. Specific HRP-conjugated antibodies were used as secondary antibody. To normalize for different protein content, we stripped the membrane from the first antibody complex and re-hybridized for GAPDH (primary antibody: Chemicon, MAB-374, 1:50.000; secondary antibody: Donkey anti-mouse, Dianova, 1:15.000) as described [3].

### 2.4. Immunofluorescence microscopy

Tissue samples were fixed in frozen section medium Neg-50 (Richard Allan Scientific). After cutting the samples into 3 μm sections with the Cryostat microtom (Jung Frigocut

Please cite this article as: Brokat S et al. Altered melusin expression in the hearts of aortic stenosis patients. Eur J Heart Fail (2007), doi:10.1016/j.ejheart.2007.02.009

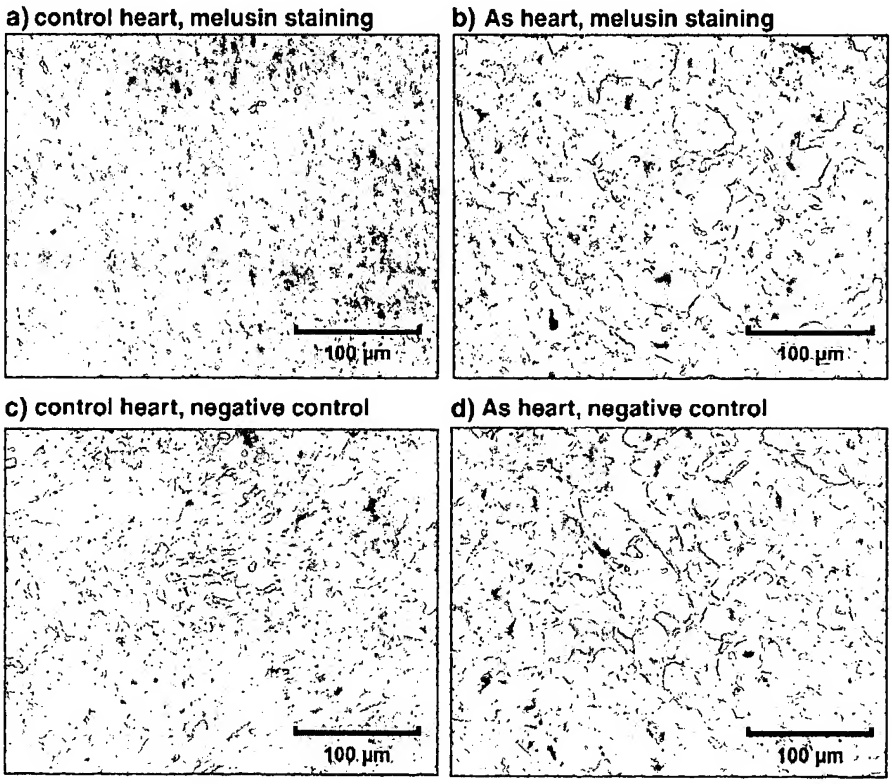


Fig. 1. Immunohistochemical staining of biopsies from a) normal human donor heart (200 fold magnification; c) negative control) and b) human AS heart with EF 50% (200 fold magnification; d) negative control). Staining of melusin in the normal hearts was clearly visible with a location within the myocytes. In the diseased heart, melusin staining was significantly weaker.

2800E; Leica), they were mounted on slides and air dried overnight. For immunohistochemistry the sections were fixed in acetone. After washing, samples were blocked in Peroxidase Blocking Reagent (K3467, Dako Cytomation, USA) and Avidin/Biotin Blocking Reagent (SP-2001, Vector Laboratories). The slides were incubated with the first antibody (melusin [4]) at final dilution of 2 µg/ml in Antibody Diluent Reagent (S3022, Dako Cytomation, USA). After washing slides, were incubated with the secondary antibody conjugated to Peroxidase-anti rabbit (711-035-152, Dianova, Germany; 1:50 in Antibody Diluent Reagent). Negative controls included sections incubated with secondary antibodies only, omitting primary antibody. After washing, slides were stained with Liquid DAB+ Substrate as described in the company protocol (K3467, Dako Cytomation, USA). Nuclei were stained with Haematoxylin. Micrographs were taken with a microscope (Zeiss Axiostar plus) and analyzed using Adobe Photoshop software.

### 2.5. Statistical methods

Values are calculated as % of controls and given as mean±SEM. For biochemical parameters, normalized gene expression or protein ratios were compared to the mean ratio of the respective control group which was set as 100%. Mean values were compared by the two-sided Student's *t*-test. Statistics were calculated with the Excel, Sigma Plot and SPSS software. A $p$-value $<0.05$ was considered to be statistically significant.

## 3. Results

Seventeen consecutive patients with chronic AS, undergoing elective aortic valve replacement were included in the study. The average age of patients was 71 years; 76% were male, 76% were hypertensive and 47% diabetic; prescribed drugs were diuretics (76%), ACE-inhibitors (41%), digitalis (24%) and β-blockers (41%). Left ventricular function was impaired (LVEF 46.0±18.2%; FS 27.0±11.0%) and the left

Table 2
Analysis of melusin protein content (melusin/GAPDH ratios) in 4 different regions of 4 normal donor hearts

| Sex | LVAW | LVLW | LVIW | Septum |
|---|---|---|---|---|
| ♂ | 8.1 | 9.6 | 9.7 | 12.7 |
| ♂ | 9.9 | 13.1 | 8.3 | 11.8 |
| ♀ | 6.3 | 6.6 | 7.0 | 7.5 |
| ♀ | 7.4 | 7.7 | 8.8 | 11.0 |
| Mean | 7.9 | 9.2 | 8.4 | 10.8 |
| SEM | 0.7 | 1.4 | 0.6 | 1.2 |

LVAW: Left ventricular anterior wall, LVLW: left ventricular free lateral wall, LVIW: left ventricular inferior wall.

Please cite this article as: Brokat S et al. Altered melusin expression in the hearts of aortic stenosis patients. Eur J Heart Fail (2007), doi:10.1016/j.ejheart.2007.02.009

ventricle was dilated (LVEDD 54.1±8.8 mm; LVESD 40.9± 11.7 mm); only 3 patients had normal LVEF and normal LVESD (Table 1).

Immunohistochemical staining of melusin was done to visualize expression changes due to cardiac hypertrophy. Melusin was found in the myocytes (Fig. 1a). Staining in the normal hearts was clearly visible (Fig. 1a; neg. control: Fig. 1c). In contrast, in the AS hearts, melusin staining was significantly weaker (Fig. 1b) and almost comparable to the negative control (Fig. 1d).

To assess the regional distribution of melusin in the heart, we analyzed melusin content in 4 different regions (septum, anterior, free lateral and inferior wall) of 4 normal donor hearts. Analysis revealed that melusin expression was homogenous in these different areas of the left ventricle (Table 2).

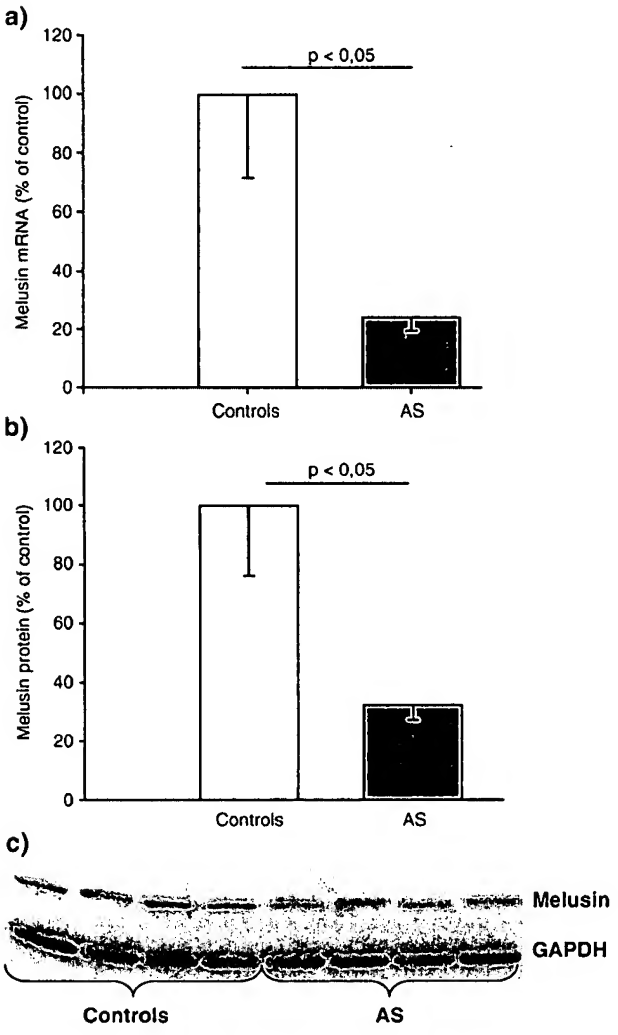


Fig. 2. Regulation of melusin a) mRNA and b) protein in human AS compared to controls. Controls were set as 100% and AS values were related to the mean value of controls. Data are presented as mean value±SEM. Controls are shown in white bars, AS in gray bars. c) Typical immunoblots showing melusin and GAPDH in patients with AS and controls.

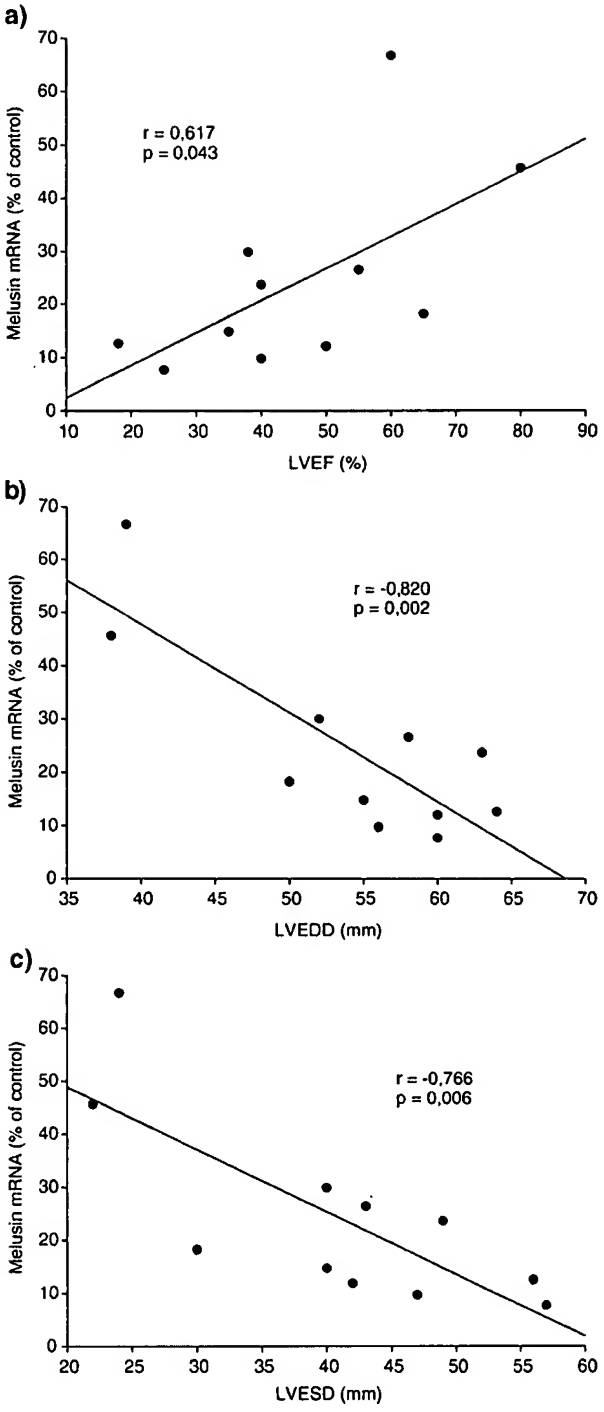


Fig. 3. Melusin was significantly correlated with parameters of LV function in human AS; positively correlated with a) LVEF ($r$=0.64, $p$=0.048) and inversely with b) LVEDD ($r$=−0.82; $p$=0.002) and c) LVESD ($r$=−0.77, $p$=0.006).

In order to quantify the changes observed by immunohistochemistry, melusin expression in the control and AS hearts was evaluated both at the mRNA and protein level. Interestingly, melusin was significantly downregulated ($p$<0.05) in our group of patients with AS. Melusin mRNA in AS

Please cite this article as: Brokat S et al. Altered melusin expression in the hearts of aortic stenosis patients. Eur J Heart Fail (2007), doi:10.1016/j.ejheart.2007.02.009

patients went down to 24.3±4.9% of control values (Fig. 2a). Concordantly, melusin protein was decreased to 32.5±5.2% of control (Fig. 2b, c). Melusin expression was positively correlated with LVEF and inversely correlated with ventricular size, i.e. LVEDD and LVESD ($p<0.05$; Fig. 3a–c).

AKT phosphorylation is located downstream from melusin. AKT phosphorylation was significantly decreased in human AS (71.2±5.2%, $p<0.001$; Fig. 4a, b) whereas AKT protein content remained unchanged (103% of control; data not shown). pAKT content was positively correlated ($r=0.61$; $p=0.022$) with melusin protein; i.e. a loss of melusin was accompanied by a parallel loss of AKT phosphorylation (Fig. 4c).

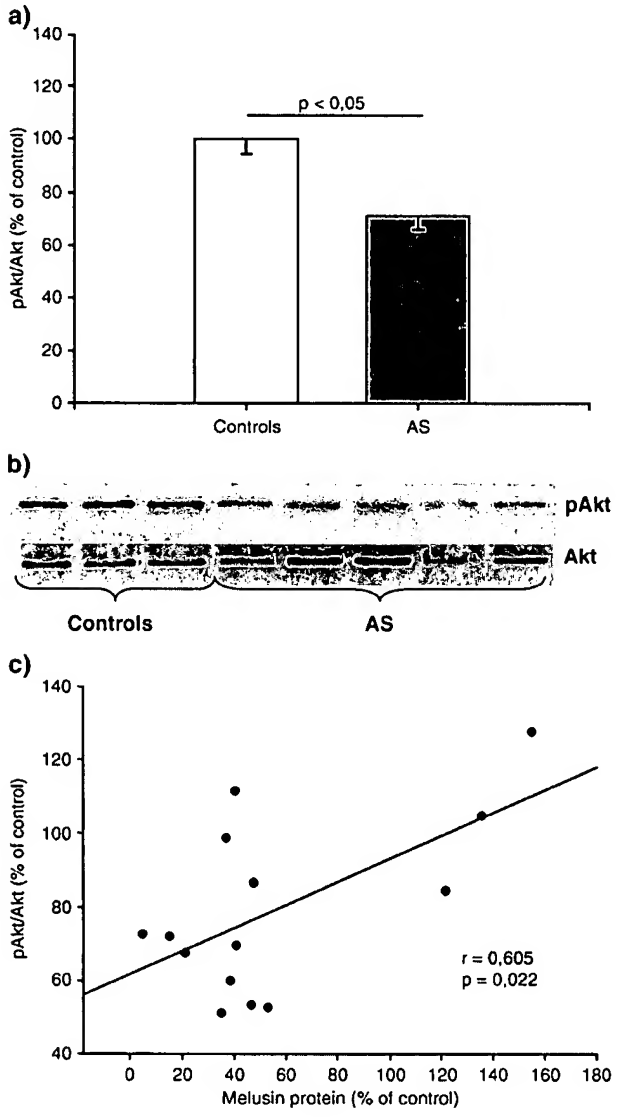


Fig. 4. a) pAKT/AKT ratios in human AS compared to controls. Controls were set as 100% and AS values were related to the mean value of controls. Data are presented as mean value±SEM. Controls are shown in white bars, AS in gray bars. b) Typical immunoblots showing pAKT and AKT in patients with AS and controls. c) Melusin protein content was significantly correlated with AKT phosphorylation ($r=0.61$, $p=0.022$).

## 4. Discussion

Rodent models suggest a major role for melusin in the preservation of cardiac function in response to biomechanical stress [3]. We describe for the first time a decrease in melusin in patients with AS, which parallels the impairment of systolic function and the increase in left ventricular size, as well as the decrease in AKT phosphorylation in human hearts.

Melusin expression was evaluated both at transcript and protein levels in samples of human hearts from control healthy individuals and from patients with aortic stenosis showing different degrees of left ventricular remodelling. Our results clearly show that in dilated hypertrophic hearts, melusin levels are lower than in healthy hearts both at the mRNA and protein level. Moreover, immunohistochemical staining showed that melusin reduction occurred in the cardiomyocytes, thus excluding the possibility that the low melusin levels in the biochemical assays was due to the increased proportion of stromal tissue. Immunohistochemical staining also indicated that melusin expression was homogenous in different regions of the control hearts. Thus, the lower melusin expression in the area beneath the septum of AS hearts, from where the biopsies were taken, probably reflects changes in the whole heart. Interestingly, when melusin levels were compared to both structural and functional parameters of the AS hearts, an inverse correlation was found between the degree of dilation of the left ventricle (both diastolic and systolic diameters) and the melusin level, with low melusin in highly dilated hearts. A direct correlation between melusin and functional parameters such as ejection fraction was also observed. These data indicate that in human AS, decreased melusin levels are associated with a greater degree of structural and functional deterioration of the heart.

This finding is consistent with the phenotype of mice in which melusin expression has either been abrogated by gene inactivation [3] or strongly increased by transgenesis [6]. In these models, lack of melusin dramatically accelerates the evolution to LV dilation and failure in conditions of pressure overload; while sustained melusin expression maintains compensatory hypertrophy and full contractility even in conditions of pressure overload which cause dilation and failure in wild type mice [3]. Based on these findings, we speculate that decreased melusin expression in humans is predictive of a worse functional state and strategies aimed at maintaining high melusin levels could be of important therapeutic value.

In line with this hypothesis, we found that melusin expression correlated with AKT phosphorylation in human AS hearts. This is in agreement with previous data showing a link between melusin expression and AKT phosphorylation in mice [3] and shows that melusin can control downstream signalling pathways in the human heart known to be involved in positive left ventricular remodelling [12].

In a previous study, increased collagen content together with decreased MMP expression was found in a group of

Please cite this article as: Brokat S et al. Altered melusin expression in the hearts of aortic stenosis patients. Eur J Heart Fail (2007), doi:10.1016/j.ejheart.2007.02.009

patients with AS [9]. These changes in collagen and MMP content occurred in the early stages of the disease. Since our patient cohort was similar to this previous study group, we compared melusin and MMP expression in a subset of 12 patients from our study. We found that melusin positively correlated with MMP1 ($r=0.75$, $p=0.005$) and MMP9 ($r=0.62$, $p=0.043$) in these 12 hearts. Parallel down-regulation of melusin and MMPs in human AS may reflect a common involvement in integrin signalling and regulation by mechanical load. In addition, it may reflect a relationship between melusin regulation, impairment of systolic function and increase in fibrosis in pressure overload in the human heart.

## 5. Limitations

A persistent limitation in studies using human heart samples is the limited availability of tissue samples. Only small intra-operative samples can be obtained in human AS and the number of unused donor hearts is limited. Thus, we were not able to study the effects of age and sex and medical therapy in a detailed manner. However, based on the analyses which were possible, comparing patients with and without a given therapy, we did not observe an effect of medical therapy on melusin gene expression.

## 6. Conclusion

Reduction in melusin expression parallels the functional impairment in human hearts with AS. Reduced melusin levels are accompanied by decreased AKT phosphorylation, suggesting a connection between the loss of melusin and the impaired systolic function. These results, together with published data in genetically modified mouse models with altered melusin expression, suggest that reversing the loss of melusin may be beneficial in human AS.

## Acknowledgements

This work has been supported by EU FP6 grant LSHM-CT-2005-018833, EUGeneHeart and by the DFG, Graduate course 754 on myocardial hypertrophy. This work was also supported with grants to GT from the Italian Ministry of University and Research (FIRB 2001 and PRIN 2003) as well as from Telethon.

## References

[1] Oakley D. General cardiology: the athlete's heart. Heart Dec 2001;86(6):722–6.
[2] Selvetella G, Hirsch E, Notte A, et al. Adaptive and maladaptive hypertrophic pathways: points of convergence and divergence. Cardiovasc Res Aug 15 2004;63(3):373–80.
[3] Brancaccio M, Fratta L, Notte A, et al. Melusin, a muscle-specific integrin beta1-interacting protein, is required to prevent cardiac failure in response to chronic pressure overload. Nat Med Jan 2003;9(1):68–75.
[4] Brancaccio M, Guazzone S, Menini N, et al. Melusin is a new muscle-specific interactor for beta(1) integrin cytoplasmic domain. J Biol Chem Oct 8 1999;274(41):29282–8.
[5] Brancaccio M, Hirsch E, Notte A, et al. Integrin signalling: the tug-of-war in heart hypertrophy. Cardiovasc Res Jun 1 2006;70(3):422–33.
[6] De Acetis M, Notte A, Accornero F, et al. Cardiac overexpression of melusin protects from dilated cardiomyopathy due to long-standing pressure overload. Circ Res May 27 2005;96(10):1087–94.
[7] Antos CL, McKinsey TA, Frey N, et al. Activated glycogen synthase-3 beta suppresses cardiac hypertrophy in vivo. Proc Natl Acad Sci U S A Jan 22 2002;99(2):907–12.
[8] Hardt SE, Sadoshima J. Glycogen synthase kinase-3beta: a novel regulator of cardiac hypertrophy and development. Circ Res May 31 2002;90(10):1055–63.
[9] Fielitz J, Leuschner M, Zurbrugg HR, et al. Regulation of matrix metalloproteinases and their inhibitors in the left ventricular myocardium of patients with aortic stenosis. J Mol Med Dec 2004;82(12):809–20.
[10] Nordmeyer J, Eder S, Mahmoodzadeh S, et al. Upregulation of myocardial estrogen receptors in human aortic stenosis. Circulation Nov 16 2004;110(20):3270–5.
[11] Martinka P, Fielitz J, Patzak A, et al. Mechanisms of blood pressure variability-induced cardiac hypertrophy and dysfunction in mice with impaired baroreflex. Am J Physiol Regul Integr Comp Physiol Mar 2005;288(3):R767–76.
[12] Matsui T, Li L, Wu JC, et al. Phenotypic spectrum caused by transgenic overexpression of activated Akt in the heart. J Biol Chem Jun 21 2002;277(25):22896–901.
[13] Braunwald E. Heart disease, a textbook of cardiovascular medicine. 5th ed. W B Saunders Company; 2001.

Please cite this article as: Brokat S et al. Altered melusin expression in the hearts of aortic stenosis patients. Eur J Heart Fail (2007), doi:10.1016/j.ejheart.2007.02.009

RESEARCH ARTICLE

# Cloned rabbits produced by nuclear transfer from adult somatic cells

Patrick Chesné[1], Pierre G. Adenot[1], Céline Viglietta[1], Michel Baratte[2], Laurent Boulanger[1], and Jean-Paul Renard[1]*

We have developed a method to produce live somatic clones in the rabbit, one of the mammalian species considered up to now as difficult to clone. To do so, we have modified current cloning protocols proven successful in other species by taking into account both the rapid kinetics of the cell cycle of rabbit embryos and the narrow window of time for their implantation after transfer into foster recipients. Although our method still has a low level of efficiency, it has produced several clones now proven to be fertile. Our work indicates that cloning can probably be carried out successfully in any mammalian species by taking into account physiological features of their oocytes and embryos. Our results will contribute to extending the use of rabbit models for biomedical research.



The rabbit is gaining attention in biotechnology because it offers several advantages over other laboratory animals for the study of several human physiological disorders[1,2]. Not only can physiological manipulations in this species be more easily carried out than in mice because of its larger size, but it is also phylogenetically closer to primates than are rodents[3]. Currently, the use of rabbits is limited to large-scale production of foreign proteins[4]. Thus cloning, associated with the genetic modifications of donor cells, would greatly enhance the possible use of this species in biotechnology. In contrast to several other mammalian species, however, the rabbit has not been very amenable to somatic cloning[5,6], despite its pioneer role in defining nuclear transfer (NT) methods in mammals[7]. Here we describe a method that has allowed us to produce several healthy and fertile somatic clones of rabbit at about the same frequency as other mammalian species. Our results will contribute to extending the use of rabbit models for biotechnological applications.

## Results and discussion

Rabbit NT embryos were reconstructed by electrofusion of freshly collected cumulus cells with recipient enucleated metaphase II (MII) ooplasm. We chose this type of nuclear donor cells because they had been initially used as models to demonstrate the feasibility of somatic cloning[8,9]. Confocal observations of reconstructed embryos, fixed 1 h after electrofusion, showed that donor nuclei exposed to MII ooplasm had condensed into chromosomes[10] (Fig. 1A). Instead of orderly chromosome arrays typical of MII oocytes, we observed misaligned metaphase plates, very similar to those previously shown in the mouse to be compatible with full-term development[8]. We therefore activated NT embryos through a second set of electrostimulation and incubated them in the presence of cycloheximide (CHX; a protein synthesis inhibitor) and 6-dimethylaminopurine (6-DMAP; a kinase inhibitor), two drugs known to facilitate the exit from artificially activated MII stage, but with potential detrimental side effects on the cell cycle[11,12]. Because the rabbit zygote enters S phase very early after activation[13], we focused on reducing the time of exposure to these inhibitors. We observed that they accelerated pronuclear formation in artificially activated rabbit oocytes, but also caused high rates of parthenogenetic development to the blastocyst stage (90%, $n = 130$), even when the time of incubation was reduced to 1 h. Upon removal of the inhibitors, 72% ($n = 25$) of NT embryos exhibited interphasic structures (Fig. 1B), and 1 h later all were in interphase (Fig. 1C). When left in culture, 47% ($n = 135$) developed into blastocysts at day 3 (D3). Their growth as determined from cell number counts at D3 and D4 was slower than that of blastocysts derived from *in vivo* or *in vitro* zygotes. At D4, the number of cells in NT blastocysts was similar to that of *in vivo* or *in vitro* zygotes at D3 (Fig. 2A).

In rabbits, a rapid and significant expansion of blastocysts occurs *in vivo* and stretches the surrounding walls of the uterus so that their individual positions on the uterine horns become easily recognizable as "implantation sites" as early as D6 (ref. 14). Implantation, however, starts only at D7.5, with the progressive dissolution of blastocyst coverings apposed during the transit of the embryo through the female genital tract, thereby contributing to the narrow window of implantation in this species. Upon dissection of the uterine horns at D8, we found that NT embryos could form some implantation sites (7 out of the 91 embryos transferred, 7.7%) following their transfer into synchronous recipients mated with a vasectomized male at the same time as donor females were mated. However, no embryonic structures were seen. Transfer into asynchronous recipients mated 16 h after the donor females were mated resulted in an increase in the implantation rate, which became only slightly lower than controls (12/59 or 20.3%, and 15/54 or 27.8%, respectively). Under these conditions we could recover embryos at the advanced blastocyst stage (see photo in Fig. 2B), but still surrounded by thin coverings of extracellular material, and thus, equivalent to D7 normal embryos[14]. None of the recipients transplanted either synchronously or asynchronously (–16 h) could be diagnosed pregnant at midgestation (Table 1), even when co-transferred with unmanipu-

[1]*Unité de Biologie du Développement et Biotechnologie, Institut National de la Recherche Agronomique, F-78352 Jouy-en-Josas, France.* [2]*Unité Commune d'Expérimentation Animale, Institut National de la Recherche Agronomique, F-78352 Jouy-en-Josas, France.* **Corresponding author: (renard@jouy.inra.fr).*

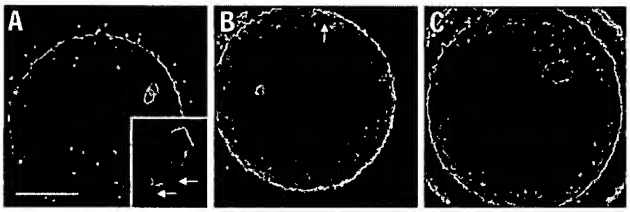


**Figure 1.** Confocal images of unicellular NT embryos immunolabeled with the anti-α-tubulin antibody (green) and DNA stained with propidium iodide (red). (A) Before the second set of electrostimulation, a misaligned metaphase plate was associated with the spindle, and sometimes individual chromosomes (arrows in the insert) were localized near the spindle poles (insert: 3-fold magnified view of the spindle region). (B) Upon removal of CHX and 6-DMAP, 72% of NT embryos ($n$ = 25) showed a small nucleus and an interphasic microtubular network (arrow). (C) One hour after removal of the drugs, all NT embryos were in interphase and 71% ($n$ = 17) exhibited a single and large pronucleus-like nucleus like those observed in normal rabbit zygotes (not shown). Bar, 50 μm.

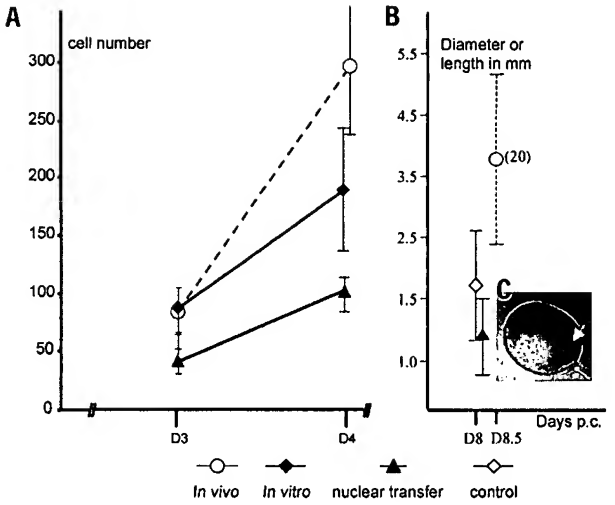


**Figure 2.** Development of rabbit blastocysts reconstructed with cumulus cells or derived from *in vivo*–fertilized embryos. (A) *In vitro* increase in cell number (mean ± s.e.) between D3 and D4 of embryos either recovered directly from donors (*in vivo*, $n$ = 27), or cultured from the one-cell stage (~20 h post-hCG) after either natural mating (*in vitro*, $n$ = 44) or nuclear transfer (NT, $n$ = 31). (B) Mean diameters or lengths (in mm ; ± s.e.) of the embryonic disks of D8 blastocysts recovered directly from donors (*in vivo*)[20], following transfer into recipients at the one-cell stage after natural mating (control, $n$ = 9), or resulting from NT ($n$ = 7). (C) Example of a retarded NT blastocyst recovered at D8 after transfer at the four-cell stage into a –16 h asynchronous recipient; embryonic disk (large arrow) is visible but the blastocyst is still surrounded by a thin layer of embryo covering (small arrow) that should normally have disappeared at D7 (ref. 14).

lated "helper" embryos of another strain (Fauve-de-Bourgogne), or transferred with an excess of NT embryos (up to 39 per female; data not shown). These observations suggested that only very few NT blastocysts could implant because their development was too delayed. In one case, we could observe a D8 NT blastocyst already adhering to the uterine epithelium and very similar in size to normal implantation controls. We therefore extended the asynchrony between donor and recipient females from 16 to 22 h. Such a marked asynchrony at early cleavage stages of development had not been attempted previously with NT embryos, but can be compatible with full-term development of fertilized eggs[15,16]. Under these conditions, 10 out of 27 (37%) of the –22 h asynchronized recipients were diagnosed pregnant after palpation at D14. Four of these gave birth at D31 to six live kits (Fig. 3) weighing 30–90 g (mean value, 65 g). Such variability is also observed with kits born from reduced litter sizes (one to four fetuses) occasionally obtained in our facilities. Expression of a green fluorescent protein (GFP) transgenic marker from hair follicles (Fig. 3) and from lymphocytes (not shown) confirmed that kits resulted from NT of cumulus cells. Two kits of normal morphological appearance (respective weights 90 and 30 g) died one day after birth, for one of whom we suspect failure in the adoptive process from the lactating mother. The four others are developing normally, and two of them (Fig. 3, B1), when tested for fertility by natural mating, gave birth to seven and eight healthy kits, respectively.

In conclusion, our results show that the former limitations to successful rabbit somatic cloning have been overcome by taking into account species differences in oocyte physiology and early embryonic development. Both a shortened timing for otherwise classical activation procedures and the transfer of reconstructed embryos into recipients retarded by nearly one day had a decisive influence on the *in vivo* development of NT embryos. The maximization of the developmental response of rabbit oocytes to external activating stimuli, through controlled $Ca^{2+}$ stimulation regimes[17] and characterization of the embryonic signals that regulate rabbit uterine epithelial responsiveness at implantation[18], should help to improve term survival rates of embryos reconstructed with different types of somatic and cultured cells.

**Table 1. *In vivo* development of rabbit somatic nuclear transfer embryos**

| Type of recipients | Synchronous | Asynchronous (–16 h) | Asynchronous (–22 h) |
|---|---|---|---|
| Stage of embryos | 1-cell | 1-cell | 4-cell |
| No. of reconstructed embryos | 554 | 523 | 775 |
| [No. of replicates] | [19] | [18] | [27] |
| No. of fused embryos | 427 | 346 | 612 |
| [% from reconstructed] | [77.1] | [66.2] | [79.0] |
| Total transferred | 367 | 346 | 371 |
| [% from fused] | [100.0] | [100.0] | [60.6] |
| No. of recipients transferred | 19 | 18 | 27 |
| No. of recipients pregnant at day 14 | 0 | 0 | 10 |
| [% from transferred] | | | [37.0] |
| No. of recipients delivering | 0 | 0 | 4[a] |
| [% from transferred] | | | [14.8] |
| No. of kits born | | | 6 |
| [% from embryos transferred] | | | [1.6] |
| Alive at weaning | | | 4 |
| Mean weight of kits at birth (g) | | | 65 ± 20[b] |

[a]Abortions between day 15 and day 29 of pregnancy (13 cotyledons and degenerated fetuses recovered).
[b]Mean weight of kits at birth in our facilities: 55.8 ± 17.0 g (sample size, $n$ = 51).

## Experimental protocol

**Source of oocytes and cumulus cells.** MII oocytes were collected from superovulated does of New-Zealand breed 16 h after human chorionic gonadotrophin (hCG) injection and mating to a vasectomized male. They were incubated in 0.5% hyaluronidase (catalog no. H3506; Sigma, St. Louis, MO) for 15 min to remove cumulus cells by gentle pipetting. For nuclear transfer, oocytes were enucleated as described[19]. All manipulations were done in M199 (Life Technologies, Rockville, MD), 20 mM HEPES (Sigma), supplemented with 10% vol/vol FCS (Life Technologies).

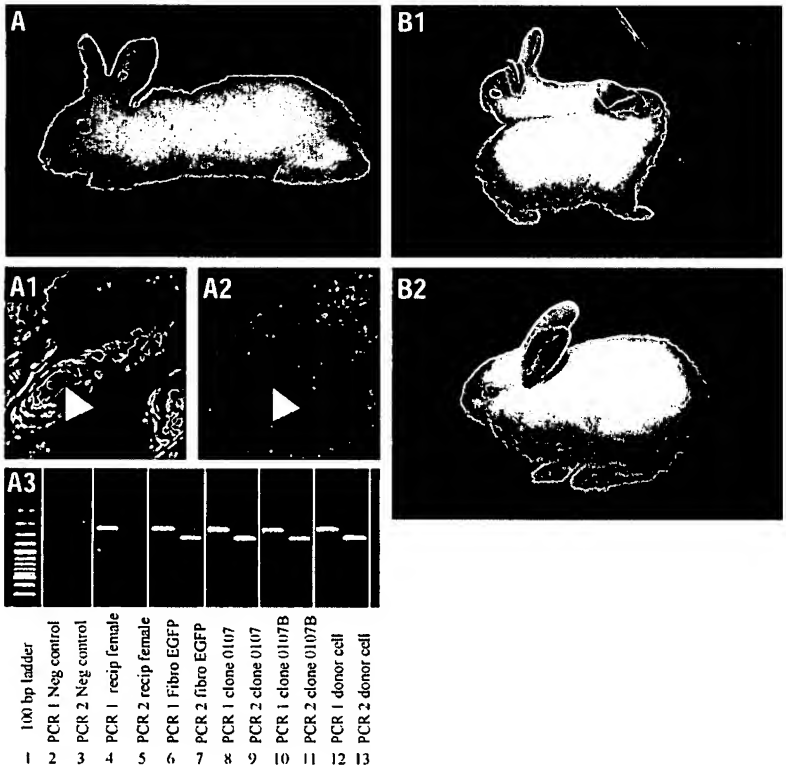


**Figure 3.** Rabbits born from somatic nuclear transfer. (A) Cloned rabbit 0107 with corresponding controls: (A1) expression of the EGFP protein fluorescence (arrowhead) detected by confocal microscopy from hair follicles obtained from an ear biopsy at 1 month of age; (A2) the same under transmission light; (A3) amplifications of the *EGFP* transgene (PCR 2) and of the exon 10 of the *CFTR* gene used as DNA quality control (PCR 1) with expected fragment sizes of 240 bp for the *CFTR* gene and 350 bp for the *EGFP* transgene. This confirms that rabbit 0107 and its littermate 107b (who died 1 day after birth) were derived from the donor cumulus cell. (B1, B2) Three other rabbits from two different litters; rabbits in B1 have now proved to be fertile.

Contemporary cumulus cells were obtained from the New Zealand breed or F1 New Zealand × Fauve-de-Bourgogne or F1 transgenic New Zealand females harboring a DNA construct with the coding sequence of the enhanced green fluorescent protein (EGFP) placed under the control of an elongation factor 1 (EF1) promoter. EGFP fluorescence and PCR amplification were used as markers of donor cumulus cells. These were kept at 38°C in $Ca^{2+}$,$Mg^{2+}$-free PBS supplemented with 1% polyvinylpyrrolidone (PVP) 40,000 (Sigma) before being used as a source of nuclei.

Oocyte activation and nuclear transfer. To reconstruct NT embryos, individual cumulus cells were inserted by micromanipulation under the zona pellucida of the enucleated oocytes. NT embryos and MII oocytes were activated 18–20 h post-hCG as follows. Two sets of electrical stimulation were applied 1 h apart with a BTX stimulator (Biotechnologies & Experimental Research Inc., San Diego, CA) (3 DC pulses of 3.2 kV/cm for 20 µs each in mannitol 0.3 M in water containing 0.1 mM $CaCl_2$ and 0.1 mM $MgCl_2$). The first set induced the cumulus cell–oocyte fusion. Reconstructed em-bryos and oocytes were then incubated for 1 h in M199 at 38°C. Then, the second set of pulses was applied to induce activation. NT embryos and oocytes were incubated for 1 h at 38°C in M199 containing 5 µg/ml CHX (Sigma) and 2 mM 6-DMAP (Sigma), then ret-urned to culture in a 50 µl microdrop of B2 medium (Laboratoire CCD, Paris, France) supplemented with 2.5% FCS under mineral oil (catalog no. M8410; Sigma) at 38°C under 5% $CO_2$ in air.

Analysis of preimplantation stages. Microtubule organization and chromatin in one-cell NT embryos were observed as already described[19], except that fixation lasted 20 min at 37°C and the mounting medium was Vectashield (Vector Laboratories, Burlingame, CA). Development rates until blastocyst stage were assessed after *in vitro* culture for 3 and 4 days. For cell number evaluation, embryos were fixed as above, stained with Hoechst 33342 at a concentration of 1 µg/ml, then mounted on well slides in Vectashield and monitored under epifluorescence.

Analysis of peri-implantation stages and *in vivo* development. Recipient females were mated to vasectomized males either at the same time (synchronous recipients), or 16 h or 22 h after the oocyte donors (asynchronous recipients). NT embryos were transplanted surgically through the infundibulum into each oviduct of recipients either at the one-cell stage (1–3 h post-activation) or at the four-cell stage (after an overnight culture). Implantation rate was assessed after killing of recipients at day 8 (D8). When visible, embryonic disks of blastocysts were measured microscopically (160×). Pregnancy was determined by palpation 13 or 14 days after embryo transplantation and the pregnant recipients delivered by caesarian section at 31 days post mating.

PCR analysis. The presence of the GFP transgenic marker was detected by PCR using a sense (5′-GAGTTTG-GATCTTGGTTCAT-3′) and an antisense (5′-GGCACGGGCAGCTTGCCGGTGG-3′) primer (Genset, Paris, France). To control the DNA quality, PCR was performed on 300–400 ng of DNA prepared with tissue extraction kit (Qiagen, Valencia, CA) with the sense primer, 5′-TTTTCCTGGATCATGCCTGGCAC-3′, and the antisense primer, 5′-CTACCTGTAGCAGCTTACCCA-3′, covering the exon 10 of the rabbit *CFTR* gene (Genset). Negative controls were double-distilled water and recipient female DNA, while positive controls were DNA from transgenic cultured fibroblasts.

*Acknowledgments*

*We thank C. Thibault for his constant support to our work, C. Viebahn for stimulating discussions, the staff from our rabbit facility for their critical role in the care of recipients and cloned kits, C. Poirier for assistance in embryo transfer, E. Campion for the recovery and fixation of D8 embryos, and C. Young and B. Nicolas for help during the preparation of the manuscript. This work was supported by a grant from the Association Française de Lutte contre la Mucoviscidose (AFLM).*

*Competing interests statement*

*The authors declare that they have no competing financial interests.*

Received 18 October 2001; accepted 23 January 2002

1. Hoeg, J.M. *et al.* Overexpression of lecithin: cholesterol acyltransferase in transgenic rabbits prevents diet-induced atherosclerosis. *Proc. Natl. Acad. Sci. USA* **93**, 11448–11453 (1996).
2. Chen, J.M. *et al.* A combined analysis of the cystic fibrosis transmembrane conductance regulator: implications for structure and disease models. *Mol. Biol. Evol.* **18**, 1771–1788 (2001).
3. Graur, D., Duret, L. & Gouy, M. Phylogenetic position of the order Lagomorpha (rabbits, hares and allies). *Nature* **379**, 333–335 (1996).
4. Stinnackre, M.G., Massoud, M., Viglietta, C. & Houdebine, L.M. The preparation of recombinant proteins from mouse and rabbit milk for biomedical and pharmaceutical studies. In *Trangenic animals, generation and use;* (ed. Houdebine, L.M.) 461–463 (Harwood Academic Publishers, Amsterdam 1997).
5. Yin, X.J., Tani, T., Kato, Y. & Tsunoda, Y. Development of rabbit parthenogenetic oocytes and nuclear-transferred oocytes receiving cultured cumulus cells. *Theriogenology* **54**, 1460–1476 (2000).
6. Dinnyés, A. *et al.* Development of cloned embryos from adult rabbit fibroblasts: effect of activation treatment and donor cell preparation. *Biol. Reprod.* **64**, 257–263 (2001).

7. Bromhall, J.D. Nuclear transplantation in the rabbit egg. *Nature* **258**, 719–722 (1975).
8. Wakayama, T., Perry, A.C., Zuccotti, M., Johnson, K.R. & Yanagimachi, R. Full-term development of mice from enucleated oocytes injected with cumulus cell nuclei. *Nature* **394**, 369–374 (1998).
9. Wells, D.N., Misica, P.M. & Tervit, H.R. Production of cloned calves following nuclear transfer with cultured adult mural granulosa cells. *Biol. Reprod.* **60**, 996–1005 (1999).
10. Campbell, K.H.S., Loi, P., Otaegui, P.J. & Wilmut, I. Cell cycle co-ordination in embryo cloning by nuclear transfer. *Rev. Reprod.* **1**, 40–46 (1996).
11. Soloy, E. *et al.* Time course of pronuclear deoxyribonucleic acid synthesis in parthenogenetically activated bovine oocytes. *Biol. Reprod.* **57**, 27–35 (1997).
12. Meyer, L. & Kim, S.H. Chemical inhibitors of cyclin-dependent kinases. *Methods Enzymol.* **283**, 113–128 (1997).
13. Szöllösi, D. Time and duration of DNA synthesis in rabbit eggs after sperm penetration. *Anat. Rec.* **154**, 209–212 (1966).
14. Denker, H.W. Implantation: the role of proteinases and blockage of implantation by proteinase inhibitors. *Adv. Anat. Embryol. Cell Biol.* **53**, 1–123 (1981).
15. Heape, W. Preliminary note on the transplantation and growth of mammalian ova within a uterine foster-mother. *Proc. R. Soc. Lond. A/B* **48**, 457–458 (1890).
16. Chang, M.C. Development and fate of transferred rabbit ova or blastocysts in relation to the ovulation time of recipients. *J. Exp. Zool.* **114**, 197–226 (1950).
17. Ozil, J.P. & Huneau, D. Activation of rabbit oocytes: the impact of the $Ca^{2+}$ signal regime on development. *Development* **128**, 917–928 (2001).
18. Hoffman, L.H., Olson G.E., Carson, D.D. & Chilton, B.S. Progesterone and implanting blastocysts regulate MUC1 expression in rabbit uterine epithelium. *Endocrinology* **139**, 266–271 (1998).
19. Adenot, P.G., Szöllösi, M.S., Chesné, P., Chastant, S. & Renard, J.P. *In vivo* aging of oocytes influences the behavior of nuclei transferred to enucleated rabbit oocytes. *Mol. Reprod. Dev.* **46**, 325–336 (1997).
20. Gottschewski, G.H.M. & Zimmermann, W. *Die Embryonalentwicklung des Hauskaninchens. Normogenese und Teratogenese.* Ch. 3.3,103–117 (M. & H. Schaper, Hannover; 1973).

# Targeted disruption of the α1,3-galactosyltransferase gene in cloned pigs

Yifan Dai[1]*, Todd D. Vaught[1], Jeremy Boone[1], Shu-Hung Chen[1], Carol J. Phelps[1], Suyapa Ball[1], Jeff A. Monahan[1], Peter M. Jobst[1], Kenneth J. McCreath[2], Ashley E. Lamborn[1], Jamie L. Cowell-Lucero[1], Kevin D. Wells[1], Alan Colman[2], Irina A. Polejaeva[1], and David L. Ayares[1]

Galactose-α1,3-galactose (α1,3Gal) is the major xenoantigen causing hyperacute rejection in pig-to-human xenotransplantation. Disruption of the gene encoding pig α1,3-galactosyltransferase (α1,3GT) by homologous recombination is a means to completely remove the α1,3Gal epitopes from xenografts. Here we report the disruption of one allele of the pig α1,3GT gene in both male and female porcine primary fetal fibroblasts. Targeting was confirmed in 17 colonies by Southern blot analysis, and 7 of them were used for nuclear transfer. Using cells from one colony, we produced six cloned female piglets, of which five were of normal weight and apparently healthy. Southern blot analysis confirmed that these five piglets contain one disrupted pig α1,3GT allele.



Galactose-α1,3-galactose (α1,3Gal) epitopes are a common carbohydrate structure on the cell surface of almost all mammals with the exception of humans, apes, and Old World monkeys[1]. Synthesis of the α1,3Gal epitope is catalyzed by the enzyme α(1,3)galactosyltransferase (α1,3GT)[2]. Humans do not have a functional copy of the α1,3GT gene, and hence do not show α1,3Gal surface expression. The presence of the α1,3Gal antigen on the surface of pig cells and tissues is the major cause of hyperacute rejection (HAR) in pig-to-human xenotransplantation[2-4]. It has been reported that, in humans, up to 1% of the total circulating IgG is anti-α1,3Gal natural antibody[5]. A number of strategies have been used to reduce or eliminate α1,3Gal-induced HAR. These methods[2-4] include overexpression of α2,3-sialyltransferase or α1,2-fucosyltransferase in pig cells to compete with α1,3GT; treatment of pig organs with α-galactosidase to remove surface α1,3Gal epitopes; expression of complement inhibitor genes, such as human decay-accelerating factor (DAF), in transgenic pig organs to suppress the complement reaction; and temporary depletion of natural anti-α1,3Gal antibody from recipients before transplantation. All these methods only partially or temporarily remove the α1,3Gal from the surface of the xenografts, however, and the residual α1,3Gal molecules are still sufficient to activate the complement cascade and cause destruction of the grafts[2-4]. Complete elimination of α1,3Gal epitopes from the donor organs should be achievable by removal of the α1,3GT gene. α1,3GT knockout mice have been made by a number of groups[6-7]. When tissues from these mice are exposed to human serum, they bind substantially less human anti-Gal xenoantibody than do tissues from normal mice, resulting in a significant decrease in human complement activation[6].

The cloning of sheep[8], goat[9], cattle[10], and pigs[11] by somatic cell nuclear transfer provides an alternative means of disrupting or deleting genes in mammals other than mice. The production of cloned sheep with targeted insertions at the ovine α1(I)-procollagen (*COL1A1*) locus showed that viable animals can be produced via nuclear transfer with gene-targeted cultured fibroblasts[12]. The α1,3GT gene has recently been successfully deleted in sheep fibroblasts and in fetuses cloned from targeted cells[13]. Although no viable animals resulted, these experiments showed that it is feasible to disrupt the α1,3GT gene using nuclear transfer techniques in livestock. Lai *et al.* have recently described the disruption of one allele of the α1,3GT gene in pig fibroblasts and in four live piglets cloned from these cells[14]. However, the only evidence of gene targeting offered in this report was PCR analysis of recombination junctions. Here we present genomic Southern blot analyses showing successful disruption of one copy of the α1,3GT gene in cultured male and female porcine fetal fibroblasts. To date we have produced five apparently healthy α1,3GT knockout female piglets by nuclear transfer.

## Results and discussion

Because the α1,3GT gene is expressed well in porcine fetal fibroblasts (PPL Therapeutics, unpublished data), it is possible to enrich for homologous recombination events using a promoter-trap knockout-vector strategy[12]. Two similar knockout vectors, pPL654 and pPL657, were constructed from isogenic DNA of SLA1-10 and PCFF4-2 cells, respectively, by inserting an *IRES-neo*-poly A cassette into the 5′ end of exon 9 (Fig. 1A). Because the majority of the coding region of the pig α1,3GT gene, including the sequences encoding the catalytic domain, is located in exon 9, successful targeting using these vectors is expected to result in functional inactivation of the gene[6-7].

Four different early-passage (P2 or P3) primary porcine fetal fibroblasts cell lines were used for transfection: the male cell lines SLA1-10, PCFF4-2, and PCFF4-3 and the female cell line PCFF4-6. SLA1-10 cells were transfected with the isogenic vector pPL654, and PCFF4-2 cells were transfected with the isogenic vector pPL657. The PCFF4-3 and PCFF4-6 cell lines were derived from sibling fetuses of the fetus used to derive PCFF4-2, and therefore were transfected with the pPL657 vector. G418-resistant colonies were screened by 3′ PCR with neo442S (a sequence from the 3′ end of *neo*) and αGTE9A2 (a sequence from the 3′ end of exon 9 in sequences located outside the 3′ recombination

[1]*PPL Therapeutics Inc., 1700 Kraft Drive, Blacksburg, Virginia 24060, USA.* [2]*PPL Therapeutics Ltd., Roslin, Midlothian EH25 9PP, UK.*
**Corresponding author (ydai@ppl-therapeutics.com).*

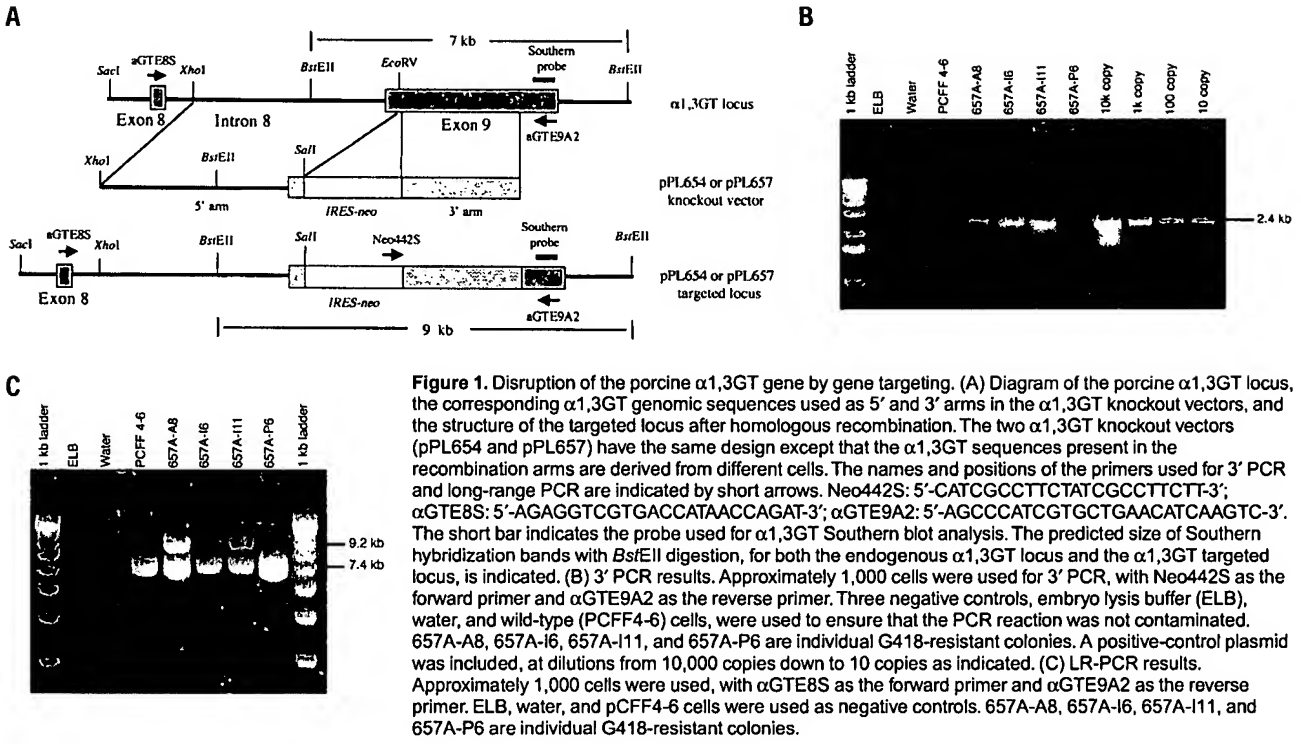


**Figure 1.** Disruption of the porcine α1,3GT gene by gene targeting. (A) Diagram of the porcine α1,3GT locus, the corresponding α1,3GT genomic sequences used as 5′ and 3′ arms in the α1,3GT knockout vectors, and the structure of the targeted locus after homologous recombination. The two α1,3GT knockout vectors (pPL654 and pPL657) have the same design except that the α1,3GT sequences present in the recombination arms are derived from different cells. The names and positions of the primers used for 3′ PCR and long-range PCR are indicated by short arrows. Neo442S: 5′-CATCGCCTTCTATCGCCTTCTT-3′; αGTE8S: 5′-AGAGGTCGTGACCATAACCAGAT-3′; αGTE9A2: 5′-AGCCCATCGTGCTGAACATCAAGTC-3′. The short bar indicates the probe used for α1,3GT Southern blot analysis. The predicted size of Southern hybridization bands with *Bst*EII digestion, for both the endogenous α1,3GT locus and the α1,3GT targeted locus, is indicated. (B) 3′ PCR results. Approximately 1,000 cells were used for 3′ PCR, with Neo442S as the forward primer and αGTE9A2 as the reverse primer. Three negative controls, embryo lysis buffer (ELB), water, and wild-type (PCFF4-6) cells, were used to ensure that the PCR reaction was not contaminated. 657A-A8, 657A-I6, 657A-I11, and 657A-P6 are individual G418-resistant colonies. A positive-control plasmid was included, at dilutions from 10,000 copies down to 10 copies as indicated. (C) LR-PCR results. Approximately 1,000 cells were used, with αGTE8S as the forward primer and αGTE9A2 as the reverse primer. ELB, water, and pCFF4-6 cells were used as negative controls. 657A-A8, 657A-I6, 657A-I11, and 657A-P6 are individual G418-resistant colonies.

arm) as forward and reverse primers (Fig. 1A). Thus, only through successful targeting at the α1,3GT locus would the expected 2.4-kb PCR product be obtained. From a total of seven transfections in four different cell lines, 1,105 G418-resistant colonies were picked, of which 100 (9%) were positive for α1,3GT gene disruption in the initial 3′ PCR screen (range 2.5–12%; Table 1). Figure 1B shows the 3′ PCR results for a representative group of G418-resistant colonies. Colonies 657A-A8, 657A-I6, and 657A-I11 showed the expected 2.4-kb band, whereas control PCFF4-6 cells and another G418-resistant colony, 657A-P6, did not. A portion of each 3′ PCR–positive colony was frozen immediately in several small aliquots for future use in nuclear transfer experiments, and the rest of the cells were expanded for long-range PCR (LR-PCR) and Southern blot analysis.

From our and others' experience[15–16], we expected that DNA analysis by PCR, or mRNA analysis by reverse transcription PCR, to detect recombination junctions would be prone to generating false-positive results. Therefore, to further confirm successful targeting at the α1,3GT locus, we carried out an LR-PCR experiment encompassing the entire targeted region. The LR-PCR covered the 7.4-kb α1,3GT genomic sequence from exon 8 to the end of exon 9, with both primers (aGTE8S and aGTE9A2) located outside the recombination region (Fig. 1A). The control PCFF4-6 cells and the 3′ PCR–negative colony, 657A-P6, showed only the endogenous 7.4-kb band from the wild-type α1,3GT locus (Fig. 1C). In contrast, three of the 3′ PCR–positive colonies, 657A-A8, 657A-I6, and 657A-I11, showed both the 7.4-kb endogenous band and a new band of 9.2 kb, the size expected for targeted insertion of the 1.8-kb *IRES-neo* cassette into the α1,3GT locus. As some 3′ PCR–positive signals may come from PCR artifacts, the LR-PCR assay is crucial to confirm successful knockout events. As evidence of this fact, only 30% of the 3′ PCR–positive colonies could be confirmed by LR-PCR (Table 1).

Approximately half (17/30) of the LR-PCR-positive colonies were successfully expanded to yield enough cells ($1 \times 10^6$) for Southern blot analysis. We expected that the colonies would be heterozygous for knockout at the α1,3GT locus and thus would have one normal copy and one disrupted copy of the α1,3GT gene. With *Bst*EII digestion, the α1,3GT knockout cells should show two bands: a 7-kb band of the size expected for the endogenous α1,3GT allele and a 9-kb band characteristic of insertion of the *IRES-neo* sequences at the α1,3GT locus (Figs. 1A, 2). Southern blot analysis confirmed knockout of the gene in all 17 LR-PCR-positive colonies. The same membranes were re-probed with sequences specific for *neo*, and the 9-kb band was detected with the *neo* probe (data not shown), confirming the targeted insertion of the *IRES-neo* cassette at the disrupted α1,3GT locus. Table 1 summarizes the results of transfection, 3′ PCR, LR-PCR, and Southern blot analysis. Recombination frequencies were highest in the PCFF4-2 and PCFF4-6 cell lines. On the basis of the LR-PCR results, the overall α1,3GT knockout rate in G418-resistant colonies was 6% for PCFF4-2 cells, 3% for PCFF4-6 cells, and 0.5% for PCFF4-3 cells. The fact that PCFF4-2 cells gave the highest recombination frequency may be related to isogenicity

**Table 1. Summary of 3′ PCR, LR-PCR, and Southern analysis results of G418-resistant colonies**

| Cells (sex) | Knockout vectors | No. of G418$^R$ colonies | No. of 3′ PCR$^+$ colonies (%) | No. of LR-PCR$^+$ colonies(%) | No. of Southern$^+$ colonies(%) |
|---|---|---|---|---|---|
| SLA1-10 (M) | pPL654 | 127 | 4 (3%) | 0 | 0 |
| PCFF4-2 (M) | pPL657 | 179 | 22 (12%) | 11 (6%) | 2 (1%) |
| PCFF4-3 (M) | pPL657 | 200 | 5 (2.5%) | 1 (0.5%) | 1 (0.5%) |
| PCFF4-6 (F) | pPL657 | 599 | 69 (11.5%) | 18 (3%) | 14 (2%) |

Results for SLA1-10, PCFF4-2, and PCFF4-6 cells are from two individual transfections for each cell; result for PCFF4-3 cells is from one transfection.

of these cells with the pPL657 GT knockout vector. When compared with PCFF4-2 cells, PCFF4-6 cells had a very similar knockout efficiency even though they were transfected with vector made from non-isogenic DNA. As both the PCFF4-2 and PCFF4-6 cell lines were derived from sibling fetuses of the same pregnancy, it is possible that they share a common allele.

We used seven Southern blot–confirmed α1,3GT-knockout single colonies for nuclear transfer. All cells used for nuclear transfer were from the aliquots that had been frozen immediately after the initial 3′ PCR screening. The karyotype of each colony was checked; all had chromosome numbers in a range similar to that of freshly isolated porcine fetal fibroblast cells (~70% of spreads with 38 chromosomes). On average, approximately 150 reconstructed nuclear-transfer embryos were transferred to the oviducts of each estrus-synchronized recipient female. All seven colonies used for nuclear transfer resulted in very high initial pregnancy rates at day 25 (50%–86%) (Table 2). However, all pregnancies established from colonies 657A-A8 and 657A-F12 were lost between days 25 and 45. In contrast, the other five colonies resulted in pregnancy rates in excess of 50% at day 45.

One spontaneously aborted day 38 fetus from a 657A-A8 nuclear transfer recipient was recovered. LR-PCR and Southern blot analysis confirmed that the fetus contained a disrupted α1,3GT locus (data not shown). Southern blot results from 657A-I11 cells showed that the 9-kb knockout band was less intense than the 7-kb endogenous α1,3GT band, indicating that this was most likely a mixed colony containing both wild-type and heterozygous knockout cells. There was some concern that fetuses derived from wild-type cells in the mixed colony could affect the development of, or outcompete, *in utero* fetuses derived from the α1,3GT-knockout cells. To test this, we terminated by hysterectomy a day 32 pregnancy derived from nuclear transfer with 657A-I11 cells. Seven fetuses were recovered, of which six were of normal size and one substantially smaller. Southern blot analysis showed that six of the seven fetuses contained a disrupted α1,3GT locus (Fig. 2A). Notably, it was the smaller fetus (fetus no. 2) that was wild type, and all six normal-sized fetuses contained an α1,3GT knockout allele. These results suggested that there was no discrimination against the heterozygous α1,3GT knockout fetuses *in utero*.

Six live piglets derived from the 657A-I11 cells were born on December 25, 2001. Five were of normal size and weight (Fig. 3); one (no. 2) was stunted, weighing less than 1 pound. Southern blot analysis indicated that five of the six offspring were α1,3GT heterozygous knockouts (Fig. 2B). Again, the one negative (wild-type) piglet was the underdeveloped runt. These results, when considered along with the analysis of the seven day 32 fetuses from 657A-I11 cells, suggested that the colony 657A-Ill was indeed a mixed population contaminated with wild-type cells. All fetuses and offspring obtained from the α1,3GT knockout cells in the 657A-I11 population were developmentally normal. Physical examination of the five knockout piglets at one month of age found no abnormalities. This contrasts with the

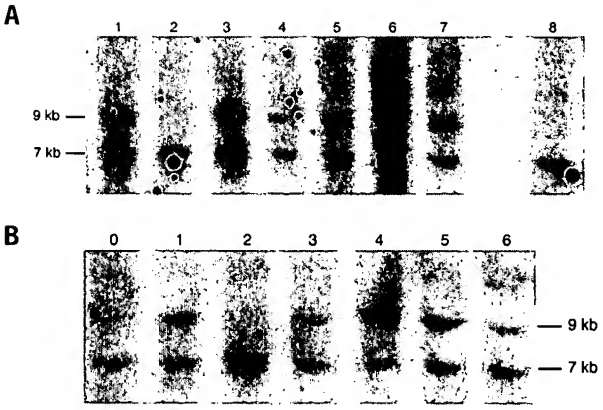


**Figure 2.** Southern blot analysis of α1,3GT gene knockout fetuses and piglets. (A) Southern analysis of DNA from seven day 32 fetuses. Lane 1–7 are *Bst*EII-digested genomic DNA from seven day 32 fetuses derived from 657A-I11 cells. Lane 8 contains normal pig DNA digested with *Bst*EII as a negative control. The 7-kb band represents the endogenous α1,3GT gene and the 9-kb band the disrupted α1,3GT locus. (B) Southern analysis of DNA from six piglets. Lane 0 is the normal pig DNA digested with *Bst*EII. Lanes 1–6 are *Bst*EII-digested DNA from six piglets cloned from 657A-I11 cells. The 7-kb band represents the endogenous α1,3GT gene and the 9-kb band represents the disrupted α1,3GT locus.

report by Lai *et al.*[14], in which only four of seven piglets survived for more than a month and three of the surviving piglets had mild physical abnormalities. These differing outcomes may have been due to many factors, including different pig breeds, different condition of cells used for nuclear transfer, and different embryo manipulation methods.

We have produced apparently healthy heterozygous α1,3GT knockout piglets by nuclear transfer. We have an additional 16 ongoing second- and third- trimester pregnancies beyond day 45 from two female and three male α1,3GT knockout colonies (Table 2). We expect that most will go to term as we have never lost any pregnancies of cloned pigs after 45 days of gestation (data not shown). The next step is to obtain homozygous pigs with both α1,3GT alleles inactivated. This could be done either through natural breeding of male and female heterozygous knockout animals or through gene targeting with heterozygous knockout cells to disrupt the second α1,3GT allele before a second round of nuclear transfer. As we already have six lines of early-passage heterozygous α1,3GT gene–disrupted fetal fibroblasts, obtained from the day 32 657A-I11 fetuses, it will probably be considerably faster to create the second knockout in these cells *in vitro* and obtain homozygous knockout animals by nuclear transfer. Natural breeding to homozygosity will also be used, but this method will take considerably longer because of the gestation time of the male knockout clones *in utero* and the time to sexual maturity.

Live births have been reported in cattle from recloning experiments that used fibroblasts obtained from cloned fetuses[17]. Recloning experiments by our group, using wild-type porcine fetal fibroblasts derived from a day 40 cloned fetus, have shown an 80% pregnancy rate at day 45 (PPL Therapeutics, unpublished data). These data suggest that it will be feasible to obtain homozygous α1,3GT knockout pigs by a second knockout and recloning

**Table 2. Summary of nuclear transfer results from α1,3GT knockout primary fibroblast cells**

| Nuclear donor cell line | PCFF4-6 | PCFF4-6 | PCFF4-6 | PCFF4-6 | PCFF4-2 | PCFF4-2 | PCFF4-3 |
|---|---|---|---|---|---|---|---|
| Cell clone | 657A-I11 | 657A-A8 | 657A-F12 | 657A-I6 | 657F-J10 | 657F-C11 | 657B-K8 |
| Sex | F | F | F | F | M | M | M |
| Embryos transferred to recipients | 1097 | 825 | 591 | 976 | 1009 | 775 | 1105 |
| Recipients | 7 | 5 | 4 | 6 | 6 | 4 | 7 |
| Pregnancies at day 25 | 6 | 3 | 2 | 5 | 5 | 2 | 6 |
| Pregnancies at day 45 | 3[a] | 0 | 0 | 4 | 4 | 2 | 4[b] |
| Piglets at birth[c] | 6 | 0 | 0 | Pending | Pending | Pending | Pending |

[a]Based on 6 recipients since one day 32 pregnancy was terminated for fetal fibroblast isolation. [b]Based on 6 recipients since one day 39 pregnancy was terminated for fetal fibroblast isolation. [c]As dated on January 25, 2002. Six piglets were born from one 657A-I11 recipient on December 25, 2001. Another 16 recipients beyond day 45 of pregnancy are due after January 25, 2002.

**Figure 3.** Five α1,3GT gene knockout piglets at 2 weeks of age.

strategy. In mice, the homozygous knockout of α1,3GT gene is not an embryonic lethal mutation, although such mice have developed cataracts[6]. Pig cells express significantly more α1,3Gal epitopes on their surface than do mouse cells, and it has therefore been proposed that α1,3GT may have some additional, unknown role in pigs[18]. Although heterozygous α1,3GT knockout pigs are developmentally normal, it is not known if complete deletion of both alleles of α1,3GT will be more (or less) problematic in pigs than in mice.

Complete removal of the α1,3Gal epitope, the major xenoantigen, combined with transgenic expression of complement regulatory proteins should prevent the hyperacute rejection of pig xenografts even in the presence of a low background of non-α1,3Gal xenoantigens. The success of xenotransplantation will also depend on risk assessment of safety factors such as porcine endogenous retroviruses and on the development of strategies that address delayed vascular and T-cell-mediated rejection. Together, these approaches may provide a near-term solution to the chronic shortage of human organs (such as heart and kidneys) and valuable tissues such as insulin-producing islet cells.

## Experimental protocol

Isolation and transfection of primary porcine fetal fibroblasts. PCFF4-1 to PCFF4-10 fetal fibroblast cells were isolated from 10 fetuses of the same pregnancy at day 33 of gestation. After removing the head and viscera, fetuses were washed with Hanks' balanced salt solution (HBSS; Gibco-BRL, Rockville, MD), placed in 20 ml of HBSS, and diced with small surgical scissors. The tissue was pelleted and resuspended in 50-ml tubes with 40 ml of DMEM and 100 U/ml collagenase (Gibco-BRL) per fetus. Tubes were incubated for 40 min in a shaking water bath at 37°C. The digested tissue was allowed to settle for 3–4 min and the cell-rich supernatant was transferred to a new 50-ml tube and pelleted. The cells were then resuspended in 40 ml of DMEM containing 10% fetal calf serum (FCS), 1× nonessential amino acids, 1 mM sodium pyruvate (Gibco-BRL), and 2 ng/ml basic fibroblast growth factor (bFGF; Roche Molecular Biochemicals, Indianapolis, IN) and seeded into 10-cm dishes. All cells were cryopreserved upon reaching confluence. SLA1-1 to SLA1-10 cells were isolated from 10 fetuses at day 28 of pregnancy. Fetuses were mashed through a 60-mesh metal screen (Sigma, St. Louis, MO) using curved surgical forceps slowly so as not to generate excessive heat. The cell suspension was then pelleted and resuspended in 30 ml of DMEM containing 10% FCS, 1× nonessential amino acids, 2 ng/ml bFGF, and 10 μg/ml gentamycin. Cells were seeded in 10-cm dishes, cultured one to three days, and cryopreserved. For transfections, 10 μg of linearized vector DNA was introduced into 2 million cells by electroporation. Forty-eight hours after transfection, the transfected cells were seeded into 48-well plates at a density of 2,000 cells per well and were selected with 250 μg/ml of G418 (Gibco-BRL).

Knockout vector construction. Two a1,3GT knockout vectors, pPL654 and pPL657, were constructed from isogenic DNA of two primary porcine fetal fibroblasts, SLA1-10 and PCFF4-2 cells. A 6.8-kb α1,3GT genomic fragment, which includes most of intron 8 and exon 9, was generated by PCR from purified DNA of SLA1-10 cells and PCFF4-2 cells, respectively. The unique *Eco*RV site at the 5′ end of exon 9 was converted into a *Sal*I site and a 1.8-kb *IRES-neo*-poly A fragment was inserted into the *Sal*I site. IRES (internal ribosome entry site) functions as a translation initial site for neo protein. Thus, both vectors have a 4.9-kb 5′ recombination arm and a 1.9-kb 3′ recombination arm (Fig. 1A).

3′PCR and long-range PCR. Approximately 1,000 cells were resuspended in 5 μl embryo lysis buffer (ELB) (40 mM Tris, pH 8.9, 0.9% Triton X-100, 0.9% Nonidet P-40, 0.4 mg/ml proteinase K), incubated at 65°C for 15 min to lyse the cells, and heated to 95°C for 10 min to inactivate the proteinase K. For 3′ PCR analysis, fragments were amplified using the Expand High Fidelity PCR system (Roche Molecular Biochemicals) in 25 μl reaction volume with the following parameters: 35 cycles of 1 min at 94°C, 1 min at 60°C, and 2 min at 72°C. For LR-PCR, fragments were amplified by using TAKARA LA system (Panvera/Takara, Madison, WI) in 50 μl reaction volume with the following parameters: 30 cycles of 10 s at 94°C, 30 s at 65°C, 10 min + 20 s increase/cycle at 68°C; and one final cycle of 7 min at 68°C. 3′ PCR and LR-PCR conditions for purified DNA was same as for cells except that 1 μl of purified DNA (30 μg/ml) was mixed with 4 μl ELB.

Southern blot analysis of cell samples. Approximately $10^6$ cells were lysed overnight at 60°C in lysis buffer (10 mM Tris, pH 7.5, 10 mM EDTA, 10 mM NaCl, 0.5% (w/v) Sarcosyl, 1 mg/ml proteinase K) and the DNA precipitated with ethanol. The DNA was then digested with *Bst*EII and separated on a 1% agarose gel. After electrophoresis, the DNA was transferred to a nylon membrane and probed with the 3′-end digoxigenin-labeled probe. Bands were detected using a chemiluminescent substrate system (Roche Molecular Biochemicals).

Southern blot analysis of pig tissues. Fetal tissues and piglet tails were lysed overnight at 60°C in a shaking incubator with approximately 1 ml lysis solution (50 mM Tris, pH 8.0, 0.15 M NaCl, 10 mM EDTA, 1% SDS, 25% sodium perchlorate, 1% 2-mercaptoethanol, and 200 μg/ml proteinase K) per 175 mg tissue. DNA was subjected to phenol/chloroform extraction and precipitated with isopropyl alcohol. Resolubilized DNA was treated with RNase A (1 mg/ml) and RNase T1 (1,000 U/μl) at 37°C for 1 h, with proteinase K (20 mg/ml) at 55°C for 1 h, then extracted with phenol/chloroform, precipitated with ethanol, and resuspended in TE buffer. About 10 mg DNA was digested with *Bst*EII and separated on an 1% agarose gel. Following electrophoresis, the DNA was transferred to a nylon membrane and probed with the 3′-end digoxigenin-labeled probe. Bands were detected using a chemiluminescent substrate system.

Nuclear transfer procedure. Enucleation of *in vitro*-matured oocytes (BioMed, Madison, WI) was begun between 40 and 42 h post-maturation as described previously[11]. A single fibroblast cell was placed under the zona pellucida in contact with each enucleated oocyte. Fusion and activation were induced by application of an AC pulse of 5 V for 5 s followed by two DC pulses of 1.5 kV/cm for 60 μs, each using an ECM2001 Electrocell Manipulator (BTX Inc., San Diego, CA). Fused embryos were cultured in NCSU-23 medium for 1–4 h at 38.6°C in a humidified atmosphere of 5% $CO_2$, and then transferred to the oviduct of an estrus-synchronized recipient gilt. Crossbred gilts (large white/Duroc/landrace) (280–400 lbs) were synchronized as recipients by oral administration of 18–20 mg Regu-Mate (Altrenogest, Hoechst, Warren, NJ) mixed into their feed. Regu-Mate was fed for 14 consecutive days. Human chorionic gonadotropin (hCG, 1,000 units; Intervet America, Millsboro, DE) was administered intramuscularly 105 h after the last Regu-Mate treatment. Embryo transfers were done 22–26 h after the hCG injection.

*Acknowledgments*

*We thank B. Gragg, W. Lucero, T. Akers, H. Bishop, and J. McPherson for technical contributions to embryo transfer and animal husbandry; A. Garst and J. Hencke for help in nuclear transfer; C. Koike and T. E. Starzl at the University of Pittsburgh for providing us with porcine α1,3GT gene genomic sequence; M. Moore, A. Kind, and A. Schnieke for valuable contributions in discussions; and staff at the Virginia Maryland Regional Veterinary College for prenatal care of some of the nuclear transfer recipients and physical examination of piglets. This research was funded in part by a grant from the National Institute of Standards and Technology (NIST) Advanced Technology Program (ATP).*

*Competing interests statement*

*The authors declare that they have no competing financial interests.*

Received 8 January 2002; accepted 22 January 2002

1. Galili, U., Shohet, S.B., Kobrin, E., Stults, C.L. & Macher, B.A. Man, apes, and Old World monkeys differ from other mammals in the expression of α-galactosyl epitopes on nucleated cells. *J. Biol. Chem.* **263**,17755–17762 (1988).
2. Joziasse, D.H. & Oriol, R. Xenotransplantation: the importance of the Galα1,3Gal epitope in hyperacute vascular rejection. *Biochim. Biophys. Acta* **1455**, 403–418 (1999).
3. Galili, U. The α-Gal epitope (Galα1-3Galβ1-4GlcNAc-R) in xenotransplantation. *Biochimie* **83**, 557–563 (2001).
4. Sandrin, M.S. & McKenzie, I.F.C. Galα(1,3)Gal, the major xenoantigen(s) recognised in pigs by human natural antibodies. *Immunol. Rev.* **141**, 169–190 (1994).
5. Galili, U., Macher, B.A., Buehler, J. & Shohet, S.B. Human natural anti-α-galactosyl IgG. II. The specific recognition of α(1-3)-linked galactose residues. *J. Exp. Med.* **162**, 573–582 (1985).
6. Tearle, R.G. *et al.* The α-1,3-galactosyltransferase knockout mouse. Implications for xenotransplantation. *Transplantation* **61**, 13–19 (1996).
7. Thall, A.D., Maly, P. & Lowe, J.B. Oocyte Galα1,3Gal epitopes implicated in sperm adhesion to the zona pellucida glycoprotein ZP3 are not required for fertilization in the mouse. *J. Biol. Chem.* **270**, 21437–21440 (1995).
8. Wilmut, I., Schnieke, A.E., McWhir, J., Kind, A.J. & Campbell, K.H.S. Viable offspring derived from fetal and adult mammalian cells. *Nature* **385**, 810–813 (1997).
9. Baguisi, A. *et al.* Production of goats by somatic cell nuclear transfer. *Nat. Biotechnology* **17**, 456–461 (1999).
10. Cibelli, J.B. *et al.* Cloned transgenic calves produced from nonquiescent fetal fibroblasts. *Science* **280**, 1256–1258 (1998).
11. Polejaeva, I.A. *et al.* Cloned pigs produced by nuclear transfer from adult somatic cells. *Nature* **407**, 86–90 (2000).
12. McCreath, K.J. *et al.* Production of gene-targeted sheep by nuclear transfer from cultured somatic cells. *Nature* **405**, 1066–1069 (2000).
13. Denning, C. *et al.* Deletion of the α(1,3)galactosyl transferase (GGTA1) gene and the prion protein (PrP) gene in sheep. *Nat. Biotechnol.* **19**, 559–562 (2001).
14. Lai, L. *et al.* Production of α-1,3-galactosyltransferase knockout pigs by nuclear transfer cloning. *Science* **295**, 1089–1092 (2002).
15. Kim, H.S., Popovich, B.W., Shehee, W.R., Shesely, E.G. & Smithies, O. Problems encountered in detecting a targeted gene by the polymerase chain reaction. *Gene* **103**, 227–233 (1991).
16. Shuldiner, A.R., Tanner, K., Moore, C.A. & Roth, J. RNA template-specific PCR: an improved method that dramatically reduces false positives in RT-PCR. *Biotechniques* **11**, 760–763 (1991).
17. Zakhartchenko, V. *et al.* Nuclear transfer in cattle with non-transfected and transfected fetal or cloned transgenic fetal and postnatal fibroblasts. *Mol. Reprod. Dev.* **60**, 362–369 (2001).
18. Tanemura, M., Maruyama, S. & Galili, U. Differential expression of α-Gal epitopes (Galα1-3Galβ1-4GlcNAc-R) on pig and mouse organs. *Transplantation* **69**, 187–190 (2000).

# Cardiac Overexpression of Melusin Protects From Dilated Cardiomyopathy Due to Long-Standing Pressure Overload

Marika De Acetis,* Antonella Notte,* Federica Accornero,* Giulio Selvetella, Mara Brancaccio, Carmine Vecchione, Mauro Sbroggiò, Federica Collino, Beniamina Pacchioni, Gerolamo Lanfranchi, Alessandra Aretini, Roberta Ferretti, Angelo Maffei, Fiorella Altruda, Lorenzo Silengo, Guido Tarone, Giuseppe Lembo

*Abstract*—We have previously shown that genetic ablation of melusin, a muscle specific $\beta$ 1 integrin interacting protein, accelerates left ventricle (LV) dilation and heart failure in response to pressure overload.

Here we show that melusin expression was increased during compensated cardiac hypertrophy in mice subjected to 1 week pressure overload, but returned to basal levels in LV that have undergone dilation after 12 weeks of pressure overload. To better understand the role of melusin in cardiac remodeling, we overexpressed melusin in heart of transgenic mice. Echocardiography analysis indicated that melusin over-expression induced a mild cardiac hypertrophy in basal conditions (30% increase in interventricular septum thickness) with no obvious structural and functional alterations. After prolonged pressure overload (12 weeks), melusin overexpressing hearts underwent further hypertrophy retaining concentric LV remodeling and full contractile function, whereas wild-type LV showed pronounced chamber dilation with an impaired contractility. Analysis of signaling pathways indicated that melusin overexpression induced increased basal phosphorylation of GSK3$\beta$ and ERK1/2. Moreover, AKT, GSK3$\beta$ and ERK1/2 were hyper-phosphorylated on pressure overload in melusin overexpressing compared with wild-type mice. In addition, after 12 weeks of pressure overload LV of melusin overexpressing mice showed a very low level of cardiomyocyte apoptosis and stromal tissue deposition, as well as increased capillary density compared with wild-type. These results demonstrate that melusin overexpression allows prolonged concentric compensatory hypertrophy and protects against the transition toward cardiac dilation and failure in response to long-standing pressure overload. (***Circ Res.* 2005;96:1087-1094.**)

**Key Words:** melusin ■ cardiac hypertrophy ■ heart failure ■ signal transduction ■ fibrosis

Mechanical stretching imposed on cardiac walls by hemodynamic overload generated by several cardiovascular diseases, such as aortic stenosis, hypertension and myocardial infarction, triggers left ventricular hypertrophy (LVH), a process aimed to increase cardiac pumping function and normalize wall stress. This response is achieved via signaling pathways, which trigger increased synthesis of sarcomeric proteins and growth of cardiomyocyte mass. In addition, LVH is accompanied by release and secretion of neurohumoral mediators, growth factors, and cytokines that, contribute to the growth of cardiomyocytes, as well as blood vessels and interstitial connective tissue. Consistent with this general picture, a variety of different signaling pathways have been implicated in the hypertrophic growth of cardiac muscle.[1,2]

Although LVH provides increased contractile power, several clinical and experimental studies have demonstrated that cardiac hypertrophy is frequently associated with an increased risk of heart failure. Following chronic pressure overload, in fact, compensatory hypertrophy can evolve to decompensated hypertrophy with cardiac dilation and loss of contractile function, representing the typical features of heart failure. This unfavorable evolution can be accounted for by several causes, including abnormal accumulation of stromal tissue, poor development of capillary vascular bed, myocyte apoptosis, inadequate cardiomyocyte growth, and defective $Ca^{2+}$ cycling.[2] The molecular mechanisms responsible for this transition are still poorly defined and identification of genes and signaling pathways involved represents a major challenge of molecular cardiology.

Original received October 4, 2004; revision received April 19, 2005; accepted April 19, 2005.

From the Department of Genetics, Biology (M.DA, F.A., M.B., M.S., F.C., R.F., F.A., L.S., G.T.), and Biochemistry, Turin University, Turin; Dept. of Angiocardioneurology (A.N., G.S., C.V., A.A., A.M., G.L.), I.R.C.C.S. "Neuromed", Pozzilli (IS); Experimental Medicine Research Center (F.A., L.S., G.T.), San Giovanni Battista Hospital, Turin; Dept. of Experimental Medicine and Pathology (G. Lembo), "La Sapienza" University of Rome; Dept. of Biology and CRIBI Biotechnology Centre (B.P., G. Lanfranchi).

*These authors contributed equally to this work.

Correspondence to Guido Tarone, Dept. of Genetics, Biology, and Biochemistry, Turin University, Via Santena, 5bis, 10126 Turin, Italy. E-mail guido.tarone@unito.it; or Giuseppe Lembo, Department of Angiocardioneurology, I.R.C.C.S. "Neuromed", 86077 Pozzilli (IS), Italy. E-mail lembo@neuromed.it



*Circulation Research* is available at http://www.circresaha.org DOI: 10.1161/01.RES.0000168028.36081.e0

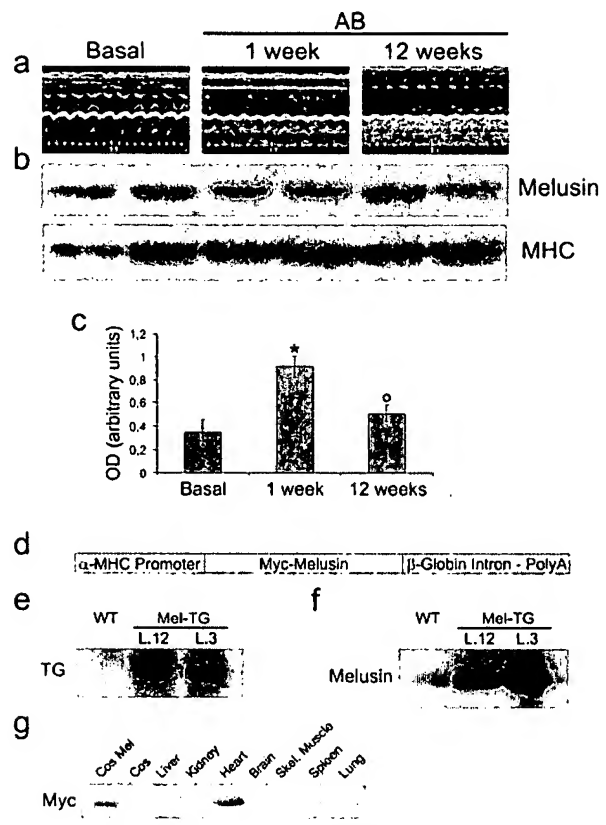


**Figure 1.** Melusin expression in LV after AB and characterization of Mel-TG mice. Echocardiography of WT mice in basal conditions and after 1 or 12 weeks AB (a). Western blot on LV proteins with melusin, or myosin heavy chain (MHC) antibodies as loading control (b). Densitometric analysis of melusin expression, relative to total protein loading (n=5 per group) (c). DNA construct used for generation of transgenic mice (d). Two independent Mel-TG lines were analyzed (L.12 and L.3). Southern blot of genomic DNA from WT and Mel-TG mice probed with human melusin cDNA (e). Western blot of proteins from WT and Mel-TG LV probed with melusin antibodies (f). Western blot of different tissues from L.12 transgenic line probed with Myc antibodies specific for the transgenic protein. COS cells transfected with myc-tagged melusin cDNA (Cos mel) as positive control (g). (*): $P<0.05$ versus basal conditions, (°): $P<0.05$ versus 1 week AB.

We have previously identified melusin as a new muscle-specific protein binding to the cytoplasmic domain of integrins[3] and acting as mechanical stretch sensor. Targeted inactivation of melusin gene in mice caused impaired LVH with accelerated development of dilated cardiomyopathy in response to chronic pressure overload.[4]

Here we report that cardiac selective overexpression of melusin in transgenic mice allows retainment of concentric compensatory hypertrophy and proper contractile function in conditions of prolonged pressure overload leading to LV dilation and contractile dysfunction in control wild-type (WT).

## Materials and Methods

### Generation of Transgenic Mice

Alpha-MHC promoter[5] was cloned upstream the myc-tagged human melusin cDNA followed by β-globin intron and poly-A (Figure 1D). The DNA construct described previously was microinjected in FVB fertilized eggs and transgenic integration was confirmed by Southern blot (Figure 1E). The use of animals was in compliance with European Community guidelines and was approved by the Animal Care and Use Committee of Turin University.

### LV Pressure Overload

A chronic pressure overload was imposed to the LV through transverse aortic banding (AB), as previously described.[4] Systolic pressure gradient (SPG) was measured by selective cannulation of left and right carotid arteries during the hemodynamic analysis at 12 weeks of AB.[4]

### LV Echocardiographic and Hemodynamic Analysis

Conscious blood pressure and heart rate were measured in unrestrained conditions by radiotelemetry as previously described.[6] Serial echocardiographic evaluations were assessed in mice in basal conditions and during chronic pressure overload (4, 8, and 12 weeks after banding) as described.[4] Hemodynamic measurements were performed in anesthetized aortic-banded and sham-operated mice after 12 weeks from AB, as described.[4]

### Histological Analysis

Histological analysis was performed as described.[4] Fibrosis was quantified by Picrosirius red followed by ImageProPlus software analysis. Apoptotic cells were detected by TUNEL. Capillaries were identified by anti von Willebrand factor antibodies (Sigma).

### Isolation of Adult Cardiomyocytes and Morphometric Analysis

Cardiomyocytes were enzymatically dissociated from hearts as described.[7] Freshly isolated cardiomyocytes were photographed at 20x phase contrast and cell areas were measured using ImageProPlus software.

### Embryonic Cardiomyocyte Isolation and Transduction

Ventricular cardiomyocytes were prepared from Sprague-Dawley rat hearts as described.[8] Final cultures contained >95% cardiomyocytes as determined by actin staining.

Lentiviral vector coding for myc-tagged human melusin, and a control vector coding for GFP, were prepared as described.[9] Forty-eight hours after plating, cardiomyocyte were incubated overnight with lentivirus. Infection efficiency was ≈80%. After washing, cells were further incubated for 72 hours with or without 50 μmol/L MEK-1 inhibitor (PD98059, Calbiochem) or 20 μmol/L AKT inhibitor (1L-6-hydroxymethyl-chiro-inositol-2(R)-2-O-methyl-3-O-octadecylcarbonate, Calbiochem). Cells were fixed and stained with FITC–labeled phalloidin (Sigma) or subjected to Western blot analysis.

### Northern and Western Blot Analysis

Northern blots with LV RNA were performed as described[4] and probed with atrial natriuretic factor (ANF) and alpha-skeletal actin (SkA) radiolabeled probes. Western blots on LV protein extracts were performed as described.[4] Polyclonal antibodies to melusin were prepared as described.[3]

### Transcriptome Analysis

Gene expression profile was performed on a mouse microarray platform with a collection of 13,443 70mer oligonucleotides (Qiagen-Operon, version 1.1). Preparation of the microarray, RNA labeling, hybridization and detection of differentially expressed transcripts are described in online supplementary information at http://www.circresaha.org.

### Statistical Analysis

Results are presented as mean±S.E. Differences between groups were compared using 2-way ANOVA followed by Bonferroni *post-hoc* test. A value of $P<0.05$ was considered significant.

**TABLE 1. Haemodynamic Parameters in Sham- and AB-Operated Mel-TG and WT Control Mice**

| | WT | | Mel-TG | |
|---|---|---|---|---|
| | Sham n=6 | AB 12w n=7 | Sham n=6 | AB 12w n=7 |
| BW, g | 30.6±0.6 | 29.3±0.3 | 31.2±0.7 | 28.4±0.7 |
| HR | 350±9 | 322±22 | 362±9 | 344±24 |
| SPG, mm Hg | — | 77.5±3.2 | — | 81.2±3.1 |
| EDV, μL | 95.2±43.7 | 118±2[b] | 91.3±4.2 | 96.0±5.8[a] |
| ESV, μL | 64±6.5 | 93.5±2.5[b] | 60.5±4 | 60±5[a] |
| ESP, mm Hg | 88.8±7.2 | 155.6±9.2[b] | 93.7±4.3 | 161.2±8.0[b] |
| EDP, mm Hg | 6.9±2.3 | 15.2±3.5[b] | 6.8±1 | 4.5±1[a] |
| $dP/dT_{max}$ | 6077±601 | 4017±504[b] | 7102±612 | 7377±577[a] |
| $dP/dT_{min}$ | −4544±443 | −3366±413[b] | −5343±797 | −3697±316[b] |
| EDPVR | 0.13±0.03 | 0.17±0.07 | 0.12±0.09 | 0.08±0.04 |
| τ(Glanz) (ms) | 17.6±1.8 | 25.5±5 | 18.8±4 | 25.7±4 |
| Emax | 2.6±0.7 | 1.8±0.6 | 2.5±1.3 | 5.4±1.6[a] |

[a]$P<0.05$ vs WT.

[b]$P<0.05$ vs basal conditions.

BW, body wt; HR, heart rate; SPG, systolic pressure gradient; ESV, end-systolic volume; EDV, end-diastolic volume; ESP, end-systolic pressure; EDP, end-diastolic pressure; $dp/dt_{max}$, maximal rate of pressure development; Emax, maximum chamber elasticity; $dp/dt_{min}$, maximal rate of pressure decay; τ(Glanz), monoexponential time constant of relaxation; EDPVR, end diastolic pressure-volume relationship.

## Results

### Melusin Expression in Pressure Overloaded Hearts

To investigate whether melusin expression is modified by pressure overload, WT were subjected to AB for different times. Whereas after 1 week LV showed a concentric hypertrophic remodeling, at 12 weeks the chamber was clearly dilated (Figure 1a). Melusin expression increased by 2.6-fold over basal ($P<0.05$ in 5 hearts) in the first week of AB (Figure 1b,c). However, after 12 weeks of AB, melusin expression in LV was decreased as compared with 1 week of AB ($P<0.05$, n=5) and not significantly different from basal levels. Thus, melusin expression is regulated during the LV remodeling induced by chronic pressure overload.

These data, together with the finding that inactivation of melusin gene in mice causes premature evolution toward dilated cardiomyopathy in response to pressure overload,[4] led us to test whether forced melusin expression can prevent cardiac dilation in conditions of chronic pressure overload.

### Generation of Mice Overexpressing Melusin in Heart

Two lines (L.3 and L.12) of transgenic FVB mice selectively expressing myc-tagged melusin transgene in the heart were selected (Mel-TG) (Figure 1G). Melusin expression was increased ≈15-fold and 8-fold in L.3 and L.12 lines respectively compared with WT littermates as detected by western blot (Figure 1F).

Transgenic mice were born in a normal Mendelian distribution, excluding lethal developmental abnormalities. They exhibit normal reproductive rate and gender distribution and did not demonstrate any difference in longevity over 2 years. All experiments reported were performed with male mice and both transgenic lines displayed comparable phenotype, ruling out the possibility that the alterations detected are due to insertional mutagenesis.

### Melusin Overexpressing Mice Show LVH in Basal Conditions

Mel-TG mice exhibited a slight LVH as compared with WT (LVW/BW: 3.12±0.11 versus 2.84±0.08, n=11 per group, $P<0.05$), even with comparable systolic and diastolic blood pressure (SBP: 108±4 versus 110±3; DBP: 84±1 versus 85±1 mm Hg) and heart rate (579±50 versus 552±37 bpm) as detected by radiotelemetric measurements in conscious mice. Furthermore, LV contractile function and diastolic relaxation, evaluated by dP/dt max and by dP/dt min and τ Glantz, respectively, were also comparable between Mel-TG and WT mice (Table 1).

However, echocardiography showed a different basal LV geometry between the 2 mouse strains (Table 2). Both interventricular septum and LV posterior wall thickness were significantly increased in Mel-TG as compared with WT, resulting in significantly higher relative wall thickness. LV histological analysis indicated that myocyte cross-sectional areas were ≈30% higher in Mel-TG hearts compared with WT (Figure 2A,B). This level of hypertrophy was confirmed by analysis of cardiomyocytes isolated from adult hearts (Figure 2C,D). No histological signs of stromal tissue deposition were observed, suggesting that LVH in Mel-TG mice can be ascribed to increased cardiomyocyte size.

Therefore, in basal conditions, melusin overexpression does not affect cardiac function, but induces a significant concentric LVH.

In addition, Northern blot analysis showed increased ANF, but reduced SkA expression in Mel-TG LV (Figure 2E,F) indicating a specific pattern of LVH.

**TABLE 2. Echocardiographic Parameters in Basal Conditions and After AB in WT and Mel-TG Mice**

| | WT | | | | Mel-TG | | | |
|---|---|---|---|---|---|---|---|---|
| | Basal n=11 | AB 4w n=11 | AB 8w n=11 | AB 12w n=10 | Basal n=8 | AB 4w n=8 | AB 8w n=8 | AB 12w n=7 |
| BW, g | 26.4±0.5 | 27.6±0.7[b] | 28.7±0.5[bc] | 29.5±0.3 | 26.3±0.4 | 27.0±0.4[b] | 28.4±0.6[bc] | 28.4±0.7[b] |
| HR, bpm | 624±9 | 625±10 | 608±10 | 621±12 | 622±10 | 615±10 | 623±13 | 619±13 |
| LVEDD, mm | 3.32±0.06 | 2.89±0.66[b] | 3.64±0.17[c] | 4.20±0.20[bc] | 3.11±0.14 | 2.74±0.21 | 2.67±0.24[a] | 2.97±0.30[a] |
| LVESD, mm | 1.46±0.04 | 1.25±0.10 | 2.13±0.18[bc] | 2.87±0.22[bc] | 1.36±0.06 | 1.15±0.11 | 1.18±0.16[a] | 1.41±0.24[a] |
| IVSTD, mm | 0.66±0.02 | 1.26±0.05[b] | 0.89±0.05[bc] | 0.72±0.04[c] | 0.86±0.06[a] | 1.44±0.07[ab] | 1.47±0.06[ab] | 1.38±0.08[ab] |
| PWTD, mm | 0.64±0.02 | 1.24±0.05[b] | 0.91±0.05[bc] | 0.72±0.03[c] | 0.86±0.06[a] | 1.45±0.07[ab] | 1.48±0.06[ab] | 1.44±0.08[ab] |
| RWT | 0.39±0.01 | 0.88±0.05[b] | 0.51±0.04[bc] | 0.35±0.02[c] | 0.57±0.06[a] | 1.10±0.10[ab] | 1.17±0.13[ab] | 1.02±0.16[ab] |
| LVMi | 2.59±0.17 | 5.20±0.41[b] | 4.29±0.33[bc] | 3.99±0.42[b] | 3.36±0.21[a] | 6.35±0.78[b] | 5.96±0.53[ab] | 6.48±0.83[ab] |
| FS% | 56.1±0.7 | 57.3±1.7 | 42.3±2.8[bc] | 32.3±2.3[bc] | 56.1±0.5 | 58.3±1.0 | 56.7±1.9[a] | 54.0±3.6[a] |

[a]$P<0.05$ vs WT.

[b]$P<0.05$ vs basal conditions.

[c]$P<0.05$ vs the previous examination.

BW indicates body wt, HR, heart rate, LVEDD, left ventricle end-diastolic diameter, LVESD, left ventricle end-systolic diameter, IVSTD, interventricular septum thickness in end-diastole, PWTD, posterior wall thickness in end-diastole, RWT, relative wall thickness, LVMi, left ventricular mass index, FS%, percent fractional shortening.

## Melusin Overexpression Protects from Dilated Cardiomyopathy in Response to Long-Standing Pressure Overload

Mel-TG and WT mice were subjected to AB for 12 weeks, and serial echocardiography was performed to progressively monitor cardiac structure and function (Figure 3a).

Four weeks after banding, both mice strains showed increased interventricular septum, LV posterior wall thickness and LV mass index (Table 2). Concomitantly, LV end-diastolic diameter was decreased. Therefore, an increase in relative wall thickness was achieved in both mice groups (Table 2, Figure 3a,c). This remodeling represents a typical pattern of concentric hypertrophy, an adaptive compensatory mechanism to sustained hypertensive conditions. Although Mel-TG still showed a higher LV mass index, LVH response was similar in both mice groups (Δ % LVMI 92±23% versus 103±16%).

At 8 weeks of AB, WT mice showed reduction in LV wall thickness with a concomitant increase in LV end-diastolic

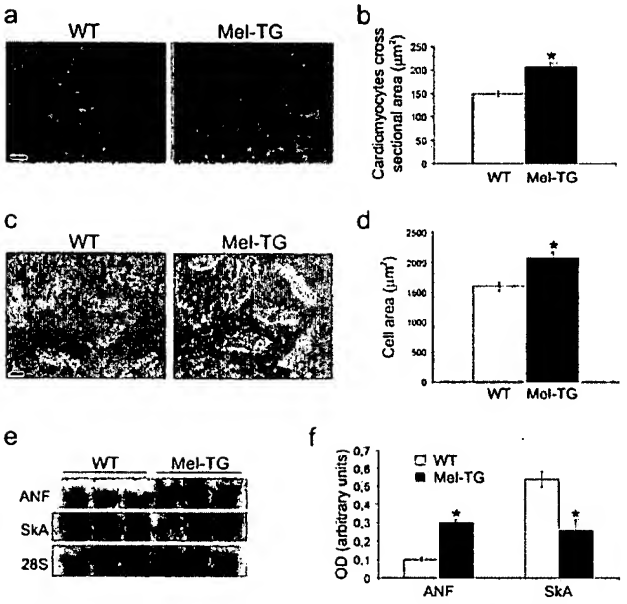


**Figure 2.** Melusin overexpression induces LV hypertrophy in basal condition. (a) Histological sections from WT and Mel-TG mice stained with hematoxylin-eosin. Scale bar:20 μm. (b) Cardiomyocyte cross-sectional area (30 sections from 3 mice per genotype). (c) Phase-contrast images of cardiomyocytes isolated from adult WT and Mel-TG hearts. Scale bar:20 μm. (d) Cell area (100 cardiomyocytes from 4 mice per genotype). (e) Northern blot for atrial natriuretic factor (ANF) and α-skeletal actin (SkA) on LV RNA. 28S rRNA as loading control. (f) Densitometric analysis on 6 mice per genotype normalized on 28S. (*): $P<0.05$ vs WT mice.

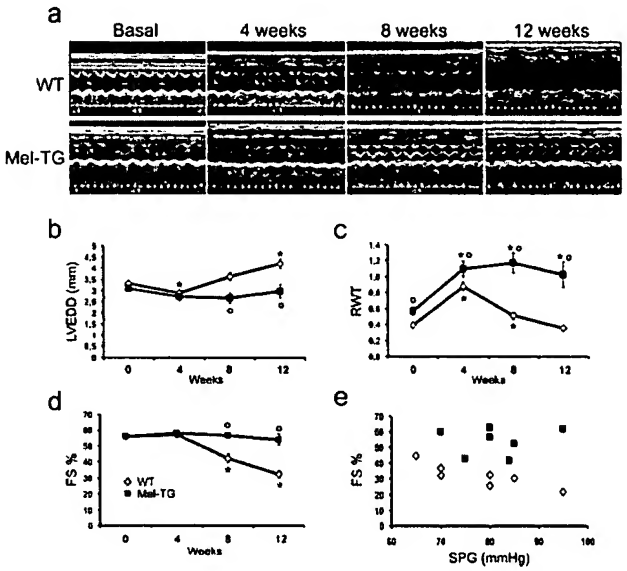


**Figure 3.** Melusin overexpression prevents LV dilation on prolonged pressure overload. (a) Representative M-mode LV echocardiographic recording of WT and Mel-TG in basal condition and after 4, 8, and 12 weeks of AB. Echocardiographic LV end diastolic diameter (LVEDD) (b), relative wall thickness (RWT) (c), and percent fractional shortening (FS%) (d). Relationship between systolic pressure gradient (SPG) and FS% in Mel-TG and WT mice after 12 weeks of AB (e). (*): $P<0.05$ vs basal conditions; (°):$P<0.05$ vs WT mice.

diameter (Table 2, Figure 3b) indicating an initial eccentric hypertrophic remodeling. Mel-TG mice, on the other hand, maintained values of LV wall thickness and diameters comparable to those developed after 4 weeks of AB. More importantly, systolic contractile function, as measured by fractional shortening (FS), was fully retained in Mel-TG, while significantly impaired in WT (Table 2, Figure 3d).

At 12 weeks of AB, WT mice showed a further dilation of the LV chamber combined with a greater thinning of the walls (Table 2, Figure 3a). These alterations were associated with a further reduction of contractile function, thus realizing the transition toward heart failure. In contrast, Mel-TG mice retained the LV concentric hypertrophy and systolic function detected at 8 weeks (Table 2, Figure 3). Hemodynamic evaluations indicated that, whereas WT mice showed a significantly reduced systolic function in terms of dP/dt max, Mel-TG preserved contractile function (Table 1). Moreover, maximum chamber elasticity (Emax) showed a significant increase in Mel-TG, but not in WT mice, further demonstrating a better contractile function in transgenic animals. Nevertheless, pressure overloaded LVs of both mice strains showed an impaired diastolic function, as detected by dP/dt min and $\tau$ Glantz.

SPG measured at 12 weeks of AB was similar in both study groups (Table 1). Finally, the relationship between SPG and FS revealed that Mel-TG mice show higher FS at any SPG studied, revealing the ability of melusin to protect against cardiac dysfunction in a wide range of pressure overload (Figure 3e).

All together these data indicate the ability of melusin overexpression to maintain concentric compensatory hypertrophic remodeling and to prevent the onset of heart failure.

## Melusin Overexpression Induces Increased Phosphorylation of AKT/GSK3$\beta$ and ERKs

Western blot analysis was performed to investigate the signaling events affected by melusin overexpression. Unstimulated LVs of Mel-TG mice showed increased Ser9 phosphorylation of GSK3$\beta$ as compared with WT (Figure 4a,b). Mel-TG hearts also showed increased level of ERK1/2 phosphorylation after normalization on total ERK1/2 which were expressed at higher levels in Mel-TG mice.

We then tested the activation of these pathways in response to AB. After 10 minutes of AB, GSK3$\beta$ was phosphorylated at a much higher level in Mel-TG compared with WT LV (Figure 4c,d). Similar differences were also observed for AKT, consistent with its role as a major kinase involved in Ser9 phosphorylation of GSK3$\beta$. ERK1/2 were also strongly phosphorylated in transgenic mice compared with WT. On the other hand, p38 phosphorylation in response to AB was not significantly different between the 2 mouse strains.

Increased phosphorylation of these signaling proteins in Mel-TG versus WT LVs persisted for the whole period of AB (Figure 4e,f). Increased phosphorylation of AKT in Mel-TG LVs at 12 weeks of AB was also detected by immunostaining of heart histological sections (not shown).

## AKT and ERKs Signaling Mediate Melusin-Induced Cardiomyocyte Growth

In order to test if AKT and ERK have a causative role in melusin-induced cardiomyocyte hypertrophy, in vitro experiments were performed. To induce melusin overexpression, cultured rat embryo cardiomyocytes were infected with a lentiviral vector coding for melusin (Figure 5a). Consistent with in vivo experiments in transgenic hearts, melusin overexpressing cardiomyocytes underwent pronounced hypertrophy as assessed by surface area measurements (Figure 5b,c). This response was strongly blunted by treatment either with PD98059, a MEK-1 inhibitor that prevented ERK1/2 phosphorylation (85% inhibition), or with a phosphatidylinositol analog inhibiting AKT (73% inhibition). These data indicate that, AKT and ERK play a crucial role in the hypertrophy response induced by melusin overexpression.

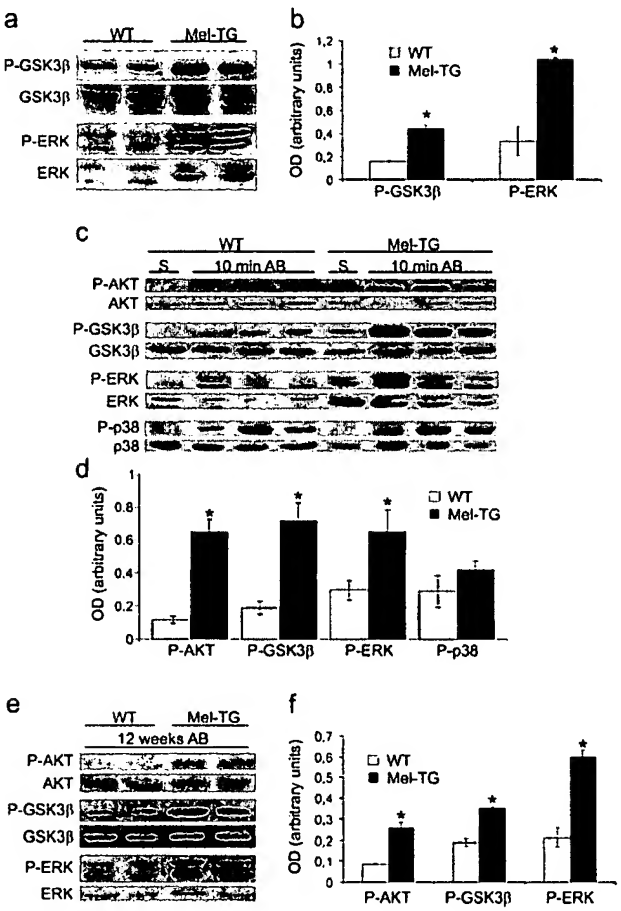


**Figure 4.** Melusin overexpression enhances phosphorylation of AKT, GSK3$\beta$, and ERK1/2. Representative western blot of WT and Mel-TG mice performed using antibodies to the indicated signaling molecules and their phosphorylated (P-) forms (a,c,e). Densitometric mean values of the phosphorylated species normalized to the expression level of the corresponding proteins (n=7 per genotype) (b,d,f). LV in basal conditions (a,b), of sham-operated mice (S) and mice subjected to 10 minutes (c,d) or 12 weeks of AB (e,f). (*): $P<0.05$ vs WT.

## Melusin Overexpression Protects From Apoptosis and Fibrosis Induced by Long-Standing Pressure Overload

As AKT, GSK3$\beta$, and ERK signaling can protect from apoptosis, we measured apoptotic index in hearts subjected to 12 weeks of pressure overload. WT LVs showed a high number of TUNEL-positive cells (Figure 6a,b), consistent

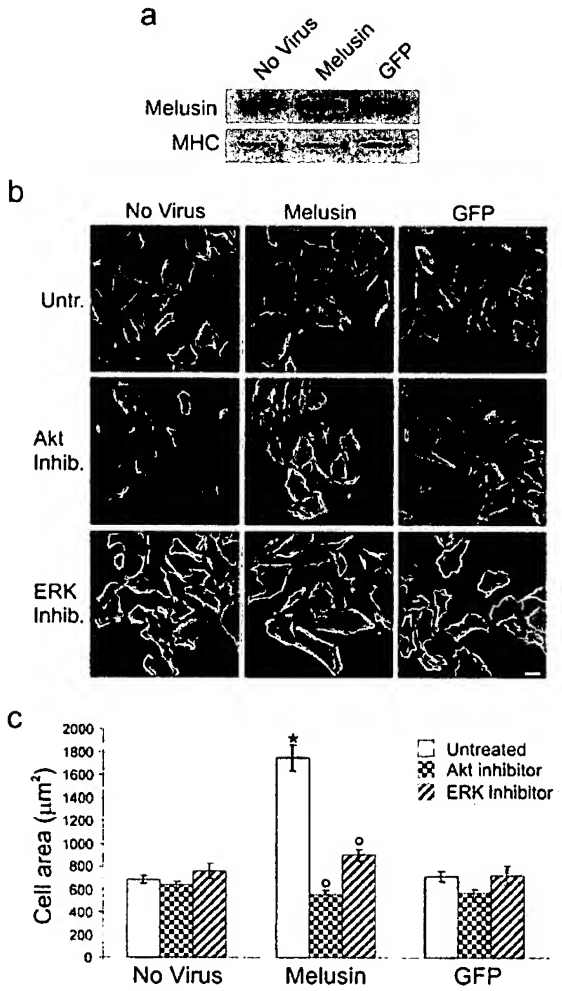


**Figure 5.** AKT and ERK signaling are required for melusin-induced cardiomyocyte growth. Rat embryo cardiomyocytes were infected with a lentiviral vector coding for melusin or GFP as control. Melusin expression detected by western blot analysis (a). Cardiomyocytes hypertrophy as assessed by surface area measurements (b,c). Melusin-induced hypertrophy was strongly blunted by treatment for 72 hours with either 50 μmol/L PD98059, an ERK1/2 inhibitor, or 20 μmol/L phosphatidylinositol analog inhibiting AKT phosphorylation (b,c). Cell areas were calculated on 70 cardiomyocytes for each group in 3 independent experiments. (*): $P<0.01$ versus no virus, (°): $P<0.01$ vs melusin untreated. Scale bar: 20 μm.

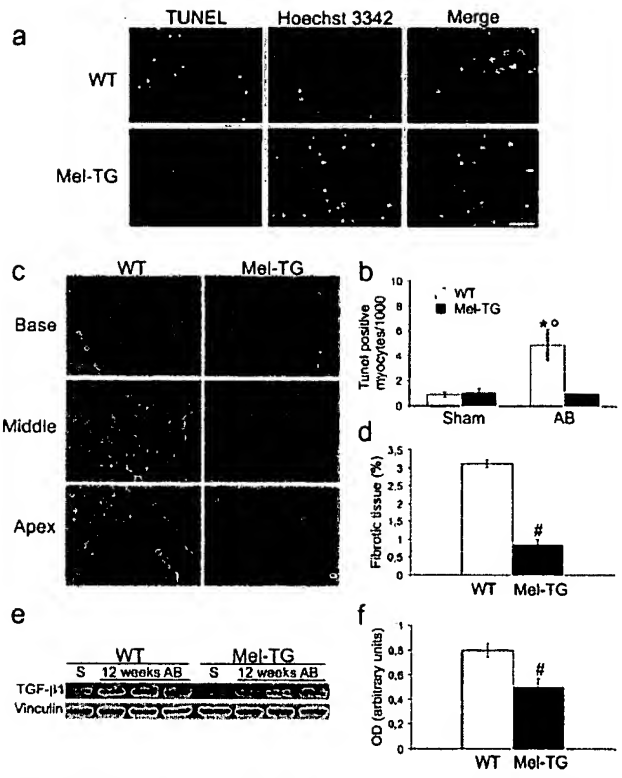


**Figure 6.** Melusin overexpression protects from cardiomyocyte apoptosis and prevents fibrotic tissue deposition induced by pressure overload. (a) TUNEL staining (red) on histological sections from WT and Mel-TG hearts subjected to 12 weeks of AB. Nuclei were counterstained with Hoechst-3342 (blue). Scale bars:100 μm and 10 μm (insets). (b) TUNEL-positive cardiomyocytes were quantified by counting only nuclei within myocytes. 30 histological sections from 3 different hearts per genotype. (c) Picrosirius red staining on histological sections from WT and Mel-TG LV after 12 weeks of AB. Scale bar:100 μm. (d) Fibrotic area quantified by image-analyzing system on histological sections from 3 different hearts per genotype (10 sections/mouse) and expressed as percentage of LV wall area. (e) Western blot analysis of TGF-β1 from WT and Mel-TG LV after sham operation (S) and 12 weeks of AB. Vinculin was used as sample loading control. Three representative mice per genotype are shown. (f) Mean values of TGF-β 1 expression from 7 banded hearts per genotype obtained by densitometric analysis. (*): $P<0.05$ vs sham; (°): $P<0.05$ versus Mel-TG after AB. (#): $P<0.05$ vs WT.

with previous reports indicating that apoptosis is a major event involved in the onset of heart failure on prolonged pressure overload.[10] In contrast, Mel-TG LV subjected to 12 weeks of pressure overload showed a number of TUNEL-positive cardiomyocytes not significantly different from that of sham-operated mice.

Heart sections were also stained with Picrosirius red to detect fibrosis. Deposition of stromal connective tissue was strongly reduced in melusin transgenic LV after 12 weeks of pressure overload compared with WTs (Figure 6c and 6d). Western blot analysis further indicated that after AB levels of TGF-β1, a major pro-fibrotic cytokine, were 47% lower in Mel-TG LV (Figure 6e and 6f).

After 12 weeks of pressure overload, capillary density, a parameter that participates in heart remodeling, was 26.3% higher in Mel-TG LV compared with WT ($P<0.05$).

## Melusin Overexpression Regulates Genes Involved in Fibrosis and Inflammation

Global transcriptome analysis in WT and Mel-TG LV subjected to AB for 12 weeks was performed using an oligonucleotide array representing ≈13 000 mouse genes. LV samples from 2 different Mel-TG mice were compared in competitive hybridization to WT, and experiments were repeated twice. Comparison of the expression profile revealed 110 differentially expressed genes, 68 underexpressed and 42 overexpressed in Mel-TG hearts compared with WT. The complete dataset is reported at http://muscle.cribi.unipd.it/microarrays/melusin/. Genes coding for extracellular matrix proteins, leukocyte markers, and cytokines were the largest functionally related gene clusters differentially expressed in the 2 mice strains. This strongly indicates that fibrosis and inflammation are significantly depressed in Mel-TG versus WT LVs subjected to chronic pressure overload (Online

Table 1). Interestingly, kallikrein, a protease capable of releasing kinins and inducing collagen breakdown, was upregulated in Mel-TG consistently with its role as an antifibrotic gene.[11,12] Moreover, SkA was greatly reduced in Mel-TG versus WT banded hearts, thus confirming that reduced expression of SkA is characteristically retained during the 12 weeks of hypertrophic remodeling.

## Discussion

Here we report that overexpression of melusin, a recently described integrin-binding protein,[3] in hearts of transgenic mice, induceds a modest, but significant, level of LVH in basal condition. Moreover, in response to chronic pressure overload, melusin overexpression allows sustained compensatory LVH and prevents the transition toward heart failure. Because loss of melusin causes reduced LVH followed by heart dilation and failure in response to hemodynamic overload,[4] we conclude that melusin is an important molecule controlling beneficial remodeling of LV.

The protection against heart failure observed in Mel-TG subjected to aortic constriction could be influenced, at least initially, by the presence of a basal LVH leading to reduced wall stress. Recent experimental evidence, however, indicate that normalization of wall stress is not crucial to prevent the evolution toward cardiac dysfunction in response to pressure overload. In fact, mice defective for Gq signaling and for norepinephrine synthesis do not develop heart failure despite markedly blunted cardiac growth response to pressure overload and abnormally higher wall stress.[13] Thus, normalization of wall stress is not the main variable in the evolution of overloaded hearts toward heart failure, but other factors such as the quality of cardiac hypertrophy can play a crucial role.

LV adaptive hypertrophy induced by melusin overexpression showed specific molecular features. In particular, analysis of LVH markers indicated that SkA, a prominent fetal actin isoform, is downregulated in Mel-TG heart versus WT both in basal conditions and after 12 weeks of AB. Consistent with the hypothesis of melusin acting as a stretch sensor downstream integrin signaling, SkA gene promoter is silenced in cultured fibroblast stretched by mechanical force applied to $\beta$1 integrin with collagen-coated magnetic beads.[14] In contrast, SkA is upregulated in experimental mouse models of chronic pressure overload and in human heart failure,[15] but downregulated or unchanged in exercise-induced cardiac hypertrophy.[16] The finding that SkA was downregulated in Mel-TG versus WT LV suggests that, in conditions of pressure overload, cardiac hypertrophy in Mel-TG partially mimics that observed in exercise-induced cardiac hypertrophy.

An additional feature of LVH of Mel-TG mice is absence of fibrosis as detected by both histological analysis and gene profiling experiments. This could be ascribed to negative regulation of well-known profibrotic factors such as TGF-$\beta$ 1, and to upregulation of antifibrotic factors such as kallikrein. In this respect it is worth noting that forced expression of kallikrein gene in heart of diabetic rats prevents fibrosis and ameliorates ventricle function.[14] Accumulation of stromal tissue represents a deleterious feature of LVH affecting the viscoelastic properties of the myocardium, impairing diastolic function and favoring the transition toward heart failure. The reduced fibrosis in Mel-TG overloaded LV could lead to improvement of diastolic function. This, however, was not the case since impairment of LV diastolic function was comparable in Mel-TG and WT mice in conditions of pressure overload. Indeed, fibrosis is only one of several determinants of diastolic function,[17] and hypertensive conditions represent another crucial factor, evoking an impairment of LV diastolic function independently of their impact on cardiac hypertrophic remodeling.[18] Thus, the hypertensive conditions imposed by AB in both Mel-TG and WT mice may mask the impact on diastolic function of reduced fibrosis.

Finally, additional important features of AB-induced heart remodeling in Mel-TG mice are reduced inflammatory reaction and increased capillary density, two additional features of the exercise-induced hypertrophy.[19]

Previous findings have shown that melusin ablation impairs phosphorylation of AKT and GSK3$\beta$[4] in response to pressure overload. Here we show that, in basal conditions, Mel-TG hearts display higher GSK3$\beta$ and ERK1/2 phosphorylation. Moreover, these phosphorylations are further increased in Mel-TG LV after pressure overload and maintain a higher level over WT after 12 weeks of AB. Interestingly, inhibitors of AKT and ERK1/2 block melusin-induced hypertrophy in cultured rat embryo cardiomyocytes. These data, although obtained in a cell culture model with growth features different from those of adult cardiomyocytes, support a causative role for AKT and ERK1/2 in melusin-induced LVH. The mechanisms by which melusin controls AKT phosphorylation are unknown at present. Several examples of adaptor proteins devoid of enzymatic activity, such as Shc and Grb2, and p130Cas are known to regulate different kinases. The most likely hypothesis is that melusin can function as an adaptor molecule interacting with proteins regulating AKT activation. AKT controls phosphorylation of mTor, p70S6K and GSK3$\beta$, three serine/threonine kinases responsible for increased protein synthesis. Forced expression of constitutively active AKT in the heart of transgenic mice induces increased cardiomyocyte size and concentric hypertrophy in the absence of fibrosis with preserved systolic function.[20] In addition expression of a nonphosphorylable form of GSK3$\beta$ prevents LVH in response to pressure overload as well as other hypertrophic stimuli.[21] In agreement with these findings, lack of GSK3$\beta$ phosphorylation in response to pressure overload is associated with reduced LVH and development of dilated cardiomyopathy,[4,22] pointing to an important role of melusin-induced AKT and GSK3$\beta$ overphosphorylation to sustain an adaptive concentric LVH.

A number of studies implicate ERK1/2 signaling as an important regulator of LVH.[23] In particular, overexpression of MEK1, an upstream activator of ERK1/2, in transgenic mice leads to development of compensatory LVH.[24] The increased ERK1/2 phosphorylation observed in Mel-TG heart, both in basal condition and after AB is, thus, in line with the compensated hypertrophy phenotype observed in our transgenic mice.

AKT, GSK3$\beta$, and ERK1/2 are among the main signaling proteins involved in the anti apoptotic machinery.[25] AKT inhibits caspase 9 and the proapoptotic molecule Bad, stimulates the prosurvival factor Bcl-2, and phosphorylates fork-

head transcription factors, repressing their ability to promote proapoptotic genes. In addition, transgenic mice overexpressing MEK1 in the heart show reduced cardiomyocyte apoptosis in a model of ischemia-reperfusion injury.[26] GSK3$\beta$ is also involved in protecting cardiomyocytes against apoptosis by regulating the mitochondrial permeability transition pore complex, which plays a central role in mitochondria-mediated cell death.[27] Involvement of these signaling molecules downstream melusin can, thus, explain the protection from apoptosis observed in transgenic hearts subjected to pressure overload.

In conclusion these data indicate that melusin overexpression allows sustained concentric compensatory cardiac hypertrophy in response to chronic pressure overload. LV remodeling in Mel-TG mice displays several features observed in hearts undergoing hypertrophy in response to physical training such as reduced fibrosis, apoptosis and inflammation and increased capillary density. This is likely to occur through the regulation of protective pathways maintaining a proportional balance between cardiac muscle and stromal tissue in overloaded LV. Because melusin expression increases in compensated hypertrophic LV subjected to pressure overload, but returns to basal level in dilated heart, upregulation of melusin expression could represent a novel strategy to activate beneficial signaling in LV remodeling and prevent the transition toward heart failure in response to hemodynamic overload.

## Acknowledgments

This work was supported by grants from: Telethon to GT; Ministry of University and Research (FIRB, and PRIN) to GT and GL; Ministry of Health to GL. We wish to thank Ornella Azzolino, Immacolata Carfora and Giovanni Russo for technical assistance; Daniela Bongioanni, for helping in some experiments; Luigi Naldini and Elisa Vigna for providing lentiviral vectors and helping in virus production.

## References

1. Hunter JJ, Chien KR. Signaling pathways for cardiac hypertrophy and failure. *N Engl J Med.* 1999;341:1276–1283.
2. Frey N, Olson EN. Cardiac hypertrophy: the good, the bad, and the ugly. *Annu Rev Physiol.* 2003;65:45–79.
3. Brancaccio M, Guazzone S, Menini N, Sibona E, Hirsch E, De Andrea M, Rocchi M, Altruda F, Tarone G, Silengo L. Melusin is a new muscle-specific interactor for beta(1) integrin cytoplasmic domain. *J Biol Chem.* 1999;274:29282–29288.
4. Brancaccio M, Fratta L, Notte A, Hirsch E, Poulet R, Guazzone S, De Acetis M, Vecchione C, Marino G, Altruda F, Silengo L, Tarone G, Lembo G. Melusin, a muscle-specific integrin beta1-interacting protein, is required to prevent cardiac failure in response to chronic pressure overload. *Nat Med.* 2003;9:68–75.
5. Gulick J, Subramaniam A, Neumann J, Robbins J. Isolation and characterization of the mouse cardiac myosin heavy chain genes. *J Biol Chem.* 1991;266:9180–9185.
6. Vecchione C, Fratta L, Rizzoni D, Notte A, Poulet R, Porteri E, Frati G, Guelfi D, Trimarco V, Mulvany MJ, Agabiti-Rosei E, Trimarco B, Cotecchia S, Lembo G. Cardiovascular influences of alpha1b-adrenergic receptor defect in mice. *Circulation.* 2002;105:1700–1707.
7. Wolska BM, Solaro RJ. Method for isolation of adult mouse cardiac myocytes for studies of contraction and microfluorimetry. *Am J Physiol.* 1996;271:H1250—H1255.
8. Kaddoura S, Firth JD, Boheler KR, Sugden PH, Poole-Wilson PA. Endothelin-1 is involved in norepinephrine-induced ventricular hypertrophy in vivo. Acute effects of bosentan, an orally active, mixed endothelin ETA and ETB receptor antagonist. *Circulation.* 1996;93:2068–2079.
9. Bonci D, Cittadini A, Latronico MV, Borello U, Aycock JK, Drusco A, Innocenzi A, Follenzi A, Lavitrano M, Monti MG, Ross J Jr, Naldini L, Peschle C, Cossu G, Condorelli G. 'Advanced' generation lentiviruses as efficient vectors for cardiomyocyte gene transduction in vitro and in vivo. *Gene Ther.* 2003;10:630–636.
10. Condorelli G, Morisco C, Stassi G, Notte A, Farina F, Sgaramella G, de Rienzo A, Roncarati R, Trimarco B, Lembo G. Increased cardiomyocyte apoptosis and changes in proapoptotic and antiapoptotic genes bax and bcl-2 during left ventricular adaptations to chronic pressure overload in the rat. *Circulation.* 1999;99:3071–3078.
11. Tschope C, Walther T, Koniger J, Spillmann F, Westermann D, Escher F, Pauschinger M, Pesquero JB, Bader M, Schultheiss HP, Noutsias M. Prevention of cardiac fibrosis and left ventricular dysfunction in diabetic cardiomyopathy in rats by transgenic expression of the human tissue kallikrein gene. *Faseb J.* 2004;18:828–835.
12. Gallagher AM, Yu H, Printz MP. Bradykinin-induced reductions in collagen gene expression involve prostacyclin. *Hypertension.* 1998;32:84–88.
13. Esposito G, Rapacciuolo A, Naga Prasad SV, Takaoka H, Thomas SA, Koch WJ, Rockman HA. Genetic alterations that inhibit in vivo pressure-overload hypertrophy prevent cardiac dysfunction despite increased wall stress. *Circulation.* 2002;105:85–92.
14. Lew AM, Glogauer M, McUlloch CA. Specific inhibition of skeletal alpha-actin gene transcription by applied mechanical forces through integrins and actin. *Biochem J.* 1999;341(Pt 3):647–653.
15. Haase D, Lehmann MH, Korner MM, Korfer R, Sigusch HH, Figulla HR. Identification and validation of selective upregulation of ventricular myosin light chain type 2 mRNA in idiopathic dilated cardiomyopathy. *Eur J Heart Fail.* 2002;4:23–31.
16. Diffee GM, Seversen EA, Stein TD, Johnson JA. Microarray expression analysis of effects of exercise training: increase in atrial MLC-1 in rat ventricles. *Am J Physiol Heart Circ Physiol.* 2003;284:H830—H837.
17. Zile MR, Brutsaert DL. New concepts in diastolic dysfunction and diastolic heart failure: Part II: causal mechanisms and treatment. *Circulation.* 2002;105:1503–1508.
18. Gelpi RJ, Pasipoularides A, Lader AS, Patrick TA, Chase N, Hittinger L, Shannon RP, Bishop SP, Vatner SF. Changes in diastolic cardiac function in developing and stable perinephritic hypertension in conscious dogs. *Circ Res.* 1991;68:555–567.
19. Brodal P, Ingjer F, Hermansen L. Capillary supply of skeletal muscle fibers in untrained and endurance-trained men. *Am J Physiol.* 1977;232:H705–H712.
20. Condorelli G, Drusco A, Stassi G, Bellacosa A, Roncarati R, Iaccarino G, Russo MA, Gu Y, Dalton N, Chung C, Latronico MV, Napoli C, Sadoshima J, Croce CM, Ross J Jr. Akt induces enhanced myocardial contractility and cell size in vivo in transgenic mice. *Proc Natl Acad Sci U S A.* 2002;99:12333–12338.
21. Antos CL, McKinsey TA, Frey N, Kutschke W, McAnally J, Shelton JM, Richardson JA, Hill JA, Olson EN. Activated glycogen synthase-3 beta suppresses cardiac hypertrophy in vivo. *Proc Natl Acad Sci U S A.* 2002;99:907–912.
22. Badorff C, Ruetten H, Mueller S, Stahmer M, Gehring D, Jung F, Ihling C, Zeiher AM, Dimmeler S. Fas receptor signaling inhibits glycogen synthase kinase 3 beta and induces cardiac hypertrophy following pressure overload. *J Clin Invest.* 2002;109:373–381.
23. Bueno OF, Molkentin JD. Involvement of extracellular signal-regulated kinases 1/2 in cardiac hypertrophy and cell death. *Circ Res.* 2002;91:776–781.
24. Bueno OF, De Windt LJ, Tymitz KM, Witt SA, Kimball TR, Klevitsky R, Hewett TE, Jones SP, Lefer DJ, Peng CF, Kitsis RN, Molkentin JD. The MEK1-ERK1/2 signaling pathway promotes compensated cardiac hypertrophy in transgenic mice. *Embo J.* 2000;19:6341–6350.
25. Datta SR, Brunet A, Greenberg ME. Cellular survival: a play in three Akts. *Genes Dev.* 1999;13:2905–2927.
26. Lips DJ, Bueno OF, Wilkins BJ, Purcell NH, Kaiser RA, Lorenz JN, Voisin L, Saba-El-Leil MK, Meloche S, Pouyssegur J, Pages G, De Windt LJ, Doevendans PA, Molkentin JD. MEK1-ERK2 signaling pathway protects myocardium from ischemic injury in vivo. *Circulation.* 2004;109:1938–1941.
27. Juhaszova M, Zorov DB, Kim SH, Pepe S, Fu Q, Fishbein KW, Ziman BD, Wang S, Ytrehus K, Antos CL, Olson EN, Sollott SJ. Glycogen synthase kinase-3beta mediates convergence of protection signaling to inhibit the mitochondrial permeability transition pore. *J Clin Invest.* 2004;113:1535–1549.

# Deletion of the α(1,3)galactosyl transferase (*GGTA1*) gene and the prion protein (*PrP*) gene in sheep

C. Denning†, S. Burl†, A. Ainslie, J. Bracken, A. Dinnyes, J. Fletcher, T. King, M. Ritchie, W. A. Ritchie, M. Rollo, P. de Sousa, A. Travers, I. Wilmut, and A. J. Clark*

Nuclear transfer offers a cell-based route for producing precise genetic modifications in a range of animal species. Using sheep, we report reproducible targeted gene deletion at two independent loci in fetal fibroblasts. Vital regions were deleted from the α(1,3)galactosyl transferase (*GGTA1*) gene, which may account for the hyperacute rejection of xenografted organs, and from the prion protein (*PrP*) gene, which is directly associated with spongiform encephalopathies in humans and animals. Reconstructed embryos were prepared using cultures of targeted or nontargeted donor cells. Eight pregnancies were maintained to term and four $PrP^{-/+}$ lambs were born. Although three of these perished soon after birth, one survived for 12 days. These data show that lambs carrying targeted gene deletions can be generated by nuclear transfer.



Gene targeting in embryonic stem (ES) cells is a powerful tool for modifying the genome of mice[1]. In other species, ES cells that contribute to the germline are not available, limiting widespread use of the technique. With the development of nuclear transfer in livestock species[2–4], genetically engineered somatic cells can be used to modify the genome. Previously, transgenic sheep expressing the human Factor IX gene in the mammary gland were produced by this route after random integration of the transgene into donor cell nuclei[4]. More recently, viable animals have been produced after gene targeting was used to precisely insert human α1-antitrypsin (AAT) sequences into the *COL1A1* locus[5], although the insertion site was specifically selected so as not to disrupt type 1 collagen protein function or expression. Targeted gene disruption is essential when complete deletion of gene function is required.

Animals potentially offer an alternative source of tissue for transplantation. A major barrier to successful xenotransplantation is presented by preformed antibodies that recognize the disaccharide galactose-α(1,3)-galactose, leading to hyperacute rejection[6]. Synthesis of galactose-α(1,3)-galactose is catalyzed by the enzyme α(1,3)galactosyl transferase, which is present in all organisms except catarrhines (Old World monkeys, apes, and humans). The hypothesis that deletion of this gene from the germline of donor species may eliminate a substantial component of hyperacute rejection needs to be tested in a large-animal model. Although the pig has been highlighted as the ideal choice for xenotransplantation, concerns have been raised about anatomical incompatibilities with humans[7] and the retroviral load of the porcine genome[8]. Sheep lacking α(1,3)galactosyl transferase could be used to determine the importance of galactose-α(1,3)-galactose in graft rejection, to develop immunosuppression regimes, and to provide tissues for xenotransplantation.

Prions, encoded by the *PrP* gene, are a novel form of infectious agent that cause spongiform encephalopathies in humans and animals[9]. Prions have assumed tremendous importance because of the bovine spongiform encephalopathy (BSE) epidemic and the concern that there has been cross-species transmission to humans, resulting in a new and highly lethal form of Creutzfeld–Jacob disease. Experiments with *PrP* gene knockout mice have shown that these animals do not replicate the prion gene and are resistant to scrapie[10,11]. Because sheep, and particularly cattle, have functional *PrP* genes and are used to produce biomedical products such as gelatin, collagen, and, increasingly, human proteins after genetic modification, it may be appropriate to produce prion-resistant populations.

We therefore selected the *GGTA1* and *PrP* genes as candidates for deletion from sheep. In addition, genetically engineered mice without one or the other of these genes show no gross deleterious effects[12–14], indicating that they would be appropriate targets to develop gene disruption technology in livestock. Here we report use of nuclear transfer to produce sheep that have targeted gene deletions.

## Results and discussion

The ovine *PrP* gene has previously been cloned and characterized. Three exons span 21 kilobases of genomic DNA, with the 770 base pair coding region contained entirely within the final exon[15]. Comparable data for the *GGTA1* gene were not available, although the coding sequence was known for other species[16,17]. Using primers that functioned across species in a reverse transcriptase–polymerase chain reaction (RT-PCR), we isolated an 1,110 base pair ovine *GGTA1* complementary DNA (cDNA), which showed 83% and 95% homology to murine and bovine sequences, respectively. A 193 base pair 5′-untranslated region was extended by rapid amplification of cDNA ends (RACE) PCR, although it appears to be truncated compared with the corresponding region in the mouse gene.

To generate targeting vectors, we used *GGTA1* or *PrP* DNA probes to screen a genomic library prepared from tissue culture cells derived from a day 35 Black Welsh fetus. The coding exons of the *GGTA1* gene span ~20 kilobases of genomic DNA and were designated 4 to 9 (Fig. 1), because translation initiation occurs in exon 4 of the well-characterized mouse gene[16]. The *PrP*-hybridizing phage were analyzed and had the same sequence and restriction pattern as in the published data[15].

The *GGTA1* and *PrP* genes are expressed in fetal fibroblasts (data not shown), permitting use of the promoter trap targeting strategy[18]. In the vectors constructed, the neomycin phosphotransferase (*neo*) gene was

*Department of Gene Expression and Development, Roslin Institute, Roslin, Midlothian EH25 9PS, United Kingdom. *Corresponding author (John.Clark@bbsrc.ac.uk). †These two authors contributed equally to this work.*

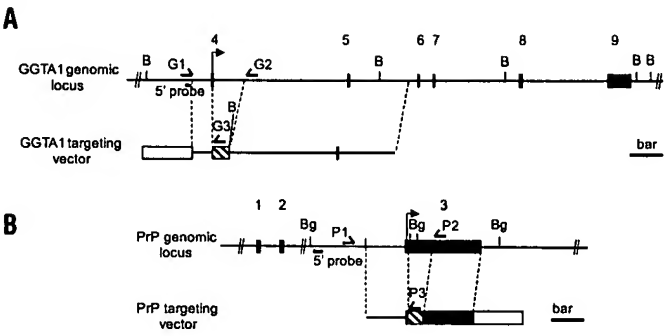


**Figure 1.** Organization of the genomic loci of ovine (A) *GGTA1* or (B) *PrP* genes and the promoterless targeting vectors used for disruption. Numbering of the exons in *GGTA1* is based on the mouse; translation initiates in exon 4 and terminates in exon 9. Targeting deletes exon 4 and 1.4 kb of intron 4, and a *Bam*HI site (labeled B) is inserted. The coding sequence of *PrP* is entirely within exon 3; targeting deletes this region and two *Bgl*I sites (labeled Bg). Arrows indicate translation initiation sites. Black boxes represent exons, hatched boxes represent *neo*-pA sequence, and open box represents pBlueScript sequence. Location of PCR primers (*GGTA1* uses G1/2 and G1/3; *PrP* uses P1/2 and P1/3) and the 5′ external probes for Southern blot analysis are shown. Scale bar represents 2 kb.

placed directly adjacent to the initiation codon of the target genes (Fig. 1). The *PrP* targeting vector does not delete the splice acceptor site of exon 3, a component of the gene that must be retained to generate knockout mice that are clinically healthy and do not have a grossly aberrant phenotype[14]. Linearized *GGTA1* or *PrP* vectors (10 μg) were transfected into early-passage BW6F2 karotypically normal male (54XY) cells. After 12 days of G418 selection, 877 and 533 colonies had grown in the *GGTA1* and *PrP* experiments, respectively (Table 1).

Initially, we used two independent PCR reactions to detect targeting events for each construct. Using this strategy, we demonstrated that 1.1% (10) or 10.3% (55) of the *GGTA1* or *PrP* BW6F2 neomycin-resistant ($neo^R$) colonies contained correctly targeted cells (Table 1). However, in terms of selecting a clonal targeted population with a stable karyotype that could be expanded for use in several nuclear transfer (NT) experiments, only one colony ($PrP^{-/+}$, termed YH6) was suitable (Table 1; Fig. 2B, lane 1). Many targeted colonies also contained nontargeted cells, as indicated by the greater intensity of the PCR band from the nontargeted allele compared with that of the targeted allele. More importantly, a substantial number of colonies (4/5 *PrP* and 8/8 *GGTA1*) with only targeted cells senesced before they could be prepared for nuclear transfer (Table 1). The high attrition rate of targeted clonal populations suitable for nuclear transfer (Table 1) represents one of the major hurdles of gene targeting in primary somatic cells.

Targeting experiments at the *GGTA1* locus were continued using a different primary cell culture, 7G65F4, isolated from a Finn Dorset fetus. These cells were in culture for 6 days before electroporation, compared with ~14 days for the BW6F2 cells used before. Targeting events were detected at a frequency of 6.2% (35 of 568). Ultimately, two *GGTA1*-targeted colonies (3C6 and 5E1) suitable for nuclear transfer were isolated (Table 1; Fig. 2A, lanes 1 and 4).

We have shown targeting frequencies in $neo^R$ clones of 1.1 and 6.2% for the *GGTA1* locus and of 10.3% for the *PrP* locus. These are upper estimates, as the data include a substantial proportion of mixed clones, but correspond to an overall targeting frequency of 1–10 per $10^6$ cells. Recently McCreath and colleagues[5] reported targeting efficiencies of 7.1, 13.8, and 65.7% in the ovine *COL1A1* locus in Poll Dorset fetal fibroblasts. The high average efficiency in these experiments may be attributable to high endogenous expression or intrinsic recombinogenic activity at this locus. Alternatively, the vector used by these workers had contiguous regions of homology with the chromosomal locus and did not delete any of the *COL1A1* gene. By contrast, to ensure effective disruption of the *GGTA1* and *PrP* genes, we deleted endogenous coding sequence with *neo*-polyA sequence using noncontiguous regions of homology.

Targeted (3C6, 5E1, or YH6) and control cells (4H2, with a random integration of the *GGTA1* targeting vector: Fig. 2A, lane 7; 7G65F4, nontransfected parental line) were prepared for nuclear transfer by culturing in low- (0.5%) serum medium for three to five days. Donor cells were fused to enucleated Poll Dorset oocytes, as described[2]. A total of 120 morulae or blastocysts were transferred to 78 Finn Dorset final recipients, which produced 39 pregnancies at day 35. The oldest *GGTA1*-targeted fetuses died *in utero* at 118 and 130 days (term 148 days). Eight pregnancies were maintained to term (two 7G65F4, one 4H2, five YH6), resulting in four live births derived from the *PrP*-deleted line, YH6. Three of these lambs perished soon after birth. One lived for 12 days (Table 2; Fig. 3) but was euthanized after developing dyspnea due to pulmonary hypertension and right-sided heart failure, common abnormalities in cloned sheep.

The high incidence of mortality reported here may indicate that genetic modification or prolonged culture is detrimental to development. Although comparison of the developmental stages revealed similar efficiencies of progression from targeted cells, nontargeted cells with random integration, and untransfected cultures (blastocyst, 10–31%; day 35, 3.3–6.7%; day 60, 0–4.4%, referenced to embryos transferred or cultured; Table 2), we observed a high incidence of mortality at and soon after birth. This contrasts with other studies using unmodified, early-passage sheep cells[2–4]. However, it is consistent with a recent report[5] of gene insertion in sheep; although two targeted animals survived beyond three months, there was a high incidence of perinatal and postnatal mortality. Thus prolonged culture, in combination with the stringent selection required for somatic gene targeting, may produce cell lines that are less competent at producing viable clones.

When possible, autopsies were performed. The range of abnormalities found was consistent among the different groups. The predominant findings were hydroallantois, distention of the liver caused by congestion (suggestive of cardiac insufficiency), insufficient placentation indicated by reduced numbers and size of cotyledons, and kidney dysplasia manifested by enlarged renal pelvis with narrowed cortex and medulla. All these defects have been described in other nuclear transfer experiments with nontrans-

**Table 1. Efficiency of gene targeting in ovine somatic cells**

| Parental primary culture | Target gene | G418-resistant colonies | Total targeting events detected[a] | Mixed colonies[b] | Senesced[c] | Unstable[d] karyotype | Targeted colonies suitable for NT |
|---|---|---|---|---|---|---|---|
| BW6F2 | *GGTA1* | 877 | 10 | 2 | 8 | 0 | 0 |
| BW6F2 | *PrP* | 533 | 55 | 50 | 4 | 0 | 1 (YH6) |
| 7G65F4 | *GGTA1* | 568 | 35 | 17 | 15 | 1 | 2 (3C6, 5E1) |

[a]Total number of targeting events detected by the initial PCR screens.
[b]Colonies were scored as mixed when the amplified band from the nontargeted locus was more intense than the targeted locus in the second PCR screen.
[c]Colonies were scored as senesced when cell numbers could not be seen to increase after seven days.
[d]The normal karyotype of these cells was 54XY.

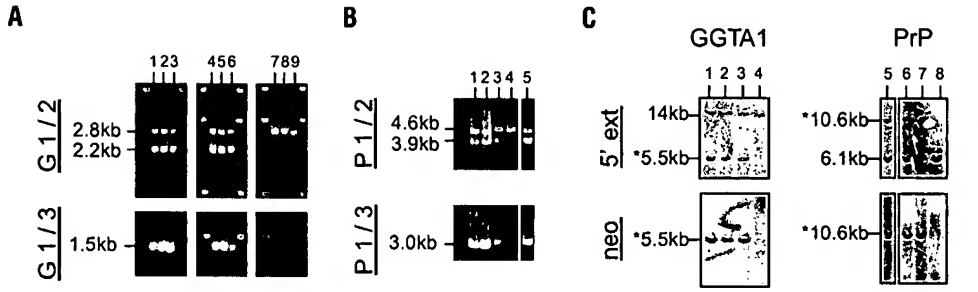


**Figure 2.** Targeted mutations are retained through development. DNA was isolated from cells before nuclear transfer or from derived fetuses, then analyzed by PCR and Southern blot. Samples with a targeted allele are indicated by an asterisk (*). See Figure 1 for location of primers and probes. (A) *GGTA1* PCR. Lanes 1, 2, and 3 show 3C6* cells, and fetuses at day 85* and day 118*. Lanes 4, 5, and 6 show 5E1* cells, and fetuses at day 49* and day 49*. Lanes 7, 8, and 9 show 4H2 cells, and fetuses at day 49 and day 148. (B) *PrP* PCR. Lane 4 shows nontargeted parental cells. Lane 1 shows YH6* cells. Lanes 2 and 3 show lambs carried to term*. Lane 5 shows the targeted lamb that survived to 12 days*. (C) Southern blot analysis. *GGTA1* samples were digested with *Bam*HI. The targeted allele hybridizes with the 5′ and neo probes; lanes 1, 2, and 3 show samples from fetuses at day 118*, day 49*, and day 49*. Lane 4 shows a nontargeted sample. *PrP* samples were digested with *Bgl*I. Lane 5 shows the targeted lamb that survived to 12 days*. Lanes 6 and 7 show samples from fetuses at term*. Lane 8 shows a nontargeted sample.

**Figure 3.** $PrP^{-/+}$ lamb photographed at six days postpartum.

fected cells[2,5,19,20]. We did not expect abnormal phenotypes as a direct result of the gene disruption because we modified only one allele at a dominant locus. Furthermore, null mice for *GGTA1* or *PrP* are healthy[12–14].

Tissue was recovered from fetuses and lambs for both PCR and Southern blot analysis. Data are shown for fetuses ranging from day 49 to 148 (term) of pregnancy. The two PCR screens for each locus revealed patterns consistent with targeting (Fig. 2) in all the samples that were recovered. In Southern blot analyses, both 5′ (external) and neo coding sequence (internal) probes hybridized to restriction fragments of the correct size. The location of probes and restriction sites is shown in Figure 1; representative Southern blots are shown in Figure 2. These data show that lambs carrying targeted gene deletions can be generated by nuclear transfer.

Our results, together with the recent report of sequence insertion at the ovine *COL1A1* locus[5], indicate that targeted homologous recombination has been demonstrated at three independent loci in cells derived from different breeds of sheep. This suggests that the technology can be used to disrupt many different genes in the ovine genome. We found, however, that the number of targeted clones suitable for nuclear transfer was low. A major barrier was that many of the clonal populations reached proliferative senescence. The bulk populations of the primary cultures we used divide ~100 times before senescing, a large excess compared to the estimated 45 doublings required for targeting and preparation for nuclear transfer[21]. A likely explanation is that there is considerable heterogeneity of life span in the culture, with many of the selected colonies having a life span considerably shorter than 100 doublings.

The death of the targeted fetuses and lambs emphasizes the need to improve the efficiency of the technology. Once this is achieved, effective ablation of gene function will usually require both alleles to be disrupted. Given the limited proliferative capacity of cells currently used in nuclear transfer, achieving this from a single clonal population will be difficult. Alternatively, conventional breeding could be used with animals surviving to reproductive maturity. However, this would take a minimum of 18 months in sheep, even if the modification were introduced simultaneously into male and female cells and the cloned animals interbred. A different approach would be to clone by nuclear transfer from the cells in which the first allele has been targeted, re-isolate cell lines from the cloned fetal material, and then target the second locus in these cells[22,23]. Ultimately, however, the fastest route to multiple genetic changes would be to extend the window to achieve targeting, either by increasing the overall efficiency of targeting or by using cells with an extended life span that still retain their totipotency for nuclear transfer.

**Table 2. Nuclear transfer from gene-targeted primary cells[a]**

| Stage of nuclear transfer | Cells used for nuclear transfer | | | | |
|---|---|---|---|---|---|
| | 3C6 | 5E1 | 4H2 | 7G65F4 | YH6 |
| Embryos transferred into temporary recipients[b] (*in vitro* cultured) | 87 (25) | 0 (30) | 92 (31) | 55 (71) | 273 (181) |
| Embryos recovered from temporary recipients | 85 | – | 62 | 55 | 214 |
| Morula or blastocyst[b]: *in vivo* (*in vitro*) | 18 (7) | 0 (3) | 19 (8) | 12 (27) | 44 (3) |
| Embryos transferred to final recipients | 18 | 3 | 23 | 33 | 43 |
| Final recipients | 12 | 3 | 17 | 18 | 28 |
| Fetuses at day 35 | 7 | 2 | 4 | 8 | 18 |
| Fetuses at day 60 | 5 | 0 | 2 | 5 | 8 |
| Lambs at birth: live (dead) | 0 | 0 | 0 (1) | 0 (2) | 3 (1) |
| Lambs alive at one week | 0 | 0 | 0 | 0 | 1 |

[a]Data are shown for various cultures: 3C6 and 5E1 (*GGTA1* correctly targeted), 4H2 (randomly integrated *GGTA1* targeting vector), and 7G65F4 (untransfected cells) were of Finn Dorset origin; YH6 (*PrP* correctly targeted) was of Black Welsh origin. Poll Dorset oocytes were used as recipient cytoplasts throughout.
[b]Reconstructed embryos were transferred to temporary recipients, unless the number of oocytes recovered was low or fusion could not be seen and *in vitro* culture (additional embryos shown in parentheses) was adopted.

## Experimental protocol

Isolation, culture, and transfection of primary fibroblasts. Black Welsh (BW6F2) or Finn Dorset (7G65F4) fibroblasts were recovered from day 35 fetuses as described[2]. Cells were cultured in BHK21 medium (Sigma, St. Louis, MO) supplemented with 2 mM glutamine, 1 mM sodium pyruvate, 1× nonessential amino acids (Life Technologies, Rockville, MD), and 10% FCS (Globe Farm, Gilford, Surrey, UK) in a humidified environment with 5% $CO_2$. Linearized targeting construct (10 μg) was electroporated to passage one 7G65F4 (125 μF/350 V, *GGTA1*) or passage six BW6F2 (250 μF/400 V, *PrP*) cells ($5 \times 10^6$), which were then seeded in 96-well plates ($2.5 \times 10^3$ cells/well). G418 selection (400 μg/ml) was applied after 24 h. At subconfluence, resistant colonies were replica plated to two 96-well plates for DNA analysis or cryopreservation.

Targeting constructs. Promoterless vectors, with *neo-pA* sequence (Stratagene, La Jolla, CA) adjacent to the endogenous gene start codon, were used to target the *GGTA1* and *PrP* loci. The *GGTA1* vector was constructed by amplifying a truncated left arm (300 bp; using primers 199001, 5′-ACGTGGCTCCAAGAATTCTCCAGGCAAGAGTACTGG-3′ and 199006, 5′-CATCTTGTTCAATGGCCGATCCCATTATTTTCTCCTGGGAAAAGAAAAG-3′, with tail complementary to the start of neo coding sequence) and neo-polyA sequence (using primers 199005, 5′-CTTTTCTTTTCCCAGGAGAAAATAATGGGATCGGCCATTGAACAAGATG-3′, with tail complementary to left arm, and 199004, 5′-CAGGTCGACGGATCCGAACAAAC-3′). These fragments were used to prime from each other to give a 1.2 kb fusion product. This was ligated to intron 3 sequence (1 kb *Eco*RV-*Eco*RI fragment), to extend the left arm, and to ~9 kb (*Eco*RV partial digest–*Not*I) of 3′ sequence to create the right arm.

The *PrP* vector was constructed by amplifying the left arm (2.4 kb; using primers prp6F, 5′-CCGAGCTCGCCAATTTCATGGCTGCAGTCACC-3′; and prp7R, 5′-CGATCCCATGATGACTTCTCTGCAAAATAAAG-3′, with tail complementary to the start of neo coding sequence) and neo-polyA sequence (using primers prp10F, 5′-GAGAAGTCATCATGGGATCGGCCATTGAACA-3′, with tail complementary to left arm; and prp8R, 5′-TGCAGGTCGACGGATCCGAA-3′). These fragments were used to prime from each other to give a 3.3 kb fusion product, which was ligated to a 3 kb *Kpn*I fragment to complete the vector.

The *GGTA1 or PrP* vectors were linearized with *Not*I or *Sac*I, respectively, before electroporation.

DNA analysis. Drug-resistant colonies were screened for targeting events by PCR. DNA was isolated in 96-well plates by overnight lysis (50 mM Tris, pH 8, 20 mM ethylenediamine tetraacetate, 100 mM NaCl, 0.3% sodium dodecyl sulfate, 10 mg/ml proteinase K), then isopropanol precipitated, and pellets were resuspended in 50 μl TE (10 mM Tris-HCl, 1 mM EDTA, pH 8). Amplification was performed using Roche Expand HiFi kit, with 1 μl DNA template. Primer locations are indicated in Figure 2: G1 (5′-CAGCTGTGTGGGTATGGGAGGG-3′); G2 (5′-CTGAACTGAATGTTTATCCAGGCCATC–3′); G3 / P3 (5′-AGCCGATTGTCTGTTGTGCCCAGTCAT–3′); PR1 (5′-TTCAGTCGCTCTGTTGTGTC CCA-3′); P2 (5′-AGCATCCCTC CTGCCTTCAG TTCTTC-3′). Cycling conditions for *GGTA1* were 94°C, 2 min/94°C, 30 s / 65°C, 30 s / 68°C, 2.5 min (10 cycles); 94°C, 30 s / 65°C, 30 s / 68°C, 2.5 min + 5 s per cycle (20 cycles); 68°C, 7 min. For *PrP* the elongation phase was increased to 4 min. Products were analyzed by agarose gel electrophoresis.

For Southern blot analysis, genomic DNA was digested with *Bam*HI or *Bgl*I (*GGTA1* or *PrP*, respectively) and blotted to Ambion bright star membrane according to manufacturer's instructions. Diagnostic bands were detected using Ultrahyb (Ambion, Austin, TX) with DNA probes corresponding to *neo* sequence (Stratagene), *GGTA1* 5′ probe (a 100 bp fragment was produced by PCR using forward [CAGCTGTGTGGGTATGGGAGGG] and reverse [CTAACTACGTGCTCCGCCGTTCA] primers) or *PrP* 5′ probe (corresponding to 16,701–17,151 bp of accession no. U67922, Entrez, NCBI).

Nuclear transfer. Somatic cell nuclear transfer was based on the method of Wilmut[2]. Oocytes were collected from superovulated Poll Dorset ewes in PBS with 1% FCS and transferred immediately to calcium-free HEPES-buffered synthetic oviduct fluid[19] (SOF) for removal of cumulus and enucleation. If necessary, cumulus was removed by pipetting in 600 IU/ml hyaluronidase. Oocytes were exposed to 5 μg/ml Hoechst 33248 and 7.5 μg/ml cytochalasin B. Sheep fetal fibroblasts were cultured for three to five days in serum-deficient medium (0.5% FCS) before use as karyoplast donors. Simultaneous fusion of donor cells and recipient oocytes, and activation of the recipient oocytes, was achieved by three consecutive 80 μs pulses of 1.25 kV/cm² in 0.3 M mannitol, 0.1 $MgCl_2$, and 0.05 mM $CaCl_2$. Reconstructed embryos were incubated for six days (*in vitro* culture) or overnight (*in vivo* culture) in SOF solution supplemented with BSA in an atmosphere consisting of 5% $O_2$, 5% $CO_2$, and 90% $N_2$ at 38°C. For *in vivo* culture, following the overnight culture, embryos were embedded in 1% agar chips in PBS and transferred into the ligated oviduct of an estrus-synchronized recipient ewe for an additional six days. Morula and blastocyst stage embryos were recovered seven days post-activation to the uteri of estrus-synchronized ewes (one to two embryos/recipient). Pregnancies were monitored using subcutaneous ultrasound scanning.

*Acknowledgments*

*The authors would like to thank J. Bowering, W. Bosma, P. Johnson, T. Ferrier, D. McGavin, B. Gasparrini, and L. Harkness for technical support, and Jane Lebkowski for reading the manuscript. The Biotechnology and Biological Sciences Research Council and the Geron Corporation provided financial support.*

Received 28 February 2001; accepted 6 April 2001

1. Capecchi, M.R. Altering the genome by homologous recombination. *Science* **244**, 1288–1292 (1989).
2. Wilmut, I., Schnieke, A.E., McWhir, J., Kind, A.J. & Campbell, K.H.S. Viable offspring derived from fetal and adult mammalian cells *Nature* **385**, 810–813 (1997).
3. Campbell, K.H.S., McWhir, J., Ritchie, W.A. & Wilmut, I. Sheep cloned by nuclear transfer from a cultured cell line. *Nature* **380**, 64–66 (1996).
4. Schnieke, A.E. *et al.* Human factor IX transgenic sheep produced by transfer of nuclei from transfected fetal fibroblasts. *Science* **278**, 2130–2133 (1997).
5. McCreath, K.J. *et al.* Production of gene-targeted sheep by nuclear transfer from cultured somatic cells. *Nature* **405**, 1066–1069 (2000).
6. Galili, U., Shohet, S.B., Kobrin, E., Stults, C.L. & Macher, B.A. Man, apes, and Old World monkeys differ from other mammals in the expression of alpha-galactosyl epitopes on nucleated cells. *J. Biol. Chem.* **263**, 17755–17762 (1988).
7. Crick, S.J., Sheppard, M.N., Ho, S.Y., Gebstein, L. & Anderson, R.H. Anatomy of the pig heart: comparisons with normal human cardiac structure. *J. Anat.* **193**, 105–119 (1998).
8. van der Laan, L.J. *et al.* Infection by porcine endogenous retrovirus after islet xenotransplantation in SCID mice. *Nature* **407**, 90–94 (2000).
9. Prusiner, S.B. & Scott, M.R. Genetics of prions. *Annu. Rev. Genet.* **31**, 139–175 (1997).
10. Prusiner, S.B. *et al.* Ablation of the prion protein (PrP) gene in mice prevents scrapie and facilitates production of anti-PrP antibodies. *Proc. Natl. Acad. Sci. USA* **90**, 10608–10612 (1993).
11. Weissmann, C. *et al.* PrP-deficient mice are resistant to scrapie. *Ann NY Acad. Sci.* **724**, 235–240 (1994).
12. Tearle, R.G. *et al.* The alpha-1,3-galactosyltransferase knockout mouse. Implications for xenotransplantation. *Transplantation* **61**, 13–19 (1996).
13. Bueler, H. *et al.* Mice devoid of PrP are resistant to scrapie. *Cell* **73**, 1339–1347 (1993).
14. Weissmann, C. & Aguzzi, A. PrP's double causes trouble. *Science* **286**, 914–915 (1999).
15. Lee, I.Y. *et al.* Complete genomic sequence and analysis of the prion protein gene region from three mammalian species. *Genome Res.* **8** 1022–1037 (1998).
16. Joziasse, D.H., Shaper, N.L., Kim, D., Van den Eijnden, D.H. & Shaper, J.H. Murine alpha 1,3-galactosyltransferase. A single gene locus specifies four isoforms of the enzyme by alternative splicing. *J. Biol. Chem.* **267**, 5534–5541 (1992).
17. Joziasse, D.H., Shaper, J.H., Van den Eijnden, D.H., Van Tunen, A.J. & Shaper, N.L. Bovine alpha 1,3-galactosyltransferase: isolation and characterization of a cDNA clone. Identification of homologous sequences in human genomic DNA. *J. Biol. Chem.* **264**, 14290–14297 (1989).
18. Sedivy, J. Gene targeting in human cells without isogenic DNA. *Science* **283**, 9a (1999).
19. DeSousa, P.A. *et al.* Evaluation of gestational deficiencies in cloned sheep. *Theriogenology* **53**, 214 (2000).
20. Hill, J.R. *et al.* Clinical and pathologic features of cloned transgenic calves and fetuses (13 case studies). *Theriogenology* **51**, 1451–1465 (1999).
21. Clark, A.J., Burl, S., Denning, C. & Dickinson, P. Gene targeting in livestock; a preview. *Transgenic Res.* **9**, 263–275 (2000).
22. Cibelli, J.B. *et al.* Cloned transgenic calves produced from nonquiescent fetal fibroblasts. *Science* **280**, 1256–1258 (1998).
23. Lanza, R.P. *et al.* Extension of cell life-span and telomere length in animals cloned from senescent somatic cells. *Science* **288**, 665–669 (2000).

*Am J Physiol Heart Circ Physiol* 292: H2324–H2332, 2007.
First published January 12, 2007; doi:10.1152/ajpheart.00392.2006.

# Impact of acute and enduring volume overload on mechanotransduction and cytoskeletal integrity of canine left ventricular myocardium

**Dirk W. Donker,[1] Jos G. Maessen,[2] Fons Verheyen,[3] Frans C. Ramaekers,[3] Roel L. H. M. G. Spätjens,[1] Helma Kuijpers,[3] Christian Ramakers,[5] Paul M. H. Schiffers,[4] Marc A. Vos,[6] Harry J. G. M. Crijns,[1] and Paul G. A. Volders[1]**

*Departments of [1]Cardiology, [2]Cardiothoracic Surgery, [3]Molecular Cell Biology, and [4]Pharmacology and Toxicology, Cardiovascular Research Institute Maastricht, Academic Hospital Maastricht and Maastricht University, Maastricht; [5]Department of Anatomy and Embryology, Experimental and Molecular Cardiology Group, Academic Medical Centre, University of Amsterdam, Amsterdam; and [6]Department of Medical Physiology, University Medical Center Utrecht, Utrecht, The Netherlands*

Submitted 13 April 2006; accepted in final form 5 January 2007

**Donker DW, Maessen JG, Verheyen F, Ramaekers FC, Spätjens RL, Kuijpers H, Ramakers C, Schiffers PM, Vos MA, Crijns HJ, Volders PG.** Impact of acute and enduring volume overload on mechanotransduction and cytoskeletal integrity of canine left ventricular myocardium. *Am J Physiol Heart Circ Physiol* 292: H2324–H2332, 2007. First published January 12, 2007; doi:10.1152/ajpheart.00392.2006.—It is poorly understood how mechanical stimuli influence in vivo myocardial remodeling during chronic hemodynamic overload. Combined quantitation of ventricular mechanics and expression of key proteins involved in mechanotransduction can improve fundamental understanding. Adult anesthetized dogs ($n$ = 20) were studied at sinus rhythm (SR) and 0, 3, 10, and 35 days of complete atrioventricular block (AVB). Serial left ventricular (LV) myofiber mechanics were measured. Repeated LV biopsies were analyzed for mRNA and/or protein expression of $\beta_{1D}$-integrin, melusin, Akt, GSK3β, muscle LIM protein (MLP), four-and-a-half LIM protein 2 (fhl2), desmin, and calpain. Upon AVB, increased ejection strain (0.29 ± 0.01 vs. 0.13 ± 0.02, SR) and end-diastolic stress (4.8 ± 1.1 vs. 2.7 ± 0.4 kPa) dominated mechanical changes. Brain natriuretic peptide plasma levels were correspondingly high (33 ± 4 vs. 19 ± 1 pg/ml, SR). $\beta_{1D}$-Integrin protein expression increased chronically after AVB. Melusin was temporarily overexpressed (+33 ± 9%, 3 days AVB vs. SR), followed by elevated ratios of phosphorylated (P)-Akt to Akt and P-GSK3β to GSK3β (+26 ± 6% and +30 ± 8% at 10 days AVB vs. SR). These changes corresponded to peak hypertrophic growth at 3 to 10 days. MLP increased gradually to maxima at chronic AVB (+36 ± 7%). In contrast, fhl2 (−22 ± 3%, 3 days) and desmin (−30 ± 9%, 10 days AVB) transiently declined but recovered at chronic AVB. Calpain protein expression remained unaltered. In conclusion, volume overload after AVB causes a transient compromise of cytoskeletal integrity based, at least partly, on transcriptional downregulation. Subsequent cytoskeletal reorganization coincides with the upregulation of melusin, P-Akt, P-GSK3β, and MLP, indicating a strong drive to compensated hypertrophy.

hemodynamics; myofiber mechanics; serial intramural ventricular biopsies; cardiomyocyte remodeling; ventricular hypertrophy

IT IS STILL POORLY UNDERSTOOD how mechanical signals are sensed by the myocardium and transduced into cellular-biological responses. Mechanical load imposed on the myocardium can be dissected into stress, which is the force per cross-sectional area of tissue, and strain, the resultant cellular deformation. Stress and strain exhibit cyclic beat-to-beat variations in the normal heart, and they are both stimuli for and responders to remodeling induced by pathological overload.

Recently, we described the time course of left ventricular (LV) myocardial mechanics in dogs with bradycardia-induced volume overload due to complete atrioventricular block (AVB) (11). Early after AVB, increased end-diastolic myofiber stress and ejection strain are imposed on the myocardium, and they coincide with peak hypertrophic growth, suggesting their role as primary stimuli for mechanotransduction.

Besides ventricular hypertrophy, the AVB model is characterized by important electrical, contractile, and structural remodeling, yet an exact relation with mechanical overload is currently unknown.

In the present study, we examined the time-dependent effects of increased load on myocardial remodeling during AVB, focusing specifically on the expression of key proteins involved in mechanotransduction and cytoskeletal integrity, i.e., laminin, $\beta_{1D}$-integrin, $\beta_{1D}$-integrin-interacting protein melusin, Akt (protein kinase B), GSK3β, muscle LIM protein (MLP), four-and-a-half LIM protein 2 (fhl2), and desmin. Serial analysis of myofiber mechanics was combined with the determination of plasma levels of brain natriuretic peptide (BNP), a biochemical marker of load. Repetitive sampling of intramural LV biopsies was applied to analyze protein expressions in individual dogs over time.

## METHODS

Experiments were conducted in accordance with the European Directive for the Protection of Vertebrate Animals Used for Experimental and Other Scientific Purposes (86/609/EU). The Committee for Experiments on Animals of Maastricht University approved the experiments.

### *Model of Complete Atrioventricular Block*

Twenty adult mongrel dogs of either sex weighing 25 ± 1 kg were used. After dogs were fasted overnight, premedication (1 ml/10 kg im Acetadon containing 1.5 mg/ml acepromazine, 4 mg/ml methadone, and 0.6 mg/ml atropine) was administered. Complete anesthesia was induced by thiopental sodium (20 mg/kg iv) and maintained with

Address for reprint requests and other correspondence: P. G. A. Volders, Dept. of Cardiology, Cardiovascular Research Institute Maastricht, Academic Hospital Maastricht, P. O. Box 5800, 6202 AZ, Maastricht, The Netherlands (e-mail: p.volders@cardio.unimaas.nl).

The costs of publication of this article were defrayed in part by the payment of page charges. The article must therefore be hereby marked "*advertisement*" in accordance with 18 U.S.C. Section 1734 solely to indicate this fact.

Table 1. *Hemodynamic and electrocardiographic measurements*

| | SR | AAVB | 3 days | 10 days | 35 days |
|---|---|---|---|---|---|
| LV pressure | | | | | |
| Peak systole, kPa | 12.5±1.1 | 10.0±0.7 | 12.4±2.0 | 12.1±0.6 | 12.3±0.8 |
| End diastole, kPa | 0.8±0.1 | 1.5±0.3* | 1.3±0.2 | 1.1±0.2 | 0.8±0.1 |
| Maximum rise, kPa/s | 142±9 | 141±20 | 244±44* | 238±21* | 236±41* |
| Heart rate, beats/min | 107±5 | 44±9* | 45±4* | 46±4* | 48±4* |
| Cardiac output, l/min | 3.1±0.4 | 1.4±0.4* | 1.8±0.3 | 2.0±0.3 | 2.2±0.1 |
| Ejection fraction, % | 48±4 | 62±5 | 70±2* | 77±3* | 75±3* |

Values are means ± SE. SR, sinus rhythm (control); AAVB, acute atrioventricular block; LV, left ventricular. *$P < 0.05$ vs. SR.

halothane (0.5–1%) and $O_2$-$N_2O$ (1:2). AVB was induced by radiofrequency catheter ablation of the His bundle. Animals were studied serially at sinus rhythm (SR; control) and at 0, 3, 10, and 35 days AVB. A standard six-lead ECG was registered. After the animals were killed (35 days AVB), the hearts were excised and weighed.

*LV Mechanics*

LV mechanics were quantified as myofiber stress and strain by applying serial transthoracic echocardiography synchronized with recordings of LV cavity pressure using a validated mathematical model (2), as we have recently described in detail (11). Plasma levels of BNP were determined in peripheral venous blood, collected in chilled EDTA tubes, centrifuged (1,600 *g*, 10 min, 4°C), and stored at −80°C until measured in duplicate by a radioimmunoassay specific for canine BNP-32 (Phoenix Pharmaceuticals, Mountain View, CA).

*Serial Percutaneous Sampling of LV Intramural Biopsies*

Intramural LV needle biopsies were taken serially in dogs at SR and after 3, 10, and 35 days AVB. A 16-gauge biopsy needle (Accut, TSK Laboratory) was percutaneously inserted into the apicolateral LV wall, under fluoroscopic guidance. At least two samples (~10 $mm^3$) were obtained per experiment. Tissue quality was optimal in most biopsies (>98%). All animals were followed by transthoracic echocardiography after biopsy sampling to exclude cardiac tamponade, although in our experience the closed-chest approach is generally uncomplicated (>95%) and fatal outcome is rare (<3%). Such complications did not occur in this study.

*Light and Electron Microscopy*

For light (LM) and electron microscopy (EM), biopsies were processed and analyzed as described before (4). Briefly, tissue was fixed in 3% glutaraldehyde and embedded in epoxy resin. LM analysis was performed on periodic acid-Schiff (PAS)-/Toluidine blue-stained sections to depict cardiomyocyte glycogen content, sarcomeres, mitochondria, and nuclei. PAS positivity and absence of contractile filaments in >10% of the cell surface area of transversely sectioned cardiomyocytes were considered abnormal.

*Immunohistochemistry*

Indirect immunohistochemistry was performed on briefly fixed tissue (3% glutaraldehyde or 3.7% formaldehyde) using primary antibodies directed against desmin (DE-R-11, 1:10) (Dako Cytomation, Glostrup, Denmark), MLP (1:80) (1), vimentin (K36, 1:10) (Frans C. Ramaekers, Maastricht University), and laminin (L9393, 1:150) (Sigma, St. Louis, MO). Specific labeling was visualized using appropriate secondary antibodies applying immunoperoxidase or immunofluorescence techniques. Nuclei were stained using Mayers hemalum or propidium iodide. For negative control, the primary antibodies were omitted. Immunofluorescent labeling was analyzed using confocal laser scanning microscopy (Bio-Rad MRC600, Bio-Rad, Hercules, CA).

*Real-Time PCR*

Total RNA was isolated from the biopsies with the use of the RNEasy Mini kit (Qiagen/Westburg, Leusden, The Netherlands). Fluorescence-based kinetic real-time PCR was performed with a LightCycler system (Roche Diagnostics, Almere, The Netherlands), and amplicons were quantified relative to the constitutively active 18S rRNA by using the LinRegPCR method (31).

*Western Blotting*

Total homogenates were derived from unfixed cryosections (5 μm) dissolved for 30 min on ice in lysis buffer (62 mmol/l Tris, 1.25 mmol/l EDTA, 2% Nonidet P-40, 2.5 mmol/l phenylmethylsulfonyl chloride, 12.5 mg/ml leupeptin, 12.5% glycerol, 100 mg/ml aprotinin, 0.5 mM sodium orthovanadate, and 2.3% SDS) and sample buffer for

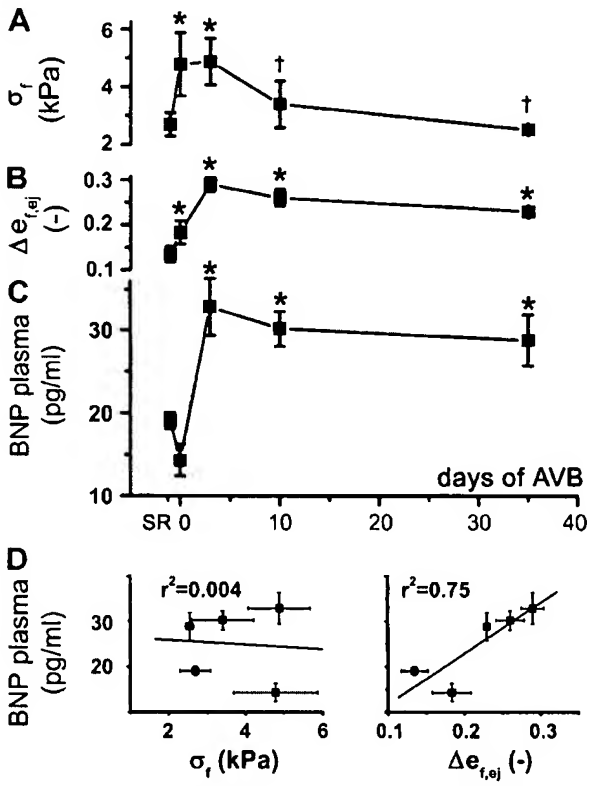


Fig. 1. Time course of mechanical overload before and after atrioventricular block (AVB). Average curves ($n$ = 5 dogs) of end-diastolic stress ($\sigma_f$; *A*), ejection strain ($\Delta e_{f,ej}$, *B*), and plasma levels of brain natriuretic peptide (BNP; *C*) are shown. Changes of ejection strain (*D*, *right*), and not of end-diastolic stress (*D*, *left*), correlate well with altering BNP plasma levels. *$P < 0.05$ vs. sinus rhythm (SR); †$P < 0.05$ vs. 3 days AVB.

4 min at 95°C (62 mmol/l Tris, 2.3% SDS, 10% glycerol, 5% β-mercaptoethanol, and 0.05% bromophenol blue). Equal amounts of total protein (7.5–30 μg/lane), determined by protein assay (Bio-Rad), were loaded on 10% SDS-PAGE gels, transferred to nitrocellulose membranes, and controlled by Coomassie brilliant blue, Ponceau S staining, and GAPDH immunoblotting. Membranes were blocked in BSA (3%, 1 h) in Tween buffer (TWB), containing PBS and Tween 20 (0.05%), and incubated with the primary antibody in BSA (0.5%, 1 h) against desmin (DE-R-11, 1:5,000), $\beta_{1D}$-integrin (2B1, 1:100) (Mubio, Maastricht, The Netherlands), melusin (1:500) (7), MLP (1:500) (1), fhl2 (1:500) (24), Akt (9272, 1:1000), phosphorylated (P)-Akt (Ser473, 1:1000), GSK3β (9315, 1:1000), P-GSK3β (Ser9, 1:1000) (Cell Signaling Technology, Danvers, MA), and the regulatory subunit of calpain I and II (P1, 1:1100) (Chemicon, Temecula, CA). After blots were washed in TWB, they were incubated (1 h) using the appropriate secondary antibodies, washed again, and visualized on X-ray films (Fujifilm, Rotterdam, The Netherlands) with enhanced chemiluminescence (Amersham Biosciences, Amersham, UK). Densitometric quantification was performed with Quantity One software using a GS-800 scanner (Bio-Rad). All immunoblots were performed in duplicate.

### *Statistical Analysis*

Data are presented as means ± SE. Data were compared by using Student's *t*-test for unpaired or paired data. Serial data were tested by repeated-measures ANOVA using Bonferroni's post test comparison. Differences were considered statistically significant if $P < 0.05$.

## RESULTS

### *Temporal Aspects of Mechanical Overload and BNP Expression*

For information regarding hemodynamic changes after AVB in this study, we refer to Table 1. Consistent with our previous study (11), LV mechanical load was characterized by early increases of end-diastolic myofiber stress (4.8 ± 1.1 vs. 2.7 ± 0.4 kPa at SR, $P < 0.01$) and ejection strain [0.29 ± 0.01 vs. 0.13 ± 0.02 (no units) at SR, $P < 0.01$]. End-diastolic stress normalized after 35 days AVB (Fig. 1, *A* and *B*). Systolic myofiber stress did not change during AVB [37.3 ± 3.6 vs. 38.0 ± 4.3 kPa at SR, $P$ = not significant (NS)].

The impact of increased stress and strain on the myocardium was reflected by maximally elevated plasma levels of BNP as early as 3 days after AVB (32.9 ± 3.5 vs. 19.1 ± 1.0 pg/ml at SR; $P < 0.01$). BNP remained high throughout the experimental period (Fig. 1*C*). Temporal changes of plasma BNP correlated well with ejection strain ($r^2 = 0.75$), whereas only a weak correlation with end-diastolic stress was found ($r^2 = 0.004$) (Fig. 1*D*).

### *Dynamic Cardiomyocyte Remodeling After AVB*

The presence of cardiac hypertrophy was confirmed at autopsy after 35 days. Total heart weight (270 ± 12 g) and heart weight-to-body weight ratio (10.7 ± 0.6 g/kg) were larger than in a matching control population of dogs with SR (202 ± 12 g and 8.0 ± 0.4 g/kg, respectively; both $P < 0.05$).

*Key proteins involved in mechanotransduction.* Western blot analysis revealed a significant increase of $\beta_{1D}$-integrin expression after AVB when compared with SR (Fig. 2*A*), whereas its extracellular ligand laminin did not alter (Fig. 3*A*). Time-dependent expression of melusin, a protein directly interacting with the cytoplasmic domain of $\beta_{1D}$-integrin at the Z disk, was characterized by an early peak at 3 days AVB (+33 ± 9% vs. SR, $P < 0.05$), which gradually declined thereafter (Fig. 2*B*).

The P-Akt-to-Akt (P-Akt/Akt) ratio increased at 10 days AVB (+26 ± 6% vs. SR, $P < 0.05$) (Fig. 4*A*). The Akt substrate GSK3β was phosphorylated along with Akt, reaching peak values of the P-GSK3β-to-GSK3β (P-GSK3β/GSK3β) ratio at 10 days (+30 ± 8% vs. SR, $P < 0.05$) (Fig. 4*B*). This higher degree of Akt and GSK3β phosphorylation was transient, because the P-Akt/Akt and P-GSK3β/GSK3β ratios at 35 days AVB were not different from control.

The cardiac LIM domain proteins MLP and fhl2, which both act at the Z disk downstream from $\beta_{1D}$-integrin-melusin, showed divergent expression patterns during AVB. MLP grad-

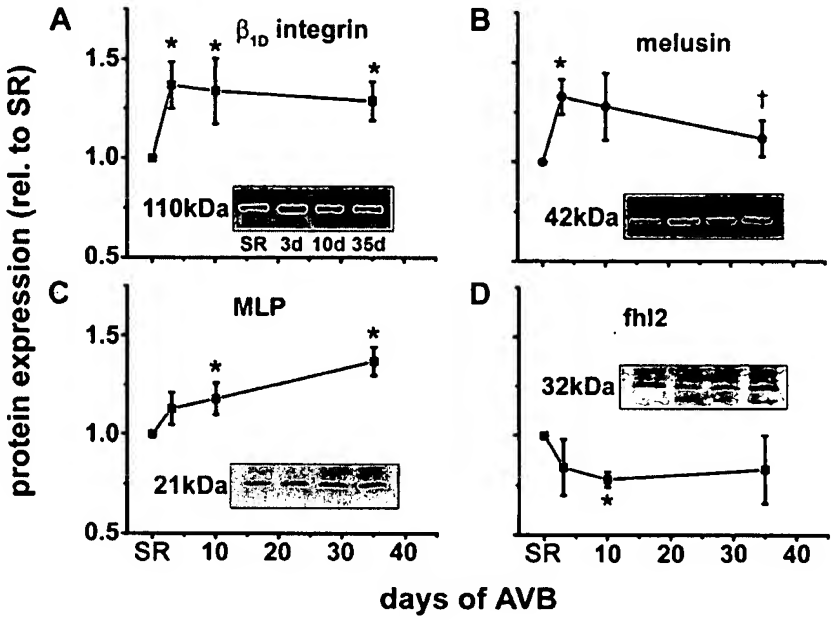


Fig. 2. Time course of Z-disk protein expression before and after AVB. Serial Western blot analysis of $\beta_{1D}$-integrin (*A*), melusin (*B*), muscle LIM protein (MLP; *C*), and four-and-a-half LIM protein 2 (fhl2; *D*) is shown. Average values ($n = 7$ dogs) are standardized to SR; rel, relative. *$P < 0.05$ vs. SR; †$P < 0.05$ vs. 3 days (3d) AVB.

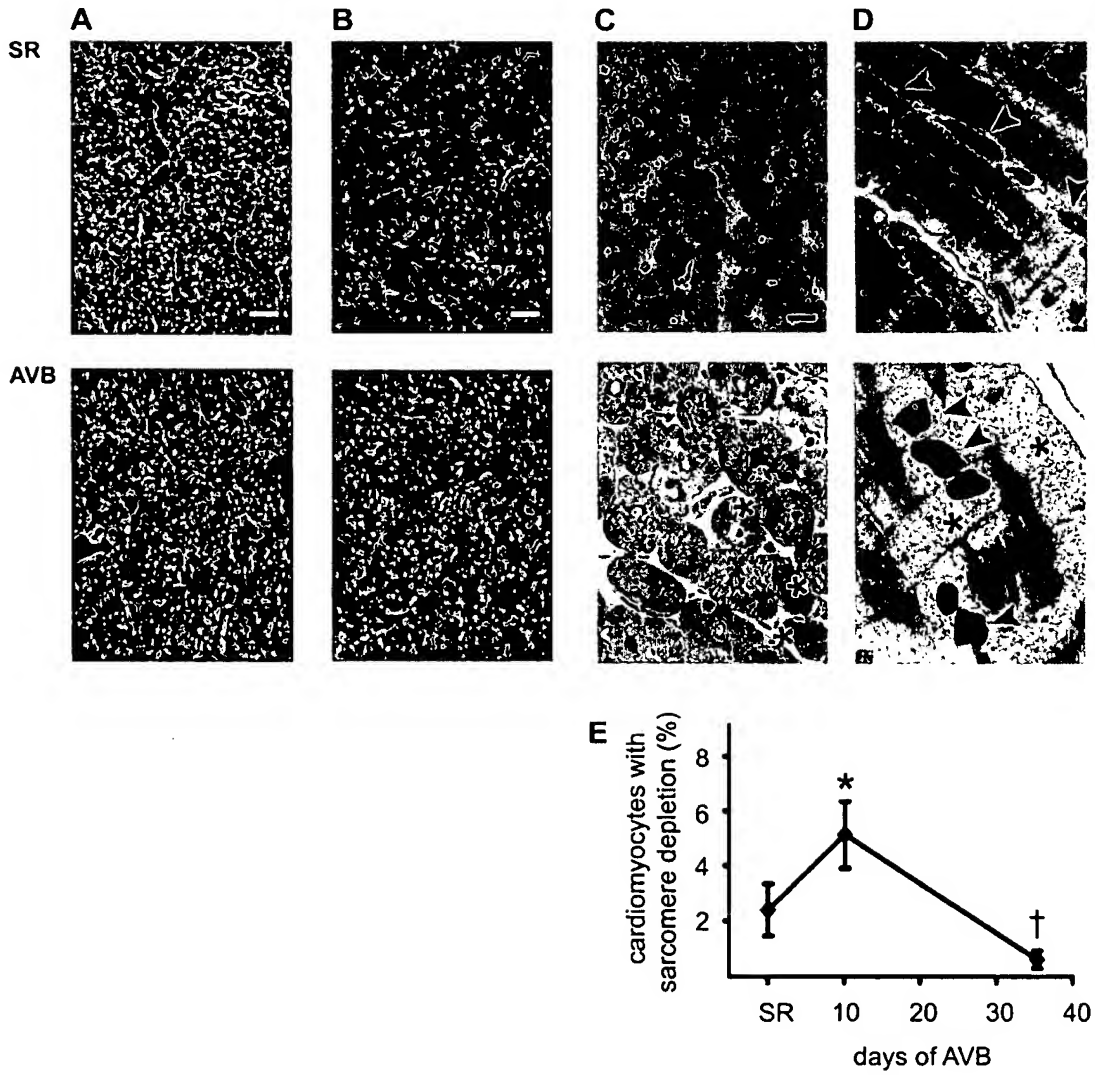


Fig. 3. Time course of structural remodeling before and after AVB. Immunofluorescent double staining for desmin (green) and laminin (red) (*A*) and desmin (green) and vimentin (red) (*B*) showing no differences between SR and AVB. *C*: light microscopy (LM) photomicrographs of periodic acid-Schiff-/Toluidine blue-stained left ventricular (LV) myocardium from serial biopsies of one individual dog showing increased cytoplasmic glycogen content during AVB (asterisks), which was absent at SR. *D*: electron microscopy photomicrographs illustrating ultrastructural details, as glycogen accumulation in areas with depletion of sarcomeres and remnants of myofibrils (asterisks) altered mitochondrial shape and size as compared with SR (arrowheads). *E*: relative number of cardiomyocytes showing depletion of sarcomeres. Scale bars in *A–C* indicate 10 μm. *$P < 0.05$ vs. SR; †$P < 0.05$ vs. 10 days AVB.

ually increased to maxima at chronic AVB (+36 ± 7% at 35 days vs. SR, $P < 0.01$; Fig. 2*C*), whereas fhl2 exhibited an early decline (−22 ± 3% vs. SR, $P < 0.01$) (Fig. 2*D*). Immunohistochemical studies revealed that, during AVB, MLP expression increased throughout the cytoplasm and was also prominently expressed in the nucleus (Fig. 5). The temporal expression of MLP correlated highly with increasing echographic LV mass (in grams) over the weeks after AVB (Fig. 6). In addition, we found a good correlation between the expression of melusin, the ratiometric expression of P-Akt/Akt and P-GSK3β/GSK3β, and the degree of hypertrophic growth (LV mass increase per time in g/day; Fig. 6).

*Time course of cytoskeletal and sarcomeric changes.* (Immuno)histological analysis revealed a normal compact myocardial texture and no alteration of the extracellular space during AVB (Fig. 3) in line with earlier work (37). The extracellular space was characterized by unaltered expressions of the $\beta_{1D}$-integrin-interacting extracellular protein laminin (Fig. 3*A*) and the fibroblast intermediate filament vimentin (Fig. 3*B*). Micromorphometry of cardiomyocyte cross sections showed comparable diameters between SR (23 ± 1 μm), 10 days (24 ± 1 μm, $P$ = NS), and 35 days AVB (25 ± 1 μm, $P$ = NS), supporting previous data showing predominant cellular lengthening after AVB (11, 37).

Cytoskeletal integrity was further explored by analysis of the intermediate filament desmin (Fig. 7). During SR, quantitative analysis of mRNA and protein expression showed a downregulation at 3 and 10 days AVB and subsequent normalization (Fig. 7, *A* and *B*). Desmin immunolabeling was in agreement with the mRNA and protein data and exhibited a normal cross-striated pattern at the Z line and prominent expression at the intercalated disk. At 3 and 10 days AVB, desmin labeling

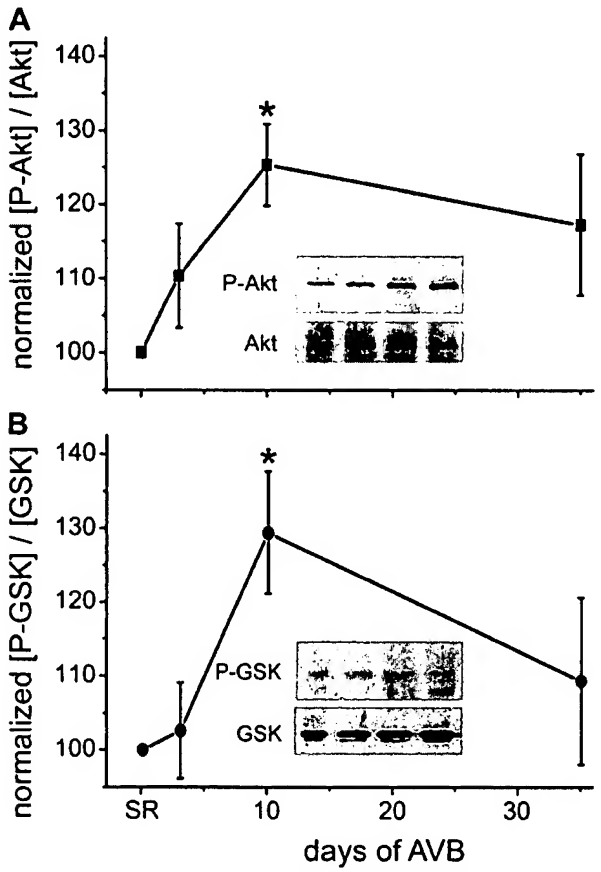


Fig. 4. Time course of Akt and GSK3β protein expression and phosphorylation before and after AVB. Serial Western blot analysis and normalized ratio of phosphorylated (P) to total protein expression of Akt (*A*) and GSK3β (*B*) are shown. Average values ($n$ = 5 dogs) are standardized to SR. *$P < 0.05$ vs. SR.

at the intercalated disk clearly decreased compared with the Z-line labeling. After 35 days, desmin expression was restored, particularly at the intercalated disks (Fig. 7, *C* and *D*).

To determine whether the early decrease of desmin was also reflected by derangements of sarcomeric structures, we analyzed the cardiomyocyte ultrastructure by EM (Fig. 3*D*). We found cytoplasmic areas largely devoid of sarcomeric structures, notably at 10 days AVB. These areas exhibited remnants of myofibrils and were filled with glycogen and with healthy-appearing, abnormally large- and small-sized mitochondria. We did not observe mitochondrial swelling, loss of intramatricial granules, disrupted mitochondrial cristae, mega-mitochondria with lipid-like inclusion, cytoplasmic vacuolization or edema, tortuous nuclei, intramatricial glycogen clumps, membrane disruption, or whorl-like myelin structures indicating the absence of ischemia or degeneration during AVB (4) (Fig. 3*D*).

To quantify these abnormalities by LM, we performed PAS staining to depict the glycogen accumulation observed during EM analysis. The number of abnormal glycogen-stuffed cardiomyocytes per microscopic section area was increased at 10 days AVB (5 ± 2% vs. 2 ± 1% at SR, $P < 0.05$) and had normalized again at 35 days AVB (Fig. 3*E*).

Finally, to examine whether the $Ca^{2+}$-dependent protease calpain could be involved in the loss of cytoskeletal and contractile elements, serial Western blot analyses of the regulatory subunits of calpain I and II were performed, which showed an unaltered protein expression throughout the experimental period.

## DISCUSSION

### *Time Course of Myofiber Mechanics and Plasma BNP*

In the present study we have confirmed previous results (11) that both end-diastolic stress and ejection strain are driven to maximal amplitudes within the first week of AVB. As a first new finding, this acute and enduring volume overload is reflected by a parallel release of the load biomarker BNP. Absolute plasma levels of BNP after AVB were comparable to those in dogs with compensated overload of different cause, varying roughly between 25 (16) and 40 pg/ml (3). Correlation analysis suggests that BNP release after AVB is mainly driven by systolic ejection strain. In vitro studies support that mechanical stimuli applied during systole can be even more capable of increasing BNP transcription than diastolic stimuli (40). Nevertheless, diastolic load may well contribute to the BNP release after AVB, despite a weak temporal correlation. Diastolic mechanical stimuli have been shown to trigger BNP release in other animal models (15) and in humans with overload (25).

### *Dynamic Expression of Key Mechanotransduction Proteins After AVB*

Key proteins located at the Z-disk level have been proposed to sense and transduce mechanical stimuli (13, 22, 30). Among those, integrins are obvious candidates that span the sarcolemma (32). In cardiomyocytes, $\beta_{1D}$-integrin is dominantly expressed (36) and has been shown to be relevant for mechanotransduction under basal (i.e., normal load) conditions and pathological overload (33). Its increased expression has been observed during hypertrophy after adrenergic stimulation in vitro (28, 32) and during chronic aortic constriction in mice (5). During AVB, $\beta_{1D}$-integrin expression was increased from 3 days onward. This early and sustained upregulation is in line with findings in other models of hypertrophy (5, 28, 32). Interestingly, the immunoexpression of laminin, the primary extracellular $\beta_{1D}$-integrin ligand (32), and vimentin, a fibroblast marker, were found unaltered (Fig. 3*B*). These findings suggest that the cardiomyocyte protein $\beta_{1D}$-integrin, and not components of the extracellular matrix, is among the first upstream elements ("initiators") activated by mechanical stimuli in this model.

At its cytoplasmic domain, $\beta_{1D}$-integrin binds to melusin, a striated muscle-specific protein involved in mechanical signaling, promoting cardiac compensation and preventing failure (6, 10). The latter was concluded from experiments in mice after aortic constriction. Melusin-null animals exhibited less hypertrophy and more rapid LV dilation and failure (6), whereas transgenic mice overexpressing melusin showed a prolonged phase of compensated hypertrophy in the absence of fibrosis as compared with wild-type animals (10). In wild-type mice, aortic constriction led to an overexpression of melusin after 1 wk during compensated hypertrophy, whereas melusin returned to baseline, when LV dilation and impaired contractility ensued after 12 wk (10). Interestingly, we found a similar temporal expression pattern of melusin after AVB, with an

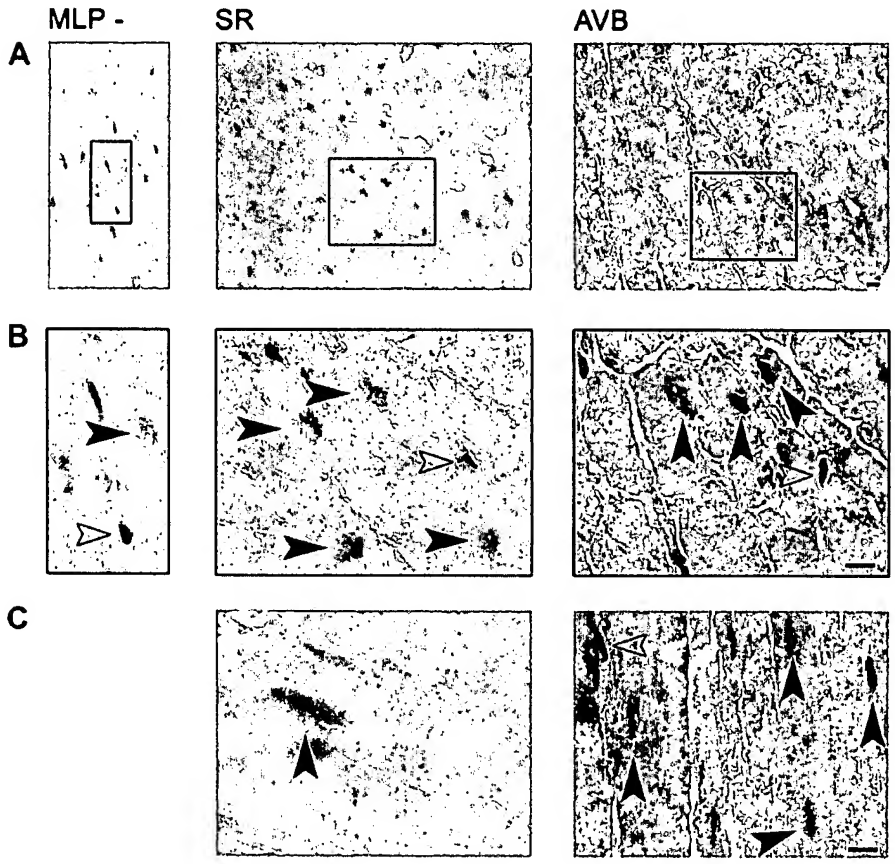


Fig. 5. Cardiomyocyte expression pattern of MLP before and after AVB. LM photomicrographs show immunohistochemical expression of MLP in LV myocardium at low (*A*) and high (*B* and *C*) magnification, in transversely (*A* and *B*) and longitudinally (*C*) sectioned cardiomyocytes. At control (SR), a mild MLP expression was observed within the cytoplasm and the nucleus (*B* and *C*; solid arrowheads). Note that noncardiomyocyte nuclei (*B* and *C*, open arrowhead) stain blue, whereas cardiomyocyte nuclei show MLP labeling (*B* and *C*, solid arrowhead). In negative control (MLP−), both cardiomyocyte nuclei (*B* and *C*, solid arrowhead) and noncardiomyocyte nuclei (*B* and *C*, open arrowheads) stain blue, indicating the absence of MLP labeling. During AVB, both cardiomyocyte cytoplasmic and nuclear expression of MLP are increased (*B* and *C*). Scale bars indicate 10 μm.

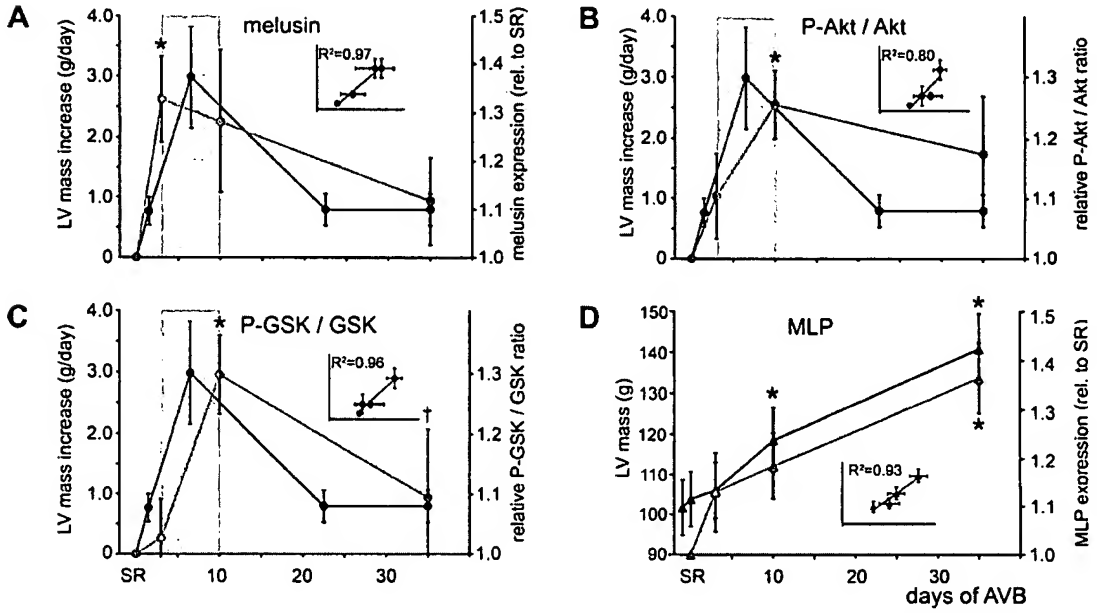


Fig. 6. Temporal expression of melusin, P-Akt/Akt, P-GSK3β/GSK3β, and MLP related to LV hypertrophy. The time course of melusin, P-Akt/Akt, and P-GSK3β/GSK3β expression (*A–C*, shaded lines) correlated (*insets*) highly with the echocardiographically determined increase of LV mass per time, a measure of hypertrophic growth (*A–C*, solid lines), whereas the time course of MLP expression (*D*, shaded line) correlated (*inset*) highly with the time course of the echographic LV mass after AVB (*D*, solid line) ($n$ = 5 dogs). Shaded bars (*A–C*) indicate time interval of peak hypertrophic growth. *$P < 0.05$ vs. SR; †$P < 0.05$ vs. 3 days AVB.

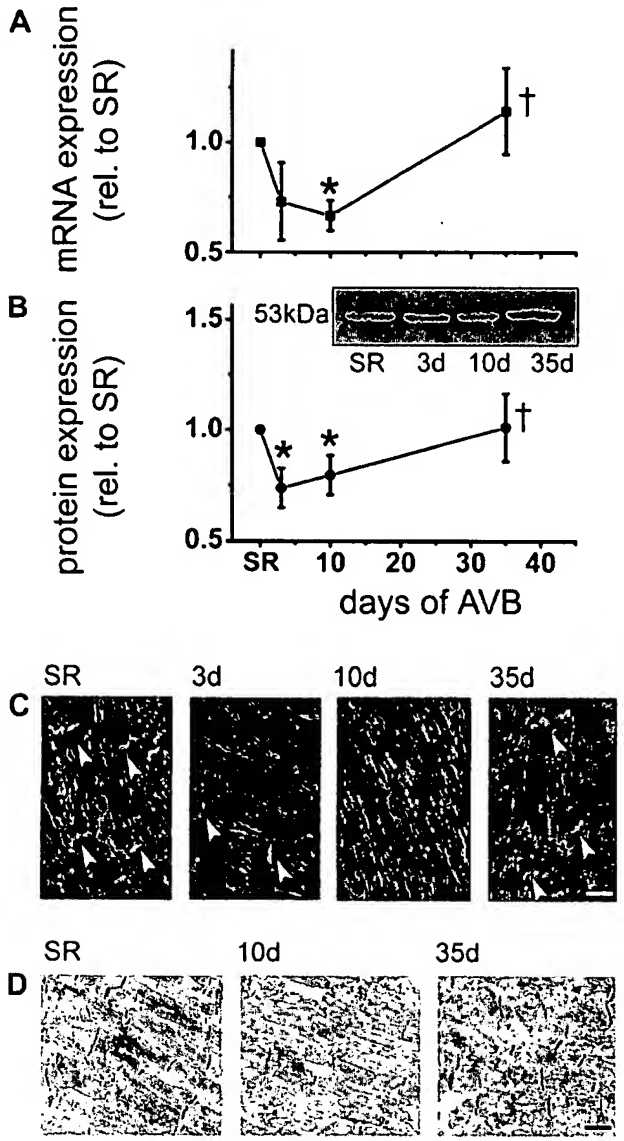


Fig. 7. Time course of desmin expression before and after AVB. Serial real-time PCR (*A*) and Western blot analysis (*B*) show average values standardized to SR ($n$ = 9 dogs). Immunofluorescent labeling of desmin (green) and nuclei (red) (*C*) and LM photomicrographs (*D*) show immunohistochemical expression of desmin in serial biopsies. Scale bars indicate 25 μm. *$P <$ 0.05 vs. SR; †$P < 0.05$ vs. 3 days AVB.

upregulation at 3 days AVB and a gradual decline thereafter. It is tempting to speculate that, early after AVB, increased melusin expression promotes compensated hypertrophy through mechanisms that remain to be elucidated. This procompensatory effect of melusin appeared closely related to the stimulation of hypertrophic growth (6), which could also hold for the AVB model, where melusin overexpression coincides with measures of peak hypertrophic growth (Fig. 6*A*).

In downstream hypertrophic signaling, melusin is involved in the phosphorylation of Akt and GSK3β in response to mechanical load (6, 10). We found that the overexpression of melusin coincided with the ratiometric increase of P-Akt/Akt and P-GSK3β/GSK3β during a phase of maximal mechanical load (Fig. 1, *A* and *B*) and hypertrophic growth (Fig. 6). Phosphorylation inhibits the constitutively active antihypertrophic effect of GSK3β and, thereby, likely stimulates different transcriptional events (14).

MLP is another key Z-disk protein involved in mechanotransduction and -sensing. It interacts with $\beta_{1D}$-integrin via α-actinin, is associated with the actin cytoskeleton, and was recently identified as a crucial element of the "cardiac mechanical stretch sensor machinery" consisting of a MLP-titin-telethonin protein chain (22). It has been postulated that a defective chain, as in MLP-null mice and a subset of patients with reduced MLP levels and heart failure (41), leads to dilated cardiomyopathy due to malfunctioning mechanosensing (22). In dogs with AVB, MLP expression gradually increased to significant levels at chronic AVB, which suggests that the MLP-titin-telethonin chain is likely not defective in this model. This is further supported by the finding of BNP release after AVB, which requires, according to a recent study (22), an intact MLP-titin-telethonin chain as prerequisite for BNP increase during mechanical overload. It has recently been shown that MLP plays an important role in the stimulation of cardiomyocyte hypertrophy via activation of the calcineurin-nuclear factor of activated T-cell pathway (17, 18). MLP may act as a scaffold protein to facilitate sarcomere assembly (17) and stimulate further downstream signaling (22). These findings of a procompensatory role of MLP in other models of hypertrophy (17, 18, 22) are in agreement with the high correlation of the temporal expression patterns of MLP and increased LV mass after AVB (Fig. 6). We found that, after AVB, MLP expression increased in both the cardiomyocyte cytoplasm and nucleus (Fig. 5). These subcellular localizations have been described for MLP and other LIM proteins (21). Nuclear relocation in conjunction with MLP downregulation has been linked to a "phenoconversion" toward heart failure (12). However, in our model with compensated hypertrophy, the nuclear translocation is associated with increased MLP levels, suggesting increased transcriptional activity, as also postulated for other LIM proteins (21).

The other Z-disk LIM domain protein that we studied, fhl2, also colocalizes with $\beta_{1D}$-integrin, α-actinin, and the actin cytoskeleton and is relevant for cardiomyocyte differentiation and myofibrillogenesis (20), as described for MLP. In contrast, fhl2 expression during AVB is transiently reduced around 10 days of AVB. This implicates a different role for fhl2 in the AVB model, which should be analyzed in more detail in future experiments. Importantly, fhl2 and MLP have a divergent protein structure, which is compatible with a different functional role (21). In contrast with MLP, fhl2 is regarded as a repressor of hypertrophy (29). It interacts with ERK2, an element of the MAP kinase signaling pathway. Hypertrophic responses induced by adrenergic stimulation, and mediated via ERK2, are partially antagonized by fhl2, which attenuates transcription (29). In line with this finding, fhl2-null mice, which exhibit a normal cardiac phenotype, show increased hypertrophic growth after catecholamine infusion, supporting repressor-like activity of fhl2 in the overloaded myocardium (23). ERK2 interacts with fhl2, but it does not interact with MLP, which underscores the protein-specific action of LIM proteins (29). The early transient downregulation of fhl2 after AVB coincides with an enhanced adrenergic tone (34) and maximal hypertrophic growth in the first 10 days after atrioventricular block. It could well be that hypertrophy is partly

caused by enhanced adrenergic stimulation and mediated via MAP kinase/ERK2. The latter pathway could be incompletely repressed by the fhl2 reduction at this stage, promoting hypertrophy.

### *Transitory Changes of Cytoskeletal Elements After AVB*

The depletion of sarcomeres and glycogen accumulation at 10 days AVB was similar but less extensive than reported in chronic hibernating myocardium (~30%) (4). These morphological changes have been interpreted as signs of myocardial dedifferentiation (4). Interestingly, glycogen accumulation after AVB coincided with the ratiometric increase of P-GSK/GSK, which interacts with glycogen synthase, promoting glycogen synthesis and accumulation (14). Whether this observation is a purely metabolic phenomenon or a sign of beneficial cardiomyocyte remodeling remains to be elucidated.

The critical changes of the early phase after AVB are further characterized by the transient downregulation of desmin, which is the most important intermediate filament in cardiomyocytes and essential for their structural integrity and function, as recently reviewed (9). It forms a scaffold that interconnects adjacent myofibrils at the Z disks, serving as a physical link between the sarcolemma, cytoskeleton, and the nuclear envelope (9, 22, 30). A transient downregulation of desmin early during acquired mechanical overload has not been reported in the literature, but it could be a consequence of the abrupt mechanical impact of AVB exhibiting aspects of mild heart failure. In ventricular hypertrophy, desmin expression has been reported to be either unaltered (35) or increased (19, 38), but from studies in desmin knockout mice it has become clear that the absence of desmin is associated with cardiac hypertrophy and failure (9, 26). Our data suggest that the reduced desmin expression is regulated at the transcriptional level. We could not find a dominant role for calpain as a posttranslational modifier, which has been suggested with respect to the depletion of sarcomeres (8) and desmin disintegration (27), although we have only analyzed protein levels of the regulatory subunit of calpain I and II and not its protease activity, nor other proteases.

Importantly, during chronic AVB the degree of sarcomere depletion, glycogen accumulation, and total desmin content had normalized and desmin was even upregulated in a subset of dogs, especially at the intercalated disk. Since contractile activity has been reported to increase desmin expression by increased gene transcription (39), it could well be that the persistently high levels of ejection strain contribute to the normalization of desmin expression in the chronic phase of AVB.

### *Conclusions*

The mechanical load acutely imposed on the ventricular myocardium after AVB causes a transient compromise of cytoskeletal integrity. This is based, at least partly, on transcriptional downregulation. By yet unknown molecular mechanisms, the dog with AVB is able to prevent serious disruption of sarcomeric elements and further downregulation of the important intermediate filament protein desmin. Toward chronic AVB a gradual structural reorganization and a strong drive to functionally compensated hypertrophy are attended by the early upregulation of melusin and MLP, known as procompensatory proteins in other models of ventricular hypertrophy and failure.

## ACKNOWLEDGMENTS

The authors thank Monique de Jong, Department of Cardiology; Theo van der Nagel, Department of Cardiothoracic Surgery; Marcel Borgers and Marie-Hélène Lenders, Department of Molecular Cell Biology; Ramon Langen, Department of Respiratory Medicine; and Iwan de Jong, IDEE, Maastricht University, for support and technical assistance. The authors are very grateful to Dr. Mara Brancaccio (melusin), Dr. Pico Caroni (MLP), and Dr. Sabina Kupershmidt (fhl2) for generously providing antibodies.

## GRANTS

D. W. Donker was financially supported by Medtronic, The Netherlands. P. G. A. Volders was supported by The Netherlands Organization for Health Research and Development (ZonMW 906-02-068) and the "Stichting Hartsvrienden Rescar," Maastricht, The Netherlands.

## REFERENCES

1. **Arber S, Halder G, Caroni P.** Muscle LIM protein, a novel essential regulator of myogenesis, promotes myogenic differentiation. *Cell* 79: 221–231, 1994.
2. **Arts T, Bovendeerd PH, Prinzen FW, Reneman RS.** Relation between left ventricular cavity pressure and volume and systolic fiber stress and strain in the wall. *Biophys J* 59: 93–102, 1991.
3. **Asano K, Masuda K, Okumura M, Kadosawa T, Fujinaga T.** Plasma atrial and brain natriuretic peptide levels in dogs with congestive heart failure. *J Vet Med Sci* 61: 523–529, 1999.
4. **Ausma J, Thone F, Dispersyn GD, Flameng W, Vanoverschelde JL, Ramaekers FC, Borgers M.** Dedifferentiated cardiomyocytes from chronic hibernating myocardium are ischemia-tolerant. *Mol Cell Biochem* 186: 159–168, 1998.
5. **Babbitt CJ, Shai SY, Harpf AE, Pham CG, Ross RS.** Modulation of integrins and integrin signaling molecules in the pressure-loaded murine ventricle. *Histochem Cell Biol* 118: 431–439, 2002.
6. **Brancaccio M, Fratta L, Notte A, Hirsch E, Poulet R, Guazzone S, De Acetis M, Vecchione C, Marino G, Altruda F, Silengo L, Tarone G, Lembo G.** Melusin, a muscle-specific integrin beta1-interacting protein, is required to prevent cardiac failure in response to chronic pressure overload. *Nat Med* 9: 68–75, 2003.
7. **Brancaccio M, Guazzone S, Menini N, Sibona E, Hirsch E, De Andrea M, Rocchi M, Altruda F, Tarone G, Silengo L.** Melusin is a new muscle-specific interactor for beta(1) integrin cytoplasmic domain. *J Biol Chem* 274: 29282–29288, 1999.
8. **Brundel BJ, Ausma J, van Gelder IC, Van der Want JJ, van Gilst WH, Crijns HJ, Henning RH.** Activation of proteolysis by calpains and structural changes in human paroxysmal and persistent atrial fibrillation. *Cardiovasc Res* 54: 380–389, 2002.
9. **Capetanaki Y.** Desmin cytoskeleton in healthy and failing heart. *Heart Fail Rev* 5: 203–220, 2000.
10. **De Acetis M, Notte A, Accornero F, Selvetella G, Brancaccio M, Vecchione C, Sbroggio M, Collino F, Pacchioni B, Lanfranchi G, Aretini A, Ferretti R, Maffei A, Altruda F, Silengo L, Tarone G, Lembo G.** Cardiac overexpression of melusin protects from dilated cardiomyopathy due to long-standing pressure overload. *Circ Res* 96: 1087–1094, 2005.
11. **Donker DW, Volders PG, Arts T, Bekkers BC, Hofstra L, Spatjens RL, Beekman JD, Borgers M, Crijns HJ, Vos MA.** End-diastolic myofiber stress and ejection strain increase with ventricular volume overload—Serial in-vivo analyses in dogs with complete atrioventricular block. *Basic Res Cardiol* 100: 372–382, 2005.
12. **Ecarnot-Laubriet A, De Luca K, Vandroux D, Moisant M, Bernard C, Assem M, Rochette L, Teyssier JR.** Downregulation and nuclear relocation of MLP during the progression of right ventricular hypertrophy induced by chronic pressure overload. *J Mol Cell Cardiol* 32: 2385–2395, 2000.
13. **Ervasti JM.** Costameres: the Achilles' heel of Herculean muscle. *J Biol Chem* 278: 13591–13594, 2003.
14. **Hardt SE, Sadoshima J.** Negative regulators of cardiac hypertrophy. *Cardiovasc Res* 63: 500–509, 2004.
15. **Hautala N, Tenhunen O, Szokodi I, Ruskoaho H.** Direct left ventricular wall stretch activates GATA4 binding in perfused rat heart: involvement of autocrine/paracrine pathways. *Pflügers Arch* 443: 362–369, 2002.

16. **He KL, Dickstein M, Sabbah HN, Yi GH, Gu A, Maurer M, Wei CM, Wang J, Burkhoff D.** Mechanisms of heart failure with well preserved ejection fraction in dogs following limited coronary microembolization. *Cardiovasc Res* 64: 72–83, 2004.
17. **Heineke J, Kempf T, Kraft T, Hilfiker A, Morawietz H, Scheubel RJ, Caroni P, Lohmann SM, Drexler H, Wollert KC.** Downregulation of cytoskeletal muscle LIM protein by nitric oxide: impact on cardiac myocyte hypertrophy. *Circulation* 107: 1424–1432, 2003.
18. **Heineke J, Ruetten H, Willenbockel C, Gross SC, Naguib M, Schaefer A, Kempf T, Hilfiker-Kleiner D, Caroni P, Kraft T, Kaiser RA, Molkentin JD, Drexler H, Wollert KC.** Attenuation of cardiac remodeling after myocardial infarction by muscle LIM protein-calcineurin signaling at the sarcomeric Z-disc. *Proc Natl Acad Sci USA* 102: 1655–1660, 2005.
19. **Heling A, Zimmermann R, Kostin S, Maeno Y, Hein S, Devaux B, Bauer E, Klovekorn WP, Schlepper M, Schaper W, Schaper J.** Increased expression of cytoskeletal, linkage, and extracellular proteins in failing human myocardium. *Circ Res* 86: 846–853, 2000.
20. **Johannessen M, Moller S, Hansen T, Moens U, Van Ghelue M.** The multifunctional roles of the four-and-a-half-LIM only protein FHL2. *Cell Mol Life Sci* 63: 268–284, 2006.
21. **Kadrmas JL, Beckerle MC.** The LIM domain: from the cytoskeleton to the nucleus. *Nat Rev Mol Cell Biol* 5: 920–931, 2004.
22. **Knoll R, Hoshijima M, Hoffman HM, Person V, Lorenzen-Schmidt I, Bang ML, Hayashi T, Shiga N, Yasukawa H, Schaper W, McKenna W, Yokoyama M, Schork NJ, Omens JH, McCulloch AD, Kimura A, Gregorio CC, Poller W, Schaper J, Schultheiss HP, Chien KR.** The cardiac mechanical stretch sensor machinery involves a Z disc complex that is defective in a subset of human dilated cardiomyopathy. *Cell* 111: 943–955, 2002.
23. **Kong Y, Shelton JM, Rothermel B, Li X, Richardson JA, Bassel-Duby R, Williams RS.** Cardiac-specific LIM protein FHL2 modifies the hypertrophic response to beta-adrenergic stimulation. *Circulation* 103: 2731–2738, 2001.
24. **Kupershmidt S, Yang IC, Sutherland M, Wells KS, Yang T, Yang P, Balser JR, Roden DM.** Cardiac-enriched LIM domain protein fhl2 is required to generate I(Ks) in a heterologous system. *Cardiovasc Res* 56: 93–103, 2002.
25. **Maeda K, Tsutamoto T, Wada A, Hisanaga T, Kinoshita M.** Plasma brain natriuretic peptide as a biochemical marker of high left ventricular end-diastolic pressure in patients with symptomatic left ventricular dysfunction. *Am Heart J* 135: 825–832, 1998.
26. **Milner DJ, Taffet GE, Wang X, Pham T, Tamura T, Hartley C, Gerdes AM, Capetanaki Y.** The absence of desmin leads to cardiomyocyte hypertrophy and cardiac dilation with compromised systolic function. *J Mol Cell Cardiol* 31: 2063–2076, 1999.
27. **Papp Z, van der Velden J, Stienen GJ.** Calpain-I induced alterations in the cytoskeletal structure and impaired mechanical properties of single myocytes of rat heart. *Cardiovasc Res* 45: 981–993, 2000.
28. **Pham CG, Harpf AE, Keller RS, Vu HT, Shai SY, Loftus JC, Ross RS.** Striated muscle-specific $\beta_{1D}$-integrin and FAK are involved in cardiac myocyte hypertrophic response pathway. *Am J Physiol Heart Circ Physiol* 279: H2916–H2926, 2000.
29. **Purcell NH, Darwis D, Bueno OF, Muller JM, Schule R, Molkentin JD.** Extracellular signal-regulated kinase 2 interacts with and is negatively regulated by the LIM-only protein FHL2 in cardiomyocytes. *Mol Cell Biol* 24: 1081–1095, 2004.
30. **Pyle WG, Solaro RJ.** At the crossroads of myocardial signaling: the role of Z-discs in intracellular signaling and cardiac function. *Circ Res* 94: 296–305, 2004.
31. **Ramakers C, Vos MA, Doevendans PA, Schoenmakers M, Wu YS, Scicchitano S, Iodice A, Thomas GP, Antzelevitch C, Dumaine R.** Coordinated down-regulation of KCNQ1 and KCNE1 expression contributes to reduction of $I_{Ks}$ in canine hypertrophied hearts. *Cardiovasc Res* 57: 486–496, 2003.
32. **Ross RS.** Molecular and mechanical synergy: cross-talk between integrins and growth factor receptors. *Cardiovasc Res* 63: 381–390, 2004.
33. **Shai SY, Harpf AE, Babbitt CJ, Jordan MC, Fishbein MC, Chen J, Omura M, Leil TA, Becker KD, Jiang M, Smith DJ, Cherry SR, Loftus JC, Ross RS.** Cardiac myocyte-specific excision of the beta1 integrin gene results in myocardial fibrosis and cardiac failure. *Circ Res* 90: 458–464, 2002.
34. **Stengl M, Ramakers C, Donker DW, Nabar A, Rybin AV, Spatjens RL, van der Nagel T, Wodzig WK, Sipido KR, Antoons G, Moorman AF, Vos MA, Volders PG.** Temporal patterns of electrical remodeling in canine ventricular hypertrophy: focus on $I_{Ks}$ downregulation and blunted beta-adrenergic activation. *Cardiovasc Res* 72: 90–100, 2006.
35. **Tagawa H, Koide M, Sato H, Zile MR, Carabello BA, Cooper GT.** Cytoskeletal role in the transition from compensated to decompensated hypertrophy during adult canine left ventricular pressure overloading. *Circ Res* 82: 751–761, 1998.
36. **Van der Flier A, Kuikman I, Baudoin C, van der Neut R, Sonnenberg A.** A novel beta 1 integrin isoform produced by alternative splicing: unique expression in cardiac and skeletal muscle. *FEBS Lett* 369: 340–344, 1995.
37. **Volders PG, Sipido KR, Vos MA, Kulcsar A, Verduyn SC, Wellens HJ.** Cellular basis of biventricular hypertrophy and arrhythmogenesis in dogs with chronic complete atrioventricular block and acquired torsade de pointes. *Circulation* 98: 1136–1147, 1998.
38. **Wang X, Li F, Campbell SE, Gerdes AM.** Chronic pressure overload cardiac hypertrophy and failure in guinea pigs: II. Cytoskeletal remodeling. *J Mol Cell Cardiol* 31: 319–331, 1999.
39. **Watson PA, Hannan R, Carl LL, Giger KE.** Desmin gene expression in cardiac myocytes is responsive to contractile activity and stretch. *Am J Physiol Cell Physiol* 270: C1228–C1235, 1996.
40. **Yamamoto K, Dang QN, Maeda Y, Huang H, Kelly RA, Lee RT.** Regulation of cardiomyocyte mechanotransduction by the cardiac cycle. *Circulation* 103: 1459–1464, 2001.
41. **Zolk O, Caroni P, Bohm M.** Decreased expression of the cardiac LIM domain protein MLP in chronic human heart failure. *Circulation* 101: 2674–2677, 2000.

ELSEVIER

Cardiovascular Research 39 (1998) 60–76

Cardiovascular Research

Review

# Animal models of human cardiovascular disease, heart failure and hypertrophy

Gerd Hasenfuss*

*Abteilung Kardiologie und Pneumologie, Universität Göttingen, Robert-Koch-Str. 40, 37075 Göttingen, Germany*

Received 5 January 1998; accepted 23 March 1998

**Abstract**

The progress made in our understanding of the pathophysiology and treatment of congestive heart failure (CHF) would not have been possible without a number of animal models of heart failure and hypertrophy, each one having unique advantages as well as disadvantages. The species and interventions used to create CHF depends on the scientific question as well as on factors such as ethical and economical considerations, accessibility and reproducibility or the model. How closely the model should mimic the human syndrome of CHF depends on the scientific question under investigation. If the goal is to study pathophysiological processes like remodeling or the function of subcellular systems such as excitation contraction-coupling processes, contractile protein function or energetics, the model of heart failure should mimic the clinical setting as closely as possible. However, if defined causal connections are under investigation such as structure–function analyses or regulation of gene expression, exact reflection of the clinical setting by the animal model may be less important. In this review, animal models of heart failure are discussed with particular focus on similarities between the animal model and the failing human heart regarding myocardial function as well as molecular and subcellular mechanisms. In addition, new models of heart failure and hypertrophy, and finally some recent animal models of myocarditis are reviewed. 

*Keywords:* Hypertrophy; Heart failure; Animal models; Calcium

## 1. Introduction

During the last decade, considerable advances in our understanding and management of heart failure have been made. However, with increasing life expectancy and decreasing mortality of acute myocardial infarction and other conditions that may cause heart failure, the incidence, prevalence, mortality and economic costs of the disease are steadily increasing. The overall prevalence of congestive heart failure (CHF) is 1 to 2% in middle-aged and older adults, reaches 2 to 3% in patients older than age 65 years, and is 5 to 10% in patients beyond the age of 75 years [1]. Survival of patients suffering from heart failure depends on the duration and severity of the disease, on gender, as well as on therapeutic strategies. In the Framingham study, the overall 5-year survival rates were 25% in men and 38% in women [2]. In recent clinical trials with selected patients under state-of-the-art medical therapy, 1 year mortality ranged between 35% in patients with severe congestive heart failure (NYHA IV) in the Consensus trial [3] to 9 and 12% in patients with moderate CHF (NYHA II–III) in the second Vasodilator Heart Failure Trial [4] and the Studies of Left Ventricular Dysfunction (SOLVD) trial [5]. Mechanisms of death include sudden death in about 40%, worsening of heart failure in about 40% and other factors in 20% of the patients.

## 2. What are the characteristics of human heart failure?

Human heart failure has many underlying causes, the frequencies of which have changed considerably during the last decades. At present, the leading cause is coronary heart disease which accounted for 67% of CHF cases in

*Tel.: +49 (551) 39 6351; Fax: +49 (551) 39 8918; E-mail: hasenfus@ruf.uni-freiburg.de

Time for primary review 31 days.

0008-6363/98/$19.00 
PII: S0008-6363(98)00110-2

the 1980s according to the Framingham heart study [2]. Most of these patients also had a history of arterial hypertension (57%). Valvular heart disease underlies failure in about 10% of the patients, and 20% of heart failure cases are attributable to primary myocardial diseases, of which dilated cardiomyopathy predominates. Regardless of the original cardiac abnormality, however, the advanced heart failure syndrome presents a complex picture including disturbed myocardial function, ventricular remodeling, altered hemodynamics, neurohumoral activation, cytokine overexpression, as well as vascular and endothelial dysfunction.

### 2.1. Neurohumoral and cytokine activation

Independent of the etiology of heart failure, activation of the neurohumoral and the cytokine system seems to play a critical role in the prognosis in CHF [6–8]. Activation of the neurohumoral systems occurs stepwise and is organ specific. It was shown recently, that increased cardiac adrenergic drive precedes generalized sympathetic activation in patients with mild CHF [9]. This results from increased norepinephrine release and decreased norepinephrine reuptake and seems to be associated with early attenuation of cardiac and arterial baroreceptor control of sympathetic tone [10,11]. Similarly, atrial natriuretic peptide is activated early in heart failure, and it was shown that atrial natriuretic peptide is elevated in asymptomatic patients with left ventricular dysfunction [12]. Although activation of local renin–angiotensin systems may occur early, plasma-renin activity and vasopressin release are only increased in patients with symptomatic heart failure [12].

Recent studies have identified the importance of cytokines as mediators of disease progression by mechanisms including necrotic and/or apoptotic myocyte cell death, myocardial fibrosis, and depression of myocardial function (for review see [13]). The influence of the vasoconstrictor peptide, endothelin has been extensively investigated. Both mature endothelin-1 and its precursor, big endothelin-1, are increased in the peripheral circulation in relation to the hemodynamic and functional severity of heart failure, and plasma levels of big endothelin-1 are correlated with the prognosis of patients with heart failure [14]. Similarly, circulating levels of tumor necrosis factor-α (TNF), of TNF receptors and of interleukin-6 are increased and positively related to the severity of heart failure [8]. TNF is expressed in the failing but not in the nonfailing human heart whereas TNF receptors (TNFR1 and TNFR2) are expressed in failing and nonfailing myocardium [7].

### 2.2. Hemodynamic abnormalities

Hemodynamic abnormalities in patients with advanced congestive heart failure include elevated filling pressures, reduced cardiac output and increased pulmonary and systemic vascular resistance. There is considerable evidence that endothelial dysfunction contributes to altered hemodynamics during rest and particularly to altered hemodynamics during exercise (for review see [15]). Endothelial dysfunction appears to result from remodeling of resistance arterioles and capillaries, from increased synthesis of endothelin, and from decreased synthesis of nitric oxide [16,17].

### 2.3. Myocardial alterations

At the level of the myocardium, characteristic functional, biochemical and molecular alterations occurring in end-stage heart failure have been described. Several studies have suggested that disturbed excitation–contraction coupling processes may underlie disturbed myocardial function [18–24]. This may be related to disturbed sarcoplasmic reticulum function due to decreased expression and activity of the sarcoplasmic reticulum calcium pump and increased expression and function of the sarcolemmal sodium–calcium exchanger (for review see [25]). In addition, disturbed energy metabolism may be involved in decreased sarcoplasmic-reticulum calcium transport [26].

Although myosin content may be decreased by about 20% due to replacement by connective tissue [18], maximum calcium-activated force was suggested to be similar in failing and nonfailing human myocardium [27,28]. This may be because force–time integral production of the individual crossbridge cycle is increased in the failing heart, associated with a reduced myofibrillar ATPase activity [18,29]. Previous studies suggested that unlike the situation in small mammals, alteration of crossbridge function may not be related to a myosin isoform shift, because it was observed that the ß-myosin heavy-chain isoform predominates in the left ventricle of nonfailing and failing human hearts [30]. This is in contrast to more recent studies in which at the level of mRNA ventricular expression of α-myosin heavy-chain isoform was observed in nonfailing hearts, which was decreased in failing human hearts [31,32]. Alternatively to a myosin isoform shift, the alteration in crossbridge function may, however, be related to changes in troponin T isoforms or alterations in myosin light chains [33,34]. Controversy exists regarding alteration of myofilament calcium sensitivity as measured in myofibrillar preparations which was suggested to be unchanged [35,36] or increased [37]. Wolff et al. suggested that calcium sensitivity is increased in failing myocardium from hearts with dilated cardiomyopathy which may be due in part to a reduction of protein kinase A-dependent phosphorylation of myofibrillar regulatory proteins [38].

Many studies have shown that the β-adrenergic signal transduction pathway is altered in the failing human heart. This results from a decrease in myocardial β1-adrenoceptor density which is partly due to decreased expression of the β1-adrenoceptor gene demonstrated both at the

mRNA and protein levels [39,40]. In addition, $G_{i\alpha}$ mRNA and protein concentrations are increased which may further inhibit adenylyl cyclase activity in failing human hearts [41].

Regarding extracellular matrix in human CHF, it was shown that connective tissue content is increased and that changes in collagen composition occur [42,43].

## 3. Animal models of heart failure and hypertrophy

During the period from 1993–1997, 1943 papers have been published on studies performed in animal models of heart failure (Table 1) and hypertrophy (Table 2). Most studies have been performed in rats with different interventions to induce hypertrophy and heart failure.

## 4. Rat models of heart failure

### *4.1. What are the advantages and disadvantages of using a rat model of heart failure?*

Rat models are relative inexpensive and because of short gestation periods, a large sample size can be produced in a relatively short period of time. Therefore, rat models have been extensively used to study long-term pharmacological interventions including long-term survival studies [44,45]. However, there are several limitations to the use of rat models regarding differences in myocardial function compared to the human heart: (1) Rat myocardium exhibits a very short action potential which normally lacks a plateau phase [46]. (2) Calcium removal from the cytosol is predominated by the activity of the sarcoplasmic reticulum calcium pump whereas $Na^+/Ca^{2+}$-exchanger activity is less relevant [46,47]. (3) In normal rat myocardium, α-myosin heavy-chain isoform predominates and a shift towards the β-myosin isoform occurs with hemodynamic load or hormonal changes [48]. (4) Resting heart rate is five times that of humans and the force–frequency relation is inverse [46].

### *4.2. Rat coronary ligation model*

Myocardial infarction following coronary artery ligation in Sprague–Dawley rats is a widely used rat model of heart failure. If the left coronary artery is not completely ligated, heart failure may occur as a consequence of chronic myocardial ischemia [49]. Complete occlusion of the left coronary artery results in myocardial infarction of variable sizes with occurrence of overt heart failure after 3–6 weeks in a subset of animals with large infarcts. The impairment of left ventricular function is related to the loss of myocardium. Failure is associated with left ventricular dilatation, reduced systolic function and increased filling pressures [44,50]. The progression of left ventricular dysfunction and myocardial failure is associated with neurohumoral activation similar to that seen in patients with CHF [51–54]. In particular, it was shown that ACE activity in the left ventricle correlated inversely with left ventricular function and that ACE activity in the kidney was only increased late after the induction of heart failure [55]. Depressed myocardial function is associated with altered calcium transients [56]. The density of L-type calcium channels, as evaluated by antagonist binding was shown to be decreased in moderate to severe stages of congestive heart failure [57,58]. Furthermore, it was shown that after 4, 8 and 16 weeks following coronary artery ligation, SR-$Ca^{2+}$-ATPase mRNA and protein levels decrease continuously with increasing severity of congestive heart failure. Interestingly, SR-$Ca^{2+}$-ATPase activity was found to be more depressed than expected from the reduction in protein levels [59].

Although a high initial mortality and induction of mild failure in most cases may be a disadvantage of this model it seems to be very useful for long-term studies of pharmacological interventions on the neurohumoral activation.

Of note, it was recently shown that ligation of the left descending coronary artery in Lewis inbred rats produces a uniformly large infarct with low mortality. This model, therefore, may be of advantage over the Sprague–Dawley rat model [60].

### *4.3. Rat aortic banding*

Suprarenal aortic coarctation results in a very short reactive hyperreninemia of less than 4 days. Thereafter, the circulating renin–angiotensin system is no longer activated, but the ventricular ACE activity begins to rise. After a period of several weeks, ventricular ACE activity may decrease again to normal values which may be related to normalization of wall stress with increasing hypertrophy [61]. Numerous studies have been performed using aortic banding in rats to evaluate different aspects of left ventricular hypertrophy. Furthermore, after several months, a subset of animals goes into failure. In a recent study, chronic experimental aortic constriction imposed by banding of the ascending aorta in weanlings resulted in compensated left ventricular hypertrophy of the adult rats for several weeks. After 20 weeks of aortic banding two distinct groups could be identified: rats without change in LV systolic pressure development and those with a significant reduction in left ventricular systolic pressure [62]. The latter group exhibited increased left ventricular volumes, reduced ejection fraction and clinical signs of overt heart failure [63]. Left ventricular hypertrophy and failure was associated with increased β-myosin heavy chain mRNA and atrial natriuretic factor mRNA. Interestingly, a decrease in SR-$Ca^{2+}$-ATPase mRNA levels by the polymerase chain reaction occurred in left ventricular myocardium from failing animals after 20 weeks of banding but

Table 1
Animal models of heart failure

| Species and technique | Selected references | Comments |
|---|---|---|
| **Rat** | 1028* | |
| Coronary ligation | [44,49,59,60] | Clinical characteristics similar to human CHF; survival studies |
| Aortic banding | [62–64] | Studies of transition from hypertrophy to failure; survival studies |
| Salt-sensitive hypertension | [66,67] | Studies of transition from hypertrophy to failure |
| Spontaneous hypertension | [68–71] | Extracellular matrix changes; apoptosis; studies of transition from hypertrophy to failure |
| SH–HF/Mcc-facp | [72–76] | Altered NOS expression; altered calcium triggered calcium release |
| Aorto-caval fistula | [184,185] | Left ventricular hypertrophy; moderate LV dysfunction |
| Toxic cardiomyopathy | [186–189] | Decreased myocardial performance; myocyte loss with chronic ethanol application. Cardiomyopathy following catecholamine infusion or associated with *Diabetes mellitus* |
| **Dog** | 148* | |
| Pacing tachycardia | [79–89,100–106] | Studies of remodeling and neurohumoral activation; studies on molecular mechanism of subcellular dysfunction; no hypertrophy |
| Coronary artery ligation | [111–115] | Studies on progression of heart failure; high mortality and arrhythmias |
| Direct-current shock | [115] | Studies of neurohumoral mechanisms |
| Volume overload<br>-aorto-caval fistula<br>-mitral regurgitation | [116–120] | Studies of neurohumoral mechanisms and therapeutic interventions |
| Vena caval constriction | [189] | Low cardiac output failure |
| Toxic cardiomyopathy | [190] | Left ventricular dysfunction |
| Genetic | [98] | Spontaneous cardiomyopathy in Doberman Pinscher dogs |
| **Pig** | 43* | |
| Pacing tachycardia | [107–110] | Comparable with dog model for most aspects |
| Coronary artery ligation | [191] | Congestive heart failure; altered myocardial energetics |
| **Rabbit** | 43* | |
| Volume and pressure overload | [122–126] | Myocardial alterations similar to failing human myocardium |
| Pacing tachycardia | [127–131,192] | Myocardial alteration similar to failing human myocardium |
| Toxic cardiomyopathy | [132] | Studies of functional consequences of altered ryanodine receptors |
| **Guinea pig** | 31* | |
| Aortic banding | [134,135,193] | Myocardial function and alteration of calcium handling similar to human heart failure |
| **Syrian hamster** | 10* | |
| Genetic | [136–147] | Hypertrophy and failure; alterations critically dependent on strain and age |
| **Cat** | 11* | |
| Pulmonary artery constriction | [194,195] | Transition from compensated right ventricular hypertrophy to failure |
| **Turkey** | 9* | |
| Toxic cardiomyopathy | [196] | Alteration of calcium handling and myocardial energetics |
| **Bovine** | 25* | |
| Genetic | [197] | Similar to human heart failure regarding changes in β-adrenergic system |
| **Sheep** | 17* | |
| Pacing tachycardia | [198,199] | Similar to dog and swine model of pacing tachycardia |
| Aortic constriction | [200] | Transition from compensated hypertrophy to left ventricular dysfunction |

* Total number of references in this species (failure and animal species) 1993–1997.

Table 2
Animal models of hypertrophy

| Species and technique | Number of references 1993–1997 | Selected references |
|---|---|---|
| **Rat** | 1082 | |
| Aortic constriction | | [62,63] |
| Pulmonary artery constriction | | [201] |
| Hypertension | | |
| -Renal ischemia | | [202] |
| -DOCA | | [203] |
| -Dahl salt-sensitive | | [66,67] |
| -SHR | | [68,69] |
| Arteriovenous fistula | | [204] |
| Hyperthyroidism | | [205] |
| Hypoxia | | [205] |
| Catecholamines | | [205] |
| Exercise | | [206,207] |
| **Rabbit** | 96 | |
| Aortic insufficiency/constriction | | [122–124] |
| Pulmonary constriction | | [121] |
| Hyperthyroidism | | [121] |
| **Dog** | 75 | |
| Aortic constriction | | [208] |
| Valvular aortic stenosis | | [209] |
| Tricuspid regurgitation | | [210] |
| **Pig** | 67 | |
| Pulmonary artery constriction | | [211] |
| **Cat** | 24 | |
| Pulmonary artery constriction | | [194] |
| **Hamster** | 28 | |
| Genetic | | [136] |
| **Ferret** | 9 | |
| Pulmonary artery constriction | | [212,213] |
| **Sheep** | 26 | |
| Aortic constriction | | [214] |
| **Baboon** | 3 | |
| Hyperthyroidism | | [215] |
| Renal ischemia | | [216] |
| **Guinea pig** | | |
| Aortic constriction | | [193,133–135,217] |
| **Mouse** | 165 | |
| Renal ischemia | | [218] |
| Exercise | | [219] |
| Aortic constriction | | [220] |
| **Transgenic animals** | | see Table 3 |

not in nonfailing hypertrophied hearts. From this data, it was suggested that the decrease in SR-$Ca^{2+}$-ATPase mRNA levels may be a marker of the transition from compensatory hypertrophy to failure in these animals [62]. During compensated hypertrophy, while catecholamine levels are normal, there is activation of the local myocardial renin–angiotensin system, which may be important for the development of myocardial failure [64]. With the development of heart failure, plasma catecholamine levels can increase [65].

This model seems to be well suited for studying the transition from hypertrophy to failure at the level of the myocardium. Nevertheless, one should keep in mind that considerable differences in the function of subcellular systems exist between rat and human myocardium [46].

### *4.4. Dahl salt-sensitive rats*

Another animal model which may be suited to study the transition from compensated hypertrophy to failure is the Dahl salt-sensitive rat [66,67]. This strain of rats develops systemic hypertension after receiving a high-salt diet. This

results in concentric left ventricular hypertrophy at 8 weeks, followed by marked left ventricular dilatation and overt clinical heart failure at 15–20 weeks. Failing rats die within a short period of time. Heart failure is associated with reduced myocardial performance as shown in isolated muscle strip preparations [67].

### 4.5. Spontaneous hypertensive rats (SHR)

The spontaneous hypertensive rat (SHR) is a well-established model of genetic hypertension in which cardiac pump function is preserved at 1 year of age [68]. At 18–24 months, cardiac failure develops which includes reduced myocardial performance and increased fibrosis. In this model, although altered calcium cycling was observed, no decrease in mRNA of the sarcoplasmic reticulum calcium pump was found during the transition from compensated hypertrophy to failure [69,70]. It was suggested that the transition to failure is associated with significant alterations in the expression of genes encoding extracellular matrix [70]. Furthermore, an increased number of apoptotic myocytes was observed, and it was suggested that apoptosis might be a mechanism involved in the reduction of myocyte mass that accompanies the transition from stable compensation to heart failure in the model. Interestingly, the angiotensin-converting enzyme inhibitor captopril was associated with reduction in the exaggerated apoptosis that accompanied CHF [71].

### 4.6. SH–HF rats

Spontaneously hypertensive rats which develop failure before 18 months of age have been selectively bred (SH–HF). Development of heart failure occurs earlier in SH–HF rats which carry the *facp* (corpulent) gene, which encodes a defective leptin receptor (SH–HF/Mcc-facp) [72]. In these animals, renin-plasma activity, atrial natriuretic peptide, and aldosterone levels progressively increase with age, and renin-plasma activity is independently correlated to cardiac hypertrophy [73]. Interestingly, hearts from the SH—HF rat exhibit a more negative force–frequency relationship than control rats [74]. In a recent study performed in SH–HF, Gómez at al. suggested that calcium current density, density and function of ryanodine receptors, and sarcoplasmic reticulum calcium uptake are normal. However, they showed that the relationship between calcium current density and the probability of evoking a spark was reduced indicating that calcium influx is less effective at inducing SR calcium release. It was speculated that these changes may be related to spacial remodeling between L-type calcium channels and ryanodine receptors [75]. Of note, a recent report showed that $Ca^{2+}$-dependent NOS activity and expression of endothelial NOS is increased in hypertensive SH–HF rats [76].

## 5. Dog models of heart failure

### 5.1. What are the advantages and disadvantages of using dog models of heart failure?

Generally, dog and other large animal models of heart failure may allow the study of left ventricular function and volumes more accurately than rodent models. In particular, they better allow chronic instrumentation. Furthermore, in dog, like in human myocardium, the β-myosin heavy-chain isoform predominates and excitation–contraction coupling processes seem to be similar to the human myocardium [77]. The force–frequency relation, as evaluated by $E_{max}$, the slope of the end-systolic pressure–volume relation, was shown to be positive in autonomically intact awake dogs as well as during autonomic blockade [78]. On the other hand, dog models are costly and require substantial resources with respect to housing and care.

### 5.2. Chronic rapid pacing

Chronic rapid pacing at heart rates above 200 beats per minute in previously healthy dogs within several weeks produces the syndrome of congestive heart failure [79–81]. In the majority of studies, chronic pacing tachycardia results in progressive biventricular chamber dilatation over a 3–4 week period. This is associated with a significant decrease in ejection fraction and diastolic dysfunction, followed by decreased cardiac output and increased systemic vascular resistance [80,82,83]. It is important to note that the changes in LV geometry and function are not accompanied by significant changes in LV mass and hypertrophy [80,81]. In addition, heart failure has been shown to be reversible with respect to clinical, hemodynamic and neurohumoral abnormalities when pacing is stopped [84]. The exact pathogenesis in this model is still unclear.

Similar to human heart failure, there are time-dependent changes in neurohumoral activation with an early sympathetic activation, increase in catecholamine plasma levels and attenuation of parasympathetic tone [85,86]. In addition plasma ANP levels are elevated early in the development of left ventricular dysfunction [87]. Systemic activation of the renin–angiotensin system is seen with progressive pump failure [86,88]. Furthermore, endothelial dysfunction with decreased agonist-stimulated and flow stimulated nitric-oxide mediated coronary vasodilation has been observed similar to the situation in patients with heart failure [89].

Consistent with the findings in failing human hearts, force–frequency relation is blunted or inversed in the pacing tachycardia failure dog model [90,91]. Altered force–frequency relation in this model was also observed at the level of the isolated myocyte [92]. Komamura et al. observed that failing animals do not further augment stroke volume by an acute increase in preload, suggesting that the

Frank–Starling reserve is exhausted under in vivo conditions [93].

At the level of the myocardium, contractile force has been shown to be decreased and calcium transients were prolonged [94]. Furthermore, Zile et al. showed that relaxation is impaired in isolated myocytes from failing hearts [95].

This may be related to altered expression and function of calcium-handling proteins. Although, an earlier report suggested that SR-$Ca^{2+}$-ATPase mRNA levels measured in left ventricular endocardial biopsies at baseline and at the onset of pacing tachycardia-induced failure do not significantly change [96], more recent data indicates that expression of SR-$Ca^{2+}$-ATPase is decreased. Similar to changes that occur in the failing human heart, O'Rourke et al. recently reported that mRNA and protein levels of sarcoplasmic reticulum calcium ATPase are decreased and that mRNA and protein levels of the sarcolemmal $Na^+$/$Ca^{2+}$-exchanger are significantly increased [97]. The latter findings are consistent with measurements from Cory et al. showing a decreased activity of the SR calcium pump in mongrel dogs with pacing-induced heart failure and in Doberman Pinscher dogs with dilated cardiomyopathy [98]. Thus altered calcium handling may result from reduced SR calcium uptake and accumulation and increased calcium sequestration into the extracellular space. In addition, a decreased number of ryanodine receptors has been suggested in a study by Cory et al. [98]. Consistently, Vatner et al. showed that in the pacing tachycardia failure model, [$^3$H]ryanodine receptor binding is depressed. However, this depression occurred as early as 1 day after pacing and remained at this depressed level up to 4–7 weeks of pacing when heart failure was manifest [99]. In the same study, dihydropyridine binding was not altered in the failing animals [99].

Whether altered myofilament calcium sensitivity contributes to altered myocardial function in this model is not clear [100,101].

Considerable changes seem to occur in myocyte shape, in cytoskeleton and in the extracellular matrix. In contrast to findings in human heart failure, collagen content was shown to be decreased and its structure was altered which may result in decreased collagen support [102]. Changes in cytoskeleton and extracellular matrix were suggested to be a major factor for ventricular remodeling, and apoptotic cell death was also suggested to play a key role in the development of CHF [103,102].

Significant alterations have been observed in the β-adrenoceptor–adenylyl-cyclase system. These include decreased β-adrenergic receptor density [102]. Unlike the situation in human heart failure, mRNA levels of adenylyl-cyclase have been shown to be reduced consistent with reduced basal and forskolin-stimulated adenylyl cyclase activity [104].

Similar to human CHF, this model was shown to be associated with malignant arrhythmias and sudden cardiac death which may be related to prolongation of the action potential [105]. Interestingly, action potential prolongation could be reversed by adenovirus mediated transfer of potassium channels (AdShK) in isolated myocytes from failing dog hearts [106].

In summary, the pacing-tachycardia dog model seems very valuable for studying neurohumoral mechanisms and peripheral circulatory alterations, both of which closely resemble that observed in human heart failure. Furthermore, alterations in myocardial function and molecular changes in calcium-handling proteins underlying altered myocardial function show considerable similarities to the failing human heart. This may allow the study of the transition from a compensated state of left ventricular dysfunction to overt failure with respect to alterations in calcium homeostasis. The model also provides temporal and mechanistic information on left ventricular remodeling and allows the study of pharmacologic interventions to influence the remodeling process. The limitations of the rapid pacing model include an uncertain pathogenesis, and lack of long-term stability because heart failure is reversible when pacing is stopped. Furthermore, unlike clinical forms of CHF, the development of CHF by chronic rapid pacing is not associated with hypertrophy or increased collagen content. Loss of collagen support may considerably contribute to ventricular remodeling in this model.

The technique of tachycardia pacing to induced heart failure has also been used in pigs and sheep and findings similar to those in dogs have been observed with respect to clinical, hemodynamic and neurohumoral changes [107–110].

### *5.3. Coronary artery ligation and microembolization*

Coronary artery ligation and microembolization have been used to produce myocardial infarction and CHF in dogs. In closed-chest dogs, approximately up to 7 embolization procedures are performed 1–3 weeks apart. Three months after the final microembolization, there are clinical signs of heart failure, there is left ventricular dilatation, decreased ejection fraction, and neurohumoral activation similar to that observed in humans [111]. A decreased number of β-adrenoceptors and L-type calcium channels have been observed 3 months after the final embolization procedure [112]. Furthermore, sarcoplasmic reticulum $Ca^{2+}$-ATPase activity and protein levels were reduced in left ventricular myocardium from failing animals [113]. With this model, the progression from left ventricular dysfunction to heart failure and the influence of pharmacological interventions can be studied [114].

The model has several disadvantages. Because of extensive collateral circulation, there are important differences in the pattern of infarction between the human and the dog. The model is time consuming, technically demanding and expensive. The model is associated with high mortality and with a high incidence of arrhythmias.

### 5.4. Transmyocardial direct-current shock

A number of transmyocardial direct-current shocks applied through a catheter into the left ventricular chamber in anesthetized dogs, results in left ventricular hypertrophy and dilatation, decreased ejection fraction and decreased cardiac output over a 4-months period [115]. This is associated with increased plasma catecholamines but with no change in plasma renin activity [115].

### 5.5. Volume overload

In dogs, volume overload has been produced by creation of an arteriovenous fistula or by destruction of the mitral valve [116,117]. Chronic experimental mitral regurgitation produced in closed-chest dogs by disruption of mitral chordae or leaflets using an arterially placed grasping forceps results in left ventricular hypertrophy and dilatation within 3 months and development of overt clinical heart failure occurs in this model [117]. Neurohumoral activation including local activation of the RAS was observed which is associated with depressed myocardial function [118–120]. The model has been used to study the influence of chronic β-adrenoceptor blockade on myocyte and left ventricular function which both significantly improved with this treatment [120].

## 6. Rabbit models of heart failure

### 6.1. What are the advantages and disadvantages of using a rabbit model of heart failure?

Rabbit models are less expensive than dog models. In addition, nonfailing rabbit myocardium exhibits interesting similarities to the human heart: (1) The β-myosin heavy-chain isoform predominates in adult animals, (2) the sarcoplasmic reticulum contributes by about 70% and the $Na^+/Ca^{2+}$-exchanger contributes by about 30% to calcium elimination, (3) the force–frequency relation is positive [121,46,47].

### 6.2. Volume and pressure overload

Volume overload, pressure overload and the combination of both are used to induce heart failure in rabbits. Chronic severe aortic regurgitation in rabbits, created by aortic valve perforation with a catheter, produces left ventricular hypertrophy, followed by systolic dysfunction and heart failure after a period of months [122]. Occurrence of heart failure is more consistently and rapidly observed when aortic regurgitation is combined with aortic constriction. In the model developed by Ezzaher et al., aortic insufficiency is produced by destroying the aortic valve with a catheter introduced through the carotid artery. After 14 days, aortic constriction is performed just below the diaphragm. Heart failure occurs about 4 weeks after the initial procedure [123,124]. Heart failure is associated with alterations in the β-adrenoceptors system similar to those in humans [123]. Furthermore, in this model there is inversion of the force–frequency relation and alteration of post-rest potentiation which closely resembles the situation in the human heart [125]. Interestingly, protein and mRNA levels of $Na^+/Ca^{2+}$-exchanger were significantly increased in failing compared to nonfailing animals whereas sarcoplasmic reticulum $Ca^{2+}$-ATPase was not significantly altered [126]. This may indicate that increased transsarcolemmal calcium loss by increased $Na^+/Ca^{2+}$-exchanger activity my decrease calcium availability to contractile proteins and decrease myocardial function even without direct alteration of sarcoplasmic reticulum function.

Because this model closely mimics alterations of myocardial function observed in the end-stage failing human myocardium, this model may be well suited to study alterations in excitation–contraction coupling processes occurring during the transition from compensated hypertrophy to failure.

### 6.3. Tachycardia-pacing

Recently, chronic rapid pacing at rates between 350 and 400 beats per minute over a period of several weeks in rabbits was shown to produce myocardial depression as well as clinical, hemodynamic and neurohumoral signs of heart failure [127–129]. Regarding myocardial function, force–frequency relation was severely depressed and inverted at higher stimulation rates [130]. This is similar to the alteration of the force–frequency relation observed in failing human hearts. As was observed in the tachycardia-pacing dog failure model, no left ventricular hypertrophy is developed in the rabbit model. Interestingly, Eble et al. recently showed that although the rate of myosin heavy chain (MHC) synthesis was increased, left ventricular MHC content was not increased [131]. The authors suggested that accelerated degradation may contribute to the failure of myocardial hypertrophy in this model [131]. These findings may also be relevant for pathophysiology of tachycardia-pacing induced CHF in other animal species

### 6.4. Doxorubicin cardiomyopathy

Doxorubicin exhibits acute and chronic cardiotoxicity and has been used to induce failure in various animal species. Several different mechanisms involved in the pathophysiology of doxorubicin-induced heart failure have been suggested including free radical generation and lipid peroxidation, reactive sulfhydryl groups, binding to channel regulatory sites, or inhibition of mRNA and protein synthesis [132].

In a recent study, doxorubicin, given intravenously twice weekly for 6–9 weeks resulted in myocardial failure, the

degree of which was correlated with decreased [$^3$H]ryanodine binding. Furthermore a decreased number of ryanodine receptors was indicated from Western Blot data. These findings may suggest that this model is suited to study functional consequences of altered ryanodine receptor expression [132].

## 7. Guinea pig models

### *7.1. Aortic banding*

Following 8 weeks of banding of the descending thoracic aorta in guinea pigs, overt heart failure develops in a subgroup of animals [133–135]. Alteration of myocardial function in this guinea pig model has some similarities with end-stage failing human myocardium. Siri et al. showed that the force–frequency relation is blunted in isolated myocytes from failing hearts [133]. Furthermore, a decrease in SR-$Ca^{2+}$-ATPase protein levels and phospholamban protein levels was observed in failing guinea pig hearts following 8 weeks of banding of the descending thoracic aorta as compared to an age-matched banded group without clinical signs of heart failure [134]. Regarding myosin isoforms, guinea pig myocardium, like the human ventricular myocardium, contains predominantly the β-myosin heavy chain with small amounts of α-myosin. This is shifted completely to β-myosin without any α-myosin heavy chain present in hypertrophied and failing hearts [135].

These studies show that this guinea pig model has similarities to human heart failure with respect to calcium cycling, myosin isoforms and myocardial function. This model may be suited to study the transition from cardiac hypertrophy to failure with respect to alterations in excitation–contraction coupling systems.

## 8. Syrian hamster

### *8.1. Cardiomyopathic hamster*

Cardiomyopathic strains of the Syrian hamster have been widely used as a model for cardiac hypertrophy and heart failure [136]. The model exhibits an autosomal recessive mode of inheritance [136,137]. The cardiac disease proceeds progressively in several histologic and clinical phases during the life of the animal and overt heart failure develops after 7–10 months. Histologically, necrotic, calcified myocardial lesions are observed initially in the development of the disease. Microvascular spasms and disturbed calcium handling have been suggested to be relevant for the pathophysiology in this model and beneficial effects of verapamil have been observed [138–140]. The density of L-type calcium channels seems to be increased in younger animals before morphological evidence for the myopathy is present, however, when there is fully developed myopathy, there seems to be no appreciable difference between control and myopathic hamsters [141,142]. Kuo et al. showed decreased gene expression of sarcoplasmic reticulum calcium pump in Syrian hamsters. Interestingly, this alteration in gene expression preceded any noticeable myocyte damage [143]. On the other hand, Whitmer et al. observed that sarcoplasmic reticulum calcium uptake is decreased in 9-month-old animals exhibiting heart failure but not in hypertrophic hearts without signs of heart failure [140]. Enhanced activity of the $Na^+/Ca^{2+}$-exchanger in failing animals was recently suggested from electrophysiological measurements [144]. Furthermore, time-dependent changes in myosin isoform expression has been observed [145].

Recently, a genetic linkage map localized the cardiomyopathy locus on hamster chromosome 9qa2.1-b1 [146]. Furthermore, it was shown that the cardiomyopathy results from a mutation in the delta-sarcoglycan gene [147].

In summary, the advantages of this model are (1) absence of surgical manipulations, (2) low costs and (3) the ease with which large numbers of animals can be studied. It is important to state that there are differences among the strains, and in the time course of the pathologic changes, and therefore, the time point at which measurements are performed is critically important in this model. Furthermore, subcellular alterations underlying myocardial failure seem to be different from those in failing human hearts.

## 9. Recent models of CHF in mice

The recent development of techniques to alter specifically the expression of genes greatly improved our understanding of the pathophysiology of heart failure. Moreover, several genetic models of heart failure by addition or deletion of genes in mice have been developed and miniaturized physiological techniques to evaluate the resulting cardiac phenotypes have been established [148,149]. These models allow the identification of genes that are causative for heart failure and to evaluate molecular mechanisms responsible for the development and progression of the disease (Table 3).

Gene-targeted disruption of the muscle LIM protein (MLP) in mice is a new model of dilated cardiomyopathy and heart failure [150]. MLP is a regulator of myogenic differentiation. Mice which are homozygous for the MLP knockout develop dilated cardiomyopathy associated with myocardial hypertrophy, interstitial cell proliferation and fibrosis. Adult mice show clinical and hemodynamic signs of heart failure similar to those in humans. Because of these similarities, it was suggested that molecular mechanisms resulting in MLP dysfunction may be involved in

Table 3
Transgenic models of heart failure and hypertrophy

| Intervention | Phenotype | Reference |
|---|---|---|
| **Gene overexpression** | | |
| C-myc | Myocardial hyperplasia | [221] |
| Epstein-Barr virus nuclear antigen | Dilated cardiomyopathy | [157] |
| Polyomavirus large T-antigen | Cardiomyopathy | [158] |
| Calmodulin | Myocardial hypertrophy and hyperplasia | [166] |
| Myogenic factor 5 | Cardiomyopathy and failure | [151] |
| $G_{s\alpha}$ | Cardiomyopathy and failure | [152] |
| $\alpha_1$-Adrenergic receptor | Myocardial hypertrophy | [168] |
| p21-ras | Myocardial hypertrophy; myofibrillar disarray | [222] |
| Interleukin β and interleukin β receptor | Hypertrophy | [167] |
| Nerve growth factor | Cardiomyopathy | [155] |
| Insulin-like growth factor 1 | Cardiomyopathy; hyperplasia | [156] |
| β-adrenergic receptor kinase | Reduced contractility | [154] |
| G protein coupled receptor kinase | Reduced contractility | [223] |
| TGR (m Ren 2)27 | Hypertrophy in rats | [224] |
| **Gene mutation** | | |
| α-cardiac myosin heavy chain | Hypertrophic cardiomyopathy | [162] |
| Lack of β-myosin light chain binding domain | Hypertrophic cardiomyopathy | [163] |
| **Knockout of gene** | | |
| Muscle LIM protein | Dilated cardiomyopathy and failure | [150] |
| Adenine nucleotide translocator | Hypertrophy | [169] |
| Transforming growth factor β | Myocarditis and failure | [182] |
| Interferon regulatory factor 1 | Myocarditis and failure | [181] |

the development of human dilated cardiomyopathy and CHF [150].

Development of cardiomyopathy was also observed in mice with knockout of myogenic factor 5 [151].

Another mouse model of dilated cardiomyopathy is overexpression of the cardiac stimulatory G protein α subunit ($G_{s\alpha}$). In this model, chronic sympathetic stimulation was suggested to be the cause of cardiomyopathy. Older mice exhibited left ventricular dilatation and dysfunction and increased mortality [152].

Transgenic mice overexpressing either β-adrenergic receptor kinase or G protein-coupled receptor kinase 5, resulting in uncoupling of the β-adrenergic receptors, also exhibit reduced contractility but without clinical signs of overt CHF [153,154].

Myocyte hyperplasia and dilated cardiomyopathy have been observed in animals with overexpression of the insulin-like growth factor 1 gene, and the nerve growth factor (NGF) [155,156].

Cardiomyopathy was also observed in a tropomodulin-overexpression model and in transgenic mice expressing Epstein-Barr virus nuclear antigen-leader protein or polyoma virus large T-antigen [157,158]. Tropomodulin is a component of the thin filament proteins which determines sarcomeric-actin filament length. A recent model of transgenic overexpression of tropomodulin exhibited dilated cardiomyopathy 2–4 weeks after birth with reduced contractile function and heart failure. This was associated with loss of myofibrillar organization [159].

## 10. Recent animal models of hypertrophy

Numerous animal models have been developed in the past and applied to study molecular mechanisms and functional aspects of myocardial hypertrophy (Table 2). Comparison of these models with different forms of myocardial hypertrophy in humans is difficult because unlike end-stage failing myocardium available from cardiac transplantation surgery, nonfailing hypertrophied human myocardium is not readily available.

Animal models of hypertrophy which allow the study of the transition from compensated hypertrophy to heart failure have been discussed in the sections above and hypertrophy associated with hypertension is addressed in the review by Pinto and Ganten [160]. Therefore, in the following section, only newer aspects of animal models of hypertrophy will be discussed.

### *10.1. Hypertrophic cardiomyopathy*

Hypertrophic cardiomyopathy is a complex cardiac disease in humans which is caused by a genetic malformation of the heart. The disease can be caused by a mutation in at least one of four genes that encode proteins of the cardiac sarcomere: the β-myosin heavy chain, cardiac troponin T, α-tropomyosin and myosin-binding protein C gene. In addition, mutations in the two genes encoding the myosin light chains that may cause a rare form of the disease, have been reported and other genes that cause the disease are likely to be found. Clinically the disease is characterized by asymmetrical left ventricular hypertrophy, myofiber disarray, diastolic left ventricular dysfunction, and increased incidence of sudden death. The clinical course varies markedly depending on the type of mutation and other unknown factors (for review see [161]).

A transgenic mouse model of the disease (a point mutation of the $Arg^{403}$-Gln in the α-myosin heavy-chain gene) has been developed which exhibits similarities to human familial hypertrophic cardiomyopathy [162]. A similar phenotype was recently observed in transgenic mice lacking the light chain binding domain of the β-myosin heavy chain [163]. These models will allow the

study of the still unknown pathophysiological mechanisms of the disease.

### *10.2. Transgenic models of hypertrophy*

Other transgenic mice models of hypertrophy have been developed (Table 3). Overexpression of the H-*ras* gene targeted to ventricles with the MLC2v promotor causes ventricular hypertrophy including myofiber disarray, obstruction of the left ventricular outflow tract, and diastolic dysfunction [164,165].

Overexpression of calmodulin, a calcium-binding protein, can also induce cardiac hypertrophy in transgenic mice [166].

Hypertrophy was also induced in transgenic mice overexpressing interleukin 6 and the interleukin 6 receptor associated with activation of gp130, the latter was suggested to mediate hypertrophic response in this model [167].

Chronic activation of the $\alpha_1$-adrenergic receptor pathway also results in hypertrophy in transgenic mice overexpressing the $\alpha_1$-adrenergic receptor [168].

Recently, a mouse transgenic model for mitochondrial myopathy exhibiting skeletal muscle myopathy and cardiac hypertrophy has been reported. This model was created by knockout of the heart/muscle isoform of the adenine nucleotide translocator (Ant1) [169].

## 11. Recent animal models of myocarditis

Several animal models of myocarditis have been developed and progression to dilated cardiomyopathy and heart failure occurs in some of those [170–174]. Congestive heart failure develops after an acute phase of myocarditis induced by the M variant of the encephalomyocarditis virus [175]. Myocyte necrosis and biventricular dilatation occur during the phase of viremia, and signs of CHF were observed at 7 to 14 days after inoculation. Altered myocardial function is associated with neurohumoral activation. Potential mechanisms contributing to the progression of CHF include a persistence of the viral RNA within the myocardium, viral-mediated cytokine production with continued myocytolysis, a prolonged immune response, and continued fibrosis and abnormalities in microcirculatory function. Interestingly, tumor necrosis factor (TNF) was elevated in this model and an exogenously administered anti-TNF antibody improved survival and reduced the myocardial lesion, suggesting the importance of TNF in the pathogenesis [176].

Another widely used model is based on experimental autoimmune myocarditis [177]. This model has been applied to different species. The model resembles human giant cell myocarditis. It was shown that myocarditis and hemodynamic deterioration developed within 21 days after immunization of rats with cardiac myosin. This was associated with increased activity and expression of iNOS, and an inhibitor of iNOS effectively attenuated histopathological changes. Accordingly, it was concluded that NO may play an important role in mediating pathophysiological changes in myocarditis of autoimmune origin [177].

Autoimmune myocarditis has also been induced with various intracellular antigens. When CAF1/J mice were immunized with a monoclonal anti-dog sarcoplasmic reticulum, $Ca^{2+}$-ATPase antibody myocarditis developed [178]. Furthermore, myocarditis and decreased cardiac function was observed after immunization of guinea pigs with the isolated ADP/ATP carrier protein [179].

Recently, transgenic knockout models of different components of the immune system have provided useful insights in the pathogenesis of viral myocarditis (for review see [180]). An interesting mouse myocarditis model was established by knocking out the gene encoding the interferon regulatory factor-1. This factor plays an important role in the regulation of interferon expression. Inactivation of the gene in mice leads to a pronounced susceptibility to Coxsackie-viral myocarditis [181].

Knockout of the gene of transforming growth factor $\beta 1$ in mice was shown to result in severe perimyocarditis resembling viral myocarditis or autoimmune diseases [182,183].

## 12. Animal models of heart failure and hypertrophy in the past, present and future

Besides basic ethical and philosophical questions, the use of animal models of heart failure and hypertrophy needs careful consideration because of at least two reasons: (1) the disease may be associated with discomfort and pain to the animal, and (2) results from animal studies are not readily transferable to the situation in patients with heart failure.

In the past, a large number of studies have been performed in animals with overt clinical heart failure to evaluate pathophysiology from the level of the intact instrumented animal to the tissue homogenate. These kind of studies brought a lot of information on hemodynamics, neurohumoral activation, myocardial function and subcellular and molecular alterations in the failing heart. There are great differences between species and models and only some models mimic human heart failure in some aspects. These kind of studies seem to be less important in the presence because with recent invasive and noninvasive technologies hemodynamics can be studied in patients. Furthermore, with cardiac transplantation surgery, end-stage failing human myocardium became available for functional, biochemical and molecular biology studies allowing the evaluation of alterations which are present in end-stage failure in the human heart itself. However, it is rather difficult or impossible to study myocardial changes

during compensated, less-severe stages of CHF, during the transition from hypertrophy to failure or during the process of remodeling. Therefore, in order to study transition processes occurring in heart failure, animal models are critically important. Furthermore, animal models of heart failure may be relevant to study the effects of new pharmacologic strategies on hemodynamics, neurohumoral activation, and survival under preclinical conditions.

At present, transgenic animal models of hypertrophy and heart failure are critically important for understanding the molecular alterations underlying the development of the disease. Addition or deletion of genes in transgenic mice together with miniaturized physiological techniques to evaluate the resulting cardiac phenotypes allow the identification of genes that are causative for heart failure and to evaluate molecular mechanisms responsible for the development and progression of the disease. Hypertrophy and heart failure models in mice will be used in the future to study rescue or repair by knockout or overexpression of specific genes. Finally, animal models of heart failure which mimic distinct features of human heart failure will be critically important to the study of the consequences of gene transfer and molecular techniques to correct disturbed subcellular processes in the failing heart. These kind of studies are a prerequisite to the development and introduction of molecular strategies for the treatment of CHF in patients.

## Acknowledgements

The author greatly appreciates the valuable contribution of Christine Baumann in preparing this manuscript.

## References

[1] Yamani M, Massie BM. Congestive heart failure: insights from epidemiology, implications for treatment. Mayo Clin Proc 1993;68:1214–1218.

[2] Ho KKL, Anderson KM, Kannel WB, Grossman W, Levy D. Survival after the onset of congestive heart failure in Framingham Heart Study subjects. Circulation 1993;88:107–115.

[3] The Consensus Trial Study Group. Effects of enalapril on mortality in severe congestive heart failure. Results of the Cooperative North Scandinavian Enalapril Survival Study (CONSENSUS). N Engl J Med 1987;316:1429–1435.

[4] Cohn JN, Johnson G, Ziesche S, Cobb F, Francis G, Tristani F, et al. A comparison of enalapril with hydralazine-isosorbide dinitrate in the treatment of chronic congestive heart failure. N Engl J Med 1991;325:303–310.

[5] The SOLVD Investigators. Effect of enalapril on survival in patients with reduced left ventricular ejection fractions and congestive heart failure. N Engl J Med 1991;325:293–302.

[6] Francis GS, Cohn JN, Johnson G, et al. Plasma norepinephrine, plasma-renin activity, and congestive heart failure. Relations to survival and the effects of therapy in V-HeFT II. The V-HeFT VA Cooperative Studies Group. Circulation 1993;87(Suppl VI):40–48.

[7] Torre-Amione G, Kapadia S, Lee J, et al. Tumor necrosis factor-alpha and tumor necrosis factor receptors in the failing human heart. Circulation 1996;93:704–711.

[8] Torre-Amione G, Kapadia S, Benedict C, et al. Proinflammatory cytokine levels in patients with depresses left ventricular ejection fraction: a report from the study of left ventricular dysfunction (SOLVD). J Am Coll Cardiol 1996;27:1201–1206.

[9] Rundqvist B, Elam M, Bergmann-Sverrisdottir Y, Eisenhofer G, Friberg P. Increased cardiac adrenergic drive precedes generalized sympathetic activation in human heart failure. Circulation 1997;95:169–175.

[10] Eisenhofer G, Friberg P, Rundqvist B, et al. Cardiac sympathetic nerve function in congestive heart failure. Circulation 1996;3:1667–1676.

[11] Grassi G, Seravalle G, Cattaneo BM, et al. Sympathetic activation and loss of reflex sympathetic control in mild congestive heart failure. Circulation 1995;92:3206–3211.

[12] Francis GS, Benedict C, Johnstone DE, et al. Comparison of neuroendocrine activation in patients with left ventricular dysfunction with and without congestive heart failure. A substudy of the Studies of Left Ventricular Dysfunction (SOLVD). Circulation 1990;82:1724–1729.

[13] Shan K, Kurrelmeyer K, Seta Y, et al. The role of cytokines in disease progression in heart failure. Curr Opin Cardiol 1997;12:218–223.

[14] Pacher R, Stanek B, Hulsmann M, et al. Prognostic impact of big endothelin-1 plasma concentrations compared with invasive hemodynamic evaluation in severe heart failure. J Am Coll Cardiol 1996;27:633–641.

[15] Katz SD. Mechanisms and implications of endothelial dysfunction in congestive heart failure. Curr Opin Cardiol 1997;12:259–264.

[16] Wroblewski H, Sindrup JH, Norgaard T, Haunso S, Kastrup J. Effects of orthotopic cardiac transplantation on structural microangiopathy and abnormal hemodynamics in idiopathic dilated cardiomyopathy. Am J Cardiol 1996;77:281–285.

[17] Katz SD, Krum H, Khan T, Knecht M. Exercise-induced vasodilation in forearm circulation of normal subjects and patients with congestive heart failure: role of endothelium-derived nitric oxide. J Am Coll Cardiol 1996;28:585–590.

[18] Hasenfuss G, Mulieri LA, Leavitt BJ, et al. Alteration of contractile function and excitation–contraction coupling in dilated cardiomyopathy. Circ Res 1992;70:1225–1232.

[19] Beuckelmann DJ, Nabauer M, Erdmann E. Intracellular calcium handling in isolated ventricular myocytes from patients with terminal heart failure. Circulation 1992;85:1046–1055.

[20] Gwathmey JK, Copelas L, MacKinnon R, et al. Abnormal intracellular calcium handling in myocardium from patients with end-stage heart failure. Circ Res 1987;61:70–76.

[21] Pieske B, Kretschmann B, Meyer M, et al. Alterations in intracellular calcium handling associated with the inverse force–frequency relation in human dilated cardiomyopathy. Circulation 1995;92:1169–1178.

[22] Hasenfuss G, Holubarsch C, Hermann HP, et al. Influence of the force–frequency relationship on haemodynamics and left ventricular function in patients with non-failing hearts and in patients with dilated cardiomyopathy. Europ Heart J 1994;15:164–170.

[23] Pieske B, Sutterlin M, Schmidt-Schweda S. Diminished post-rest potentiation of contractile force in human dilated cardiomyopathy. Functional evidence for alterations in intracellular $Ca^{2+}$ handling. J Clin Invest 1996;98:764–776.

[24] Piot C, Lemaire S, Albat B. High frequency-induced upregulation of human cardiac calcium currents. Circulation 1996;93:120–128.

[25] Hasenfuss G. Alterations of calcium-regulatory proteins in heart failure. Cardiovasc Res 1998;37:279–289.

[26] Neubauer S, Horn M, Cramer M, et al. Myocardial phosphocreatine-to-ATP ratio is a predictor of mortality in patients with dilated cardiomyopathy. Circulation 1997;96:2178–2182.

[27] Ginsburg R, Bristow MR, Billingham ME, et al. Study of the normal

and failing isolated human heart: decreased response of failing heart to isoproterenol. Am Heart J 1983;106:535–540.
[28] Feldman MD, Copelas L, Gwathmey JK, et al. Deficient production of cyclic AMP: pharmacologic evidence of an important cause of contractile dysfunction in patients with end-stage heart failure. Circulation 1987;75:331–339.
[29] Alpert NR, Gordon MS. Myofibrillar adenosine triphosphatase activity in congestive heart failure. Am J Physiol 1962;202:940–946.
[30] Mercadier JJ, Bouveret P, Gorza L, et al. Myosin isoenzymes in normal and hypertrophied human ventricular myocardium. Circ Res 1983;53:52–62.
[31] Nakao K, Minobe W, Roden R, Bristow MR, Leinwand LA. Myosin heavy-chain gene expression in human heart failure. J Clin Invest 1997;100:2362–2370.
[32] Lowes BD, Minobe W, Abraham WT, et al. Changes in gene expression in the intact human heart. Downregulation of α-myosin heavy chain in hypertrophied, failing ventricular myocardium. J Clin Invest 1997;100:2315–2324.
[33] Anderson PA, Malouf NN, Oakeley AE, Pagani ED, Allen PD. Troponin T isoform expression in humans. A comparison among normal and failing adult heart, fetal heart, and adult and fetal skeletal muscle. Circ Res 1991;69:1226–1233.
[34] Margossian SS, White HD, Caulfield JB, et al. Light chain 2 profile and activity of human ventricular myosin during dilated cardiomyopathy. Identification of a causal agent for impaired myocardial function. Circulation 1992;85:1720–1733.
[35] Hajjar RJ, Gwathmey JK, Briggs GM, Morgan JP. Differential effect of DPI 201-106 on the sensitivity of the myofilaments to $Ca^{2+}$ in intact and skinned trabeculae from control and myopathic human hearts. J Clin Invest 1988;82:1578–1584.
[36] D'Agnolo A, Luciani GB, Mazzucco A, Galluci V, Salviati G. Contractile properties and $Ca^{2+}$ release activity of the sarcoplasmic reticulum in dilated cardiomyopathy. Circulation 1992;85:518–525.
[37] Schwinger RH, Bohm M, Koch A, et al. The failing human heart is unable to use the Frank–Starling mechanism. Circ Res 1994;74:959–969.
[38] Wolff MR, Buck SH, Stoker SW, Greaser ML, Mentzer RM. Myofibrillar calcium sensitivity of isometric tension is increased in human dilated cardiomyopathies: role of altered beta-adrenergically mediated protein phosphorylation. J Clin Invest 1996;98:167–176.
[39] Bristow MR, Minobe WA, Raynolds MV, et al. Reduced beta-1 receptor messenger RNA abundance in the failing human heart. J Clin Invest 1993;92:2737–2745.
[40] Ungerer M, Bohm M, Elce JS, Erdmann E, Lohse MJ. Altered expression of beta-adrenergic receptor kinase and beta1-adrenergic receptors in the failing human heart. Circulation 1993;87:454–463.
[41] Brodde OE, Michel MC, Zerkowski HR. Signal transduction mechanisms controlling cardiac contractility and their alterations in chronic heart failure. Cardiovasc Res 1995;30:570–584.
[42] Marijianowski MMH, Teeling P, Mann J, Becker AE. Dilated cardiomyopathy is associated with an increase in the type I/type III collagen ratio: a quantitative assessment. J Am Coll Cardiol 1995;25:1263–1272.
[43] Schaper J, Froede R, Hein S, et al. Impairment of the myocardial ultrastructure and changes of the cytoskeleton in dilated cardiomyopathy. Circulation 1991;83:504–514.
[44] Pfeffer MA, Pfeffer JM, Fishbein MC, et al. Myocardial infarct size and ventricular function in rats. Circ Res 1979;44:503–512.
[45] Sakai S, Miyauchi T, Kobayashi M, et al. Inhibition of myocardial endothelin pathway improves long-term survival in heart failure. Nature 1996;384:353–355.
[46] Bers DM. Control of cardiac contraction by SR-Ca release and sarcolemmal-Ca fluxes. In: Bers DM, editor. Excitation–contraction coupling and cardiac contractile force. Developments in cardiovascular medicine, vol. 122. Dordrecht, Boston, London: Kluver Academic Publishers, 1991:149–170.
[47] Pieske B, Maier LS, Weber T, Bers DM, Hasenfuss G. Alterations in sarcoplasmic reticulum $Ca^{2+}$-content in myocardium from patients with heart failure. Circulation 1997;96(Suppl I):199.
[48] Swynghedauw B. Developmental and functional adaptation of contractile proteins in cardiac and skeletal muscles. Physiol Rev 1986;66:710–771.
[49] Kajstura J, Zhang X, Reiss K, et al. Myocyte cellular hyperplasia and myocyte cellular hypertrophy contribute to chronic ventricular remodeling in coronary artery narrowing-induced cardiomyopathy in rats. Circ Res 1994;74:383–400.
[50] Litwin SE, Katz SE, Morgan JP, Douglas PS. Serial echocardiographic assessment of left ventricular geometry and function after large myocardial infarction in the rat. Circulation 1994;89:345–354.
[51] van Veldhuisen DJ, van Gilst WH, de Smet BJ, et al. Neurohumoral and hemodynamic effects of ibopamine in a rat model of chronic myocardial infarction and heart failure. Cardiovasc Drugs Ther 1994;8:245–250.
[52] Hodsman GP, Kohzuki M, Howes LG, et al. Neurohumoral responses to chronic myocardial infarction in rats. Circulation 1988;78:376–381.
[53] Teerlink JR, Loffler BM, Hess P, et al. Role of endothelin in the maintenance of blood pressure in conscious rats with chronic heart failure. Acute effects of the endothelin receptor-antagonist Ro 47-0203 (Bosentan). Circulation 1994;90:2510–2518.
[54] Yamagishi H, Kim S, Nishikimi T, Takeuchi K, Takeda T. Contribution of cardiac renin–angiotensin system to ventricular remodelling in myocardial-infarcted rats. J Mol Cell Cardiol 1993;25:1369–1380.
[55] Pinto YM, de Smet BG, van Gilst WH, et al. Selective and time-related activation of the cardiac renin–angiotensin system after experimental heart failure: relation to ventricular function and morphology. Cardiovasc Res 1993;27:1933–1938.
[56] Litwin SE, Morgan JP. Captopril enhances intracellular calcium handling and beta-adrenergic responsiveness of myocardium from rats with postinfarction failure. Circ Res 1992;71:797–807.
[57] Dixon IM, Lee SL, Dhalla NS. Nitrendipine binding in congestive heart failure due to myocardial infarction. Circ Res 1990;66:782–788.
[58] Gopalakrishnan M, Triggle DJ, Rutledge A, et al. Regulation of $K^+$ and $Ca^{2+}$ channels in experimental cardiac failure. Am J Physiol 1991;261:H1979–H1987.
[59] Zarain-Herzberg A, Afzal N, Elimban V, Dhalla NS. Decreased expression of cardiac sarcoplasmic reticulum $Ca^{2+}$-pump ATPase in congestive heart failure due to myocardial infarction. Mol Cell Biochem 1996;163–164:285–290.
[60] Liu YH, Yang XP, Nass O, et al. Chronic heart failure induced by coronary artery ligation in Lewis inbred rats. Am J Physiol 1997;272:H722–727.
[61] Holtz J, Studer R, Reinecke H, Just H. Modulation of myocardial sarcoplasmic reticulum $Ca^{2+}$-ATPase in cardiac hypertrophy by angiotensin converting enzyme?. Basic Res Cardiol 1992;87(Suppl II):191–204.
[62] Feldman AM, Weinberg EO, Ray PE, Lorell BH. Selective changes in cardiac gene expression during compensated hypertrophy and the transition to cardiac decompensation in rats with chronic aortic banding. Circ Res 1993;73:184–192.
[63] Weinberg EO, Schoen FJ, George D, et al. Angiotensin-converting enzyme inhibition prolongs survival and modifies the transition to heart failure in rats with pressure overload hypertrophy due to ascending aortic stenosis. Circulation 1994;90:1410–1422.
[64] Schunkert H, Lorell BH. Role of angiotensin II in the transition of left ventricular hypertrophy to cardiac failure. Heart Failure 1994;10:142–149.
[65] Elsner D, Riegger GA. Characteristics and clinical relevance of animal models of heart failure. Curr Opin Cardiol 1995;10:253–259.
[66] Dahl LK, Heine M, Tassinari L. Role of genetic factors in susceptibility to experimental hypertension due to chronic excess salt ingestion. Nature 1962;194:480–482.

[67] Inoko M, Kihara Y, Morii I, Fujiwara H, Sasayama S. Transition from compensatory hypertrophy to dilated, failing left ventricles in Dahl salt-sensitive rats. Am J Physiol 1994;267:H2471–H2482.
[68] Okamoto K, Aoki K. Development of a strain of spontaneously hypertensive rats. Jpn Circ J 1963;27:282–293.
[69] Bing OH, Brooks WW, Conrad CH, et al. Intracellular calcium transients in myocardium from spontaneously hypertensive rats during the transition to heart failure. Circ Res 1991;68:1390–1400.
[70] Boluyt MO, O'Neill L, Meredith AL, et al. Alterations in cardiac gene expression during the transition from stable hypertrophy to heart failure. Marked upregulation of genes encoding extracellular matrix components. Circ Res 1994;75:23–32.
[71] Li Z, Bing OH, Long X, Robinson KG, Lakatta EG. Increased cardiomyocyte apoptosis during the transition to heart failure in the spontaneously hypertensive rat. Am J Physiol 1997;272:H2313–H2319.
[72] Chua Jr. SC, Chung WK, Wu-Peng XS. Phenotypes of mouse diabetes and rat fatty due to mutations in the OB (leptin) receptor. Science 1996;271:994–996.
[73] Holycross BJ, Summers BM, Dunn RB, McCune SA. Plasma-renin activity in heart failure-prone SHHF/Mcc-facp rats. Am J Physiol 1997;273:H228–H233.
[74] Narayan P, McCune SA, Robitaille PM, Hohl CM, Altschuld RA. Mechanical alternans and the force–frequency relationship in failing rat hearts. J Mol Cell Cardiol 1995;27:523–530.
[75] Gomez AM, Valdivia HH, Cheng H, et al. Defective excitation–contraction coupling in experimental cardiac hypertrophy and heart failure. Science 1997;276:800–806.
[76] Khadour FH, Kao RH, Park S, et al. Age-dependent augmentation of cardiac endothelial NOS in a genetic rat model of heart failure. Am J Physiol 1997;273:H1223–H1230.
[77] Lompre AM, Mercadier JJ, Wisnewsky C, et al. Species and age-dependent changes in the relative amounts of cardiac myosin isozymes in mammals. Dev Biol 1981;84:286–290.
[78] Freeman GL, Little WC, O'Rourke RA. Influence of heart rate on left ventricular performance in conscious dogs. Circ Res 1987;61:455–464.
[79] Whipple GH, Sheffield LT, Woodman EG, Thoephilis C, Friedman S. Reversible congestive heart failure due to rapid stimulation of the normal heart. Proc New Eng Cardiovasc Soc 1961;20:39–40.
[80] Armstrong PW, Stopps TP, Ford SE, de Bold AJ. Rapid ventricular pacing in the dog: pathophysiologic studies of heart failure. Circulation 1986;74:1075–1084.
[81] Wilson JR, Douglas P, Hickey WF, et al. Experimental congestive heart failure produced by rapid ventricular pacing in the dog: cardiac effects. Circulation 1987;75:857–867.
[82] Ohno M, Cheng CP, Little WC. Mechanism of altered patterns of left ventricular filling during the development of congestive heart failure. Circulation 1994;89:2241–2250.
[83] Kiuchi K, Shannon RP, Sato N, et al. Factors involved in delaying the rise in peripheral resistance in developing heart failure. Am J Physiol 1994;267:H211–H216.
[84] Armstrong PW, Gordon WM. The development of and recovery from pacing-induced heart failure. In: Spinale FG, editor. Pathophysiology of tachycardia-inuced heart failure. Armonk, NY: Futura Publishing Company, 1996;45–59.
[85] Eaton GM, Cody RJ, Nunziata E, Binkley PF. Early left ventricular dysfunction elicits activation of sympathetic drive and attenuation of parasympathetic tone in the paced canine model of congestive heart failure. Circulation 1995;92:555–561.
[86] Travill CM, Williams TD, Pate P, et al. Haemodynamic and neurohumoral response in heart failure produced by rapid ventricular pacing. Cardiovasc Res 1992;26:783–790.
[87] Redfield MM, Aarhus LL, Wright RS, Burnett Jr. JC. Cardiorenal and neurohumoral function in a canine model of early left ventricular dysfunction. Circulation 1993;87:2016–2022.
[88] Luchner A, Stevens TL, Borgeson DD, et al. Angiotensin II in the evolution of experimental heart failure. Hypertension 1996;28:472–477.
[89] Wang J, Seyedi N, Xu XB, Wolin MS, Hintze TH. Defective endothelium-mediated control of coronary circulation in conscious dogs after heart failure. Am J Physiol 1994;266:H670–H680.
[90] Ohno M, Cheng CP, Little WC. Altered left ventricular systolic and diastolic force–frequency relation in heat failure. Circulation 1994;90(Suppl I):112.
[91] Cheng CP, Noda T, Nozawa T, Little WC. Effect of heart failure on the mechanism of exercise-induced augmentation of mitral valve flow. Circ Res 1993;72:795–806.
[92] Ravens U, Davia K, Davies Ch, et al. Tachycardia-induced failure alters contracile properties of canine ventricular myocytes. Cardovasc Res 1996;32:613–621.
[93] Komamura K, Shannon RP, Ihara T, et al. Exhaustion of Frank–Starling mechanism in conscious dogs with heart failure. Am J Physiol 1993;265:H1119–H1131.
[94] Perreault CL, Shannon RP, Komamura K, Vatner SF, Morgan JP. Abnormalities in intracellular calcium regulation and contractile function in myocardium from dogs with pacing-induced heart failure. J Clin Invest 1992;89:932–938.
[95] Zile MR, Mukherjee R, Clayton C, Kato S, Spinale FG. Effects of chronic supraventricular pacing tachycardia on relaxation rate in isolated cardiac muscle cells. Am J Physiol 1995;268:H2104–H2113.
[96] Williams RE, Kass DA, Kawagoe Y, et al. Endomyocardial gene expression during development of pacing tachycardia-induced heart failure in the dog. Circ Res 1994;75:615–623.
[97] O'Rourke B, Fan Peng Ling, Tomaselli GF, Marban E. Excitation contraction coupling alterations in canine tachycardia-induced heart failure. Circulation 1997;96(Suppl I):238.
[98] Cory CR, Shen H, O'Brien PJ. Compensatory asymmetry in down-regulation and inhibition of the myocardial $Ca^{2+}$ cycle in congestive heart failure produced in dogs by idiopathic dilated cardiomyopathy and rapid ventricular pacing. J Mol Cell Cardiol 1994;26:173–184.
[99] Vatner DE, Sato N, Kiuchi K, Shannon RP, Vatner SF. Decrease in myocardial ryanodine receptors and altered excitation–contraction coupling early in the development of heart failure. Circulation 1994;90:1423–1430.
[100] Wolff MR, Whitesell LF, Moss RL. Calcium sensitivity of isometric tension is increased in canine experimental heart failure. Circ Res 1995;76:781–789.
[101] O'Leary EL, Colston JT, Freeman GL. Maintained length-dependent activation of skinned myocardial fibers in tachycardia heart failure. Circulation 1992;86(suppl I):284.
[102] Spinale FG, Holzgrefe HH, Mukherjee R, et al. Angiotensin-converting enzyme inhibition and the progression of congestive cardiomyopathy. Effects on left ventricular and myocyte structure and function. Circulation 1995;92:562–578.
[103] Liu Y, Cigola E, Cheng W, et al. Myocyte nuclear mitotic division and programmed myocyte cell death characterize the cardiac myopathy induced by rapid ventricular pacing in dogs. Lab Invest 1995;73:771–787.
[104] Ishikawa Y, Sorota S, Kiuchi K, et al. Downregulation of adenylylcyclase types V and VI mRNA levels in pacing-induced heart failure in dogs. J Clin Invest 1994;93:2224–2229.
[105] Pak PH, Nuss HB, Kaab S, et al. Repolarization abnormalities, arrhythmia and sudden death in canine tachycardia induced cardiomyopathy. J Am Coll Cardiol 1997;30:576–584.
[106] Nuss HB, Johns DC, Kaab S, et al. Reversal of potassium channel deficiency in cells from failing hearts by adenoviral gene tranfer: a prototype for gene therapy for disorders of cardiac excitability and contractility. Gene Ther 1996;3:900–912.
[107] Spinale FG, Fulbright BM, Mukherjee R, et al. Relation between ventricular and myocyte function with tachycardia-induced cardiomyopathy. Circ Res 1992;71:174–187.
[108] Spinale FG, Hendrick DA, Crawford FA, et al. Chronic supraven-

tricular tachycardia causes ventricular dysfunction and subendocardial injury in swine. Am J Phys 1990;259:H218–H229.
[109] Spinale FG, Tomita M, Zellner JL, et al. Collagen remodeling and changes in LV function during development and recovery from supraventricular tachycardia. Am J Physiol 1991;261:H308–H318.
[110] Spinale FG, Tempel GE, Mukherjee R, et al. Cellular and molecular alterations in the beta adrenergic system with cardiomyopathy induced by tachycardia. Cardiovasc Res 1994;28:1243–1250.
[111] Sabbah HN, Stein PD, Kono T, et al. A canine model of chronic heart failure produced by multiple sequential coronary microembolizations. Am J Physiol 1991;260:H1379–H1384.
[112] Gengo PJ, Sabbah HN, Steffen RP, et al. Myocardial beta adrenoceptor and voltage-sensitive calcium channel changes in a canine model of chronic heart failure. J Mol Cell Cardiol 1992;24:1361–1369.
[113] Gupta RC, Shimoyama H, Tanimura M, et al. SR $Ca^{2+}$-ATPase activity and expression in ventricular myocardium of dogs with heart failure. Am J Physiol 1997;273:H12–H18.
[114] Sabbah HN, Shimoyama H, Kono T, et al. Effects of long-term monotherapy with enalapril, metoprolol, and digoxin on the progression of left ventricular dysfunction and dilation in dogs with reduced ejection fraction. Circulation 1994;89:2852–2859.
[115] McDonald KM, Francis GS, Carlyle PF, et al. Hemodynamic, left ventricular structural and hormonal changes after discrete myocardial damage in the dog. J Am Coll Cardiol 1992;19:460–467.
[116] McCullagh WH, Covell JW, Ross Jr. J. Left ventricular dilatation and diastolic compliance changes during chronic volume overloading. Circulation 1972;45:943–951.
[117] Kleaveland JP, Kussmaul WG, Vinciguerra T, Diters R, Carabello BA. Volume overload hypertrophy in a closed-chest model of mitral regurgitation. Am J Physiol 1988;254:H1034–H1041.
[118] Dell'Italia LJ. The canine model of mitral regurgitation. Heart Failure 1995;11:208–218.
[119] Nagatsu M, Zile MR, Tsutsui H, et al. Native beta-adrenergic support for left ventricular dysfunction in experimental mitral regurgitation normalizes indexes of pump and contractile function. Circulation 1994;89:818–826.
[120] Tsutsui H, Spinale FG, Nagatsu M, et al. Effects of chronic beta-adrenergic blockade on the left ventricular and cardiocyte abnormalities of chronic canine mitral regurgitation. J Clin Invest 1994;93:2639–2648.
[121] Hasenfuss G, Mulieri LA, Blanchard EM, et al. Energetics of isometric force development in control and volume-overload human myocardium. Comparison with animal species. Circ Res 1991;68:836–846.
[122] Magid NM, Opio G, Wallerson DC, Young MS, Borer JS. Heart failure due to chronic experimental aortic regurgitation. Am J Physiol 1994;267:H556–H562.
[123] Gilson N, el Houda Bouanani N, Corsin A, Crozatier B. Left ventricular function and beta-adrenoceptors in rabbit failing heart. Am J Physiol 1990;258:H634–H641.
[124] Ezzaher A, Bouanani NEH, Su JB, Hittinger L, Crozatier B. Increased negative inotropic effect of calcium channel blockers in hypertrophied and failing rabbit hearts. J Pharmacol Exp Ther 1991;257:466–471.
[125] Ezzaher A, Boudanani NEH, Crozatier B. Force-frequency relations and response to ryanodine in failing rabbit hearts. Am J Physiol 1992;263:H1710–H1715.
[126] Pogwizd SM, Qi M, Samarel AM, Bers DM. Upregulation of $Na^+/Ca^{2+}$-exchanger gene expression in an arrhythmogenic model of nonischemic cardiomyopathy in the rabbit. Circulation 1997;96(Suppl I):8.
[127] Freeman GL, Colston JT. Myocardial depression produced by sustained tachycardia in rabbits. Am J Physiol 1992;262:H63–H67.
[128] Masaki H, Imaizumi T, Ando S, et al. Production of chronic congestive heart failure by rapid ventricular pacing in the rabbit. Cardiovasc Res 1993;27:828–831.
[129] Masaki H, Imaizumi T, Harasawa Y, Takeshita A. Dynamic arterial baroreflex in rabbits with heart failure induced by rapid pacing. Am J Physiol 1994;267:H92–H99.
[130] Ryu KH, Tanaka N, Dalton N, et al. Force–frequency relations in the failing rabbit heart and responses to adrenergic stimulation. J Card Fail 1997;3:27–39.
[131] Eble DM, Walker JD, Mukherjee R, Samarel AM, Spinale FG. Myosin heavy chain synthesis is increased in a rabbit model of heart failure. Am J Physiol 1997;272:H969–H978.
[132] Dodd DA, Atkinson JB, Olson RD, et al. Doxorubicin cardiomyopathy is associated with a decrease in calcium release channel of the sarcoplasmic reticulum in a chronic rabbit model. J Clin Invest 1993;91:1697–1705.
[133] Siri FM, Krueger J, Nordin C, Ming Z, Aronson RS. Depressed intracellular calcium transients and contraction in myocytes from hypertrophied and failing guinea pig hearts. Am J Phys 1991;261:H514–H530.
[134] Kiss E, Ball NA, Kranias EG, Walsh RA. Differential changes in cardiac phospholamban and sarcoplasmic reticulum $Ca^{2+}$-ATPase protein levels. Effects on $Ca^{2+}$ transport and mechanics in compensated pressure-overload hypertrophy and congestive heart failure. Circ Res 1995;77:759–764.
[135] Malhotra A, Siri FM, Aronson R. Cardiac contractile proteins in hypertrophied and failing guinea pig heart. Cardiovasc Res 1992;26:153–161.
[136] Bajusz E. Hereditary cardiomyopathy: a new disease model. Am Heart J 1969;7:686–696.
[137] Forman R, Parmley WW, Sonnenblick EH. Myocardial contractility in relation to hypertrophy and failure in myopathic Syrian hamsters. J Mol Cell Cardiol 1972;4:203–211.
[138] Jasmin G, Proschek L. Hereditary polymyopathy and cardiomyopathy in the Syrian hamster. I. Progression of heart and skeletal muscle lesions in the UM-X7.1 line. Muscle Nerve 1982;5:20–25.
[139] Rouleau JL, Chuck LH, Hollosi G, et al. Verapamil preserves myocardial contractility in the hereditary cardiomyopathy of the Syrian hamster. Circ Res 1982;50:405–412.
[140] Whitmer JT, Kumar P, Solaro RJ. Calcium transport properties of cardiac sarcoplasmic reticulum from cardiomyopathic Syrian hamsters (BIO 53.58 and 14.6): evidence for a quantitative defect in dilated myopathic hearts not evident in hypertrophic hearts. Circ Res 1988;62:81–85.
[141] Finkel MS, Marks ES, Patterson RE, et al. Correlation of changes in cardiac calcium channels with hemodynamics in Syrian hamster cardiomyopathy and heart failure. Life Sci 1987;41:153–159.
[142] Wagner JA, Reynolds IJ, Weisman HF, et al. Calcium antagonist receptors in cardiomyopathic hamster: selective increases in heart, muscle, brain. Science 1986;232:515–518.
[143] Kuo TH, Tsang W, Wang KK, Carlock L. Simultaneous reduction of the sarcolemmal and SR calcium ATPase activities and gene expression in cardiomyopathic hamster. Biochim Biophys Acta 1992;1138:343–349.
[144] Hatem SN, Sham JS, Morad M. Enhanced $Na^+/Ca^{2+}$ exchange activity in cardiomyopathic Syrian hamster. Circ Res 1994;74:253–261.
[145] Malhotra A, Karell M, Scheuer J. Multiple cardiac contractile protein abnormalities in myopathic Syrian hamsters (BIO 53: 58). J Mol Cell Cardiol 1985;17:95–107.
[146] Okazaki Y, Okuizumi H, Osumi T, et al. A genetic linkage map of the Syrian hamster and localization of cardiomyopathy locus on chromosome 9qa2.1-b1 using RLGS spot-mapping. Nat Genet 1996;13:87–90.
[147] Nigro V, Okazaki Y, Belsito A, et al. Identification of the Syrian hamster cardiomyopathy gene. Hum Mol Gen 1997;6:601–607.
[148] Hoit BD, Khoury SF, Kranias EG, Ball N, Walsh RA. In vivo echocardiographic detection of enhanced left ventricular function in gene-targeted mice with phospholamban deficiency. Circ Res 1995;77:632–637.

[149] Rockman HA, Ono S, Ross RS, et al. Molecular and physiological alterations in murine ventricular dysfunction. Proc Natl Acad Sci USA 1994;91:2694–2698.
[150] Arber S, Hunter JJ, Ross Jr. J, et al. MLP-deficient mice exhibit a disruption of cardiac cytoarchitectural organization, dilated cardiomyopathy, and heart failure. Cell 1997;88:393–403.
[151] Edwards JG, Lyons GE, Micales BK, Malhotra A, Factor S, Leinwand LA. Cardiomyopathy in trangenic myf5 mice. Circ Res 1996;78:379–387.
[152] Iwase M, Uechi M, Vatner DE, et al. Cardiomyopathy induced by cardiac Gs alpha overexpression. Am J Phys 1997;272:H585–H589.
[153] Koch WJ, Rockman HA, Samama P, et al. Cardiac function in mice overexpressing the β-adrenergic receptor kinase or a βARK inhibitor. Science 1995;268:1350–1353.
[154] Rockman HA, Hamilton R, Rahman NU, et al. Dampened cardiac function in vivo in transgenic mice overexpression GRK5, a G protein-coupled receptor kinase. Circulation 1995;92(Suppl I):240.
[155] Hassankhani A, Steinhelper ME, Soonpaa MH, et al. Overexpression of NGF within the heart of transgenic mice causes hyperinnervation, cardiac enlargement, and hyperplasia of ectopic cells. Dev Biol 1995;169:309–321.
[156] Reiss K, Cheng W, Ferber A, et al. Overexpression of IGF-1 in the heart is coupled with myocyte proliferation in transgenic mice. Circulation 1995;92(Suppl I):370.
[157] Huen DS, Fox A, Kumar P, Searle PF. Dilated heart failure in transgenic mice expression the Epstein-Barr virus nuclear antigen-leader protein. J Gen Virol 1993;74:1381–1391.
[158] Chalifour LE, Gomes ML, Wang NS, Mes Masson AM. Polyomavirus large T-antigen expression in heart of transgenic mice causes cardiomyopathy. Oncogene 1990;5:1719–1726.
[159] Sussman MA, Welch S, Klevitsky R, Hewett TE, Cambon N. Lethal cardiomyopathy in juvenile mice caused by tropomodulin overexpression. Circulation 1997;98(Suppl I):571.
[160] Pinto YM, Ganten D. Animal models of hypertension. Cardiovasc Res this issue.
[161] Spirito P, Seidman CE, McKenna WJ, Maron BJ. The management of hypertrophic cardiomyopathy. N Engl J Med 1997;336:775–785.
[162] Geisterfer-Lowrance AAT, Christe M, Conner DA, et al. A mouse model of familial hypertrophic cardiomyopathy. Science 1996;272:731–734.
[163] Welikson RE, Vikstrom KL, Factor SM, Weinberger HD, Leinwand LA. Heavy chains lacking the light chain binding domain cause genetically dominant cardiomyopathy in mice. Circulation 1997;96(Suppl I):571.
[164] Hunter JJ, Tanaka N, Rockman HA, Ross Jr. J, Chien KR. Ventricular expression of a MLC-2v-ras fusion gene induces cardiac hypertrophy and selective diastolic dysfunction in transgenic mice. J Biol Chem 1995;270:23173–23178.
[165] Gottstall KR, Hunter JJ, Tanaka N, et al. Ras dependent pathways induce obstructive hypertrophy in echo-selected trangenic mice. Proc Natl Acad Sci USA 1997;94:4710–4715.
[166] Gruver CL, DeMayo F, Goldstein MA, Means AR. Targeted developmental overexpression of calmodulin induces proliferative and hypertrophic growth of cardiomyocytes in trangenic mice. Endocrinology 1993;133:376–388.
[167] Hirota H, Yoshida K, Kishimoto T, Taga T. Continuous activation of gp130, a signal-retransducing receptor component for interleukin 6-related cytokines, cause myocardial hypertrophy in mice. Proc Natl Acad Sci USA 1995;92:4862–4866.
[168] Milano CA, Dolber PC, Rockman HA, et al. Myocardial expression of a constitutively active α1b-adrenergic receptor in trangenic mice induces cardiac hypertrophy. Proc Natl Acad Sci USA 1994;91:10109–10113.
[169] Graham BH, Waymire KG, Cottrell B, et al. A mouse model for mitochondrial myopathy and cardiomyopathy resulting from a deficiency in the heart/muscle isoform of the adenine nucleotide translocator. Nat Genet 1997;16:226–234.
[170] Kawai C, Matsumori A, Fujiwara H. Myocarditis and dilated cardiomyopathy. Annu Rev Med 1987;38:221–239.
[171] Tanaka A, Matsumori A, Wang W, Sasayama S. An angiotensin II receptor antagonist reduces myocardial damage in an animal model of myocarditis. Circulation 1994;90:2051–2055.
[172] Martino TA, Liu P, Sole MJ. Viral infection and the pathogenesis of dilated cardiomyopathy: time to revisit the virus. Heart Failure 1993;9:218–226.
[173] Lane JR, Neumann DA, Lafond-Walker A, Herskowitz A, Rose NR. Role of IL-1 and tumor necrosis factor in coxsackie virus-induced autoimmune myocarditis. J Immunol 1993;151:1682–1690.
[174] Huber SA. Coxsackievirus-induced myocarditis is dependent on distinct immunopathogenic responses in different strain of mice. Lab Invest 1997;76:691–701.
[175] Matsumori A, Kawai C. An experimental model for congestive heart failure after encephalomyocarditis virus myocarditis in mice. Circulation 1982;65:1230–1235.
[176] Matsumori A, Sasayama S. Immunomodulating agents for the management of heart failure with myocarditis and cardiomyopathy – lessons from animal experiments. Eur Heart J 1995;(Suppl 0):140–143.
[177] Hirono S, Islam MO, Nakazawa M, et al. Expression of inducible nitric oxide synthase in rat experimental autoimmune myocarditis with special reference to changes in cardiac hemodynamics. Circ Res 1997;80:11–20.
[178] Sharaf AR, Narula J, Nicol PD, Southern JF, Khaw BA. Cardiac sarcoplasmic reticulum calcium ATPase, an autoimmune antigen in experimental cardiomyopathy. Circulation 1994;89:1217–1228.
[179] Schulze K, Schultheiss HP. The role of the ADP/ATP carrier in the pathogenesis of viral heart disease. Eur Heart J 1995;16(Suppl O):64–67.
[180] Liu P, Penninger J, Aitken K, Sole M, Mak T. The role of transgenic knockout models in defining the pathogenesis of viral heart disease. Eur Heart J 1995;16(Suppl O):25–27.
[181] Aitken K, Penninger J, Mak T, et al. Increased susceptibility to coxsackie viral myocarditis in IRF-1 transgenic knockout mice. Circulation 1994;90(Suppl I):139.
[182] Shull MM, Ormsby I, Kier AB, et al. Targeted disruption of the mouse tranforming growth factor-β 1 gene results in multifocal inflammatory disease. Nature 1992;359:693–699.
[183] Kulkarni AB, Huh CG, Becker D, et al. Transforming growth factor β-1 null mutation in mice causes excessive inflammatory response and early death. Proc Natl Acad Sci USA 1993;90:770–774.
[184] Jannini JP, Spinale FG. The identification of contributory mechanisms for the development and progression of congestive heart failure in animal models. J Heart Lung Transplant 1996;15:1138–1150.
[185] Liu Z, Hilbelink DR, Crockett WB, Gerdes AM. Regional changes in hemodynamics and cardiac myocyte size in rats with aortocaval fistulas. Developing and established hypertrophy . Circ Res 1991;69:52–58.
[186] Fein FS, Sonnenblick EH. Diabetic cardiomyopathy. Cardiovasc Drugs Ther 1994;8:65–73.
[187] Teerlink JR, Pfeffer JM, Pfeffer MA. Progressive ventricular remodeling in response to diffuse isoproterenol-induced myocardial necrosis in rats. Circ Res 1994;75:105–113.
[188] Capasso JM, Li P, Guideri G, et al. Myocardial mechanical, biochemical and structural alterations induced by chronic ethanol ingestion in rats. Circ Res 1992;71:346–356.
[189] Wei CM, Clavell AL, Burnett JC. Atrial and pulmonary endothelin mRNA is increased in a canine model of chronic low cardiac output. Am J Physiol 1997;273:R838–844.
[190] Magovern JA, Christlieb IY, Badylak SF, Lantz GC, Kao RL. A

model of left ventricular dysfunction caused by intracoronary adriamycin. Ann Thorac Surg 1992;53:861–863.
[191] Zhang J, Wilke N, Wang Y, et al. Functional and bioenergetic consequences of postinfarction left ventricular remodeling in a new porcine model. MRI and 31 P-MRS study. Circulation 1996;94:1089–1100.
[192] Colston JT, Kumar P, Chambers JP, Freeman GL. Altered sarcolemmal calcium-channel density and $Ca^{2+}$-pump ATPase activity in tachycardia heart failure. Cell Calcium 1994;16:349–356.
[193] Siri FM, Nordin C, Factor SM, Sonnenblick E, Aronson R. Compensatory hypertrophy and failure in gradual pressure-overloaded guinea pig heart. Am J Physiol 1989;257:H1016–H1024.
[194] Tagawa H, Koide M, Sato H, Cooper 4th G. Cytoskeletal role in the contractile dysfunction of cardiocytes from hypertrophied and failing right ventricular myocardium. Proc Assoc Am Physicians 1996;108:218–229.
[195] Kent RL, Rozich JD, McCollam PL, et al. Rapid expression of the $Na^+/Ca^{2+}$ exchanger in response to cardiac pressure overload. Am J Physiol 1993;265:H1024–H1029.
[196] Genao A, Seth K, Schmidt U, Carles M, Gwathmey JK. Dilated cardiomyopathy in turkeys: an animal model for the study of human heart failure. Lab Anim Sci 1996;46:399–404.
[197] Eschenhagen T, Diederich M, Kluge SH, et al. Bovine hereditary cardiomyopathy: an animal model of human dilated cardiomyopathy. J Mol Cell Cardiol 1995;27:357–370.
[198] Rademaker MT, Charles CJ, Lewis LK, et al. Beneficial hemodynamic and renal effects of adrenomedullin in an ovine model of heart failure. Circulation 1997;96:1983–1990.
[199] Rademaker MT, Charles CJ, Espiner EA, et al. Natriuretic peptide responses to acute and chronic ventricular pacing in sheep. Am J Physiol 1996;270:H594–H602.
[200] Aoyagi T, Fujii AM, Flanagan MF, et al. Transition from compensated hypertrophy to intrinsic myocardial dysfunction during development of left ventricular pressure-overload hypertrophy in conscious sheep. Systolic dysfunction precedes diastolic dysfunction. Circulation 1993;88:2415–2425.
[201] Julian FJ, Morgan DL, Moss RL, Gonzalez M, Dwivedi P. Myocyte growth without physiological impairment in gradually induced rat cardiac hypertrophy. Circ Res 1981;49:1300–1310.
[202] Goldblatt H, Lynch J, Hanzak RF, Summerville WW. Studies of experimental hypertension; I. Production of persistent elevation of systolic blood pressure by means of renal ischemia. J Exp Med 1934;59:347–379.
[203] Besse S, Robert V, Assayag P, Delcayre C, Swynghedauw B. Nonsynchronous changes in myocardial collagen mRNA and protein during aging: effect of DOCA-salt hypertension. Am J Physiol 1994;267:H2237–2244.
[204] Dart Jr. CH, Holloszy JO. Hypertrophied non-failing rat heart; partial biochemical characterization. Circ Res 1969;25:245–253.
[205] Bartosova D, Chvapil M, Korecky B, et al. The growth of the muscular and collagenous parts of the rat heart in various forms of cardiomegaly. J Physiol (Lond) 1969;200:285–295.
[206] Hickson RC, Hammons GT, Holloszy JO. Development and regression of exercise-induced cardiac hypertrophy in rats. Am J Physiol 1979;236:H268–H272.
[207] Rupp H, Jacob R. Response of blood pressure and cardiac myosin polymorphism to swimming training in the spontaneously hypertensive rat. Can J Physiol Pharmacol 1982;60:1098–1103.
[208] Koide M, Nagatsu M, Zile MR, et al. Premorbid determinants of left ventricular dysfunction in a novel model gradually induced pressure overload in the adult canine. Circulation 1997;95:1601–1610.
[209] Roitstein A, Cheinberg BV, Kedem J, et al. Reduced effect of phenylephrine on regional myocardial function and $O_2$ consumption in experimental LVH. Am J Physiol 1995;268:H1202–H1207.
[210] Dolber PC, Bauman RP, Rembert JC, Greenfield Jr. JC. Regional changes in myocyte structure in model of canine right atrial hypertrophy. Am J Physiol 1994;267:H1279–H1287.
[211] Carroll SM, Nimmo LE, Knoepfler PS, White FC, Bloor CM. Gene expression in a swine model of right ventricular hypertrophy: intercellular adhesion molecule, vascular endothelial growth factor and plasminogen activators are upregulated during pressure overload. J Mol Cell Cardiol 1995;27:1427–1441.
[212] Do E, Baudet S, Verdys M, et al. Energy metabolism in normal and hypertrophied right ventricle of the ferret heart. J Mol Cell Cardiol 1997;29:1903–1913.
[213] Wang J, Flemal K, Qiu Z, et al. $Ca^{2+}$ handling and myofibrillar $Ca^{2+}$ sensitivity in ferret cardiac myocytes with pressure-overload hypertrophy. Am J Physiol 1994;267:H918–H924.
[214] Charles CJ, Kaaja RJ, Espiner EA, et al. Natriuretic peptides in sheep with pressure overload left ventricular hypertrophy. Clin Exp Hypertens 1996;18:1051–1071.
[215] Hoit BD, Pawloski-Dahm CM, Shao Y, Gabel M, Walsh RA. The effects of a thyroid hormone analog on left ventricular performance and contractile and calcium cycling proteins in the baboon. Proc Assoc Am Physicians 1997;109:136–145.
[216] Hoit BD, Shao Y, Gabel M, Walsh RA. Disparate effects of early pressure overload hypertrophy on velocity-dependent and force-dependent indices of ventricular performance in the conscious baboon. Circulation 1995;91:1213–1220.
[217] Tweedie D, Henderson CG, Kane KA. Assessment of subrenal banding of the abdominal aorta as a method of inducing cardiac hypertrophy in the guinea pig. Cardioscience 1995;6:115–119.
[218] Wiesel P, Mazzolai L, Nussberger J, Pedrazzini T. Hypertension 1997;29:1025–1030.
[219] Kaplan ML, Cheslow Y, Vikstrom K, et al. Cardiac adaptations to chronic exercise in mice. Am J Physiol 1994;267:H1167–H1173.
[220] Dorn 2nd GW, Robbins J, Ball N, Walsh RA. Myosin heavy chain regulation and myocyte contractile depression after LV hypertrophy in aortic-banded mice. Am J Physiol 1994;267:H400–H405.
[221] Jackson T, Allard MF, Sreenan CM, et al. The c-*myc* proto-oncogene regulates cardiac development in transgenic mice. Mol Cell Biol 1990;10:3709–3716.
[222] Hunter JJ, Tanaka N, Rockman HA, Ross J, Chien KR. Ventricular expression of a MLC-2v-*ras* fusion gene induces cardiac hypertrophy and selective diastolic dysfunction in transgenic mice. J Biol Chem 1995;270:23173–23178.
[223] Bertin B, Mansier P, Makeh I, et al. Specific atrial over-expression of G protein coupled human $\beta_1$-adrenoceptors in transgenic mice. Cardiovasc Res 1993;27:1606–1612.
[224] Langheinrich M, Lee MA, Bohm M, et al. The hypertensive Ren-2 transgenic rat TGR (mREN2)27 in hypertension research. Characteristics and functional aspects. Am J Hypertens 1996;9:506–512.

lation with anti-CD28 enhanced NFATc nuclear accumulation (Fig. 4B), in keeping with the finding that $T_H2$ cytokine induction in wild-type $T_H$ cells requires costimulation (Fig. 2C). In contrast, anti-CD3 treatment alone led to an increase in nuclear NFATc in *Jnk1*$^{-/-}$ $T_H$ cells and a decrease in cytoplasmic NFATc (Fig. 4, A and B), consistent with the high $T_H2$ cytokine production by CD3-activated *Jnk1*$^{-/-}$ cells (Fig. 2C). The enhanced accumulation of nuclear NFATc in *Jnk1*$^{-/-}$ $T_H$ cells was observed in cells 8, 24, and 48 hours after stimulation, but was not observed in nonactivated cells (*10*). NFATc accumulation was specific because the amount of nuclear NFATp, a proposed negative regulator of $T_H2$ cytokine genes (*21*), was the same in wild-type and *Jnk1*$^{-/-}$ cells (Fig. 4A). Enhanced nuclear accumulation of NFATc in *Jnk1*$^{-/-}$ T cells was not blocked by anti–IL-4 (Fig. 4A); hence, increased IL-4 production and NFATc nuclear localization is intrinsic to T cell receptor signaling and is not secondary to IL-4 production. Because NFATc can bind to the IL-4 promoter and is required for IL-4 production and $T_H2$ differentiation (*20, 22*), the greatly enhanced amount of nuclear NFATc could account for the increased IL-4 production in CD3-activated *Jnk1*-deficient mice.

The mechanism by which JNK1 negatively regulates NFATc nuclear accumulation remains to be resolved. The isoform NFAT4 is phosphorylated and negatively regulated by JNK, leading to nuclear exclusion (*23*). This regulation appears to be specific to the NFAT4 isoform; evidence for JNK regulation of NFATc was not reported (*23*). An indirect mechanism may therefore account for the altered regulation of NFATc in *Jnk1*$^{-/-}$ $T_H$ cells. NFATc and NFATp can bind to the IL-4 promoter NFAT sites (*22*). Both *Jnk1* and *NFATp* knockout mice have enhanced T cell proliferation and $T_H2$ cytokine production (*21, 24*), precisely the opposite of the NFATc knockout. It is therefore possible that these two NFAT factors antagonize each other in the regulation of the IL-4 gene. The apparent similarity between *NFATp*$^{-/-}$ and *Jnk1*$^{-/-}$ phenotypes supports a functional linkage between JNK1 and NFAT.

Our results further reveal a novel mechanism by which TCR signaling negatively regulates $T_H2$ cytokines through JNK1. Positive and negative regulation of JNK1 activity may affect the decision of $T_H$ cells to differentiate into $T_H1$ or $T_H2$ effectors, and therefore may affect the type of immune response that is initiated. The function of JNK1 demonstrated in this study is distinct from that of JNK2, which is required for IFN-γ production in $T_H1$ cells (*14*). Moreover, the related p38 mitogen-activated protein kinase pathway is $T_H1$ specific and drives IFN-γ transcription (*25*). Together, these pathways potentiate the $T_H1$ response and provide a potential target for pharmaceutical intervention.

### References and Notes


1. K. M. Murphy, *Curr. Opin. Immunol.* **10**, 226 (1998); A. O'Garra, *Immunity* **8**, 275 (1998).
2. S. L. Constant and K. Bottomly, *Annu. Rev. Immunol.* **15**, 297 (1997).
3. A. J. Whitmarsh and R. J. Davis, *J. Mol. Med.* **74**, 589 (1996); M. Karin, Z. Liu, E. Zandi, *Curr. Opin. Cell Biol.* **9**, 240 (1997).
4. Y. T. Ip and R. J. Davis, *ibid.* **10**, 205 (1998).
5. M. Rincón and R. A. Flavell, *EMBO J.* **13**, 4370 (1994); B. Su *et al.*, *Cell* **77**, 727 (1994).
6. C. Y. Chen, F. Del Gatto-Konczak, Z. Wu, M. Karin, *Science* **280**, 1945 (1998).
7. M. Rincón, B. Dérijard, C.-W. Chow, R. J. Davis, R. A. Flavell, *Genes Funct.* **1**, 51 (1997).
8. J. W. Rooney, T. Hoey, L. H. Glimcher, *Immunity* **2**, 473 (1995); J. Jain, C. Loh, A. Rao, *Curr. Opin. Immunol.* **7**, 333 (1995); S. J. Szabo, L. H. Glimcher, I. C. Ho, *ibid.* **9**, 776 (1997); V. C. Foletta, D. H. Segal, D. R. Cohen, *J. Leukocyte Biol.* **63**, 139 (1998).
9. The murine *Jnk1* locus was isolated from a 129/Sv mouse genomic library (Stratagene) using the human *Jnk1* cDNA as a probe. An internal 5.5-kb genomic fragment containing four exons was replaced by a PGK-hyg (hygromycin phosphotransferase) cassette. The knockout vector was electroporated into W9.5 ES cells, and 15 targeted clones were identified by Southern blot analysis of genomic DNA, three of which gave germ line transmission of the disrupted allele. Heterozygous (+/–) mice were intercrossed to generate homozygous wild-type and mutant mice, which were independently bred; their age- and sex-matched offspring were used for experiments.
10. C. Dong, D. D. Yang, M. Wysk, A. J. Whitmarsh, R. J. Davis, R. A. Flavell, unpublished data.
11. The data are shown at *Science* Online (www.sciencemag.org).
12. Total spleen cells or purified CD4 T cells were stimulated as triplicates with Con A (2.5 μg/ml), plate-bound anti-CD3 with or without anti-CD28 (plates were precoated with antibody at 10 μg/ml). IL-2 production was measured by enzyme-linked immunosorbent assay (ELISA; Pharmingen) 24 hours after stimulation. Proliferation was assayed after 3 days of treatment by adding [$^3$H]thymidine to the culture for the last 8 hours. At day 4, the supernatant of stimulated cells was removed and $T_H$ cytokine production was measured by ELISA. In activation-induced cell death experiments, CD4 T cells were stimulated with Con A for 4 days, extensively washed, and restimulated with immobilized anti-CD3 for 48 hours. Apoptosis was determined by staining the cells with 7-aminoactinomycin D (7-AAD) and Annexin V (Pharmingen); dead cells were scored as Annexin$^+$ 7-AAD$^+$. The data are shown at *Science* Online (www.sciencemag.org).
13. CD4 T cells were isolated from 6- to 8-week-old mice by depletion of major histocompatibility class II$^+$, CD8$^+$, and NK1.1$^+$ cells using magnetic beads. The CD44$^{lo}$CD45RB$^{hi}$ naïve cells were further purified by a FACS sorter (Becton Dickinson). APCs were prepared from spleen by complement-mediated lysis of Thy1$^+$ T cells.
14. D. D. Yang *et al.*, *Immunity* **9**, 575 (1998).
15. J. Chen *et al.*, *ibid.* **1**, 65 (1994).
16. Naïve or total CD4 T cells (10$^6$ cells/ml) were differentiated in the presence of irradiated APCs (10$^6$ cells/ml), immobilized anti-CD3, and IL-2 (30 U/ml). IL-12 (3.5 ng/ml) and anti–IL-4 (4 μg/ml) were added for $T_H1$ differentiation, and IL-4 (1000 U/ml) and anti–IFN-γ (4 μg/ml) for $T_H2$ differentiation. After 4 days, the cells were extensively washed, counted, and restimulated with plate-bound anti-CD3 for 24 hours. Cytokine production was measured by ELISA (Pharmingen) in triplicates or by competitive reverse transcription polymerase chain reaction (RT-PCR) (*17*).
17. S. L. Reiner, S. Zheng, D. B. Corry, R. M. Locksley, *J. Immunol. Methods* **165**, 37 (1993).
18. A total of 20 6- to 8-week-old mice (in three independent experiments) were immunized with KLH (50 μg/ml) precipitated with alum in the footpads (100 μl each). After 9 days, the draining lymph nodes were removed and the cells were stimulated as triplicates with or without KLH peptide for 4 days, and cytokine production was determined by ELISA (Pharmingen).
19. Nuclear and cytosolic fractions of $T_H$ cells were prepared [E. Schreiber, P. Matthias, M. M. Muller, W. Shaffner, *Nucleic Acids Res.* **17**, 6419 (1989)], and amounts of protein were determined by Bio-Rad protein assay to ensure equal protein loading for the analysis. Antibodies to GATA-3, Stat-6, JunB, and NFATp were from Santa Cruz Biotechnology and anti-NFATc was from Affinity Bioreagents.
20. A. M. Ranger *et al.*, *Immunity* **8**, 125 (1998); H. Yoshida *et al.*, *ibid.*, p. 115.
21. M. R. Hodge *et al.*, *ibid.* **4**, 397 (1996); A. Kiani, J. P. Viola, A. H. Lichtman, A. Rao, *ibid.* **7**, 849 (1997).
22. L. A. Timmerman *et al.*, *J. Immunol.* **159**, 2735 (1997).
23. C.-W. Chow, M. Rincón, J. Cavanagh, M. Dickens, R. J. Davis, *Science* **278**, 1638 (1997).
24. S. Xanthoudakis *et al.*, *ibid.* **272**, 892 (1996).
25. M. Rincón *et al.*, *EMBO J.* **17**, 2817 (1998).


26. We thank D. Y. Loh and C. L. Stewart for providing reagents; T. Barrett, L. Evangelisti, D. Butkus, C. Hughes, and J. Stein for technical assistance; B. Li for helpful suggestions; and F. Manzo for secretarial work. Supported in part by NIH grants CA65861 and CA72009 and by the Howard Hughes Medical Institute.

11 August 1998; accepted 6 November 1998




# Eight Calves Cloned from Somatic Cells of a Single Adult

**Yoko Kato, Tetsuya Tani, Yusuke Sotomaru, Kazuo Kurokawa, Jun-ya Kato, Hiroshi Doguchi, Hiroshi Yasue, Yukio Tsunoda***

**Eight calves were derived from differentiated cells of a single adult cow, five from cumulus cells and three from oviductal cells out of 10 embryos transferred to surrogate cows (80 percent success). All calves were visibly normal, but four died at or soon after birth from environmental causes, and postmortem analysis revealed no abnormality. These results show that bovine cumulus and oviductal epithelial cells of the adult have the genetic content to direct the development of newborn calves.**

Nuclear transfer is an efficient technique for assessing the developmental potential of a nucleus and for analyzing the interactions between the donor nucleus and the recipient cytoplasm. In amphibians, successful nuclear transfer was first reported by Briggs and King who used blastula cells for nuclear transfer to oocytes, which proceeded to develop into

tadpoles (*1*) and later juvenile frogs (*2*). Other cell types, including germ cells and somatic cells from tadpoles, have also been shown to have developmental totipotency (*3*): their nuclei directed the formation of fertile amphibians. However, despite extensive studies in amphibians, progeny could not be generated from adult cell nuclei (*3*). This obstacle was recently overcome in sheep (*4*) and mice (*5*), and nuclei from fetal fibroblast cells have directed the formation of lambs (*4, 6*) and calves (*7*). Wakayama *et al.* (*5*) used nuclear transfer to produce fertile mice from cumulus cells collected from metaphase II oocytes. Here, we report cloning of calves at a high rate using cumulus cells and oviductal epithelial cells that were passaged several times in vitro.

Oviducts and ovaries used as the donor nuclear source were obtained from a local slaughterhouse from a single cow of Japanese beef cattle in an unknown stage of the estrous cycle. Cumulus cells from ovarian oocytes at the germinal vesicle stage and oviductal epithelial cells (*8, 9*) were collected and cultured for several passages (*10*), and cells quiescent in the $G_0$-$G_1$ phase by serum starvation for 3 to 4 days (*4, 11*) were used for nuclear transfer (*12*). The characteristics of donor cells were determined by labeling with vimentin and cytokeratine (Fig. 1).

Forty-seven percent of the enucleated oocytes fused with cumulus cells and 63% did so with oviductal epithelial cells (Table 1). Among these constructs, 37 cumulus and 88 oviductal nuclear transplants were selected for culture in vitro for 8 to 9 days, by which time 49% of the cumulus-derived and 23% of the oviductal-derived nuclear transplants had developed into blastocysts. A total of 10 blastocysts originating from both cell types were nonsurgically transferred into surrogate cows at day 7 or 8 after the onset of estrous. Six blastocysts derived from cumulus cells were transferred into three females, and four from oviductal cells were placed into two females. All five females became pregnant. Two of the three surrogates containing cumulus nuclear transplants and one of the two with oviductal transplants had multiple pregnancies. Of the 10 blastocysts transferred to cows, 8 cloned female fetuses completed gestation and were born (Table 2). Calves OVI-1, -2, CUM-3, -4, -5, -6, -7, and OVI-8 were delivered 242, 242, 266, 267, 267, 276, 276, and 287 days of gestation, respectively (OVI and CUM indicate origin from oviductal or cumulus cells). All calves were born vaginally except calf OVI-8, which was delivered by cesarean section because of dystocia. The average length of pregnancy of Japanese beef cattle with a female fetus is 286.6 ± 0.9 days and the average body weight at birth is 27.0 ± 0.8 kg. The pregnancy period is often shorter when there are two fetuses. The calves of OVI-1 and OVI-2 were born prematurely.

Four of the eight calves died. Postmortem analysis did not reveal any abnormality; however, environmental factors appeared to account for their deaths. Calf CUM-3 died 3 days after birth from pneumonia apostematosa stemming from heatstroke, CUM-4 and -5 died just after birth from drawing in superfluous amniotic fluid, and OVI-8 died at birth from dystocia and delayed delivery. The other four calves were healthy. In addition, most surrogate mothers showed no or few symptoms of parturition such as labor pains and mammary development. On 1 November 1998, OVI-1 and -2 calves were 120 days old and CUM-6 and -7 calves were 85 days old. The results of microsatellite-typing (*13*) indicated that the genomes of the cloned calves were identical to those of the donor cells, and different from those of the surrogate mothers (Table 3).

Nuclear transfer of adult somatic cells from farm animals is the most efficient technique for obtaining large numbers of genetically identical animals. Although preimplantation embryonic cells and fetal fibroblasts are also useful for cloning, the economic potential of the donor is not predictable. In contrast, adult somatic cells can be selected from animals already proven to be ideal milk or meat producers. In particular, cumulus cells are especially appropriate for cloning females, because they can be easily obtained without injury to the animals.

In our study, the percentage of nuclear transplants developing into blastocysts was quite high (23% from oviductal cells and 49% from cumulus cells) compared with that of bovine fetal fibroblasts (12%) reported by Cibelli *et al.* (*7*). Our higher efficiency may relate to our culture system in which 30% of the control oocytes matured and fertilized in vitro developed into blastocysts (*14*). Thus, our nuclear transplants were about equal to the controls in developmental ability to the

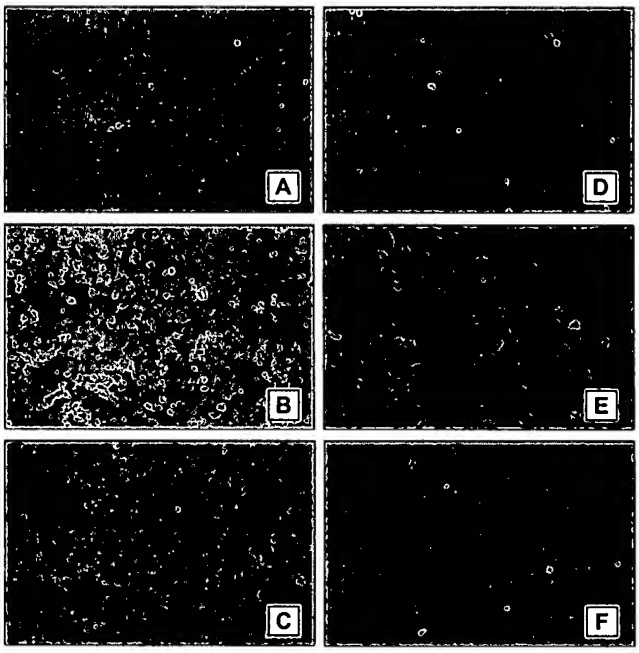


**Fig. 1.** Labeling of bovine oviductal (A to C) and cumulus (D to F) cells with vimentin B and E and cytokeratin (C and F). Panels (A) and (D) are negative controls. All oviductal epithelial cells were visually positive for a marker of epithelial cells, cytokeratin (C) (detected with rabbit antiserum to keratin), and for vimentin (B) (detected with rabbit antibody to vimentin) (*19*). All cumulus cells were also visually positive for vimentin (E) and cytokeratin (F), though the latter was very weak. Original magnification, × 100.

**Table 1.** Developmental potential of somatic nuclear transplants in vitro.

| Origin of donor cells | No. of oocytes | | No. of oocytes developed to | | | |
|---|---|---|---|---|---|---|
| | Fused/total | Cultured | Two-cell | Eight-cell | Morula | Blastocyst |
| Cumulus | 47/99 | 37 | 31 | 25 | 21 | 18 |
| Oviduct | 94/150 | 88 | 77 | 58 | 39 | 20 |

Y. Kato, Y. Sotomaru, Y. Tsunoda, Laboratory of Animal Reproduction, College of Agriculture and Research Institute for Animal Developmental Biotechnology, Kinki University, 3327-204, Nakamachi, Nara, 631-8505, Japan. T. Tani, Laboratory of Animal Reproduction, College of Agriculture, Kinki University, 3327-204, Nakamachi, Nara, 631-8505, Japan. K. Kurokawa and J. Kato, Division of Molecular Oncology, Nara Institute of Science and Technology, 8916-5, Takayama, Ikoma, Nara, 630-0101, Japan. H. Doguchi and H. Yasue, Department of Animal Breeding and Genetics, National Institute of Animal Industry, Ministry of Agriculture, Forestry, and Fisheries (MAFF), Tsukuba, Ibaraki 305-0901 Japan.

*To whom correspondence should be addressed. E-mail: tsunoda@nara.kindai.ac.jp

blastocyst stage. Furthermore, the quality of the nuclear transplant blastocysts was evidenced by the fact that they had normal cell numbers (69 to 114 cells) (*14*).

The high percentage of nuclear transplant embryos developing to term may be due to a number of factors. First, both donor cell populations maintained an apparent normal karyotype during the in vitro culture before use for nuclear transfer (*15*). Second, nucleo cytoplasmic interactions might be more compatible in this bovine experiment than in previous mouse experiments where the genetic type of the donor nucleus was critically important for later development (*16*). Third, although it was hypothesized that the donor cytoplasm of some somatic cell types might interfere with the development of nuclear transplants (*5*), the cumulus cytoplasm used in this study may have been compatible with the oocyte cytoplasm. The precursor cells of cumulus cells were connected by cytoplasmic bridges of microvilli and processes, through which cytoplasmic factors were exchanged. This exchange of factors might account for the higher percentage of nuclear transplant blastocysts from cumulus cell (49%) compared with oviductal cells (23%). Although, the telomerase activity of bovine cumulus cells is unclear, human cumulus cells, known to exhibit telomerase activity (*17*), might suffer fewer aging affects than other cell types and serve as an ideal adult donor cell for cloning. Fourth, twinning all embryos may have improved the survival rates of the embryos.

**Table 2.** Calves cloned from somatic cells. OVI and CUM designate the origin of the donor cells: oviduct and cumulus cells, respectively.

| Calf number | Born at day | Weight at birth (kg) | Status |
|---|---|---|---|
| OVI-1 | 242 | 18.2 | Living |
| OVI-2 | 242 | 17.3 | Living |
| CUM-3 | 266 | 32.0 | Dead (day 3) |
| CUM-4 | 267 | 17.3 | Dead (day 0) |
| CUM-5 | 267 | 34.8 | Dead (day 0) |
| CUM-6 | 276 | 23.0 | Living |
| CUM-7 | 276 | 27.5 | Living |
| OVI-8 | 287 | 30.1 | Dead (day 0) |

A problem for investigation concerns the cytoplasmic contribution of the oocyte to the properties of the clone. Bovine ovaries are often obtained from a slaughterhouse and the genetic background of the oocytes is unknown. In mice, cytoplasmic factors do affect the phenotype of nuclear transplants (*16*), but whether the effect stems from mitochondrial or maternal gene products is unknown. Two technical factors regarding the donor cells also require consideration, namely, freezing and the cell cycle stage. Large-scale cloning requires freezing of the donor cells. In our study, both donor cell types were freshly prepared and used before freezing. Although freezing of donor cells does not affect the in vitro development of nuclear transplants (*14*), the later developmental potential of such transplants is unknown. As cells are often damaged during freezing and thawing, this process should be carefully examined.

The application of somatic cell nuclear transfer to animal breeding poses many unanswered questions. Future studies are needed to reduce the death rate from environmental causes and also to reveal whether surviving calves grow normally into fertile adults. The low survival rate of calves might also be in part due to an epigenic component resulting from cloning and related procedures such as culture conditions, because the previous study on cloning bovine by nuclear transfer of embryonic nuclei reported similar postnatal problems (*18*). Whether these problems were caused by the nuclear transfer procedure or other factors is not known. Also, yet to be determined is whether other adult cell types can be reprogrammed to direct the development of fertile animals.

**Table 3.** DNA microsatellite analysis. The values indicate the fragment size in base pairs. DIK024, AG223, DIK069, DIK089, AG035, AG233, AG053, DIK106, DIK096, DIK020, DIK097, AG310, DIK102, AG119, DIK039, AG133, AG140, AG273, AG147, DIK010, AG160 and DIK068 are on the chromosome 1, 2, 3, 4, 5, 6, 7, 8, 9, 10, 11, 12, 13, 15, 17, 19, 20, 21, 22, 23, 24, 26, and 28, respectively. ND, not determined.

| | DIK024 | AG223 | DIK069 | DIK089 | AG035 | AG233 | AG053 | DIK106 | DIK096 | DIK020 | DIK023 | DIK097 |
|---|---|---|---|---|---|---|---|---|---|---|---|---|
| OVI cells | 234, 240 | 87, 87 | 160, 164 | 81, 90 | 166, 166 | 186, 186 | 285, 289 | ND | 251, 256 | 242, 242 | 100, 100 | 197, 201 |
| CUM cells | 234, 240 | 87, 87 | 160, 164 | 81, 90 | 166, 166 | 186, 186 | 285, 289 | ND | 251, 256 | 242, 242 | 100, 100 | 197, 201 |
| OVI-1 | 234, 240 | 87, 87 | 160, 164 | 81, 90 | 166, 166 | 186, 186 | 285, 289 | ND | 251, 256 | 242, 242 | 100, 100 | 197, 201 |
| OVI-2 | 234, 240 | 87, 87 | 160, 164 | 81, 90 | 166, 166 | 186, 186 | 285, 289 | ND | 251, 256 | 242, 242 | 100, 100 | 197, 201 |
| mother | 241, 243 | 82, 82 | 155, 164 | 88, 98 | 166, 166 | 192, 192 | 287, 292 | ND | 248, 248 | 242, 242 | 93, 108 | 192, 197 |
| CUM-3 | 234, 240 | 87, 87 | 160, 164 | 81, 90 | 166, 166 | 186, 186 | 285, 289 | ND | 251, 256 | 242, 242 | 100, 100 | ND |
| mother | 233, 237 | 82, 82 | 166, 166 | 93, 98 | 166, 168 | 192, 192 | 287, 290 | ND | 250, 254 | 241, 241 | 93, 95 | ND |
| CUM-4 | 234, 240 | 87, 87 | 160, 164 | 81, 90 | 166, 166 | 186, 186 | 285, 289 | ND | 251, 256 | 242, 242 | 100, 100 | ND |
| CUM-5 | 234, 240 | 87, 87 | 160, 164 | 81, 90 | 166, 166 | 186, 186 | 285, 289 | ND | 251, 256 | 242, 242 | 100, 100 | ND |
| mother | ND | ND | ND | ND | ND | ND | ND | ND | ND | ND | ND | ND |
| CUM-6 | 234, 240 | 87, 87 | 160, 164 | 81, 90 | 166, 166 | 186, 186 | 285, 289 | ND | 251, 256 | ND | 100, 100 | ND |
| CUM-7 | 234, 240 | 87, 87 | 160, 164 | 81, 90 | 166, 166 | 186, 186 | 285, 289 | ND | 251, 256 | 242, 242 | 100, 100 | ND |
| mother | 233, 239 | 82, 82 | 154, 154 | 85, 93 | 166, 166 | 187, 192 | 289, 289 | ND | 244, 254 | 230, 232 | 84, 95 | ND |
| OVI-8 | 234, 240 | 87, 87 | 160, 164 | 81, 90 | 166, 166 | 186, 186 | 285, 289 | ND | 251, 256 | 242, 242 | 100, 100 | ND |
| mother | 237, 248 | 82, 82 | 158, 160 | 87, 97 | 166, 168 | 185, 185 | 289, 289 | ND | 254, 254 | 243, 250 | 90, 99 | ND |

| | AG310 | DIK102 | AG119 | DIK039 | AG133 | AG140 | AG273 | AG147 | DIK010 | AG160 | DIK068 |
|---|---|---|---|---|---|---|---|---|---|---|---|
| OVI cells | ND | ND | 233, 246 | 188, 194 | 135, 139 | 150, 156 | 114, 114 | 194, 211 | 185, 195 | 246, 246 | 147, 153 |
| CUM cells | ND | ND | 233, 246 | 188, 194 | 135, 139 | 150, 156 | 114, 114 | 194, 211 | 185, 195 | 246, 246 | 147, 153 |
| OVI-1 | ND | ND | 233, 246 | 188, 194 | 135, 139 | 150, 156 | 114, 114 | 194, 211 | 185, 195 | 246, 246 | 147, 153 |
| OVI-2 | ND | ND | 233, 246 | 188, 194 | 135, 139 | 150, 156 | 114, 114 | 194, 211 | 185, 195 | 246, 246 | 147, 153 |
| mother | ND | ND | 233, 233 | 188, 194 | 135, 144 | 146, 148 | 100, 114 | 186, 191 | 185, 192 | 239, 241 | 146, 146 |
| CUM-3 | ND | ND | 233, 246 | 188, 194 | 135, 139 | 150, 156 | 114, 114 | 194, 211 | 185, 195 | 246, 246 | 147, 153 |
| mother | ND | ND | 233, 233 | ND | 135, 149 | 149, 156 | 100, 110 | 192, 200 | 192, 196 | 243, 246 | 143, 149 |
| CUM-4 | ND | ND | 233, 246 | 188, 194 | 135, 139 | 150, 156 | 114, 114 | 194, 211 | 185, 195 | 246, 246 | 147, 153 |
| CUM-5 | ND | ND | 233, 246 | 188, 194 | 135, 139 | 150, 156 | 114, 114 | 194, 211 | 185, 195 | ND | 147, 153 |
| mother | ND | ND | ND | ND | ND | ND | ND | ND | ND | ND | ND |
| CUM-6 | ND | ND | 233, 246 | 188, 194 | 135, 139 | 150, 156 | 114, 114 | ND | 185, 195 | 246, 246 | 147, 153 |
| CUM-7 | ND | ND | 233, 246 | 188, 194 | 135, 139 | 150, 156 | 114, 114 | ND | 185, 195 | 246, 246 | 147, 153 |
| mother | ND | ND | 229, 233 | 184, 188 | 137, 149 | 149, 150 | 110, 114 | 191 | 194, 196 | 238, 244 | 146, 147 |
| OVI-8 | ND | ND | 233, 246 | 188, 194 | 135, 139 | 150, 156 | 114, 114 | ND | 185, 195 | 246, 246 | 147, 153 |
| mother | ND | ND | 229, 233 | 194, 194 | 135, 149 | 147, 149 | 101, 114 | 185, 200 | 192, 195 | 240, 240 | 147, 147 |


**References and Notes**

1. R. Briggs and T. J. King, *Proc. Natl. Acad. Sci. U.S.A.* **38**, 455 (1952).
2. ———, *Dev. Biol.* **2**, 252 (1960).
3. M. A. Di Berardino, in *Genomic Potential of Differentiated Cells* (Columbia Univ. Press, New York, 1997).
4. I. Wilmut, A. E. Schnieke, J. McWhir, A. J. Kind, K. H. S. Campbell, *Nature* **385**, 810 (1997).
5. T. Wakayama, A. C. F. Perry, M. Zuccotti, K. R. Johnson, R. Yanagimachi, *ibid.* **394**, 369 (1998).
6. A. E. Schnieke *et al.*, *Science* **278**, 2130 (1997).
7. J. B. Cibelli *et al.*, *ibid.* **280**, 1256 (1998).
8. M. S. Joshi, *J. Reprod. Fertil.* **83**, 249 (1988).
9. Epithelial cell clusters from the mucosal tissue were squeezed from the oviduct and cultured.
10. They were passaged six times for cumulus and four times for oviductal epithelial cells. D-ME medium modified for mouse embryonic stem cell culture (ES-D-MEM) and supplemented with 10% fetal bovine serum (FBS) was used for the cell culture [E. J. Robertson, Ed., *Teratocarcinomas and Embryonic Stem Cells* (IRL Press, Oxford, 1987).
11. Cells cultured in 0.5% or less FBS for longer than 3 days attained a quiescent state (*14*).
12. For nuclear transfer, in vitro–matured oocytes were enucleated at 22 to 24 hours after maturation. A single donor cell was electrically fused with an oocyte immediately after enucleation with two pulses of 150 v/mm of dc for 25 μs in Zimmerman fusion medium. Pulses were repeated twice with an interval

of 15 min until fusion occurred. Fused oocytes were again electrically stimulated (20-v/mm dc pulses for 20 μs) to ensure activation. Nuclear transplant oocytes were immediately treated with cyclohexamide (10 μg/ml) in CR1-aa medium [C. F. Rosenkraus and N. L. First, *Theriogenology* **35**, 266 (abstr.) (1991)] with 3 mg of bovine serum albumin (fatty acid free) for 5 to 6 hours. After treatment, the oocytes were cultured in cyclohexamide-free medium. On day 3 (day 1 being the day of nuclear transfer), the nuclear transplant embryos were transferred to dishes containing CR-1aa medium supplemented with 10% FBS and mouse fetal fibroblast cells pretreated with mitomycin C (10 μg/ml) for 2.5 hours. On days 8 and 9 of in vitro culture, visually normal blastocysts were selected and transferred to recipient cows.

13. Genomes of recipient cows, nuclear donor cells, and cloned calves were typed for microsatellites by means of 23 primer sets that were provided by Shirakawa Institute of Animal Genetics, Livestock Technology Association of Japan [M. M. Inoue *et al.*, *Anim. Sci. Technol.* **68**, 443 (1997)].
14. Y. Kato *et al.*, unpublished data.
15. Even after 8 to 15 passages when they stopped dividing, most (71 to 82%) maintained normal diploid chromosomes.
16. W. Reik *et al.*, *Development* **119**, 933 (1993).
17. M. Dorland, S. Hol, R. J. van Kooij, E. R. te Velde, *J. Reprod. Fertil.* **20** (abstr.), 31 (1997).
18. F. B. Garry, R. Adams, J. P. McCann, K. G. Odde, *Theriogenology* **45**, 141 (1996).
19. The antiserum to keratin was obtained from Transformation Research, Farmingham, MA (catalog number 1007), and antibody to vimentin was from Diagnostic BioSystems, Freemont, CA (catalog number PDR 001).
20. We thank M. DiBerardino for the critical review of the manuscript and M. Kita, G. Tachiura, and other staff members of the Ishikawa Prefecture Livestock Station and Animal Public Health Center for embryo transfer, assistance and management of recipient animals, and assistance in postmortem analyses. This work was supported by grants from the Program for Promotion of Basic Research Activities for Innovative Biosciences (PROBRAIN) and the Special Coordination Funds for Promoting Science and Technology from the Ministry of Science and Technology.

11 September 1998; accepted 3 November 1998

# Elevating the Vitamin E Content of Plants Through Metabolic Engineering

**David Shintani and Dean DellaPenna***

α-Tocopherol (vitamin E) is a lipid-soluble antioxidant synthesized only by photosynthetic organisms. α-Tocopherol is an essential component of mammalian diets, and intakes in excess of the U.S. recommended daily allowance are correlated with decreased incidence of a number of degenerative human diseases. Plant oils, the main dietary source of tocopherols, typically contain α-tocopherol as a minor component and high levels of its biosynthetic precursor, γ-tocopherol. A genomics-based approach was used to clone the final enzyme in α-tocopherol synthesis, γ-tocopherol methyltransferase. Overexpression of γ-tocopherol methyltransferase in *Arabidopsis* seeds shifted oil compositions in favor of α-tocopherol. Similar increases in agricultural oil crops would increase vitamin E levels in the average U.S. diet.

The chloroplasts of higher plants produce numerous compounds that not only perform vital functions but also are important from agricultural and nutritional perspectives. Tocopherols, the lipid-soluble antioxidants known collectively as vitamin E, are one such group of compounds. The four naturally occurring tocopherols, α-, β-, γ- and δ-tocopherol, differ only in the number and position of methyl substituents on the aromatic ring (*1*). In addition to their role as antioxidants (*1*), tocopherols stabilize polyunsaturated fatty acids within lipid bilayers by protecting them from lipoxygenase attack (*2*).

Of tocopherol species present in foods, α-tocopherol is the most important to human health, has the highest vitamin E activity (*3*), and occurs as a single (*R,R,R*)-α-tocopherol isomer (*4*). Although all tocopherols are absorbed equally during digestion, only (*R,R,R*)-α-tocopherol is preferentially retained and distributed throughout the body (*5*).

The most recent U.S. recommended daily allowance (RDA) suggests that 10 to 13.4 international units (IU) of vitamin E [equal to 7 to 9 mg of (*R,R,R*)-α-tocopherol] be consumed daily (*6*). Because of the abundance of plant-derived components in most diets, this RDA is often met in the average diet. However, daily intake of vitamin E in excess of the RDA (100 to 1000 IU) is associated with decreased risk of cardiovascular disease and some cancers, improved immune function, and slowing of the progression of a number of degenerative human conditions (*5*). Obtaining these therapeutic levels of vitamin E from the average diet is nearly impossible unless a concerted effort is made to ingest large quantities of specific foods enriched in vitamin E.

In the United States, approximately 60% of dietary vitamin E intake is from vegetable oils (*7*). In soybean oil, which accounts for 80 and 25% of the edible oil consumed in the United States and the world, respectively (*8*), α-tocopherol and its immediate biosynthetic precursor γ-tocopherol account for 7 and 70%, respectively, of the total tocopherol pool (*9*). The other major oilseed crops—corn, canola, cottonseed, and palm oils—have similarly low α- to γ-tocopherol ratios (*4*).

Substantial increases in the α-tocopherol content of major food crops are needed to provide the public with dietary sources of vitamin E that can approach the desired therapeutic levels. The observation that many oilseeds contain relatively high levels of γ-tocopherol, the biosynthetic precursor to α-tocopherol, suggests that the final step of the α-tocopherol biosynthetic pathway, catalyzed by γ-tocopherol methyltransferase (γ-TMT), is limiting in these tissues. Therefore, it may be possible to convert the large pool of γ-tocopherol present in seeds such as soybeans to α-tocopherol by targeted overexpression of

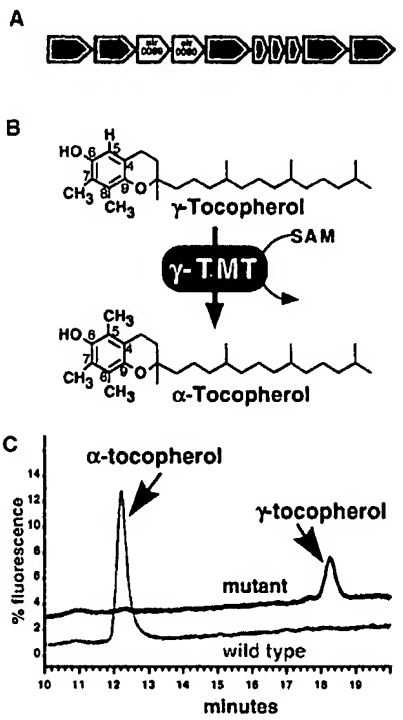


**Fig. 1.** γ-TMT in *Synechocystis* PCC6803. (**A**) Putative tocopherol biosynthetic operon from *Synechocystis* (*15*). SLR0089 encodes γ-TMT and SLR0090 encodes *p*-hydroxyphenylpyruvate dioxygenase. (**B**) γ-TMT enzymatic reaction. γ-TMT adds a methyl group to ring carbon 5 of γ-tocopherol. (**C**) HPLC profiles of tocopherols in wild-type *Synechocystis* PCC6803 and the γ-TMT null mutant. Total lipid extracts were isolated from each line, and tocopherols were analyzed by HPLC (*21*).

Department of Biochemistry, Mail Stop 200, University of Nevada, Reno, NV 89557, USA.

*To whom correspondence should be addressed. E-mail: della_d@med.unr.edu

BIOLOGY OF REPRODUCTION 64, 849–856 (2001)

# Generation of Dwarf Goat (*Capra hircus*) Clones Following Nuclear Transfer with Transfected and Nontransfected Fetal Fibroblasts and In Vitro-Matured Oocytes[1]

C.L. Keefer,[2,3] H. Baldassarre,[3] R. Keyston,[3] B. Wang,[3] B. Bhatia,[3] A.S. Bilodeau,[3] J.F. Zhou,[3] M. Leduc,[3] B.R. Downey,[4] A. Lazaris,[3] and C.N. Karatzas[3]

*Nexia Biotechnologies Inc.,[3] Ste Anne de Bellevue, Quebec, Canada H9X 3R2*
*Department of Animal Science,[4] McGill University, Ste Anne de Bellevue, Quebec, Canada H9X 3V9*

## ABSTRACT

**The developmental potential of caprine fetal fibroblast nuclei after in vitro transfection and nuclear transfer (NT) into enucleated, in vitro-matured oocytes was evaluated. Fetal fibroblasts were isolated from Day 27 to Day 30 fetuses from a dwarf breed of goat (BELE: breed early lactate early). Cells were transfected with constructs containing the enhanced green fluorescent protein (eGFP) and neomycin resistance genes and were selected with G418. Three eGFP lines and one nontransfected line were used as donor cells in NT. Donor cells were cultured in Dulbecco minimum Eagle medium plus 0.5% fetal calf serum for 4–8 days prior to use in NT. Immature oocytes were recovered by laparoscopic ovum pick-up and matured for 24 h prior to enucleation and NT. Reconstructed embryos were transferred as cleaved embryos into synchronized recipients. A total of 27 embryos derived from transgenic cells and 70 embryos derived from nontransgenic cells were transferred into 13 recipients. Five recipients (38%) were confirmed pregnant at Day 35 by ultrasound. Of these, four recipients delivered five male kids (7.1% of embryos transferred) derived from the nontransfected line. One recipient delivered a female kid derived from an eGFP line (7.7% of embryos transferred for that cell line). Presence of the eGFP transgene was confirmed by polymerase chain reaction, Southern blotting, and fluorescent in situ hybridization analyses. Nuclear transfer derivation from the donor cells was confirmed by single-strand confirmation polymorphism analysis. These results demonstrate that both in vitro-transfected and nontransfected caprine fetal fibroblasts can direct full-term development following NT.**

*assisted reproductive technology, developmental biology, embryo, gamete biology, gene regulation, ovum*

## INTRODUCTION

Live offspring have been obtained following nuclear transfer (NT) of embryonic, fetal, and adult cells in cattle, sheep, goats, pigs, and mice [1–11]. This cloning process involves transfer of a donor cell nucleus into an enucleated oocyte. The source and treatment of the donor cell and recipient oocyte are key factors in the successful outcome of this process. In vivo-matured oocytes were used initially as the recipients for blastomeres for embryo cloning in cattle [1, 12]. However, the high cost of in vivo-sourced bovine oocytes propelled the switch to in vitro-matured oocytes [13, 14]. Cloning in cattle now involves a totally in vitro approach: Recipient oocytes are derived from in vitro-matured oocytes obtained from slaughterhouse ovaries and resulting NT embryos are cultured to the blastocyst stage in vitro prior to transfer [7, 15]. In other species, including sheep, goat, and mice, in vivo-matured oocytes are used predominately [8, 9, 16]. Although the use of in vitro-matured ovine oocytes in NT was reported in one study, a lower production of lambs from NT embryos derived from in vitro-matured oocytes was achieved than from in vivo-matured oocytes (2.3% vs. 6.5% of embryos transferred; [17]). Despite these results, the use of in vitro-matured oocytes in small ruminants could provide similar advantages as those seen in the bovine system. While the quality and quantity of oocytes obtained from slaughterhouse-derived ovaries of small ruminants can be affected by season, immature oocytes can be readily obtained year round from hormone-primed animals by either laparoscopy or laparotomy [18]. As we show in this study, the laparoscopic approach provides a minimally invasive, efficient means of obtaining immature oocytes for subsequent use in NT.

Freshly isolated cells [8], short-term culture of fetal and adult cells [5, 15, 16], and established embryonic stem cell lines [10] have all been successfully used in NT. In a few cases, transgenic cells have been used as donor cells in order to produce transgenic offspring. This includes propagation of transgenic animals (goat [9]) and the in vitro transfection and selection of transgenic donor cells (sheep [19] and cattle [7]). Furthermore, there has been a recent report of transgenic lambs resulting from the application of homologous recombination techniques to the donor cells [20]. In transgenic animal production programs, the ability to transfect and select cells prior to animal production results in transgenic animals of the desired gender and overcomes the problem of founder animals being mosaic. Therefore, in contrast to production of transgenic animals by pronuclear injection that results in less than 10% of offspring carrying the transgene, production of a transgenic animal can be ensured by confirming integration site(s) prior to use in NT.

In this study, we demonstrate that NT embryos derived from goat fetal cells transfected in vitro can support development to term following NT using in vitro-matured oocytes. Furthermore, we demonstrate that the BELE (breed early lactate early) system of transferring dwarf goat embryos into standard-sized goats (e.g., Alpine, Saanen, and Nubian) is suitable for the production of NT-derived, transgenic offspring. In earlier studies, the advantages of this system were demonstrated by the production of transgenic dwarf offspring following transfer of pronuclear-injected, dwarf zygotes into standard-sized dairy goats [21]. These dwarf goats provide advantages in their small size (reduced

[1]Preliminary reports of this work were presented at the 32nd Annual Meeting of the Society for the Study of Reproduction, July 1999, Pullman, WA, and the Transgenic Animal Research Conference, August 1999, Tahoe City, CA.

[2]Correspondence: Carol L. Keefer, Nexia Biotechnologies Inc., 21025 Trans Canada Highway, Ste-Anne-de-Bellevue, PQ, Canada H9X 3R2. FAX: 514 457 6151; e-mail: ckeefer@nexiabiotech.com

Received: 16 August 2000.
First decision: 15 September 2000.
Accepted: 11 October 2000.

ISSN: 0006-3363. http://www.biolreprod.org

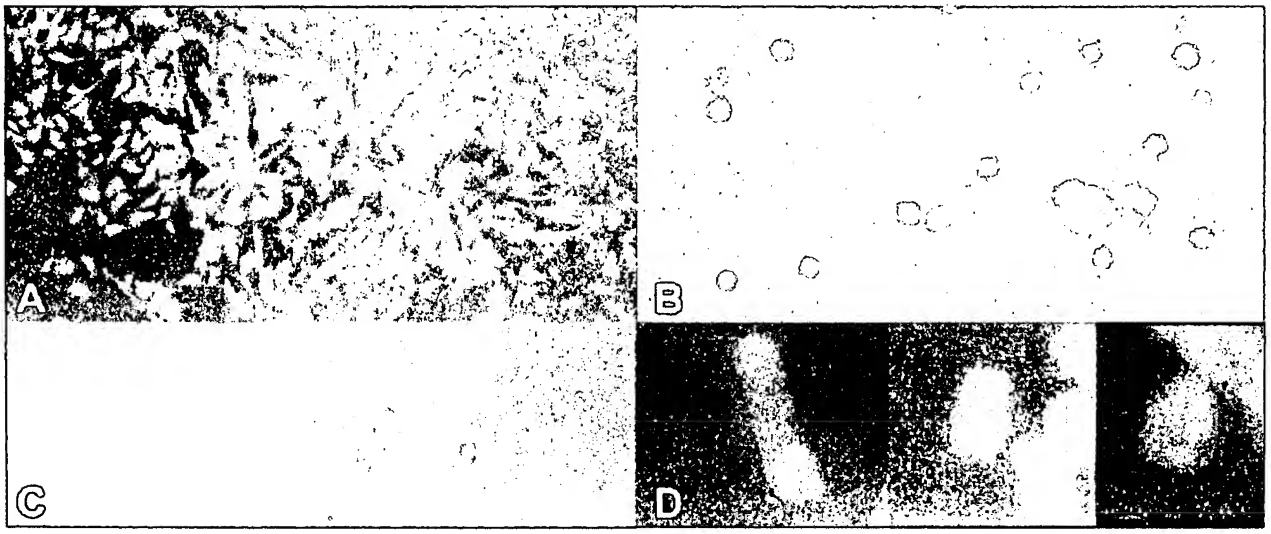


FIG. 1. A) The in vitro-transfected fetal fibroblast line FF3-eGFP demonstrating GFP expression under blue light. B) Expression of GFP in donor FF3-eGFP cells at time of NT. C) Expression of GFP after 5-azacytidine treatment of cells obtained from the transgenic female. D) Fluorescence in situ hybridization analysis using a biotin-labeled probe containing the CEeGFP plasmid demonstrating integration of the transgene in cells obtained from the transgenic FF3-eGFP female clone. Original magnification ×25 (A), ×200 (B and C), ×1000 (D).

housing and feed) and early sexual maturity (reduced time lines) [22]. Furthermore, the ability to utilize both standard dairy breeds and dwarf breeds as recipients simplifies recipient herd management.

## MATERIALS AND METHODS

### *Isolation of Donor Cell Lines*

Fetal cells were isolated from Day 27 to Day 30 fetuses recovered surgically from a dwarf breed of goat (BELE). After removal of the head and internal organs, the remaining tissues were mechanically dissociated. Explants were cultured in Dulbecco modified Eagle medium (DMEM; Gibco, Canadian Life Technologies, Burlington, ON, Canada) supplemented with 20% fetal bovine serum (FBS) and 20 μg/ml gentamycin at 38°C in 5% $CO_2$. While the explant cultures contained a mixed population of cells, fetal fibroblasts were predominant. When the cells from the explants reached 70% confluency, they were removed with 0.05% trypsin-EDTA treatment, counted, and frozen into aliquots in 10% DMSO + 90% FBS, or plated in chamber slides (Labtek, Canadian Life Technologies, Burlington, ON, Canada) for cytogenetic analysis. Frozen aliquots of cells with a normal chromosome number were thawed and either prepared for use in NT or were transfected with the DNA construct to generate stable lines.

### *Generation of Transfected Cells*

Stable cell lines were generated through lipid-mediated gene transfer. The CEeGFP plasmid (kindly provided by Dr. T. Takada, National Childrens' Medical Research Center, Tokyo, Japan) contained the enhanced, humanized version of the green fluorescent protein reporter gene driven by the human elongation factor-1α promoter and cytomegalovirus enhancer, and the neomycin selection marker under the control of the simian virus-40 promoter [23, 24]. This plasmid was delivered into the cells using lipofectamine (Gibco) according to the manufacturer's instructions. A number of stable clones were generated by selection under G418 for 20 days and assessed for expression of the reporter gene by visualization of the fluorescent signal under blue light (Zeiss Filter Set 09; Carl Zeiss Canada Ltd., North York, ON, Canada). Stable lines were either used as donor cells in NT or were frozen into small aliquots for later use. Four lines were subsequently used in NT: a non-transfected male line (FF4), a transfected male line (FF4-eGFP), and two transfected female lines (FF1-eGFP and FF3-eGFP; Fig. 1A).

### *Donor Cell Preparation*

Fetal fibroblast cells (0.5 to 1 × $10^5$) were plated into 24- or 96-well plates and cultured in DMEM + 10% FBS until they reached 100% confluency. The medium was then replaced with low serum media (DMEM + 0.5% FBS + 20 μg/ml gentamycin), and the cells were incubated at 38°C, 5% $CO_2$ for 4–8 days until day of NT [25]. Just prior to cell transfer, the donor cells were collected by trypsinization using 0.05% trypsin-EDTA, washed twice, and resuspended in EmCare containing 1% BSA.

### *Oocyte Maturation and Preparation*

Ten to fifteen cumulus-oocyte complexes (COCs) were cultured per 50-μl drops of maturation medium covered with an overlay of mineral oil (Sigma, St. Louis, MO) and incubated at 38.5–39°C in 5% $CO_2$. The maturation medium consisted of M199 supplemented with bovine LH (0.02 U; Sioux Biochemicals, Sioux Center, IA), bovine FSH (0.02 U; Sioux Biochemicals), estradiol-17β (1 μg/ml; Sigma), 0.2 mM sodium pyruvate, kanamycin (50 μg/ml), and 10% heat-inactivated goat serum (Sigma), or FBS (Immunocorp, PQ, Canada). The FBS was used as the serum source in five sessions, whereas, goat serum was used in seven sessions. After 23–24 h of maturation, the cumulus cells were removed from the matured oocytes by vortexing the COCs for 1–2 min in EmCare (Immuno-Chemical Products, Auckland, NZ) containing 1 mg/ml hyaluronidase (Sigma). The denuded oocytes were washed in handling medium (EmCare supplemented with 1% FBS) and were returned to maturation medium. The enucleation process

was initiated within 1 h of oocyte denuding. Prior to enucleation, the oocytes were incubated for 20–30 min in 5 μg Hoeschst 33342 (Sigma) per ml handling medium at 30–36°C in air atmosphere.

### *Enucleation*

Oocytes stained with Hoechst were enucleated following brief exposure of the cytoplasm to UV light (Zeiss Filter Set 01) to determine the location of the chromosomes. Oocytes were manipulated at room temperature (24–26°C) in handling medium (EmCare supplemented with 1% FBS) without the addition of cytochalasin B. Stage of nuclear maturation was observed and recorded during the enucleation process. The removed cytoplasm was checked for the presence of chromosomes and polar body by exposure to UV light.

### *Donor Cell Transfer and Fusion*

The enucleated oocytes and dispersed donor cells were manipulated in handling medium. Small (<20 μm) donor cells with smooth plasma membranes were picked up with a manipulation pipette and slipped into the perivitelline space of the enucleated oocytes. Cell-cytoplast couplets were fused immediately after cell transfer. Groups of four to six couplets were manually aligned between the electrodes of a 500-μm gap fusion chamber (BTX, San Diego, CA) overlaid with sorbitol fusion medium (0.25 M sorbitol, 100 μM calcium acetate, 0.5 mM magnesium acetate, 0.1% BSA). A brief fusion pulse (15 μsec) at 2.39 kV/cm was administered by a BTX Electrocell Manipulator 200. After the couplets had been exposed to the fusion pulse they were placed into 25-μl drops of culture medium overlaid with mineral oil (Sigma). Culture medium consisted of either a low phosphate (0.35 mM) modification of SOFaa [26] or G1.2 (Colorado Center for Reproductive Medicine, Englewood, CO [27]) supplemented with 8 mg/ml BSA. Fused couplets were incubated at 38.5–39°C in 5% $CO_2$, 7% $O_2$, 88% $N_2$. After 1 h, couplets were observed on a stereomicroscope for fusion. Unfused couplets were administered a second fusion pulse as described above.

### *Activation and Culture*

Two to three hours after application of the fusion pulse, the couplets were activated using the calcium ionomycin and 6-dimethylaminopurine (6-DMAP; Sigma) method of Susko-Parrish et al. [28]. Activated couplets were cultured for 2.5–4 h in DMAP, then washed in handling medium, and placed into 25-μl culture drops consisting of low phosphate SOFaa or G1.2 under an oil overlay. While group size ranged from 4 to 27 embryos per drop, the average number was 10. Cleavage development (2- to 4-cell stages) was observed at 36 h. Embryos were transferred on Day 2 (Day 0 = day of fusion) into synchronized recipients on Day 1 of their cycle (D0 = estrus). Visual observations of the reconstructed embryos for GFP expression were not made prior to embryo transfer to reduce further manipulations of the embryos.

### *Donor and Recipient Animals*

Oocyte recoveries and embryo transfers were performed during the months of October, November, and December 1998. The donor herd consisted of 32 does (Alpine, Saanen, Nigerian Dwarf, and Pygmy). Twenty of the donors underwent two or three laparoscopic ovum pick-up (LOPU) sessions. Intravaginal sponges containing 60 mg of medroxyprogesterone acetate (Veramix; Upjohn Co., Orangeville, ON, Canada) were inserted into the vagina of donor goats and left in place for 7–10 days with an injection of 125 μg cloprostenol (Estrumate; Schering Canada Inc., Pointe-Claire, PQ, Canada) given 36–48 h before sponge removal. Priming of the ovaries was achieved by the use of gonadotropin preparations including FSH and eCG. The following hormonal regimes were used: a total dose equivalent to 120 mg NIH-FSH-P1 of Ovagen (Immuno-Chemical Products, Auckland, New Zealand) given twice daily in decreasing doses (35, 35, 25, and 25 mg) starting 48 h before sponge removal, or a total dose equivalent to 70 mg NIH-FSH-P1 (Follitropin-V; Vetrepharm, London, ON, Canada) given together with 400 IU of eCG (Equinex; Ayerst Laboratories, Canada) 36–48 h before oocyte recovery. Both regimes resulted in similar numbers of follicles and COCs recovered (data not shown).

Recipients (Alpine, Saanen, Nubian, LaMancha, and Toggenburg) were synchronized using intravaginal sponges containing 60 mg of medroxyprogesterone acetate. An injection of 125 μg cloprostenol was given 36–48 h before sponge removal. An injection of 400 IU of eCG was given at sponge removal on the same day as LOPU.

### *Laparoscopic Oocyte Pick-Up and Embryo Transfer*

Donor goats were fasted 24 h prior to laparoscopy. Anesthesia was induced with i.v. administration of diazepam (0.35 mg/kg body weight) and ketamine (5 mg/kg body weight) and was maintained with isofluorane via endotrachial intubation. Cumulus-oocyte complexes were recovered by aspiration of follicular contents under laparoscopic observation [18].

Recipient goats were fasted and anesthetized in the same manner as the donors. A laparoscopic exploration was performed to confirm if the recipient had one or more recent ovulations or corpora lutea (CL) present on the ovaries. Four to 11 cleavage-staged embryos (2-cell to 8-cell stages) were transferred into the oviduct ipsilateral to ovulation(s) by means of a TomCat catheter threaded into the oviduct by way of the fimbria. Donors and recipients were monitored following surgical procedures. Antibiotics and analgesics were administered according to approved procedures.

### *Determination of Fetal Survival and Kidding*

All recipient goats were examined by ultrasonography on Day 35 and 60 of gestation to record fetal development. Parturition was induced with three injections of 8 mg dexamethasone (Azium) given at 12-h intervals with 125 μg of clorprostenol (Estrumate) given with the third injection. The first injection was administered on Day 147 or 148 of gestation. Cotyledon number and birth weights were recorded.

### *Cytogenetic Analysis (Chromosome Counts, Sexing, and Fluorescence In Situ Hybridization)*

Normal chromosome number (2n = 60) was determined prior to use of cells in NT. Slides for cytogenetic analysis were prepared by standard techniques [29, 30]. Briefly, fetal fibroblasts were cultured with colcemid in order to increase the number of cells in mitotic metaphase. Spreads were stained with Giemsa and assessed for chromosome number and sex.

TABLE 1. Nuclear transfer efficiencies using caprine fetal fibroblast cells.

| Donor cell (sex) | Passage | No. NTs produced | No. NTs transferred | No. recipients | No. pregnant (%) | No. kids born (%) |
|---|---|---|---|---|---|---|
| FF4 (male) | 2 | 254 | 70 | 8 | 4 (50%) | 5 (7.1%) |
| FF4-eGFP (male) | 5 | 13 | 5 | 1 | 0 | 0 |
| FF3-eGFP (female) | 5 | 30 | 13 | 2 | 1 (50%) | 1 (7.7%) |
| FF1-eGFP (female) | 6 | 69 | 9 | 2 | 0 | 0 |

Chromosomal integration of the transgene into transfected stable lines was demonstrated by fluorescent in situ hybridization (FISH) techniques. The transgene hybridization signal was visualized using a biotin-labeled probe containing the entire CEeGFP construct. The chromosome spreads were stained with propidium iodide [29, 31, 32].

### *Genotyping and Polymerase Chain Reaction Analysis of Cloned Animals*

Genomic DNA was isolated (QIAmp DNA Blood Mini Kit; Qiagen Inc., Mississauga, ON, Canada) from blood samples collected from the cloned animals, the surrogate dams, the biological dams and sire, and the donor cells. Each nontransgenic animal was analyzed by polymerase chain reaction (PCR)-single strand confirmation polymorphism (SSCP) to confirm that the clones were derived from the NT procedure. Briefly, a 286-base pair (bp) fragment of the goat major histocompatibility complex (MHC) class II DRB gene [33] was amplified using two primers (ACB0445, 5′-TATCCCGTCTCTGCAGCACATTTC-3′; ACB0446, 5′-ATCGCCGCTGCACACTGAAACTC-3′). The identity of the PCR product was confirmed by DNA sequencing analysis (Mobix, Hamilton, Canada). The PCR product was analyzed by SSCP [34, 35] in order to identify the relationship between animals.

Genomic DNA from the goat derived from a transgenic cell line was analyzed by PCR for the presence of the transgene using two different primer sets. The first set (ACB411, 5′-AGACTGAAGTTAGGCCAGCTTGG-3′ and ACB412, 5′-GTCTTGTAGTTGCCCGTCGTCCTT-3′) amplified a 490-bp fragment that spanned the elongation factor-1α promoter and the GFP reporter gene. A second set of primers amplified a 360-bp portion of the endogenous β-casein that provided a positive control to ensure that the extracted DNA was amplifiable by PCR.

### *Induction of GFP Expression*

A skin biopsy was obtained from the lower edge of the ear using a 6-mm biopsy punch. The cells were dispersed by cutting the sample into small fragments and incubating them in digestion medium (Gibco) at 37°C in a 5% $CO_2$ incubator. After 16 h, the tissue digest was pipetted up and down, and the dissociated cells were centrifuged, washed, resuspended in DMEM supplemented with 10% FBS and 0.02 mg/ml gentamycin (Gibco), and plated in a culture vessel. Once the cells reached 70–80% confluency, they were trypsinized, counted, centrifuged, resuspended in cryomedia (90% dimethylsulfoxide, 10% FBS) at a concentration of $1 \times 10^6$ cells per ml, and frozen in aliquots. An aliquot was thawed and the cells incubated at 37°C in 5% $CO_2$. Upon reaching 70–80% confluency, the cells were trypsinized, counted, and plated for drug treatment in 12-well plates at a concentration of $1 \times 10^4$ cells per well. These cells were treated with either 5-azacytidine, a cytidine analog that inhibits methylation when incorporated into DNA [36], or sodium butyrate that nonspecifically inhibits histone deacetylase enzyme [36, 37]. Twenty-four hours after plating, 5-azacytidine (Sigma) was added to the cells at either 0, 3, 6, or 10 μM concentrations. After an additional 24 h, the drug was removed from the cells, and they were observed daily under blue light for the presence of GFP fluorescence. Similarly, the cells were plated in 12-well plates at a concentration of $1 \times 10^4$ cells per well, and 24 h later they were treated with either 0, 50, or 100 mM sodium butyrate (Sigma). The drug was removed 24 h later, and the cells were observed daily under blue light for the presence of GFP fluorescence.

### *Animal Ethics*

This project was approved by the McGill Animal Ethics and Animal Care Committees.

### *Statistical Analysis*

The proportional data for oocyte nuclear maturation, cell fusion, in vitro development, pregnancy rates, and NT efficiencies (offspring produced per embryo transferred) were analyzed by contingency tables using InStat (GraphPad, San Diego, CA). Birth weight and cotyledon number were analyzed using the Student's *t*-test (GraphPad).

## RESULTS

In 11 sessions, 781 oocytes were recovered from 57 donor aspirations (13.7 per donor). Following maturation, 734 in vitro-matured oocytes were denuded of cumulus cells and assessed for nuclear maturation. Significantly fewer oocytes matured to metaphase II in maturation medium supplemented with FBS, than for oocytes matured with goat serum, 69% (235/338) versus 86% (341/396), respectively ($P < 0.01$). A total of 366 karyoplast-cytoplast couplets were produced using donor cells from one nontransfected and three eGFP-transfected fetal fibroblast cell lines (Table 1). At the time of cell transfer the donor cells from all three lines were mosaic for expression of the transgene as determined by visual observation (Fig. 1B).

Due to the small size of the donor cell, fusion was difficult to assess; however, 54% of the karyoplast-cytoplast couplets appeared to have fused. As culture group size was known to affect developmental rates [26], fused and nonfused couplets were not separated at assessment and were cultured together in order to prevent the generation of small subsets of embryos. Forty-three percent of the couplets underwent initial cleavage (2-cell to 8-cell stages). No differences were observed in fusion or initial cleavage rates when NT embryos were cultured in SOF or G1.2 ($P > 0.05$; data not shown). A total of 97 reconstructed embryos were transferred into 13 recipients (Table 1) with each recipient receiving on average 7.5 ± 0.6 embryos. Number of embryos transferred per recipient did not significantly affect the pregnancy rate.

Five of the recipients (38%) receiving cleavage-staged embryos were confirmed pregnant by ultrasound. These

TABLE 2. Cell line treatment and birth data of NT-derived kids.

| Name | Donor cell | Passage | Days low serum | Type of delivery (length of gestation) | Birth weight (kg) | No. cotyledons | Status |
|---|---|---|---|---|---|---|---|
| FF4-01 | FF4 | 2 | 4 | C-section (150 days) | 1.5 | 32 | Live (>1 yr) |
| FF4-02 | FF4 | 2 | 4 | Induced | 3.1 | 50 | Dead (1 mo) |
| FF4-03 | | | | (150 days) | 2.7 | | Live (>1 yr) |
| FF4-04 | FF4 | 2 | 4 | Induced (150 days) | 2.1 | 83 | Dead (1 day) |
| FF4-05 | FF4 | 2 | 4 | Induced (149 days) | 2.4 | 65 | Dead (3 mo) |
| FF3-eGFP-01 | FF3-eGFP | 5 | 6 | Induced (149 days) | 2.1 | 48 | Live (>1 yr) |

pregnancies resulted from transfers of reconstructed embryos from two of the four cell lines. In both cases the pregnancy rate was 50%, four of eight recipients receiving embryos derived from the nontransfected FF4 male line and one of two recipients receiving embryos derived from the FF3-eGFP positive female line (Table 1). Transfers involving the other two cell lines did not result in pregnancies. The FF4 pregnancies resulted from transfer of cleavage stage NT embryos derived from donors cells at passage 2 that had been maintained in low serum for 4 days. The FF3-eGFP pregnancy resulted from transfer of cleavage-stage NT embryos derived from donor cells at passage 5 that had been maintained in low serum for 6 days. The source of the oocyte, Dwarf/Pygmy or Saanen/Alpine, affected neither the initial pregnancy rate (37.5% vs. 25%, respectively) nor the NT efficiency (4.6% vs. 4.5%, respectively, $P > 0.05$).

One kid was delivered by cesarean section on Day 150; the remaining kids were born on Days 149 and 150 by vaginal delivery approximately 36–48 h following initiation of induction (Table 2). Four of the recipients delivered five male kids derived from the nontransfected FF4 line. Average birth weight (±SEM) was 2.36 ± 0.27 kg (range 1.5–3.1 kg). Four placentas were recovered and had an average of 57 cotyledons (range 32–83). One kid subsequently died within 24 h of birth, one died at 1 mo of age, and one died at 3 mo of age, all three succumbed to bacterial infections affecting the lungs. The remaining two males are healthy (Fig. 2B). One recipient delivered a healthy female kid (2.1 kg birth weight) derived from the eGFP-positive line (Fig. 2A). The placenta was recovered and had 48 cotyledons. The birth weights and cotyledonary numbers were not significantly different from those of dwarf goat kids produced by natural breeding at Nexia Biotechnologies Caprine Production Facility that averaged 2.35 ± 0.15 kg at birth (n = 11) with recovered placentas having an average cotyledon number of 60 (n = 5; N. Kafidi, personal communication).

### *Chromosome Number, SSCP, FISH, PCR, and GFP Expression Analyses*

All four cell lines used in NT had a normal chromosome count consisting of 60 chromosomes (60XX or 60XY). The PCR-SSCP analysis for the polymorphic MHC class II DRB gene confirmed that all the cloned kids were derived from their donor cell lines, whereas the surrogate dams carried different alleles. The cloned goats differ from the surrogate dams at the analyzed locus but have the same allelic information as the donor lines and biological dam (Fig. 2C).

Presence of the CEeGFP transgene in the genomic DNA of the transgenic female was confirmed by PCR, Southern blotting (data not shown), and FISH (Fig. 1D). The Southern blotting and FISH analyses both indicated that there were three integration sites. Based on banding patterns, the transgene integration sites were located on 10q34, 23q12, and 25q15. However, neither epithelial cells taken from a mouth swab nor skin fibroblasts expressed the GFP protein as determined by observation under blue light. Western blot analysis of cytoplasmic extracts of cultured fibroblasts from skin biopsies also indicated that the protein was not expressed (data not shown). Expression of GFP was induced in a subpopulation of the skin fibroblast cells (<1%) after a 24-h drug treatment with either 3, 6, or 10 μM 5-azacytidine (Fig. 1C). This expression persisted for over a week and then declined slowly if drug treatment was not repeated. Cells that were treated repeatedly retained GFP expression in a subpopulation of cells. Expression of GFP was not observed in any of the cells that were treated with sodium butyrate or in the controls (data not shown).

## DISCUSSION

In this study, in vitro-matured caprine oocytes supported full term development when used as recipient cytoplasts in NT. Both in vitro-transfected and nontransfected fetal fibroblasts were used successfully as donor cells. Polymerase chain reaction and FISH analyses confirmed the presence of the transgene in the FF3-eGFP-derived female; however, expression was not detected either visually or by Western analysis in skin fibroblastic cells. One possible explanation for lack of expression could be that the transgene had been silenced by epigenetic regulatory mechansims (e.g., methylation, histone deacetylation) [36]. Treatment of cells with 5-azacytidine, a cytidine analogue that inhibits methylation when incorporated into DNA, resulted in expression of the transgene in a cell subpopulation. Although position-dependent expression cannot be ruled out, this expression indicates the presence of a functional transgene that may have been silenced by epigenetic mechanisms. Furthermore, at the time of NT the donor cells demonstrated mosaic expression of the transgene as determined by visual observation (Fig. 1B). The mosaic expression observed at the time of NT may indicate that the process of transgene methylation had commenced during in vitro culture. At this time it is not certain if the epigenetic mechanisms affected the promoter or the GFP transgene or both. Incorporation of insulator elements, locus control regions, matrix-attachment regions into the construct design, or the use of artificial chromosomes or gene targeting could alleviate problems of nonexpression due to transcriptional regulation [36, 38]. While the GFP protein was not expressed in the animal itself, these results demonstrated the production of a trans-

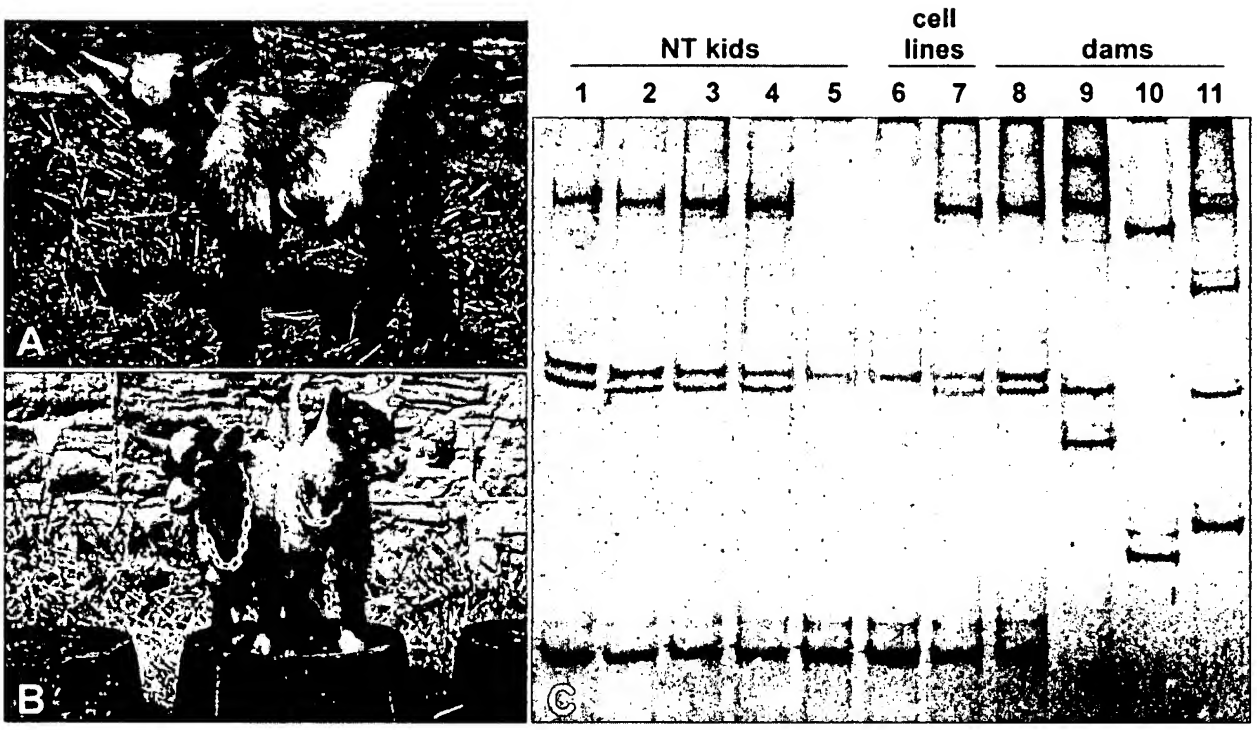


FIG. 2. A) Female kid produced by NT using in vitro-transfected FF3-eGFP fetal fibroblasts. B) Male FF4 kids produced by NT using fetal fibroblasts. C) A PCR-SSCP analysis of the second exon of the caprine MHC class II DRB gene: lanes 1–4, male FF4 kids; lane 5, FF3-CEeGFP kid; lane 6, FF3 cell line; lane 7, FF4 cell line; lane 8, biological dam of FF3 and FF4 fetuses; lanes 9, 10, and 11, surrogate dams.

genic goat through in vitro transfection and NT confirming similar work in cattle and sheep [7, 19].

Fetal fibroblasts were chosen as the source of donor cells owing to their potential for longer term culture required in the transfection and selection processes. Optimization of culture, transfection conditions, and selection treatments may permit utilization of other sources, adult or fetal, as the targeted donor cell. Recent reports indicate that some adult cell lines can be maintained sufficiently long enough for homologous recombination events to take place [20, 39, 40]. In this study, serum starvation was utilized in order to synchronize the donor cells in $G_0/G_1$ arrest [25]. While there are conflicting reports on the necessity of serum starvation, $G_0/G_1$-arrested cells may be more receptive to reprogramming than other stages of the cell cycle [7, 25, 41, 42]. The number of recipients per cell line was too small in this study to determine any real differences in NT efficiencies between the cell lines; however, the longer period of culture necessitated for in vitro transfection and/or the in vitro transfection treatments themselves may have affected the viability of the transfected lines. The ability to correlate success (live offspring) with type, stage, or donor cell treatment has been limited by the low efficiencies currently achieved in NT [43]. However, with the current level of interest and the application of NT techniques to divergent species, some of the intriguing questions regarding cell cycle and nuclear reprogramming should be resolved.

A 50% pregnancy rate was achieved following embryo transfer of NT embryos derived from both the transgenic FF3-eGFP line and the FF4 nontransgenic line. This is similar to the pregnancy rates reported for standard-sized recipients receiving DNA-injected dwarf goat zygotes [21]. Unlike reports in sheep and cattle [17, 19, 42], we did not observe any prenatal loss. This is similar to the report by Baguisi and coworkers [9] for somatic cell NT in goats, in which no losses were observed after confirmation of fetal heartbeats at Day 40. However, at earlier observations (Day 30) a high proportion of recipient does (55–78%) exhibited vesicle formation that were subsequently resorbed. In their work, NT-derived kids were produced using in vivo-matured oocytes and transgenic fetal fibroblasts obtained from a transgenic donor animal. In both their report and in our study, NT-derived embryos were transferred at early cleavage stages. In sheep and cattle, an increased incidence of large offspring following transfer of embryos cultured in the presence of serum has been observed [44, 45], demonstrating the possible effects of in vitro culture on fetal development. It may be that avoidance of longer term culture may have alleviated some of the detrimental effects of in vitro culture. Contrarily, this lack of prenatal loss may be a species-related phenomenon reflected in the cytoplast's ability to reprogram the donor nucleus. Compatibility between nucleus and cytoplasm may be limited to closely related breeds such as those used in this study and those involving Enderly Island [6], Zebu [46], and Holstein breeds, while more diverse relationships may result in early embryonic loss [47, 48]. In this study, both dairy and dwarf goat oocytes were used as recipient cytoplasts with similar efficiencies. In mice, gene expression and adult body weight were affected by epigenetic events resulting from pronuclear exchange between two different strains [49]. Furthermore, strain has been shown to have significant effects on efficiencies following NT [50]. As compatibility between the recipient ooplasm and the donor nucleus must be reflected in some part in the overall effectiveness of nuclear reprogramming, nucleocytoplasmic interactions may be responsible for some of the detrimental effects observed following NT.

All pregnancies were full term with recipients showing mammary gland development prior to initiation of induction. The first cloned kid was delivered by c-section due to concern for the well-being of the kid and not to any difficulties associated with the dam itself. Birth weights and number of cotyledons on the recovered placentas were within normal range for dwarf goats (Table 2). While the shape and distribution of the cotyledons appeared slightly irregular, further studies are needed to confirm these observations. Despite the apparent normalcy of the pregnancies and births, a high postnatal loss (50%) was observed. While three of the six cloned kids were lost, only one of these occurred within a day of birth. The other two occurred at 1 and 3 mo of age. These postnatal losses are similar to those reported in sheep [16, 19] and cattle [51, 52]. Renard and coworkers [52] reported the sudden loss of a cloned calf after 6 wk of apparent normal development. While these losses may be overcome by application of intensive perinatal monitoring and kid management [11], continued long-term monitoring of resulting clones is needed.

Nuclear transfer may be successful in some cases due to the convergence of several factors including oocyte viability, nucleocytoplasmic compatibility, and cell cycle synchronization. In other cases, reprogramming may be incomplete, resulting in embryonic loss, abortion, or abnormal development. It is remarkable that efficiencies of animal production based on number of NT embryos produced and transferred are similar in many reports. Average efficiencies in cattle, sheep, and mouse have ranged between 1% and 10% of transferred NT embryos [5, 8, 10, 15, 43]. While a few reports present higher efficiencies, these generally represent small sets of data [51]. Whether the low efficiencies observed for NT-derived embryos is due to incomplete reprogramming and/or to procedural elements remains to be resolved. Nevertheless, NT is a viable technique for the production of transgenic animals. Further studies are needed in order to gain a better understanding of the intricacies involved in the processes of NT, reprogramming, and epigenetic regulatory mechanisms.

## ACKNOWLEDGMENTS

We gratefully acknowledge Dr. T. Tanaka for the gift of the GFP vector. We also gratefully acknowledge the technical and animal health staff on the Macdonald farm campus and from Nexia Biotechnologies, Inc. for their assistance. We are especially grateful to Nathalie Chrétien, Denyse Laurin, Mélanie Gauthier, and Dr. N. Kafidi for their assistance.

## REFERENCES

1. Willadsen SM. Cloning of sheep and cow embryos. Genome 1989; 31:956–962.
2. Prather RS, Sims MM, First NL. Nuclear transplantation in early pig embryos. Biol Reprod 1989; 41:414–418.
3. Kono T. Nuclear transfer and reprogramming. Rev Reprod 1997; 2: 74–80.
4. Yong Z, Yuqiang L. Nuclear-cytoplasmic interaction and development of goat embryos reconstructed by nuclear transplantation: production of goats by serially cloning embryos. Biol Reprod 1998; 58:266–269.
5. Wilmut I, Schnieke AE, McWhir J, Kind AJ, Campbell KH. Viable offspring derived from fetal and adult mammalian cells. Nature 1997; 385:810–813.
6. Wells DN, Misica PM, Tervit HR, Vivanco WH. Adult somatic cell nuclear transfer is used to preserve the last surviving cow of the Enderby Island cattle breed. Reprod Fertil Dev 1998; 10:369–378.
7. Cibelli JB, Stice SL, Golueke PJ, Kane JJ, Jerry J, Blackwell C, Ponce de Leon FA, Robl JM. Cloned transgenic calves produced from nonquiescent fetal fibroblasts. Science 1998; 280:1256–1258.
8. Wakayama T, Perry ACF, Zucotti M, Johnson KR, Yanagimachi R. Full term development of mice from enucleated oocytes injected with cumulus cell nuclei. Nature 1998; 394:369–374.
9. Baguisi A, Behboodi E, Melican DT, Pollock JS, Destrempes MM, Cammuso C, Williams JL, Nims SD, Porter CA, Midura P, Palacios MJ, Ayres SL, Denniston RS, Hayes ML, Ziomek CA, Meade HM, Godke RA, Gavin WG, Overstrom EW, Echelard Y. Production of goats by somatic cell nuclear transfer. Nat Biotechnol 1999; 17:456–461.
10. Wakayama T, Rodriguez I, Perry AC, Yanagimachi R, Mombaerts P. Mice cloned from embryonic stem cells. Proc Natl Acad Sci U S A 1999; 96:14984–14989.
11. Keefer CL, Keyston R, Bhatia B, Lazaris A, Begin I, Kafidi N, Bilodeau A, Wang B, Tao T, Laurin D, Zhou FJ, Downey B, Baldassarre H, Karatzas C. Efficient production of viable goat offspring following nuclear transfer using adult somatic cells. Biol Reprod 2000; 62:192.
12. Prather RS, Barnes FL, Sims MM, Robl JM, Eyestone WH, First NL. Nuclear transplantation in the bovine embryo: assessment of donor nuclei and recipient oocyte. Biol Reprod 1987; 37:859–866.
13. Barnes F, Endebrock M, Looney C, Powell R, Westhusin M, Bondioli K. Embryo cloning in cattle: the use of in vitro-matured oocytes. J Reprod Fertil 1993; 97:317–320.
14. Keefer CL, Stice SL, Dobrinsky J. Effect of follicle-stimulating hormone and luteinizing hormone during bovine in vitro maturation on development following in vitro fertilization and nuclear transfer. Mol Reprod Dev 1993; 36:469–474.
15. Wells DN, Misica PM, Tervit HR. Production of cloned calves following nuclear transfer with cultured adult mural granulosa cells. Biol Reprod 1999; 60:996–1005.
16. Wells DN, Misica PM, Day AM, Peterson AJ, Tervit HR. Cloning sheep from cultured embryonic cells. Reprod Fertil Dev 1998; 10: 615–626.
17. Wells DN, Misica PM, Day TA, Tervit HR. Production of cloned lambs from an established embryonic cell line: a comparison between in vivo- and in vitro-matured cytoplasts. Biol Reprod 1997; 57:385–393.
18. Baldassarre H, Furnus CC, Matos DG, de Pessi H. In vitro production of sheep embryos using laparoscopic folliculocentresis: alternative gonadotrophin treatment for stimulation of oocyte donors. Theriogenology 1996; 45:707–717.
19. Schnieke AE, Kind AJ, Ritchie WA, Mycock K, Scott AR, Ritchie M, Wilmut I, Colman A, Campbell KH. Human factor IX transgenic sheep produced by transfer of nuclei from transfected fetal fibroblasts. Science 1997; 278:2130–2133.
20. McCreath KJ, Howcroft J, Campbell KHS, Colman A, Schnieke AE, Kind AJ. Production of gene-targeted sheep by nuclear transfer from cultured somatic cells. Nature 2000; 405:1066–1069.
21. Baldassarre H, Wang B, Gauthier M, Neveu N, Mellor S, Pika J, Loiselle M, Duguay F, Zhou J, Keyston R, Lazaris A, Karatzas C, Keefer C. Embryo transfer in a commercial transgenic production program using BELE goat embryos. Theriogenology 1999; 51:415.
22. Karatzas CN, Turner JD. Toward altering milk composition by genetic manipulation: current status and challenges. J Dairy Sci 1997; 80: 2225–2232.
23. Cormack B, Valdivia K, Falkow S. FACS-optimized mutants of the green fluorescent protein (GFP). Gene 1996; 173:33–38.
24. Takada T, Iida K, Awaji T, Itoh K, Takahashi R, Shibui A, Yoshida K, Sugano S, Tsujimoto G. Selective production of transgenic mice using green fluorescent protein as a marker. Nat Biotechnol 1997; 15: 458–461.
25. Campbell KH, Loi P, Otaegui PJ, Wilmut I. Cell cycle co-ordination in embryo cloning by nuclear transfer. Rev Reprod 1996; 1:40–46.
26. Gardner DK, Lane M, Spitzer A, Batt PA. Enhanced rates of cleavage and development for sheep zygotes cultured to the blastocyst stage in vitro in the absence of serum and somatic cells: amino acids, vitamins, and culturing embryos in groups stimulate development. Biol Reprod 1994; 50:390–400.
27. Gardner DK, Lane M. Culture and selection of viable blastocysts: a feasible proposition for human IVF? Hum Reprod Update 1997; 3: 367–382.
28. Susko-Parrish JL, Leibfried-Rutledge ML, Northey DL, Schutzkus V, First NL. Inhibition of protein kinases after an induced calcium transient causes transition of bovine oocytes to embryonic cycles without meiotic completion. Dev Biol 1994; 166:729–739.
29. Bilodeau AS, Lazaris A, Zhou JF, Duguay F, Keefer CL, Keyston R, Baldassarre H, Wang B, Karatzas CN. Localization of transgene integration in four dwarf BELE (breed early lactate early) founder goats by FISH analysis. Cytogenet Cell Genet 1999; 85:91 (abstract P363).

30. Freshney RI. Culture of Animal Cells: A Manual of Basic Technique. New York: Wiley-Liss; 1994: 197–217.
31. Lemieux N, Dutrillaux B, Viegas-Pequignot E. A simple method for simultaneous R- or G-banding and fluorescence in situ hybridization of small single-copy genes. Cytogenet Cell Genet 1992; 59:311–312.
32. Viegas-Pequignot E, Dutrillaux B, Magdelenat H, Coppey-Moisan M. Mapping of single-copy DNA sequences on human chromosomes by in situ hybridization with biotinylated probes: enhancement of detection sensitivity by intensified-fluorescence digital-imaging microscopy. Proc Natl Acad Sci U S A 1989; 86:582–586.
33. Amills M, Francino O, Sanchez A. Nested PCR allows the characterization of TaqI and PstI RFLPs in the second exon of the caprine MHC class II DRB gene. Vet Immunol Immunopathol 1995; 48:313–321.
34. Orita M, Iwahana H, Kanazawa H, Sekiya T. Detection of polymorphism of human DNA by gel electrophoresis as single stand confirmation polymorphisms. Proc Natl Acad Sci U S A 1989; 86:2766–2770.
35. Orita M, Suzuki Y, Sekiya T, Hayashi K. A rapid and sensitive detection of point mutations and DNA polymorphisms using the polymerase chain reaction. Genomics 1989; 5:874–879.
36. Pikaart M, Recillas-Targa F, Felsenfeld G. Loss of transcriptional activity of a transgene is accompanied by DNA methylation and histone deacetylation and is prevented by insulators. Genes Dev 1998; 12: 2852–2862.
37. Chen WY, Bailey EC, McCune SL, Dong J-Y, Townes TM. Reactivation of silenced, virally transduced genes by inhibitors of histone deacetylase. Proc Natl Acad Sci U S A 1997; 94:5798–5803.
38. Kioussis D, Festenstein R. Locus control regions: overcoming heterochromatin-induced gene inactivation in mammals. Curr Opin Genet Dev 1997; 7:614–619.
39. Kubota C, Yamakuchi H, Todoroki J, Mizoshita K, Tabara N, Barber M, Yang X. Six cloned calves produced from adult fibroblast cells after long-term culture. Proc Natl Acad Sci U S A 2000; 97:990–995.
40. Polejaeva IA, Campbell KH. New advances in somatic cell nuclear transfer: application in transgenesis. Theriogenology 2000; 53:117–26.
41. Galli C, Duchi R, Moor RM, Lazzari G. Mammalian leukocytes contain all the genetic information necessary for the development of a new individual. Cloning 1999; 1:161–170.
42. Zakhartchenko V, Durcova-Hills G, Stojkovic M, Schernthaner W, Prelle K, Steinborn R, Muller M, Brem G, Wolf E. Effects of serum starvation and re-cloning on the efficiency of nuclear transfer using bovine fetal fibroblasts. J Reprod Fertil 1999; 115:325–31.
43. Dominko T, Ramalho-Santos J, Chan A, Moreno RD, Luetjens CM, Simerly C, Hewitson L, Takahashi D, Martinovich C, White JM, Schatten G. Optimization strategies for production of mammalian embryos by nuclear transfer. Cloning 1999; 1:143–152.
44. Young LE, Sinclair KD, Wilmut I. Large offspring syndrome in cattle and sheep. Rev Reprod 1998; 3:155–163.
45. van Wagtendonk-de Leeuw A, Mullaart E, de Roos APW, Merton J, den Daas J, Kemp B, de Ruigh L. Effects of different reproduction techniques: AI, MOET or IVP, on health and welfare of bovine offspring. Theriogenology 2000; 53:575–597.
46. Smith LC, Bordignon V, Garcia JM, Meirelles FV. Mitochondrial genotype segregation and effects during mammalian development: application to biotechnology. Theriogenology 2000; 53:35–46.
47. Dominko T, Mitalipova M, Haley B, Beyhan Z, Memili E, McKusick B, First NL. Bovine oocyte cytoplasm supports development of embryos produced by nuclear transfer of somatic cell nuclei from various mammalian species. Biol Reprod 1999; 60:1496–502.
48. White KL, Bunch TD, Mitalipov S, Reed WA. Establishment of pregnancy after the transfer of nuclear transfer embryos produced from the fusion of Argali (*Ovis ammon*) nuclei into domestic sheep (*Ovis aries*) enucleated oocytes. Cloning 1999; 1:47–54.
49. Reik W, Romer I, Barton S, Surani M, Howlett S, Klose J. Adult phenotype in the mouse can be affected by epigenetic events in the early embryo. Development 1993; 119:933–942.
50. Rideout WM, Wakayama T, Wutz A, Eggan K, Jackson-Grusby L, Dausman J, Yanagimachi R, Jaenisch R. Generation of mice from wild-type and targeted ES cells by nuclear cloning. Nat Genet 2000; 24:109–110.
51. Kato Y, Tani T, Sotomaru Y, Kurokawa K, Kato J, Doguchi H, Yasue H, Tsunoda Y. Eight calves cloned from somatic cells of a single adult. Science 1998; 282:2095–2098.
52. Renard JP, Chastant S, Chesne P, Richard C, Marchal J, Cordonnier N, Chavatte P, Vignon X. Lymphoid hypoplasia and somatic cloning. Lancet 1999; 353:1489–1491.

data demonstrate that compound **4** is a potent LFA-1 antagonist, which binds LFA-1, blocks the binding of ICAM-1, and inhibits LFA-1 mediated lymphocyte proliferation and adhesion in vitro. It achieves this with a potency significantly greater than cyclosporine A, and demonstrates its equivalence to anti-CD11a in the level of its inhibition of the immune system's response in vivo.

Compounds **1** through **4** emerged from considerations of the ICAM-1 epitope via kistrin, the RGDMP peptides and $H_2N$-CGY$^{(m)}$DMPC-COOH. Each of these LFA-1 ligands was able to compete with a fluorescein-conjugated analog of compound **3** for LFA-1 binding. SAR similarities suggest a common presention of a carboxylic acid moiety to a binding site on LFA-1 as the basis of this competition. A comparison of the structures and molecular functionality of compound **4** and ICAM-1 responsible for their LFA-1 binding reveals that the carboxylic acid, sulfide, phenol, and carboxamide groups of the ICAM-1 epitope are embodied in compound **4** (Fig. 3) (*14*). This allows us to propose that compounds **2** through **4** are mimics of ICAM-1 resulting from the transfer of the ICAM epitope to a small molecule. A definitive proof of this mimicry will require the determination of the structures of LFA-1 and its complexes with ICAM-1 and compounds **2** through **4**.

We believe the work presented here (*23, 24*) represents the first reduction of a nonlinear, discontinuous but contiguous protein epitope (encompassing five residues spanning three different β strands across the face of a protein surface) from a protein to a small molecule. In contrast to more traditional approaches, this rational, structurally directed hypothesis and information driven lead discovery process utilized molecular modeling and structure activity relationships to identify pharmacophoric similarities within ICAM-1, kistrin, the peptides, and ultimately compounds **1** through **4**. This provided the perspective to recognize compound **1** as a viable lead and rapidly elaborate it into compounds **2** through **4**, and demonstrates the value of antibodies, protein mutagenesis, and structural (SAR) data for native protein ligands as leads in the identification of pharmaceutical agents, which block large protein-protein interactions. What remains to be seen with these small-molecule LFA-1 antagonists is a clinical evaluation of their safety and effectiveness in the control of human diseases relative to humanized anti-CD11a and other small-molecule agents discovered by other means (*25–28*).

### References and Notes


1. R. W. McMurray, *Semin. Arthritis Rheumatism* **25**, 215 (1996).
2. J. H. Spragg, in *Molecular Biology of Cell Adhesion Molecules*, M. A. Horton, Ed. (Wiley, New York, 1996), chap. 8, pp. 131–154.
3. N. Oppenheimer-Marks, P. E. Lipsky, *Clin. Immunol. Immunopathol.* **79**, 203 (1996).
4. M. K. Connolly, E. A. Kitchens, B. Chan, P. Jardieu, D. Wofsy, *Clin. Immunol. Immunopathol.* **72**, 198 (1994).
5. K. Kakimoto *et al.*, *Cell. Immunol.* **142**, 326 (1992).
6. E. K. Nakakura *et al.*, *Transplantation* **55**, 412 (1993).
7. W. A. Werther *et al.*, *J. Immunol.* **157**, 4986 (1996).
8. A. Gottlieb *et al.*, *J. Am. Acad. Dermatol.* **42**, 428 (2000).
9. H. Granlund, in *Curr. Opin. Anti-Inflammatory Immunomodulatory Invest. Drugs* **2**, 332 (2000).
10. Single-letter abbreviations for the amino acid residues are as follows: A, Ala; C, Cys; D, Asp; E, Glu; F, Phe; G, Gly; H, His; I, Ile; K, Lys; L, Leu; M, Met; N, Asn; P, Pro; Q, Gln; R, Arg; S, Ser; T, Thr; V, Val; W, Trp; and Y, Tyr. X indicates any residue.
11. K. L. Fisher *et al.*, *Mol. Biol. Cell* **8**, 501 (1997).
12. J. M. Casasnovas, T. Stehle, J.-h. Liu, J.-h. Wang, T. A. Springer, *Proc. Natl. Acad. Sci. U.S.A.* **95**, 4134 (1998).
13. D. E. Staunton, M. L. Dustin, H. P. Erickson, T. A. Springer, *Cell* **61**, 243 (1990).
14. Supplementary material is available at *Science* Online at www.sciencemag.org/cgi/content/full/295/5557/1086/DC1
15. M. S. Dennis *et al.*, *Proc. Natl. Acad. Sci. U.S.A.* **87**, 2471 (1989).
16. M. Adler, P. Carter, R. A. Lazarus, G. Wagner, *Biochemistry* **32**, 282 (1993).
17. S. C. Bodary, P. Gribling, W. P. Lee, unpublished data.
18. M. S. Dennis, P. Carter, R. A. Lazarus, *Proteins Struct. Funct. Genet.* **15**, 312 (1993).
19. R. S. McDowell *et al.*, *J. Am. Chem. Soc.* **116**, 5069 (1994).
20. R. S. McDowell, T. R. Gadek, *J. Am. Chem. Soc.* **114**, 9245 (1992).
21. R. S. McDowell *et al.*, *J. Am. Chem. Soc.* **116**, 5077 (1994).
22. D. J. Burdick, in *PCT Int. Appl.* (Genentech, USA). WO 9949856 (1999), p. 9.
23. Experimental methods for an LFA-1 ELISA assay (p. 65), the mixed lymphocyte reaction (MLR) (p. 67) and the synthesis of compounds **2** through **4** (p. 68) are found in D. J. Burdick, *PCT Int. Appl.* (Genentech, USA). WO 9949856 (1999).
24. In the course of the studies presented here, several reports appeared describing small molecule antagonists of LFA-1/ICAM (*25–27*). Two have identified compounds which interact with LFA-1's allosteric I domain site (*26, 27*). Preliminary studies with compound **4** indicate that it binds at a different site on LFA-1, and that the allosteric site antagonist(s) do not inhibit the binding of compound **4** to LFA-1.
25. T. A. Kelly *et al.*, *J. Immunol.* **163**, 5173 (1999).
26. J. Kallen *et al.*, *J. Mol. Biol.* **292**, 1 (1999).
27. G. Liu *et al.*, *J. Med. Chem.* **44**, 1202 (2001).
28. G. Liu, *Expert Opin. Ther. Patents* **11**, 1383 (2001).
29. J. Bella, P. R. Kolatkar, C. W. Marlor, J. M. Greve, M. G. Rossman, *Proc. Natl. Acad. Sci. U.S.A.* **95**, 4140 (1998).


30. We thank P. Barker, C. Quan, J. Tom, and M. Struble for help with peptide synthesis and compound purification, S. Spencer for protein preparation and purification, and J. Burnier, R. Lazarus, and R. G. Hammonds for helpful discussions in the preparation of the manuscript.

17 September 2001; accepted 20 December 2001


# Production of α-1,3-Galactosyltransferase Knockout Pigs by Nuclear Transfer Cloning


**Liangxue Lai,[1] Donna Kolber-Simonds,[3] Kwang-Wook Park,[1] Hee-Tae Cheong,[1,4] Julia L. Greenstein,[3] Gi-Sun Im,[1,5] Melissa Samuel,[1] Aaron Bonk,[1] August Rieke,[1] Billy N. Day,[1] Clifton N. Murphy,[1] David B. Carter,[1,2] Robert J. Hawley,[3] Randall S. Prather[1]***



The presence of galactose α-1,3-galactose residues on the surface of pig cells is a major obstacle to successful xenotransplantation. Here, we report the production of four live pigs in which one allele of the α-1,3-galactosyltransferase locus has been knocked out. These pigs were produced by nuclear transfer technology; clonal fetal fibroblast cell lines were used as nuclear donors for embryos reconstructed with enucleated pig oocytes.


Clinical transplantation has become one of the preferred treatments for end-stage organ failure since the introduction of chronic immunosuppressive drugs in the mid-1980s. One of the novel approaches to dealing with the limited supply of human organs is the use of alternative species as a source of organs (xenotransplantation). The pig is considered the primary alternative species because of ethical considerations, breeding characteristics, infectious disease concerns, and its compatible size and physiology (*1*).

A major barrier to progress in pig-to-primate organ transplantation is the presence of terminal α-1,3-galactosyl (Gal) epitopes on the surface of pig cells. Humans and Old World monkeys have lost the corresponding galactosyltransferase activity in the course of


[1]Department of Animal Science, [2]Department of Veterinary Pathobiology, University of Missouri, Columbia, MO 65211, USA. [3]Immerge BioTherapeutics Inc., Charlestown, MA 02129, USA. [4]Department of Veterinary Medicine, College of Animal Resource Science, Kangwon National University, Chunchon 200-701, Korea. [5]National Livestock Research Institute, Suwon 441-350, Korea.

*To whom correspondence should be addressed. E-mail: pratherR@missouri.edu

evolution and therefore produce preformed natural antibodies to the epitope, which are responsible for hyperacute rejection of porcine organs. The temporary removal of recipient antibodies to Gal through affinity adsorption and expression of complement regulators in transgenic pigs has allowed survival of pig organs beyond the hyperacute stage. However, returning antibody and residual complement activity are believed to be responsible for the acute and delayed damage that severely limit organ survival even in the presence of high levels of immunosuppressive drugs and other clinical intervention (*2*). Competitive inhibition of galactosyltransferase in α-1,2-fucosyl-transferase transgenic pigs has resulted in only partial reduction in epitope numbers (*3*). Similarly, attempts to block expression of Gal epitopes in *N*-acetylglucosaminyltransferase III transgenic pigs also resulted in partial reduction of Gal epitope number but failed to substantially extend graft survival in primate recipients (*4*). Given the large number of Gal epitopes present on pig cells (*5*), it seems unlikely that any dominant transgenic approach of this nature can provide sufficient protection from damage mediated by antibodies to Gal. In contrast, a genetic knockout of the α-1,3-galactosyltransferase (GGTA1) locus in pigs would provide permanent and complete protection.

Viable α-1,3-galactosyltransferase knockout mice have been produced by embryonic stem cell technology (*6*). The development of nuclear transfer technology has provided a means for locus-specific modification of large animals, as demonstrated by the production of viable sheep by means of in vitro targeted somatic cells (*7*). Successful cloning (*8–11*) and production of transgenic pigs by nuclear transfer of genetically modified somatic cells (*12*) have been reported. Attempts at targeting the GGTA1 locus in pigs (*11*) and sheep (*13*) have also been reported, but these failed to result in live birth of animals with the desired modification. In both cases, difficulties in obtaining viable targeted donor cell clones were encountered.

We chose to knock out the GGTA1 locus in a highly inbred, major histocompatibility complex–defined miniature pig line. Descendant from lines long used for xenotransplantation studies (*14, 15*), this line is an ideal size match for eventual use in clinical transplantation and has animals that consistently test negative for transmission of porcine endogenous retrovirus (PERV) to human cells in vitro (*16*). Cells were isolated from one male (F9) and three female (F3, F6, and F7) fetuses at day 37 of gestation for production of donor cell lines (*17*). A gene trap targeting vector, pGalGT, was used for homologous replacement of an endogenous GGTA1 allele (Fig. 1). The vector contains about 21 kb of homology to the GGTA1 locus, with the coding region upstream of the catalytic domain disrupted by insertion of a selection cassette consisting of a Bip internal ribosome entry site followed by sequences encoding G418 resistance. After transfection and 14 days of G418 selection, viable cell clones (*18*) were passaged in triplicate for further analysis and cryopreservation (*19*).

A reverse transcription polymerase chain reaction (RT-PCR) was performed on crude cell lysates the day after passage with a forward primer from exon 7 (upstream of the 5′ end of the targeting vector) and a reverse primer from the selection cassette (*20*). Dot blot hybridization of the RT-PCR products with an exon 8 probe detected targeting in 22 of 159 clones analyzed.

The structure of the GGTA1 locus was analyzed in two overlapping PCR reactions (*21*). Clones with a targeted insertion of the cassette relative to vector external primer sites both upstream and downstream of the cassette, indicative of a replacement-type targeting event, were considered candidates for use in nuclear transfer. Of 17 clones analyzed, 8 were found to have undergone the desired recombination event, and one from each fetus (F3-C5, F6-C3, F7-H6, and F9-J7) was used for nuclear transfer.

Nuclear transfer was performed with the use of in vitro matured oocytes and, except for 4 of 28 embryo transfers, cryopreserved donor cells without further culture (*22*). Asynchronous embryo transfer—that is, transfer to a surrogate at an earlier stage of the estrus cycle than the embryos themselves—had previously been used with minimally manipulated (*23*), pronuclear microinjected (*24*), and nuclear transfer (NT)–derived embryos (*10–12*). The observed benefit of asynchronous transfer suggests that any manipulation may result in a delay in early embryonic development. Because the manipulations required for nuclear transfer are quite extensive, and because previous reports suggest that miniature swine embryos of the NIH strain used here may normally develop at a relatively slower rate (*25*), naturally cycling large white gilts that had displayed standing estrus but had not yet completed ovulation were used as surrogates (*26*). [For detailed information on all 28 embryo transfers, see (*18*).]

A minimum of four viable embryos is required for establishment of pregnancy in pigs (*27*). Thus, we used two methods to increase the likelihood of establishing pregnancies with NT-derived embryos. Although pregnancy was established in five of seven surrogates receiving parthenogenetic "carrier" embryos, no live births resulted. Therefore, we transferred reconstructed embryos to a mated surrogate. In the one embryo transfer performed in this group, the surrogate (O212) was mated on the first day of standing estrus and received NT-derived embryos the same day. Although any fertilized embryos would theoretically be 43 to 55 hours behind development of the transferred NT-derived embryos, the actual in vivo development rate for NT-derived embryos is unknown. Early pig embryos have a lower rate of survival when present in a surrogate along with embryos at a slightly more advanced stage (*25*). Thus, an apparent embryonic asynchrony may be advantageous should NT-derived embryos develop at a slower rate than naturally fertilized embryos.

Seven piglets, four females and three males (Table 1), were delivered by cesarean section at term (*28*). Microsatellite analysis (*29*) revealed that six of six haplotypes for one female piglet (O212-2) were iden-

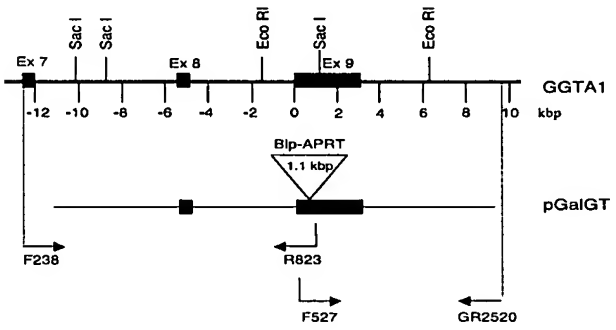


**Fig. 1.** pGalGT targeting vector and genomic PCR assays for targeting (*35*).

**Table 1.** Pregnancies carried to term after transfer of embryos reconstructed with GGTA1 knockout cell lines.

| Surrogate (estrus day) | Donor line | NT embryos | Outcome |
|---|---|---|---|
| O212 (0) | F7-H6 | 116 | Mated surrogate<br>Seven born 9/21/01<br>One NT-derived female piglet |
| O226 (1) | F3-C5 | 92 | Four NT-derived female piglets born 10/19/01 |
| O230 (1) | F7-H6 cultured | 130 | Two NT-derived female piglets born 10/15/01 |

tical to that of the F7 fetal cell line from which knockout donor line F7-H6 was derived (*18*). Furthermore, three of six haplotypes of O212-2 were not compatible with mating of the surrogate. All other piglets had at least four haplotype mismatches with the F7 line and were compatible with mating of the surrogate.

We performed 20 additional transfers of only NT-derived embryos to unmated surrogates. Pregnancy was confirmed by ultrasound in six of these surrogates, with two continuing to cesarean section at term. Two live piglets were delivered from surrogate O230 (Table 1), one of which (O230-2) died from respiratory distress syndrome shortly after delivery. Four live piglets were delivered from surrogate O226 (Table 1), again with one (O226-4) dying shortly after birth from respiratory distress syndrome. Microsatellite haplotypes of all six piglets from the two litters were identical to the F7 and F3 donor parental cell lines, respectively.

Genomic targeting analysis was performed on DNA samples from all NT-derived piglets, the untransfected F3 and F7 donor parental cell lines, and surrogates (Fig. 2). For all piglets except O230-2, analysis of both ends of the GGTA1 locus revealed the presence of one replacement-type targeted allele. Whether O230-2 was derived from an untargeted miniature swine cell in the F7-H6 donor line or had a GGTA1 rearrangement incompatible with detection by the targeting assays performed has yet to be determined.

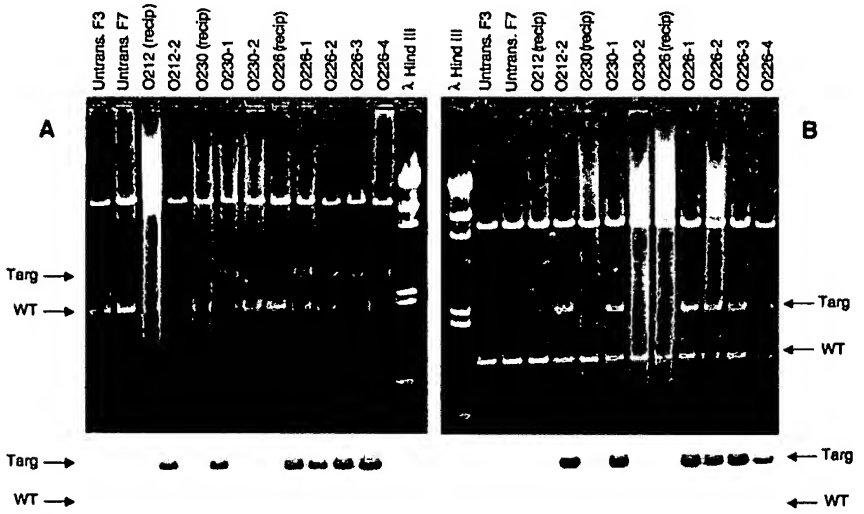


**Fig. 2.** Targeting analysis of NT-derived piglets, parental miniature swine fetal cell lines F3 and F7, and surrogate sows. See Fig. 1 for a description of the assays. (**A**) Upstream genomic PCR analysis with primers F238 and R823. (**B**) Downstream genomic PCR analysis with primers F527 and GR2520. After transfer, digested reactions were probed with an oligonucleotide (Bip419) from the IRES portion of the selection cassette. The analysis of all offspring, with the exception of O230-2, is consistent with a replacement-type targeting event at one GGTA1 allele.

Table 2 presents a health summary for the seven NT-derived piglets. Four of the five piglets surviving beyond the immediate postpartum period remain healthy, with a normal growth rate for miniature swine. The fifth, O226-3, died suddenly at 17 days of age during a routine blood draw. Necropsy revealed a dilated right ventricle and thickening of the heart wall. Another animal, O230-1, has shown cardiac defects similar to those reported in NT-derived animals of other species (*7, 12, 30, 31*).

A number of other abnormalities were noted at birth among surviving piglets, none of which appear to affect their overall health and well-being. Flexure tendon deformities similar to those reported here have been observed in previous NT-derived commercial strain pigs (*32*). It is unlikely that the abnormalities we have seen are related to the genetic modification, as there is not a consistent phenotype and only one allele has been targeted, but rather are the result of improperly reprogrammed epigenetic factors. With the exception of O212-2, the four surviving piglets were somewhat undersized, with birth weights of 450 to 650 g (strain average 860 g).

Under our growth and selection conditions, miniature swine fetal fibroblasts maintain a steady doubling time of about 24 hours. Clonal lines senesce after 30 to 32 days of culture on average. The ability to quickly select clonal lines for nuclear transfer is likely to be a requirement for introduction of other complex genetic alterations into the pig genome. The ability to use cryopreserved donor cells without further culture, demonstrated by two of our litters, is also advantageous, as it extends the number of potential donor lines available for use in nuclear transfer. Our efficiencies in producing NT-derived GGTA1 knockout animals are similar to those previously reported in which extensively cultured primary fetal cells were used as

**Table 2.** Health summary of NT-derived miniature swine piglets. H, healthy; NG, normal growth; D, dead.

| Piglet | Physical findings | Birth weight (g) | Clinical symptoms/cardiac exam findings |
|---|---|---|---|
| O212-2 (H, NG) | Ocular defect, small ear flaps with no patent ear canals | 1100 | No clinical symptoms; no significant echocardiogram findings |
| O230-1 (H, NG) | Flexure deformity of distal interphalangeal joint at birth* | 450 | Mild abdominal ascites; right ventricular enlargement and pulmonary hypertension |
| O230-2 (D) | Flexure deformity of distal interphalangeal joint at birth; dysmaturity at birth | 115 | Died shortly after delivery of respiratory distress syndrome; no gross lesions observed at necropsy |
| O226-1 (H, NG) | Normal | 600 | No clinical symptoms; no significant echocardiogram findings |
| O226-2 (H, NG) | Flexure deformity of distal interphalangeal joint at birth† | 650 | No clinical symptoms; low-velocity regurgitation at center of tricuspid valve |
| O226-3 (D) | Flexure deformity of distal interphalangeal joint at birth* | 550 | Death during routine blood draw 17 days after birth; dilated right ventricle with thickening of heart wall observed at necropsy |
| O226-4 (D) | Cleft palate; dysmaturity at birth | 250 | Died shortly after delivery of respiratory distress syndrome; no gross lesions observed at necropsy |

*Responded to physical therapy. †Responded to physical therapy plus splinting.

nuclear donors (*10, 11*), despite the nearly fourfold difference in adult size between the miniature swine strain modified here and the commercial oocyte donor and surrogate strains used. The ability to use readily available oocyte donors and surrogates in a nuclear transfer program is essential when modification of less commonly available animals is required.

The next step will be to create α-1,3-galactosyltransferase–null (homozygous knockout) pigs, either by breeding to a heterozygous male produced by nuclear transfer or by sequential nuclear transfer modification of cell lines produced from the four female pigs reported here. Because α-1,3-galactosyltransferase–null mice have already been produced (*6*), it is not anticipated that this genetic modification will be lethal in the null animals. We hope that α-1,3-galactosyltransferase–null pigs will not only eliminate hyperacute rejection but also ameliorate later rejection processes, and (in conjunction with clinically relevant immunosuppressive therapy) will permit long-term survival of transplanted porcine organs. At a minimum, the availability of galactosyltransferase-null pigs will allow a clearer evaluation of approaches currently in development aimed at overcoming potential delayed and chronic rejection mechanisms in porcine xenotransplantation.

### References and Notes


1. R. W. Evans, in *Xenotransplantation*, J. L. Platt, Ed. (ASM Press, Washington, DC, 2001), pp. 29–51.
2. D. Lambrigts, D. H. Sachs, D. K. S. Cooper, *Transplantation* **66**, 547 (1998).
3. C. Costa *et al.*, *FASEB J.* **13**, 1762 (1999).
4. S. Miyagawa *et al.*, *J. Biol. Chem.* **276**, 39310 (2001).
5. U. Galili, *Curr. Opin. Organ Trans.* **6**, 30 (2001).
6. A. D. Thall, P. Maly, J. B. Lowe, *J. Biol. Chem.* **270**, 21437 (1995).
7. K. J. McCreath *et al.*, *Nature* **405**, 1066 (2000).
8. I. A. Polejaeva *et al.*, *Nature* **407**, 86 (2000).
9. A. Onishi *et al.*, *Science* **289**, 1188 (2000).
10. J. Betthauser *et al.*, *Nature Biotechnol.* **18**, 1055 (2000).
11. K. Bondioli, J. Ramsoondar, B. Williams, C. Costa, W. Fodor, *Mol. Reprod. Dev.* **60**, 189 (2001).
12. K. W. Park *et al.*, *Anim. Biotech.*, **12**, 173 (2001).
13. C. Denning *et al.*, *Nature Biotechnol.* **19**, 559 (2001).
14. D. H. Sachs *et al.*, *Transplantation* **22**, 559 (1976).
15. Fetuses for derivation of cell lines used here were the product of six generations of brother-sister mating and have an estimated inbreeding coefficient of 0.86. Two additional sib-mated generations have been produced from this inbred line, with no apparent decrease in fitness.
16. B. A. Oldmixon *et al.*, in preparation.
17. Primary fibroblasts were isolated from miniature swine fetuses by collagenase-trypsin digestion of minced tissue. Dissociated cells were plated at $2 \times 10^5$ cells/cm$^2$ on collagen-coated plates in Ham's F10 medium containing 20% fetal bovine serum (FBS) and antibiotics. Adherent cells were frozen the following day.
18. For supplementary data, see *Science* Online (www.sciencemag.org/cgi/content/full/1068228/DC1).
19. Fetal fibroblasts were thawed and cultured for 3 days to subconfluence before transfection. About $2 \times 10^7$ fibroblasts were electroporated at 260 V, 960 μFD in 0.8 ml of Hepes-buffered saline containing pGalGT (0.5 pmol/ml). The vector was restriction-digested at both ends of the GATA1 homologous sequences before use. Transfected cells were cultured in bulk for 2 days without selection, then plated in collagen-coated 96-well plates at $2 \times 10^4$ cells per well in Ham's nutrient mixture F10 containing 20% FBS and G418 (100 μg/ml). The low selection concentration was made possible by the absence of cells transiently expressing G418 resistance; untransfected cells were uniformly killed by G418 (50 to 75 μg/ml) after 5 to 7 days. After 14 days of selection in G418, growing cultures were passaged in triplicate for cryopreservation of donor cells, RT-PCR screening for targeting, and DNA isolation. Subconfluent donor cell cultures were trypsinized and frozen in 20-μl aliquots containing 1000 to 2000 cells each.
20. Lysates were prepared from 96-well cultures of selected clones the day after passage by three rounds of freezing and thawing in 10 μl of 2 mM dithiothreitol containing placental ribonuclease inhibitor (1 U/μl). The lysate was amplified in a one-tube amplification reaction using rTth polymerase, exon 7 forward primer F291 (5′-ACAACAGAGGAGAGCTTCCG) and reverse primer Bip419 (5′-CTCTCACACTCGCGAAACAC). PCR products were alkaline-denatured and transferred to nylon membranes before hybridization with an exon 8 oligonucleotide probe (5′-GGTCGTGACCATAACCAGATG).
21. Clones identified as putatively targeted in the RT-PCR screening assay were expanded into 24-well plates, and DNA was isolated for genomic analysis. About 250 ng of DNA was amplified in reactions with LA Taq DNA polymerase (Panvera, Madison, WI). Targeting was assessed by two PCR assays, each incorporating a primer outside of the vector homologous region. Upstream analysis used exon 7 forward primer F238 (5′-TTACCACGAAGAAGAAGACGC) and exon 9 reverse primer R823 (5′-AGGATGTGCCTTGTACCACC). Upon digestion with Eco RI, fragments of 2.0 kb (WT locus), 3.1 kb (targeted locus), and 10.4 kb (either locus) are produced. Downstream analysis used exon 9 forward primer F527 (5′-GGTTGGCCACAAAGTCATC) and reverse primer GR2520 (5′-CACTATTTGGAGGACAGGGTC). Upon digestion with Sac I, fragments of 1.2 kb (WT locus), 2.3 kb (targeted locus), and 8.1 kb (either locus) are produced. Southern blots of digested reactions were hybridized to internal ribosome entry site (IRES) region probe Bip419.
22. Oocytes derived from slaughtered gilts were matured in defined protein medium [TCM 199 supplemented with 0.1% polyvinyl alcohol, cysteine (0.1 mg/ml), epidermal growth factor (10 ng/ml), 0.91 mM Na-pyruvate, 3.05 mM D-glucose, follicle-stimulating hormone (0.5 μg/ml), luteinizing hormone (0.5 μg/ml), penicillin (75 μg/ml), and streptomycin (50 μg/ml)]. Oocytes from sow ovaries were purchased from BoMed Inc. (Madison, WI) and shipped overnight in their commercial maturation medium. After maturation, oocytes were freed of cumulus cells and were kept in TCM/BSA [TCM 199 supplemented with bovine serum albumin (BSA, 4 mg/ml)] until use. Enucleation of metaphase II oocytes was performed in medium supplemented with cytochalasin B (7.5 μg/ml), without staining the chromatin (as this may be detrimental to subsequent development) (*33*). Cryopreserved donor cells were thawed at 37°C and 10 volumes of FBS were added. The suspension was kept at room temperature for 30 min, and four volumes of TCM/BSA were added and the cells pelleted. Fibroblast cells were resuspended and directly used for NT. For NT-derived embryos transferred to four surrogates (O230, O203, O291, and O221), the cells were cultured for 1 week as above, then overnight in medium containing 0.5% serum before use in NT. All cells with an intact membrane were used, as the limited number of targeted cells did not permit selection. Nuclear transfer, fusion, and activation were performed as in Park *et al.* (*12*). Embryos were kept in TCM/BSA for another 30 to 60 min before the fusion rate was evaluated. Fused embryos were cultured in NCSU 23 supplemented with BSA (4 mg/ml) overlaid with mineral oil. The surviving embryos (intact plasma membrane) were selected for transfer into surrogates.
23. C. Polge, *Control of Pig Reproduction* (Butterworth, London, 1981), pp. 283–285.
24. M. J. Martin, C. A. Pinkert, *Transgenic Animal Technology* (Academic Press, New York, 1994), pp. 315–333.
25. W. F. Pope, S. Xie, D. M. Broermann, K. P. Nephew, *J. Reprod. Fertil. Suppl.* **40**, 251 (1990).
26. Potential surrogates were checked for estrus twice a day. Depending on the exact time of estrus, NT-derived embryo transfers were performed 5 to 17 hours or 20 to 36 hours after the actual onset of estrus for day 0 and day 1 surrogates, respectively. In prior control experiments using in vitro produced embryos cultured for 22 hours after fertilization and then transferred to a day 1 surrogate, 19 of 100 embryos recovered on day 6 were at blastocyst stage, with an average nuclear number of 65. For surgery, gilts were induced with Pentothal (Abbott Laboratories) and anesthesia was maintained with 2% Halothane (Halocarbon Laboratories, River Edge, NJ). A midventral laparotomy was performed, and embryos were loaded into a 3½ Fr. tomcat catheter and deposited into the oviduct. Examination of the ovaries during embryo transfer confirmed that none of the surrogates had completed ovulation.
27. C. Polge, L. E. A. Rowson, M. C. Chang, *J. Reprod. Fertil.* **12**, 395 (1966).
28. Surrogates displayed few if any signs of impending parturition, similar to findings reported in other species (*31, 34*). They also lacked mammary gland development and colostrum production. The surrogates all displayed mild signs of vulvar enlargement and elongation, but much less than would normally be expected. This would appear to indicate a defect in the signaling mechanism between the fetuses and dam, and would most likely result from an abnormality in placental function. These observations were made even in the mated recipient.
29. Microsatellite reactions were amplified with fluorescent primers kindly provided by the USDA-supported U.S. Pig Genome Coordination Project and analyzed by Lark Technologies Inc. (Houston, TX).
30. J. B. Cibelli *et al.*, *Science* **280**, 1256 (1998).
31. J. R. Hill *et al.*, *Theriogenology* **51**, 1451 (1999).
32. L. Lai *et al.*, unpublished data.
33. T. Tao, Z. Machaty, L. R. Abeydeera, B. N. Day, R. S. Prather, *Zygote* **8**, 69 (2000).
34. D. N. Wells, P. M. Misica, H. R. Tervit, *Biol. Reprod.* **60**, 996 (1999).
35. GGTA1 homologous sequences in the pGalGT vector begin ~0.8 kb downstream of exon 7 and continue to ~6.8 kb downstream of the end of exon 9. A selection cassette—consisting of a Bip internal ribosome entry site, APRT coding sequences (encoding G418 resistance), and flanking stop codons—is inserted into an Eco RV site upstream of the GGTA1 catalytic domain in exon 9. Targeting is assessed with two PCR assays, each incorporating a primer outside of the vector homologous region. Upstream genomic structure is assessed with primers F238 (exon 7, upstream of the 5′ end of the pGalGT vector) and R823 (exon 9 downstream of the selection cassette insertion site). Upon digestion with Eco RI, fragments of 2.0 kb (WT locus), 3.1 kb (targeted locus), and 10.4 kb (either locus) are produced. Downstream genomic structure is assessed with primers F527 (exon 9 upstream of the selection cassette insertion site) and GR2520 (downstream of the 3′ end of the pGalGT vector). Upon digestion with Sac I, fragments of 1.2 kb (WT locus), 2.3 kb (targeted locus), and 8.1 kb (either locus) are produced.



36. We thank E. Brown and D. Liske for care of the surrogate gilts during gestation; T. Cantley for help with surgical embryo transfers; J. C. Lattimer for echocardiography; K. Whitworth, R. Woods, J. Luth, L. Overman, R. Cabot, and D. Wax for helping to care for the piglets after delivery; S. Arn for miniature swine management and assistance; M. Baetscher and D. Akiyoshi for their contributions to the early phases of cell engineering work; and C. Patience for comments on the manuscript. Supported by the F. B. Miller fund, Department of Animal Sciences, University of Missouri–Columbia (H.-T.C.), NIH grant T32 RR07004 (D.B.C.), and NIH National Center for Research Resources grant R44 RR15198.

20 November 2001; accepted 17 December 2001
Published online 3 January 2002;
10.1126/science.1068228
Include this information when citing this paper.

# Production of gene-targeted sheep by nuclear transfer from cultured somatic cells

K. J. McCreath, J. Howcroft, K. H. S. Campbell*, A. Colman, A. E. Schnieke & A.J. Kind

*PPL Therapeutics Ltd, Roslin, Edinburgh, EH25 9PP, UK*
** Present address: University of Nottingham, School of Biological Sciences, Division of Animal Physiology, Loughborough, LE12 5RD, UK*

**It is over a decade since the first demonstration that mouse embryonic stem cells could be used to transfer a predetermined genetic modification to a whole animal[1]. The extension of this technique to other mammalian species, particularly livestock, might bring numerous biomedical benefits, for example, ablation of xenoreactive transplantation antigens, inactivation of genes responsible for neuropathogenic disease and precise placement of transgenes designed to produce proteins for human therapy. Gene targeting has not yet been achieved in mammals other than mice, however, because functional embryonic stem cells have not been derived. Nuclear transfer from cultured somatic cells provides an alternative means of cell-mediated transgenesis[2,3]. Here we describe efficient and reproducible gene targeting in fetal fibroblasts to place a therapeutic transgene at the ovine α1(I) procollagen (*COL1A1*) locus and the production of live sheep by nuclear transfer.**

We previously showed that transfection of fetal fibroblasts with nuclear transfer offers an efficient and practical method of producing sheep carrying randomly integrated transgenes[3], and similar work has been reported in cattle[4]. Gene targeting is a more powerful method of genetic manipulation and requires essentially the same procedures of transfection and drug selection of cultured cells. Although experimental gene targeting was first carried out in somatic cell lines[5,6], the use of embryonic stem (ES) cells now predominates; however, there has been no definitive comparison of gene targeting efficiency in primary somatic cells and ES cells (but see ref. 7 for review). We wished to determine whether practically useful gene targeting could be achieved in primary ovine fetal fibroblasts, and whether these cells could produce viable animals by nuclear transfer. The ovine *COL1A1* gene represented a suitable target with which to establish gene targeting in fetal fibroblasts for three reasons. First, we expected that gene-targeting events would be very rare compared with random integrations. *COL1A1* is highly expressed in fibroblasts, allowing promoter-trap enrichment of gene-targeting events. Second, few ovine genes have been cloned and characterized. *COL1A1* is well studied and highly conserved in several species, facilitating molecular cloning and construction of ovine gene-targeting vectors. Third, mutations in *COL1A1* can cause connective tissue disorders in humans, for example, *osteogenesis imperfecta*[8,9]. The ability to generate models of human genetic disorders by gene targeting in animals other than mice might be valuable for clinical research; however, we chose to target a site that would not significantly affect type I collagen protein function or expression to avoid affecting fetal development.

We used two gene-targeting vectors to target ovine *COL1A1* (Fig. 1). Each vector incorporated two regions of *COL1A1* homology, derived from a contiguous fragment of Poll Dorset fetal fibroblast[3] (PDFF2) genomic DNA. COLT-1 was designed to insert a promoterless *neo* selectable marker between the *COL1A1* translational stop and polyadenylation signal, such that transcription of the targeted locus resulted in a bicistronic messenger RNA. An internal ribosomal entry site (IRES)[10] immediately 5′ of *neo* facilitated translation. COLT-2 had the same structure, but included a transgene as a separate transcription unit located 3′ of *neo*. This transgene, termed AATC2, comprised human α1-antitrypsin (AAT) complementary DNA within an ovine β-lactoglobulin (BLG) expression vector designed to direct expression in the lactating mammary gland[11].

We transfected COLT-1 DNA into early passage PDFF2 female and PDFF5 male ovine primary fetal fibroblasts; we transfected COLT-2 DNA into PDFF2 cells. Stable G418 resistant clones

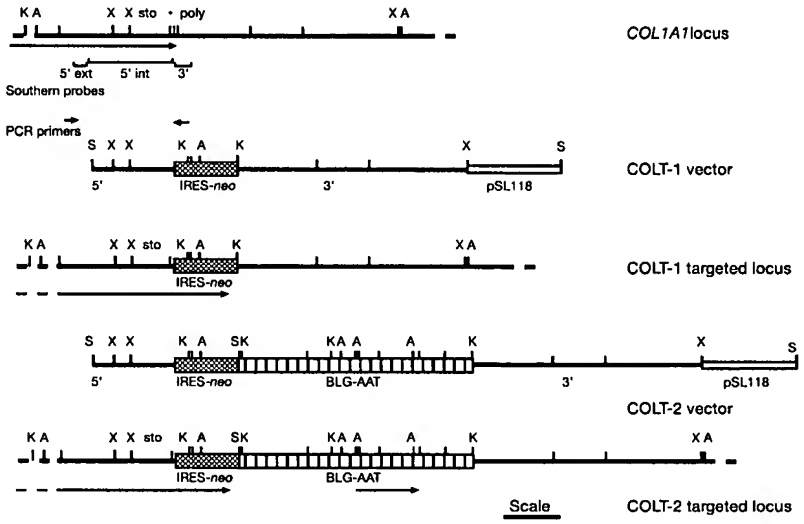


**Figure 1** Diagrams of ovine *COL1A1*, COLT-1 and COLT-2 targeting vectors and targeted *COL1A1* locus. The map of ovine *COL1A1* shows the translational stop and polyadenylation sites, the direction of transcription and extent of the *COL1A1* mRNA is indicated by an arrow, an asterisk marks an *Ssp*1 site where the targeted gene insertions were made. Southern hybridization probes and PCR primers are indicated. The maps of the COLT-1 and COLT-2 vectors and the targeted *COL1A1* locus show the IRES–*neo* cassette as a shaded box, the BLG driven AAT transgene by a striped box, and the bacterial vector pSL1180 by an open box. The direction and predicted extent of the *COL1A1* / IRES–*neo* bicistronic mRNA and the AAT transgene mRNA are shown as arrows. The scale bar represents 2 kb. Restriction enzyme sites: A, *Asp*I; B, *Bam*HI; Sc, *Sac*II; S, *Sal*I; K, *Kpn*I; X, *Xho*I.

were derived. About 30 days of culture elapsed between fetal disaggregation and cryopreservation of gene-targeted cell clones. DNA samples of each cell clone were initially screened by polymerase chain reaction (PCR) using primers designed to amplify a 3.4-kilobase (kb) fragment across the 5′ junction of the targeted locus (Fig. 1). In each case, a high proportion of G418 resistant cell clones were found to have undergone gene targeting (5 out of 36 PDFF2 COLT-1, 4 out of 56 PDFF5 COLT-1, and 46 out of 70 PDFF2 COLT-2 cell clones analysed). We called COLT-1 cell clones 'PDCOL' and COLT-2 cell clones 'PDCAAT'. The DNA sequence of PCR products amplified from three PDCOL and two PDCAAT cell clones was determined across the 5′ junction; each was consistent with gene targeting (data not shown).

Figure 2a shows Southern analysis of the 5′ junctions of a series of PDCAAT cell clones. All samples showed the presence of a 7-kb *Bam*HI fragment from the normal *COL1A1* locus. Each clone identified as positive by PCR also showed a diagnostic 4.7-kb *Bam*HI fragment spanning the 5′ junction of the COLT-2 targeted locus. This is consistent with the presence of one targeted and one normal *COL1A1* allele. PDCAAT cell clones 87 and 99 also showed the presence of additional bands, indicating additional integrations of COLT-2.

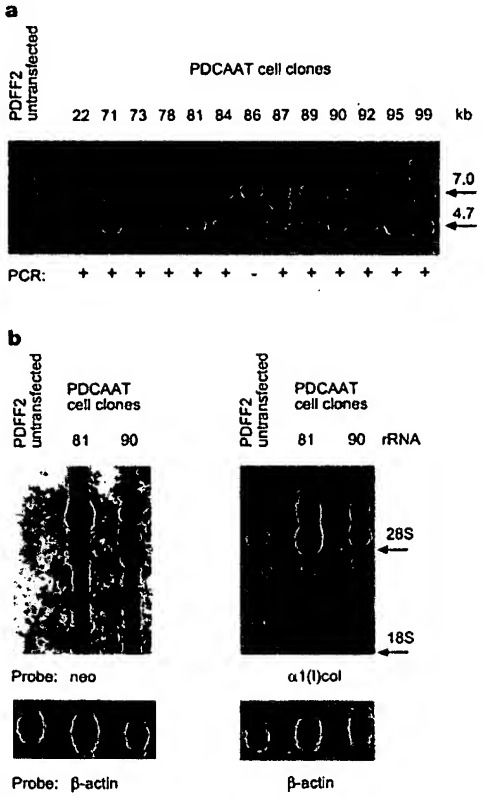


**Figure 2** Analysis of COLT-2 transfected (PDCAAT) cell clones. **a**, Southern analysis. Each lane contains *Bam*HI digested genomic DNA from cell samples hybridized with a 3-kb *COL1A1 Sal*I, *Ssp*I fragment corresponding to the 5′ homologous arm of COLT-1 and COLT-2 (see Fig. 1). The cell clone is indicated above each lane and results of the PCR screen are shown below each lane. The positions of the 7-kb *Bam*HI fragment from the non-targeted ovine *COL1A1* locus and the 4.7-kb *Bam*HI fragment from the COLT-2 targeted locus are marked. **b**, Northern analysis. Each lane contains 10 μg total RNA extracted from PDFF2 cells and targeted cell clones PDCAAT81 and PDCAAT90 as indicated. Duplicate blots were hybridized with a *neo* probe (upper left), and full-length human α1(I) procollagen cDNA (upper right). The positions of the 28S and 18S rRNA bands are indicated. The lower two autoradiographs show rehybridization of the same blots with mouse β-actin cDNA as an indication of the amount of total RNA loaded.

PDFF5 cells were also targeted at high frequency with COLT-1. PDFF2 and PDFF5 cells have different parentage from within the PPL outbred flock of Poll Dorset sheep. This indicates that it may not always be essential to isolate DNA from the same individual, or an animal of the same inbred strain, to achieve efficient gene targeting[12]; however, the degree of sequence divergence, if any, between the targeted *COL1A1* alleles in these cells has not yet been determined.

Northern analysis of cell clones PDCAAT 81 and 90 is shown in Fig. 2b. Hybridization with human α1(I) procollagen cDNA detected a 4.8-kb mRNA species in both non-transfected cells and PDCAAT cell clones, consistent with expression of normal *COL1A1*. A larger species of about 6.8 kb was present only in the PDCAAT cell clones, consistent with a bicistronic *COL1A1*–IRES–*neo* fusion mRNA. Hybridization of the same RNA samples with a *neo* probe also detected a 6.8-kb mRNA in the targeted clones, again consistent with a bicistronic mRNA. These results confirmed that gene targeting had occurred. This analysis also showed that, unlike mouse, rat and human, which express two endogenous α1(I) procollagen mRNA species from different polyadenylation sites[13,14], sheep express a single mRNA species.

Although these experiments were designed to avoid disruption of *COL1A1* gene expression, the mRNA from the targeted locus is less abundant than the wild type (Fig. 2b). Whether this reflects different mRNA stability or transcriptional activity has yet to be determined. However, elements which affect transcription have been identified at the 3′ end of *COL1A1* in other species[15,16], and targeted DNA insertion may affect their function.

We carried out northern analysis to determine whether placement of the AATC2 transgene adjacent to the highly expressed *COL1A1* gene resulted in aberrant expression of the BLG promoter in fibroblasts. Hybridization with human AAT cDNA failed to detect AAT mRNA expression in either PDCAAT81 or 90 cells (data not shown), indicating no apparent loss of BLG promoter specificity.

Four targeted cell clones, all derived from PDFF2 female cells (PDCOL6, PDCOL13, PDCAAT81 and PDCAAT90), were selected for nuclear transfer on the basis of their vigour and normal metaphase chromosome number. Nuclear transfer was carried out on twelve occasions and the results are summarized in Table 1. Fourteen lambs were live-born: seven died within 30 hours of birth, and one each after 3 days, 8 days, 7.5 weeks and 12 weeks. Three lambs are currently alive and thriving at almost one year of age. The first two live-born lambs are shown in Fig. 3.

*Post mortem* examination of lambs that died *in utero* or after birth revealed a range of abnormalities. Although there was no consistent pattern, we observed a high incidence of kidney defects (frequently renal pelvis dilation), liver and brain pathology. These findings are similar to a previous nuclear transfer study using the same cells[3],

**Table 1 Summary of nuclear transfer results**

| Nuclear donor cells | PDCOL 6 | PDCOL 13 | PDCAAT 81 | PDCAAT 90 |
|---|---|---|---|---|
| Reconstructed embryos | 109 | 154 | 71 | 83 |
| Embryos recovered from temporary recipient | 104 | 149 | 62 | 78 |
| Embryos developed to morula or blastocyst | 14 | 43 | 4 | 19 |
| Embryos transferred to final recipients | 14 | 43 | 4 | 19 |
| Final recipients | 8 | 22 | 2 | 10 |
| Fetuses at day 60 | 5* | 10* | 2 | 3* |
| Live-born lambs | 4 | 8 | 0 | 2 |
| Lambs alive beyond 1 week | 2 | 3 | 0 | 1 |
| Lambs alive beyond 6 months (lamb ID) | 1 (ID 990502) | 1 (ID 990504) | 0 | 1 (ID 990507) |

*One twin pregnancy.

and are therefore probably due to some aspect of the cell treatment or nuclear transfer procedure and not a consequence of gene targeting *per se*. Several researchers have reported developmental abnormalities associated with somatic cell nuclear transfer[4,17,18]. Although there is some indication that inappropriate expression of imprinted genes may be involved[19], definitive investigations have yet to be carried out. Understanding and rectifying this problem is a continuing priority.

Figure 4 shows Southern analysis of 5′ and 3′ junctions of the *COL1A1* targeted locus in representative nuclear transfer lambs. Hybridization with the same 5′ and 3′ probes used to analyse PDCAAT cell clones revealed fragments consistent with the presence of one targeted and one normal *COL1A1* allele in the two lambs shown. This was confirmed using a 5′ probe external to the vector.

Sixteen lambs and fetuses were analysed by Southern blot, of which fifteen confirmed the presence of a targeted allele. One lamb (990504), derived from PDCOL13, showed only the normal *COL1A1* gene, which probably indicates that the cell isolate was oligoclonal. Non-transfected cells have been detected within some G418 selected cell isolates in previous experiments (unpublished data).

Lamb 990507 derived from clone PDCAAT90 was hormonally induced to lactate and milk samples analysed by western blotting (data not shown). AAT was detected at a concentration of 650 $\mu g\,ml^{-1}$, which compares favourably with the highest level previously reported for an AAT cDNA transgene in sheep carrying multiple random gene inserts (18 $\mu g\,ml^{-1}$)[20]. This indicates that the *COL1A1* locus supports transgene expression even though it is not actively expressed in mammary epithelium[21].

We have shown that gene targeting can be carried out efficiently in somatic cells and that viable animals can be produced by nuclear transfer. We have also obtained preliminary data (that is, PCR fragment size and sequence) indicating similarly efficient targeting at the α-1,3-galactosyl-transferase locus in porcine fibroblasts (unpublished data). Notably, the use of nuclear transfer does not require embryonic stem or embryonic germ cells, and circumvents the generation of chimaeric animals, which would be costly and time consuming in livestock. Fibroblasts are also being used in clinical trials to provide a protein production system after *ex vivo* gene therapy in human patients[22], and it has been suggested that the introduction of therapeutic transgenes by homologous recombination could avoid undesirable effects arising from random integration[23]. Nuclear transfer in animals such as sheep provides a rigorous means of testing the suitability of specific loci for transgene placement. If the *COL1A1*-targeted sheep continue to show no locus-related deleterious effects, this would indicate that this target locus may provide a permissive and benign environment for the insertion of therapeutically useful genes. □

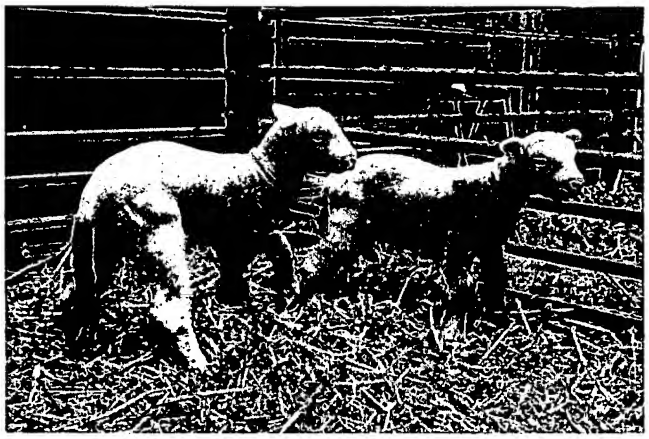

**Figure 3** Gene-targeted lambs. Lambs 990502 and 990503, both derived by transfer of nuclei from gene-targeted cell clone PDCOL6.

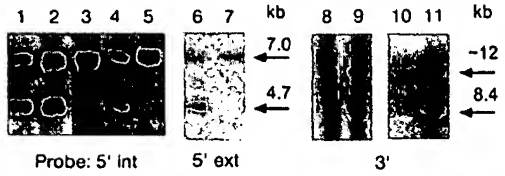


**Figure 4** Southern analysis of nuclear transfer lambs. Lanes 1—7 show *Bam*HI-digested genomic DNA samples hybridized with 5′ internal and external probes as indicated. Arrows indicate the 7-kb *Bam*HI fragment from the non-targeted ovine *COL1A1* locus, and the 4.7-kb fragment from the COLT-1 and COLT-2 targeted locus. Lanes 8–11 show *Kpn*I, *Asp*I double-digested genomic DNA samples hybridized with the 3′ probe. Arrows indicate the ~12-kb *Asp*I fragment from the non-targeted locus and the 8.4-kb *Kpn*I, *Asp*I fragment from the COLT-1 and COLT-2 targeted locus. Lane 1, nuclear transfer (n.t.) lamb from cell clone PDCOL6; lane 2, n.t. lamb from cell clone PDCAAT90; lane 3, normal lamb; lane 4, cell clone PDCAAT90; lanes 5, 7 and 8, non-targeted PDFF2 cells; lane 6, n.t. lamb from cell clone PDCOL6; lane 9, cell clone PDCAAT90; lane 10, normal lamb; lane 11, n.t lamb from cell clone PDCOL6.

## Methods

### Gene-targeting vectors

The promoter trap vector COLT-1 comprised a 3-kb region of the 3′ end of the ovine *COL1A1* gene from a point roughly 2.9-kb 5′ of the translation stop site to an *Ssp*I site 131-bp 3′ of the stop site; a 0.6-kb IRES region[10] corresponding to bases 1,247–1,856 of the pIREShyg vector (Clontech); a 1.7-kb region containing the bacterial *neomycin* gene and a portion of the 3′ end of the human growth hormone gene containing the polyadenylation site, essentially as described[24]; an 8.3-kb region of the 3′ end and flanking region of the ovine *COL1A1* gene from an *Ssp*I site 131-bp 3′ of the translational stop site to a *Xho*I site roughly 8.4-kb 3′ of the stop site; and the bacterial cloning vector pSL1180 (Pharmacia). DNA fragments homologous to the ovine *COL1A1* gene were derived from a single genomic clone isolated from a library of genomic fragments of PDFF2 in bacteriophage λ. The promoter trap transgene placement vector COLT-2 was constructed by inserting an *Mlu*I fragment containing the AATC2 transgene into COLT-1 at a unique *Eco*RV site at the 3′ end of the IRES–*neo* region.

### Preparation, culture and transfection of primary fibroblasts

Derivation of ovine PDFF2 and PDFF5 cells has been described[3]. PDFF cells were grown throughout in BHK 21 (Glasgow MEM) medium supplemented with 2 mM glutamine, 1 mM sodium pyruvate, 1X non-essential amino acids and 10% fetal calf serum in standard tissue-culture vessels in a humidified atmosphere composed of 2% $CO_2$, 5% $O_2$ and 93% $N_2$, and were passaged by standard trypsinization. PDFF cells were used at passage three, and had undergone 5–6 days of culture following fetal disaggregation. Cells were plated at $5 \times 10^5$ cells in a 25-$cm^2$ flask and transfected the next day with either 6 μg of *Sal*I linearized COLT-1 or *Sac*II linearized COLT-2, using lipofectAMINE (Gibco, BRL Life Technologies) according to the manufacturer's guidelines. G418 selection (0.8 mg $ml^{-1}$) was applied 48 h after transfection. On average ~200 G418′ colonies were derived per $5 \times 10^5$ cells transfected. Well separated G418′ colonies were isolated, expanded and cryopreserved by standard procedures.

### Nuclear transfer

Ovine cell clones were prepared for nuclear transfer by culture in medium containing reduced (0.5%) serum for either 2 or 4 days. Transfer of cell nuclei into Poll Dorset oocytes was carried out essentially as described[3].

### Nucleic acid analysis

Putative targeted cell clones were screened by PCR amplification across the 5′ short arm of homology. The position of PCR primers is shown in Fig. 1. Samples of cell clones for screening were lysed in PCR lysis buffer (50 mM KCl, 1.5 mM $MgCl_2$,10 mM Tris-HCl pH 8.5, 0.5% Nonidet P40, 0.5% Tween, 400 $\mu g\,ml^{-1}$ Proteinase K) at 65 °C for 30 min. Proteinase K was inactivated at 95 °C for 10 min, and PCR amplification was performed using the 'Expand long template PCR system' (Boehringer) according to the manufacturer's recommended conditions. PCR primer sequences were: COLTPCR4 primer, 5′-GGTTTGTTCCCAGGTGCTCA-3′; COLTPCR8 primer, 5′-GACCTTG-CATTCCTTTG GCGAGAG-3′. Thermal cycling conditions were: 94 °C, 2 min; 10 cycles of 94 °C, 10 s, 55 °C, 30 s, 68 °C, 2 min; 20 cycles of 94 °C, 10 s, 60 °C, 30 s, 68 °C, 2 min + 20 s per cycle; followed by 68 °C, 7 min. PCR products were analysed by agarose gel electrophoresis.

Ovine genomic DNA was prepared from cell pellets, tail samples of live lambs and umbilical cord samples of dead lambs. Southern analysis was carried out by standard procedures. Three hybridization probes were used: a 5′ internal probe, a 3-kb *COL1A1* *SalI*, *SspI* fragment corresponding to the 5′ homologous arm of COLT-1 and 2 (Fig. 1); a 5′ external probe, a 520-bp ovine *COL1A1* fragment directly adjacent to but outside the 5′ homologous arm; a 3′ internal probe, a 0.7-kb *COL1A1* *SalI*, *PstI* fragment immediately 3′ of the integration site (Fig. 1). The diagnostic fragments detected were: a 4.7-kb *Bam*HI fragment extending across the 5′ junction of the targeted locus from a *Bam*HI site within the IRES–*neo* region to a *Bam*HI site in the *COL1A1* gene 5′ of the region contained in the vector; a 8.4-kb *Kpn*I, *Asp*I fragment extending across the 3′ junction of the targeted locus from a *Kpn*I site within the vector to an *Asp*I site in the *COL1A1* gene flank 3′ of the region contained in the vector.

### Hormonal induction of lactation

Milk samples were obtained from immature ewes by hormonal induction of lactation, essentially as described[25].

Received 28 January; accepted 5 May 2000.


1. Thompson, S., Clarke, A. R., Pow, A. M., Hooper, M. L. & Melton, D. W. Germ line transmission and expression of a corrected HPRT gene produced by gene targeting in embryonic stem cells. *Cell* 56, 313–321 (1989).
2. Campbell, K. H. S., McWhir, J., Ritchie, W. A. & Wilmut, I. Sheep cloned by nuclear transfer from a cultured cell line. *Nature* 389, 64–66 (1996).
3. Schnieke, A. S. *et al.* Human Factor IX transgenic sheep produced by transfer of nuclei from transfected fetal fibroblasts. *Science* 278, 2130–2133 (1997).
4. Cibelli, J. B. *et al.* Cloned transgenic calves produced from nonquiescent fetal fibroblasts. *Science* 280, 1256–1258 (1998).
5. Lin, F. L., Sperle, K. & Sternberg, N. Recombination in mouse L cells between DNA introduced into cells and homologous chromosomal sequences. *Proc. Natl Acad. Sci. USA* 82, 1391–1395 (1985).
6. Smithies, O., Gregg, R. G., Boggs, S. S., Koralewski, M. A. & Kucherlapati, R. S. Insertion of DNA sequences into the human chromosomal β-globin locus by homologous recombination. *Nature* 317, 230–234 (1985).
7. Yanez, R. J. & Porter, A. C. Therapeutic gene targeting. *Gene Ther.* 5, 149–159 (1998).
8. Prockop, D. J. & Kivirikko, K. I. Collagens: molecular biology, diseases, and potentials for therapy. *Annu. Rev. Biochem.* 64, 403–434 (1995).
9. Stacey, A. *et al.* Perinatal lethal osteogenesis imperfecta in transgenic mice bearing an engineered mutant pro-alpha 1(I) collagen gene. *Nature* 332, 131–136 (1988).
10. Jang, S. K. *et al.* A segment of the 5′ nontranslated region of encephalomyocarditis virus RNA directs internal entry of ribosomes during in vitro translation. *J. Virol.* 62, 2636–2643 (1988).
11. Carver, A. S. *et al.* Transgenic livestock as bioreactors: stable expression of human alpha-1-antitrypsin by a flock of sheep. *Bio/Technology* 11, 1263–1270 (1993).
12. Sedivy, J. M. & Dutriaux, A. Gene targeting and somatic cell genetics: a rebirth or coming of age? *Trends Genet.* 15, 88–90 (1999).
13. Mooslehner, K. & Harbers, K. Two mRNAs of mouse pro a1(I) collagen differ in the size of the 3′-untranslated region. *Nucleic Acids Res.* 16, 773 (1988).
14. Chu, M. L., de Wet, W., Bernard, M. & Ramirez, F. Fine structural analysis of the human pro-alpha 1 (I) collagen gene. Promoter structure, AluI repeats, and polymorphic transcripts. *J. Biol. Chem.* 260, 2315–2320 (1985).
15. Rippe, R. A., Umezawa, A., Kimball, J. P., Breindl, M. & Brenner, D. A. Binding of upstream stimulatory factor to an E-box in the 3′-flanking region stimulates alpha1(I) collagen gene transcription. *J. Biol. Chem.* 272, 1753–1760 (1998).
16. Määttä, A., Ekholm, E. & Penttinen, R. P. Effect of the 3′-untranslated region on the expression levels and mRNA stability of alpha 1(I) collagen gene. *Biochim. Biophys. Acta* 1260, 294–300 (1995).
17. Renard, J. P. *et al.* Lymphoid hypoplasia and somatic cloning. *Lancet* 353, 1489–1491 (1999).
18. Hill, J. R. *et al.* Clinical and pathologic features of cloned transgenic calves and fetuses (13 case studies). *Theriogenology* 51, 1451–1465 (1999).
19. Kono, T. Influence of epigenetic changes during oocyte growth on nuclear reprogramming after nuclear transfer. *Reprod. Fertil. Dev.* 10, 593–598 (1998).
20. McClenaghan, M. *et al.* Production of human $\alpha_1$-antitrypsin in the milk of transgenic sheep and mice targeting expression of cDNA sequences to the mammary gland. *Anim. Biotechnol.* 2, 161–176 (1991).
21. Warburton, M. J., Kimbell, R., Rudland, P. S., Ferns, S. A. & Barraclough, R. Control of type IV collagen production in rat mammary epithelial and myoepithelial-like cells. *J. Cell. Physiol.* 128, 76–84 (1986).
22. Kay, M. A. & High, K. Gene therapy for the hemophilias. *Proc. Natl Acad. Sci. USA* 96, 9973–9975 (1999).
23. Lai, L-W. & Lien, Y-H. Homologous recombination based gene therapy. *Exp. Nephrol.* 7, 11–14 (1999).
24. McWhir, J. *et al.* Selective ablation of differentiated cells permits isolation of embryonic stem cell lines from murine embryos with a non-permissive genetic background. *Nat. Genet.* 14, 223–226 (1996).
25. Ebert, K. D. *et al.* Induction of human tissue plasminogen activator in the mammary gland of transgenic goats. *Bio/Technology* 12, 699–702 (1994).



### Acknowledgements

We would like to acknowledge the contributions of Y. Gibson and K. Mycock for embryo manipulation; E. Emslie and L. Hutchison for molecular biology technical assistance; T. Johnston for protein analysis; and the PPL Therapeutics large animal team for animal husbandry and veterinary procedures. We thank I. Garner and D. Ayares for useful discussions.


Correspondence and requests for materials should be addressed to A.J.K. (e-mail: akind@ppl-therapeutics.com).

# Gigantism in mice lacking suppressor of cytokine signalling-2

**Donald Metcalf, Christopher J. Greenhalgh, Elizabeth Viney, Tracy A. Willson, Robyn Starr, Nicos A. Nicola, Douglas J. Hilton & Warren S. Alexander**

*The Walter and Eliza Hall Institute of Medical Research and The Cooperative Research Centre for Cellular Growth Factors, Post Office, Royal Melbourne Hospital, Victoria 3050, Australia*

**Suppressor of cytokine signalling-2 (SOCS-2) is a member of the suppressor of cytokine signalling family, a group of related proteins implicated in the negative regulation of cytokine action through inhibition of the Janus kinase (JAK) signal transducers and activators of transcription (STAT) signal-transduction pathway[1]. Here we use mice unable to express SOCS-2 to examine its function *in vivo*. SOCS-2$^{-/-}$ mice grew significantly larger than their wild-type littermates. Increased body weight became evident after weaning and was associated with significantly increased long bone lengths and the proportionate enlargement of most organs. Characteristics of deregulated growth hormone and insulin-like growth factor-I (IGF-I) signalling, including decreased production of major urinary protein, increased local IGF-I production, and collagen accumulation in the dermis, were observed in SOCS-2-deficient mice, indicating that SOCS-2 may have an essential negative regulatory role in the growth hormone/IGF-I pathway.**

We isolated genomic clones corresponding to three independent loci from two murine libraries using a SOCS-2 coding region complementary DNA as hybridization probe. Comparison of sequence from these clones with that of the SOCS-2 cDNA revealed that one locus, which consisted of three exons and two introns, encoded the predicted SOCS-2 RNA (Fig. 1a). The two other loci

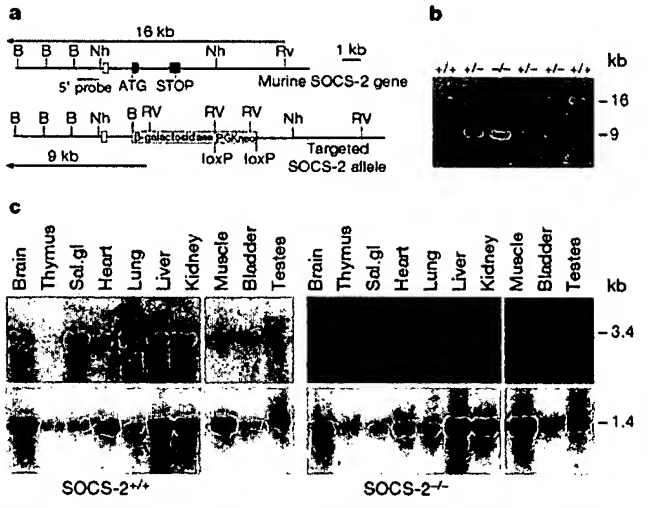


**Figure 1** Disruption of the SOCS-2 locus by homologous recombination. **a**, The functional murine SOCS-2 gene (B, *Bam*HI; Nh, *Nhe*I; RV, *Eco*RV) with the exons containing the coding region as shaded boxes. In the targeted allele, the entire SOCS-2 coding region was replaced by a β-gal-PGKneo cassette in which the β-galactosidase coding region was fused to the SOCS-2 initiation codon. **b**, Southern blot of *Eco*RV-digested genomic DNA from the tails of mice derived from a cross between SOCS-2$^{+/-}$ mice. The blot was hybridized with the 5′ genomic SOCS-2 probe, which distinguishes between endogenous (16 kb) and mutant SOCS-2 (9 kb) alleles. **c**, Northern blot showing lack of SOCS-2 expression in organs of SOCS-2$^{-/-}$ mice. Top, the blot was hybridized with a coding region probe, which detects the 3.4-kb SOCS-2 transcript[1]; bottom, the integrity of the RNA was confirmed by hybridization with GAPDH (1.4-kb transcript). Sal gl, salivary gland.

Nature Ref. N0614E-- — KIND —(ERR)

erratum

# Production of gene-targeted sheep by nuclear transfer from cultured somatic cells

K. J. McCreath , J. Howcroft, K. H. S. Campbell, A. Colman, A. E. Schnieke & A. J. Kind

*Nature* **405**, 1066–1069 (2000).

An incomplete version of Figure 1 was printed in this Letter. The correct Figure is reproduced below. □

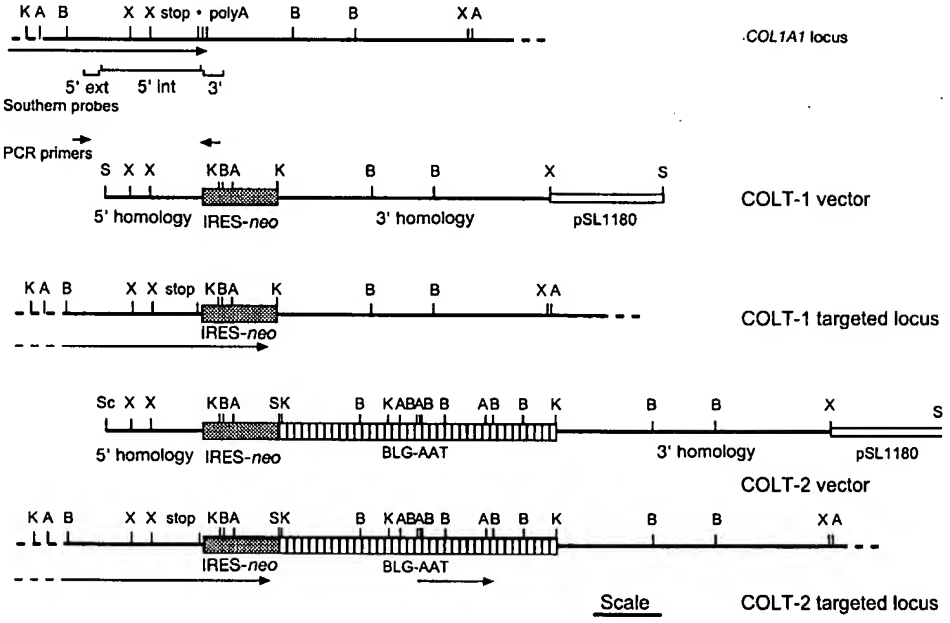


**Figure 1** Diagrams of ovine *COL1A1*, COLT-1 and COLT-2 targeting vectors and targeted *COL1A1* locus. The map of ovine *COL1A1* shows the translational stop and polyadenylation sites, the direction of transcription and extent of the *COL1A1* mRNA is indicated by an arrow, an asterisk marks an *Ssp*1 site where the targeted gene insertions were made. Southern hybridization probes and PCR primers are indicated. The maps of the COLT-1 and COLT-2 vectors and the targeted *COL1A1* locus show the IRES–*neo* cassette as a shaded box, the BLG driven AAT transgene by a striped box, and the bacterial vector pSL1180 by an open box. The direction and predicted extent of the *COL1A1* / IRES–*neo* bicistronic mRNA and the AAT transgene mRNA are shown as arrows. The scale bar represents 2 kb. Restriction enzyme sites: A, *Asp*I; B, *Bam*HI; Sc, *Sac*II; S, *Sal*I; K, *Kpn*I; X, *Xho*I.

Development 119, 485-499 (1993)
Printed in Great Britain © The Company of Biologists Limited 1993



# Defects in heart and lung development in compound heterozygotes for two different targeted mutations at the N-*myc* locus

**Cecilia B. Moens[1,3], Brian R. Stanton[2], Luis F. Parada[2] and Janet Rossant[1,3,*]**

[1]Division of Molecular and Developmental Biology, Samuel Lunenfeld Research Institute, 600 University Ave, Toronto, Ontario, M5G 1X5, Canada
[2]Molecular Embryology Section, ABL-Basic Research Program, National Cancer Institute - Frederick Cancer Research and Development Center, Frederick, Maryland 21702-1201, USA
[3]Department of Molecular and Medical Genetics, University of Toronto

*Author for correspondence

## SUMMARY

**Two types of mutant allele, one leaky and one null, have been generated by gene targeting at the N-*myc* locus in embryonic stem cells and the phenotypes of mice homozygous for these mutations have been described. These mutations have shown that N-*myc* has a number of functions during development, including a role in branching morphogenesis in the lung, which manifests itself at birth in mice homozygous for the leaky allele, and roles in the development of the mesonephric tubules, the neuroepithelium, the sensory ganglia, the gut and the heart, which become evident at midgestation in embryos homozygous for the null allele. In an attempt to define roles for N-*myc* at other stages of development, we have combined the two types of N-*myc* mutant allele in a compound heterozygote that as a result contains approximately 15% of normal levels of N-Myc protein. Compound heterozygotes died during gestation at a time intermediate to the times of death of embryos homozygous for either mutation individually, and their death appeared to result from cardiac failure stemming from hypoplasia of the compact subepicardial layer of the myocardium. Investigation of the expression pattern of N-*myc* and various markers of differentiation in wild-type and compound heterozygote mutant hearts has suggested that N-*myc* may function in maintaining the proliferation and/or preventing the differentiation of compact layer myocytes. This study illustrates the importance of generating different mutations at a given locus to elucidate fully the function of a particular gene during development.**

Key words: N-myc, heart development, targeted mutagenesis, mouse mutant

## INTRODUCTION

N-*myc* is a member of the *myc* family of proto-oncogenes, which includes N-*myc*, c-*myc*, and L-*myc*. Myc proteins are site-specific DNA-binding proteins (Blackwell et al., 1990; Prendergast and Ziff, 1991; Alex et al., 1992), belonging to the basic-helix-loop-helix class of transcription factors, which includes genes that control cell fate determination in such diverse processes as myogenesis, neurogenesis and sex determination (reviewed in Garrell and Campuzano, 1991).

Deregulated expression of *myc* genes has been implicated in the genesis or progression of a number of naturally occurring tumours, in the transformation of cells in culture and in the formation of tumours in transgenic mice (reviewed in DePinho et al., 1991). In general, the sites of expression of a given *myc* gene in vivo reflect the types of tumours associated with its elevated expression. Thus N-*myc* is expressed predominantly in the embryo where it is restricted to undifferentiated subsets of cells in the central and peripheral nervous system, lung, kidney and eye (Mugrauer et al., 1988; Hirning et al., 1991; Zimmerman et al., 1986) and overexpression of N-*myc* has been associated with tumours of embryonic origin such as neuroblastoma (Kohl et al., 1983; Schwab et al., 1983), small-cell lung cancer (Nau et al., 1986; Wong et al., 1986), Wilm's tumour (Nisen et al., 1986) and retinoblastoma (Lee et al., 1984). N-*myc* is also expressed in the skin (Mugrauer et al., 1988), in the epithelial layer of the intestine (Hirning et al., 1991) and, earlier in development, in the heart, sclerotome and visceral arches (Katoh et al., 1991).

The functioning of a Myc protein in vivo should depend not only on its own level of expression, but also on the levels of Max, a protein which, like the Myc proteins, possesses a basic-helix loop helix-leucine zipper (bHLH-LZ) domain (Blackwood and Eisenman, 1991), and which associates with N-Myc, L-Myc and c-Myc proteins in vivo (Blackwood et al., 1992; Wenzel et al., 1991; Mukherjee et al., 1992). Max is required for specific DNA binding by Myc proteins (Blackwood and Eisenman, 1991; Prendergast and Ziff, 1991; Kato et al., 1992; Barrett et al., 1992), and has

been shown to be required for transcriptional activation (Amati et al., 1992) and transformation (Amati et al., 1993) by c-*myc*. Unlike Myc proteins, Max is able to form homodimers in vitro and thereby to bind the *myc*-binding site (Prendergast and Ziff, 1991; Kato et al., 1992). However Max does not transactivate downstream genes on its own (Amati et al., 1992; Kretzner et al., 1992) because it lacks a transactivation domain (Kato et al., 1992) which Myc proteins possess (Kato et al., 1990). Both transformation of fibroblasts by c-*myc* and N-*myc* (Mukherjee et al., 1992; Makela et al., 1992; Prendergast et al., 1992) and transcriptional transactivation by c-*myc* (Amati et al., 1992; Kretzner et al., 1992) have been shown to be enhanced by low levels of Max and inhibited by excess Max, suggesting that Myc function is indeed influenced by levels of Max. Recently, bHLH-LZ proteins have been isolated which also bind the Myc recognition site and which suppress transcription as heterodimers with Max (Ayer et al., 1993; Zervos et al., 1993). One of these, Mad (Ayer et al., 1993), has been shown to compete with Myc for Max in vitro and in transfected cells. Thus high levels of expression of Max dimerization partners may indirectly affect Myc function in vivo by competing for available Max protein and for DNA-recognition sites. Finally, Myc function in vivo may be affected by the levels of other Myc proteins (Mukherjee et al., 1992; Resar et al., 1993).

In an effort to understand the function of *myc* genes in embryogenesis, leaky and null mutations were made in N-*myc* in embryonic stem cells by homologous recombination (Charron et al., 1990; Stanton et al., 1990; Sawai et al., 1991; Moens et al., 1992). These mutations have allowed a description of the function of N-*myc* at different stages of development. Mice homozygous for the null mutations die at midgestation (Stanton et al., 1992; Charron et al., 1992) while mice homozygous for the leaky mutation survive until birth, when they die due to a defect in lung branching morphogenesis (Moens et al., 1992). The latter phenotype is consistent with the normal expression of N-*myc* in the developing lung epithelium, and has led us to postulate that N-*myc* plays a role in the response of the lung epithelium to the signals from the lung mesenchyme that induce epithelial branching.

There have been two detailed reports of the phenotype of mice carrying null mutations in N-*myc* (Stanton et al., 1992; Charron et al., 1992). In the homozygous condition, these mutations cause embryonic death at around 11.5 days p.c. and cause hypoplasia in a number of components of the embryo, different aspects of which have been emphasized by the two groups. The developing genitourinary system shows a reduced number of mesonephric tubules in mutant embryos, which is consistent with N-*myc*'s normal expression in the newly induced epithelium of the meso- and metanephric tubules (Katoh et al., 1991; Mugrauer et al., 1988). The genital ridge is also hypoplastic. Stanton et al. (1992) also describe a defect in the development of the stomach and intestine, consistent with N-*myc*'s expression in the epithelium of these tissues (Hirning et al., 1991). Homozygotes also have reduced cranial and spinal ganglia and a thin neuroepithelium in the telencephalon; both of these are sites of N-*myc* expression in the embryo. Finally, homozygotes have a defect in heart development in which the heart appears to cease development at 9.5 days p.c. (Charron et al., 1992) and as a result is poorly compartmentalized and appears not to have undergone the normal epithelial-to-mesenchymal transitions that result in the formation of the septa and valves. This is again consistent with a previous description of N-*myc* expression in the myocardium of the 9.5 day embryo (Katoh et al., 1991).

By combining leaky and null alleles of N-*myc* in a compound heterozygote, we hoped to investigate N-*myc* function in the mouse embryo at a stage intermediate to those identified by the null and leaky alleles individually. We find that compound heterozygotes indeed survive longer than null homozygotes, but that they die before birth. The mutant phenotype includes a more severe defect in branching morphogenesis of the lung, as well as a cardiac myocyte hypoplasia in the compact subepicardial layer of the ventricular myocardium. We show that, consistent with this phenotype, N-*myc* expression in the developing myocardium is restricted to the compact layer. A role for *myc* genes in the control of myocyte differentiation in the heart is discussed.

## MATERIALS AND METHODS

### PCR genotyping of embryos

Yolk sacs from dissected embryos were washed several times in fresh PBS and placed in 100-200 μl of proteinase K buffer with non-ionic detergents (50 mM KCl, 10 mM Tris pH 8.3, 2.0 mM $MgCl_2$, 0.1 mg/ml gelatin, 0.45% Nonidet P-40, 0.45% Tween-20). 10 μg of proK was added to each tube and samples were incubated at 55°C overnight. 10 μl of the mixture was placed in a PCR tube with 30 μl sterile water and heated to 94°C for 10 minutes before cooling to 62°C. 0.1 μg of each primer, 200 μM dNTPs, 10× reaction buffer and Taq polymerase (Promega) were added and PCR was run with an annealing temperature of 62°C (1 minute), an extension temperature of 72°C (2 minutes), and a denaturing temperature of 94°C (1 minute). Each consecutive cycle was extended by 2 seconds. The oligonucleotide primers used for the PCR detection of 9a, BRP and wild-type alleles of N-*myc* are shown in Fig. 1. Their sequences are as follows: primer a (N-*myc* intron 1): 5′-GGTAGTCGCGCTAGT AAGAG-3′; primer b (N-*myc* exon 2): 5′-GGCGTGGGCA GCAGCTCAAAC-3′; primer c (N-*myc* intron 2): 5′-CCGAGCATCTGTCGCCAAGTC-3′; primer d (neo): 5′-GACCGCTATCAGGACATAGCG-3′.

### Western blotting

An anti-human N-*myc* monoclonal antibody, NCMII 100 (Ikegaki et al., 1986), was generously provided by Dr R. Kennett. 11.5 days p.c. embryos from 9a/+×BRP/+ crosses were dissected and homogenized in several volumes of 1× sample buffer without bromophenol blue (60 mM Tris, pH 6.8, 2% SDS, 0.1 M DTT, 0.32% pharmalyte 3-10 (Pharmacia)). Samples were boiled for 5 minutes and chromosomal DNA was sheared by repeated passage through a 26-gauge needle before freezing at −20°C for future use. Yolk sacs were washed several times in PBS and were prepared for and typed by PCR as described above. After typing, extracts of embryos of each genotype were pooled and the concentration of protein in each sample was determined by the Bradford assay (protein assay reagent from Biorad). Approximately 20 μg of protein from each genotype in 2× loading buffer (0.1 M Tris pH 6.8, 20% glycerol, 4% SDS, 0.2% bromophenol blue, 0.2 M DTT) was run in a 10% SDS-PAGE. Protein was transferred onto PVDF membrane (Immobilon-P, Millipore). Application of primary antibody and fixation of the primary antibody to the blot with 0.2%

glutaraldehyde was performed as described (Ikegaki and Kennett, 1989). Horseradish peroxidase-conjugated goat anti-mouse secondary antibody and reagents for the chemiluminescent detection of HRP activity were obtained in the ECL western blotting kit (Amersham) and were used as suggested by the manufacturer.

### Histology

Dissected embryos were fixed in 10% buffered formalin overnight at room temperature, then were dehydrated and cleared by soaking sequentially in 70%, 80%, 90% and 95% ethanol, 1:1 ethanol:xylene, xylene, 1:1 xylene:paraffin wax, (TissuePrep 2, Fisher Scientific) each for 1 hour. Embryos were then oriented and embedded in paraffin wax. Mutant embryos and control littermates were oriented either for sagittal or frontal sections. 5 μm sections were placed on slides, which were dried overnight at 37°C. Slides were dewaxed, rehydrated, and stained with hematoxylin and eosin. To analyse mutant phenoypes, sections throughout wild-type and mutant embryos were carefully examined in order to find those sections that passed through corresponding regions of the different embryos. Mutant embryos were always compared to non-mutant littermates rather than to non-mutant embryos from other litters, in order to rule out differences due to age.

### RNA in situ hybridizations

Probes for in situs were as follows. N-*myc*: a 541 bp *Pst*1-*Sca*1 fragment of the N-*myc* genomic clone N7.7 (DePinho et al., 1986), including largely 3'-untranslated sequence; c-*myc*: a 351 bp *Hae*III fragment including the untranslated first exon (Bossone et al., 1992); *flk-1*: an 800 bp fragment spanning the transmembrane domain and part of the extracellular ligand-binding domain (Yamaguchi et al., 1993) and α-cardiac actin, a 130 bp *Bam*HI fragment including the first untranslated exon of the mouse α-cardiac actin gene (Sassoon et al., 1988). In situ hybridization was carried out essentially as described (Frohman et al., 1990) with the following modifications: in vitro-transcribed, α-$^{35}$S-labeled RNA probes were used at $5\times10^4$ disintegrations/minute per 1 μl of hybridization solution for the α-cardiac actin probe, and at $1\times10^5$ disintegrations/minute per 1 μl of hybridization solution for c-*myc*, N-*myc* and *flk-1* probes. Slides were hybridized at 53°C overnight, and were washed in the presence of 0.1% β-mercaptoethanol as a reducing agent. High stringency washes were in 50% formamide, 0.1% β-mercaptoethanol, and 1× SSC at 65°C. Final rinses in 2× and 0.1× SSC were at 65°C for 15 minutes. Slides were exposed for either 6 days (for α-cardiac actin probe) or for 14 days (for N-*myc*, *flk-1* and c-*myc* probes). After developing and photographing with dark-field illumination, slides were stained with hematoxylin and eosin and were rephotographed with bright-field illumination.

## RESULTS

### Time of death of N-*myc* compound heterozygotes

The leaky mutation that was generated in N-*myc* (Moens et al., 1992) was termed N-$myc^{9a}$ and the null allele of N-*myc* used in this study was named N-$myc^{BRP}$ (Stanton et al., 1992). Both the N-$myc^{9a}$ mutation and the N-$myc^{BRP}$ mutation are lethal in the homozygous condition. Therefore, N-$myc^{9a/BRP}$ embryos were generated by crossing N-$myc^{9a/+}$ females to N-$myc^{BRP/+}$ males, with the expected ratio of embryos being 1 N-$myc^{+/+}$: 1 N-$myc^{9a/+}$: 1 N-$myc^{BRP/+}$: 1 N-$myc^{9a/BRP}$. The reciprocal cross was also performed: no differences in mutant phenotypes were observed.

In order to expedite the genotypic analysis of offspring from this cross, a PCR strategy was designed that used four oligonucleotide primers to distinguish 9a, BRP, and wild-type alleles of N-*myc* (Fig. 1). 161 live offspring from N-$myc^{9a/+}$×N-$myc^{BRP/+}$ crosses were typed by PCR between 1 day and 3 weeks after birth. Among these pups, 59 were N-$myc^{+/+}$, 53 were N-$myc^{9a/+}$ and 49 were N-$myc^{BRP/+}$. No live animals were N-$myc^{9a/BRP}$. No pups were observed to die postnatally as occurred in the case of N-$myc^{9a/9a}$ newborns, suggesting that the N-$myc^{9a/BRP}$ phenotype was indeed more severe than the N-$myc^{9a/9a}$ phenotype.

We dissected embryos from N-$myc^{9a/+}$×N-$myc^{BRP/+}$ crosses at various stages of gestation in order to determine the time during gestation when N-$myc^{9a/BRP}$ embryos died. Between 8.5 and 11.5 days p.c., N-$myc^{9a/BRP}$ embryos were phenotypically normal and constituted approximately 25% of the total number of embryos, by PCR analysis. Of 268 embryos dissected between 8.5 and 11.5 days p.c., 61 (23%) were N-$myc^{9a/BRP}$ embryos. This is clearly different from the situation in N-$myc^{BRP/BRP}$ embryos, which were all found to be dead by 11.5 days p.c. (Stanton et al., 1992). The observed differences in phenotype among the various mutants were unlikely to be due to different genetic background effects, since all mutant phenotypes were analysed in outbred mice.

Occasionally, N-$myc^{9a/BRP}$ embryos at 11.5 days were slightly smaller than their littermates but were otherwise indistinguishable from their wild-type or single heterozygote littermates. However, by 12.5 days, most N-$myc^{9a/BRP}$ embryos were distinguishable from their littermates either because they were dead and necrotic, or because they were alive but had a characteristic edema of the body wall in the neck area (Fig. 2). Subsequent histological analysis identified this swelling as likely being the result of extravasion of fluid from the vascular compartment into the connective tissue, since the jugular veins are dilated in these embryos (Fig. 7g,h). Of 230 embryos dissected at 12.5 days p.c., 42 (18%) were N-$myc^{9a/BRP}$, but among these, 12 were dead and necrotic, 23 had the characteristic edema described above, two were smaller than normal and five were phenotypically normal. After 12.5 days p.c., live N-$myc^{9a/BRP}$ embryos were progressively less frequent and all were phenotypically abnormal. N-$myc^{9a/BRP}$ embryos that survived until 14.5 days p.c. were always smaller than normal and had a large edema in the neck area. Live N-$myc^{9a/BRP}$ embryos were not observed after 14.5 days p.c. Coincident with the loss of N-$myc^{9a/BRP}$ embryos there was an increase in the number of resorptions visible in the uterus. These resorptions were not typed, but presumably were derived from N-$myc^{9a/BRP}$ embryos, since the sum of the number of N-$myc^{9a/BRP}$ embryos and the number of resorptions added up to approximately 25% of the total number of embryos and resorptions at each stage of gestation. These data are shown graphically in Fig. 3.

### N-Myc protein levels in mutant embryos

Although we have previously shown reduced N-*myc* mRNA levels in N-$myc^{9a/9a}$ embryos (Moens et al., 1992), N-Myc protein levels have not been determined in mice bearing either the leaky or the null N-*myc* alleles. In the present study, we have used western blot analysis to assess N-Myc protein levels in embryos with the various N-*myc* genotypes. Fig. 4 shows a western blot performed on

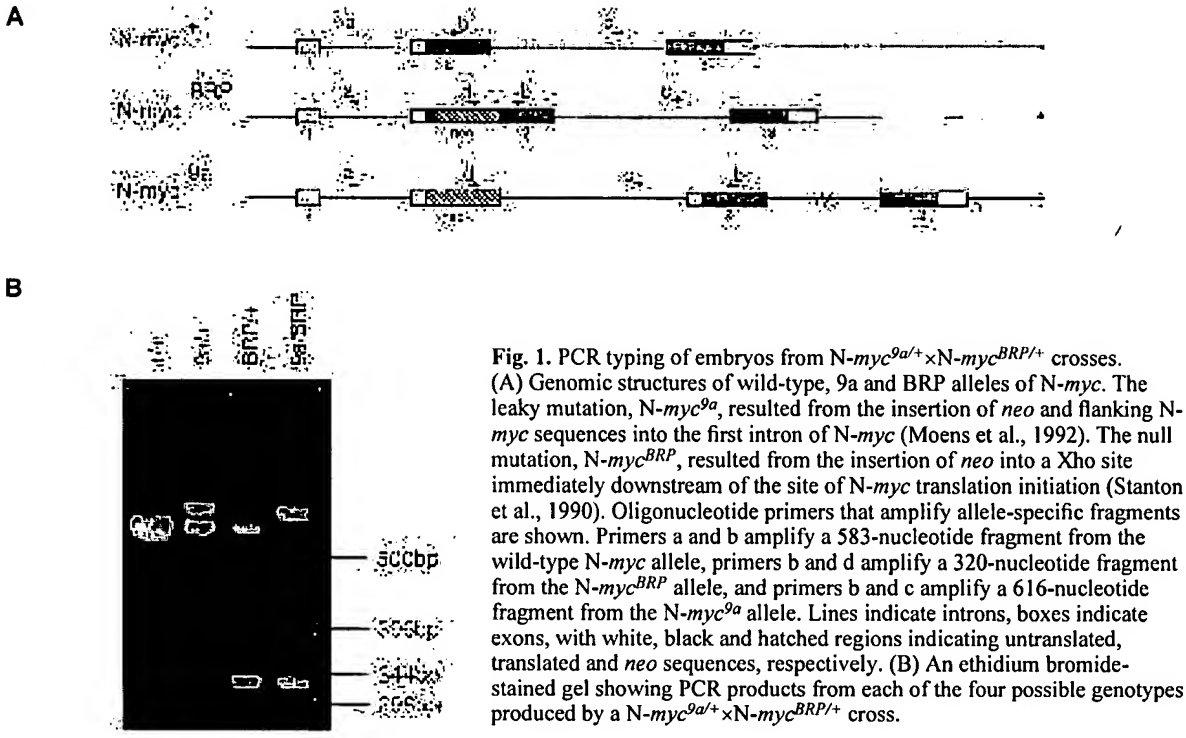


Fig. 1. PCR typing of embryos from N-*myc*$^{9a/+}$×N-*myc*$^{BRP/+}$ crosses. (A) Genomic structures of wild-type, 9a and BRP alleles of N-*myc*. The leaky mutation, N-*myc*$^{9a}$, resulted from the insertion of *neo* and flanking N-*myc* sequences into the first intron of N-*myc* (Moens et al., 1992). The null mutation, N-*myc*$^{BRP}$, resulted from the insertion of *neo* into a Xho site immediately downstream of the site of N-*myc* translation initiation (Stanton et al., 1990). Oligonucleotide primers that amplify allele-specific fragments are shown. Primers a and b amplify a 583-nucleotide fragment from the wild-type N-*myc* allele, primers b and d amplify a 320-nucleotide fragment from the N-*myc*$^{BRP}$ allele, and primers b and c amplify a 616-nucleotide fragment from the N-*myc*$^{9a}$ allele. Lines indicate introns, boxes indicate exons, with white, black and hatched regions indicating untranslated, translated and *neo* sequences, respectively. (B) An ethidium bromide-stained gel showing PCR products from each of the four possible genotypes produced by a N-*myc*$^{9a/+}$×N-*myc*$^{BRP/+}$ cross.

extracts of whole 11.5 days p.c. embryos from a N-*myc*$^{9a/+}$×N-*myc*$^{BRP/+}$ cross, using a monoclonal antibody that was raised against human N-Myc protein (Ikegaki et al., 1986), but which also recognizes mouse N-Myc protein. N-Myc protein runs at approximately $65\times10^3$ $M_r$. This N-*myc* antibody also showed binding to a protein of approximately $100\times10^3$ $M_r$. The relative intensities of this cross-reacting band between lanes matched the relative intensities of a ubiquitously expressed protein phosphatase, *syp* (not shown), so this band was used as a loading control in scanning densitometry. The amount of N-Myc protein in N-*myc*$^{9a/BRP}$ embryos was considerably lower than in their wild-type or singly heterozygous littermates. While N-*myc*$^{9a/9a}$ embryos had approximately 25% of wild-type levels of N-Myc protein (not shown), N-*myc*$^{9a/BRP}$ embryos had approximately 15% of wild-type levels, as determined by scanning densitometry of this and several other, similar Western blots. This is consistent with the more severe phenotype of N-*myc*$^{9a/BRP}$ embryos. N-*myc*$^{BRP+}$ embryos had approximately 50% of wild-type levels of N-Myc protein, consistent with the N-*myc*$^{BRP}$ mutation being a null mutation.

## Histological analysis of N-*myc*$^{9a/BRP}$ embryos

In order to determine more precisely the phenotype of N-*myc*$^{9a/BRP}$ embryos, histological analysis of hematoxylin and eosin-stained, sectioned embryos was performed at various stages of development. We examined a total of 42 N-*myc*$^{9a/BRP}$ embryos and 50 N-*myc*$^{+/+}$ littermates in this manner (5 N-*myc*$^{9a/BRP}$ embryos at 14.5 days p.c., 28 at 12.5 days p.c., 3 at 11.5 days p.c., and 6 at 10.5 days p.c.). Younger embryos were analyzed without sectioning, after whole-mount RNA in situ hybridization with various probes (data not shown). Occasionally, N-*myc*$^{9a/+}$ embryos were used as controls since we have previously shown that the N-*myc*$^{9a}$ mutation has no phenotypic effect in the heterozygous condition. N-*myc*$^{9a/BRP}$ embryos not used for histology were used for N-*Myc* protein analysis and RNA in situ analysis.

Before 12.5 days p.c., N-*myc*$^{9a/BRP}$ embryos were apparently normal and could not generally be distinguished from their littermates either by gross morphology or by histological examination of sectioned embryos. The first signs of lethality occurred at 12.5 days, when 12 out of 42 N-*myc*$^{9a/BRP}$ were clearly in the process of resorption. Aside from the edema in the neck area, described above, and their slightly smaller size, live N-*myc*$^{9a/BRP}$ embryos at 12.5 days were still not grossly abnormal. However careful examination of specific organ systems did reveal particular defects.

## Lung development

N-*myc*$^{9a/9a}$ mice die at birth due to a defect in lung branching morphogenesis, consistent with the observation that N-*myc* is expressed in the lung epithelium at early stages of lung development (Moens et al., 1992). Specifically, at 12.5 days p.c., when wild-type lungs have tertiary and quaternary branches, N-*myc*$^{9a/9a}$ lungs had only the beginnings of tertiarybranches. The further reduction in the amount of N-Myc protein in N-*myc*$^{9a/BRP}$ embryos led to an enhancement of this phenotype, as predicted. Branching morphogenesis in N-*myc*$^{9a/BRP}$ lungs was all but blocked (Fig. 5A,B), N-*myc*$^{9a/BRP}$ embryos having only the beginnings of secondary branches. Interestingly, the *pattern* of branching was normal, as can be observed by the presence of a rudimentary right postcaval lobe extending to the left

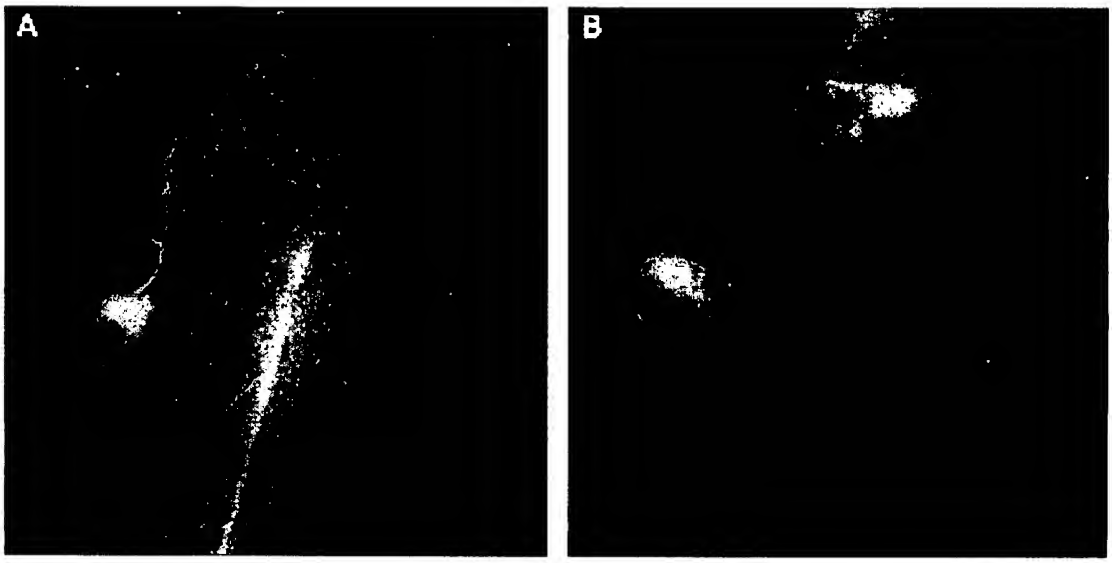


**Fig. 2.** N-$myc^{9a/BRP}$ embryos are edematous in the region of the neck. (A) Wild-type 12.5 days p.c. embryo, dorsal view. (B) N-$myc^{9a/BRP}$ embryo, showing swelling of the tissue and expanded, blood-filled jugular veins.

side of the N-$myc^{9a/BRP}$ embryo (Fig. 5B). The lungs begin their development by budding from the trachea into the surrounding mesenchyme and are visible as two pouches at 10.5 days of development. This early phase of lung development occurred normally in N-$myc^{9a/BRP}$ embryos (not shown).

In order to determine whether aspects of lung development other than the branching of the lung epithelium were affected by the reduction in N-Myc protein levels, we performed RNA in situ hybridizations on wild-type and N-$myc^{9a/BRP}$ lungs at 12.5 days p.c. (Fig. 6). *Flk-1*, which encodes a tyrosine kinase receptor for vascular endothelial

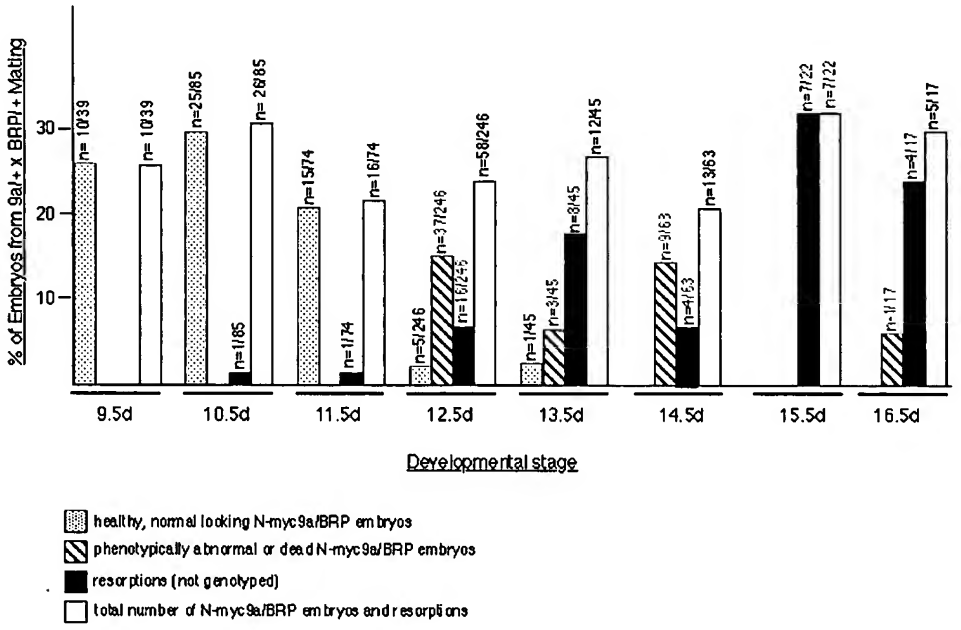


**Fig. 3.** Percentage of embryos in a N-$myc^{9a/+}$×N-$myc^{BRP/+}$ litter that are N-$myc^{9a/BRP}$, as a function of developmental stage. N-$myc^{9a/BRP}$ embryos are separated into two groups: (1) healthy, phenotypically normal embryos (stippled bars), and (2) phenotypically abnormal or dead embryos (hatched bars). Resorption sites visible in the uterus but not typed with respect to N-*myc* are included as a separate category (black bars). Note that the total of resorptions, abnormal N-$myc^{9a/BRP}$ embryos and normal N-$myc^{9a/BRP}$ embryos adds up to approximately 25% of the offspring at each time point (white bars). Numbers are given as a fraction of the total number of embryos dissected from N-$myc^{9a/+}$×N-$myc^{BRP/+}$ crosses at that developmental stage.

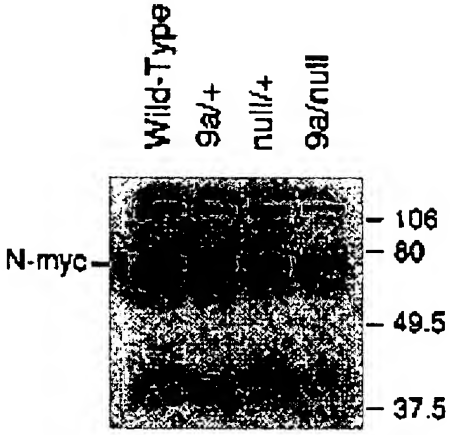


Fig. 4. Western analysis of N-Myc protein levels in extracts of 11.5 days p.c. embryos of the four possible types of offspring from an N-*myc*$^{9a/+}$×N-*myc*$^{BRP/+}$ cross. Each lane contains approximately 20 μg of protein. The N-Myc protein runs at approximately $65\times10^3$ $M_r$. A cross-reacting band appears at approximately $100\times10^3$ $M_r$.

growth factor, marks endothelial cells in the developing capillaries and blood vessels in the mouse (Yamaguchi et al., 1993; Millauer et al., 1993), and as such is expressed in a punctate manner throughout the lung mesenchyme where the lung vasculature is developing (Fig. 6C). The pattern and intensity of *flk-1* expression was not affected in N-*myc*$^{9a/BRP}$ lungs (Fig. 6G), indicating that the development of the lung vasculature is not affected by the reduction in N-Myc protein observed in N-*myc*$^{9a/BRP}$ embryos. Fig. 6B,F shows the pattern of expression of N-*myc* in wild-type and N-*myc*$^{9a/BRP}$ lungs, respectively, at 12.5 days p.c., reconfirming that expression is restricted to the lung epithelium and showing that the reduced N-Myc protein levels in N-*myc*$^{9a/BRP}$ embryos did not lead to a complete loss of N-*myc*-expressing cells in the lung epithelium. N-*myc*$^{9a/BRP}$ lungs appeared to express more than 15% of normal levels of N-*myc* RNA (Fig. 6F). This is because the N-*myc*$^{BRP}$ allele encodes a transcript that includes the entire N-*myc* open reading frame, but which contains stop codons that prevent translation of any part of the N-*myc* protein (Stanton et al., 1990). Fig. 6D,H demonstrate that levels of c-*myc* mRNA at the cellular level were not affected by the reduction in N-Myc protein in the lungs of N-*myc*$^{9a/BRP}$ embryos. C-*myc* is normally expressed in the lung mesenchyme (Fig. 6D, Hirning et al., 1991) and the pattern and level of c-*myc* expression was not altered in the N-*myc*$^{9a/BRP}$ lung, despite its reduced size (Fig. 6H).

## Heart development

The other clearly visible defect in N-*myc*$^{9a/BRP}$ embryos examined at 12.5 days p.c. was in the morphology of the heart. While N-*myc*$^{9a/BRP}$ hearts had the normal four-chamber structure, normal endocardial cushions, valves and septa, the heart was small and the myocardium was abnormally thin (Fig. 7A-D). The latter defect was particularly apparent in the 'compact', or subepicardial layer of the ventricular myocardium while the atrial myocardium and the inner trabecular layer of the ventricles were less severely affected. In mammals, trabeculation occurs early during heart development and, at later stages, growth occurs largely in the compact layer (Rumyantsev, 1991). In N-*myc*$^{9a/BRP}$ embryos, this growth of the compact layer appeared not to occur, so that the N-*myc*$^{9a/BRP}$ myocardium at 12.5 days p.c. was no thicker than it had been at 10.5 days p.c.

Occasionally, N-*myc*$^{9a/BRP}$ embryos survived until 14.5 days p.c. These embryos were always grossly abnormal, with large edemas in the neck area, and were smaller than their littermates. Fig. 7E and F compares wild-type and N-*myc*$^{9a/BRP}$ hearts at this stage, showing that the compact layer of the myocardium of the compound heterozygote was still no more developed than it had been at 10.5 days.

It seems likely that this failure in the proliferation of the ventricular myocardium leads to a failure of the circulatory system and ultimately in fetal death. The inefficient function of the heart was demonstrated by the hugely expanded

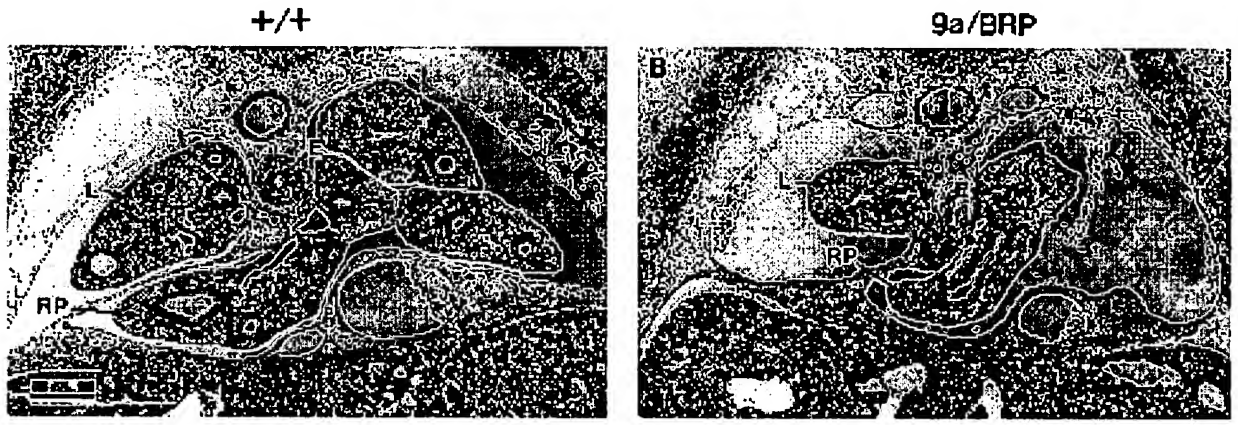


Fig. 5. Comparison of lung development in wild-type (A) and compound heterozygote N-*myc*$^{9a/BRP}$ (B) embryos at 12.5 days p.c. Comparable frontal sections were taken at the level of the right postcaval lobe. E, esophagus; L, left lung; RP; right lung, postcaval lobe. Bar, 200 μm.

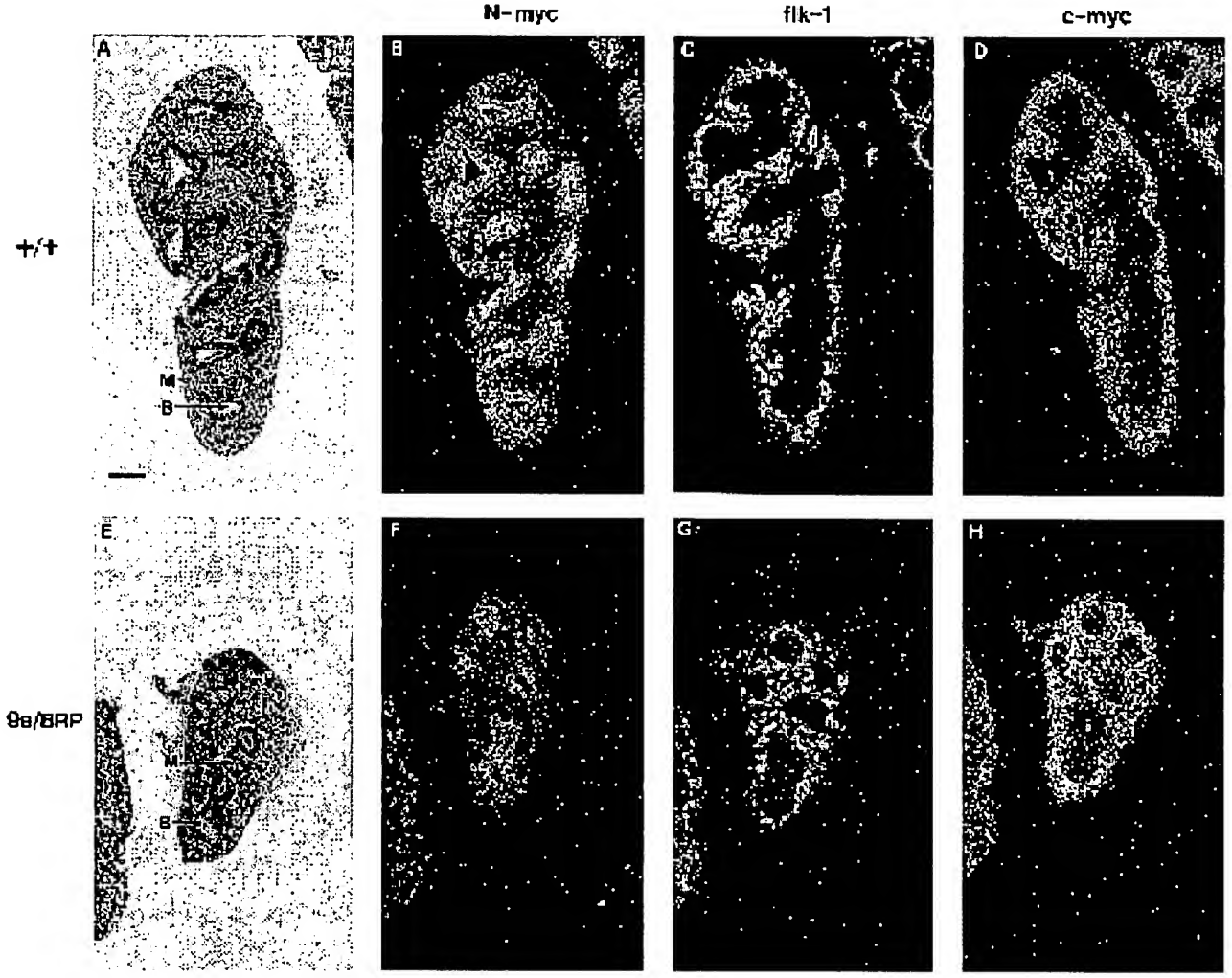


**Fig. 6.** Expression of N-*myc*, *flk-1*, and c-*myc* in wild-type and N-$myc^{9a/BRP}$ lungs at 12.5 days p.c.. (A,E) Bright-field photomicrographs of sagittal sections of the left lung of +/+ (A) and compound heterozygote N-$myc^{9a/BRP}$ (E) embryos. Wild-type (B-D) and N-$myc^{9a/BRP}$ (F-H) serial sections hybridized to the RNA probes shown, were photographed in dark field. B, bronchiole; M, lung mesenchyme. Bar, 100 μm.

jugular veins of N-$myc^{9a/BRP}$ embryos (Fig. 7G,H), since the lack of a highly muscularized ventricular myocardium pumping blood from the heart could lead to a back-up of blood in the major veins. However, it should be noted that we did not see this marked distension in the other major veins that lead into the heart.

We wished to determine whether the observed defect in the development of the compact layer of the ventricular myocardium correlated with N-*myc* expression in the heart. Expression of N-*myc* in the heart at 9.5 days p.c. has been described (Katoh et al., 1991), and we have confirmed this by whole-mount RNA in situ hybridization (data not shown). However the differentiation of trabecular and compact layers has only just begun at this stage, and N-*myc* expression was not shown to be restricted to one specific layer. Our experiments indicate that, by 10.5 days p.c., N-*myc* expression in the heart is largely confined to the compact layer and not to the trabecular layer of the developing ventricular myocardium (Fig. 8B). For comparison, α-cardiac actin, a marker of differentiated myocytes in the developing heart (Sassoon et al., 1988), is expressed in both the trabeculae and the compact layer (Fig. 8C). We observed continued N-*myc* expression in the compact layer at the time when a mutant phenotype was first observed in the heart (12.5 days p.c., Fig. 9B,G). This higher level of of N-*myc* expression in the compact layer compared to the trabecular layer is consistent with a direct role in the development of the mutant phenotype we have observed in N-$myc^{9a/BRP}$ embryos.

Considerable N-*myc* expression was detected in the compact layer of 12.5 days p.c. N-$myc^{9a/BRP}$ hearts (Fig. 9B,G) because the N-$myc^{BRP}$ mutation prevents translation but not transcription of N-*myc*, as noted above. However, as expected, the layer of N-*myc*-expressing cells was narrower in the ventricular myocardium of compound heterozygotes than in the wild-type myocardium (compare Figs 9B and

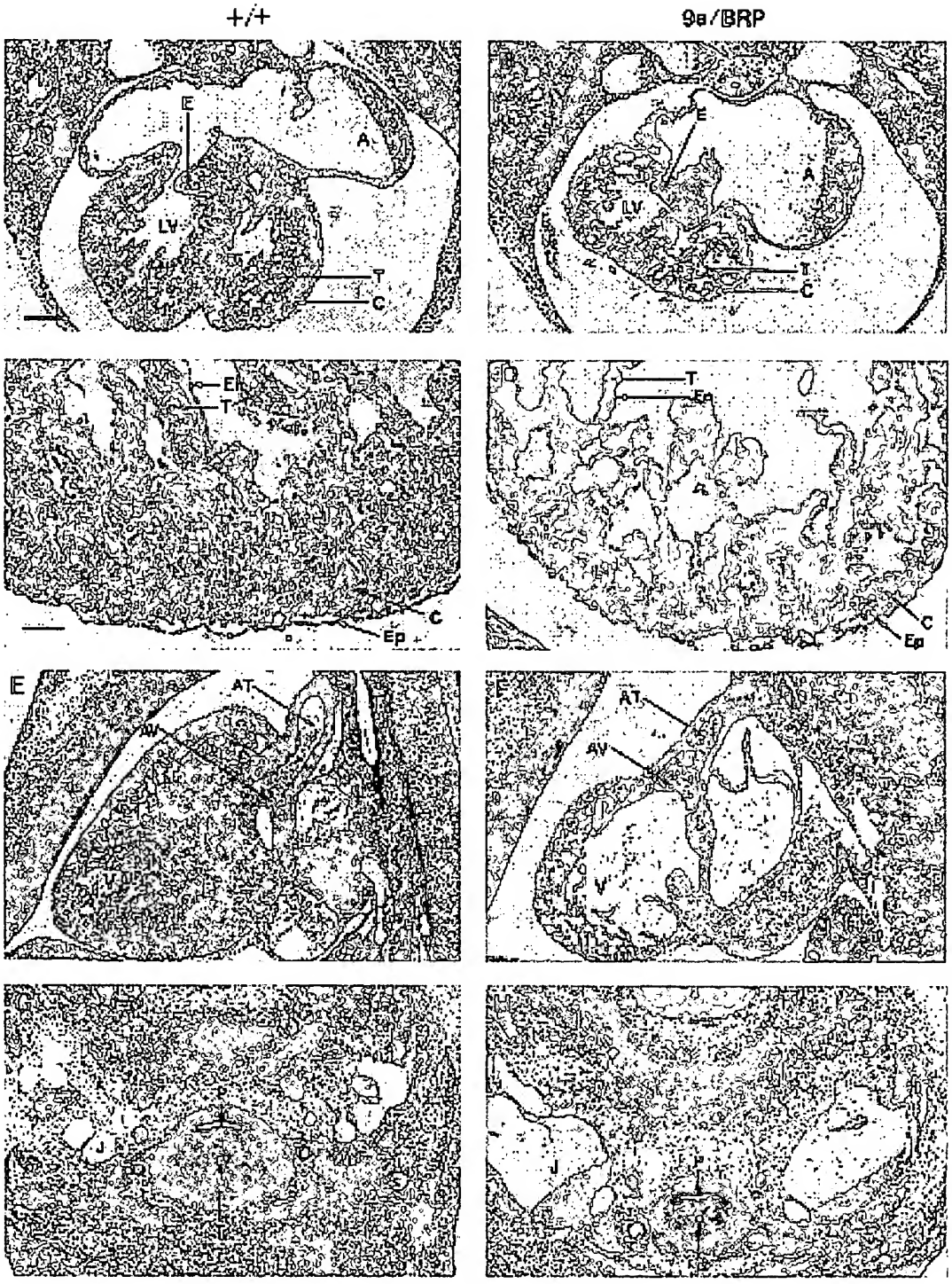


**Fig. 7.** Comparison of heart development in wild-type and compound heterozygote N-*myc*$^{9a/BRP}$ embryos at 12.5 and 14.5 days p.c. Left-hand photographs show wild-type embryos, and right-hand photographs show N-*myc*$^{9a/BRP}$ embryos. (A,B) Low-power magnification photomicrographs of frontal sections of 12.5 days p.c. hearts taken at the level of the left atrioventricular canal. (C,D) High-power magnification of the ventricle of 12.5 day hearts. (E,F) Sagittal sections of 14.5-day hearts. (G,H) Frontal sections through the jugular veins at 12.5 days. A, atrium; AT, aortic trunk; AV, aortic valve; C, compact layer; E, endocardial cushion; En, endocardium; Ep, epicardium; J, jugular veins; LV, left ventricle; P, pharynx; V, ventricle; T, trabeculae; Tr, trachea. For A,B,E,F,G,H: bar, 250 μm; for C,D: bar, 50 μm.

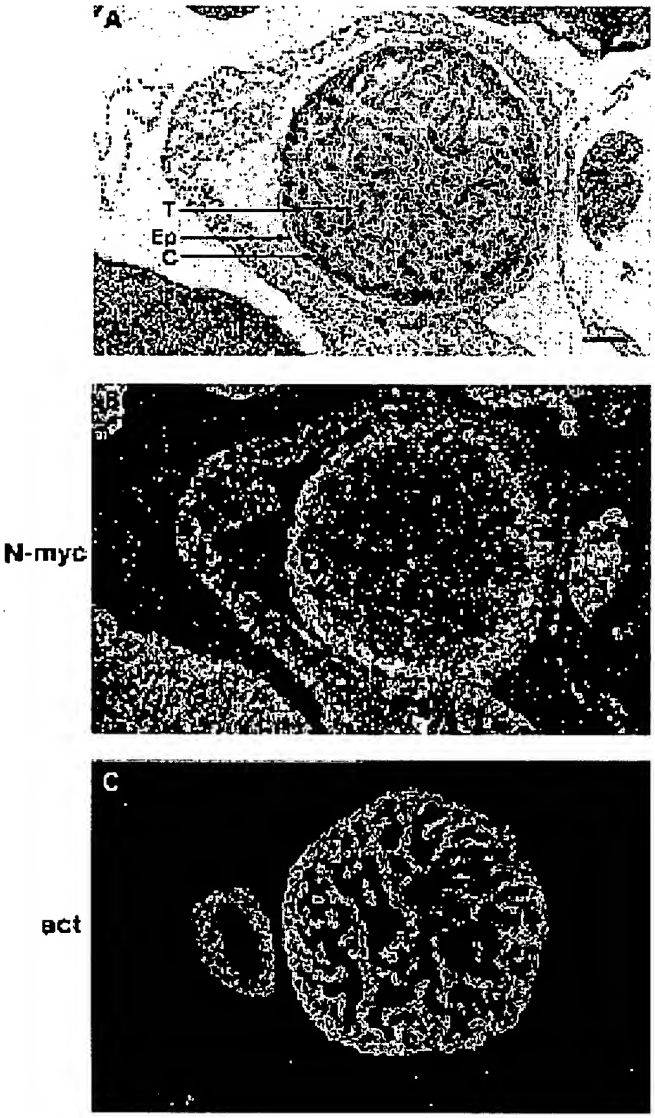


**Fig. 8.** Expression patterns of N-*myc* and α-cardiac actin in the heart at 10.5 days p.c. (A) Bright-field photomicrograph of a hematoxylin and eosin-stained parasagittal section of a wild-type ventricle. (B,C) Dark-field photomicrographs of serial sections showing N-*myc* (B) and α-cardiac actin (C) expression by RNA in situ hybridization. C, compact subepicardial layer; T, trabeculae; Ep, epicardium. Bar, 100 μm.

8B). The observation that the mutant alleles continue to be transcribed in the N-$myc^{9a/BRP}$ myocardium suggests that cells that normally express N-*myc* are present but in reduced numbers.

*Flk-1*, the endothelial cell marker described above, is expressed in the endocardium (Yamaguchi et al., 1993), which is the mesodermally derived inner lining of the heart that later contributes to the endocardial cushion and heart valves through an epithelial-to-mesenchymal transition (Fig. 9D,I; Markwald et al., 1990). The differentiation of the endocardium was not affected in N-$myc^{9a/BRP}$ embryos, as demonstrated by the continued expression of *flk-1* in the endocardium (compare Figs 10D,I and 8D,I). The N-$myc^{9a/BRP}$ genotype also did not prevent the differentiation of cardiac myocytes in the myocardium, as indicated by the strong expression of α-cardiac actin in both the compact and trabecular layers of the mutant myocardium (compare Figs 10C,H and 9C,H).

The finding that reduction in N-*myc* expression in the compact layer of the heart caused a myocyte hypoplasia evident at 12.5 days p.c. was interesting, in that overexpression of the closely related c-*myc* proto-oncogene in the heart of transgenic mice has been described to cause a hyperplasia of the myocytes which is also evident during development (Jackson et al., 1990). The normal expression pattern of c-*myc* in the heart has not been described, so the relative roles of these two genes in myocyte proliferation in vivo was not clear. Fig. 9E,J demonstrates that c-*myc* is expressed at low levels in the heart, and that its pattern of expression is different, and to some extent complementary to that of N-*myc*. While N-*myc* is expressed in the compact layer of the ventricular myocardium, c-*myc* expression is largely restricted to cells adjacent to and on the outside of the compact layer, and to isolated cells or clusters of cells adjacent to and on the inside of the compact layer. The expression on the outer surface of the heart is similar to that of *flk-1* (Fig. 8D,I) and probably represents expression in the capillaries that run between the myocardium and epicardium (Viragh and Challice, 1981). The small foci of grains on the inner surface of the myocardium also appears to represent c-*myc* expression in endocardial cells, as they are found specifically in the vicinity of red-blood-cell-containing capillaries. c-*myc* mRNA was also observed in endothelial cells lining the endocardial cushion. c-*myc* is only expressed at low levels in the myocardium itself, in spite of the fact that when it is expressed ectopically in the myocardium it causes myocytic hyperplasia (Jackson et al., 1990). In N-$myc^{9a/BRP}$ hearts, the expression of c-*myc* did not appear to be affected (Fig. 10E,J).

### Other tissues

Careful examination of N-$myc^{9a/BRP}$ embryos between 10.5 and 14.5 days p.c. gave no evidence of defects in the kidney or brain, both of which are major sites of N-*myc* expression in the embryo, and both of which are affected in N-$myc^{BRP/BRP}$ embryos (Stanton et al., 1992; Charron et al., 1992). In four N-$myc^{9a/BRP}$ embryos that survived until 14.5 days p.c., the kidneys were small but were structurally normal (not shown). N-$myc^{BRP/BRP}$ mice have also been described as having reduced genital ridges (Stanton et al., 1992) and cranial and spinal ganglia. However, these structures were indistinguishable in N-$myc^{9a/BRP}$ embryos from those of their wild-type littermates (not shown).

## DISCUSSION

We have generated mice that carry two different mutant alleles of the N-*myc* proto-oncogene in order to identify functions for N-*myc* that were not revealed in mice homozygous for each mutation individually. The N-$myc^{9a}$ allele is a leaky mutation which in the homozygous condition causes perinatal lethality due to a defect early in lung branching

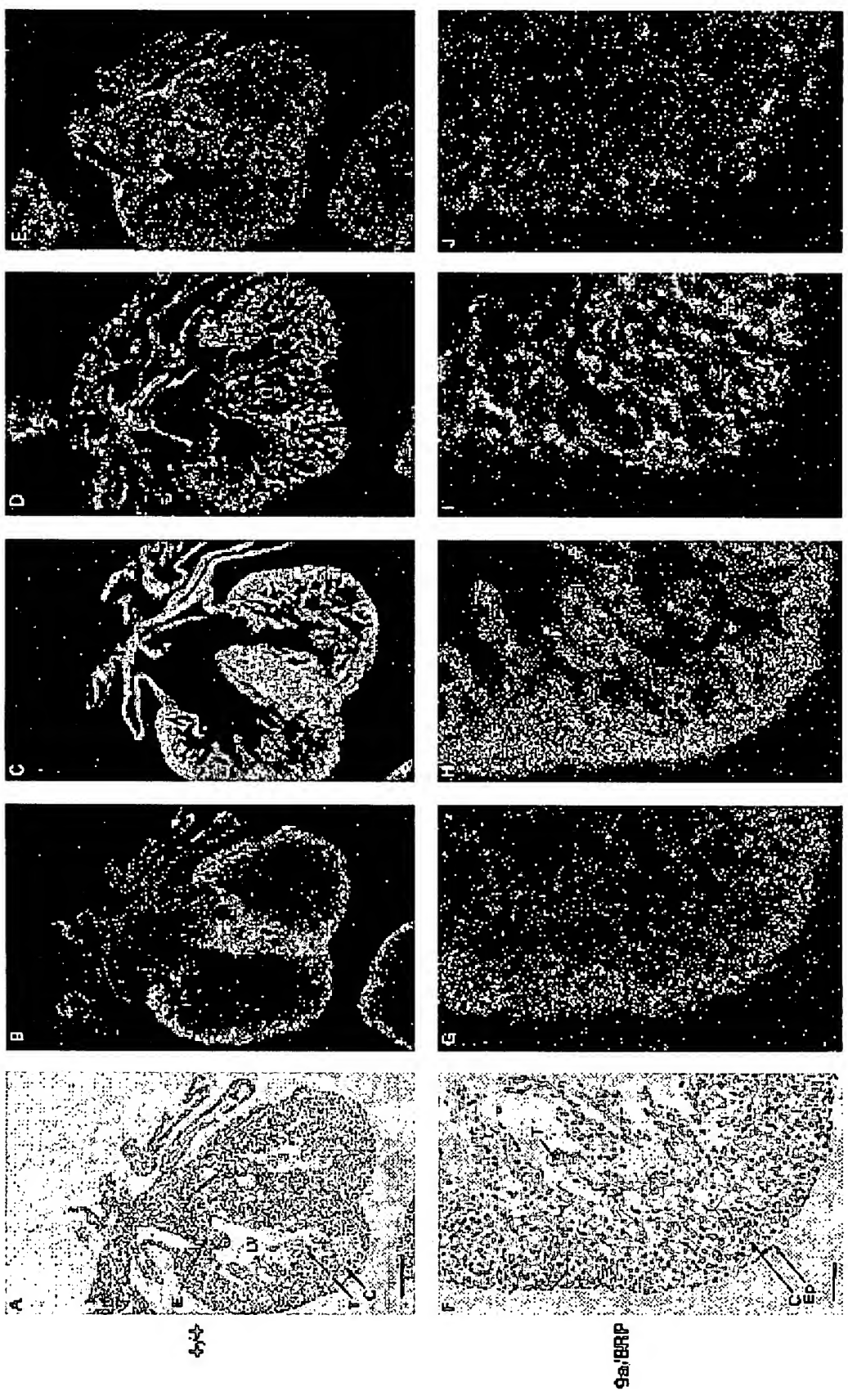


Fig. 9. Expression of N-*myc*, α-cardiac actin, *flk-1* and c-*myc* in the wild-type heart at 12.5 days p.c. (A) Bright-field photomicrograph of a hematoxylin and eosin-stained frontal section in the region of the left atrioventricular canal. (F) High power magnification of the section shown in a, through the ventricle. (B-E) Dark-field photomicrographs of serial sections hybridized to the RNA probes shown above. (G-J) High power detail of the sections shown in B-E. Act, α-cardiac actin; A, atrium; C, compact layer; E, endocardial cushion; Ep, epicardium; LV, left ventricle; T, trabeculae. For A-E, bar, 200 μm; for F-J, bar, 50 μm.

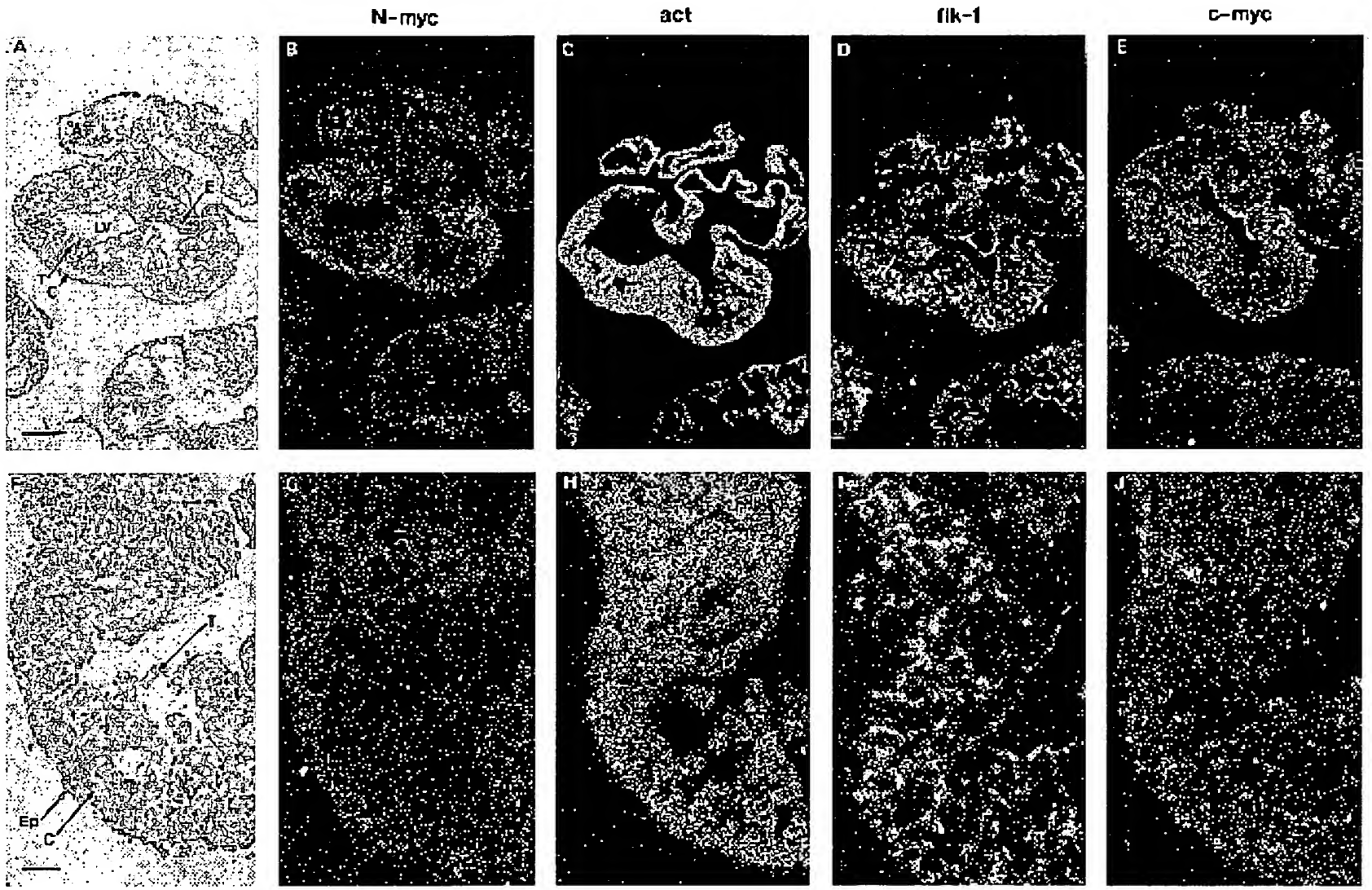


**Fig. 10.** Expression of N-*myc*, α-cardiac actin, *flk-1* and c-*myc* in compound heterozygote N-*myc*$^{9a/BRP}$ heart at 12.5 days p.c. (A) Bright-field photomicrograph of a hematoxylin and eosin-stained frontal section in a region comparable to that shown in Fig. 9. (F) High power magnification of the section shown in A, through the ventricle. (B-E) Dark-field photomicrographs of serial sections hybridized to the RNA probes shown. (G-J) High power detail of the sections shown in B-E. Act, α-cardiac actin; A, atrium; C, compact layer; E, endocardial cushion; Ep, epicardium; LV, left ventricle; T, trabeculae. For A-E, bar, 200 μm, for F-J, bar, 50 μm

morphogenesis. The levels of residual N-Myc protein (approximately 25% of normal levels) are presumably sufficient to support the normal development of other tissues in which N-*myc* normally functions. The N-$myc^{BRP}$ allele is likely to be a mutation which, in the homozygous condition, results in embryonic lethality at approximately 11.5 days p.c., at which point the epithelial component of the mesonephros, brain, lung, stomach and intestine are all hypoplastic (Stanton et al., 1992). The phenotype of N-$myc^{9a/BRP}$ compound heterozygotes is intermediate to the two homozygous mutant phenotypes, consistent with the observation that the N-$myc^{9a/BRP}$ heterozygotes contain lower levels of N-Myc protein than are present in N-$myc^{9a/9a}$ embryos. N-$myc^{9a/BRP}$ embryos die between 12 and 15 days p.c., and a number of tissues that are affected in N-$myc^{BRP/BRP}$ homozygotes, such as the kidney, brain and cranial and spinal sensory ganglia, appear to be normal. The lungs, which are the main organ affected in N-$myc^{9a/9a}$ homozygotes, are even more severely affected in N-$myc^{9a/BRP}$ embryos. Compound heterozygotes also showed a defect in the development of the compact subepicardial layer of the heart, and appeared to die from a failure of heart function caused by a hypoplasia of ventricular myocytes in the compact layer. These results indicate a critical role for N-*myc* in the development of the heart.

## N-*myc* in heart development

The reduced levels of N-Myc protein found in N-$myc^{9a/BRP}$ embryos result in a considerable thinning of the subepicardial compact layer of the myocardium by 12.5 days of development. Consistent with this phenotype, N-*myc* expression is expressed much more strongly in the compact layer of the heart at 10.5 and 12.5 days p.c. than in the trabecular layer of the myocardium or in the endothelium. Trabeculation, or formation of the myocardial projections that form a lattice of contractile cells throughout much of the ventricles of the embryonic heart, occurs early during heart development in the mouse, beginning around day 9.5 of gestation (Challice and Viragh, 1973). By a number of ultrastructural and cytochemical criteria, the myocytes within the trabeculae are more highly differentiated than the myocytes in the compact layer (Rumyantsev, 1991). Thus compact layer myocytes are more basophilic and richer in RNA, while trabecular myocytes contain more mitochondria, ribosomes and granular endoplasmic reticulum. Myofibrils in trabecular myocytes are thicker and more highly organized than in compact layer myocytes, where myofibrils are present but are scattered randomly relative to one another in the cytoplasm. Consistent with this picture is the observation that the rate of cell proliferation in the compact layer is 2- to 3-fold higher than in the trabeculae (Rumyantsev, 1977; Tokuyasu, 1990). The highly differentiated myocytes in the trabecular layer have been postulated to be responsible for the early beating of the heart while, at later stages, the thickened compact layer becomes the major contractile force. The cardiac hypoplasia that we observe in N-$myc^{9a/BRP}$ embryos is more apparent in the compact layer. This may explain our observation that embryonic lethality does not occur until later during heart development, when heart function may depend more on the compact layer than on the trabecular layer.

Our observation of N-*myc* expression in the compact layer and the absence of development in the compact layer in N-$myc^{9a/BRP}$ mice suggests that N-*myc* is required either for the proliferation of myocytes in the compact layer, and/or for preventing the differentiation of these cells, although there are other possible explanations, such as that they are dying prematurely. The simplest explanation is the former. However, the second hypothesis, in which N-*myc* expression prevents the terminal differentiation of compact layer myocytes into trabecular-type myocytes, is consistent with previous descriptions of N-*myc* expression in the embryo, in which N-*myc* expression is correlated with cells in an undifferentiated state in the kidney, brain and skin, regardless of their proliferative state, and the further differentiation of these cells is correlated with down-regulation of N-*myc* (Mugrauer et al., 1988).

In their description of embryos homozygous for a null mutation in N-*myc*, Charron et al. (1992) noted a defect in the development in the heart, visible as early as 9.5 days p.c., in which development was apparently slowed as evidenced by the absence of endocardial cushion tissue and of interatrial and interventricular septa. It was postulated that N-*myc* is involved in the generation of the inductive signal sent by the myocardium to the endocardium to induce the epithelial-to-mesenchymal transition of the endocardium, which forms these anlagen of the cardiac valves and septa. Our results confirm a function for N-*myc* in the development in the heart, but tend to support a role for N-*myc* within the myocardium itself, although this could presumably have a secondary impact on endocardial differentiation in more severe mutants. We have not observed defects in the formation of septal or endocardial cushion tissue in N-$myc^{9a/BRP}$ embryos.

## c-*myc* in heart development

When c-*myc* is overexpressed in the heart of RSV/c-*myc* transgenic mice, these mice develop a fetal cardiac myocyte hyperplasia and at birth have more than twice the normal number of cardiac myocytes (Jackson et al., 1990). This has suggested that endogenous c-*myc* may play a role in cardiac myocyte proliferation in vivo. However, we have demonstrated that c-*myc* is only expressed at low levels in the heart at 12.5 days p.c. and that this expression is largely in endothelial cells and not in the myocardium. Background levels of c-*myc* expression in the heart were also observed in mouse embryos at 13.5 days p.c. (Stanton et al., 1992) and in first trimester human embryos (Pfeifer-Ohlsson et al., 1985). N-*myc*, in contrast, is expressed at high levels in the compact layer of the ventricular myocardium at 10.5 and 12.5 days. Combined with the hypoplasia of the myocardium that we have observed in N-$myc^{9a/BRP}$ embryos, these data suggest that N-*myc* rather than c-*myc* may play a primary role in the regulation of proliferation and/or differentiation of ventricular myocytes during heart development, and that the effect of c-*myc* in these transgenic mice may reflect the possibility that in this instance c-*myc* can mimic the normal effects of N-*myc*. It has previously been observed that different *myc* family genes can cause the same tumour types in transgenic mice when they are overexpressed using identical promoters, even though this expression may be ectopic (Rosenbaum et al., 1989; Dildrop

et al., 1989; Adams et al., 1985). Furthermore, high levels of expression of one *myc* gene in transgenic mice can repress transcription of itself and of other *myc* genes (Rosenbaum et al., 1989; Dildrop et al., 1989; Adams et al., 1985). These results have suggested that at high levels, the various *myc* genes may be able to mimic each other's effects on downstream targets. This hypothesis has been strengthened by the observations that N-Myc and c-Myc proteins bind the same core DNA sequence in vitro, and that N-, L- and c-*myc* all form heterodimers with Max in vivo (Blackwood et al., 1992; Wenzel et al., 1991; Mukherjee et al., 1992), and all transform cells in culture through their interaction with Max (Mukherjee et al., 1992). We are presently crossing RSV/c-*myc* mice with the N-*myc* mutant mice to generate N-$myc^{9a/BRP}$ embryos that also express this c-*myc* transgene in the heart. If c-*myc* in these transgenics truly mimicks the normal role of N-*myc*, the cardiac myocyte hypoplasia of compound heterozygous embryos is expected to be rescued by the transgene.

Recently, Davis et al. (1993) have described the phenotype of mice that bear a null mutation in c-*myc*. These embryos die before 10.5 days p.c. and exhibit, among other abnormalities, an enlargement of the heart and a dilated, fluid-filled pericardium. This is unexpected in light of the observation, described above, that mice with ectopic expression of c-*myc* in the heart have enlarged hearts. However, it is still unclear whether the heart abnormality in the c-*myc* null mutants is a direct result of the mutation or is secondary to other defects that are causing the embryo to die.

In spite of the possibility that c-*myc* expression may be able to replace N-*myc* function, we observe no up-regulation of c-*myc* in either the compact layer of the myocardium or in the lung epithelium of N-$myc^{9a/BRP}$ mice. This may be because cross-regulation of the *myc* family genes does not normally occur in these tissues as it does when they are overexpressed in transformed cells or in transgenic mice. Stanton et al. (1992) showed that c-*myc* is expressed in the telencephalon of N-$myc^{BRP/BRP}$ embryos, and this observation was interpreted to indicate cross regulation of N-*myc* and c-*myc* in the neuroepithelium.

## N-*myc* in lung development

Mice homozygous for the N-$myc^{9a}$ mutation die at birth due to a defect in lung morphogenesis which is visible as early as 12.5 days p.c. (Moens et al., 1992). We have postulated that N-*myc* is required for the lung epithelium to respond to local inductive signals emanating from the lung mesenchyme, which cause branching to occur. N-$myc^{9a/BRP}$ embryos have more severely affected lungs, with only a rudimentary branching pattern at 12.5 days. However, the earliest events of lung development, in which two buds are induced to grow from the trachea by surrounding mesenchyme (Spooner and Wessells, 1970), occur normally in N-$myc^{9a/BRP}$ and indeed in N-$myc^{BRP/BRP}$ embryos (Stanton et al., 1992). We and others (Hirning et al., 1991; Moens et al., 1992) have shown that N-*myc* is expressed in the lung epithelium and, further, that expression is largely restricted to bronchioles and is present at very low levels in the trachea and bronchi. These results suggest that N-*myc* is involved in branching morphogenesis in the lung but not in the initial induction of budding of the tracheal epithelium. Experimental manipulations in vitro have suggested that there are different mechanisms for budding versus branching of the lung epithelium. A number of different stimuli, including salivary gland mesenchyme and bronchial mesenchyme, can induce supernumerary buds in tracheal epithelium, but only bronchial mesenchyme is able to induce those buds to branch (Wessells, 1970; Spooner and Wessells, 1970). The phenotypes of mice bearing mutations in N-*myc* provide genetic evidence for such a mechanism for lung development and provide a candidate gene that is involved in the control of one process (branching) and not the other (budding).

## Tissue-specific effects of N-myc mutant alleles

Only a subset of the tissues that normally express N-*myc* are visibly affected in N-$myc^{9a/BRP}$ embryos. N-$myc^{9a/9a}$ embryos have approximately 25% of wild-type levels of N-Myc protein and, in these embryos, the lungs and spleen are the only tissues affected (Moens et al., 1992). N-$myc^{9a/BRP}$ embryos have approximately 15% of wild-type levels of N-Myc protein and, in these embryos, the heart is also affected. However, 15% of normal levels of N-Myc protein appear to be sufficient for normal genitourinary and nervous system development. The molecular basis for this remains to be determined. It is possible that different tissues within the embryo make different amounts of normal protein relative to the amounts in wild-type embryos. We have previously attempted to correlate the relative levels of normal N-*myc* mRNA in different tissues of N-$myc^{9a/9a}$ embryos with the presence or absence of a mutant phenotype (Moens et al., 1992) and, although there were differences among the tissues examined, no strong correlation could be established. Another explanation for the tissue-specific effects of N-*myc* mutant alleles is that different tissues are affected differently by approximately the same reduction in N-Myc protein because of differences in the ratio of N-Myc protein to Max (Blackwood and Eisenman, 1991), to Max-associated proteins such as Mad and Mxi1 (Ayer et al., 1993; Zervos et al., 1993), or to other Myc proteins.

Myc proteins require dimerization with Max for DNA binding (Blackwood and Eisenman, 1991; Prendergast and Ziff, 1991; Kato et al., 1992). A number of lines of evidence have suggested that Max overexpression can inhibit transformation (Mukherjee et al., 1992; Makela et al., 1992; Prendergast et al., 1992) and transactivation (Kretzner et al., 1992; Amati et al., 1992) by *myc* genes. Mad, cloned by virtue of its ability to dimerize with Max, has been shown to compete with Myc for binding to Max, and to thereby inhibit transactivation by Myc (Ayer et al., 1993). Mxi1 (Zervos et al., 1993) and other, as yet unidentified, Max partners presumably act in a similar manner and are also likely thereby to inhibit N-*myc* function. Also, L-Myc, a poorly transforming member of the Myc family, has been shown to prevent transformation by other *myc* genes, presumably by competing for and forming less active DNA-bound complexes with Max (Mukherjee et al., 1992). In cell types where a number of Max-associated and Myc proteins compete with N-Myc protein for dimerization with Max and sites on DNA, an 85% reduction in N-Myc protein is expected to reduce the response of downstream targets of N-

Myc more strongly than in cells where there are no competitors for Max binding. Interestingly, L-*myc* is co-expressed with N-*myc* in the lung, perhaps in the same cell type (Zimmerman et al., 1986), but the two genes are not co-expressed in the kidney (Mugrauer and Ekblom, 1991), where neither the N-*myc*$^{9a/9a}$ nor the N-*myc*$^{9a/BRP}$ embryos have an abnormal phenotype. It will be interesting to compare the detailed expression patterns of the various interacting factors with the tissues affected by the N-*myc* mutations.

## Conclusions

We have generated a third N-*myc* mutant phenotype by combining leaky and null alleles in a compound heterozygote. These mice have allowed us to study the function of N-*myc* at a stage in development that is not reached in embryos homozygous for the null allele (Stanton et al., 1992) and that is not affected in embryos homozygous for the leaky allele (Moens et al., 1992). Classical genetic studies of development in a number of systems have demonstrated the importance of studying the phenotypic effects of different mutant alleles and combinations of mutant alleles in a given gene in order to determine its multiple roles in the course of development. Our results have shown that the technique of gene targeting by homologous recombination in the mouse can be used to the same ends. The clear delineation of a function for N-*myc* in both lung branching morphogenesis and myocardial development also provides target tissues in which to search for the elusive downstream genes in the N-*myc* signaling pathway.

## Note added after acceptance

Recently, a third description of embryos homozygous for a putative null allele of N-*myc* has been published (Sawai et al., 1993). The overall phenotype of these mutant embryos is very similar to those described by Stanton et al. (1992) and Charron et al. (1992), but the defect in heart development is shown to be primarily in the myocardium.

We wish to thank Dr R. Kennett for the anti-N-*myc* antibody, Dr M. Buckingham for the α-cardiac actin probe, T. Yamaguchi for the *flk-1* probe, Dr C. Asselin for the c-*myc* probe and Dr R. DePinho for the N-*myc* genomic clone from which probes for RNA in situ hybridization were subcloned. Our gratitude also to Dr Arch Perkins for his help in the phenotypic analysis of N-*myc*$^{9a/BRP}$ mutants, to Alexandra Joyner for her critical reading of the manuscript, and to Valerie Prideaux, Chi-Chong Hui, Benny Motro and Ester Ivanyi for their generous assistance in various aspects of this work. This work was supported by a Terry Fox program project grant from the National Cancer Institute of Canada. C. B. M. was supported by a Natural Sciences and Engineering Research Council of Canada 'Centennial' Scholarship and a Medical Research Council of Canada Studentship. J. R. is an International Scholar of the Howard Hughes Medical Institute and a Terry Fox Cancer Research Scientist of the National Cancer Institute of Canada. B. R. S. and L. F. P. are sponsored by the NCI-DHHS under contract NO1-CO-74101 with ABL.

## REFERENCES

**Adams, J. M., Harris, A. W., Pinkert, C. A., Corcoran, L. M., Alexander, W. S., Cory, S., Palmiter, R. D. and Brinster, R. L.** (1985). The c-myc oncogene driven by immunoglobulin enhancers induces lymphoid malignancy in transgenic mice. *Nature* **318**, 533-538.

**Alex, R., Soezeri, O., Meyer, S. and Dildrop, R.** (1992). Determination of the DNA sequence recognized by the bHLH-zip domain of the N-Myc protein. *Nucleic Acids Res.* **20**, 2257-2263.

**Amati, B., Dalton, S., Brooks, M. W., Littlewood, T. D., Evan, G. I. and Land, H.** (1992). Transcriptional activation by the human c-Myc oncoprotein in yeast requires interaction with Max. *Nature* **359**, 423-426.

**Amati, B., Brooks, M. W., Levy, N., Littlewood, T. D., Evan, G. I. and Land, H.** (1993). Oncogenic activity of the c-Myc protein requires dimerization with Max. *Cell* **72**, 233-245.

**Ayer, D. E., Kretzner, L. and Eisenman, R. N.** (1993). Mad: a heterodimeric partner for Max that antagonizes Myc transcriptional activity. *Cell* **72**, 211-222.

**Barrett, J., Birrer, M. J., Kato, G. J., Dosaka-Akita, H. and Dang, C. V.** (1992). Activation domains of L-Myc and c-Myc determine their transforming potencies in rat embryo cells. *Mol. Cell Biol.* **12**, 3130-3137.

**Blackwell, T. K., Kretzner, L., Blackwood, E. M., Eisenman, R. N. and Weintraub, H.** (1990). Sequence-specific DNA binding by the c-Myc protein. *Science* **250**, 1149-1151.

**Blackwood, E. M., Luescher, B. and Eisenman, R. N.** (1992). Myc and Max associate in vivo. *Genes Dev.* **6**, 71-80.

**Blackwood, E. M. and Eisenman, R. N.** (1991). Max: a helix-loop-helix zipper protein that forms a sequence-specific DNA-binding complex with Myc. *Science* **251**, 1211-1217.

**Bossone, S. A., Asselin, C., Patel, A. J. and Marcu, K. B.** (1992). Maz, a zinc finger protein, binds to c-MYC and C2 gene sequences regulating transcriptional initiation and termination. *Proc. Natl. Acad. Sci. USA* **89**, 7452-7456.

**Challice, C. E. and Viragh, S.** (1973). The architectural development of the early mammalian heart. *Tissue Cell* **6**, 447-462.

**Charron, J., Malynn, B. A., Robertson, E. J., Goff, S. P. and Alt, F. W.** (1990). High-frequency disruption of the N-myc gene in embryonic stem and pre-B cell lines by homologous recombination. *Mol. Cell Biol.* **10**, 1799-1804.

**Charron, J., Malynn, B. A., Fisher, P., Stewart, V., Jeannotte, L., Goff, S. P., Robertson, E. J. and Alt, F. W.** (1992). Embryonic lethality in mice homozygous for a targeted disruption of the N-myc gene. *Genes Dev.* **6**, 2248-2257.

**Davis, A. C., Wims, M., Spotts, G. D., Hann, S. R. and Bradley, A.** (1993). A null c-*myc* mutation causes lethality before 10.5 days of gestation in homozygotes and reduced fertility in heterozygous female mice. *Genes Dev.* **7**, 671-682.

**DePinho, R. A., Legouy, E., Feldman, L. B., Kohl, N. E., Yancopoulos, G. D. and Alt, F. W.** (1986). Structure and expression of the murine N-myc gene. *Proc. Natl. Acad. Sci. USA* **83**, 1827-1831.

**DePinho, R. A., Schreiber-Agus, N. and Alt, F. W.** (1991). myc family oncogenes in the development of normal and neoplastic cells. *Adv. Cancer Res.* **57**, 1-46.

**Dildrop, R., Ma, A., Zimmerman, K., Hsu, E., Tesfaye, A., DePinho, R. A. and Alt, F. W.** (1989). IgH enhancer-mediated deregulation of N-myc gene expression in transgenic mice: generation of lymphoid neoplasias that lack c-myc expression. *EMBO J.* **8**, 1121-1128.

**Frohman, M. A., Boyle, M. and Martin, G. R.** (1990). Isolation of the mouse Hox-2.9 gene; Analysis of embryonic expression suggests that positional information along the anterior-posterior axis is specified by mesoderm. *Development* **110**, 589-607.

**Garrell, J. and Campuzano, S.** (1991). The helix-loop-helix domain: A common motif for bristles, muscles and sex. *BioEssays* **13**, 493-498.

**Hirning, U., Schmid, P., Schulz, W. A., Rettenberger, G. and Hameister, H.** (1991). A comparative analysis of N-myc and c-myc expression and cellular proliferation in mouse organogenesis. *Mech. Dev.* **33**, 119-126.

**Ikegaki, N., Bukovsky, J. and Kennett, R. H.** (1986). Identification and characterization of the NMYC gene product in human neuroblastoma cells by monoclonal antibodies with defined specificities. *Proc. Natl. Acad. Sci. USA* **83**, 5929-5933.

**Ikegaki, N. and Kennett, R. H.** (1989). Glutaraldehyde fixation of the primary antibody-antigen complex on nitrocellulose paper increases the overall sensitivity of immunoblot assay. *J. Immunol. Met.* **124**, 205-210.

**Jackson, T., Allard, M. F., Sreenan, C. M., Doss, L. K., Bishop, S. P. and Swain, J. L.** (1990). The c-myc proto-oncogene regulates cardiac development in transgenic mice. *Mol. Cell Biol.* **10**, 3709-3716.

**Kato, G. J., Barrett, J., Villa-Garcia, M. and Dang, C. V.** (1990). An

amino-terminal c-Myc domain required for neoplastic transformation activates transcription. *Mol. Cell Biol.* **10**, 5914-5920.

**Kato, G. J., Lee, W. M. F., Chen, L. and Dang, C. V.** (1992). Max: Functional domains and interaction with c-Myc. *Genes Dev.* **6**, 81-92.

**Katoh, K., Kanamori, A., Wakamatsu, Y., Sawai, S. and Kondoh, H.** (1991). Tissue distribution of N-myc expression in the early organogenesis period of the mouse embryo. *Dev. Growth Diff.* **33**, 29-36.

**Kohl, N. E., Kanda, N., Schrenck, R. R., Bruns, G., Latt, S. A., Gilbert, F. and Alt, F. W.** (1983). Transposition and amplification of oncogene-related sequences in human neuroblastomas. *Cell* **35**, 359-367.

**Kretzner, L., Blackwood, E. M. and Eisenman, R. N.** (1992). Myc and Max proteins possess distinct transcriptional activities. *Nature* **359**, 426-429.

**Lee, W. H., Murphree, A. L. and Benedict, W. F.** (1984). Expression and amplification of the N-myc gene in primary retinoblastoma. *Nature* **309**, 458-460.

**Makela, T. P., Koskinen, P. J., Vastrik, I. and Alitalo, K.** (1992). Alternative forms of Max as enhancers or suppressors of Myc-Ras cotransformation. *Science* **256**, 373-377.

**Markwald, R. R., Mjaatvedt, C. H., Krug, E. L. and Sinning, A. R.** (1990). Inductive interactions in heart development: role of cardiac adherons in cushion tissue formation. *Ann. NY Acad. Sci.* **588**, 13-25.

**Millauer, B., Wizigmann-Voos, S., Schnurch, H., Martinez, R., Moller, N. P. H., Risau, W. and Ullrich, A.** (1993). High affinity VEGF binding and developmental expression suggest Flk-1 as a major regulator of vasculogenesis and angiogenesis. *Cell* **72**, 835-846.

**Moens, C. Bernelot, Auerbach, A. B., Conlon, R. A., Joyner, A. L. and Rossant, J.** (1992). A targeted mutation reveals a role for N-myc in branching morphogenesis in the embryonic mouse lung. *Genes Dev.* **6**, 691-704.

**Mugrauer, G., Alt, F. W. and Ekblom, P.** (1988). N-myc proto-oncogene expression during organogenesis in the developing mouse as revealed by in situ hybridization. *J. Cell Biol.* **107**, 1325-1335.

**Mugrauer, G. and Ekblom, P.** (1991). Contrasting expression patterns of three members of the myc family of protooncogenes in the developing and adult mouse kidney. *J. Cell Biol.* **112**, 13-25.

**Mukherjee, B., Morgenbesser, S. D. and DePinho, R. A.** (1992). Myc family oncoproteins function through a common pathway to transform normal cells in culture: cross-interference by Max and trans-acting dominant mutants. *Genes Dev.* **6**, 1480-1492.

**Nau, M. M., Brooks, B. J., Jr., Carney, D. N., Gazdar, A. F., Battey, J. F., Sausville, E. A. and Minna, J. D.** (1986). Human small-cell lung cancers show amplification and expression of the N-myc gene. *Proc. Natl. Acad. Sci. USA* **83**, 1092-1096.

**Nisen, P. D., Zimmerman, K., Cotter, S. V., Gilbert, F. and Alt, F. W.** (1986). Enhanced expression of the N-myc gene in Wilms' tumours. *Cancer Res.* **46**, 6217-6222.

**Pfeifer-Ohlsson, S., Rydnert, J., Goustin, A. S., Larsson, E., Betsholtz, C. and Ohlsson, R.** (1985). Cell-type-specific pattern of myc protooncogene expression in developing human embryos. *Proc. Natl. Acad. Sci. USA* **82**, 5050-5054.

**Prendergast, G. C., Lawe, D. and Ziff, E. B.** (1991). Association of Myn, the murine homolog of Max, with c-Myc stimulates methylation-sensitive DNA binding and Ras cotransformation. *Cell* **65**, 395-407.

**Prendergast, G. C., Hopewell, R., Gorham, B. J. and Ziff, E. B.** (1992). Biphasic effect of Max on Myc cotransformation activity and dependence on amino- and carboxy-terminal Max functions. *Genes Dev.* **6**, 2429-2439.

**Prendergast, G. C. and Ziff, E. B.** (1991). Methylation-sensitive sequence-specific DNA binding by the c-myc basic region. *Science* **251**, 186-189.

**Resar, L. M. S., Dolde, C., Barrett, J. F. and Dang, C. V.** (1993). B-myc inhibits neoplastic transformation and transcriptional activation by c-myc. *Mol. Cell Biol.* **13**, 1130-1136.

**Rosenbaum, H., Webb, E., Adams, J. M., Cory, S. and Harris, A. W.** (1989). N-myc transgene promotes B lymphoid proliferation, elicits lymphomas and reveals cross-regulation with c-myc. *EMBO J.* **8**, 749-755.

**Rumyantsev, P. P.** (1977). Interrelations of the proliferation and differentiation processes during cardiac myogenesis and regeneration. *Int. Rev. Cytol.* **51**, 187-273.

**Rumyantsev, P. P.** (1991). *Growth and Hyperplasia of Cardiac Muscle Cells*. London: Harwood Academic Publishers.

**Sassoon, D. A., Garner, I. and Buckingham, M.** (1988). Transcripts of α-cardiac and α-skeletal actins are early markers for myogenesis in the mouse embryo. *Development* **104**, 155-164.

**Sawai, S., Shimono, A., Hanaoka, K. and Kondoh, H.** (1991). Embryonic lethality resulting from disruption of both N-myc alleles in mouse zygotes. *New Biologist* **3**, 861-869.

**Sawai, S., Shimono, A., Wakamatsu, Y., Palmes, C., Hanaoka, K., and Kondoh, H.** (1993). Defects of embryonic organogenesis resulting from targeted disruption of the N-*myc* gene in the mouse. *Development* **117**, 1445-1455.

**Schwab, M., Alitalo, K., Klempnauer, K., Varmus, H. E., Bishop, J. M., Gilbert, F., Brodeur, G. M., Boldstein, M. and Trent, J.** (1983). Amplified DNA with limited homology to myc cellular oncogene is shared by human neuroblastoma cell lines and a neuroblastoma tumour. *Nature* **305**, 245-248.

**Spooner, B. S. and Wessells, N. K.** (1970). Mammalian lung development: interactions in primordium formation and bronchial morphogenesis. *J. Exp. Zool.* **175**, 445-454.

**Stanton, B. R., Reid, S. W. and Parada, L. F.** (1990). Germ line transmission of an inactive N-myc allele generated by homologous recombination in mouse embryonic stem cells. *Mol. Cell Biol.* **10**, 6755-6758.

**Stanton, B. R., Perkins, A. S., Tessarollo, L., Sassoon, D. A. and Parada, L. F.** (1992). Loss of N-myc function results in embryonic lethality and failure of the epithelial component of the embryo to develop. *Genes Dev.* **6**, 2235-2247.

**Tokuyasu, K. T.** (1990). Co-development of embryonic myocardium and myocardial circulation. In *Developmental Cardiology: Morphogenesis and Function* (ed. E. B. Clark and A. Takao), pp. 205-218. Mount Kisko, NY: Futura Publishing Co., Inc.

**Viragh, S. and Challice, C. E.** (1981). The origin of the epicardium and the embryonic myocardial circulation in the mouse. *Anat. Rec.* **201**, 157-168.

**Wenzel, A., Cziepluch, C., Hamann, U., Schuermann, J. and Schwab, M.** (1991). The N-myc oncoprotein is associated in vivo with the phosphoprotein Max(p20/22) in human neuroblastoma cells. *EMBO J.* **10**, 3703-3712.

**Wessells, N. K.** (1970). Mammalian lung development: interactions in the formation and morphogenesis of tracheal buds. *J. Exp. Zool.* **175**, 455-466.

**Wong, A. J., Ruppert, J. M., Eggleston, J., Hamilton, S. R., Baylin, S. B. and Vogelstein, B.** (1986). Gene amplification of c-myc and N-myc in small cell carcinoma of the lung. *Science* **233**, 461-464.

**Yamaguchi, T. P., Dumont, D. J., Conlon, R. A., Breitman, M. and Rossant, J.** (1993). Flk-1, a flt-1-related receptor tyrosine kinase is an early marker for heart and blood for endothelial cell precursors. *Development* in press,

**Zervos, A. S., Gyuris, J. and Brent, R.** (1993). Mxi1, a protein that specifically interacts with Max to bind Myc-Max recognition sites. *Cell* **72**, 223-232.

**Zimmerman, K., Yancopoulos, G. D., Collum, R. G., Smith, R. K., Kohl, N. E., Denis, K. A., Nau, M. M., Witte, O. N., Toran-Allerand, D., Gee, C. E., Minna, J. D. and Alt, F. W.** (1986). Differential expression of myc family genes during murine development. *Nature* **319**, 780-783.

(Accepted 30 June 1992)

Development 122, 2339-2348 (1996)
Printed in Great Britain © The Company of Biologists Limited 1996
DEV2073



# Long-term in vitro culture and characterisation of avian embryonic stem cells with multiple morphogenetic potentialities

**B. Pain[1,*], M. E. Clark[2], M. Shen[2], H. Nakazawa[3], M. Sakurai[4], J. Samarut[1] and R. J. Etches[2]**

[1]Laboratoire de Biologie Moléculaire et Cellulaire, Ecole Normale Supérieure de Lyon, UMR 49 CNRS/ENS, LA INRA 913, Lyon, France
[2]Animal and Poultry Science Department, University of Guelph, Ontario, Canada
[3]International Agency for Research on Cancer, World Health Organisation, Lyon, France
[4]National Institute of Animal Health, Tsukuba, Japan

*Author for correspondence (e-mail: bpain@ens-lyon.fr)

## SUMMARY

**Petitte, J. N., Clarck, M. E., Verrinder Gibbins, A. M. and R. J. Etches (1990; *Development* 108, 185-189) demonstrated that chicken early blastoderm contains cells able to contribute to both somatic and germinal tissue when injected into a recipient embryo. However, these cells were neither identified nor maintained in vitro. Here, we show that chicken early blastoderm contains cells characterised as putative avian embryonic stem (ES) cells that can be maintained in vitro for long-term culture. These cells exhibit features similar to those of murine ES cells such as typical morphology, strong reactivity toward specific antibodies, cytokine-dependent extended proliferation and high telomerase activity. These cells also present high capacities to differentiate in vitro into various cell types including cells from ectodermic, mesodermic and endodermic lineages. Production of chimeras after injection of the cultivated cells reinforced the view that our culture system maintains in vitro some avian putative ES cells.**

Key words: embryonic stem cells, ES cells, chicken, quail, in vitro culture

## INTRODUCTION

Experimental modification of the genome of animal species is one of the major tools to investigate embryonic development, gene expression and tissue differentiation and to develop new approaches of animal selection. Two strategies have been used to date: (1) injecting DNA into oocytes and (2) genetically engineered embryonic stem cells. In avian species the injection of DNA into oocytes successfully generated transgenic chickens but the technique is tedious and the yield of transgenic animals is low (Love et al., 1994). The development of ES cells would provide invaluable tools to manipulate the genome of avian species.

ES cells were first isolated in mouse in cultures of inner cell mass of preimplantation embryos (Evans and Kaufman, 1981; Nichols et al., 1990). When implanted into host blastocysts, these cultured cells can participate in the development of all cell lineages including the germ line. Numerous mouse ES cell lines from several strains have been isolated and maintained in vitro using various protocols (Smith, 1991; Robertson, 1987; Kawase et al., 1994). Recently, ES-like cells, designated as EG, were derived in culture from murine PGC (Matsui et al., 1992; Donovan, 1994). These cells are distinct from mouse Embryonic Carcinoma (EC) cells derived from teratocarcinomas, although the ability to contribute to all somatic tissues and the germ line is shared by ES and EG cells (Bradley et al., 1984, Robertson, 1987). Cultures of EC cells or ES-like cells have been developed to date from mink (Sukoyan et al., 1993), hamster (Doetschman et al., 1988), rat (Iannaccone et al., 1994), pig (Wheeler, 1994) and bovine (First et al., 1994), and recently from monkey (Thomson et al., 1995) and zebra fish (Sun et al., 1995). Although these cells share several features with murine ES cells, they have not yet been shown to reconstitute the germ line.

Cells derived from the early chick blastoderm will contribute to the somatic and the germ line when injected into recipient embryos to form chimeras (Thoraval et al., 1994; Carsience et al., 1993; Watanabe et al., 1992; Petitte et al., 1990). To date, blastodermal cells have been maintained in vitro for only brief periods (Etches et al., 1996) and have not yet been cytologically identified.

In the present work, we characterised embryonic stem cells derived from culture of chicken and quail embryos. The culture system allows long-term LIF-dependent growth of cells with histochemical and antigenic markers and morphogenetic potentialities similar to those described for murine ES cells.

## MATERIALS AND METHODS

### Medium

ESA medium was composed of Glasgow-MEM (Gibco, UK) containing 10% foetal bovine serum (Techgen batch no F 93246, France),

2% chicken serum (Valbiotech, France), 1% bovine serum albumin (Boëhringer, Germany), 20 ng/ml conalbumin (Sigma, USA), 1 mM sodium pyruvate (Gibco, UK), 1% non-essential amino acid (Gibco, UK), 1 μM of each nucleotide adenosine, guanosine, cytidine, uridine, thymidine (Sigma, USA), 10 mM Hepes pH 7.6 (Gibco, UK), 0.16 mM β-mercaptoethanol (Sigma, USA), 100 U/ml penicillin (Gibco, UK), 100 μg/ml streptomycin (Gibco, UK) and 10 ng/ml gentamycin (Boehringer, Germany). ESA medium refers to as medium without addition of growth factors. ESA complete medium refers to as medium supplemented with 10 ng/ml bFGF, 20 ng/ml h-IGF-1, 1% vol/vol avian-SCF and 1% vol/vol h-LIF, 1% vol/vol h-IL-11.

### Growth factors

bFGF, IGF-1, m-SCF, IL-6, CNTF and OSM were purchased from PeproTech Inc. (NJ, USA) or from R&D Systems (UK), ESGRO from Gibco (UK) and IL-11 was kindly provided by Genetics Institute (MA, USA).

For routine maintenance, some growth factors were provided as supernatants of transfected Cos-7 cells. Expression vectors of the cDNAs of avian SCF (Zhou et al., 1993), LIF (kindly provided by A. Smith, Edinburgh, UK), IL-11 and IL-6 (kindly provided by Genetics Institute, Cambridge, MA, USA) were transiently transfected in Cos-7 cells (ATCC collection) by a calcium precipitate procedure and, 3 days later, conditioned medium was filtered and stored in aliquots at −20°C.

### Anti-retinoic acid monoclonal antibody (ARMA)

ARMA hybridoma (kindly provided by Dr Ide, Tohoku University, Japan) was maintained in RPMI 1640 with 10% FBS, 1% glutamine and 100 U/ml penicillin (Gibco, UK) and 100 μg/ml streptomycin (Gibco, UK). The IgG fraction was purified from the conditioned medium through an affinity column of protein G Sepharose 4 Fast Flow (Pharmacia, Sweden).

### Preparation of culture dishes and feeder cells

Dishes (Costar or Nunc) were coated with 0.25% sterile bovine skin gelatine (Sigma, USA) solution. STO feeder cells (ATCC collection) were maintained at 37°C in 7.5% $CO_2$ in the presence of DMEM containing 4.5 g/l of glucose, 10% FBS, 2 mM L-glutamine, 100 U/ml penicillin and 100 μg/ml streptomycin, and treated with 10 μg/ml of Mitomycin C (Sigma) for 90 minutes at 37 °C or irradiated by exposure to 45 Gy (Cobalt source). Cells were used at $10^5$ cells/cm $^2$ as feeder.

### Blastodermal cells

Freshly laid unincubated eggs from Barred Rock or White Leghorn chicken or *Coturnix coturnix japonica* quail were used. The stages of the chicken embryos were estimated according to Eyal-Giladi and Kochav, (1976). Only embryos at stage IX-XI were used to prepare the blastodermal cells. The quail embryos were estimated to be at the equivalent stage X to XI at laying. The entire blastoderm was removed by gentle aspiration with a Pasteur pipette in PBS containing 5.6 mM D-glucose (PBS-G) at room temperature. Embryos were pooled at 1 embryo per ml and centrifuged at 400 *g* twice. The cell pellet was then slowly mechanically dissociated in ESA medium. Cells were seeded in ESA complete medium on gelatine precoated dish or on inactivated STO feeder cells at a final concentration of 1 embryo per ml or as indicated.

### Murine ES cells

The CGR-8 ES cell line (kindly provided by A. Smith, Edinburgh, UK) was maintained according to Smith (1991).

### Culture

The blastodermal cells were maintained at 37°C in 7.5% $CO_2$ and 90% humidity. Half of the medium was partially replaced after 24 hours in culture. Fresh blastodermal cells were added in half of the original volume of ESA complete medium 48 hours later. The medium was then changed partially (50%) on the third day and totally every day thereafter. To recover the cells, cultures were washed with PBS-G and incubated in a solution of pronase (0.025% w/v, Boehringer, Germany). Dissociated cells were seeded on new feeder cells or on gelatine-coated dishes for longer culture or laid on LSM gradient (Nycoprep, Norway). The density gradients were centrifuged at 2500 *g* and the interface was collected to isolate putative stem cells for injection into recipient embryos.

### Development of embryoid bodies in vitro

Cells were enzymatically dissociated after several passages, washed in PBS-G and plated in non-tissue-culture dishes at $10^5$ cells/ml of ESA medium without LIF. Fresh medium was added every 2 days. After 7 days, floating masses of cells were collected, washed carefully and plated into wells to allow them to attach and differentiate.

### Alkaline phosphatase reaction

After washing, cultured cells were fixed with cold 4% paraformaldehyde for 15 minutes at 4°C. Alkaline phosphatase staining solution containing 100 mM NaCl, 100 mM Tris-HCl pH 9.5, 5 mM $MgCl_2$, 1 mg/ml NBT, 0.1 mg/ml BCIP was added after washing and incubating at 37°C. The reaction was incubated for 5-30 minutes at 37°C, stopped by addition of 10 mM EDTA and the wells were washed with PBS. Coloured colonies were scored using a inverted microscope (Leica, Germany).

### Immunofluorescence analysis

Cultured cells were fixed with cold 4% paraformaldehyde for 15 minutes at 4°C. Reactions were performed with cold PBS-containing 1mg/ml BSA at 4°C. The first diluted antibody was added overnight. After washing, the second antibody DFAT-labelled (Jackson Laboratories, USA) was added for 1 hour and the cells were rewashed and then observed using an inverted Leica fluorescence microscope.

### Cytofluorometry analysis

Blastodermal cells were dissociated into a monocellular suspension with pronase and then washed and incubated in complete ESA medium for 1 hour at 37°C until the epitopes were reconstituted. Cells were then washed again in PBS-G buffer and fixed with cold 4% paraformaldehyde. Immunofluorescence was analysed using a FACSCAN (Becton Dickinson), equipped with an argon laser (488 nm) and a band pass filter at 530 nm. Data were analysed using the CellQuest program (Becton Dickinson).

### Antibodies

Antibodies were bought from the Developmental Studies Hybridoma Bank (Iowa University, USA) for SSEA-1, SSEA-3 (Solter and Knowles, 1978) and TROMA-1 (Brulet et al., 1980) or kindly provided by Dr R. Kemler (Freiburg, Germany) for ECMA-7 (Kemler et al., 1981), by Dr A. Eddy (NIH, NC) for EMA-1 and EMA-6 (Hahnel and Eddy, 1986), by Dr J. L. Duband (Paris, France) for N-CAM, by Dr C. Ziller (Nogent/Marne, France) for 13F4 and by Dr T. Graf (Heidelberg, Germany) for MEP21 (Graf et al., 1992).

### Telomerase activity

Cells from various passages were dissociated by pronase, counted and washed extensively. Cell pellet ($5\times10^4$ cells) was washed with 1 ml PBS, then with ice-cooled telomere-repeat-amplification-protocol (TRAP) washing buffer (Kim et al., 1994). Dried pellets could be stored at −80°C. 100 μl of ice-cooled TRAP lysis buffer was added to fresh or dried pellets. Samples were homogenised 3 times on ice with a plastic pestle for 1 minute each and kept on ice for 30 minutes. After the lysates were cleared by centrifugation at 70 000 revs/minute for 30 minutes at 4°C, the supernatants were collected and kept at −80°C until use. PCR-based TRAP assay was performed as described by Kim et al. (1994). The PCR products (15 μl out of 50 μl) were

electrophoresed on a 8% polyacrylamide gel, run for 1 hour at 200 V. The gel was then dried, exposed for 2-3 hours and analysed by a phosphoimager (with scanner Control) and ImageQuant soft wares, Molecular Dynamics.

### RT-PCR

CEFs (primary chicken embryonic fibroblasts), prepared as previously described (Gandrillon et al., 1989), embryoid bodies and 9-day-old embryonic blood cells were used for extraction of RNA by guanidinium thiocyanate acidic phenol procedure. 2 μg of heat-denatured total RNA were reverse transcribed for 1 hour at 37°C in 20 μl 1× RT buffer (Promega) containing 1 mM each dNTP, 200 pM $d(N)P_6$, 1 U RNAsin (Promega), 10 U M-MVL RT (Promega). 5 μl of mixture were then used for PCR amplification in 1× GoldStar buffer (Eurogentec, Belgium) containing 2 mM $MgCl_2$, 1 mM each dNTP, 1 μg of each oligonucleotide and 0.3 U Goldstar thermostable polymerase (Eurogentec, Belgium). Oligonucleotides (5′ to 3′) were purchased from Genset (France): α-globin 9(s) GCTGCTGACAAGAACAACG, α-globin 307(as) CCAATGCTTCCTGGTGGT (Dogson and E, 1983), β-globin 425(s) TCTCCCAACTGTCCGAAC, β-globin 1415(as) TAGGTGCTCCGTATCTT (Dolan et al., 1983), ε-globin 332(s) GGGTCCGTGCTCATGGTAAG, ε-globin 1575(as) CTATGGCCAGGCTGTGCTG (Dogson and Engel, 1983), c-S17 61(s) TACACCCGTCTGGGCAACGAC, c-S17 169(as) CCGCTGGATGCGCTTCATCAG (Trueb et al., 1988), c-vil 301(s) TCTGTGGCCGTGCAGCAC, c-vil 840 (as) GACCAGTATGTTCTCCAT (Bazari et al., 1988). Reaction was performed on a Perkin Elmer 9600 thermocycler during 25 cycles for c-S17, α-globin, β-globin and ε-globin and 30 cycles for c-villin. Parameters were 30 seconds at 94°C for denaturation, 30 seconds at 62°C (S17, β-globin) or 30 seconds at 60°C (α-globin and ε-globin), 30 seconds at 58°C (c-villin) for annealing and 30 seconds at 72°C for elongation. The last step of elongation was realised for 5 minutes. PCR products were analysed on an agarose gel (2% Nusieve, 1% agarose).

### Injection into recipient embryo

Stage X White Leghorn embryos from newly laid eggs were used as recipient embryos for the Barred Rock cultured cells. Recipient embryos were irradiated at 6 Gy (Cobalt source), according to Carsience et al. (1993). A small window was made on the lateral part of the egg and shell membrane was removed. Between 1 and 3 μl of cell suspension at $2\times10^5$ cells/ml were injected into the subgerminal cavity using a micropipet (20 μl borosilicate capillaries, Denmark). The window was then closed with two layers of shell membrane and sealed with cement for plastic model (Testors, USA). When dried, the closure was reinforced with one piece of Opsite (Smith and Nephew, UK), before the eggs were incubated for 3.5 days and rotated through 90° per hour. The fourth day, the well-developed embryos were transferred into a surrogate shell derived from an egg 25 g bigger than the original. The embryos were then incubated until the 20th day with rotation of 60° per hour. On the 20th day, the embryos were transferred to a hatcher. The percentage of somatic chimerism was estimated visually from the percentage of black feather pigmentation. The germ-line contribution of donor cells was assessed by mating the chimeras to Barred Rocks chickens.

## RESULTS

In an attempt to develop cultures of avian totipotent embryonic cells (potentially ES cells), we started from chicken or quail blastoderms collected at stage X according to Eyal-Giladi and Kochav (1976), which are known to contain cells that contribute to the germ line in chimeras (Carsience et al., 1993; Petitte et al., 1990). After dissociation, the cells were plated in culture, passed several times and the growing cells, designated as Chicken or Quail Embryonic Cells (CEC and QEC respectively), cultured under optimal culture conditions.

Since avian ES cells have not yet been cytologically characterised, we followed in culture the expression of several histochemical markers previously used to identify mouse ES cells.

### Cultured CEC and QEC express alkaline phosphatase activity

Alkaline phosphatase has been shown previously to be a marker of mouse PGC and teratocarcinoma cells (Strickland et al., 1980). As shown in Fig. 1A, mouse embryonic stem cells exhibit a strong endogenous alkaline phosphatase activity that is lost as these cells differentiate in culture. CEC cultures also contained alkaline-phosphatase-positive colonies as shown in Fig. 1B. Similar cells were found in QEC cultures (not shown). This positive reaction with endogenous alkaline phosphatase was used as the first criterion to identify putative non-differentiated embryonic progenitor cells and to set up culture conditions for the growth of positive cells.

### Requirement of specific growth factors and cytokines for CEC and QEC cultures

In order to define the growth factor requirement for proliferation of alkaline-phosphatase-positive cells, quail blastodermal cells were plated at a final concentration of 0.75 embryo/ ml in ESA medium on a gelatine-coated dish. Different growth factors were then added to the medium as indicated in Fig. 2A. After 3 days of culture, cells were fixed and stained for alkaline phosphatase activity and the positive colonies with a compact and round morphology were scored. When added alone, none of the factors significantly increased the number of positive colonies. However, the combination of h-LIF, bFGF and either avian or murine SCF strongly enhanced the number of alkaline-phosphatase-positive colonies. This combination of growth factors was also shown to induce the growth of alkaline-phosphatase-positive cells in CEC cultures (data not shown). These culture conditions were then used to develop routinely CEC or QEC cultures.

LIF belongs to a family of cytokines (Piquet-Pellorce et al., 1994) including ciliary neurotrophic factor (CNTF), oncostatin (OSM), interleukin-6 (IL-6) and interleukin-11 (IL-11). Since all of the members of the family of cytokines are known to provide their stimulatory transduction signal through very similar receptors and associated molecules (Kishimoto et al., 1994; Yoshida et al., 1994), the effects of OSM, CNTF, LIF; IL-11 and IL-6 on avian embryonic cells were evaluated. The cultures were grown on gelatine-coated dishes either in the presence or absence of STO feeders. The data illustrated in Fig. 2B and C indicate that, in both conditions, OSM, LIF, IL-11 and IL-6 added individually provided the greatest enhancement of the number of alkaline-positive colonies. We further observed that LIF and IL-11 had a slight synergistic effect on the growth of alkaline-phosphatase-positive cells (data not shown) and these two cytokines were then routinely used in combination. As shown in Fig. 2C, the STO feeder strongly promoted the development of alkaline-positive colonies (Fig. 2B).

When comparing different natures of feeder, it appeared that the mitomycin C or irradiated inactivated STO feeder provided the most regular and reproducible morphology and highest number of alkaline-phosphatase-positive colonies. Avian

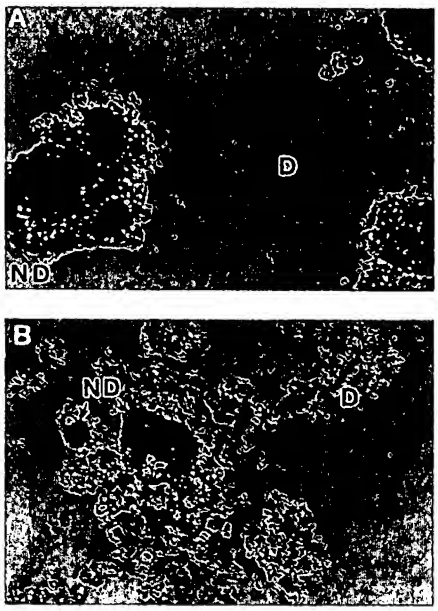


**Fig. 1.** Endogenous alkaline phosphatase activity in ES and CEC cultures. (A) Murine ES cells plated at low density. Spontaneously differentiated cells (D) were observed between areas of non-differentiated cells (ND). Cells were stained for alkaline phosphatase activity. (B) Alkaline-phosphatase-positive colonies in CEC culture grown for 5 days.

feeders, like primary CEFs or QEFs, or established cells QT6 (Moscovici et al., 1977), QBr-3 (Guilhot et al., 1993) or LMH (Kawaguchi et al, 1987) also provided high numbers of alkaline phosphatase colonies. Because of their highly transformed phenotype, QT6, QBr-3 and LMH cells are inappropriate for generation of stable adherent feeders.

### Effect of anti-retinoic acid antibody on CEC growth

Retinoic acid is a strong inducer of differentiation especially on the murine ES cells, which then rapidly lose their totipotency. In order to neutralise endogenous retinoic acid in the culture medium, we added a monoclonal antibody against retinoic acid (ARMA; Tamura et al., 1990). This procedure has been used successfully to maintain selfrenewing hematopoietic cells in culture (Gandrillon et al., 1994; unpublished data). As shown in Fig. 2D, the addition of a low concentration of this antibody (1 μg/ml) into the CEC cultures enhanced the number of alkaline-phosphatase-positive colonies. In contrast, the addition of an excess of retinoic acid ($10^{-6}$ M final) into the medium for 2 days completely abolished the presence of alkaline-phosphatase-positive colonies (data not shown). Depletion of retinoic acid using activated charcoal or anionic exchange resin strongly decreased the ability of treated sera to sustain the growth of blastodermal cells. Therefore, the media were routinely supplemented with ARMA.

### Characterisation of epitopes expressed by grown blastodermal cells

Cells maintained in CEC cultures were characterised using antibodies known to identify murine ES cells. Blastodermal cells were plated in ESA complete medium. After 5 days, the cultures were fixed and analysed for expression of both alkaline phosphatase and epitopes known to be specific of murine ES cells. Cultures of murine ES cells were used as controls. The epitopes recognised by the monoclonal antibodies ECMA-7 (Kemler et al., 1981) and SSEA-1 (Solter and Knowles, 1978) which are expressed by non-differentiated murine ES cells were also expressed on colonies in CEC cultures (Fig. 3A-D). Another antibody, SSEA-3, which recognises a specific epitope on murine ES cells also labelled CEC in culture (not shown). The EMA-1 and EMA-6 antibodies recognise epitopes specifically on primordial germ cells (PGC) in both mouse and chicken (Hahnel and Eddy, 1986; Urven et al., 1988). We observed that these two antibodies also label murine ES cells (Fig. 3E,F, and data not shown) and CEC cultures (Fig. 5G,H). In general, the epitopes expressed by undifferentiated cells disappeared following exposure to retinoic acid within 12-18 hours for ECMA-7, 24 hours for

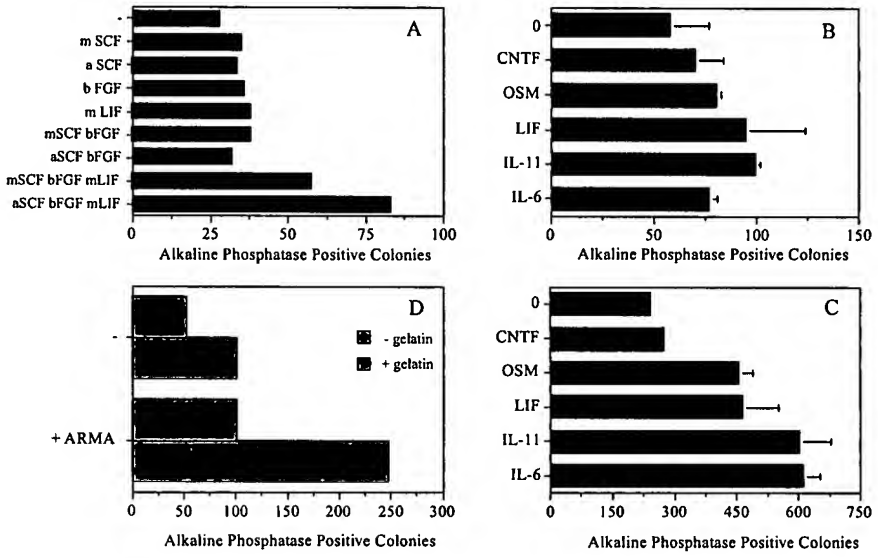


**Fig. 2.** Effect of culture conditions on the development of alkaline phosphatase colonies. (A) QEC (0.75 embryo/ml) were plated in the presence or absence of growth factors as indicated (10 ng/ml for bFGF, 10 ng/ml for mSCF, 1% V/V aSCF and 1% hLIF. After 3 days, alkaline-phosphatase-positive colonies were scored. (B,C) CEC (1 embryo/ml) were plated in complete ESA medium on gelatine-coated dishes in the presence (C) or absence (B) of inactivated STO feeder cells. Cytokines were added as indicated. After 5 days, alkaline-phosphatase-positive colonies were numbered. (D) QEC (0.75 embryo/ml) were plated in ESA complete medium in the presence or absence of ARMA (1 μg/ml) on non-coated (– gelatine) or gelatine-coated (+ gelatine) dishes. After 5 days, alkaline-phosphatase-positive colonies were numbered.

SSEA-1 and 36-48 hours for EMA-1 (not shown). The TROMA-1 antigen is specifically expressed on cells derived from differentiation-induced murine ES cells. This antigen was also observed on CEC cells 48 hours following treatment with RA.

We observed that the expression of ECMA-7, SSEA-1 and EMA-1 was localised in the alkaline-positive CEC colonies, as illustrated on Fig. 3A and B for ECMA-7. However, in primary culture, around 20 % and 40% of the alkaline-phosphatase-positive foci were labelled by the ECMA-7 and EMA-1 antibodies, respectively. As the cultures were passaged, the frequencies of ECMA-7 and EMA-1-positive foci increased strongly making the cultures phenotypically more homogeneous (not shown).

### LIF is necessary for long-term in vitro growth of CEC with ES-like markers

LIF is necessary for the growth and long-term maintenance of murine ES cells in culture (Nichols et al., 1990). We therefore tested its importance in CEC culture. CEC cultures were initiated in ESA complete medium and then passed every 4 to 7 days by subculturing. After 12 passages, one half of the culture was subcultured for several passages in identical conditions. The other half was seeded in ESA complete medium devoid of LIF and regularly subcultured in this same medium. Growth kinetics were then followed in each conditions. As shown in Fig. 4A, the cultures devoid of LIF showed a much slower growth and the number of cells was more than ten times lower than in LIF-supplemented cultures. The phenotype of the cultures was also progressively altered in the absence of LIF as the colonies became less compact, cells became flat, lost their nucleoli and increased their nucleocytoplasmic ratio. In addition, the expression of antigenic epitopes was profoundly altered by deprivation of LIF. As shown in Fig. 4B, the cultures maintained in the presence of LIF contained 10-15 times as many cells that were positive for ECMA-7, EMA-1 and SSEA-1 than cultures maintained in the absence of LIF. As a consequence, we observed that the cultures regularly maintained in the presence of LIF progressively selected a more homogeneous population of cells harbouring the ECMA-7 and EMA-1 epitopes (not shown). Growing cultures containing ECMA-7-, SSEA-1- and EMA-1-positive cells could be maintained for at least 35 passages, i.e. more than 160 days in the presence of LIF. Therefore the mammalian LIF is required for the long-term growth of avian embryonic cells and the expression of antigens characteristic of ES cells.

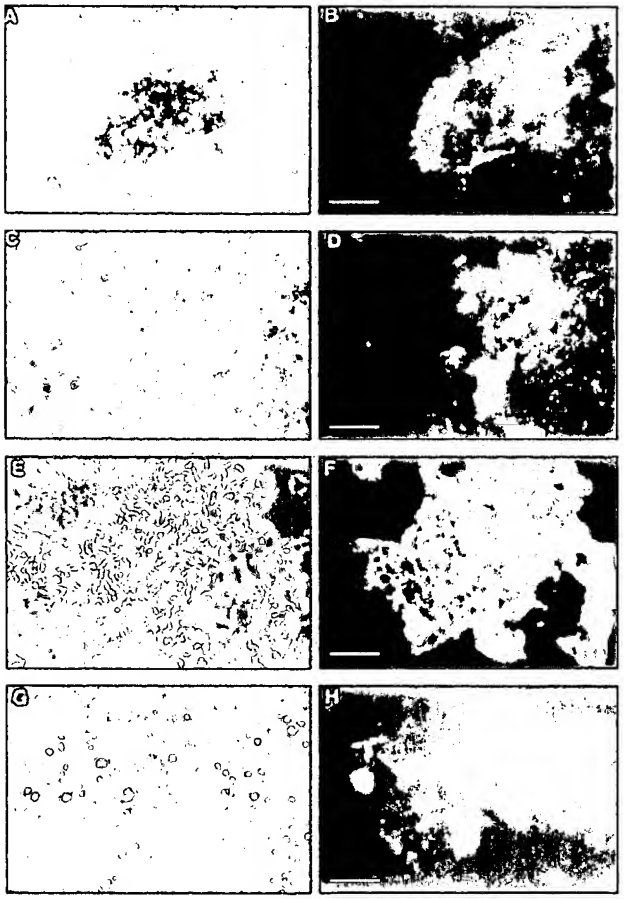


**Fig. 3.** Epitope profile of cultured CEC. Expression of various epitopes was tested on CEC after 5 days in culture. (A,B) Alkaline phosphatase staining and ECMA-7 detection; (C,D) phase contrast and SSEA-1 detection; (G,H) phase contrast and EMA-1 detection; (E,F) murine ES cells in phase contrast and stained anti-EMA-1 (scale, 20 μm).

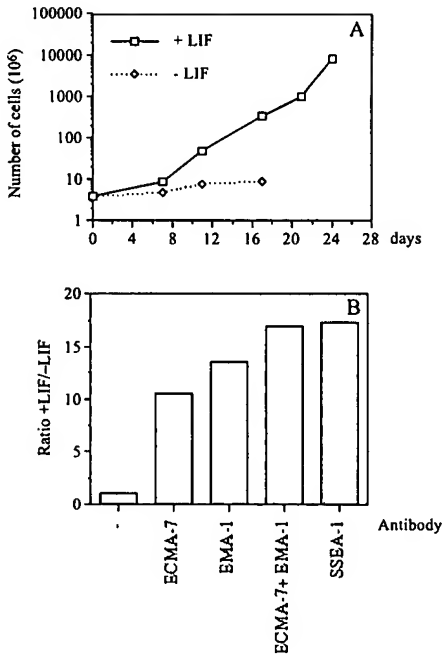


**Fig. 4.** Effect of LIF on long-term growth of CEC. (A) Kinetics of growth CEC were grown in complete ESA medium. After 11 passages, cells were plated at similar density with or without LIF. The number of cells was determined during 24 days of culture. At day 12 of culture, samples of cells were tested for epitope analysis. (B) Epitope analysis. Each bar represents the ratio between the number of labelled cells in culture with LIF versus number of labelled cells in culture without LIF.

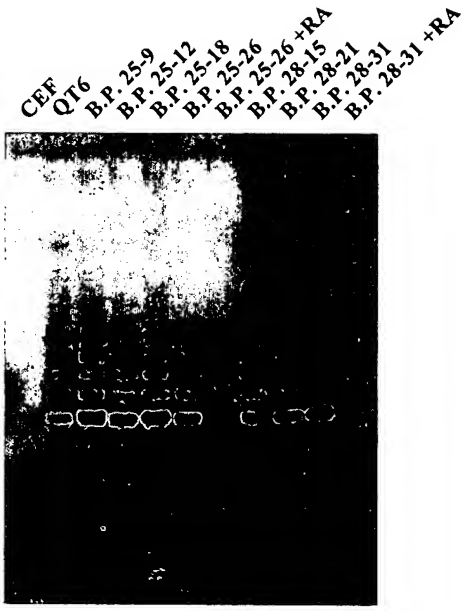


**Fig. 5.** Telomerase activity. Telomerase activity was measured in cell lysate by the TRAP assay. Primary CEF and established quail fibroblastic cells of line QT6 were used as controls. CEC from the two independent initial cultures B.P.25 and B.P.28 were collected at passages 9, 12, 18, 26 for B.P.25 and passages 12, 21 and 31 for B.P.28 and frozen until TRAP assay was performed. At passages 26 and 31 for B.P. 25 and B.P.28 respectively, cultures were treated with $10^{-6}$ M retinoic acid (+RA) for 2 days.

### CEC contain a high telomerase activity

Telomerase activity is high in human immortalised and cancer cells and in mouse germ cells and ES cells (Kim et al., 1994; Prowse and Greider, 1995; Chadeneau et al., 1995; our unpublished data). To further characterise our CEC as putative ES cells, we tested their telomerase activity and compared it to the activity of the same cells taken 48 hours after retinoic-acid-induced differentiation. Normal CEF and carcinogen-transformed established quail fibroblasts QT6 (Moscovici et al., 1977) were used on controls. The data are presented in Fig. 5.

Telomerase activity was undetectable in CEF and very high in QT6 cells. In two different CEC cultures at several passages, telomerase activity was high. This activity totally disappeared in the same cultures treated with retinoic acid. These observations therefore provide an additional marker suggesting the occurrence of stem cells in the long-term CEC cultures maintained in conditions that prevent their differentiation.

### In vitro differentiation of cultured CEC

Murine ES cells can be induced to differentiate in vitro into various lineages. One way is to remove LIF and to prevent the adhesion of ES cells to the culture dish. This procedure leads to the formation of embryonic bodies (EB) which can then be induced to attach again and to differentiate into various cell types including muscle, hematopoietic and nerve cells (Doetschman et al., 1985; Sanchez et al., 1991; Rohwedel et al., 1994; Fraichard et al., 1995).

To test whether CEC could differentiate into several lineages, we adapted this procedure to develop embryoid bodies from cultures at different passages (see Materials and Methods). When seeded in non-tissue culture dishes without LIF, CEC developed floating organised structures resembling embryoid bodies (Fig. 6). These EB-like structures could be maintained in these conditions for more than 10 days. Spontaneous differentiation occurred in these floating masses. By RT-PCR analysis (Fig. 7B), we could detect the expression of villin, an early endodermic marker (Ezzel et al., 1992; Maunoury et al., 1988). When transferred onto tissue-culture dishes, these EB-like structures attached and within a few days generated various cell phenotypes that were characterised with specific antibodies. As shown in Fig. 6C and D, some cells exhibited morphological features of nerve cells and were stained with antibodies against N-CAM. GFAP could also be detected in these conditions (not shown). Some other cells exhibited markers of muscle cells as revealed by staining with an anti-myosin antibody (Fig. 6G,H). Rhythmic contractile activity could also be observed confirming the development of functional muscle cells. Finally, immature hematopoietic cells were revealed by the expression of the antigenic marker MEP-21 (Fig. 6E,F) (Graf et al., 1992) and mature hemoglobinised erythrocytes were identified (data not shown). The presence of hemoglobin was corroborated by the detection by RT-PCR of mRNA for $\alpha$, $\beta$ and $\varepsilon$ globins (Fig. 7A). All these cell types were identified from embryoid bodies derived from cultures maintained during at least 12 passages in the presence of LIF. These results suggest that these cells were able to differentiate, at least in vitro, into endoderm, mesoderm and ectoderm lineages.

### In vivo differentiation of cultured CEC

In order to test the morphogenetic potentialities of the cultured blastodermal cells, we injected these cells into recipient embryos. For these series of experiments, the cultured CEC originated from Barred Rock black strain embryos and were maintained routinely on STO feeder in ESA complete medium. Cells were collected from cultures after 1-3 passages. 100-500 cells were injected into the subgerminal cavity of irradiated stage X White Leghorn recipient embryos. Several of the grafted embryos hatched, some of which exhibited a chimeric plumage phenotype (Fig. 8). Regardless of the number of passages, more than 50% of the hatched recipient embryos were chimeras with nearly 33% of the plumage from donor phenotype. The extent of donor phenotype in the chimeric chickens did not change appreciably with the duration of culture. To date, among a high number of chimeras tested, we have obtained 2 chickens from 7-day-old culture, which gave rise to chicks of the donor-derived phenotype demonstrating a germ-line transmission. These data thus demonstrate that some of the cultured CEC are able to provide germ-line transmission. The ability of long-term cultures to give rise to chimeric animals is currently under investigation.

## DISCUSSION

The purpose of this work was to set up culture conditions allowing the growth and characterisation of putative avian ES cells. Although the occurrence of totipotent cells in early avian embryos has been demonstrated, these cells have not yet been identified and maintained in culture. We were able to cultivate

avian embryonic cells with biochemical and biological features reminiscent of those associated with ES cells in the mouse.

Murine ES (mES) cells are characterised by their round and small shape, their large nucleus, the presence of one or two prominent nucleoli and their small cytoplasm amount (Robertson, 1987). In addition, mES cells possess strong endogenous alkaline phosphatase activity similar to the EC-derived cells (Strickland et al., 1980). In our quail and chicken blastodermal long-term cultures, we could detect large colonies of small cells, tightly packed in nests with this typical "ES-like" morphological features and a high endogenous alkaline phosphatase activity. The conclusion that the endogenous alkaline phosphatase activity, observed in colonies of blastodermal cells, reflects ES-like properties was further supported by the presence of the ECMA-7 and SSEA-1 epitopes, known to be characteristic of non-differentiated murine ES cells (Kemler et al., 1981; Solter et al., 1978). The expression of ECMA-7 and SSEA-1 epitopes has not yet been reported on avian cells and strongly suggests that ES-like features are shared by cells derived from the inner cell mass of murine embryos and the blastoderm of avian embryos. This interspecies cross reactivity suggests that these epitopes fulfil highly conserved functions in embryonic progenitor cells. The presence of EMA-1 and EMA-6 epitopes (Hahnel and Eddy, 1986) on cultured mES cells and on chicken blastodermal cells suggests that these epitopes can also be used to characterise non-differentiated embryonic stem cells (Fig. 3E,F). As soon as mES cells enter differentiation, they rapidly lose their characteristic morphology, their endogenous alkaline phosphatase activity and expression of the ECMA-7, SSEA-1 and EMA-1 epitopes. In contrast, the epitope TROMA-1 is induced in these conditions (Brulet et al., 1980). The same changes in expression of all these epitopes were observed in the CEC cultures induced to differentiate either by removal of LIF or by treatment with retinoic acid. To exclude any contamination of our CEC cultures by mES cells, we checked the karyotype of our cells. All the examined metaphases showed the expected macrochromosomes, characteristic of chicken.

The long-term growth of alkaline-phosphatase-positive cells and of cells harbouring ES-cell-specific epitopes in the CEC cultures is dependent upon specific growth factors and cytokines like bFGF, SCF and (mostly) LIF. bFGF and SCF have been previously reported to stimulate proliferation and prevent differentiation of murine EG cells and PGC (Matsui et al., 1992; Donovan, 1994). The ability of this combination to promote proliferation and to prevent differentiation is reinforced by the addition of ARMA. LIF produced either under soluble or membrane-associated form is essential for the growth of murine ES (Rathgen et al., 1990). We show here that mammalian LIF is required to maintain cells with ES features in CEC cultures. The addition of IL-11, another member of the LIF family of cytokines, also facilitates the maintenance of ES-like properties of avian blastodermal cells. The effect of LIF and IL-11 on chicken blastodermal cells may be similar to that of CNTF, which is also a member of the LIF family of cytokines and which is also active on murine ES cells (Wolf et al., 1994; Conover et al., 1993). This observation further supports the assumption that our cultures maintain embryonic stem cells very similar to ES cells. It is interesting to see that a mammalian LIF can activate a signalling pathway in avian cells, which suggests that some molecular mediators of cytokine signal transduction are structurally conserved between species. This proposal is strengthened by the recent identification of a chicken membrane receptor for GPA (GPA Rα), similar to the CNTF receptor (Heller et al., 1995).

The culture conditions, which included the use of mouse embryonic feeder cells and the inclusion of LIF, IL-11, SCF, bFGF, IGF-1 and ARMA in the medium, facilitated the proliferation of cells with an undifferentiated phenotype during more than 35 passages, i.e. more than 160 days. Life span of primary chicken cells in culture is usually limited to 30-40 generations and spontaneous immortalisation of these cells is extremely rare (Shay et al., 1991). These long-term cultures could be generated only with some strains of chickens at a frequency of more than 40% of the initial starting cultures. A

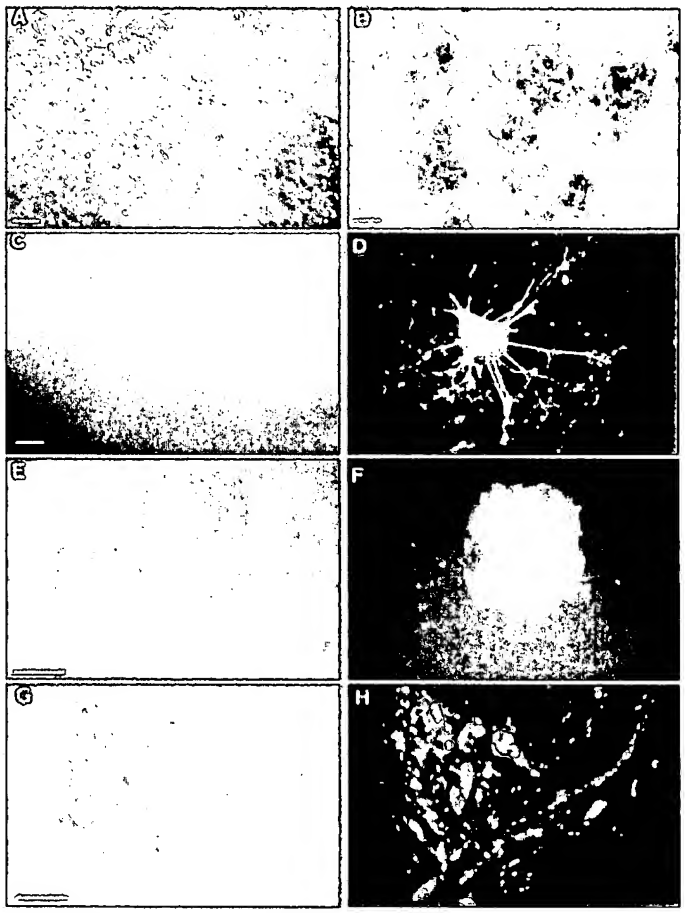


**Fig. 6.** Differentiation of CEC in culture. (A) CEC culture in the presence of LIF (scale: 10 μm); (B) embryoid body-like structures after 8 days (scale: 1.5 mm); (C,D) nerve cells in phase contrast and after staining with anti-N-CAM (scale: 1.5 mm); (E,F) hematopoietic cell colony in phase contrast and after staining with anti-MEP21 (scale, 20 μm); (G,H) muscle cells in phase contrast and after staining with anti-myosin (scale, 20 μm).

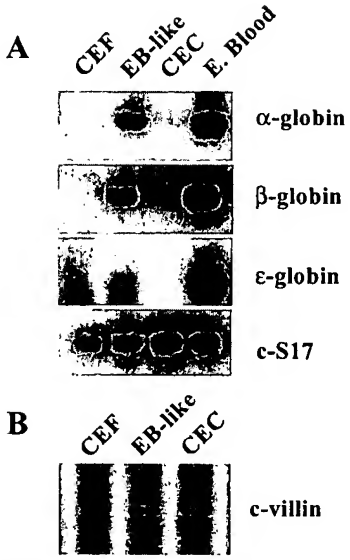


Fig. 7. RT-PCR analysis of globin and villin mRNAs. Total mRNA from CEF, EB-like structures, CEC culture and embryonic blood was tested by RT-PCR for chicken α globin, β globin and ε globin (A) and chicken villin (B). The chicken ribosomal protein S17 RNA was tested as control.

similar variation exists among mouse strains for the establishment of ES cell cultures (Kawase et al., 1994). Therefore, the culture conditions described above are likely to promote the growth of a specific kind of cells endowed with extended growth potential like ES cells. In this context, the high telomerase activity detected only in non-differentiated CEC suggests that we maintained in culture some cells with similar properties to mouse germ cells and ES cells (Kim et al., 1994; Prowse and Greider, 1995; Chadeneau et al., 1995; our unpublished data). The conclusion that the cultured CEC were undifferentiated cells was tested by providing an environment in which differentiation would be induced in vitro and in vivo. Differentiation of CEC in vitro was induced by preventing adhesion of blastodermal cells, conditions that promote formation of embryoid bodies and differentiation of cells into neural, muscular and hematopoietic lineages. Since these lineages are derived from the ectoderm and mesoderm, it can be concluded that the long-term CEC cultures contained precursors of both lineages. Moreover, detection of chicken villin mRNA in the EB-like structures suggest that cells derived from endoderm were also generated. Since the stage X embryo contains only the epiblast, it seems reasonable to conclude that cells derived in vitro from such embryo were multipotential. This conclusion was supported by the production of somatic chimeras when cultured CEC were injected into recipient embryos. Previously, similar chimeras have been produced after grafting fresh blastodermal cells and these chimeras contained donor-derived contribution to the ectoderm, mesoderm, endoderm and germ line (Kagami et al., 1995; Watanabe et al., 1992; Carsience et al., 1993; Petitte et al., 1990; Thoraval et al., 1994). In the present work, the evidence for donor-derived contributions from cultured cells was observed for the ectoderm and the germ line in at least two chickens. Even though this germ-line contribution was detected at a low frequency, it demonstrates the ability of these cells to be the equivalent of the murine ES cells. The low frequency of the germ-line transmission observed so far might have several explanations. It is possible that the germ line has already differentiated within the stage X embryo and this view is supported by the presence of cells that exhibit the SSEA-1 and EMA-1 epitopes at this stage of development (Urven et al., 1988). Alternatively, we may imagine that germ-line precursors are lost preferentially from the culture. The karyotype of chicken blastodermal cells might have been impaired during the cultivation altering the ability of CEC to generate viable germ cells, as is often observed in murine ES cell clones. The polyclonal nature of grafted cells might also block the development of functional germ cells, a hypothesis strengthened by the observation that some chimeric hens were sterile. We have been unable so far to maintain clonal growth of CEC, which could suggest that some specific avian growth factors are necessary and produced by the blastodermal cells themselves. Work is in progress to improve the culture conditions allowing clonal selection of stem cells and further work is required to improve donor-derived cells so that they can enter readily and at a high frequency into the germ line.

In conclusion, we showed in this work that cells derived from stage X avian blastoderm exhibit a morphology and epitope profiles that are similar to those of murine ES and EG cells after extended periods in culture. The cells can differentiate into at least ectodermally, mesodermally and endodermally derived tissues in vitro and into at least ectodermally derived tissues in vivo. In some cases, they can also enter and contribute to the germ line. The conditions that support prolif-

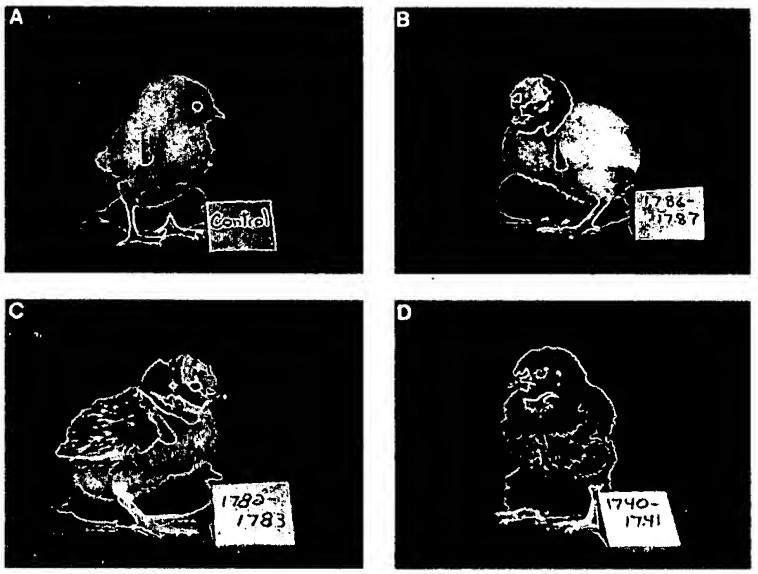


Fig. 8. Chimeric chickens generated after grafting of cultured CEC. (A) Control normal White Leghorn chick; (B-D) chimeric chicks derived from White Leghorn embryos grafted with Barred Rock CEC cultivated during 3 to 19 days.

eration and differentiation of chicken blastodermal cells have been established opening the way to isolation and utilisation of avian pluripotential embryonic stem cells.

We thank Dr A. Smith for reading the manuscript and for his comments. This work was supported by grants from ARC, INRA and the FITT programm of Region Rhone Alpes to J. S., in part by the Ontario Ministry of Agriculture, Food and Rural Affairs and an Operating Grant from the Natural Sciences and Engineering Research Council of Canada for R. E. During the tenure of this work, R. E. held the visiting Chair Marcel Merieux at ENS de Lyon, supported by the Fondation Merieux.

## REFERENCES

**Bazari, W. L., Matsudaira, P., Wallek, M., Smeal, T., Jakes, R. and Ahmed, Y. F.** (1988). Villin sequence and peptide map identify six homologs domains. *Proc. Natl. Acad. Sci. USA* **85**, 4986-4990.

**Bradley, A., Evans, M., Kaufman, M. and Robertson, E. J.** (1984). Formation of germ-line chimaeras from embryo-derived teratocarcinoma cell lines. *Nature* **309**, 255-256.

**Brulet, P., Babinet, C., Kemler, R. and Jacob, F.** (1980). Monoclonal antibodies against trophectoderm specific markers during mouse blastocyst formation. *Proc. Natl. Acad. Sci. USA* **77**, 4113-4117.

**Carsience, R. S., Clark, M. E., Verrinder Gibbins, A. M. and Etches, R. J.** (1993). Germline chimeric chickens from dispersed donor blastodermal cells and compromised recipient embryos. *Development* **117**, 669-675.

**Chadeneau, C., Siegel, P., Harley, C. B., Muller, W. J. and Bachetti, S.** (1995). Telomerase acitity in normal and malignant murine tissues. *Oncogene* **11**, 893-898.

**Conover J. C., Ip N. Y., Poueymirou W. T., Bates B., Goldfarb M. P., DeChiara T. M. and Yancopoulos, G. D.** (1993). Ciliary neurotrophic factor maintains the pluripotentiality of embryonic stem cells. *Development* **119**, 559-565.

**Doetschman, T., Williams, P. and Maeda, N.** (1988). Establishment of hamster blastocyst derived embrynoic stem (ES) cells. *Dev. Biol.* **127**, 224-227.

**Doetschman, T. C., Eistetter, H., Katz, M., Schmidt, W. and Kemler, R.** (1985). The in vitro development of blastocyst-derived embryonic stem cell lines: formation of visceral yolk sac, bood islands and myocardium. *J. Embryol. Exp. Morphol.* **87**, 27-45.

**Dogson, J. B. and Engel, J. D.** (1983). The nucleotide sequence of the adult chicken α-globin genes. *J. Biol. Chem.* **258**, 4623-4629.

**Dolan, M., Dogson, J. B. and Engel, J. D.** (1983). Analysis of the adult chicken β-globin gene. *J. Biol. Chem.* **258**, 3983-3990.

**Donovan, P. J.** (1994). Growth factor regulation of mouse primordial germ cell development. *Curr. Top. Dev. Biol.* **29**, 189-225.

**Etches, R. J., Clarck, M. E., Toner, A., Liu, G., Verrinder-Gibbins, A. M.** (1996). Contribution to somatic and germline lineages of chicken blastodermal cells maintained in culture. *Poultry Sci.* (in press).

**Evans, M. J. and Kaufman, M. H.** (1981). Establishment in culture of pluripotential cells from mouse embryos. *Nature* **292**, 154-156.

**Eyal-Giladi, H. and Kovak, S.** (1976). From cleavage to primitive streak formation: a complementary normal table and a new look at the first stages of the development of the chick; I. General Morphology. *Dev. Biol.* **49**, 321-337.

**Ezzel, R. M., Leung, J., Collins, K., Chafel, M. M., Cardozo, T. J. and Matsudaira, P. T.** (1992). Expression and localization of villin, fimbrin, and myosin I in differentiating mouse F9 teratocarcinoma cells. *Dev. Biol.* **151**, 575-585.

**First, N. L., Sims, M. M., Park, S. P. and Kent-Fisrt, M. J.** (1994). Systems for production of calves from cultures bovine embryonic cells. *Reprod. Fertil. Dev.* **6**, 553-562.

**Fraichard, A., Chassande, O., Bilbaut, G., Dehay, C., Savatier, P. and Samarut, J.** (1995). In vitro differentiation of embryonic stem cells into glial cells and functional neurons. *J. Cell. Sci.* **108**, 3181-3188.

**Gandrillon, O., Ferrand, N., Michaille, J. J., Roze, L., Zile, M. H. and Samarut, J.** (1994). C-erbAα/T3R and RARs control commitment of hemopoietic self-renewing progenitor cells to apoptosis or differentiation and are antagonized by the v-erbA oncogene. *Oncogene* **9**, 749-758.

**Gandrillon, O., Jurdic, P., Pain, B., Desbois, C., Madjar, J. J., Moscovici, M. G., Moscovici,C. and Samarut, J.** (1989). Expression of the v-erbA product, an altered nuclear hormone receptor, is sufficient to transform erythrocytic cells in vitro. *Cell* **58**, 115-121.

**Guilhot, C., Benchaibi, M., Flechon, J. E. and Samarut, J.** (1993). The 12S adenoviral E1A protein immortalizes avian cells and interacts with the avian RB product. *Oncogene* **8**, 619-624.

**Graf, T., MacNagny, K., Brady, G. and Frampton, J.** (1992). Chicken erythroid cells transformed by gag-myb-ets encoding E26 leukemia virus are multipotent. *Cell* **70**, 201-213.

**Hahnel, A. C. and Eddy, E. M.** (1986). Cell surface markers of mouse primordial germ cells defined by two monoclonal antibodies. *Gamete Research* **15**, 25-34.

**Heller, S., Finn, T. P., Huber, J., Nishi, R., Geissen, M., Puschel, A. W. and Rohrer, H.** (1995). Analysis of function and expression of the chick GPA receptor (GPAR alpha) suggests multiple roles in neuronal development. *Development* **121**, 2681-2693.

**Iannaccone, P. M., Taborn, G. U., Garton, R. L., Caplice, M. D. and Brenin, D. R.** (1994). Pluripotent embryonic stem cells from rat are capable of producing chimeraes. *Dev. Biol.* **163**, 288-292.

**Kagami, H., Clarck, M. E., Verrinder Gibbins, A. M. and Etches, R. J.** (1995). Sexual differentiation of chimeric chickens containing ZZ and ZW cells in the germline. *Mol. Reprod. Dev.* (in press).

**Kawaguchi, T., Nomura, K., Hirayama, Y. and Kitagawa, T.** (1987). Establishment and characterization of a chicken hepatocellular carcinoma cell line, LMH. *Cancer Res.* **47**, 4460-4464.

**Kawase, E., Suemori, H., Takahashi, N., Okazaki, K., Hashimoto, K. and Nakatsuji, N.** (1994). Strain difference in establishment of mouse embryonic stem (ES) cell lines. *Int. J. Dev. Biol.* **38**, 385-390.

**Kemler, R., Brulet, P., Schnebelen, M-T., Gaillard, J. and Jacob, F.** (1981). Reactivity of monoclonal antibodies against intermediate filament proteins during embryonic development. *J. Embryol. Exp. Morph.* **64**, 45-60.

**Kim, N. W., Piatyszek, M. A., Prowse, K. R., Harley, C. B., West, M. D., Ho, P. L. C., Coviello, G. M., Wright, W. E., Weinrich, S. L. and Shay, J. W.** (1994). Specific association of human telomerase activity with immortal cells and cancer. *Science* **266**, 2011-2012.

**Kishimoto, T., Taga, T. and Akira, S.** (1994). Cytokine signal transduction. *Cell* **76**, 253-262.

**Love, J., Gribbin, C., Mather, C. and Sang, H.** (1994). Transgenic birds by DNA microinjection. *Biotechnology* **12**, 60-63.

**Matsui, Y., Zsebo, K. and Hogan, B. L. M.** (1992). Derivation of pluripotential embryonic stem cells from murine primordial germ cells in culture. *Cell* **70**, 841-847.

**Maunoury, R., Robine, S., Pringault, E., Huet, C., Guenet, J. L., Gaillard, J. A. and Louvard, D.** (1988). Villin expression in the visceral endoderm and in the gut anlage during early mouse embryogenesis. *EMBO J.* **7**, 3321-3329.

**Moscovici, C., Moscovici, G. G., Jimenez, H., Lai, M. M. C., Hayman, M. J. and Vogt, P. K.** (1977). Continous tissue culture cell lines derived from chemically induced tumors of japanese quail. *Cell* **11**, 95-103.

**Nichols, J., Evans, E. P. and Smith, A. G.** (1990). Establisment of germ-line competent embryonic stem (ES) cells using differentiation inhibiting activity. *Development* **110**, 1341-1348.

**Petitte, J. N., Clarck, M. E., Verrinder Gibbins, A. M. and Etches, R. J.** (1990). Production of somatic and germline chimeraes in the chicken by transfer of early blastodermal cells. *Development* **108**, 185-189.

**Piquet-Pellorce, C., Grey, L., Mereau, A. and Heath, J. K.** (1994). Are LIF and related cytokines functionally equivalent ? *Exp. Cell. Res.* **213**, 340-347.

**Prowse, K. R. and Greider, C. W.** (1995). Developmental and tissue-specific regulation of mouse telomerase and telomere length. *Proc. Natl. Acad. Sci. USA* **92**, 4818-4822.

**Rathgen, P., Toth, S., Willis, A., Heath, J. and Smith, A. G.** (1990). Differentiation inhibiting activity is produced in matrix-associated and diffusible forms that are generated by alternate promoter usage. *Cell* **62**, 1105-1114.

**Robertson, E. J.** (1987). Embryo derived stem cell lines. In *Teratocarcinomas and Embryonic Stem Cells: A Practical Approach* (ed. E. J. Robertson), pp. 71-112. Oxford: IRL Press.

**Rohwedel, J., Maltsev, V., Bober, E., Arnold, H. H., Hescheler, J. and Wobus, A. M.** (1994). Muscle cell differentiation of embryonic stem cells reflects myogenesis in vivo: developmentally regulated expression of myogenic determination genes and functional expression of ionic currents. *Dev. Biol.* **164**, 87-101.

**Sanchez, A., Jones, W. K., Gulick, J., Doetschman, T. and Robbins, J.**

(1991). Myosin heavy chain gene expression in mouse embryoid bodies. An in vitro developmental study. *J. Biol. Chem.* **266**, 22419-22426.

**Shay, J. W., Wright, E. W. and Werbin, H.** (1991). Defining the molecular mechanisms of human immortalization. *Bioch. Bioph. Acta* **1072**, 1-7.

**Smith, A. G.** (1991). Culture and Differentiation of embryonic stem cells. *J. Tiss. Cult. Meth.* **13**, 89-94.

**Solter, D. and Knowles, B. B.** (1978). Monoclonal antibody defining a stage specific mouse embryonic antigen (SSEA-1). *Proc. Natl. Acad. Sci. USA* **75**, 5565-5569.

**Strickland, S., Smith, K. K. and Marotti, K. R.** (1980). Hormonal induction of differentiation in teratocarcinoma stem cells: generation of parietal endoderm by retinoic acid and dibutyryl cAMP. *Cell* **21**, 347-355.

**Sukoyan, M. A., Vatolin, S. Y., Golubitsa, A. N., Zhelezova, A. I., Semenova, L. A. and Serov, O. L.** (1993). Embryonic stem cells derived from morulae, inner cell mass, and blastocysts of mink: comparisons of their pluripotencies. *Mol. Repod. Dev.* **36**, 148-158.

**Sun, L., Bradford, C. S., Ghosh, C., Collodi, P. and Barnes, D. W.** (1995). ES-like cells cultures derived from early zebrafish embryos. *Mol. Mar. Biol. Biotechnol.* **4**, 193-199.

**Tamura, K., Ohsugi, K. and Ide, H.** (1990). Distribution of retinoids in the chick limb bud: analysis with monoclonal antibody. *Dev. Biol.* **140**, 20-26.

**Thomson, J. A., Kalishman, J., Golos, T. G., Durning, M., Harris, C. P., Becker, R. A. and Hearn, J. P.** (1995). Isolation of a primate embryonic stem cell line. *Proc. Natl. Acad. Sci. USA* **92**, 7844-7848.

**Thoraval, P., Lasserre, F., Coudert, F. and Dambrine, G.** (1994). Somatic and germline chicken chimeras obtained from brown and white leghorns by transfer of early blastodermal cells. *Poultry Sci.* **73**, 1897-1905.

**Trueb, B., Schreier, T. Winterhalter, K. H. and Strehler, E. E.** (1988). Sequence of a cDNA clone encoding chicken ribosomal protein S17. *Nucl. Acids. Res.* **16**, 4723-4728.

**Urven, L. E., Erickson, C. A., Abbott, U. K. and McCarrey, J. R.** (1988). Analysis of germ line development in the chick embryo using an anti mouse ES cell antibody. *Development* **103**, 299-304.

**Watanabe, M., Kinutani, M., Naito, M., Ochi, O. and Takashima, Y.** (1992). Distribution analysis of transferred donor cells in avian blastodermal chimeras. *Development* **114**, 331-338.

**Wheeler, M. B.** (1994). Development and validation of swine embryonic stem cells: a review. *Reprod. Fertil. Dev.* **6**, 563-568.

**Wolf, E., Kramer, R., Polejaeva, I., Thoenen, H. and Brem, C.** (1994). Efficient generation of chimaeric mice using embryonic stem cells after long-term culture in the presence of ciliary neurotrophic factor. *Transgenic Res.* **3**, 152-158.

**Yoshida, K., Chambers, I., Nichols, J., Smith, A., Saito, M., Yasukawa, K., Shoyab, M., Taga, T. and Kishimoto, T.** (1994). Maintenance of the pluripotential phenotype of embryonic stem cells through direct activation of gp130 signalling pathways. *Mech. Develop.* **45**, 163-171.

**Zhou, J. H., Ohtaki, M. and Sakurai, M.** (1993). Sequence of a cDNA encoding chicken stem cell factor. *Gene* **127**, 269-270.

(Accepted 24 May 1996)

Anat. Histol. Embryol. 31, 169–186 (2002)

ISSN 0340–2096

Department of Molecular Animal Breeding and Biotechnology

# Pluripotent Stem Cells – Model of Embryonic Development, Tool for Gene Targeting, and Basis of Cell Therapy

KATJA PRELLE*, NICOLA ZINK and ECKHARD WOLF

Address of authors: Department of Molecular Animal Breeding and Biotechnology, Ludwig Maximilian University Munich, Hackerstrasse 27, 85764 Oberschleissheim, Germany; *Corresponding author: Tel.: + 49-89-31573223; Fax: + 49-89-3152799; e-mail: k.prelle@gen.vetmed.uni-muenchen.de

With 7 figures

Received November 2001; accepted for publication November 2001

## Summary

Embryonic stem (ES) cells are pluripotent cell lines with the capacity of self-renewal and a broad differentiation plasticity. They are derived from pre-implantation embryos and can be propagated as a homogeneous, uncommitted cell population for an almost unlimited period of time without losing their pluripotency and their stable karyotype. Murine ES cells are able to reintegrate fully into embryogenesis when returned into an early embryo, even after extensive genetic manipulation. In the resulting chimeric offspring produced by blastocyst injection or morula aggregation, ES cell descendants are represented among all cell types, including functional gametes. Therefore, mouse ES cells represent an important tool for genetic engineering, in particular via homologous recombination, to introduce gene knock-outs and other precise genomic modifications into the mouse germ line. Because of these properties ES cell technology is of high interest for other model organisms and for livestock species like cattle and pigs. However, in spite of tremendous research activities, no proven ES cells colonizing the germ line have yet been established for vertebrate species other than the mouse (Evans and Kaufman, 1981; Martin, 1981) and chicken (Pain et al., 1996).

The *in vitro* differentiation capacity of ES cells provides unique opportunities for experimental analysis of gene regulation and function during cell commitment and differentiation in early embryogenesis. Recently, pluripotent stem cells were established from human embryos (Thomson et al., 1998) and early fetuses (Shamblott et al., 1998), opening new scenarios both for research in human developmental biology and for medical applications, i.e. cell replacement strategies. At about the same time, research activities focused on characteristics and differentiation potential of somatic stem cells, unravelling an unexpected plasticity of these cell types. Somatic stem cells are found in differentiated tissues and can renew themselves in addition to generating the specialized cell types of the tissue from which they originate. Additional to discoveries of somatic stem cells in tissues that were previously not thought to contain these kinds of cells, they also appear to be capable of developing into cell types of other tissues, but have a reduced differentiation potential as compared to embryo-derived stem cells. Therefore, somatic stem cells are referred to as multipotent rather than pluripotent. This review summarizes characteristics of pluripotent stem cells in the mouse and in selected livestock species, explains their use for genetic engineering and basic research on embryonic development, and evaluates their potential for cell therapy as compared to somatic stem cells.

## Introduction

### Pluripotent Cell Lines in the Mouse

In the very first studies conducted, pluripotent cells were isolated from teratocarcinomas, complex tumours containing a mixture of differentiated cell types including derivatives of all germ layers and undifferentiated cells, which are termed embryonic carcinoma (EC) cells due to their resemblance of early embryonic cells (Martin and Evans, 1975). EC cells are capable of multilineage differentiation but their value as a developmental model is undermined by aneuploid karyotypes which are frequently observed in EC cells, most likely due to their expansion in tumours (Martin, 1980). Consequently, EC cells rarely colonize the germ line of chimeric mice produced by blastocyst injection (Illmensee and Mintz, 1976), limiting the use of this cell type for genetic engineering. Nevertheless, studies using EC cells laid the intellectual and experimental groundwork for the establishment of embryonic stem (ES) cell cultures. Since teratocarcinomas could be generated experimentally by ectopic transplantation of mouse embryos, the next logical step was putting early embryos directly into culture, thereby avoiding a tumour environment.

Since the first murine ES cell lines sharing many features with EC cell lines were established from the inner cell mass (ICM) of blastocysts (Evans and Kaufman, 1981; Martin, 1981), others have been derived from 8-cell embryos, dissociated blastomeres of morulae, or from the pluripotent cell population of the primitive ectoderm of implantation-delayed blastocysts (reviewed in Prelle et al., 1999) (Fig. 1). ES cells correspond roughly to the cells of the early epiblast, but they are not identical to them. This is evident by the fact that ES cells depend on leukaemia inhibitory factor (LIF) *in vitro*, whereas embryos deficient for LIF or its receptor show normal development. Nevertheless, there is a requirement for LIF signalling by the ICM of delayed blastocysts (Nichols et al., 2001). Most ES cell lines were isolated from embryos of the inbred strain 129 and its various substrains. There is a strong genetic component of ES cell derivation, proving isolation of ES cell lines from other mouse strains to be very problematic (Smith, 2001). Nevertheless, selection strategies have been developed to allow isolation of ES cells also from embryos with a normally non-permissive genetic background (McWhir et al., 1996). However, usually only a minority of embryos from the same strain gives rise to ES cells, suggesting that some epigenetic event is rate-limiting.

Standard conditions for the establishment and maintenance of mouse ES cells include the use of feeder layers (mostly

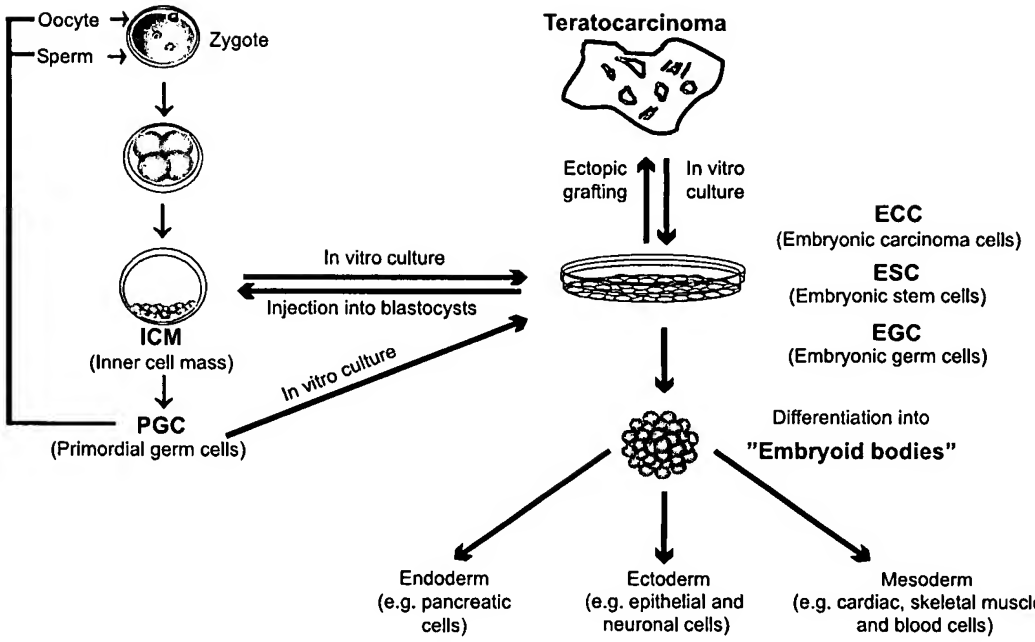


Fig. 1. Origin and determination of pluripotent cells. Embryonic stem (ES) cells are established from isolated ICM cells of blastocysts, embryonic carcinoma (EC) cells originate from malignant teratocarcinomas, and embryonic germ (EG) cells are developed of PGCs of fetal genital ridges. They can be reintroduced into host embryos via blastocyst injection and contribute to all developing tissues including the germ line. They differentiate into malignant tumours after subcutaneous injection into nude mice and differentiate *in vitro* via embryoid bodies into cells of all three germ layers.

primary mouse embryonic fibroblasts) and supplementation of culture media with LIF (Smith et al., 1988). This cytokine is able to maintain pluripotency of ES cells also in the absence of feeder cells (Nichols et al., 1990). Similarly, other cytokines acting through the gp130 signal transduction pathway, including interleukin-6 (IL-6), oncostatin M and ciliary neurotrophic factor, have been shown to preserve the undifferentiated status of mouse ES cells (Conover et al., 1993; Nichols et al., 1994; Rose and Bruce, 1994; Wolf et al., 1994).

The establishment of an ES cell culture entails the liberation of pluripotent epiblast cells from their fated differentiation. However, the point of embryo development at which the capacity to generate ES cells is lost, is not clear yet. With egg cylinder stages of mouse embryos, no successful ES cell derivation is reported to date, although these stages give rise to teratocarcinomas after transplantation under the renal capsule (Solter et al., 1970). Possibly the epithelial organization of the egg cylinder imposes constraints on epiblast cells that may be disrupted on ectopic grafting but are not erased in primary cultures. The arrest of normal development, e.g. during diapause, might preconfigure the epiblast cells for continued self-renewal by activating cytokine signalling for maintenance of pluripotency (Smith, 2001).

The fact that testicular teratocarcinomas can originate spontaneously from germ cells, forced experiments on isolation and prolonged *in vitro* culture of germ cells to obtain a third class of pluripotent cell lines. In mice these cells are derived from primordial germ cells (PGCs), which originate from the proximal epiblast of the egg cylinder. It is the proximal location of the epiblast cells that is critical for germ cell fate, rather than any intrinsic properties (Tam and Zhou, 1996). The specification depends on signals, such as bone morphogenetic protein (BMP)-4, originating from the extraembryonic ectoderm in contact with the proximal epiblast (Lawson et al., 1999). In the mouse, approximately 100 PGCs can be detected in the extraembryonic mesoderm at day 7 *post coitum* (p.c.). They migrate from the base of the allantois through the hindgut epithelium and the dorsal mesentery into the gonadal anlage (Eddy et al., 1981). After a period of intragonadal mitotic proliferation until day 12.5 p.c., the male germ cells enter a quiescent period of mitotic arrest in the testis, while the female PGCs undergo rapid mitotic divisions before entering the meiotic arrest in the ovary (reviewed in Wylie, 1993).

When PGCs begin migration into the genital ridge they contain genomic imprints, with one of the two X chromosomes being inactive in female PGCs (Tam et al., 1994). Demethylation resulting in the erasure of imprints as well as reactivation of the inactive X chromosome occurs as soon as the PGCs enter the genital ridge (Mann, 2001). Imprinting is an epigenetic modification acquired in the germ line that causes heritable but potentially reversible modifications of DNA, primarily methylation of CpG (cytosine-guanine) dinucleotides, that can ensure efficient silencing of genes (reviewed in Surani, 2001). Thus, asymmetric paternal and maternal imprints are inherited after fertilization and endure stably into adults (Ferguson-Smith and Surani, 2001). The approximate number of 45 imprinted genes identified in mice and humans are organized in clusters and contain CpG-rich differentially methylated regions (DMRs), which ensure monoallelic expression of imprinted genes (Reik and Walter, 2001).

Embryonic germ (EG) cells can be derived from pre- and post-migratory PGCs by using a combination of LIF, basic

fibroblast growth factor (bFGF), and Kit ligand (= Stem cell factor, SCF) (acting through the c-Kit receptor) in the culture medium (Matsui et al., 1992; Resnick et al., 1992). However, once established, they apparently no longer require bFGF for their growth, but Stem cell factor (SCF) (Stewart et al., 1994). EG cells are in many aspects indistinguishable from blastocyst-derived ES cells, including their capacity to differentiate *in vitro* (Rohwedel et al., 1996) and to colonize the germ line of chimeric mice (Matsui et al., 1992). However, irregularities in imprinting arising from their germ cell origin can comprise full developmental potential (Solter, 1998). The lack of imprints in EG cells, which, in contrast to ES cells, retain the unique capacity of PGCs to erase imprints, may cause developmental anomalies, such as aberrant growth and skeletal abnormalities in chimeras (Tada et al., 1998). Very recently the epigenetic state of ES cells was also found to be extremely unstable, as evidenced by remarkable differences in DNA methylation between various ES cell lines and even between different subclones of the same ES cell line (Humpherys et al., 2001).

### Characteristics of Pluripotent Embryonic Cell Lines in the Mouse

Pluripotent cells exhibit typical morphological characteristics, such as a high nuclear:cytoplasm ratio and growth in compact, multilayered colonies. They show alkaline phosphatase (AP) activity (Resnick et al., 1992) and express highly-conserved epitope markers, such as stage-specific embryonic antigen-1 (SSEA-1) (Solter and Knowles, 1978) and germ line-specific transcription factor Oct–4 (Schöler et al., 1989). In addition, a short G1 cell cycle phase (Rohwedel et al., 1996) and high levels of telomerase activity (Thomson et al., 1998) are characteristic for undifferentiated embryonic cells.

Pluripotent cells can be stimulated to differentiate *in vitro* into various cell types (reviewed in Pedersen, 1994; Wobus et al., 1994, 1997; Rohwedel et al., 1999). In suspension culture, they form embryo-like aggregates called 'embryoid bodies', consisting of derivatives of the three embryonic germ layers (Doetschman et al., 1985; Rohwedel et al., 1996) (Fig. 2).

After ectopic transplantation (e.g. under the renal capsule or into the testis) pluripotent cells give rise to teratocarcinomas, demonstrating their *in vivo* differentiation capacity (Evans and Kaufman, 1981). When combined with normal embryos via blastocyst injection (Bradley et al., 1984) or morula aggregation (Wood et al., 1993), these cells contribute to all tissues and organs including the germ line of chimeric individuals, giving rise to functional gametes (Labosky et al., 1994). When ES cells are aggregated with tetraploid embryos (Nagy et al., 1993), offspring can be obtained which are entirely ES cell-derived (Wang et al., 1997).

### Pluripotent Embryonic Cell Lines in Other Vertebrate Species

Pluripotent cell lines offer a suitable *in vitro* model of early embryonic differentiation events and a powerful tool for

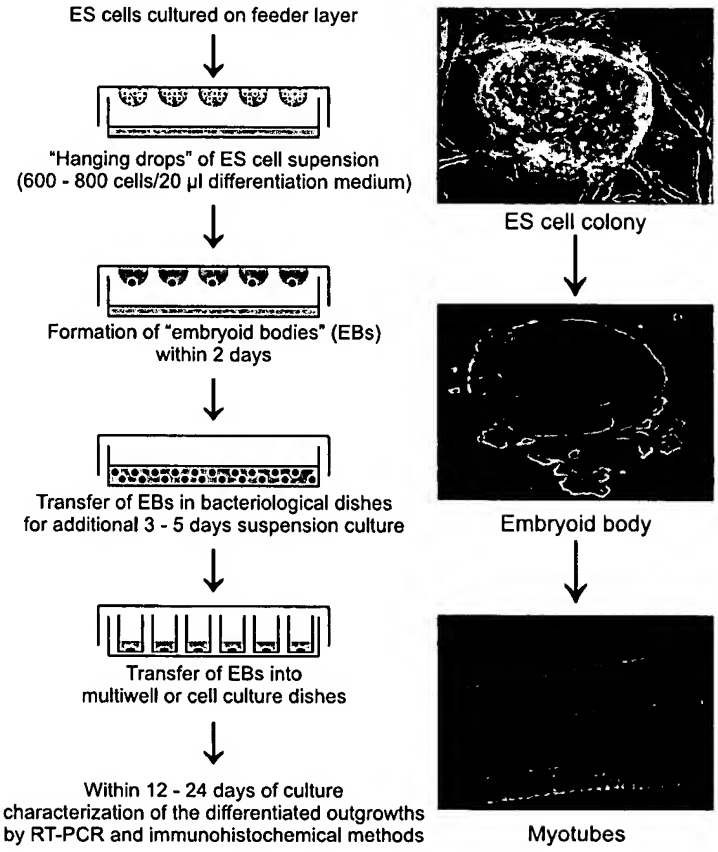


Fig. 2. *In vitro* differentiation of ES cells in 'hanging drop' suspension. Plating of EBs results in differentiated outgrowths which can be used to study events of early embryonic development, serve as material for *in vitro* cytotoxicity testing or may be used for cell transplantation.

innovative gene targeting technologies. Because of these important applications, many attempts have been made to establish ES and EG cell lines in other species than the mouse. Many of these embryo-derived cell lines resemble – at least in part – the morphology and epitope profiles of murine ES cells (Van Stekelenburg-Hamers et al., 1995; Etches et al., 1996). Some studies demonstrate the ability of the ES-like cells to differentiate *in vitro*; however, there are no published data indicating that pluripotent cells can colonize the germ line of chimeric animals in mammalian species other than the mouse (reviewed in Prelle et al., 1999) (Table 1).

*Rabbit*

Because the rabbit is an important model organism for studies of various human diseases, targeted modifications of its genome by ES cell technology would be extremely valuable.

Rabbit ICM cells were isolated from 3- to 4-day-old embryos (Giles et al., 1993; Graves and Moreadith, 1993) and cultured with murine LIF. Following injection into blastocysts, rabbit ES-like cells formed coat colour chimeras, but did not colonize the germ line (Schoonjans et al., 1996). Using these cells as karyoplasts in nuclear transfer experiments a similar proportion of developing blastocysts was achieved as when using embryonic blastomeres (Du et al., 1995).

Rabbit PGCs were isolated from gonadal cells of 18- to 22-day-old fetuses, and displayed similar characteristics as mouse PGCs regarding morphology, SSEA-1 expression and AP activity (Moens et al., 1997). Blastocyst injection of short-term cultured rabbit PGCs resulted in low chimerism of liveborn offspring, while nuclear transfer experiments using these cells yielded only blastocysts, but no implanted fetuses (Moens et al., 1996).

*Pig*

Much effort was also taken to establish porcine ICM- and PGC-derived cell lines. The failure of most attempts may be due to the prolonged preimplantation period characterized by a remarkable blastocyst elongation and simultaneously a quiescent ICM which forms the endoderm-covered embryonic disc (Notarianni et al., 1991) and finally differentiates into mesodermal cells already at day 9 p.c. (Prelle et al., 2001). Therefore, separation of ICM cells from differentiation-inducing effects prior to *in vitro* culture by immunosurgery or calcium ionophore is required (Prelle et al., 1993).

Undifferentiated ICM-derived cells of embryos between day 6 p.c. (Notarianni et al., 1990; Piedrahita et al., 1990a; Ropeter-Scharfenstein et al., 1996) up to more advanced stages at day 13 p.c. (Strojek et al., 1990; Hochereau-de Reviers and Perreau, 1993) could be maintained for prolonged periods when using recombinant human LIF and other heterologous cytokines (Moore and Piedrahita, 1997).

Most of these cell lines were capable of *in vitro* differentiation (Evans et al., 1990; Gerfen and Wheeler, 1995) and formed teratocarcinomas after transplantation into nude mice (Hochereau-de Reviers and Perreau, 1993). They showed AP activity (Talbot et al., 1993), expressed SSEA-1 (Wianny et al., 1997), but – in contrast to murine ES cells – displayed an epithelial phenotype characterized by cytokeratin expression (Piedrahita et al., 1990b). Putative porcine ES cells maintained in culture for up to 44 passages contributed to viable offspring displaying coat colour chimerism but no germ line transmission (Wheeler, 1994).

Porcine PGCs were isolated from fetal genital ridges between days 24 and 26 p.c. (Takagi et al., 1997; Piedrahita et al., 1998), but also earlier during their migration across the dorsal mesentery (Shim et al., 1997). Primary porcine PGC

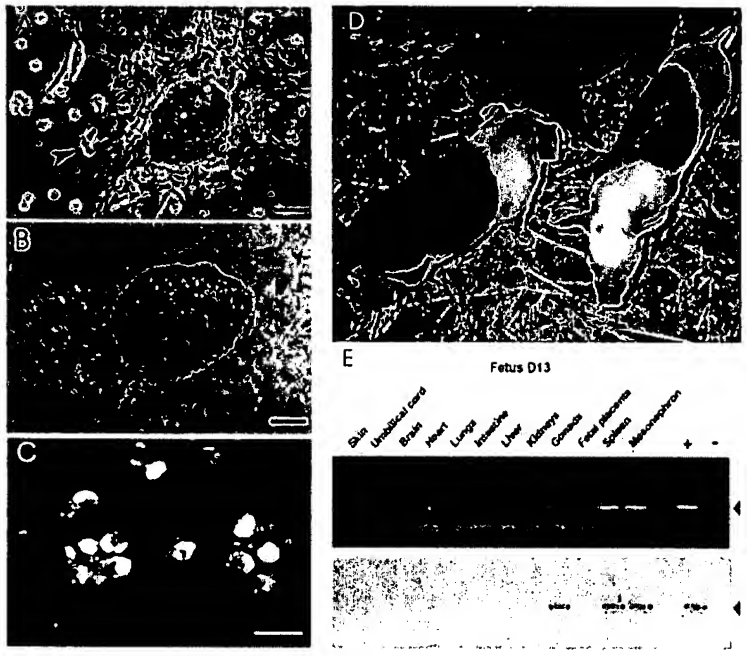


Fig. 3. Establishment of pluripotent PGC-derived cell lines in pigs. (A) Porcine PGCs as multilayered colony; (B) AP histochemical staining of porcine PGCs; (C) SSEA-1-positive PGCs at passage 17. Bar 50 μm (D) Chimeric piglets showing coat colour chimerism after blastocyst injection of Duroc PGCs into Landrace embryos. (E) PCR and hybridization analysis of DNA from a fetus developed after blastocyst injection of transgenic PGCs revealing the presence of the WAPhGH transgene in gonadal, spleen and mesonephron tissue (kindly provided by Dr. S. Müller).

cultures require STO feeder cells (Shim and Anderson, 1998), LIF, porcine SCF, but – in contrast to the mouse – no bFGF (Durcova-Hills et al., 1998). For prolonged undifferentiated proliferation they are more responsive to cell membrane-bound cytokines than to the soluble counterparts (Durcova-Hills et al., 1998).

Some cell lines were capable of *in vitro* differentiation and contributed to a liveborn chimeric piglet (Shim et al., 1997). Blastocyst injection of transfected PGCs carrying the green fluorescent protein gene (Piedrahita et al., 1998) or of WAP-hGH-transgenic EG-like cells (Mueller et al., 1999) resulted in the birth of chimeric piglets carrying the respective transgene in different tissues, but not in the germ cells (Fig. 3).

*Cattle*

In cattle, undifferentiated cells have been isolated at any stage from 16-cell embryos to hatched blastocysts (reviewed in Strelchenko, 1996). A number of different feeder cell types including granulosa cells, fetal fibroblasts of different species, and STO cells, as well as medium with murine LIF were not suitable for stimulating proliferation of embryonic cells without differentiation for an extended period of time (reviewed in Prelle et al., 1999). In contrast to other species, bovine trophectoderm-like ICM outgrowths showed AP activity (Talbot et al., 1995), while undifferentiated bovine ES-like cells were AP-negative (Cibelli et al., 1998).

Stice et al. (1996) reported several ES-like cell lines capable of embryoid body formation after more than 50 passages. Nuclear transfer embryos reconstructed with these cells initiated pregnancies, but were lost before day 60 due to incomplete placental development which was interpreted as a consequence of abnormal imprinting (Strelchenko, 1996). The aberrant placental phenotype in nuclear transfer clones could in some extent be due to a loss of function of Mash2, a maternally expressed imprinted gene (Surani, 2001). Imprinting defects in these embryos generated from PGCs demonstrate that oocytes can not initiate imprints if they are erased, but that they can only be initiated in the germ line (Kato et al., 1999). To support normal placentome formation, bovine ES-like cells could be aggregated with tetraploid embryos according to results in the mouse, where placental tissue was almost exclusively derived from the tetraploid cells (Nagy et al., 1993). However, this approach failed in the bovine because the tetraploid embryos did not develop beyond the 8-cell stage (Stice et al., 1996).

Cibelli et al. (1998) transfected putative bovine ES-like cells by DNA microinjection of a β-galactosidase-neomycin (βGeo) expression vector. Alternatively, bovine fetal fibroblasts were transfected with βGeo and used as nuclear donors to produce transgenic blastocysts and subsequently ES-like cells. Morula injection of either transfected or cloned transgenic ES-like cells yielded overall nine chimeric calves carrying the βGeo marker gene in at least one tissue, but not in the germ line.

Bovine PGCs were obtained from fetal genital ridges between days 29 and 70 p.c. (Lavoir et al., 1994, 1997) and around day 175 of gestation (Delhaise et al., 1995). They were cultured on a wide variety of feeder layers in medium supplemented with a 'cocktail' of different cytokines routinely used for murine EG cell culture (reviewed in Strelchenko, 1996). Pluripotency was evaluated by embryoid body formation and by generation of chimeric blastocysts containing FITC-labelled PGCs in their ICM shortly after re-expansion (Cherny et al., 1994). Re-cloning of nuclear transfer embryos reconstructed from PGC karyoplasts resulted in the birth of one healthy calf (Strelchenko et al., 1998). Another calf derived directly from freshly isolated PGCs died soon after delivery (Zakhartchenko et al., 1999).

*Sheep*

For the establishment of ovine ES cells, embryos were collected between days 7 and 13 p.c. and placed in culture, when the attachment and proliferation rates were higher with advanced embryonic stages (reviewed in Prelle et al., 1999). Instead of forming typical multilayered colonies, ovine ES-like cells grew as epitheloid monolayers (Notarianni et al., 1991). Their AP activity (Talbot et al., 1993) and their potential to differentiate *in vitro* (Piedrahita et al., 1990b; Meinecke-Tillmann and Meinecke, 1996) could be maintained only for a few passages, whatever feeder cell type and cytokine supplementation of the culture medium was tested (reviewed in Galli et al., 1994). Attempts to prove the pluripotent status of ovine embryo-derived cell lines by teratocarcinoma formation (Galli et al., 1994) or by germ line transmission in chimeric animals (Handyside et al., 1987) failed. However, when differentiated epithelial-like ovine ICM outgrowths were used in nuclear transfer experiments, live lambs were obtained (Campbell et al., 1996; Wells et al., 1997).

**Genetic Modification in ES cells**

Originally, ES cells have been used for the study of early developmental processes, e.g. the clonal analysis of cell lineage formation in mammals and the detection of stage- and cell-specific gene expression patterns (reviewed in Anderson, 1992). After Bradley et al. (1984) demonstrated the capacity of ES cells to colonize the germ line of chimeric mice produced by blastocyst injection, it was clear that these cells would be a most interesting vehicle for introducing targeted mutations into the mouse germ line. In 1987 it was demonstrated for the first time that a targeted mutation could be introduced into ES cells in culture by homologous recombination (Thomas and Capecchi, 1987), and the first germ line transmission of a targeted mutation via ES cells was reported by Thompson et al., (1989). ES cell-mediated transgenesis has some distinct advantages over other methods of gene transfer such as the use of viral vectors or the DNA microinjection technique which may yield unpredictable results due to the random integration of multiple copies of the introduced DNA (reviewed in Stewart, 1991). ES cell technology might significantly increase the efficiency of producing transgenic animals, as individual transfected cell clones can be screened *in vitro* for integration and eventually expression of the exogenous DNA construct before creating germ line chimeric animals (Wheeler et al., 1995). ES cell clones carrying a targeted integration of the construct DNA are identified by polymerase chain reaction (PCR) and Southern blot analysis.

Because of the rapid proliferation *in vitro*, ES cells provide an inexhaustible supply of cells capable of homologous recombination with a newly introduced mutated DNA sequence (Capecchi, 1989). This technique allows the precise modification of existing genes, including their functional inactivation and the generation of new alleles (reviewed in

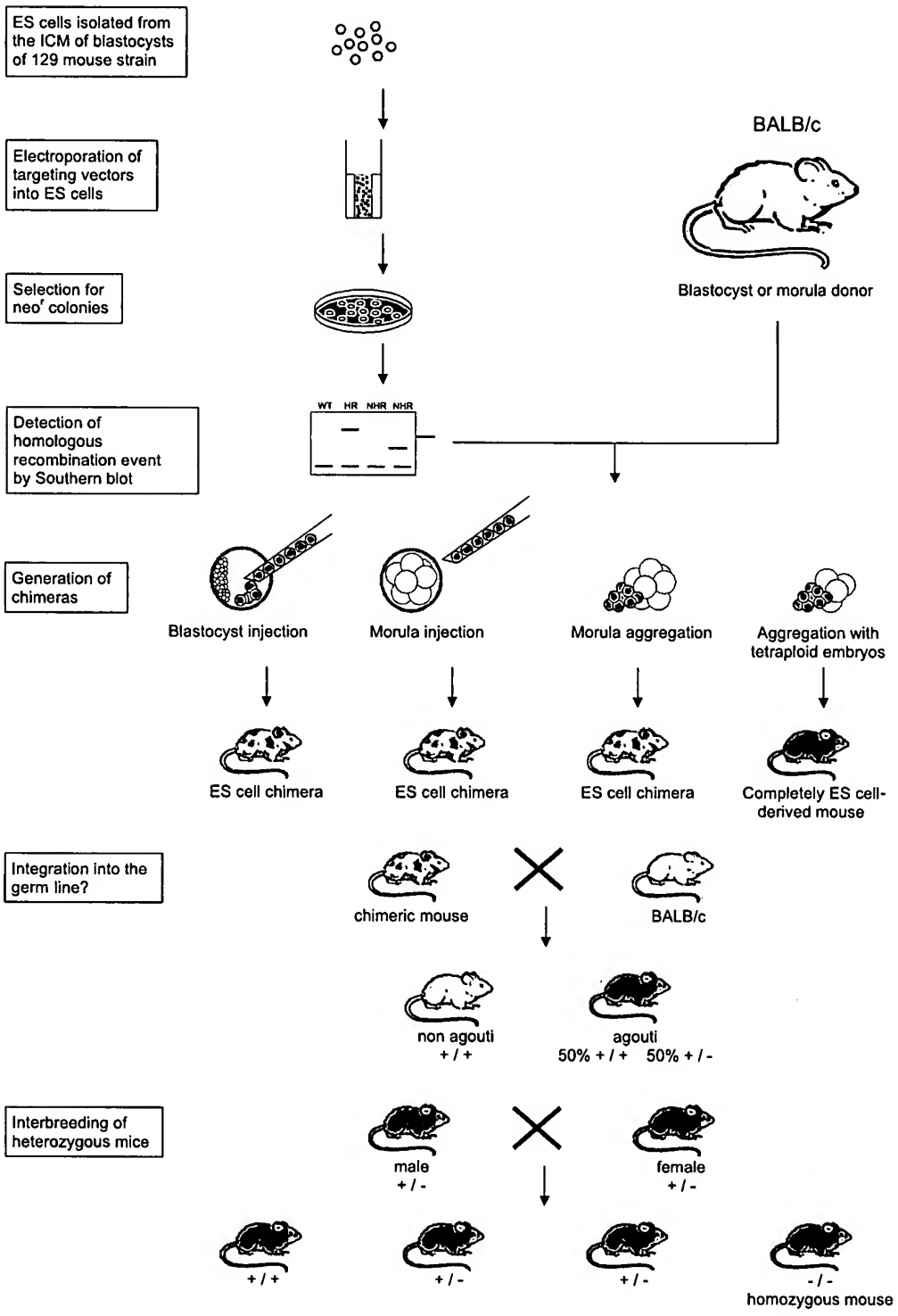


Fig. 4. Generation of mutant mice from targeted ES cells. The targeting vector is introduced by transfection into the ES cells. After selection and screening to identify transgenic ES cell clones, targeted cells are reintroduced into embryos by blastocyst injection or morula aggregation. Breeding of the chimeric mouse yields to homozygous and heterozygous offspring which are used for interbreeding to generate homozygous mutant mice, WT = wild-type; HR = homologous recombination; NHR = nonhomologous recombination.

Osterrieder and Wolf, 1998). To introduce a designed mutation into the germ line of mice, a targeting vector containing the desired mutation and a selectable marker flanked by sequences homologous to the genomic target is introduced by transfection (mostly electroporation) into an ES cell line. The targeting vector pairs with the cognate chromosomal DNA sequence and the mutated gene replaces the original wild-type sequence by homologous recombination. These altered ES cells are reintroduced into wild-type embryos and transferred to recipient mice. The resulting chimeras may be identified by coat colour chimerism and are usually bred to mice from a strain that allows the identification of ES cell-derived offspring by eye pigmentation and coat colour. For ES cells derived from the inbred strain 129, C57BL/6 and BALB/c mice are widely used as donors of host embryos and for mating with chimeras. If one allele of the target gene was mutated in the diploid ES cells, 50% of the ES cell-derived offspring are expected to be heterozygous, carrying one targeted allele (+/–). Interbreeding of heterozygous mice results in the birth of animals homozygous for the desired mutation (–/–), if the mutation is not embryonic lethal (Fig. 4).

By creating a 'loss-of-function-mutation' or so-called null genotype, the resulting knock-out mice provide the experimental evidence regarding the function of the encoded protein. They also provide useful models for human genetic diseases and for the exploration of new therapeutic protocols including gene therapy (Capecchi, 1989).

Two types of targeting vectors have been designed to recombine with, and mutate a specific chromosomal locus (reviewed in Ledermann, 2000). Replacement-type vectors contain part of the genomic target sequence interrupted by a positive selection cassette, which mutates or replaces essential parts of the target locus. These vectors are linearized outside the homologous region and recombine with the target gene by a double cross-over event, resulting in the replacement of the chromosomal DNA by the targeting construct (Thomas et al., 1986). In contrast, insertion-type vectors are linearized within the region of homology and are inserted entirely into the targeted gene locus by a single cross-over event, leading to a partial duplication of the homologous DNA.

The most commonly-used selection cassette contains the prokaryotic neomycin phosphotransferase (*neo*) gene which confers resistance to neomycin and its analogue G418. Homologous recombination occurs less frequently than non-homologous recombination. The proportion of targeted ES cell clones is influenced by the target locus itself (e.g. by its transcriptional activity), by the length and sequence identity of the homologous DNA in the targeting vector and by the penetrance of the selectable marker.

To enrich ES cell clones with a homologous recombination event, positive selection for integration of the targeting vector can be combined with an additional marker, allowing selection against cells carrying randomly integrated vector copies. In this case, the targeting construct is most frequently based on a replacement-type vector containing the positive selection marker within the region of homology and the negative selection marker at one or both ends of the homologous DNA. Genes for negative selection include the herpes simplex virus thymidine kinase gene (HSV-tk), which converts nucleoside analogues such as ganciclovir into toxic metabolites. As the terminal part should be cleaved-off by a double cross-over integration within the homologous region, this strategy can be used to enrich clones with a targeted integration event (Fig. 5).

In addition to these selection markers, reporter genes such as the *E. coli* β-galactosidase (*lacZ*) (Mansour et al., 1990) or green fluorescent protein (GFP) genes (Gagneten et al., 1997) can be included into the targeting vector to monitor expression of the target gene *in situ* throughout embryogenesis. The position of these reporter sequences in the targeting vector is chosen to allow their transcriptional activation by regulatory sequences of the target locus.

The analysis of mouse models carrying targeted mutations often revealed a less severe phenotype than expected. This might be due to functional redundancy among different genes and compensatory mechanisms between gene family members (Ledermann, 2000). Also the genetic background has a great effect on the phenotypic alterations of the knock-out mice due to polymorphic modifier genes in different strains.

The constitutive inactivation of genes in the mouse leads to animals that are constantly deficient for the deleted gene product. This may cause embryonic lethality, if a gene is crucial for development and therefore its function in later developmental stages cannot be studied. Additionally, the loss of a gene product may be compensated by other genes and the resulting phenotype may be close to the wild-type animal.

These problems associated with a constitutive gene knock-out can be avoided by tissue-specific and inducible gene

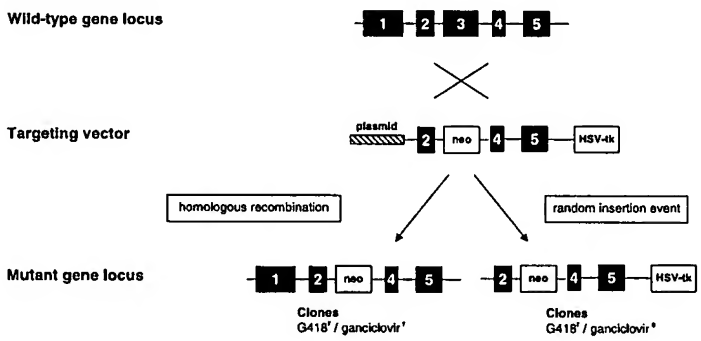


Fig. 5. Positive-negative selection. The targeting vector includes the postive selection marker *neo* (confering resistance to G418) and the negative selection marker HSV-tk (converting ganciclovir into a toxic metabolite). Upon random integration, the whole vector is inserted, rendering the cells sensitive to ganciclovir. During integration by homologous recombination HSV-tk is cleared off, resulting in cells being resistant to double selection with G418) and ganciclovir.

disruption strategies. So-called conditional knock-outs overcome problems raised when inactivation of a gene is lethal *in utero*, when the presence of a selectable marker may influence the phenotype of a mutant mouse, or when compensation may arise due to the lack of a gene product for the entire lifetime, and the interpretation of a null mutation is limited. The most widely adopted approach to achieve tissue- or developmental stage-specific gene targeting is the use of the Cre-*loxP* system (Gu et al., 1993), which offers multiple possibilities of inducible genetic engineering. The classical approach involves two steps: a genetic modification including three *loxP* (locus of crossing-over) sites flanking the gene segment of interest, and the cassette of the selectable marker is first introduced into the ES cell genome by homologous recombination. Secondly, ES cells positive for a homologous recombination event are transfected transiently with a Cre recombinase expression vector generating the desired, final structure of the targeted locus. Cre (causes recombination) excises a DNA segment flanked by *loxP* sites (Kühn and Schwenk, 1997), if the *loxP* sites are placed in the same orientation. The important application of this Cre-mediated recombination is the removal of the selection marker gene to avoid possible interference with the expression of the targeted or neighbouring genes. The specificity for the introduced *loxP* sites results in three types of deletion mutants: the first type of *neo*-sensitive ES cell clones, in which recombination between the outer *loxP* sites results in the deletion of the entire flanked region; secondly, the desired outcome, in which the selectable markers are deleted leaving the gene sequence flanked by two *loxP* sites; and thirdly, the deletion of the gene segment and the remaining of the selection markers (HSVtk and *neo*). Clones harbouring a *loxP*-flanked (floxed) allele of the target gene are used to generate chimeric mice suitable for conditional gene targeting, still carrying a functional target gene in parallel, transgenic mice are generated which express the Cre recombinase gene under a tissue-specific and/or an inducible promoter (Orban et al., 1992). The Cre-transgenic mice are then crossed with gene-target mice carrying *loxP*-flanked genomic regions of the target gene to be deleted or modified. In the progeny, the target gene remains intact until the Cre gene is expressed, which catalyses site-specific recombination between the *loxP* sites, deleting the sequences in-between and thereby leading to gene silencing (Fig. 6). Meanwhile, mutations in some hundreds of genes have been made and several databases provide a source of information for Cre transgenic mice: http://www.mshri.on.ca/nagy/cre.htm; http://www.emma.rm.cnr.it; http://www.jax.org.

The application of gene-targeting technology in mouse embryonic stem cells has enabled scientists to generate model mutant mice. The alterations range from subtle mutations, gene replacements, inversions and deletions to tissue-specific inducible gene targeting, allowing temporal and spatial control (reviewed in Lewandowski, 2001; Stanford et al., 2001).

### Gene Targeting in Other Mammalian Species

Although germ line-competent ES cells are not available for other mammalian species than the mouse, the recently developed nuclear transfer technology using transfected differentiated cells provides an alternative route for gene targeting in these species. Nuclear transfer technology involves the transfer of a donor nucleus (karyoplast) into an enucleated zygote or a MII oocyte (cytoplast) (Campbell et al., 1996). Nuclear donor cells can be transfected before nuclear transfer, as first demonstrated by the production of cloned transgenic sheep carrying expression vectors for human factor IX (Schnieke et al., 1997). Recently, a mammary gland-specific expression vector for α1-antitrypsin (AAT) was targeted into the α1(I) procollagen (*COL1A1*) locus of ovine fetal fibroblasts which were subsequently used for nuclear transfer to produce the first gene targeted sheep (McCreath et al., 2000). The target locus (*COL1A1*) was chosen since this gene is highly expressed in fetal fibroblasts, allowing the use of a promoter-trap strategy, i.e. a promoter-less *neo* selection marker which was only expressed when integrated downstream of an active promoter. Using this approach, targeting efficiencies (targeted vs. random integration events) were similar as those usually seen in mouse ES cells. Using similar strategies, the α(1,3)galactosyl transferase (*GGTA1*) gene and the prion protein (*PrP*) gene were recently targeted in sheep (Denning et al., 2001).

Transgenesis and targeted mutagenesis via nuclear transfer circumvents the need for generating chimeric animals, reduces costs and saves time, especially in larger animals, and obviously has several additional advantages: (a) sex selection is possible (e.g. female transgenic cell lines could be used for the production of valuable proteins in the milk); (b) integration and eventually expression of the transferred construct can be detected in cultured cells before nuclear transfer; (c) cell lines can be cryopreserved; (d) all cells within a cloned offspring contain the introduced gene, eliminating mosaicism and ensuring germ line transmission; (e) the number of animals required reduced since all animals generated are transgenic (reviewed in Wolf et al., 2000).

In large domestic animals, gene transfer focuses not only on the improvement of productivity traits (milk and carcass composition, growth rate and feed utilization), but also on disease resistance and reproductive performance (Wheeler et al., 1995). Other important applications include the production of pharmaceutical proteins in specific organs or body fluids of transgenic animals (gene farming) (Brem and Müller, 1994) and the genetic modification of pigs to produce cells, tissues or organs for xenotransplantation (reviewed in Platt, 1998). In addition, genetically engineered farm animals may become important animal models. The establishment of animal homologues for human diseases has proven to be an invaluable tool for studies of human genetic, infectious disorders and cancer. In particular pigs offer some distinct advantages compared to the commonly used rodent models because they are immunologically and physiologically more similar to humans and have a more diverse genetic background (Platt, 1998).

### Potential Applications of ES Cells and Nuclear Transfer in Human Biology and Medicine

Although the recent success in establishing human ES cells raised numerous ethical concerns, acceptable applications of ES cell technology in humans can be envisaged and will be based on manipulation and analysis of human ES cells *in vitro*. Bongso et al. (1994) reported for the first time the isolation of human ICM cells at day 8 post-insemination and the culture on ampullary epithelial feeder layers for 2 passages. Later, human ES cell lines were established from immunosurgically isolated ICMs and maintained undifferentiated until present (Thomson et al., 1998). Currently, 64 human ES cell lines are in existence, almost all derived from donated 'spare' IVF

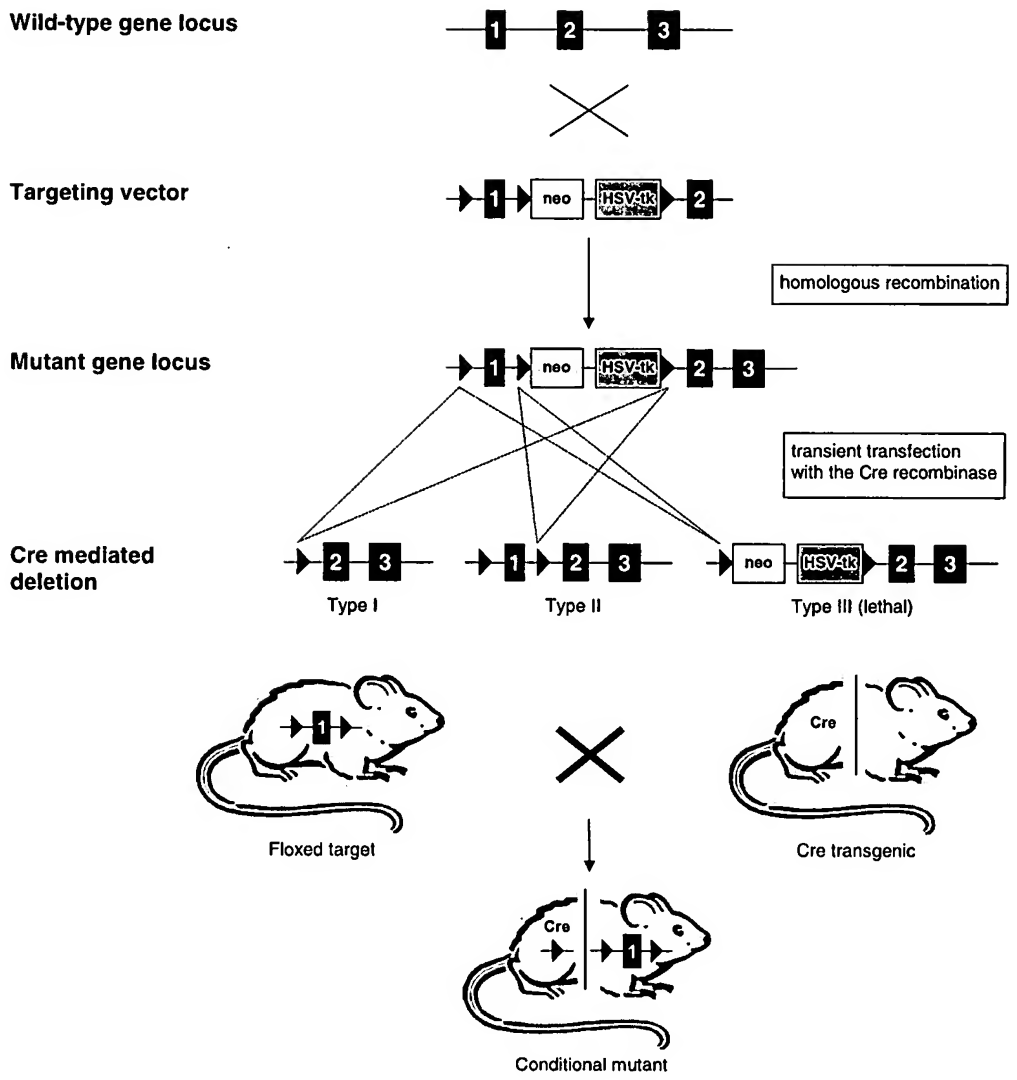


Fig. 6. Utilization of the Cre recombinase system for generation of conditional knock-outs. A genetic modification including three *loxP* (locus of crossing-over) sites (black triangles) flanking the gene segment of interest and the cassette of the selectable marker is introduced into the ES cell genome by homologous recombination. Subsequently, targeted ES cells are transiently transfected with the Cre (causes recombination) recombinase gene, resulting in three mutation types: (I) *neo*-sensitive cell clones, in which recombination between the outer *loxP* sites results in the deletion of the entire floxed region (dashed lines); (II) desired clones, in which the selectable markers are deleted leaving the floxed gene unaffected; and (III) deletion of the gene segment and remaining of the selection markers resulting in lethality under ganciclovir selection. Chimeric mice created with ES cells carrying the floxed target gene are cross-bred with transgenic mice expressing the Cre recombinase gene under control of a tissue-specific and/or inducible promoter. Resulting offspring will lack the gene of interest in cells where the Cre recombinase is expressed.

embryos (McLaren, 2001). Only one IVF clinic has derived human ES cell lines from donated oocytes fertilized for the purpose of stem cell establishment (Lanzendorf et al., 2001). ES-like characteristics were demonstrated, including surface marker expression (SSEA-3, SSEA-4), AP activity, teratocarcinoma formation in nude mice, and high telomerase activity (which is involved in the maintenance of telomere length and correlates with immortality of cells). Additionally, human primordial germ cells were derived from 5- to 9-week-old fetuses and cultured on STO cells with medium containing human LIF and bFGF. The growing EG colonies were AP-positive, expressed characteristic surface markers (SSEA-1, SSEA-3 and SSEA-4), and differentiated *in vitro* into derivatives of all three germ layers (Shamblott et al., 1998; 2001). Meanwhile, several results underline the broad *in vitro* differentiation capacity of human ES cells (Itskovitz-Eldor et al., 2000; Reubinoff et al., 2000; Schuldiner et al., 2000).

To direct this *in vitro* differentiation along chosen pathways would allow for the investigation of human developmental events including regulatory signals for cell commitment and morphogenesis, as well as the identification of target genes for new drugs and teratogenic or toxic compounds that cannot be

analysed *in vivo* due to ethical constraints (Rathjen et al., 1998; Scholz et al., 1999). ES cell technology has mainly been speculated to be useful for cell and tissue therapy in humans (Gearhart, 1998; Trounson and Pera, 1998). One key issue is the histocompatibility of the ES cells and their differentiated derivatives with every individual. Pluripotent ES cells would have the advantages of being selected out of a collection of different ES cell lines screened for matching the recipient's major histocompatibility complex (MHC) composition. Additionally, at least in mouse ES cells and their differentiated progeny, the expression of MHC proteins, which initiate immune rejection, is either absent or greatly decreased compared to adult cells (Harley et al., 2001). Immune suppression and tolerance induction routinely used in organ transplantation to date are other solutions. But the efficient and feasible genetic modification of ES cells may also facilitate to modify the MHC complex of existing human ES cell lines by homologous recombination (Amit et al., 2000). In another scenario for which the term 'therapeutic cloning' has been coined, people could provide their own somatic cells to be used as nuclear donors and be fused with their own or foreign enucleated oocytes. After blastocyst formation, autologous ES cells could be established in culture and then be induced to *in vitro* differentiation to provide patient-specific cells and tissue. Those can be used for replacement and cell therapy without rejection problems and allow lifelong treatment (Gage, 1998) (Fig. 7). However, the reprogramming of a somatic nucleus in an oocyte is still very inefficient (less than 3%) (Wakayama and Yanagimachi, 2001), and it is unclear if this is due to genetic or epigenetic anomalies. Abnormal epigenetic reprogramming has recently been shown in borine nuclear transfer embryos (Dean et al., 2001; Kang et al., 2001). While telomere size might be restored in a reprogrammed somatic nucleus (Betts et al., 2001), most DNA mutations can not be repaired and might contribute to the low efficiency of development. It is significant that transplantation of nuclei from pluripotent ES cells into oocytes results in higher rates of development to term (Rideout et al., 2000). Also the ability to derive ES cells from nuclear transfer blastocysts is an essential criteria to propagate investigation on therapeutic cloning and was approximately 4% compared to an average of 40–50% from normal blastocysts of the 129 strain (Wakayama et al., 2001). Some mutations may have no effect on reprogramming and the subsequent derivation of ES cells if they do not affect blastocyst development. Yet the consequences of some genetic mutations and epigenetic modifications may become evident later when these cells are allowed to undergo differentiation towards specific cell types desired to be used in cell therapy (Surani, 2001).

A major problem of transferring ES cell technology into clinic is that *in vitro* differentiation always results in heterogeneous mixed population of derivatives from all three germ

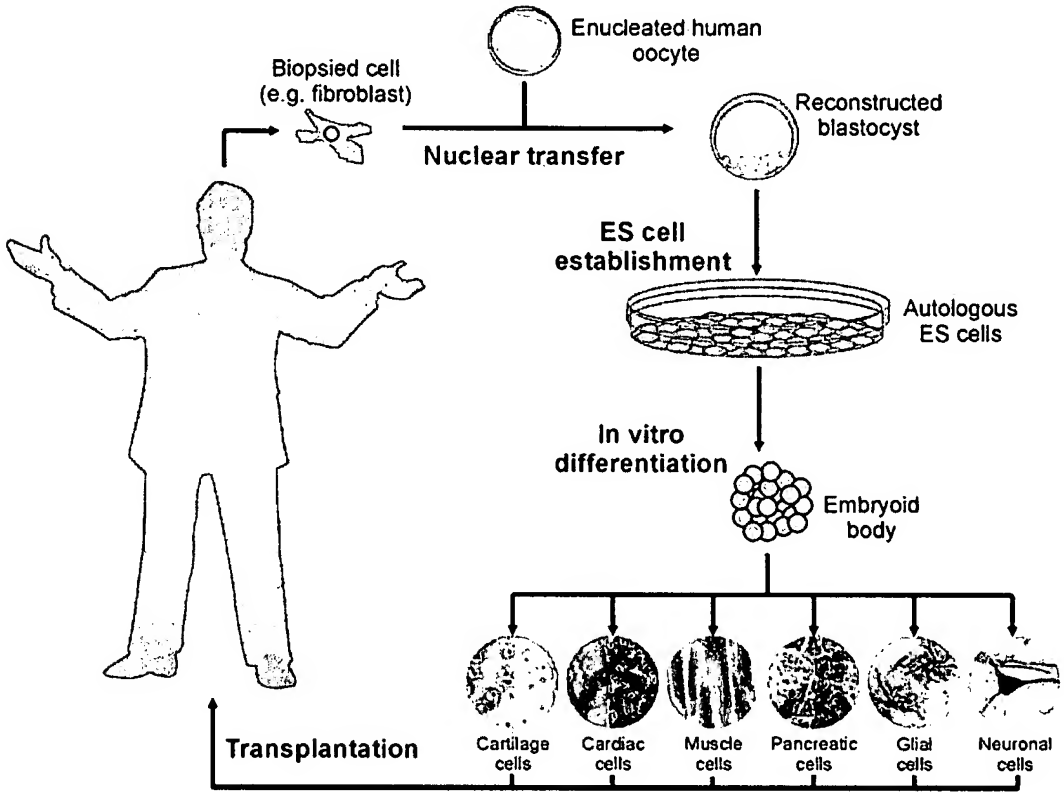


Fig. 7. Therapeutic cloning as a method of providing autologous cell transplants. A convenient somatic cell type is obtained from a patient requiring transplant therapy. Nuclear transfer generates an early embryo genetically identical to the patient, which is then used to establish embryonic stem (ES) cells. Via embryoid body formation the cell type required, e.g. neuronal or pancreatic cells, is derived by directed *in vitro* differentiation and used for transplantation.

Table 1. Establishment of pluripotent embryonic cell lines from selected animal species and humans

| Species | Cell source | ES cell-like characteristics | *In vivo* differentiation | References |
|---|---|---|---|---|
| Medaka fish | Midblastulae | AP activity, EB formation | Transgenic chimeric fry | Hong et al. (1998) |
| Chicken | Stage X blastoderm | AP activity, SSEA-1, SSEA-3 and ECMA-7 expression | Germ line chimeras | Pain et al. (1996) |
| | 5 d genital ridges | Morphology | Germ line chimeras | Chang et al. (1997) |
| Rabbit | 5 d intact embryos | EB formation | Coat colour chimeras | Schoonjans et al. (1996) |
| | 18–22 d genital ridges | SSEA-1 expression, AP activity | Coat colour chimeras | Moens et al. (1997) |
| Pig | Blastocysts | EB formation | Coat colour chimeras | Wheeler (1994) |
| | 25–27 d genital ridges | AP activity, EB formation | Transgenic chimeric piglet | Piedrahita et al. (1998) |
| Cattle | Blastocysts derived by fibroblast nuclear transfer | Morphology | Transgenic chimeric calves | Cibelli et al. (1998) |
| | 45 d genital ridges | Morphology, pseudopodia | Cloned bull calf | Strelchenko et al. (1998) |
| Sheep | 8 d blastocysts | Morphology | Cloned lambs | Wells et al. (1997) |
| Human | IFV blastocysts | Morphology, telomerase activity, AP activity, SSEA-3 and -4 expression | n.d. | Thomson et al. (1998) |
| | 5- to 9-week genital ridges | AP activity, SSEA-1, -3 and -4 expression, EB formation | n.d. | Shamblott et al. (1998) |

n.d. = not determined.

layers. For cell therapy, the desired cell population has to be sorted by traditional methods of fluorescence-activated cell sorting (FACS), by selective growth of specific cells under suitable culture conditions or by introducing a selectable marker that allows drug selection to ablate unwanted cells (reviewed in Donovan and Gearhart, 2001). Murine ES cells differentiated into insulin-producing beta cells (Assady et al., 2001; Lumelsky et al., 2001) were selected by an antibiotic resistance introduced via gene targeting. Only those cells that were activating the insulin promoter were able to survive the antibiotic supplementation and could be transplanted into diabetic mice resulting in normalized blood glucose levels (Soria et al., 2000). Also, pluripotent stem cells remaining in the differentiated outgrowth need to be erased by techniques such as genetical selection to avoid tumour formation after transplanting cells into the injured or diseased tissue or organ.

It is still unclear how the cells introduced into specific sites migrate to the correct site and do not go to the wrong place. Plus, for broad application, stem cells are needed in large quantities. Unfortunately human ES cells proliferate more slowly than their murine counterparts, differentiate more readily and their cloning efficiency is very low, but can be improved by the addition of bFGF (Amit et al., 2000).

So far, there have been few, but remarkable examples that derivatives of murine ES cells can be transplanted successfully in animal models with diseases or injuries. ES cell-derived cardiomyocytes were able to form stable, apparently functioning intracardiac grafts in mice (Klug et al., 1996). Glial precursor cells transplanted into 1-week-old rats with myelin deficiency interacted with the host neurones to produce myelin in the brain and spinal cord (Brüstle et al., 1999). Even transplanted neuronal cells differentiated from human ES cells induced recovery of motor function in rats with motor neurone injury (Donovan and Gearhart, 2001). Promising animal experiments (Studer et al., 1998, 2000) encourage the testing of the potential of human ES cells in animal models of Parkinson's disease (Bjorklund et al., 2002). Therefore, ES cells have to be differentiated into functional dopaminergic neurones either by committing them *in vitro* and mediating terminal differentiation into this neuronal cell lineage after implantation into the host brain, or by transferring less-committed cells into the damaged area and allowing 'environmental' signals to guide them to become the final replacement cell type.

### Adult Stem Cells and Stem Cell-based Therapies

Ethical concerns regarding human ES cells and the human embryos involved together with the scientific as well as public discussion about efficiency and abuse of cloning technology in humans caused an intensive search for practical alternatives. In addition, recent studies challenged the belief that stem cells, which persist after early embryonic stages, are restricted in potential to form only the cell types characteristic of the tissue they belong to, and opened up the investigations on somatic stem cells. These cells are capable of long-term self-renewal and of forming at least one, and sometimes many, specialized cell types via an intermediate cell type called precursor or progenitor cells. Somatic stem cells are committed to differentiate along a particular, but not strictly defined developmental pathway (Robey, 2000). Their primary functions are to maintain the steady state functioning of a cell (homeostasis) and to replace cells lost due to injury or disease (Holtzer, 1978). For example, only a very small proportion (1 in 15 000 cells) in the bone marrow are haematopoietic stem cells (HSCs), which are constantly generated in adult individuals, but when dispersed in tissues they differentiate into the various mature blood cell types depending on the local environment (Weissman, 2000).

Unlike ES cells, which are defined by their origin from the ICM of blastocysts, adult stem cells do not have such a definitive basis and are likely characterized by being set aside during fetal development and restrained from differentiation. But the main difference between embryo-derived pluripotent cells and soma-originated multipotent stem cells is that the latter are no longer capable of generating germ cells and may also not make the range of cell types that can be derived from embryo-originated stem cells (Donovan and Gearhart, 2001). Besides the bone marrow, other adult tissues such as peripheral blood, brain, spinal cord, skeletal muscle, epithelia of the skin and digestive system, and pancreas contain stem cells. In addition to the capability of self-renewal throughout the entire lifetime of an organism, somatic stem cells are characterized by being clonogenic (a single adult stem cell should be able to

generate a line of genetically identical cells) and being able to differentiate into cells with a mature phenotype regarding morphology, specific cell surface markers, and characteristic behaviour. Somatic stem cells and also the long-term repopulating HSC can not properly be expanded *in vitro* without losing developmental potential (Weissman, 2000). But recent studies show that at least oligodendrocyte precursor cells can be grown indefinitely in culture (Tang et al., 2001).

Somatic stem cells are often determined by labelling and tracking *in vivo* after re-transplantation or, when grown *in vitro*, they can be manipulated by adding growth factors or introducing genes to determine what differentiated cell types they will yield. It is often difficult to distinguish adult, tissue-specific stem cells from progenitor cells, which are found in fetal and adult tissues and are partly differentiated to give rise to certain cell types of a tissue.

The typical asymmetric cell division of stem cells into one identical replacement stem cell responsible for self-renewal and into one more differentiated progenitor cell is controlled by the environment provided in the so-called stem cell niche (reviewed in Spradling et al., 2001). A niche is considered to be a subset of tissue cells and extracellular substrates, e.g. integrin or laminin, which interact with the housed stem cells via cell-cell or cell-basement membrane contact or via diffuse signalling by growth factors, e.g. BMP-4 or SCF, and regulate the proportion of stem vs. differentiated cells and the rate of proliferation (Lovell-Badge, 2001). The proper functioning of niches is likely to depend on the continued presence of stem cells, therefore stem cell-based therapies may face the problem to rejuvenate or replace niches as well as stem cells (Bianco and Robey, 2001). Self-renewal of HSC and other stem cells might be regulated by pathways also involved in oncogenesis, such as Notch, Sonic hedgehog (*Shh*) and *Wnt* signalling (Taipale and Beachy, 2001), considering cancer to be a disease of unregulated self-renewal (Reya et al., 2001). However, understanding these pathways should facilitate the use of adult stem cells for regenerative medicine and the identification of cancer cell targets for anti-cancer therapies.

Recently, it became evident that stem cells from a particular tissue can also generate specialized cell types of another tissue, either derived from the same or from a different embryonic germ layer. This so-called plasticity (Krause et al., 2001) describes the ability of stem cells from one adult tissue to generate the differentiated cell types of another tissue and is also referred to as 'transdifferentiation' (Lagasse et al., 2000; Anderson et al., 2001). Most experiments demonstrating somatic stem cell plasticity involve cells derived from bone marrow, which may differentiate into another mesoderm-derived tissue such as skeletal muscle (Ferrari et al., 1998; Gussoni et al., 1999), cardiac muscle (Kocher et al., 2001; Orlic et al., 2001), or liver (Alison et al., 2000; Theise et al., 2000). While bone marrow-derived mesodermal stem cells were reported to generate ectoderm-originated neural tissue (Mezey et al., 2000), neural stem cells from adult brain tissue were found to form haematopoietic cells (Bjornson et al., 1999).

### *Neuronal Stem Cells*

Stem cells from the central nervous system, unlike bone marrow cells, are not located in a single, accessible location. Instead they are scattered in three places: the tissue around the lateral ventricles in the forebrain, a migratory pathway from there to the olfactory bulbs, and the hippocampus (Eriksson et al., 1998). Experiments with CNS stem cells involve formation of neurospheres, round aggregates that are clonally derived and have to be dissociated to study plasticity *in vitro* (McKay, 1997). To follow the differentiation fate of these cells *in vivo* they are injected in the circulatory system of the recipient animal, either after dissociation (Bjornson et al., 1999) or as compact neurospheres (Clarke et al., 2000).

Stem cells in the fetal and adult brain are recently believed to divide and give rise to more stem cells and to several types of precursor cells, regionally specified by gradients of signalling molecules (Temple, 2001). Neuronal precursors (neuroblasts) give rise to neurones, while glial precursors give rise to astrocytes and oligodendrocytes (Gage et al., 1995; Johe et al., 1996; McKay, 1997; Shihabuddin et al., 1999). Most adult neuronal stem cells are also temporally restricted, but there are rare stem cells present in the nervous system that have greater plasticity (Weissman, 2000). For example, adult spinal cord-derived stem cells, which do not normally develop neurones, form interneurones if injected into the adult hippocampus (Shihabuddin et al., 2000).

### *Haematopoietic Stem Cells*

HSCs forming all types of blood cells (Till and McCullough, 1961; Becker et al., 1963), the immune (haematolymphoid) system, and the mixed population of stromal cells generating bone, cartilage, fat, fibrous connective tissue and the reticular network (Friedenstein et al., 1966; Owen, 1988) are longer known than neural stem cells. HSC mature from the long-term self-renewing pool to multipotent progenitors, progressively losing their potential to self-renew, but become more mitotically active (Reya et al., 2001). A population of progenitor cells that differentiates into endothelial cells of blood vessels was isolated from circulating blood (Asahara et al., 1997), identified as 'originating in bone marrow' (Shi et al., 1998), and therefore discussed as a third bone marrow-derived stem cell population.

### *Stem Cells in Skeletal Muscle, Pancreas, and Liver*

Additional stem cells are found in various other adult tissues. Skeletal muscle stem cells with a specific population of so-called 'satellite cells' located at the basal lamina of mature muscle cells mediate muscle growth (Schultz, 1996). These normally non-dividing cells can be stimulated to proliferate by injury or sportive exercise. Another muscle-derived 'side population' of cells can also regenerate skeletal muscle after transplantation into Duchenne's muscular dystrophic mice (Gussoni et al., 1999).

Epithelial cells in the skin and the digestive tract are replaced constantly, while other epithelial populations of liver and pancreas turn over more slowly. But replacement of all these compartments is postulated to occur via stem cells (Slack, 2000; Taylor et al., 2000; Ghazizadeh and Taichman, 2001).

A recent study indicates that a single precursor cell derived from embryonic endoderm may generate both the ventral pancreas and the liver (Deutsch et al., 2001). However, in the adult, both of these organs contain multiple kinds of differentiated cells that may be regenerated by multiple types of stem cells (Zulewski et al., 2001). In the pancreas, endocrine

cells occur in the islets of Langerhans, including insulin-producing beta cells, glucagon-secreting alpha cells, and somatostatin-releasing cells. In the liver it is not clear whether hepatic oval cells involved in repairing severe liver damage are bone marrow-derived stem cells (Crosby and Strain, 2001) and if they actually generate new hepatocytes *in vivo*, which are responsible for the well-known regenerative capacity of the liver (Sell, 1990).

### *Clinical Applications of Adult Stem Cells*

One of the first clinical uses of HSC was the treatment of blood cancers such as leukaemia, which results from the uncontrolled proliferation of white blood cells. In these applications, cancerous haematopoietic cells destroyed via radiation are replaced by a bone marrow transplant or a HSC transplant collected from the peripheral circulation of a matched donor. Autologous stem cell transplants collected from the peripheral blood of the patient are also used to replace haematopoietic cells destroyed by chemotherapy. The plasticity of HSC described above suggests that these cells can also be used to regenerate other tissues damaged by injury, destroyed by medical therapies, or affected by inherited genetical disorders (Bittner et al., 1999; Alison et al., 2000; Krause et al., 2001).

The use of HSC is also discussed for the treatment of autoimmune diseases which may be organ-specific, like type 1 diabetes, destructing pancreatic beta islet cells, or multiple sclerosis, resulting from the breakdown of myelin covering of the nerves. First reports already showed that stem cells can support re-myelination of axons (McDonald et al., 1999; Liu et al., 2000). Yet diseases, which in contrast might be non-organ-specific and lack a single specific target for the therapy, may also be treated by HSC transplantation. The ability to generate and propagate unlimited numbers of HSCs *in vitro* – whether from adult, umbilical cord blood, or fetal source – would have a major impact on the safety, cost and availability of stem cells for transplantation. In addition, the use of genetically selected or engineered HSC may further limit the possibility of disease progression or re-emergence after *in vitro* screening. However, HSC of whichever origin have a more limited potential for self-renewal than pluripotent ES cells.

A potential therapy for diabetes patients could be based on self-renewing somatic stem cells with the potential to differentiate *in vivo* into pancreatic islet cell clusters capable of releasing an appropriate amount of insulin to maintain glucose homeostasis (Bosco and Meda, 1997). Purified and cultured fetal cells, especially adult islet progenitor cells, are very difficult to expand *in vitro* and their insulin content decreases in culture (Beattie et al., 1997; Zulewski et al., 2001).

Besides the HSC population and liver stem cells, neural stem cells are also very promising candidates for cell therapy. The discovery of a regenerative capacity in the adult central nervous system may facilitate the repair of cell-damage from neuronal degenerative diseases such as Parkinson's disease as well as from brain and spinal cord injuries resulting from stroke or trauma. Neural stem cells or committed precursor cells might be used to generate transplants either by driving these cells in culture towards the desired differentiated neuronal cell type or by implanting them directly into the affected region, and rely on signals inside the transplantation side to direct their maturation. Since the 1980s, brain tissue transplants removed from aborted human fetuses are used in therapy of Parkinson's disease, where fetal dopaminergic neurones mature within the adult host brain (Dunnett et al., 2001). However, the logistical and technical problems involved in recovering enough developing dopaminergic neurones from fetal tissue highlight the need to find a different source of cells. Parkinson's disease is only one of many disorders in the nervous system, but is a relatively promising target because a regenerative therapy needs only the replacement of one particular cell type in one part of the brain. In contrast, complete reconstruction of the spinal cord requires the replacement of many different cell types and the need for neurones growing across an injury site connecting appropriately with their target fibres.

### *Assessing Human Stem Cell Safety*

The isolation of human stem cells offers the promise of a remarkable array of novel therapeutics. For complete success, efforts to analyse and assess the safety of these cells in the clinic are most important. Transplanted human stem cells are dynamic biological units that interact strongly with – and are influenced by – the physiology of the recipient. Whether human stem cells are of embryonic, fetal or adult origin, donor sources must be carefully screened to prevent transmission of infectious diseases, but also to assess the genetic background to obtain optimal conditions for allogenic transplantation and for particular clinical situations. To ensure the integrity, uniformity, and reliability of human stem cells, rigorously controlled and standardized procedures have to be followed in establishing and maintaining stem cell lines in culture to avoid unintended alterations in intrinsic properties. The use of mouse embryonic fibroblast feeder cells to maintain human ES and EG cells in a pluripotent status and the transplantation of these cells that have been in contact with non-human cells raises concerns of the unintended transfer of animal viruses into humans. Recently, feeder-independent culture conditions for human ES cells were developed using 100% conditioned medium from feeder cells (Xu et al., 2001).

Furthermore, detailed characterization of stem cell preparations which are intended for transplantation is necessary. Useful parameters would include: (1) cell morphology; (2) cell-surface marker expression; (3) tissue-specific enzymatic activity; and (4) characteristic gene expression patterns. It is not yet clear if homogeneous populations composed of a single cell type will be more effective in cell replacement therapy than mixed populations. The formation of various cell types differentiated stem cell outgrowths may be required to ensure maximum survival and functional capability. Before transplantation, it is essential to demonstrate relevant biological activity of stem cell preparations, e.g. insulin release of islet-like cells, glycogen storage of hepatocyte-intended cells or synchronous contraction of cells used for the replacement of cardiomyocytes. Before using human stem cells in the clinic, the cells must be transplanted into animal models of human diseases which were created by chemical, surgical, immunological or gene targeting methods. Also, evidence for anatomical and functional integration, and even migration of transplanted stem cells should be provided. Questions regarding the advantages of using embryonic instead of somatic stem cells with respect to robustness and durability should also be addressed in animal transplantation models.

Because of tumorigenity caused by unregulated growth, the proliferation potential of undifferentiated ES and EG cells evokes the greatest concern. It is still unknown at which point of differentiation this risk becomes insignificant, and whether the process of stem cell differentiation occurs only in a forward direction or is reversible. All steps of this comprehensive strategy to assess human stem cell safety have to be considered before this encouraging and challenging technique can be transferred into routine therapy of various human diseases.

## References


Alison, M. R., R. Poulsom, R. Jeffery, A. P. Dhillon, A. Quaglia, J. Jacob, M. Novelli, G. Prentice, J. Williamson, and N. A. Wright, 2000: Hepatocytes from non-hepatic adult stem cells. Nature **406**, 257.

Amit, M., M. K. Carpenter, M. S. Inokuma, C. P. Chiu, C. P. Harris, M. A. Waknitz, J. Itskovitz-Eldor, and J. A. Thomson, 2000: Clonally derived human embryonic stem cell lines maintain pluripotency and proliferative potential for prolonged periods of culture. Dev. Biol. **227**, 27127–27128.

Anderson, G. B., 1992: Isolation and use of embryonic stem cells from livestock species. Anim. Biotechnol. **3**, 165–175.

Anderson, D. J., F. H. Gage, and I. L. Weissman, 2001: Can stem cells cross lineage boundaries? Nat. Med. **7**, 393–395.

Asahara, T., T. Murohara, A. Sullivan, M. Silver, R. van der Zee, T. Li, B. Witzenbichler, G. Schatteman, and J. M. Isner, 1997: Isolation of putative progenitor endothelial cells for angiogenesis. Science **275**, 964–967.

Assady, S., G. Maor, M. Amit, J. Itskovitz-Eldor, K. L. Skorecki, and M. Tzukerman, 2001: Insulin production by human embryonic stem cells. Diabetes **50**, 1691–1697.

Beattie, G. M., T. Otonkoski, A. D. Lopez, and A. Hayek, 1997: Functional beta-cell mass after transplantation of human foetal pancreatic cells: differentiation or proliferation? Diabetes **46**, 244–248.

Becker, A. J., E. A. McCullough, and J. E. Till, 1963: Cytological demonstration of the clonal nature of spleen colonies derived from transplanted mouse marrow cells. Nature **197**, 452–454.

Betts, D., V. Bordignon, J. Hill, O. Winger, M. Westhusin, L. Smith, and W. King, 2001: Reprogramming of telomerase activity and rebuilding of telomere length in cloned cattle. Proc. Natl. Acad. Sci. USA **98**, 1077–1082.

Bianco, P., and P. G. Robey, 2001: Stem cells in tissue engineering. Nature **414**, 118–121.

Bittner, R. E., C. Schofer, K. Weipoltshammer, S. Ivanova, B. Streubel, E. Hauser, M. Freilinger, H. Hoger, A. Elbe-Burger, and F. Wachtler, 1999: Recruitment of bone marrow-derived cells by skeletal and cardiac muscle in adult dystrophic mdx mice. Anat. Embryol. **199**, 391–396.

Bjorklund, L. M., R. Sanchez-Pernaute, S. Chung, T. Andersson, I. Y. Chen, K. S. McNaught, A. L. Brownell, B. G. Jenkins, C. Wahlestedt, K. S. Kim, and O. Isacson 2002: Embryonic stem cells develop into functional dopaminergic neurons after transplantation in a Parkinson rat model. Proc. Natl. Acad. Sci. USA, **99**, 2344–2349.

Bjornson, C. R., R. L. Rietze, B. A. Reynolds, M. C. Magli, and A. L. Vescovi, 1999: Turning brain into blood: a hematopoietic fate adopted by adult neural stem cells *in vivo*. Science **283**, 534–537.

Bongso, A., C.-Y. Fong, S.-C. Ng, and S. Ratnam, 1994: Isolation and culture of inner cell mass cells from human blastocysts. Hum. Reprod. **11**, 2110–2117.

Bosco, D., and P. Meda, 1997: Reconstructing islet function *in vitro*. Adv. Exp. Med. Biol. **426**, 285–298.

Bradley, A., M. Evans, M. H. Kaufman, and E. Robertson, 1984: Formation of germ line chimeras from embryo-derived teratocarcinoma cell lines. Nature **309**, 255–256.

Brem, G., and M. Müller, 1994: Large transgenic animals. In: Animals with Novel Genes (MacLean, N., ed.), Cambridge: Cambridge University Press, pp. 179–244.

Brüstle, O., K. N. Jones, R. D. Learish, K. Karram, K. Choudhary, O. D. Wiestler, I. D. Duncan, and R. D. McKay, 1999: Embryonic stem cell-derived glial precursors: a source of myelinating transplants. Science **285**, 754–756.

Campbell, K. H. S., J. McWhir, W. A. Ritchie, and I. Wilmut, 1996: Sheep cloned by nuclear transfer from a cultured cell line. Nature **380**, 64–66.

Capecchi, M. R., 1989: Altering the genome by homologous recombination. Science **244**, 1288–1292.

Chang, I.-K., D. L. Jeong, Y. H. Hong, T. S. Park, Y. K. Moon, T. Ohno, and J. Y. Han, 1997: Production of germ line chimeric chickens by transfer of cultured primordial germ cells. Cell Biol. Int. **21**, 495–499.

Cherny, R. A., T. M. Stokes, J. Merei, L. Lom, M. R. Brandon, and R. L. Williams, 1994: Strategies for the isolation and characterization of bovine embryonic stem cells. Reprod. Fertil. Dev. **6**, 569–575.

Cibelli, J. B., S. L. Stice, P. G. Golueke, J. J. Kane, J. Jerry, E. S. C. Blackwell, F. A. Ponce de Leon, and J. M. Robl, 1998: Transgenic bovine chimeric offspring produced from somatic cell-derived stem-like cells. Nat. Biotechnol. **16**, 642–646.

Clarke, D. L., C. B. Johansson, J. Wilbertz, B. Veress, E. Nilsson, H. Karlström, U. Lendahl, and J. Frisen, 2000: Generalized potential of adult neural stem cells. Science **288**, 1660–1663.

Conover, J. C., N. Y. Ip, W. T. Poueymirou, B. Bates, M. P. Goldfarb, T. M. DeChiara, and G. D. Yancopoulos, 1993: Ciliary neurotrophic factor maintains the pluripotentiality of embryonic stem cells. Development **119**, 559–565.

Crosby, H. A., and A. J. Strain, 2001: Adult liver stem cells: bone marrow, blood, or liver derived? Gut **48**, 153–154.

Dean, W., F. Santos, M. Stojkovic, V. Zakhartchenko, J. Walter, E. Wolf, and W. Reik, 2001: Conservation of methylation reprogramming in mammalian embryos: aberrant reprogramming in cloned embryos. Proc. Natl. Acad. Sci. USA, **98**, 13734–13738.

Delhaise, F., F. J. Ectors, R. De Roover, F. Ectors, and F. Dessy, 1995: Nuclear transplantation using bovine primordial germ cells from male fetuses. Reprod. Fertil. Dev. **7**, 1217–1219.

Denning, C., S. Burl, A. Ainslie, J. Bracken, A. Dinnyes, J. Fletcher, T. King, M. Ritchie, W. A. Ritchie, M. Rollo, P. de Sousa, A. Travers, I. Wilmut, and A. J. Clark, 2001: Deletion of the alpha (1,3) galactosyl transferase (*GGTA1*) gene and the prion protein (*PrP*) gene in sheep. Nat. Biotechnol. **19**, 559–562.

Deutsch, G., J. Jung, M. Zheng, J. Lora, and K. S. Zaret, 2001: A bipotential precursor population for pancreas and liver within the embryonic endoderm. Development **128**, 871–881.

Doetschman, T. C., H. R. Eistetter, M. Katz, W. Schmidt, and R. Kemler, 1985: The *in vitro* development of blastocyst-derived embryonic stem cell lines: formation of visceral yolk sac, blood islands and myocardium. J. Embryol. Exp. Morphol. **87**, 27–45.

Donovan, P. J., and J. Gearhart, 2001: The end of the beginning for pluripotent stem cells. Nature **414**, 92–97.

Du, F., J. R. Giles, R. H. Foote, K. H. Graves, X. Yang, and R. W. Moreadith, 1995: Nuclear transfer of putative rabbit embryonic stem cells leads to normal blastocyst development. J. Reprod. Fertil. **104**, 219–223.

Dunnett, S. B., A. Bjorklund, and O. Lindvall, 2001: Cell therapy in Parkinson's disease – stop or go? Nat. Rev. Neurosci. **2**, 365–369.

Durcova-Hills, G., K. Prelle, S. Müller, M. Stojkovic, J. Motlik, E. Wolf, and G. Brem, 1998: Primary culture of porcine PGCs requires LIF and porcine membrane-bound stem cell factor. Zygote **6**, 271–275.

Eddy, E. M., J. M. Clark, D. Gong, and B. A. Fenderson, 1981: Origin and migration of primordial germ cells in mammals. Gamete Res. **4**, 333–362.

Eriksson, P. S., E. Perfilieva, T. Björn-Eriksson, A. M. Alborn, C. Nordborg, D. A. Peterson, and F. H. Gage, 1998: Neurogenesis in the adult human hippocampus. Nat. Med. **4**, 1313–1317.

Etches, R. J., M. E. Clark, A. Toner, G. Liu, and A. M. Verrinder Gibbins, 1996: Contribution to somatic and germ line lineage of chicken blastodermal cells maintained in culture. Mol. Reprod. Dev. **45**, 291–298.

Evans, M. J., and M. H. Kaufman, 1981: Establishment in culture of pluripotential cells from mouse embryos. Nature **292**, 154–156.

Evans, M. J., E. Notarianni, S. Laurie, and R. M. Moor, 1990: Derivation and preliminary characterization of pluripotent cell lines from porcine and bovine blastocysts. Theriogenology **33**, 125–128.

Ferguson-Smith, A. C., and M. A. Surani, 2001: Imprinting and the epigenetic asymmetry between parental genomes. Science **293**, 1086–1089.

Ferrari, G., G. Cusella-De Angelis, M. Coletta, E. Paolucci, A. Stornaluolo, G. Cossu, and F. Mavillo, 1998: Muscle regeneration by bone marrow-derived myogenic progenitors. Science **279**, 1528–1530.

Friedenstein, A. J., I. I. Piatetzky-Shapiro, and K. V. Petrakova, 1966: Osteogenesis in transplants of bone marrow cells. J. Embryol. Exp. Morphol. **16**, 381–390.

Gage, F. H., 1998: Cell therapy. Nature **392**, 18–24.

Gage, F. H., P. W. Coates, T. D. Palmer, H. G. Kuhn, L. J. Fisher, J. O. Suhonen, D. A. Peterson, S. T. Suhr, and J. Ray, 1995: Survival and differentiation of adult neuronal progenitor cells transplanted to the adult brain. Proc. Natl. Acad. Sci. USA **92**, 11879–11883.

Gagneten, S., Y. Le, J. Miller, and B. Sauer, 1997: Brief expression of a GFP cre fusion gene in embryonic stem cells allows rapid retrieval of site-specific genomic deletions. Nucleic Acids Res. **25**, 3326–3331.

Galli, C., G. Lazzari, J. E. Flechon, and R. M. Moor, 1994: Embryonic stem cells in farm animals. Zygote **2**, 385–389.

Gearhart, J., 1998: New potential for human embryonic stem cells. Science **282**, 1061–1062.

Gerfen, R. W., and M. B. Wheeler, 1995: Isolation of embryonic cell lines from porcine blastocysts. Anim. Biotechnol. **6**, 1–14.

Ghazizadeh, S., and L. B. Taichman, 2001: Multiple classes of stem cells in cutaneous epithelium: a lineage analysis of adult mouse skin. EMBO J. **20**, 1215–1222.

Giles, J. R., X. Yang, W. Mark, and R. H. Foote, 1993: Pluripotency of cultured rabbit inner cell mass cells detected by isozyme analysis and eye pigmentation of fetuses following injection into blastocysts or morulae. Mol. Reprod. Dev. **36**, 130–138.

Graves, K. H., and R. W. Moreadith, 1993: Derivation and characterisation of putative pluripotential embryonic stem cells from preimplantation rabbit embryos. Mol. Reprod. Dev. **36**, 424–433.

Gu, H., Y.-R. Zou, and K. Rajewsky, 1993: Independent control of immunglobulin switch recombination at individual switch regions evidenced through Cre-loxP-mediated gene targeting. Cell **73**, 1155–1164.

Gussoni, E., Y. Soneoka, C. D. Strickland, E. A. Buzney, M. K. Khan, A. F. Flint, L. M. Kunkel, and R. C. Mulligan, 1999: Dystrophin expression in the mdx mouse restored by stem cell transplantation. Nature **401**, 390–394.

Handyside, A., M. L. Hooper, M. H. Kaufman, and I. Wilmut, 1987: Towards the isolation of embryonal stem cell lines. Roux, Arch. Dev. Biol. **196**, 185–190.

Hochereau-de Reviers, T. M., and C. Perreau, 1993: *In vitro* culture of embryonic disc cells from porcine blastocysts. Reprod. Nutr. Dev. **33**, 475–483.

Holtzer, H., 1978: Cell lineages, stem cells and the 'quantal' cell cycle concept. In: Stem Cells and Tissue Homeostasis (B. I. Lord, C. S. Potten, and R. J. Cole, eds), Cambridge, New York: Cambridge University Press, pp. 1–28.

Hong, Y., C. Winkler, and M. Schartl, 1998: Production of medakafish chimeras from a stable embryonic stem cell line. Proc. Natl. Acad. Sci. USA **95**, 3679–3684.

Humpherys, D., K. Eggan, H. Akutsu, K. Hochedlinger, W. M. Rideout, D. Biniszkiewicz, R. Yanagimachi, and R. Jaenisch, 2001: Epigenetic instability in ES cells and cloned mice. Science **293**, 95–97.

Illmensee, K., and B. Mintz, 1976: Totipotency and normal differentiation of single teratocarcinoma cells cloned by injection into blastocysts. Proc. Natl. Acad. Sci. USA **73**, 549–553.

Itskovitz-Eldor, J., M. Schuldiner, D. Karsenti, A. Eden, O. Yanuka, M. Amit, H. Soreq, and N. Benvenisty, 2000: Differentiation of human embryonic stem cells into embryoid bodies comprising the three embryonic germ layers. Mol. Med. **6**, 88–95.

Johe, K. K., T. G. Hazel, T. Muller, M. M. Dugich-Djordjevic, and R. D. McKay, 1996: Single factors direct the differentiation of stem cells from the foetal and adult central nervous system. Genes Dev. **10**, 3129–3140.

Kang, Y. K., D. B. Koo, J. S. Park, Y. H. Choi, A. S. Chung, K. K. Lee, and Y. M. Han, 2001: Aberrant methylation of donor genome in cloned bovine embryos. Nat. Genet. **28**, 173–177.

Kato, Y., W. M. Rideout, 3rd, K. Hilton, S. C. Barton, Y. Tsunoda, and M. A. Surani, 1999: Developmental potential of mouse primordial germ cells. Development **126**, 1823–1832.

Klug, M. G., M. H. Soonpaa, G. Y. Koh, and L. J. Field, 1996: Genetically selected cardiomyocytes from differentiating embryonic stem cells form stable intracardiac grafts. J. Clin. Invest. **98**, 216–224.

Kocher, A. A., M. D. Schuster, M. J. Szabolcs, S. Takuma, D. Burkhoff, J. Wang, S. Homma, N. M. Edwards, and S. Itescu, 2001: Neovascularization of ischemic myocardium by human bone-marrow-derived angioblasts prevents cardiomyocyte apoptosis, reduces remodelling and improves cardiac function. Nat. Med. **7**, 430–436.

Krause, D. S., N. D. Theise, M. I. Collector, O. Henegariu, S. Hwang, R. Gardner, S. Neutzel, and S. J. Sharkis, 2001: Multi-organ, multilineage engraftment by a single bone marrow-derived stem cell. Cell **1005**, 369–377.

Kühn, R., and F. Schwenk, 1997: Advances in gene targeting methods. Curr. Opin. Immunol. **9**, 183–188.

Labosky, P. A., D. P. Barlow, and B. M. L. Hogan, 1994: Mouse embryonic germ (EG) cell lines: transmission through the germ line and differences in the methylation imprint of insulin-like growth factor 2 receptor (*Igf2r*) gene compared with embryonic stem (ES) cell lines. Development **120**, 3197–3204.

Lagasse, E., H. Connors, M. Al Dhalimy, M. Reitsma, M. Dohse, L. Osborne, X. Wang, M. Finegold, I. L. Weissman, and M. Grompe, 2000: Purified hematopoietic stem cells can differentiate into hepatocytes *in vivo*. Nat. Med. **6**, 1229–1234.

Lanzendorf, S. E., C. A. Boyd, D. L. Wright, S. Muasher, S. Oehninger, and G. D. Hodgen, 2001: Use of human gametes obtained from anonymous donors for the production of human embryonic stem cell lines. Fertil. Steril. **76**, 132–137.

Lavoir, M.-C., P. K. Basrur, and K. J. Betteridge, 1994: Isolation and identification of germ cells from fetal bovine ovaries. Mol. Reprod. Dev. **37**, 413–424.

Lavoir, M.-C., N. Rumph, A. Moens, W. A. King, Y. Plante, W. H. Johnson, J. Ding, and K. J. Betteridge, 1997: Development of bovine nuclear transfer embryos made with oogonia. Biol. Reprod. **56**, 194–199.

Lawson, K. A., N. R. Dunn, B. A. Roelen, L. M. Zeinstra, A. M. Davis, C. V. Wright, J. P. Korving, and B. L. Hogan, 1999: Bmp4 is required for the generation of primordial germ cells in the mouse embryo. Genes Dev. **13**, 424–436.

Ledermann, B., 2000: Embryonic stem cells and gene targeting. Exp. Physiol. **85**, 603–613.

Lewandowski, M., 2001: Conditional control of gene expression in the mouse. Nat. Rev. Genet. **2**, 743–755.

Liu, S., Y. Qu, T. J. Stewart, M. J. Howard, S. Chakrabortty, T. F. Holekamp, and J. W. McDonald, 2000: Embryonic stem cells differentiate into oligodendrocytes and myelinate in culture and after spinal cord transplantation. Proc. Natl. Acad. Sci. USA **97**, 6126–6131.

Lovell-Badge, R., 2001: The future for stem cell research. Nature **414**, 88–91.

Lumelsky, N., O. Blondel, P. Laeng, I. Velasco, R. Ravin, and R. McKay, 2001: Differentiation of embryonic stem cells to insulin-secreting structures similar to pancreatic islets. Science **292**, 1389–1394.

Mann, J. R., 2001: Imprinting in the germ line. Stem Cells **19**, 289–294.

Mansour, S. L., K. R. Thomas, C. Deng, and M. R. Capecchi, 1990: Introduction of a *lacZ* reporter gene into the mouse int-2 locus by homologous recombination. Proc. Natl. Acad. Sci. USA **87**, 7688–7692.

Martin, G., 1980: Teratocarcinomas and mammalian embryogenesis. Science **209**, 768–776.

Martin, G., 1981: Isolation of a pluripotent cell line from early mouse embryos cultured in medium conditioned by teratocarcinoma stem cells. Proc. Natl. Acad. Sci. USA **78**, 7634–7638.

Martin, G. R., and M. J. Evans, 1975: Differentiation of clonal lines of teratocarcinoma cells: formation of embryoid bodies *in vitro*. Proc. Natl. Acad. Sci. USA **72**, 1441–1445.

Matsui, Y., K. Zsebo, and B. L. M. Hogan, 1992: Derivation of pluripotential embryonic stem cells from murine primordial germ cells in culture. Cell **70**, 841–847.

McCreath, K. J., J. Howcroft, K. H. S. Campbell, A. Colman, A. E. Schnieke, and A. J. Kind, 2000: Production of gene-targeted sheep by nuclear transfer from cultured somatic cells. Nature **405**, 1066–1069.

McDonald, J. W., X. Z. Liu, Y. Qu, S. Liu, S. K. Mickey, D. Turetsky, D. I. Gottlieb, and D. W. Choi, 1999: Transplanted embryonic stem cells survive, differentiate and promote recovery in injured rat spinal cord. Nat. Med. **5**, 1410–1412.

McKay, R., 1997: Stem cells in the central nervous system. Science **276**, 66–71.

McLaren, A., 2001: Ethical and social considerations of stem cell research. Nature **414**, 129–131.

McWhir, J., A. E. Schnieke, R. Ansell, H. Wallace, A. Colman, A. R. Scott, and A. J. Kind, 1996: Selective ablation of differentiated cells permits isolation of embryonic stem cell lines from murine embryos with a non-permissive genetic background. Nat. Genet. **14**, 223–226.

Meinecke-Tillmann, S., and B. Meinecke, 1996: Isolation of ES-like cell lines from ovine and caprine pre-implantation embryos. J. Anim. Breed. Genet. **113**, 413–426.

Mezey, E., K. J. Chandross, G. Harta, R. A. Maki, and S. R. McKercher, 2000: Turning blood into brain: cells bearing neuronal antigens generated *in vivo* from bone marrow. Science **290**, 1779–1782.

Moens, A., S. Chastant, P. Chesne, J.-E. Flechon, K. J. Betteridge, and J.-P. Renard, 1996: Differential ability of male and female rabbit fetal germ cell nuclei to be reprogrammed by nuclear transfer. Differentiation **60**, 339–345.

Moens, A., B. Flechon, J. Degrouard, X. Vignon, J. Ding, J.-E. Flechon, K. J. Betteridge, and J.-P. Renard, 1997: Ultrastructural and immunocytochemical analysis of diploid germ cells isolated from fetal rabbit gonads. Zygote **5**, 47–60.

Moore, K., and J. A. Piedrahita, 1997: The effects of human leukemia inhibitory factor (HLIF) and culture medium on *in vitro* differentiation of cultured porcine inner cell mass (PICM). In Vitro Cell Dev. Biol. Anim. **33**, 62–71.

Mueller, S., K. Prelle, N. Rieger, C. Lassnig, U. Luksch, H. Petznek, B. Aigner, M. Baetscher, E. Wolf, M. Müller, and G. Brem, 1999: Chimeric pigs following blastocyst injection of transgenic porcine primordial germ cells. Mol. Reprod. Dev. **54**, 244–254.

Nagy, A., J. Rossant, R. Nagy, W. Abramow-Newerly, and J. C. Roder, 1993: Derivation of completely cell culture-derived mice from early passage embryonic stem cells. Proc. Natl. Acad. Sci. USA **90**, 8424–8428.

Nichols, J., I. Chambers, and A. Smith, 1994: Derivation of germ line competent embryonic stem cells with combination of interleukin-6 and soluble interleukin-6 receptor. Exp. Cell Res. **215**, 237–239.

Nichols, J., I. Chambers, T. Taga, and A. Smith, 2001: Physiological rationale for responsiveness of mouse embryonic stem cells to gp130 cytokines. Development **128**, 2333–2339.

Nichols, J. F., E. P. Evans, and A. G. Smith, 1990: Establishment of germ line-competent embryonic stem (ES) cells using differentiation inhibiting activity. Development **110**, 1341–1348.

Notarianni, E., C. Galli, S. Laurie, R. M. Moor, and M. J. Evans, 1991: Derivation of pluripotent, embryonic cell lines from the pig and sheep. J. Reprod. Fertil. **43** (Supplement), 255–260.

Notarianni, E., S. Laurie, R. M. Moor, and M. J. Evans, 1990: Maintenance and differentiation in culture of pluripotential embryonic cell lines from pig blastocysts. J. Reprod. Fertil. **41** (Supplement), 51–56.

Orban, P. C., D. Chui, and J. D. Marth, 1992: Tissue and site-specific DNA recombination in transgenic mice. Proc. Natl. Acad. Sci. USA **89**, 6861–6865.

Orlic, D., J. Kajstura, S. Chimenti, I. Jakoniuk, S. M. Anderson, B. Li, J. Pickel, R. McKay, B. Nadal-Ginard, D. M. Bodine, A. Leri, and P. Anversa, 2001: Bone marrow cells regenerate infarcted myocardium. Nature **410**, 701–705.

Osterrieder, N., and E. Wolf, 1998: Lessons from gene knockouts. Rev. Sci. Tech. **17**, 351–364.

Owen, M., 1988: Marrow derived stromal stem cells. J. Cell Sci. **10** (Supplement), 63–76.

Pain, B., M. E. Clark, M. Shen, H. Nakazawa, M. Sakura, J. Samarut, and R. J. Etches, 1996: Long-term *in vitro* culture and characterisation of avian embryonic stem cells with multiple morphogenic potentialities. Development **122**, 2339–2348.

Pedersen, R. A., 1994: Studies of *in vitro* differentiation with embryonic stem cells. Reprod. Fertil. Dev. **6**, 543–552.

Piedrahita, J. A., G. B. Anderson, and R. H. BonDurant, 1990a: Influence of feeder layer type on the efficiency of isolation of porcine embryo-derived cell lines. Theriogenology **34**, 865–877.

Piedrahita, J. A., G. B. Anderson, and R. H. BonDurant, 1990b: On the isolation of embryonic stem cells: comparative behavior of murine, porcine and ovine embryos. Theriogenology **34**, 879–901.

Piedrahita, J. A., K. Moore, B. Oetama, C.-K. Lee, N. Scales, J. Ramsoondar, F. W. Bazer, and T. Ott, 1998: Generation of transgenic porcine chimeras using primordial germ cell-derived colonies. Biol. Reprod. **58**, 1321–1329.

Platt, J. L., 1998: New directions for organ transplantation. Nature **392**, 11–17.

Prelle, K., H. Füllgrabe, and W. Holtz, 1993: Isolation of the inner cell mass (ICM) for the establishment of embryonic stem cells. J. Reprod. Fertil. Abstract. Series **12**, 6.

Prelle, K., W. Holtz, and M. Osborn, 2001: Immunocytochemical analysis of vimentin expression patterns in porcine embryos suggests mesodermal differentiation from Day 9 after conception. Anat. Histol. Embryol. **30**, 339–344.

Prelle, K., I. M. Vassiliev, S. G. Vassilieva, E. Wolf, and A. M. Wobus, 1999: Establishment of pluripotent cell lines from vertebrate species – present status and future prospects. Cells Tissues Organs **165**, 220–236.

Rathjen, P. D., J. Lake, L. M. Whyatt, M. D. Bettess, and J. Rathjen, 1998: Properties and uses of embryonic stem cells: prospects for application to human biology and gene therapy. Reprod. Fertil. Dev. **10**, 31–47.

Reik, W., and J. Walter, 2001: Genomic imprinting: parental influence on the genome. Nat. Rev. Genet. **2**, 21–32.

Resnick, J. L., L. S. Bixler, L. Cheng, and P. L. Donovan, 1992: Long-term proliferation of mouse primordial germ cells in culture. Nature **359**, 550–551.

Reubinoff, B. E., M. F. Pera, C. Y. Fong, A. Trounson, and A. Bongso, 2000: Embryonic stem cell lines from human blastocysts: somatic differentiation *in vitro*. Nat. Biotechnol. **18,** 399–404.

Reya, T., S. J. Morrison, M. F. Clarke, and I. L. Weissman, 2001: Stem cells, cancer, and cancer stem cells. Nature **414,** 105–111.

Rideout, W. M. 3rd, T. Wakayama, A. Wutz, K. Eggan, L. Jackson-Grusby, J. Dausman, R. Yanagimachi, and R. Jaenisch, 2000: Generation of mice from wild-type and targeted ES cells by nuclear cloning. Nat. Genet. **24,** 109–110.

Robey, P. G., 2000: Stem cells near the century mark. J. Clin. Invest. **105,** 1489–1491.

Rohwedel, J., K. Guan, and A. M. Wobus, 1999: Induction of cellular differentiation by retinoic acid *in vitro*. Cells Tissues Organs **165,** 190–202.

Rohwedel, J., U. Sehlmeyer, J. Shan, A. Meister, and A. M. Wobus, 1996: Primordial germ cell-derived mouse embryonic germ (EG) cells *in vitro* resemble undifferentiated stem cells with respect to differentiation capacity and cell cycle distribution. Cell Biol. Int. **20,** 579–587.

Ropeter-Scharfenstein, M., N. Neubert, K. Prelle, and W. Holtz, 1996: Identification, isolation, and culture of pluripotent cells from the porcine inner cell mass. J. Anim. Breed. Genet. **113,** 427–436.

Rose, T. M., and G. Bruce, 1994: Oncostatin M is a member of a cytokine family that includes leukaemia inhibitory factor, granulocyte colony stimulating factor, and interleukin-6. Proc. Natl. Acad. Sci. USA **88,** 8641–8645.

Schnieke, A. E., A. J. Kind, W. A. Ritchie, K. Mycock, A. R. Scott, M. Ritchie, I. Wilmut, A. Colman, and K. H. S. Campbell, 1997: Human factor IX transgenic sheep produced by transfer of nuclei from transfected fetal fibroblasts. Science **278,** 2130–2133.

Schöler, H. R., A. K. Hatzopoulos, R. Balling, N. Suzuki, and P. Gruss, 1989: A family of octamer specific proteins present during mouse embryogenesis: evidence for germ line-specific expression of an Oct factor. EMBO J. **8,** 2543–2550.

Scholz, G., I. Pohl, E. Genschow, M. Klemm, and H. Spielmann, 1999: Embryotoxicity screening using embryonic stem cells *in vitro*: correlation to *in vivo* teratogenicity. Cells Tissues Organs **165,** 203–211.

Schoonjans, L., G. M. Albricht, J.-L. Li, D. Collen, and R. W. Moreadith, 1996: Pluripotential rabbit embryonic stem (ES) cells are capable of forming overt coat colour chimeras following injection into blastocysts. Mol. Reprod. Dev. **45,** 439–443.

Schuldiner, M., O. Yanuka, J. Itskovitz-Eldor, D. A. Melton, and N. Benvenisty, 2000: From the cover: effects of eight growth factors on the differentiation of cells derived from human embryonic stem cells. Proc. Natl. Acad. Sci. USA **97,** 11307–11312.

Schultz, E., 1996: Satellite cell proliferative compartments in growing skeletal muscles. Dev. Biol. **175,** 84–94.

Sell, S., 1990: Is there a liver stem cell? Cancer Res. **50,** 3811–3815.

Shamblott, M. J., J. Axelman, J. W. Littlefield, P. D. Blumenthal, G. R. Huggins, Y. Cui, L. Cheng, and J. D. Gearhart, 2001: Human embryonic germ cell derivatives express a broad range of developmentally distinct markers and proliferate extensively *in vitro*. Proc. Natl. Acad. Sci. USA **98,** 113–118.

Shamblott, M. J., J. Axelman, S. Wang, E. M. Bugg, J. W. Littlefield, P. J. Donovan, P. D. Blumenthal, G. R. Huggins, and J. D. Gearhart, 1998: Derivation of pluripotent stem cells from cultured human primordial germ cells. Proc. Natl. Acad. Sci. USA **95,** 13726–13731.

Shi, Q., S. Rafii, M. H. Wu, E. S. Wijelath, C. Yu, A. Ishida, Y. Fujita, S. Kothari, R. Mohle, L. R. Sauvage, M. A. Moore, R. F. Storb, and W. P. Hammond, 1998: Evidence for circulating bone marrow-derived endothelial cells. Blood **92,** 362–367.

Shihabuddin, L. S., P. J. Horner, J. Ray, and F. H. Gage, 2000: Adult spinal cord stem cells generate neurons after transplantation in the adult dentate gyrus. J. Neurosci. **30,** 624–627.

Shihabuddin, L. S., T. D. Palmer, and F. H. Gage, 1999: The search for neural progenitor cells: prospects for the therapy of neurodegenerative disease. Mol. Med. Today **5,** 474–480.

Shim, H., and G. B. Anderson, 1998: *In vitro* survival and proliferation of porcine primordial germ cells. Theriogenology **49,** 521–528.

Shim, H., A. Gutierrez-Adan, L. R. Chen, R. H. BonDurant, E. Behboodi, and G. B. Anderson, 1997: Isolation of pluripotent stem cells from cultured porcine primordial germ cells. Biol. Reprod. **57,** 1089–1095.

Slack, J. M., 2000: Stem cells in epithelial tissues. Science **287,** 1431–1433.

Smith, A., 2001: Embryonic stem cells. In: Stem Cell Biology, (Marshak, D. R., R. L. Gardner, and D. Gottlieb, eds) Cold Spring Harbor, New York: Cold Spring Harbor Laboratory Press, pp. 205–230.

Smith, A. G., J. K. Heath, D. D. Donaldson, G. G. Wong, J. Moreau, M. Stahl, and D. Rogere, 1988: Inhibition of pluripotential embryonic stem cell differentiation by purified polypeptides. Nature **336,** 688–690.

Solter, D., 1998: Dolly is a clone – and no longer alone. Nature **394,** 315–316.

Solter, D., and B. B. Knowles, 1978: Monoclonal antibody defining a stage-specific mouse embryonic antigen (SSEA-1). Proc. Natl. Acad. Sci. USA **75,** 5565–5569.

Solter, D., N. Skreb, and I. Damjanov, 1970: Extrauterine growth of mouse egg-cylinders results in malignant teratoma. Nature **227,** 503–504.

Soria, B., E. Roche, G. Berna, T. Leon-Quinto, J. A. Reig, and F. Martin, 2000: Insulin-secreting cells derived from embryonic stem cells normalize glycemia in streptozotocin-induced diabetic mice. Diabetes **49,** 157–162.

Spradling, A., D. Drummond-Barbosa, and T. Kai, 2001: Stem cells find their niche. Nature **414,** 98–104.

Stanford, W. L., J. B. Cohn, and S. P. Cordes, 2001: Gene-trap mutagenesis: past, present and beyond. Nat. Rev. Genet. **2,** 756–768.

Stewart, C. L., 1991: Prospects for the establishment of embryonic stem cells and genetic manipulation of domestic animals. In: Animal Applications of Research in Mammalian Development. (Pedersen, R. A., A. McLaren, and N. L. First, eds), Cold Spring Harbor, New York: Cold Spring Harbor Laboratory Press, pp. 267–283.

Stewart, C. L., I. Gadi, and H. Bhatt, 1994: Stem cells from primordial germ cells can re-enter the germ line. Dev. Biol. **161,** 626–628.

Stice, S. L., N. S. Strelchenko, C. L. Keefer, and L. Matthews, 1996: Pluripotent bovine embryonic cell lines direct development following nuclear transfer. Biol. Reprod. **54,** 100–110.

Strelchenko, N., 1996: Bovine pluripotent stem cells. Theriogenology **45,** 131–140.

Strelchenko, N., J. Betthauser, G. Jurgella, E. Farsberg, P. Damiani, and P. Golueke, 1998: Use of somatic cells in cloning. Proc. Gen. Engin. Cloning Anim., Park City, 125. pp.

Strojek, R. M., M. A. Reed, J. L. Hoover, and T. E. Wagner, 1990: A method for cultivation of morphologically undifferentiated embryonic stem cells from porcine blastocysts. Theriogenology **33,** 901–913.

Studer, L., M. Csete, S. H. Lee, N. Kabbani, J. Walikonis, B. Wold, and R. McKay, 2000: Enhanced proliferation, survival, and dopaminergic differentiation of CNS precursors in lowered oxygen. J. Neurosci. **20,** 7377–7383.

Studer, L., V. Tabar, and R. D. McKay, 1998: Transplantation of expanded mesencephalic precursors leads to recovery in Parkinsonian rats. Nat. Neurosci. **1,** 290–295.

Surani, M. A., 2001: Reprogramming of genome function through epigenetic inheritance. Nature **414,** 122–128.

Tada, T., M. Tada, K. Hilton, S. C. Barton, T. Sado, N. Takagi, and M. A. Surani, 1998: Epigenotype switching of imprintable loci in embryonic germ cells. Dev. Genes Evol. **207,** 551–561.

Taipale, J., and P. A. Beachy, 2001: The hedgehog and Wnt signaling pathways in cancer. Nature **411,** 349–354.

Takagi, Y., N. C. Talbot, C. E. Rexroad, and V. G. Pursel, 1997: Identification of pig primordial germ cells by immunocytochemistry and lectin binding. Mol. Reprod. Dev. **46,** 567–580.

Talbot, N. C., A. M. Powell, and C. E. Rexroad, 1995: *In vitro* pluripotency of epiblast derived from bovine blastocysts. Mol. Reprod. Dev. **42**, 35–52.

Talbot, N. C., C. E. Rexroad, V. G. Pursel, and A. M. Powell, 1993: Alkaline phosphatase staining of pig and sheep epiblast cells in culture. Mol. Reprod. Dev. **36**, 139–147.

Tam, P. P., and S. X. Zhou, 1996: The allocation of epiblast cells to ectodermal and germ-line lineages is influenced by the position of the cells in the gastrulating mouse embryo. Dev. Biol. **178**, 124–132.

Tam, P. I., S. X. Zhou, and S.-S. Tan, 1994: X-chromosome activity of the mouse primordial germ cells revealed by the expression of an X-linked lacZ transgene. Development **120**, 2925–2932.

Tang, D. G., Y. M. Tokumoto, J. A. Apperly, A. C. Lloyd, and M. C. Raff, 2001: Lack of replicative senescence in cultured rat oligodendrocyte precursor cells. Science **291**, 868–871.

Taylor, G., M. S. Lehrer, P. J. Jensen, T. T. Sun, and R. M. Lavker, 2000: Involvement of follicular stem cells in forming not only the follicle but also the epidermis. Cell **102**, 451–461.

Temple, S., 2001: The development of neural stem cells. Nature **414**, 112–117.

Theise, N. D., M. Nimmakayalu, R. Gardner, P. B. Illei, G. Morgan, L. Teperman, O. Henegariu, and D. S. Krause, 2000: Liver from bone marrow in humans. Hepatology **32**, 11–16.

Thomas, K. R., and M. R. Capecchi, 1987: Site-directed mutagenesis by gene targeting in mouse embryo-derived stem cells. Cell **51**, 503–512.

Thomas, K. R., K. R. Folger, and M. R. Capecchi, 1986: High frequency targeting of genes to specific sites in the mammalian genome. Cell **44**, 419–428.

Thompson, S., A. R. Clarke, A. M. Pow, M. L. Hooper, and D. W. Melton, 1989: Germ-line transmission of a corrected HPRT gene produced by gene targeting in embryonic stem cells. Cell **56**, 313–321.

Thomson, J. A., J. Itskovitz-Eldor, S. S. Shapiro, M. A. Waknitz, J. J. Swiergiel, V. S. Marshall, and J. M. Jones, 1998: Embryonic stem cell lines derived from human blastocysts. Science **282**, 1145–1147.

Till, J. E., and E. A. McCullough, 1961: A direct measurement of the radiation sensitivity of normal mouse bone marrow cells. Radiat. Res. **14**, 213–222.

Trounson, A., and M. Pera, 1998: Potential benefits of cell cloning for human medicine. Reprod. Fertil. Dev. **10**, 121–125.

Van Stekelenburg-Hamers, A. E. P., T. A. E. Van Achterberg, H. G. Rebel, J.-E. Flechon, K. H. S. Campbell, S. M. Weima, and C. L. Mummery, 1995: Isolation and characterization of permanent cell lines from inner cell mass cells of bovine blastocysts. Mol. Reprod. Dev. **40**, 444–454.

Wakayama, T., V. Tabar, I. Rodriguez, A. C. Perry, L. Studer, and P. Mombaerts, 2001: Differentiation of embryonic stem cell lines generated from adult somatic cells by nuclear transfer. Science **292**, 740–743.

Wakayama, T., and R. Yanagimachi, 2001: Mouse cloning with nucleus donor cells of different age and type. Mol. Reprod. Dev. **58**, 376–383.

Wang, Z. Q., F. Kiefer, P. Urbanek, and E. F. Wagner, 1997: Generation of completely embryonic stem cell-derived mutant mice using tetraploid blastocyst injection. Mech. Dev. **62**, 137–145.

Weissman, I. L., 2000: Stem cells: units of development, units of regeneration, and units in evolution. Cell **100**, 157–168.

Wells, D. N., P. M. Misica, T. A. M. Day, and H. R. Tervit, 1997: Production of cloned lambs from an established embryonic cell line: a comparison between *in vivo*- and *in vitro*-matured cytoplasts. Biol. Reprod. **57**, 385–393.

Wheeler, M. B., 1994: Development and validation of swine embryonic stem cells: a review. Reprod. Fertil. Dev. **6**, 563–568.

Wheeler, M. B., A. L. Rund, and G. T. Bleck, 1995: The use of embryonic stem cells in the production of transgenic livestock. Emb. Trans. News **13**, 20–25.

Wianny, F., C. Perreau, and M. T. Hochereau-de Reviers, 1997: Proliferation and differentiation of porcine inner cell mass and epiblast *in vitro*. Biol. Reprod. **57**, 756–764.

Wobus, A. M., J. Rohwedel, V. Maltsev, and J. Hescheler, 1994: *In vitro* differentiation of embryonic stem cells into cardiomyocytes or skeletal muscle cells is specifically modulated by retinoic acid. Roux's Arch. Dev. Biol. **204**, 36–45.

Wobus, A. M., J. Rohwedel, C. Strübing, J. Shan, K. Adler, V. Maltsev, and J. Hescheler, 1997: *In vitro* differentiation of embryonic stem cells. In: Methods in Developmental Toxicology and Biology (Klug, S., and R. Thiel, eds) Berlin: Blackwell Science, pp. 1–17.

Wolf, E., R. Kramer, I. Polejaeva, H. Thoenen, and G. Brem, 1994: Efficient generation of chimeric mice using embryonic stem cells after long-term culture in the presence of ciliary neurotrophic factor. Transgenic Res. **3**, 152–158.

Wolf, E., W. Schernthaner, V. Zakhartchenko, K. Prelle, M. Stojkovic, and G. Brem, 2000: Transgenic technology in farm animals – progress and perspectives. Exp. Physiol. **85**, 615–625.

Wood, S. A., N. D. Allen, J. Rossant, A. Auerbach, and A. Nagy, 1993: Non-injection methods for the production of embryonic stem cell-embryo chimeras. Nature **365**, 87–89.

Wylie, C. C., 1993: The biology of primordial germ cells. Eur. Urol. **23**, 62–67.

Xu, C., M. S. Inokuma, J. Denham, K. Golds, P. Kundu, J. D. Gold, and M. K. Carpenter, 2001: Feeder-free growth of undifferentiated human embryonic stem cells. Nat. Biotechnol. **19**, 971–974.

Zakhartchenko, V., G. Durcova-Hills, W. Schernthaner, M. Stojkovic, H.-D. Reichenbach, S. Müller, R. Steinborn, M. Müller, H. Wenigerkind, K. Prelle, E. Wolf, and G. Brem, 1999: Potential of fetal germ cells for nuclear transfer in cattle. Mol. Reprod. Dev. **52**, 421–426.

Zulewski, H., E. J. Abraham, M. J. Gerlach, P. B. Daniel, W. Moritz, B. Muller, M. Vallejo, M. K. Thomas, and J. F. Habener, 2001: Multipotential nestin-positive stem cells isolated from adult pancreatic islets differentiate *ex vivo* into pancreatic endocrine, exocrine, and hepatic phenotypes. Diabetes **50**, 521–533.

Received 11 January; accepted 31 May 2000.


1. Munson, M. A., Baumann, P. & Kinsey, M. G. *Buchnera*, new genus and *Buchnera aphidicola*, new species, a taxon consisting of the mycetocyte-associated, primary endosymbionts of aphids. *Int. J. Syst. Bacteriol.* **41**, 566–568 (1991).
2. Ishikawa, H. Biochemical and molecular aspects of endosymbiosis in insects. *Int. Rev. Cytol.* **116**, 1–45 (1989).
3. Baumann, P., Moran, N. A. & Baumann, L. in *The Prokaryotes* (ed. Dworkin, M.) (Springer, New York, 2000).
4. Komaki, K. & Ishikawa, H. Intracellular bacterial symbionts of aphids possess many genomic copies per bacterium. *J. Mol. Evol.* **48**, 717–722 (1999).
5. Charles, H. & Ishikawa, H. Physical and genetic map of the genome of *Buchnera*, the primary endosymbiont of the pea aphid *Acyrthosiphon pisum*. *J. Mol. Evol.* **48** 142–150 (1999).
6. Buchner, P. *Endosymbiosis of Animals with Plant Microorganisms* (Wiley, New York, 1965).
7. Moran, N. A., Munson, M. A., Baumann, P. & Ishikawa, H. A molecular clock in endosymbiotic bacteria is calibrated using the insect hosts. *Proc. R. Soc. Lond. B* **253**, 167–171 (1993).
8. Fraser, C. M. *et al.* The minimal gene complement of *Mycoplasma genitalium*. *Science* **270**, 397–403 (1995).
9. van Ham, R. C., Moya, A. & Latorre, A. Putative evolutionary origin of plasmids carrying the genes involved in leucine biosynthesis in *Buchnera aphidicola* (endosymbiont of aphids). *J. Bacteriol.* **179**, 4768–4777 (1997).
10. Douglas, A. E. Nutritional interactions in insect-microbial symbioses: aphids and their symbiotic bacteria *Buchnera*. *Annu. Rev. Entomol.* **43**, 17–37 (1998).
11. Moran, N. A. Accelerated evolution and Muller's rachet in endosymbiotic bacteria. *Proc. Natl Acad. Sci. USA* **93**, 2873–2878 (1996).
12. Houk, E. J. & Griffiths, G. W. Intracellular symbiotes of the Homopltera. *Annu. Rev. Entomol.* **25**, 161–187 (1980).
13. Sasaki, T. & Ishikawa, H. Production of essential amino acids from glutamate by mycetocyte symbionts of the pea aphid, *Acyrthosiphon pisum*. *J. Insect. Physiol.* **41**, 41–46 (1995).
14. Nakabachi, A. & Ishikawa, H. Provision of riboflavin to the host aphid, *Acyrothosiphon pisum*, by endosymbiotic bacteria, *Buchnera*. *J. Insect. Physiol.* **45**, 1–6 (1999).
15. Mittler, T. E. Dietary amino acid requirements of Aphid *Myzus persicae* affected by antibiotic uptake. *J. Nutr.* **101**, 1023–1028 (1971).
16. Whitehead, L. F. & Douglas, A. E. A metabolic study of *Buchnera*, the intracellular bacterial symbionts of the pea aphid *Acyrthosiphon pisum*. *J. Gen. Microbiol.* **139**, 821–826 (1993).
17. Douglas, A. E. Sulphate utilization in an aphid symbiosis. *Insect. Biochem. Mol. Biol.* **18**, 599-605 (1988).
18. Tomii, K. & Kanehisa, M. A comparative analysis of ABC transporters in complete microbial genomes. *Genome Res.* **8**, 1048–1059 (1998).
19. Kubori, T. *et al.* Supramolecular structure of the *Salmonella typhimurium* type III protein secretion system. *Science* **280**, 602–605 (1998).
20. Young, G. M., Schmiel, D. H. & Miller, V. L. A new pathway for the secretion of virulence factors by bacteria: the flagellar export apparatus functions as a protein-secretion system. *Proc. Natl Acad. Sci. USA* **96**, 6456–6461 (1999).
21. Marais, A., Bove, J. M. & Renaudin, J. Characterization of the *recA* gene regions of *Spiroplasma citri* and *Spiroplasma melliferum*. *J. Bacteriol.* **178**, 7003–7009 (1996).
22. Eisen, J. A. & Hanawalt, P. C. A phylogenomic study of DNA repair genes, proteins, and processes. *Mutat. Res.* **435**, 171–213 (1999).
23. Nogueira, T. & Springer, M. Post-transcriptional control by global regulators of gene expression in bacteria. *Curr. Opin. Microbiol.* **3**, 154–158 (2000).
24. Fleischmann, R. D. *et al.* Whole-genome random sequencing and assembly of *Haemophilus influenzae* Rd. *Science* **269**, 496–512 (1995).
25. Hattori, M. *et al.* A novel method for making nested deletions and its application for sequencing of a 300 kb region of human APP locus. *Nucleic Acids Res.* **25**, 1802–1808 (1997).
26. Yada, T. & Hirosawa, M. Detection of short protein coding regions within the cyanobacterium genome: application of the hidden Markov model. *DNA Res.* **3**, 355–361 (1996).
27. Tomb, J. F. *et al.* The complete genome sequence of the gastric pathogen *Helicobacter pylori*. *Nature* **388**, 539–547 (1997).
28. Ogata, H. *et al.* KEGG: Kyoto Encyclopedia of Genes and Genomes. *Nucleic Acids Res.* **27**, 29–34 (1999).
29. Watanabe, H., Mori, H., Itoh, T. & Gojobori, T. Genome plasticity as a paradigm of eubacteria evolution. *J. Mol. Evol.* **44** (Suppl. 1), S57–S64 (1997).
30. Riley, M. Functions of the gene products of *Escherichia coli*. *Microbiol. Rev.* **57**, 862–952 (1993).


**Supplementary information** is available on *Nature*'s World-Wide Web site (http://www.nature.com) or as paper copy from the London editorial office of *Nature*.


## Acknowledgements

We thank the technical staff of RIKEN GSC, M. Horishima, H. Ishizaki, N. Ota and Y. Seki for sequencing; T. Yada for ORF prediction; A. Toyoda for technical support on the sequence library preparation; C. Kawagoe for computer system support; and T. D. Taylor for discussion. This work was supported by a grant from the Program for Promotion of Basic Research Activities for Innovation Biosciences (ProBRAIN) of the Bio-oriented Technology Research Advancement Institution, and Grants-in-Aid for Scientific Research from the Japanese Ministry of Education, Science, Sports and Culture.


Correspondence and requests for materials should be addressed to Y.S. (e-mail: sakaki@ims.u-tokyo.ac.jp) or H.I. (e-mail: iskw@biol.s.u-tokyo.ac.jp). The complete sequence and the annotated data are available on our website (http://buchnera.gsc.riken.go.jp/). The sequence has been deposited with DDBJ under accession number AP000398, AP001070 and AP001071 for chromosome, the pTrp plasmid and the pLeu plasmid, respectively.

# Cloned pigs produced by nuclear transfer from adult somatic cells

**Irina A. Polejaeva*, Shu-Hung Chen*, Todd D. Vaught*, Raymond L. Page*, June Mullins*, Suyapa Ball*, Yifan Dai*, Jeremy Boone*, Shawn Walker*, David L. Ayares*, Alan Colman† & Keith H. S. Campbell†‡**

* *PPL Therapeutics Incorporated, 1700 Kraft Drive, Blacksburg, Virginia 24060, USA*

† *PPL Therapeutics, Roslin, Midlothian EH25 9PP, UK*

**Since the first report of live mammals produced by nuclear transfer from a cultured differentiated cell population in 1995 (ref. 1), successful development has been obtained in sheep[2,3], cattle[4], mice[5] and goats[6] using a variety of somatic cell types as nuclear donors. The methodology used for embryo reconstruction in each of these species is essentially similar: diploid donor nuclei have been transplanted into enucleated MII oocytes that are activated on, or after transfer. In sheep[2] and goat[6] pre-activated oocytes have also proved successful as cytoplast recipients. The reconstructed embryos are then cultured and selected embryos transferred to surrogate recipients for development to term. In pigs, nuclear transfer has been significantly less successful; a single piglet was reported after transfer of a blastomere nucleus from a four-cell embryo to an enucleated oocyte[7]; however, no live offspring were obtained in studies using somatic cells such as diploid or mitotic fetal fibroblasts as nuclear donors[8,9]. The development of embryos reconstructed by nuclear transfer is dependent upon a range of factors. Here we investigate some of these factors and report the successful production of cloned piglets from a cultured adult somatic cell population using a new nuclear transfer procedure.**

To date, the efficiency of somatic cell nuclear transfer, when measured as development to term as a proportion of oocytes used, has been very low (1–2%)[10]. A variety of factors probably contribute to this inefficiency. These include laboratory to laboratory variation, oocyte source and quality, methods of embryo culture (which are more advanced in some species (such as cows) than others (such as pigs)), donor cell type, possible loss of somatic imprinting in the nuclei of the reconstructed embryo, failure to reprogram the transplanted nucleus adequately, and finally, the failure of artificial methods of activation to emulate reproducibly those crucial membrane-mediated events that accompany fertilization.

In the pig, there is the additional difficulty that several ($>4$) good quality embryos are required to induce and maintain a pregnancy[11]. As fully developmentally competent embryos are rare in nuclear transfer procedures, there is every chance of squandering those good embryos unless very large numbers of reconstructed embryos are transferred back into recipients. Even if it were possible in the pig to select good quality blastocysts for transfer (after, for example, the use of a temporary recipient), most blastocysts formed from reconstructed embryos in other species are not competent to proceed to term[10]. The co-transfer of reconstructed embryos with 'helper', unmanipulated embryos, parthenotes or tetraploid embryos has been suggested as an aid to inducing and maintaining pregnancy. However, studies in mice after zygote pronuclear injection have suggested that the manipulated embryos are 'compromised' and selected against[12]. An alternative to the use of 'helper' embryos is the hormonal treatment of recipient sows to maintain pregnancy with low embryo numbers[13].

We cannot currently address all of the methodological problems, and, to improve our chances of success in pig nuclear

‡ Present address: University of Nottingham, School of Biosciences, Sutton Bonington, Leicestershire LE12 5RN, UK.

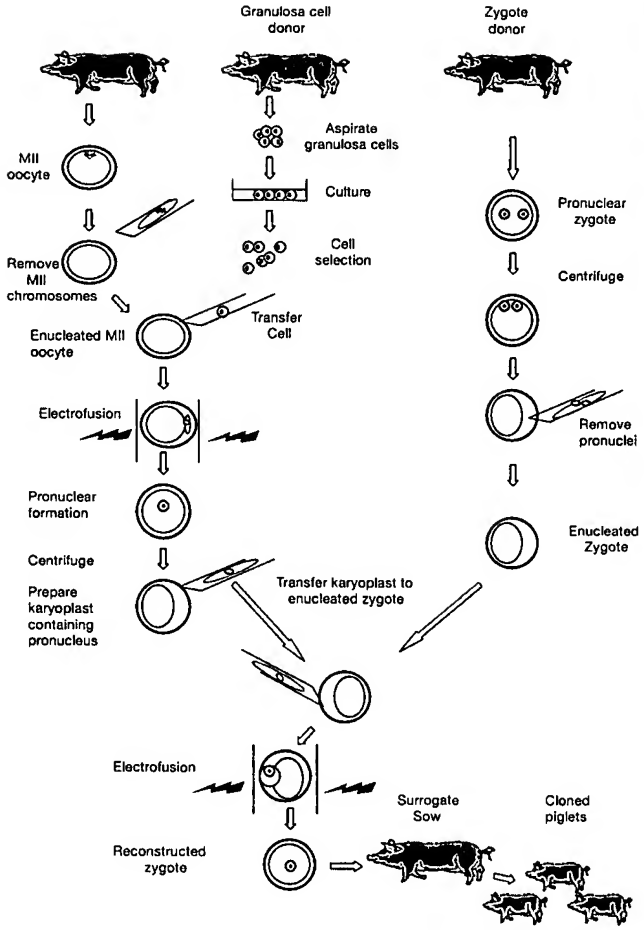


**Figure 1** Representation of the double nuclear transfer procedure for the production of viable piglets using cultured adult somatic granulosa cells as nuclear donors. The outer circle in all the oocytes and embryos denotes the zona pellucida; the inner circle denotes the cell membrane.

**Figure 2** A litter of five live piglets derived by nuclear transfer using cultured adult granulosa cells as nuclear donors. A total of 72 reconstructed embryos were transferred to the surrogate sow.

transfer, we chose to focus on four areas: activation, choice of donor cell, embryo culture, and induction and maintenance of pregnancy.

In all species, when using MII oocytes as recipients, the method of activation is crucial for subsequent development. In the pig, although current activation protocols stimulate pronuclear formation, cleavage, and development to the blastocyst stage, both the frequency of development and the quality of the embryos produced are low[14]. A system that involves the use of fertilized zygotes as cytoplast recipients would bypass the inefficiencies of artificial activation procedures and might promote more successful development. The technique of pronuclear exchange between zygotes showed that the manipulations involved were compatible with development[15]; however, when donor nuclei from later developmental stages were transferred there was restricted development[16]. One explanation is that factors required for development, which are absent in the donor nuclei, are removed with the pronuclei. But if a pronucleus-like structure could be produced from the donor nucleus, this might prove a suitable nuclear donor for transfer. Such a system was described in mice by Kwon and Kono[17], who first fused mitotically arrested blastomere nuclei with enucleated MII oocytes. The reconstructed oocytes were subsequently activated in the presence of cytochalasin B, preventing polar body extrusion and resulting in the formation of two diploid pseudo-pronuclei. Each pseudo-pronucleus was then transferred into an enucleated, *in vivo* produced zygote, which was transferred into a surrogate recipient for development to term. Effectively, this latter procedure mimics pronuclear exchange and allows the

**Table 1 Development of porcine embryos**

| | Double NT | | | | | | | Single NT | | |
|---|---|---|---|---|---|---|---|---|---|---|
| Cell isolate | Pool1 | GR5 | GR8 | GR12 | GR21Z | GR18 | GR18 | GR1 | GR8 | GR18 |
| Cell treatment | CI | CI | CI | CI | CI | SS (74) | SS (51) | CI | CI | SS (51) |
| No. of oocytes | 245 | 344 | 269 | 291 | 311 | 193 | 216 | 123 | 109 | N/A |
| No. of attempted reconstructions day 1 (%) | 183 (75) | 217 (63) | 207 (77) | 226 (78) | 221 (71) | 122 (63) | 192 (89) | 94 (76) | 83 (76) | N/A |
| No. of fused embryos day 1 (%) | 124 (68) | 153 (70) | 186 (90) | 97 (43) | 163 (74) | 90 (74) | 162 (84) | 87 (93) | 61 (73) | N/A |
| No. of day-1 embryos with single pronucleus (%) | 87 (70) | 88 (57) | 120 (64) | 62 (64) | 69 (42) | 23 (26) | 102 (63) | – | – | – |
| No. of reconstructed embryos day 2 | 74 | 57 | 105 | 61 | 55 | 22 | 45* | – | – | – |
| No. of fused embryos day 2 (%) | 72 (97) | 56 (98) | 100 (95) | 53 (87) | 54 (98) | 22 (100) | 44 (98) | – | – | – |
| No. of embryos transferred to recipient | 72 | 56 | 100 | 53 | 54 | 22 | 44 | 85 | 61 | 39† |
| Pregnancy (no. of fetuses observed) | +ve (3) | –ve | –ve | –ve | –ve | +ve (6) | –ve | –ve | –ve | –ve |
| No. of live births (%) | 5 (7) | 0 | 0 | 0 | 0 | 0 | 0 | 0 | 0 | 0 |

Development of porcine embryos reconstructed using a single or double nuclear transfer protocol with adult granulosa cells cultured to confluence (CI), or serum starved (SS) as nuclear donors.
* Insuffici9ent zygotes to reconstruct day 1 embryos.
† Due to insufficient zygote numbers 39 day-1 recosntructed embryos were transferred to a single recipient.

formation of a final reconstructed one-cell embryo whose membrane has been activated during fertilization.

The use of cultured cell populations for the production of animals by nuclear transfer is now well documented in a number of species. We have considerable experience in the production of sheep and cattle from primary cell populations and genetically modified primary cell populations. Analysis of these studies has shown considerable variation in development between individual cell populations and at present has provided no definitive method for the identification of cell populations that are suitable for nuclear transfer. Factors that are thought to influence the suitability of a particular cell population include the effects of oxidative damage associated with cellular metabolism, genome instabilities and chromosomal pathologies. All of these factors may be influenced by the method of isolation and culture, and the number of population doublings in culture. On consideration of these factors and our previous observations, we chose to use granulosa cells as nuclear donors. Granulosa cells are suitable nuclear donors in cattle[18], and require the minimum of manipulations to establish in culture. Because of differences between cell populations, we initially decided to use a pool of cells isolated from a group of four donors. In later experiments, cell populations from individual animals were also examined. To minimize the culture period, early passage, never-frozen cells were used.

For embryo reconstruction, we attempted to minimize the potential inefficiencies at each step of the nuclear transfer procedure and adopted an approach that (1) uses *in vivo* derived material, (2) seeks to avoid artificial activation, and (3) minimizes the period of *in vitro* culture of manipulated embryos. To do this we used a two-stage nuclear transfer procedure modified from Kwon and Kono[17] (Fig. 1). In the first stage, donor cells were fused to *in vivo* derived, enucleated MII oocytes obtained from superovulated crossbred gilts. The pseudo-pronucleus formed in the first nuclear transfer embryo was then subsequently transplanted into an *in vivo* produced, enucleated zygote (second nuclear transfer embryo). The second nuclear transfer reconstructed embryo was transferred to the oviduct of a synchronized sow within 2 h of fusion. Because of the expected low developmental rate, we transferred up to 100 reconstructed embryos to a single recipient. Each recipient was treated with pregnant mare serum gonadotropin (PMSG) and human chorionic gonadotropin (hCG) to maintain pregnancy[13] in the event that fewer than four reconstructed embryos were viable at implantation.

Coordination of the cell-cycle stages of the recipient cytoplasm and the donor nucleus are essential for maintaining correct ploidy and preventing DNA damage in nuclear transfer reconstructed embryos[19]. Various combinations of donor and recipient cell-cycle stages can prevent DNA damage and uncoordinated DNA replication, and result in formation of a pseudo-pronucleus. It has been suggested that the use of MII oocytes may improve 're-programming' of the donor genetic material owing to the occurrence of nuclear envelope breakdown and premature chromosome condensation, thus exposing the donor chromatin to maternally derived oocyte factors involved in early development. To take advantage of this here, we used MII oocytes as cytoplast recipients for the first nuclear transfer embryo reconstruction. To maintain ploidy in this situation, we chose diploid donor nuclei as nuclear donors.

Previous studies have suggested that diploid cells arrested in the G0 phase of the cell cycle may be beneficial[2]. Using flow cytometry, we examined the cell-cycle distribution of porcine granulosa cells under three different culture conditions: sub-confluent actively growing, 100% confluent, and cells starved of serum for 48 hours (see Figure in Supplementary Information). After serum starvation, the population contained a large proportion (7.2%) of cells with a DNA content lower than that consistent with a diploid cell (termed sub-G1). In contrast, in the population synchronized by contact inhibition, 90.3% of the cells had a diploid DNA content (G1/G0) and there were fewer sub-G1 cells (1.6%). We analysed DNA synthesis in serum-starved and contact-inhibited cell populations by 5-bromo-2'-deoxyuridine (BrdU) incorporation. These experiments revealed that 45% of the contact inhibited cell population compared with 0% of the serum-starved population incorporated BrdU. An analysis of BrdU incorporation after an additional 24 h of contact inhibition revealed that the fraction of BrdU-positive cells was reduced to 5%. These observations suggest that the diploid cells in the contact-inhibited granulosa cell population used as nuclear donors for embryo reconstruction contained a mixture of cell-cycle-arrested diploid cells (G1/G0) and unarrested diploid cells (G1), which were able to undergo a further round of DNA synthesis. In

**Table 2 Microsatellite analysis of pigs and cell donors**

| Loci | S0059 | S0070 | S0122 | S0226 | SW24 | SW72 | SW840 | SW936 | TNFB |
|---|---|---|---|---|---|---|---|---|---|
| Samples | | | | | | | | | |
| PGR1 | 152 | 275 | 178 | 178 | 103 | 102 | 129 | 95 | 161 |
| | 152 | 295 | 182 | 198 | 111 | 110 | 129 | 97 | 164 |
| PGR2 | 148 | 275 | 180 | 178 | 103 | 110 | 129 | 97 | 158 |
| | 154 | 275 | 182 | 198 | 111 | 112 | 129 | 111 | 185 |
| PGR3 | 146 | 275 | 180 | 178 | 103 | 110 | 125 | 97 | N/A |
| | 152 | 275 | 182 | 198 | 109 | 112 | 125 | 111 | |
| PGR4 | 152 | 275 | 178 | 198 | 103 | 102 | 129 | 97 | 158 |
| | 152 | 295 | 182 | 198 | 111 | 110 | 129 | 109 | 161 |
| NTP1 | 152 | 275 | 178 | 178 | 103 | 102 | 129 | 95 | 161 |
| | 152 | 295 | 182 | 198 | 111 | 110 | 129 | 97 | 164 |
| NTP2 | 152 | 275 | 178 | 178 | 103 | 102 | 129 | 95 | 161 |
| | 152 | 295 | 182 | 198 | 111 | 110 | 129 | 97 | 164 |
| NTP3 | 152 | 275 | 178 | 178 | 103 | 102 | 129 | 95 | 161 |
| | 152 | 295 | 182 | 198 | 111 | 110 | 129 | 97 | 164 |
| NTP4 | 152 | 275 | 178 | 198 | 103 | 102 | 129 | 97 | 158 |
| | 152 | 295 | 182 | 198 | 111 | 110 | 129 | 109 | 161 |
| NTP5 | 152 | 275 | 178 | 198 | 103 | 102 | 129 | 97 | 158 |
| | 152 | 295 | 182 | 198 | 111 | 110 | 129 | 109 | 161 |
| Recipient (54B) | 152 | 275 | 178 | 192 | 111 | 102 | N/A | 103 | 158 |
| | 152 | 295 | 182 | 198 | 95 | 102 | | 109 | 161 |
| Boar | 134 | 265 | 178 | 180 | 115 | 102 | 129 | 97 | 164 |
| | 156 | 273 | 182 | 180 | 115 | 112 | 129 | 109 | 185 |

Microsatellite analysis was performed on genomic DNA from the four individual populations of granulosa cells (PGR1, PGR2, PGR3, PGR4), the piglets (NTP1–5), the surrogate sow (54B) and the boar responsible for inseminating the zygote donors. Primers corresponding to nine polymorphic loci were used. Two numbers are shown for each sample at each locus, which represent the PCR product size for each of the two alleles at that particular locus.

contrast, when the serum-starved populations were used as nuclear donors most the diploid cells were cell-cycle arrested (G1/G0).

Production of the first nuclear transfer embryos requires activation of the *in vivo* derived oocytes. Activation experiments carried out in control oocytes showed that electrical stimulation applied between 51.5 and 60 h after hCG administration, promoted similar cleavage and development to blastocyst (see Table in Supplementary Information). For embryo reconstruction, MII oocytes were collected 46–54 h after hCG and the first nuclear tranfer embryo reconstruction was carried out between 50 and 58 h after hCG. Reconstructed embryos were cultured overnight in NCSU-23 medium[22]; we then checked them for the presence of a pronucleus and used them for the second nuclear transfer embryo reconstruction. The development of single nuclear transfer and double nuclear transfer embryos reconstructed from contact-inhibited and serum-starved granulosa populations were compared (see Table 1). In total, 185 single nuclear transfer embryos were transferred to 3 recipient sows and 401 double nuclear transfer embryos to 7 recipients. Two recipients of the double nuclear transfer embryos became pregnant as determined by ultrasound visualization of fetuses at day 35 of gestation. One of these maintained the pregnancy to term, and five piglets (Fig. 2) were delivered by Caesarean section on day 116 of gestation. The average birth weight of the piglets was 2.72 lb (range 2.28–3.08 lb); this is about 25% lower than that observed in the same population of pigs under natural mating conditions (average litter size average 10.9, average birth weight 3.6 lb, range 3.3–3.9 lb).

The live piglets were produced from a pooled population of cells derived from four animals. We carried out microsatellite analysis of genomic DNA from the various samples (Table 2). The comparison of the pattern of alleles in the piglets with that of the granulosa cell populations indicated that three of the nuclear transfer piglets (NTP1, NTP2 and NTP3) were derived from the porcine granulosa (PGR)1/cell line, as there was 100% identity at all nine microsatellite markers. The other 2 nuclear transfer piglets (NTP4 and NTP5) showed perfect identity with the genotype of the PGR4 cell population. All five of the nuclear transfer piglets were significantly different from the surrogate mother (54B). Some of the loci (S0059, S0070, S0122 and TNFB) were not highly polymorphic indicating a degree of homogeneity or inbreeding within the population of pigs used in these studies (all of which come from the same commercial supplier).

We think that the principal reasons for the success of this modified nuclear transfer procedure in pigs is its lack of reliance on current artificial activation protocols and *in vitro* culture techniques. Although elaborate, the double nuclear transfer does not add another major inefficiency (the second step fusion is very efficient). Direct transfer of a somatic nucleus to an enucleated zygote will not work because (in addition to reprogramming difficulties) of the loss of important factors sequestered within the removed pronuclei. The cell population used successfully as nuclear donors in these experiments were not quiesced by serum starvation. Cell-cycle analysis showed that most cells in control cultures had a diploid DNA content, and a high percentage were able to undergo a further round of DNA synthesis suggesting that most cells in the population were in the G1 phase of the cell cycle and not arrested in G0. All five of the pigs, now three months old, are extremely healthy, in contrast to the (usual) 50% postnatal loss of nuclear transfer animals[10]. It is tempting then to speculate that this modified method may have general utility in other species, even those where single nuclear transfer has been shown to work.

The successful development of nuclear transfer in pigs opens the door for the application of gene-targeting technology, thus allowing for very precise genetic modifications, including gene knockouts. We have recently reported gene targeting in cultured ovine somatic cells and the successful development to term of offspring produced by nuclear transfer using these cells[20]. In pigs, a gene of great interest for the application of knockout technology is that for α-1,3-galactosyl transferase (α-1,3-GT)—the enzyme responsible for adding the xenogeneic sugar, galactose α-1,3-galactose, to the surface of porcine cells. This gene is inactive in certain monkeys and humans, and their blood contains anti-gal antibodies, which trigger (in monkeys) early rejection of transplanted organs[21]. We have achieved targeted disruption of the α-1,3-GT gene in primary porcine cells (unpublished data) and this will allow the production of α-1,3-GT-deficient pigs, whose organs should show improved resistance to rejection. Overcoming antibody-mediated rejection is the first critical step in improving xenograft survival, towards the ultimate goal of providing an unlimited supply of compatible pig organs for human transplantation. □

## Methods

### Modified NCSU-23 medium

The published NCSU-23 medium[22] was modified for use as a phosphate-buffered benchtop medium without $NaHCO_3$. Physiological pH phosphate buffer is made using a 3:1 molar ratio of dibasic to monobasic phosphate anions. These changes induced alterations in the Na and K concentrations, which were corrected by adjusting the NaCl and KCl concentrations to maintain osmolarity and Na/K ratio (all chemicals purchased from Sigma unless otherwise noted).

### Superovulation of donor gilts for collection of oocytes and zygotes

Crossbred gilts (280–320 lbs) were synchronized by oral administration of 18–20 mg Regu-Mate (Altrenogest, Hoechst) mixed into the feed. Regu-Mate was fed for 5–14 d using a scheme dependent on the stage of the oestrous cycle. Estrumate (250 μg, Bayer) was administered intramuscularly (i.m.) on the last day of the Regu-Mate treatment. Superovulation was induced with a single i.m. injection of 1,500 IU of PMSG (Diosynth) 15–17 h after the last Regu-Mate feeding. One thousand units of hCG (Intervet America) were administered i.m. 82 h after the PMSG injection.

We collected oocytes 46–54 h after the hCG injection by reverse flush of the oviducts using pre-warmed Dulbecco's phosphate buffered saline (PBS) containing bovine serum albumin (BSA; 4 g $l^{-1}$). For the collection of zygotes, 24–36 h after the hCG injection the gilts were either artificially inseminated or bred naturally. We flushed zygotes from the oviduct 52–54 h after the hCG injection using PBS containing BSA (4 g $l^{-1}$).

### Isolation and culture of porcine granulosa cells

Follicular fluid was aspirated from 2–8-mm diameter follicles of superovulated crossbred gilts (Large White (1/2), Landrace (1/4), White Duroc (1/4)), 7–8 months old, 280–320 lb, 28–51 h post hCG injection. Granulosa cells were collected by centrifugation at 1,040 *g* for 10 min, re-suspended in DMEM (Gibco), containing 10% fetal calf serum (FCS; Summit Biotech), 0.1 mM non-essential amino acids (NEAA Gibco), 2 ng $ml^{-1}$ basic fibroblast growth factor (bFGF) (Beckton Dickinson) and 6 μl $ml^{-1}$ Gentamycin (Sigma). Cells were expanded for several days and then cryo-preserved.

For nuclear transfer, we plated the granulosa cells at $1–5 \times 10^4$ cells per 35 mm dish in DMEM medium supplemented with NEAA (0.1 mM), bFGF (2 ng $ml^{-1}$) and 10% FCS, and cultured them to 100% confluency at 37 °C. For experiments where serum starvation was evaluated, cells were starved of serum for 48–72 h in DMEM containing 0.5% FCS. We collected cells by trypsinization and stored them in suspension in modified NCSU-23 phosphate medium at 38.5 °C for 20–120 min, before use as nuclear donors.

### Activation of oocytes

Activation of control oocytes was achieved by application of two 1.0 kV $cm^{-1}$ DC electric pulses for 60 μs each at an interval of 5 s in activation medium (0.3 M D-sorbitol supplemented with 0.1 mM Mg $SO_4$ and 0.05 mM $CaCl_2$ in $H_20$).

### Reconstruction of first nuclear transfer embryo

Recovered oocytes were washed in PBS containing 4 g $l^{-1}$ BSA at 38 °C, and transferred to calcium-free phosphate-buffered NCSU-23 medium at 38 °C for transport to the laboratory. For enucleation, we incubated the oocytes in calcium-free phosphate-buffered NCSU-23 medium containing 5 μg $ml^{-1}$ cytochalasin B (Sigma) and 7.5 μg $ml^{-1}$ Hoechst 33342 (Sigma) at 38 °C for 20 min. A small amount of cytoplasm from directly beneath the first polar body was then aspirated using an 18-μM glass pipette (Humagen, Charlottesville,Virginia). We exposed the aspirated karyoplast to ultraviolet light to confirm the presence of a metaphase plate. A single granulosa cell was placed below the zona pellucida in contact with each enucleated oocyte. The couplet was transferred to a fusion chamber (model no. BT-453, BTX Inc., San Diego) containing 700 μl of 0.3 M mannitol, 0.1 mM $MgS0_4$ and 0.1 mM $CaCl_2$ in deionized water. Fusion and activation were induced by application of an AC pulse of 5 V for 5 s followed by two DC pulses of 1.5 kV $Cm^{-1}$ for 60 μs using an ECM2001 Electrocell Manipulator (BTX Inc., San Diego). Couplets were then washed in bicarbonate buffered NCSU-23 medium, and incubated in this medium for 0.5–1 h at 38.6 °C in a humidified atmosphere consisting of 5% $CO_2$ in air. We checked couplets for fusion at ×300 magnification using an inverted microscope. Fused embryos were given a second activation stimulus of two successive DC pulses of 1.2 kV $cm^{-1}$ for 60 μs each, and cultured overnight in NCSU medium[20].

### Reconstruction of second nuclear transfer embryo

Zygotes were centrifuged at 14,900 *g* for 15 min in a Biofuge 13 centrifuge and then incubated in phosphate buffered NCSU-23 medium containing 5.0 $\mu g\ ml^{-1}$ cytochalasin B (Sigma) at 38 °C for 20 min. Zygotes containing two pronuclei were enucleated using a 25–35-$\mu$m glass pipette by aspirating a membrane bound karyoplast containing both pronuclei (and the second polar body if present). Karyoplasts containing the pseudo-pronucleus were prepared from the day 1 nuclear transfer embryos as described for zygote enucleation with the modification that a 30–45-$\mu$m enucleation pipette was used for manipulation. A single karyoplast was placed into the perivitelline space of each enucleated zygote. Fusion was induced by application of an AC pulse of 5 V for 5 s followed by two DC pulses of 1.2 kV $cm^{-1}$ for 60 $\mu$s. Couplets were then washed and cultured in NCSU-23 medium for 0.5–1 h at 38.6 °C in a humidified atmosphere of 5% $CO_2$. We transferred fused couplets as soon as possible to the oviduct of an oestrus-synchronized recipient gilt.

### Treatment of recipient sows

Pregnancy was maintained by using a combination of PMSG and hCG. PMSG (1,000 IU) was injected i.m. on day 10 of the oestrous cycle (day 1 being the day of oestrus), hCG was injected i.m. 3–3.5 d later (day 13 of the cycle)[15].

### Microsatellite analysis

DNA (25 ng $\mu l^{-1}$) from each of the five piglets (24-h tail samples), the four granulosa cell lines mixed to make pool 1 (PGR1, PGR2, PGR3 and PGR4), the recipient sow (54B) and a boar, 'Ranger', that was used for artificial insemination purposes, were sent in individually coded vials to Celera-AgGEN (Davis, California), a company that specializes in parentage verification for swine. The microsatellite analysis consists of a multiplexed set of nine polymorphic porcine loci, each of which consists of different multimers of short tandem repeats (dinucleotides). The polymorphic loci are designated: S0059, S0070, S0122, S0226, SW24, SW72, SW840, SW936 and TNFB (PCR primer sequence information is proprietary to Celera-AgGEN). This multiplex set contains nine different PCR primer pairs, amplified in two PCR reactions, a five-plex and a four-plex. Ten nanograms of template DNA was amplified in each multiplex PCR. The forward primers were labelled on the 5′ end with a fluorescent dye (either FAM, JOE or TAMRA). The entire battery for each DNA sample was loaded in a single lane and co-electrophoresed with the internal size standard GeneScan 350 Rox. All multiplexing and loci evaluations were performed on an ABI PRISM 377 DNA Sequencer and analysed with Genotyper 2.0 software.

Received 12 June; accepted 27 July 2000.


1. Campbell, K. H. McWhir, J. Ritchie, W. A. & Wilmut, I. Sheep cloned by nuclear transfer from a cultured cell line. *Nature* **380**, 64–67 (1996).
2. Wilmut, I., Schnieke, A. E., McWhir, J., Kind, A. J. & Campbell, K. H. Viable offspring derived from fetal and adult mammalian cells. *Nature* **385**, 810–813 (1997).
3. Wells, D. N., Misica, P. M., Day, T. A. & Tervit, H. R. Production of cloned lambs from an established embryonic cell line: a comparison between in vivo- and in vitro-matured cytoplasts. *Biol. Reprod.* **57**, 385–393 (1997).
4. Cibelli, J. B. *et al.* Cloned transgenic calves produced from nonquiescent fetal fibroblasts. *Science* **280**, 1256–1258 (1998).
5. Wakayama, T., Perry, A. C., Zuccotti, M., Johnson, K. R. & Yanagimachi, R. Full-term development of mice from enucleated oocytes injected with cumulus cell nuclei. *Nature* **394**, 369–374 (1998).
6. Baguisi, A. *et al.* Production of goats by somatic cell nuclear transfer. *Nature Biotechnol.* **17**, 456–461 (1999).
7. Prather, R. S., Sims, M. M. & First, N. L. Nuclear transplantation in early pig embryos. *Biol. Reprod.* **41**, 414–418 (1989).
8. Tao, T. *et al.* Development of pig embryos reconstructed by microinjection of cultured fetal fibroblast cells into in vitro matured oocytes. *Anim. Reprod. Sci.* **56**, 133–141 (1999).
9. Ouhibi, N. *et al.* Nuclear transplantation in pigs: M-phase karyoplast to M-phase cytoplast fusion. *Reprod. Nutr. Dev.* **36**, 661–666 (1996).
10. Colman, A. Somatic cell nuclear transfer in mammals: Progress and applications. *Cloning* **1**, 185–200 (2000)
11. Polge, C., Rowson, L. E. A. & Chang, M. C. The effect of reducing the number of embryos during early stages of gestation on the maintenance of pregnancy in the pig. *J. Reprod. Fert.* **12**, 395–397 (1966).
12. Canseco, R. S. *et al.* Gene transfer efficiency during gestation and the influence of co-transfer of non-manipulated embryos on production of transgenic mice. *Transgenic Res.* **3**, 20–25 (1994).
13. Christenson, R. K. & Day, B. N. Maintenance of unilateral pregnancy in the pig with induced corpora lutea. *J. Anim. Sci.* **32**, 282–286 (1971).
14. Prather, R. S. *et al.* Artificial activation of porcine oocytes matured in vitro. *Mol. Reprod. Dev.* **28**, 405–409 (1991).
15. McGrath, J. & Solter, D. Nuclear transplantation in the mouse embryo by microsurgery and cell fusion. *Science* **220**, 1300–1302 (1993).
16. McGrath, J. & Solter, D. Nuclear transplantation in mouse embryos. *J. Exp. Zool* **228**, 355–362 (1993).
17. Kwon, O. Y. & Kono, T. Production of identical sextuplet mice by transferring metaphase nuclei from four-cell embryos. *Proc. Natl Acad. Sci. USA* **93**, 13010–13013 (1996).
18. Wells, D. N., Misica, P. M. & Tervit, H. R. Production of cloned calves following nuclear transfer with cultured adult mural granulosa cells. *Biol. Reprod.* **60**, 996–1005 (1999).
19. Campbell, K. H., Loi, P., Otaegui, P. J. & Wilmut, I. Cell cycle co-ordination in embryo cloning by nuclear transfer. *Rev. Reprod.* **1**, 40–46 (1996).
20. McCreath, K. J. *et al.* Homologous recombination in ovine somatic cells enables the production of gene targeted sheep by nuclear transfer. *Nature* **405**, 1066–1069 (2000).
21. Platt, J. L. Xenotransplantation:recent progress & current perspectives. *Curr. Opin. Immunol.* **8**, 721–728 (1996).
22. Petters, R. M. & Wells, K. D. Culture of pig embryos. *J. Reprod. Fertil. Suppl.* **48**, 61–73 (1993).


Supplementary information is available on *Nature*'s World-Wide Web site (http://www.nature.com) or as paper copy from the London editorial office of *Nature*.


### Acknowledgements

We thank B. Gragg, T. Akers, H. Bishop and J. McPherson for technical contributions to embryo production, embryo transfer and animal husbandry; P. Jobst for technical contributions in embryo production and nuclear transfer; W. Eyestone and K. Polson for valuable contributions in discussions; S. Pleasant and M. Crisman and their staff at the Virginia Maryland Regional Veterinary College for their critical roles in the Caesarian delivery and post-natal care of the cloned piglets. This research was funded in part by a grant from the National Institute of Science and Technology (NIST) Advanced Technology Program (ATP).



Correspondence and requests for materials should be addressed to I.P. (e-mail: ipolejaeva@ppl-therapeutics.com).


# Infection by porcine endogenous retrovirus after islet xenotransplantation in SCID mice


**Luc J.W. van der Laan*, Christopher Lockey†, Bradley C. Griffeth*, Francine S. Fraser*, Carolyn A. Wilson‡, David E. Onions§, Bernhard J. Hering ‖, Zhifeng Long†, Edward Otto†, Bruce E. Torbett* & Daniel R. Salomon***

**The Scripps Research Institute, Department of Molecular and Experimental Medicine, 10550 North Torrey Pines Road, La Jolla, California 92037, USA*
*† Genetic Therapy Inc., A Novartis Company, 9 West Watkins Mill Road, Gaithersburg, Maryland 20878, USA*
*‡ Food and Drug Administration, Centre for Biologics Evaluation and Research, 8800 Rockville Pike, Bethesda, Maryland 20892, USA*
*§ University of Glasgow, Department of Veterinary Pathology, Bearsden Road, Glasgow G61 1QH, Scotland & Q-One Biotech Ltd, Todd Campus, Glasgow G20 OXA, UK*
*‖University of Minnesota, Department of Surgery, 420 Delaware Street S.E., Minneapolis, Minnesota 55455, USA*



**Animal donors such as pigs could provide an alternative source of organs for transplantation. However, the promise of xenotransplantation is offset by the possible public health risk of a cross-species infection[1,2]. All pigs contain several copies of porcine endogenous retroviruses (PERV)[3,4], and at least three variants of PERV can infect human cell lines *in vitro* in co-culture, infectivity and pseudotyping experiments[3,5–7]. Thus, if xenotransplantation of pig tissues results in PERV viral replication, there is a risk of spreading and adaptation of this retrovirus to the human host. C-type retroviruses related to PERV are associated with malignancies of haematopoietic lineage cells in their natural hosts[8]. Here we show that pig pancreatic islets produce PERV and can infect human cells in culture. After transplantation into NOD/SCID (non-obese diabetic, severe combined immunodeficiency) mice, we detect ongoing viral expression and several tissue compartments become infected. This is the first evidence that PERV is transcriptionally active and infectious cross-species *in vivo* after transplantation of pig tissues. These results show that a concern for PERV infection risk associated with pig islet xenotransplantation in immunosuppressed human patients may be justified.**


Juvenile-onset diabetes mellitus is a major health problem and exogenous insulin therapy is only partially successful in preventing its many complications. Although islet transplantation holds great promise for a cure, the number of potential human pancreas donors are extremely unlikely to provide enough islet tissue to treat the millions of patients worldwide. The xenotransplantation of pig

BIOLOGY OF REPRODUCTION 57, 1089–1095 (1997)

# Isolation of Pluripotent Stem Cells from Cultured Porcine Primordial Germ Cells[1]

**Hosup Shim,[3] Alfonso Gutiérrez-Adán,[3] Lih-Ren Chen,[3] Robert H. BonDurant,[4] Esmail Behboodi,[3] and Gary B. Anderson[2,3]**

*Department of Animal Science[3] and Department of Population Health and Reproduction,[4] University of California, Davis, California 95616*

## ABSTRACT

**Embryonic germ (EG) cells are undifferentiated stem cells isolated from cultured primordial germ cells (PGC). To date, EG cells have been isolated only in the mouse. Murine EG cells share several characteristics with embryonic stem (ES) cells, including morphology, pluripotency, and the capacity for germline transmission. We report here the isolation of porcine EG cells. PGC collected from Day 24 or 25 porcine embryos were cultured on mitotically inactivated murine fibroblasts. Four EG cell lines were isolated from repeated subculture of porcine PGC. Porcine EG cells morphologically resembled murine ES cells and consistently expressed alkaline phosphatase activity. These cell lines maintained a normal diploid karyotype and survived after cryopreservation. Porcine EG cells were capable of differentiating into a wide range of cell types in culture, including endodermal, trophoblast-like, epithelial-like, fibroblast-like, and neuron-like cells. In suspension culture, porcine EG cells formed embryoid bodies. When injected into host blastocysts, the EG cells were able to differentiate and contribute to tissues of a chimeric piglet. Both in vitro and in vivo evidence demonstrates that the isolated EG cells were pluripotent. These cells are potentially useful for genetic manipulation in pigs.**

## INTRODUCTION

Embryonic stem (ES) cells provide not only useful models for the study of embryonic development but also can serve as vehicles for germ-line transfer of foreign DNA. Such cells were first isolated from blastocyst-stage embryos in the mouse [1, 2]. ES cells remain undifferentiated in repeated subcultures, and under the appropriate culture conditions they can differentiate into a wide range of cell types. In vivo pluripotency, demonstrated by transmission of ES cell genotypes to chimeric offspring, has been reported in the mouse [3], rat [4], rabbit [5], and pig [6]. To date, only murine ES cells have been conclusively demonstrated to colonize the germ line of chimeras [3]. Transplantation of nuclei from cultured inner cell mass (ICM) cells into enucleated oocytes has produced embryos capable of developing to term after transfer to recipients [7]. Pluripotency of embryo-derived cells from cattle [8] and sheep [9] has been demonstrated by bovine conceptus development and birth of live lambs, respectively, after nuclear transfer.

Primordial germ cells (PGC) are embryonic cells that migrate from the root of the allantois to the genital ridge, where they ultimately give rise to gametes. PGC can be distinguished throughout PGC migration from surrounding somatic tissues by expression of alkaline phosphatase (AP) activity [10]. Pluripotent stem cells have been isolated from murine PGC [11, 12]. These cells are referred to as embryonic germ (EG) cells to distinguish them from undifferentiated stem cells of blastocyst origin. EG cells share several important characteristics with ES cells, including their morphology, pluripotency, and capacity to contribute to the germ line of chimeras when injected into blastocysts [13, 14].

Because of their potential use for targeted gene manipulation, isolation of ES cells in livestock species could have numerous agricultural and biomedical applications. Use of ES cell technology in livestock may overcome current limitations to efficient gene transfer by providing an abundance of pluripotent stem cells to be genetically manipulated by conventional recombinant DNA techniques [15]. However, progress toward establishment of ES cell lines from species other than the mouse has been slow [16]. Since EG cells are highly similar to ES cells in their characteristics, PGC may provide an alternative source of pluripotent stem cells. As compared with the situation for the conventional method for isolating ES cells from ICM cells, PGC are available in large numbers per embryo.

Bovine PGC have been collected from fetal ovaries and identified by morphology and histochemistry [17]. The isolation of putative bovine EG cells has also been reported [18]. These cells were capable of in vitro differentiation, and they displayed AP activity, a murine ES cell marker. When injected into the blastocoele of blastocysts, PGC-derived cells were incorporated into the ICM of the host blastocyst. Spontaneously aborted fetuses between 38 and 60 days in gestation were recently reported [19] after transfer of nuclei from putative bovine EG cells into enucleated oocytes. To date, only results of short-term culture of PGC are available in the pig. Under conventional culture conditions, porcine PGC were reported to survive barely more than 24 h [20].

In this study, the isolation and characterization of porcine EG cells are reported. Pluripotency of isolated EG cells was tested both in vitro and in vivo.

## MATERIALS AND METHODS

### *Collection of PGC*

Embryo donors were Hampshire × Yorkshire crossbred gilts (approximately 6 mo of age) prepared as described previously [19]. Animals were slaughtered on Day 24 or 25 of gestation, and embryos were dissected from the uteri. Genital ridges, if visible, were dissected from the embryos; otherwise, dorsal mesentery was removed [21]. Isolated tissues were washed once with PBS and incubated in 0.02% EDTA solution (Sigma Chemical Co., St. Louis, MO) for 20 min at room temperature. After incubation, PGC were dissociated by gentle disruption of the tissues using fine forceps. The suspension containing dissociated cells was collected and centrifuged at 800 × *g* for 5 min. The pellet was resuspended in PGC culture medium, Dulbecco's Modified Eagle's medium (DMEM) containing 15% fetal bovine

Accepted July 8, 1997.
Received March 3, 1997.
[1]This research was supported by USDA NRICGP Grant 94-37205-1029.
[2]Correspondence. FAX: (916) 752-0175; e-mail: gbanderson@ucdavis.edu

serum, L-glutamine (1 mM), MEM nonessential amino acids (0.1 M), 2-mercaptoethanol (10 μM), penicillin (100 U/ml), and streptomycin (0.5 mg/ml). A total of 174 embryos dissected from 17 gilts were used to collect PGC and ultimately to isolate EG cell lines.

### AP Histochemistry

Prior to seeding of PGC onto feeder cells, samples of the cell suspension were assessed for presence of PGC using morphological criteria [22]. To confirm the morphological assessment, samples were stained for AP activity using an AP histochemistry kit (Sigma) according to the manufacturer's protocol. Putative EG cells were also tested for AP activity. Monolayers containing PGC-derived colonies and feeder cells were fixed with 80% ethanol [23] and stained for AP activity.

### Feeder Cells

Feeder cells were prepared and maintained as described elsewhere [24]. Briefly, STO cells (subcultures of stock provided by Dr. G.R. Martin, University of California, San Francisco) were inactivated by incubation in medium containing 10 μg/ml of mitomycin C (Sigma) for 2 h. A day before PCG were seeded, inactivated STO cells were plated at a density of $5 \times 10^4$ cells per well in a 96-well plate (Falcon, Franklin Lakes, NJ) or at $2.5 \times 10^5$ cells per well in a 4-well multidish (Nunclon, Roskilde, Denmark).

### Isolation of EG Cell Lines

For primary culture, cells collected from the embryos of the same gilt were pooled. The number of PGC equivalent to that collected from one embryo (approximately 15 000 PGC) was seeded per well of a 96-well plate containing feeder cells. Approximately 4–7 days after PCG were seeded, densely packed EG-like colonies obtained from primary culture were picked from the feeder layer and disaggregated in a microdrop of 0.25% trypsin-EDTA (Gibco BRL, Grand Island, NY) for 10–15 min at 39°C with the aid of a micropipette. The cells disaggregated from the colonies were seeded onto a fresh feeder layer in a 4-well multidish. Putative EG colonies were passed as described above for 1–3 passages until colonies reached more than 50% confluence. For further subculture, at 4- to 7-day intervals, the plates containing colonies and feeder cells were washed with PBS and treated with 0.25% trypsin-EDTA for 10–15 min at 39°C. Cells were removed from the plates and centrifuged at $800 \times g$ for 5 min, and resulting pellets were resuspended in PGC culture medium prior to plating onto a fresh feeder layer in a 4-well multidish. All cultures were maintained at 39°C in 5% $CO_2$:95% air with PGC culture medium changed every other day. EG cell lines were isolated and maintained in the medium with or without supplementation of porcine leukemia inhibitory factor (LIF; 1000 U/ml; a gift from Alexion Pharmaceuticals, New Haven, CT).

### Cryopreservation

To ensure availability of EG cells for later use, cells were cryopreserved at each passage, beginning as early as passage 3. Porcine EG cells were frozen and thawed as described elsewhere [25].

### Karyotypic Analysis

At passages 8–12, porcine EG cells in a 4-well multidish were cultured overnight in PGC culture medium containing 0.02 μg/ml colcemid (Gibco BRL) at 39°C in 5% $CO_2$:95% air. The cells were trypsinized and harvested as described above. The resulting pellet was resuspended in hypotonic solution (0.56% KCl in $H_2O$, w:v) and was incubated for 20 min at 20°C. The cells were pelleted by centrifugation at $800 \times g$ for 5 min at 20°C and fixed in cold Carnoy's fixative (3:1 vol of absolute methanol to glacial acetic acid) for 5 min. After another wash by centrifugation, the cells were resuspended in 0.5 ml of fixative. To prepare slides, the cell suspension was dropped onto microscope slides prewashed with fixative. After air drying, the slides were stained in Giemsa staining solution (Gibco BRL). The stained slides were rinsed with tap water, air dried, and observed at ×400 magnification with oil immersion. Approximately 10–20 metaphase spreads from each EG cell line were examined for the presence of structural and numerical abnormalities of chromosomes. Photographs were taken on Kodak (Eastman Kodak, Rochester, NY) Technical Pan B&W film, and karyotypes from each EG cell line were arranged as described elsewhere [26].

### In Vitro Differentiation

To induce differentiation on a monolayer, EG cells were cultured for more than 2 wk without passage. To induce differentiation in suspension culture, EG cells were passed once as described above onto a 0.1% gelatin-coated plate to eliminate possible contamination by fibroblasts. After 4–7 days in culture, colonies were gently dislodged from the plate with the aid of a micropipette and were disaggregated by incubation in 0.25% trypsin-EDTA for 10–15 min at 39°C. Dissociated cells were cultured in a microdrop of PGC culture medium containing 0.3 μM retinoic acid (Sigma) on a 35-mm nonadhesive petridish (Falcon). Suspension cultures were monitored daily for embryoid body formation, with medium changed every other day.

### Chimera Production

The ability of porcine EG cell lines to differentiate in vivo was tested by injection into host blastocysts. Duroc gilts (approximately 6 mo of age) artificially inseminated with mixed semen from 2 to 3 Duroc boars were used as host blastocyst donors. Estrus in blastocyst donors and recipient sows was induced as described previously [27]. Skin-pigmentation markers were used for preliminary identification of chimeric piglets. Porcine EG cell lines were isolated from embryos of Hampshire × Yorkshire crossbred pigs (black and white pigmentation; both are codominant alleles), and host blastocysts were Durocs (red pigmentation; recessive). Blastocysts were collected from the Duroc gilts 6 days after the first day of estrus. Porcine EG cell lines at passage 7–15 were used for injection. All cell lines used had been cryopreserved once or more prior to the blastocyst injection. Colonies of EG cells picked off the feeder layer were incubated in 0.25% trypsin-EDTA for 5–10 min and dissociated into small clumps containing approximately 10–20 cells each. One EG cell clump each was injected into the blastocoele of a host blastocyst as described previously [28]. Injected blastocysts were surgically transferred to the uteri of recipients on Day 4 of their estrous cycle (i.e., 2 days behind donor gilts). Host blastocysts were pooled across donors after injection with EG

cells to ensure a sufficient number of embryos to sustain pregnancy after transfer. At birth, piglets were examined for skin-pigmentation chimerism (i.e., black or white among red pigmentation).

### DNA Marker

A piglet with overt skin-pigmentation chimerism was subjected to analysis of DNA from various tissues. Since host blastocysts collected from 6 gilts had been pooled for the embryo transfer that produced the skin-pigmentation chimera, parentage analysis was performed to identify the sire and dam of the host blastocyst that produced the skin-pigmentation chimera. After polymerase chain reaction (PCR) amplification of microsatellites (MS) S0036, S0099, SW157, and SW871 from blood samples of the skin-pigmentation chimera and its potential parents, the amplified fragments were analyzed using PAGE [29] (primers were provided by Dr. M.F. Rothschild, Iowa State University, Ames, IA). These MS were selected for analysis on the basis of their having a high degree of polymorphism and therefore a likelihood of being the most informative. Each MS was amplified individually. Five gilts and two boars could be excluded as possible parents of the Duroc host blastocyst on the basis of MS DNA incompatibilities. The remaining gilt and boar were genetically comparable with the Duroc host blastocyst and were identified as the parents. The presumptive chimera was killed 5 days after delivery, and tissue samples were excised from the brain, pituitary gland, lung, liver, heart, spleen, kidney, muscle, testis, epididymis, pancreas, intestine, thyroid gland, and skin. After washing of tissue samples with PBS, DNA was isolated from each tissue sample and analyzed by PCR amplification of MS SW871 as described above.

## RESULTS

### Isolation of EG Cell Lines

With or without supplementation of LIF in the culture medium, porcine EG cell lines were isolated and maintained in long-term culture (Table 1). Although PGC readily formed colonies resembling murine ES cells in primary culture, most colonies were lost prior to the fourth passage (Table 1). Four EG cell lines isolated from PGC of different gilts survived in long-term culture; one cell line survived for more than 29 passages. These cells proliferated indefinitely in repeated subculture carried out over a period of more than 6 mo.

The EG cell lines produced densely packed colonies similar to murine ES cells (Fig. 1A), but porcine EG colonies were flatter and more translucent than murine ES cells. Porcine EG cells did not contain lipid-like vacuoles, which often appear in both murine and porcine ES cells [30]. The size and shape of EG colonies varied, and individual EG cells were 5–15 μm in diameter, approximately a third the size of a STO feeder cell. As described for porcine ES cells [30], each porcine EG cell contained a large nucleus with prominent nucleoli and a relatively small amount of cytoplasm. One and three cell lines were isolated from PGC collected from the dorsal mesentery and genital ridge, respectively (Table 2). Among isolated EG cell lines, no obvious differences were observed in their morphology, proliferation, and AP activity. Porcine EG cells consistently expressed AP activity (Fig. 1B) whereas STO feeder cells did not. When the EG cells differentiated in vitro, they rapidly lost AP activity. After 8–12 passages, all four isolated EG cell lines had the normal porcine complement of 38 chromosomes (36 autosomes and 2 sex chromosomes). No obvious abnormalities were found in chromosomes from the isolated EG cells. Three cell lines possessed normal diploid male karyotypes, and one cell line had a normal diploid female karyotype (Table 2). After cryopreservation, EG cells survived and proliferated without overt changes in their characteristics.

TABLE 1. Progressive loss of porcine EG cell lines after several passages in medium with and without porcine LIF.

| Growth factor supplemented | No. primary cultures* | No. cell lines surviving to passage | | | | |
|---|---|---|---|---|---|---|
| | | 1 | 2 | 3 | 4 | >14 |
| None | 10 | 9 | 7 | 6 | 3 | 3 |
| Porcine LIF | 7 | 5 | 3 | 2 | 1 | 1 |

* Each primary culture included PGC from pooled embryos of a different embryo donor.

### In Vitro Differentiation

In prolonged culture without passage, porcine EG cells occasionally differentiated into several cell types. As evidenced by morphology, the EG cells gave rise to at least five differentiated phenotypes, including endodermal, trophoblast-like, epithelial-like, fibroblast-like, and neuron-like cells. The neuron-like cells had several long neurites that emerged from cell bodies (Fig. 1C) and often formed neural rosettes. The fibroblast-like cells grew rapidly and elongated in culture (Fig. 1D). They easily mixed with feeder cells and rapidly dominated undifferentiated stem cells in culture. The epithelial-like cells formed a monolayer of polygonal cells with visible borders between cells (Fig. 1E), whereas typical undifferentiated EG cells did not show distinct boundaries between cells. The trophoblast-like cells were occasionally found in loosely packed colonies in which individual cells were larger than EG cells (Fig. 1F). When EG colonies formed tent-like protrusions with multilayers, the colonies often resulted in formation of an endodermal layer at the boundaries of the colonies (Fig. 1G). AP expression was rapidly reduced with differentiation of EG cells. Differentiation could also be induced in suspension culture. After approximately 7 days in suspension culture, the EG cells formed simple embryoid bodies (Fig. 1H), each containing an outer layer of large endodermal cells separated from a core of undifferentiated stem cells.

TABLE 2. In vivo differentiation of porcine EG cell lines after injection into blastocysts.

| | EG cell line | | | |
|---|---|---|---|---|
| | PEGC142* | PEGC273 | PEGC367 | PEGC62* |
| Origin of PGC† | GR | GR | GR | DM |
| Karyotype (2n) | 38,XY | 38,XY | 38,XY | 38,XX |
| No. of embryos transferred | 105 | 25 | 56 | NT |
| No. of recipients | 4 | 1 | 2 | NT |
| No. of pregnant recipients | 4 | 1 | 1 | NT |
| No. of piglets born | 20 | 10 | 11 | NT |
| No. of chimeras born | 1 | 0 | 0 | NT |

* Cell line was isolated with supplementation of porcine LIF in the culture medium.
† GR, genital ridge; DM, dorsal mesentery.
‡ Not tested.

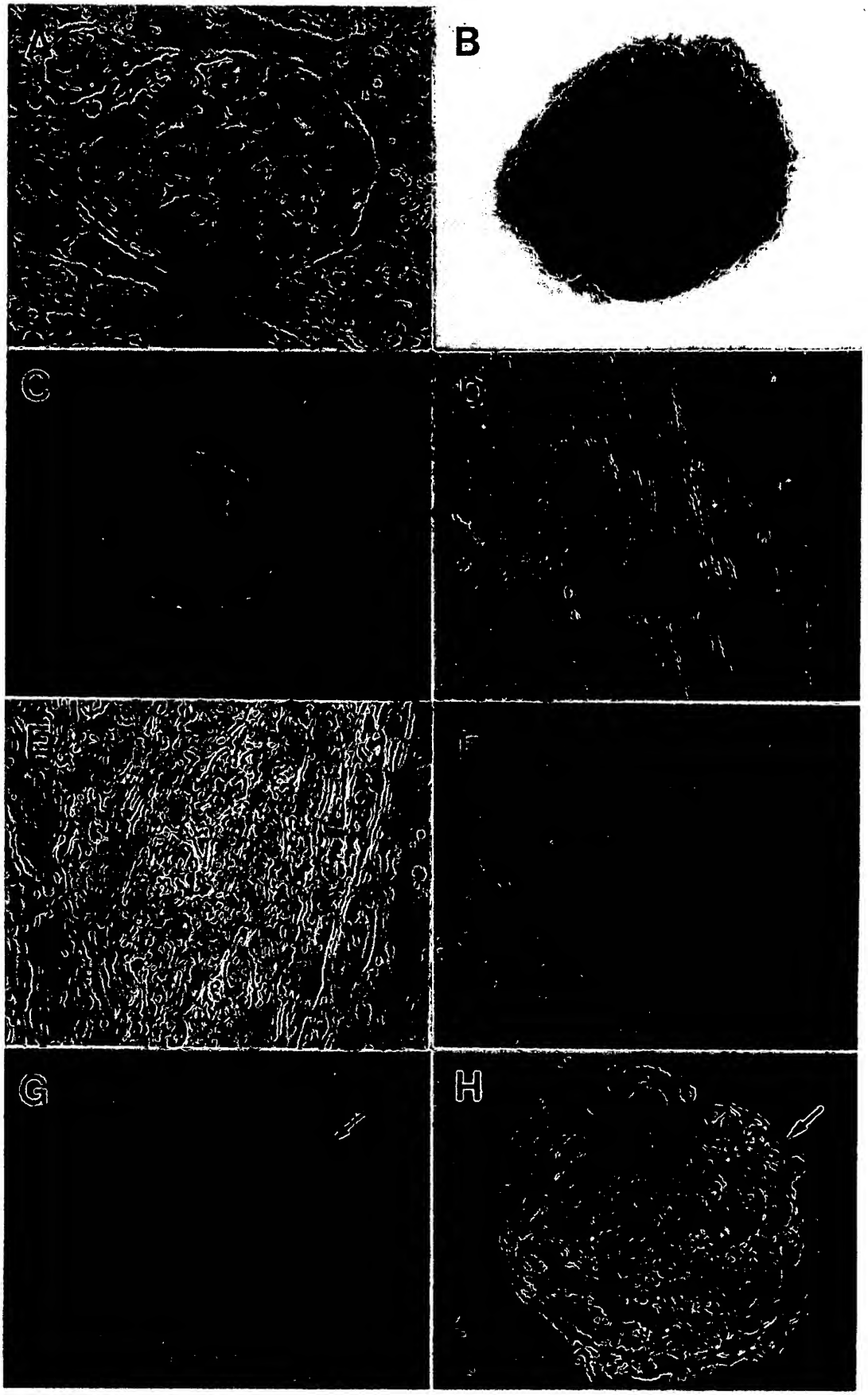
B
C
G
H

FIG. 1. Porcine EG cells. A) Colony of EG cells each with a large nucleus and prominent nucleoli. Stained with hematoxylin and eosin. ×400. B) AP histochemical staining of porcine EG cells. Dark stain represents AP activity of undifferentiated stem cells. ×200. C–G) In vitro differentiation of porcine EG cells. C) Neuron-like cells. Long neurites emerged from a cell body. ×200. D) Fibroblast-like cells elongated and mixed with feeder cells. ×100. E) Epithelial-like cells forming a monolayer of polygonal cells. ×200. F) Trophoblast-like cells. Colony was loosely packed, and individual cells were larger than EG cells. ×100. G) Endodermal cells. A layer of endodermal cuff (arrow) was differentiated at boundaries of the EG colony. ×100. H) Simple embryoid body formation induced by suspension culture of porcine EG cells. Note an outer layer of large endoderm cells (arrow). ×200. (Reproduced at 90%.)

### *Chimera Production*

Porcine EG cell lines were tested for in vivo pluripotency by injection into blastocysts that were subsequently transferred to recipients for development to term. As shown in Table 2, a total of 186 host blastocysts were injected with EG cells from three cell lines and transferred to seven recipients. Six recipients were pregnant (pregnancy rate, 86%), and 41 piglets were born (embryo survival rate, 22%; 4 were dead at birth). One male (piglet 363) showed overt skin-pigmentation chimerism resulting from the injection of the crossbred EG cell line PEGC142 into a Duroc host blastocyst. White stripes derived from the EG cells were observed on the flank and back of the piglet and most prominently on the left hind leg (Fig. 2).

The chimeric piglet failed to thrive postnatally, and at 5 days of age it was killed for collection of tissue samples. At necropsy, several developmental abnormalities were observed, including a ventricular septal defect and shortened caudate vertebrae. MS profiles of parents of the host blastocyst, the EG cell line, and tissue samples from the skin-pigmentation chimera confirmed chimerism. A 120 base-pair allele of MS SW871 was present both in the injected EG cell line (PEGC142) and in various tissues from the skin-pigmentation chimera but was absent in parents of the host blastocyst (Fig. 3). Porcine EG cells contributed to tissues derived from all three germ layers, including blood, brain, pituitary gland, lung, kidney, muscle, testis, epididymis, pancreas, intestine, thyroid gland, and skin. Contributions of the EG cells to development of the heart, liver, and spleen were not detectable.

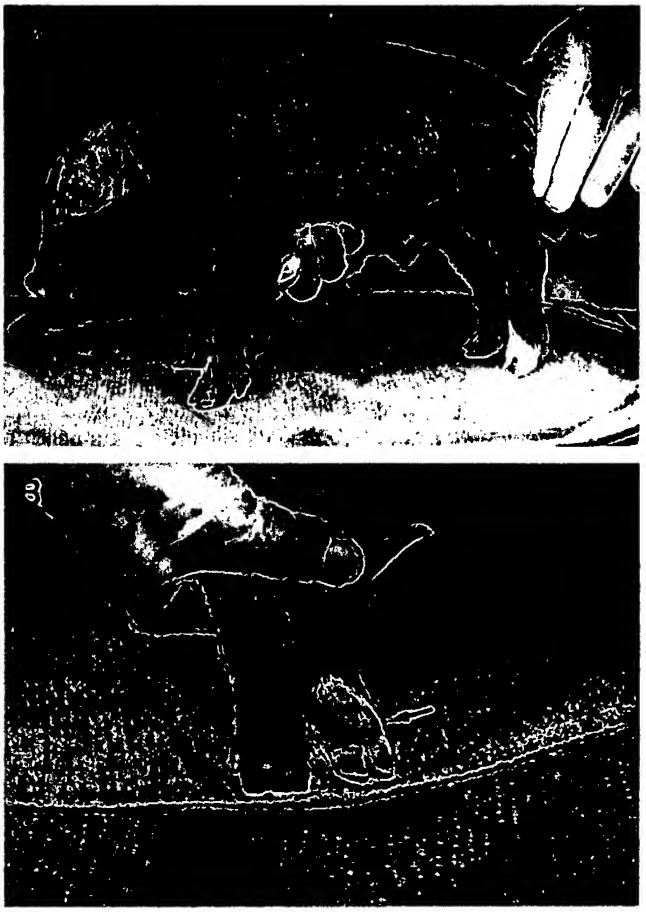

FIG. 2. Chimeric piglet (piglet 363) that developed from a Duroc blastocyst (red pigmentation) injected with Hampshire × Yorkshire (black and white pigmentation) EG cells. A) Chimeric male with white stripes interspersed among areas of red across flanks and back. B) White pigmentation derived from EG cells was most prominent on left hind leg (arrow).

## DISCUSSION

LIF has been shown to be an essential growth factor for isolation and maintenance of murine ES cells [31]. STO cells produce LIF, but cell culture medium is often supple-

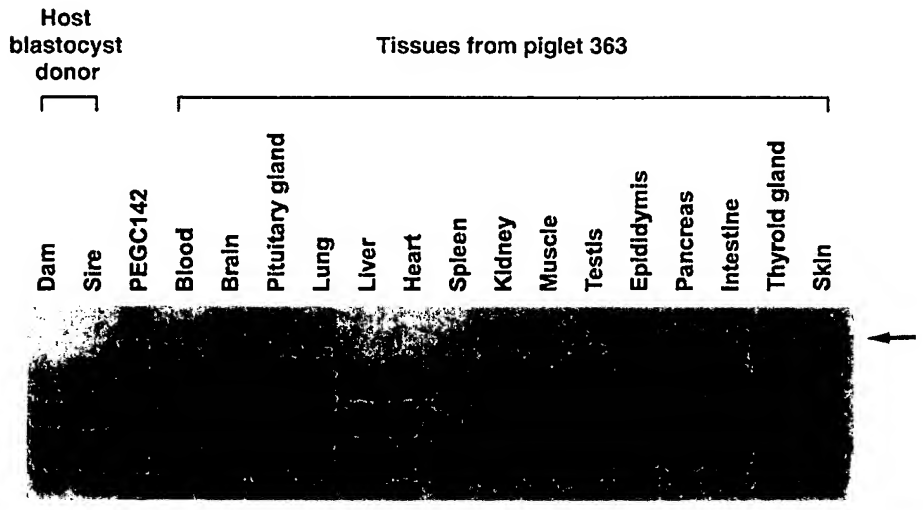


FIG. 3. PCR analysis of DNA from the parents of the Duroc host blastocyst, the EG cell line injected into the blastocyst, and tissues of piglet 363 with skin-pigmentation chimerism. A 120-bp allele (arrow) of MS SW871 was present both in the injected EG cell line PEGC142 and in various tissues of piglet 363 but absent in parents of the host blastocysts. MS profile of the piglet 363 confirms observations of overt pigmentation chimerism.

mented with additional LIF when ES cells are isolated and passed [32]. Moreover, murine EG cells have been successfully isolated only in instances in which PGC were cultured with a combination of three growth factors, including LIF, stem cell factor, and basic fibroblast growth factor [11, 12]. These three growth factors have also been used to establish bovine PGC-derived cell lines [19]. However, cell lines have also been isolated by culturing bovine PGC over a feeder layer of either murine or bovine fibroblasts without growth factor supplementation [18]. Porcine PGC can proliferate in short-term culture on STO feeder layers without supplementation of growth factors in the culture medium (unpublished results). In this long-term culture experiment, a feeder layer of STO cells provided sufficient support to allow isolation and maintenance of porcine EG cell lines. It remains to be determined whether these and other growth factors have a long-term effect on efficiency in isolation of EG cells, on contribution of EG cells to normal in vivo differentiation, and on colonization of the germ line by EG cells.

Markers for pluripotent cells are often useful to identify stem cells in culture. Expression of AP has been demonstrated in ES and ES-like cells in the mouse [33, 34], rat [35], pig [36], and cow [37]. AP activity has also been detected in murine PGC [11], murine EG cells [12, 13], and porcine PGC (unpublished results). In the present study, AP activity was consistently expressed in primary cultures and subcultures of EG cells. With in vitro differentiation of EG cells, AP activity was rapidly lost. In conjunction with morphological evaluation of EG cell colonies, AP expression was a convenient marker to identify undifferentiated stem cells in culture.

A significant proportion of newly established ES cells has been reported not to contain a normal diploid karyotype [32], a phenomenon associated with their rapid proliferation in culture. For germ-line genetic manipulation using ES cells (e.g., gene targeting), normal diploid cell lines (preferably male) are required. As evidenced by Giemsa staining and karyotypic analysis, all porcine EG cell lines in this study contained a normal diploid karyotype, and three of four cell lines were male.

Murine ES cells are capable of differentiating in vitro into multiple cell types, including skeletal muscle-, cardiac-, neuron-, and hematopoietic-like cells [2, 38, 39]. Cell lines derived from epiblast showed in vitro differentiation into a variety of cell types in the cow [37], pig [36, 40], and sheep [36]. In this study, porcine EG cells were capable of in vitro differentiation into various cell types. Formation of simple embryoid bodies with endodermal differentiation was also induced from porcine EG cells. The capacity for in vitro differentiation demonstrated by EG cells suggested that they were pluripotent.

One male piglet was confirmed by skin pigmentation and DNA analysis to be a chimera from injection of porcine EG cells into blastocysts. An association between observed developmental abnormalities and contribution of EG cells could be neither confirmed nor excluded. Congenital cardiac malformations have been observed in natural swine populations at a frequency of 4.35%; 7% of these were ventricular septal defects as seen in the chimera described here [41]. Occasional abnormalities including stunted growth, skeletal abnormalities, and sterility in chimeras derived from murine EG cells have been reported [11]. Varying degrees of chimerism observed among organs, and at times lack of chimerism in some organs, have been described in chimeric mice [42], rabbits [43], and pigs [44]. Pigmentation chimerism was not extensive throughout the body, but in vivo pluripotency of porcine EG cells was clearly demonstrated by DNA analysis. Descendants of EG cells were incorporated into several tissues derived from all three germ layers, including ectoderm (brain and skin), mesoderm (skeletal muscle, kidney, testis, and epididymis) and endoderm (lung, liver, and intestine).

The efficiency of producing chimeras appeared to be low on the basis of expression of the pigmentation markers (Table 2). Injection of fresh ICM cells into blastocysts has given rise to 10–11% chimeric pigs among offspring [27, 44], but a low efficiency (5% and 2.5%, respectively) of producing chimeras was observed after injection of rabbit ES cells [5] and PGC [43] into blastocysts. In mice, efficiency of producing chimeras and frequency of germ-line transmission vary among strains from which ES cells are derived [45]. The incidence and degree of chimerism vary among EG cell lines in the mouse [13]. It is not yet clear whether the low frequency of chimerism was due to developmental potency of porcine EG cells in general or of the particular cell lines tested, to challenges of manipulation and transfer of embryos in large animal species, or simply to the relatively smaller number of embryo transfers that is frequently feasible in large animal species as compared to mice.

In this study, porcine EG cells were successfully isolated and maintained in long-term culture. These cells demonstrated many important features of pluripotent stem cells, including AP activity, capacity of in vitro differentiation, and production of chimeric offspring with EG cells contributing to various cell lineages. This report is the first to document isolation of EG cells from a species other than the mouse. Further research is required to enhance the efficiency of chimera production and to document germ-line transmission of EG cells, but results of this study provide an important step toward targeted modification of the porcine genome.

## REFERENCES


1. Evans MJ, Kaufman MH. Establishment in culture of pluripotential cells from mouse embryos. Nature 1981; 292:154–156.
2. Martin GR. Isolation of a pluripotent cell line from early mouse embryos cultured in medium conditioned to teratocarcinoma stem cells. Proc Natl Acad Sci USA 1981; 78:7634–7638.
3. Bradley A, Evans M, Kaufman MH, Robertson E. Formation of germline chimeras from embryo-derived teratocarcinoma cell lines. Nature 1984; 309:255–256.
4. Iannaccone PM, Taborn GU, Garton RL, Caplice MD, Brenin DR. Pluripotent embryonic stem cells from the rat are capable of producing chimeras. Dev Biol 1994; 163:288–292.
5. Schoonjans L, Albright GM, LI J, Collen D, Moreadith RW. Pluripotential rabbit embryonic stem (ES) cells are capable of forming overt coat color chimeras following injection into blastocysts. Mol Reprod Dev 1996; 45:439–443.
6. Wheeler MB. Development and validation of swine embryonic stem cells: a review. Reprod Fertil Dev 1994; 6:563–568.
7. Sims M, First NL. Production of calves by transfer of nuclei from cultured inner cell mass cells. Proc Natl Acad Sci USA 1993; 90: 6143–6147.
8. Stice SL, Strelchenko NS, Keefer CL, Matthews L. Pluripotent bovine embryonic cell lines direct embryonic development following nuclear transfer. Biol Reprod 1996; 54:100–110.
9. Campbell KHS, McWhir J, Ritchie WA, Wilmut I. Sheep cloned by nuclear transfer from a cultured cell line. Nature 1996; 380:64–66.
10. Chiquoine AD. The identification, origin, and migration of the primordial germ cells. Anat Rec 1954; 118:135–146.
11. Matsui Y, Zsebo K, Hogan BL. Derivation of pluripotential embryonic stem cells from murine primordial germ cells in culture. Cell 1992: 70:841–847.

12. Resnick JL, Bixter LS, Cheng L, Donovan PJ. Long-term proliferation of mouse primordial germ cells in culture. Nature 1992; 359:550–551.
13. Stewart CL, Gadi I, Bhatt H. Stem cells from primordial germ cells can reenter the germ line. Dev Biol 1994; 161:626–628.
14. Labosky PA, Barlow DP, Hogan BLM. Mouse embryonic germ (EG) cell lines: transmission through the germline and differences in the methylation imprint of insulin-like growth factor 2 receptor (Igf2r) gene compared with embryonic stem (ES) cell lines. Development 1994; 120:3197–3204.
15. Seamark RF. Progress and emerging problems in livestock transgenesis: a summary perspective. Reprod Fertil Dev 1994; 6:653–657.
16. Stice SL, Strelchenko NS. Domestic animal embryonic stem cells: progress toward germ-line contribution. In: Miller RH, Pursel VG, Norman HD (eds.), Biotechnology's Role in the Genetic Improvement of Farm Animals. Beltsville Symposia in Agricultural Research. Savoy: American Society of Animal Science; 1996: 189–201.
17. Lavoir MC, Basrur PK, Betteridge KJ. Isolation and identification of germ cells from fetal bovine ovaries. Mol Reprod Dev 1994; 37:413–424.
18. Cherny RA, Stokes TM, Merei J, Lom L, Brandon MR, Williams L. Strategies for the isolation and characterization of bovine embryonic stem cells. Reprod Fertil Dev 1994; 6:569–575.
19. Strelchenko N. Bovine pluripotent stem cells. Theriogenology 1996; 45:131–140.
20. Leichthammer F, Baunack E, Brem G. Behavior of living primordial germ cells of livestock in vitro. Theriogenology 1990; 33:1221–1230.
21. Cooke JE, Godin I, Ffrench-Constant C, Heasman J, Wylie CC. Culture and manipulation of primordial germ cells. Methods Enzymol 1993; 225:37–58.
22. De Felici M, McLaren A. Isolation of mouse primordial germ cells. Exp Cell Res 1982; 142:476–482.
23. Buehr M, McLaren A. Isolation and culture of primordial germ cells. Methods Enzymol 1993; 225:58–77.
24. Hogan B, Beddington R, Costantini F, Lacy E. Manipulating the Mouse Embryo: A Laboratory Manual, 2nd ed. New York: Cold Spring Harbor Laboratory Press; 1994: 253–290.
25. Robertson EJ. Embryo-derived stem cell lines. In: Robertson EJ (ed.), Teratocarcinomas and Embryonic Stem Cells: A Practical Approach. Oxford: IRL Press; 1987: 71–112.
26. Eldridge FE. Cytogenetics of Livestock. Westport: AVI Publishing Company; 1985: 219–242.
27. Anderson GB, Choi SJ, BonDurant RH. Survival of porcine inner cell masses in culture and after injection into blastocysts. Theriogenology 1994; 42:204–212.
28. Butler JE, Anderson GB, BonDurant RH, Pashen RL, Penedo MCT. Production of ovine chimeras by inner cell mass transplantation. J Anim Sci 1987; 65:317–324.
29. Rohrer GA, Alexander LJ, Keele JW, Smith TP, Beattie CW. A microsatellite linkage map of the porcine genome. Genetics 1994; 136: 231–245.
30. Gerfen RW, Wheeler MB. Isolation of embryonic cell-lines from porcine blastocysts. Anim Biotech 1995; 6:1–14.
31. Williams RL, Hilton DJ, Pease S, Wilson TA, Stewart CL, Gearing DP, Wagner EF, Metcalf D, Nicola NA, Gough NM. Myeloid leukaemia inhibitory factor maintains the developmental potential of embryonic stem cells. Nature 1988; 336:684–687.
32. Abbondanzo SJ, Gadi I, Stewart CL. Derivation of embryonic stem cell lines. Methods Enzymol 1993; 225:803–823.
33. Wobus AM, Holzhausen H, Jakel P, Schoneich J. Characterization of a pluripotent stem cell line derived from a mouse embryo. Exp Cell Res 1984; 152:212–219.
34. Pease S, Braghetta P, Gearing D, Grail D, Williams RL. Isolation of embryonic stem (ES) cells in media supplemented with recombinant leukemia inhibitory factor (LIF). Dev Biol 1990; 141:344–352.
35. Ouhibi N, Sullivan NF, English J, Colledge WH, Evans MJ, Clarke NJ. Initial culture behaviour of rat blastocysts on selected feeder cell lines. Mol Reprod Dev 1995; 40:311–324.
36. Talbot NC, Rexroad CE, Purcel VG, Powell AM. Alkaline phosphatase staining of pig and sheep epiblast cells in culture. Mol Reprod Dev 1993; 36:139–147.
37. Talbot NC, Powell AM, Rexroad CE. In vitro pluripotency of epiblasts derived from bovine blastocysts. Mol Reprod Dev 1995; 42:35–52.
38. Smith AG, Hooper ML. Buffalo rat liver cells produce a diffusible activity which inhibits the differentiation of murine embryonal carcinoma and embryonic stem cells. Dev Biol 1987; 121:1–9.
39. Bain G, Kitchens D, Yao M, Huettner JE, Gottlieb DI. Embryonic stem cells express neural properties in vitro. Dev Biol 1995; 168:342–357.
40. Talbot NC, Rexroad CE, Purcel VG, Powell AM, Nel ND. Culturing the epiblast cells of the pig blastocyst. In Vitro Cell Dev Biol 1993; 29A:543–554.
41. Hsu FS, Du SJ. Congenital heart diseases in swine. Vet Pathol 1982; 19:676–686.
42. McLaren A. Mammalian Chimaeras. Cambridge: Cambridge University Press; 1976: 105–117.
43. Moens A, Betteridge KJ, Brunet A, Renard JP. Low levels of chimerism in rabbit fetuses produced from preimplantation embryos microinjected with fetal gonadal cells. Mol Reprod Dev 1996; 43:38–46.
44. Onishi A, Takeda K, Komatsu M, Akita T, Kojima T. Production of chimeric pigs and the analysis of chimerism using mitochondrial deoxyribonucleic acid as a cell marker. Biol Reprod 1994; 51:1069–1075.
45. Stewart CL. Production of chimeras between embryonic stem cells and embryos. Methods Enzymol 1993; 225:823–855.

# A cat cloned by nuclear transplantation

This kitten's coat-coloration pattern is not a carbon copy of its genome donor's.

Sheep, mice, cattle, goats and pigs have all been cloned by transfer of a donor cell nucleus into an enucleated ovum[1–5], and now we add the successful cloning of a cat (*Felis domesticus*) to this list. However, this cloning technology may not be readily extendable to other mammalian species if our understanding of their reproductive processes is limited or if there are species-specific obstacles.

As a first attempt, we isolated adult fibroblast cells from oral mucosa obtained from an adult male cat, passaged them three to seven times for expansion in culture, and then froze and stored them in liquid nitrogen. For nuclear transfer, we thawed these cells and fused them with cat ova that had matured *in vitro* and which had had their metaphase chromosomes removed by micromanipulation (see supplementary information). We then transferred cloned embryos into synchronized recipient queens for development.

We carried out 188 such nuclear-transfer procedures, which resulted in 82 cloned embryos that were transferred into seven recipient females. One queen became pregnant with a single conceptus, which ceased to develop and was surgically removed after about 44 days of gestation. Subsequent DNA analysis confirmed that the fetus was derived from a cloned embryo.

Our second attempt involved using nuclei from another cell type for transfer, which we obtained by primary culture of cumulus cells collected from an adult female cat. In a single experiment, three cloned embryos derived from cumulus cells and two cloned embryos derived from fibroblast cells were transferred into a recipient queen. Pregnancy was confirmed by ultrasonography after 22 days of gestation and a kitten was delivered by caesarian section on 22 December 2001, 66 days after the embryo was transferred. The kitten was vigorous at birth and appears to be completely normal.

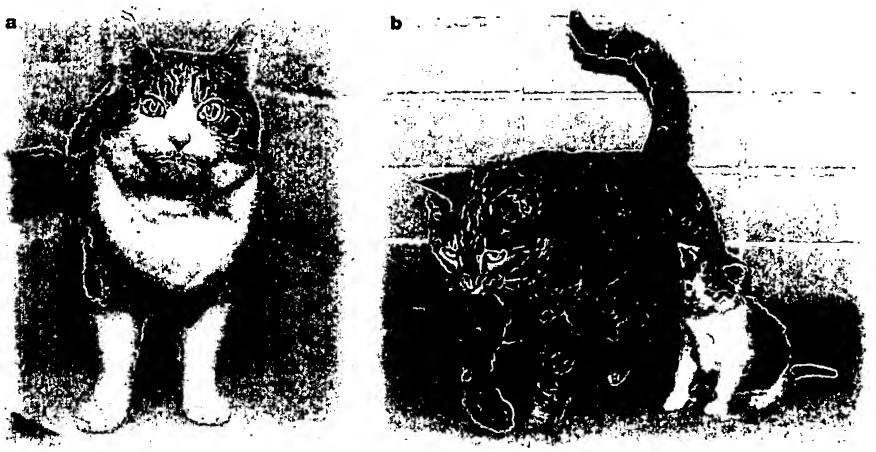


**Figure 1** Nuclear-donor cat, and cloned kitten with its surrogate mother. **a**, Adult female cat that supplied cumulus cells for nuclear transplantation. The cells were cultured in DMEM/F12 medium for 5 days at 37 °C until confluent; micromanipulation was used to enucleate ova obtained after routine ovariohysterectomy and to transfer the donor's cumulus cells into the perivitelline space. Enucleated ova and cumulus cells were fused by electrofusion; a second electropulse was applied to activate the oocytes. **b**, The surrogate mother, a synchronized recipient of three cloned embryos, produced one cloned kitten, which was delivered by caesarian section 66 days after embryonic transfer. For further details, see supplementary information.

The kitten's coat colour suggested that it was derived from a cumulus cell from the female donor (Fig. 1); we therefore analysed DNA of the cumulus cells used for nuclear transfer, as well as from leukocytes in blood samples from the donor cat and surrogate mother, and from cheek cells collected in an oral swab from the kitten. We also analysed control feline samples for comparison with a random-bred cat genetic database. Analysis of seven unlinked, highly polymorphic, feline-specific microsatellite loci confirmed that the kitten is a clone (Table 1).

As with other genetically identical animals with multicoloured coats, the cloned kitten's colour patterning is not exactly the same as that of the nuclear donor — this is because the pattern of pigmentation in multicoloured animals is the result not only of genetic factors but also of developmental factors that are not controlled by genotype.

At this point, we can only roughly evaluate the efficiency of cloning cats by nuclear transfer: 87 cloned embryos were transferred into eight recipients, resulting in one failed pregnancy and one live clone. This is comparable to the success rates obtained for other cloned species. On the other hand, the cloned kitten was born after the transfer of only three embryos derived from cumulus cells. It remains to be investigated whether this cloning efficiency is reproducible in cats.

Table 1 **Analysis of feline genetic markers**

| *Feline markers* | *Cumulus-cell donor (blood)* | *Cumulus-cell line (cultured cells)* | *Cloned kitten (cheek cells)* | *Surrogate queen (blood)* |
|---|---|---|---|---|
| FCA229 | 164/164 | 164/164 | 164/164 | 166/166 |
| FCA290 | 222/222 | 222/222 | 222/222 | 212/218 |
| FCA305 | 194/196 | 194/196 | 194/196 | 196/196 |
| FCA441 | 165/169 | 165/169 | 165/169 | 165/169 |
| FCA078 | 196/198 | 196/198 | 196/198 | 194/200 |
| FCA201 | 159/163 | 159/163 | 159/163 | 143/159 |
| FCA224 | 154/160 | 154/160 | 154/160 | 160/162 |

Values represent the sizes (in base pairs) of the two versions of the amplified microsatellite DNA markers in each sample. Statistical analysis indicates that the probability of the specific microsatellite profile of the cloned kitten matching that of an unrelated cat is $9 \times 10^{-16}$.

**Taeyoung Shin*, Duane Kraemer*, Jane Pryor*, Ling Liu*, James Rugila*, Lisa Howe†, Sandra Buck*, Keith Murphy‡, Leslie Lyons§, Mark Westhusin***

*Departments of *Veterinary Physiology and Pharmacology, †Small Animal Medicine and Surgery, and ‡Pathobiology, College of Veterinary Medicine, Texas A&M University, College Station, Texas 77843-4466, USA*

*e-mail: mwesthusin@cvm.tamu.edu*

*§Department of Population Health and Reproduction, School of Veterinary Medicine, University of California, Davis, California 95616, USA*

1. Wilmut, I., Schnieke, A. E., McWhir, J., Kind, A. & Campbell, K. *Nature* **385**, 810–813 (1997).
2. Wakayama, T., Perry, A. C., Zuccotti, M., Johnson, K. R. & Yanagimachi, R. *Nature* **394**, 369–374 (1998).
3. Kato, Y. *et al. Science* **282**, 2095–2098 (1998).
4. Baguisi, A. *et al. Nature Biotechnol.* **17**, 456–461 (1999).
5. Polejaeva, I. A. *et al. Nature* **407**, 86–90 (2000).

Published online 14 February 2002; DOI 10.1038/nature723.
**Supplementary information** accompanies the paper online.
**Competing financial interests:** declared (see online version).

BIOLOGY OF REPRODUCTION 54, 100–110 (1996)

# Pluripotent Bovine Embryonic Cell Lines Direct Embryonic Development Following Nuclear Transfer

Steven L. Stice,[1] Nick S. Strelchenko, Carol L. Keefer,[2] and Lee Matthews

*American Breeder Service, DeForest, Wisconsin 53532*

## ABSTRACT

Nuclear transfer (NT) procedures were used to determine the in vivo developmental capacity of bovine embryonic cell lines derived from both morula- and blastocyst-stage embryos. These cell lines differed in morphology from trophoblast and endoderm-like cells. Regardless of initial donor embryo stage, cells in the resulting bovine embryonic cell lines had a small cytoplasmic/nuclear volume ratio and contained cytoplasmic vesicles. Developmental rates to blastocyst stage for NT embryos were improved when smaller cells (15 μm) rather than larger cells (18 μm or 21 μm) were used in the NT procedure and the recipient oocyte was activated after the cell fusion step. NT embryos produced from these embryonic cell lines, both morula- and blastocyst-derived, initiated pregnancies following transfer into recipient females. However, all of these pregnancies were lost prior to 60 days of gestation. These NT embryos were able to direct development through organogenesis, with one NT fetus reaching 55 days before death. When viable NT embryos were recovered during early gestation (38 days), an absence of cotyledons and a hemorrhagic response in the caruncles were observed. A chimera produced by aggregating an NT embryo with two 8-cell-stage blastomeres from in vitro-produced embryos developed through the 85th day of gestation. However, this conceptus was also deficient of cotyledons. DNA markers indicated that 50% of the chimera conceptus tissues were derived from the embryonic cell line. Blastocyst- and morula-derived embryonic cell line nuclei are pluripotent in that they can direct development through organogenesis, with subsequent pregnancy loss due, at least in part, to a deficiency in placentome development.

## INTRODUCTION

The establishment of embryonic stem (ES) cells from embryos of domestic farm animals has been problematic. There have been numerous reports of embryonic cell lines derived from domestic farm animal species that exhibit in vitro pluripotent characteristics (cattle [1], sheep [2, 3], pigs [2–4]). These cell lines can maintain a normal karyotype through numerous passages and are able to differentiate and form embryoid bodies in vitro. However, evidence of in vivo developmental capacity is lacking for most of these lines. Recent phenotypical information suggests that chimeric pigs [5] and rats [6] have been produced, but the embryonic cell line contribution to the germ cells remains undetermined. One method of obtaining immediate germ-line contribution would be to utilize ES cells as donor nuclei in the nuclear transfer (NT) procedure. Reports of NT calves derived from inner cell mass (ICM) cells [7, 8] and cultured ICM cells [9] suggest that embryonic cell lines derived from ICM or blastomeres used in NT procedures might result in fetuses or offspring.

In the mouse, the particular ES cell line and embryo manipulation technique used influence the ability of ES cells to differentiate into fetal and placental tissues. Mouse ES cells showed limited potency when used as donor nuclei in NT procedures [10]. ES cell NT embryos directed development to the blastocyst stage but failed to develop further when transferred to recipient animals. Possible causes for the pregnancy losses in the mouse could not be elucidated. However, Nagy and coworkers [11] showed that mouse ES cells from one particular ES cell line formed live offspring when aggregated to a tetraploid embryo. In those experiments, the tetraploid cells gave rise to placental tissue while the ES cell contribution was almost exclusively fetal. Taken together, the minimal mouse ES cell contribution to the placental tissues in the chimera studies, and the limited development of NT embryos, suggest that ES cells may not be capable of initially differentiating into all conceptus cell types.

In the present study, we tested the potency of bovine embryonic cell lines using NT procedures. Developmental rates to blastocyst stage for NT embryos were improved through modification in NT procedures. However, the developmental potential of NT embryos beyond the blastocyst stage was limited to the period of organogenesis, with pregnancy loss due, at least in part, to a deficiency in placentome development.

## MATERIALS AND METHODS

### *Production of Embryonic Cell Lines*

Production of embryonic cell lines from blastocyst-stage embryos were described elsewhere [1] and modified in our laboratory. Briefly, primary cultures of embryonic fibroblasts were obtained from 14–16-day-old murine fetuses. After the head, liver, heart, and alimentary tract were aseptically removed, the embryos were minced and incubated for 30 min at 37°C in prewarmed trypsin EDTA solution (0.05% trypsin/0.02% EDTA; GIBCO, Grand Island, NY). Fibroblast cells were plated in tissue culture flasks and cul-

Accepted August 23, 1995.
Received March 6, 1995.

[1]Correspondence and current address: Steven L. Stice, Advanced Cell Technology Inc., 207 Paige Laboratory, University of Massachusetts, Amherst, MA 01003. FAX: (413) 545-6326; e-mail: stice@vasci.umass.edu

[2]Current address: Nexia Biotechnologies, Inc., 21,111 Lakeshore Rd., Box 183, Ste. Anne de Bellevue, Quebec, Canada H9X 3V9.

tured in alpha-MEM medium (BioWhittaker, Walkersville, MD) supplemented with 10% fetal calf serum (FCS; Hyclone, Logan, UT), penicillin (100 IU/ml), and streptomycin (50 μl/ml). Three to four days after passage, embryonic fibroblasts, in 35 × 10 Nunc culture dishes (Baxter Scientific, McGaw Park, IL), were treated with mitomycin C (10 μg/ml; Sigma Chemical Company, St. Louis, MO) in supplemented alpha-MEM for a minimum of 3 h. The fibroblasts were grown and maintained in a humidified atmosphere with 5% $CO_2$ in air at 37°C. Only culture plates that had a uniform monolayer of cells were used to culture the bovine embryonic cells.

Bovine embryos were nonsurgically collected or produced through use of in vitro procedures [12]. Blastomeres from morula, or the ICM of blastocysts, were partially disaggregated by a 10-min incubation in a 0.3% protease E (Sigma) in HEPES-buffered Hamster Embryo Culture Medium (HECM [13]) supplemented with 3 mg/ml BSA fraction V (Sigma). After removal of a majority of the trophoblast, a clump of cells containing the ICM was washed through 3 ml of HECM and plated directly onto the mitomycin C-blocked fibroblast cells. Disaggregated blastomeres were placed under the fibroblast feeder layer to initiate more contact with the feeder layer. A transfer pipette (50–100-μm diameter) was used to transfer the blastomeres between the feeder layer and culture plate. After 24 h in culture, the feeder layer usually reattached to the culture plate. The cell lines were maintained in a growth medium consisting of alpha-MEM supplemented with 10% FCS and 0.1 mM beta-mercaptoethanol (Sigma). Growth medium was exchanged every 2 to 3 days. Initial colonies were observed by the fourth day of culture and could be passaged between the seventh and tenth day. Only cells having the following three morphological features were isolated for passage: a small cytoplasmic/nuclear volume ratio, nuclei with multiple nucleoli, and cytoplasmic vesicles. Isolation of cells meeting these three criteria was accomplished by using a glass needle to cut out and separate the desired portions of the cell colony. These sections were lifted off the dish and mechanically disaggregated into clumps of cells by repeated pipetting through a small-bore pipette (50–100 μm). The disaggregated clumps were then passaged onto a new feeder layer. Only cell lines that had undergone fewer than 10 passages were used as nuclear donors in the NT procedure.

*NT Procedures*

Four NT experiments were performed to examine the time of activation and fusion, donor cell size, individual cell lines, and the ability of NT chimeras to develop in utero. NT procedures have been described previously [14, 15]. Briefly, after slaughterhouse oocytes were matured in vitro [12], the oocytes were stripped of cumulus cells and enucleated with a beveled micropipette at approximately 18 h post the beginning of maturation (hpm). Enucleation was confirmed through use of Hoechst 33342 (3 μg/ml; Sigma). Individual donor cells were then placed into the perivitelline space of the recipient oocyte. Blastomeres from morula were mechanically separated, whereas embryonic cell line cells were disaggregated by protease treatment (see above). Time of fusion varied from one experiment to another, ranging from 20 to 28 hpm. However, fusion pulse parameters were maintained at a constant 90 V for 14 μsec as described previously [15].

The procedure used to artificially activate oocytes has been described elsewhere [16]. The timing of activation was held constant (24 hpm). In brief, the activation procedure was as follows. NT embryos were exposed for 4 min to ionomycin (5 μM; CalBiochem, La Jolla, CA) in HECM supplemented with 1 mg/ml BSA and then were washed for 5 min in HECM supplemented with 30 mg/ml BSA. The NT embryos were then transferred into a microdrop of CR1aa culture medium [17] containing 0.2 μM 4-diethylaminopyridine (Sigma) and cultured at 39°C 5% $CO_2$ for 4–5 h. The embryos were washed in HECM and then placed in CR1aa medium in microdrop plates and cultured for 3–4 more days at 39°C and 5% $CO_2$. At all stages, oocytes and embryos were cultured in pre-equilibrated drops of medium (30–50 μl) under light-weight mineral oil.

After 4 days in culture, NT embryos were transferred into microdrops of CR1aa medium containing 10% FCS. At Day 7 (Day 0 = day of fusion and activation) the developmental rates to blastocyst stage was determined. On Day 7 or 8, a limited number of blastocysts from various groups were transferred into recipient females. The stage of estrous cycle of the recipient was matched with the stage of the embryo.

*Production of Chimeras*

To produce aggregate chimeras, two 8-cell-stage blastomeres were added to an 8-cell-stage NT embryo. NT embryos have reached the 8-cell stage by Day 2.5 of culture. At that time, 8-cell-stage in vitro-produced embryos (Day 2.5) were mechanically disaggregated through use of a transfer pipette, and two of the blastomeres were transferred through the slit in the zona of the NT embryo. These transferred blastomeres were placed in direct contact with the blastomeres of the NT embryo. The aggregate embryos were placed back into CR1aa supplemented with 3 mg/ml BSA and on the third or fourth day transferred into CR1aa supplemented with 10% FCS. Those embryos in which the combined cells had formed a blastocyst were transferred into recipient females.

*Pregnancy Detection and Ultrasound Observations*

Recipient females were monitored daily for return to estrus. Females not returning to estrus between 25 and 30 days of gestation were examined by ultrasound (Aloka 500, 7.5 MHz transducer; Corometrics Medical Systems, Wallingford, CT). The presence of a fetal heartbeat was the criterion for

considering a recipient to be pregnant. Those animals diagnosed as pregnant were monitored every week for the presence or absence of a fetal heartbeat. The time of pregnancy loss was arbitrarily set at midweek between the time a heartbeat was present and the time it was absent. Pregnancies were monitored weekly until Day 90 of gestation.

*DNA Markers*

DNA was isolated from the tissues of presumptive NT and chimeric fetuses (heart, muscle, skin, and placenta) and calves (blood) to determine parentage. Polymerase chain reaction amplification of cytosine/adenine repeat microsatellite markers (MGTG 4-B, TLGA 73, TLGA 57, TLGA 53, TLGA 263, TLGA 48, TLGA 122, TLGA 126, TLGA 227, TLGA 261, TLGA 325, and TLGA 245; Linkage Genetics, Salt Lake City, UT) was performed, and the amplification products were analyzed at Linkage Genetics and Grace Washington Research Group (Columbia, MD). Conceptus and calf DNA marker results were compared with the DNA marker profiles of the bulls used to produce embryos for both the established embryonic cell lines and the aggregate blastomeres. In addition, DNA marker profiles were run on the embryonic cell lines themselves and compared with those of the conceptuses and calves. In order to quantify the embryonic cell line contribution in the chimera experiment, DNA mixes composed of known ratios of DNA were used as standards for comparison with the putative chimeric tissues results.

*Sex Determination*

Sexing of embryonic cell lines was accomplished by amplification of Y chromosome-specific DNA sequences using an assay kit produced by AB Technology (Pullman, WA). Three to six cells were removed from the embryonic cell lines and from the mouse feeder layer. These cells were washed through serum-free PBS and placed into microcapillary tubes containing 10 μl sterile, deionized water. The samples were frozen-thawed to lyse the cells, and a reagent mixture containing the primers, nucleotide triphosphates, buffer solution, and *Taq* polymerase (Complete-Reaction-Mix, AB Technology) was added. The primers in the reaction mix were for a bovine-ovine-caprine-specific Y chromosome repeat sequence and for a repeated autosomal sequence (control). Capillary tubes containing the samples, the control without DNA, and male and female controls were placed into a Corbett Capillary DNA Thermal Cycler FTS-1S (AB Technology). Male and nonspecific (autosomal control) DNA bands were separated and visualized by gel electrophoresis in an ethidium bromide-3% agarose gel. No bands were visible for the mouse feeder layer cells, demonstrating that the mouse feeder layer DNA did not interfere with this bovine-specific assay.

*Histology*

Conceptuses were recovered from five recipient animals by hysterectomy via a flank incision. Histological preparations were made of recovered fetuses and placentomes. Tissue was placed in 10% buffered formalin, dehydrated in increasing concentrations of ethyl alcohol, cleared in chloroform, and infiltrated with paraffin. Tissues were sectioned and stained with hematoxylin and eosin. Slide-mounted sections were then viewed under a microscope, and comparisons between normal conceptuses and NT conceptuses were made by a veterinary pathologist.

*Statistical Analysis*

Statistical computations were made through use of chi-square analysis for all data (Instat; GraphPad Software, San Diego, CA).

## RESULTS

*Establishment of Embryonic Cell Lines*

Embryonic cell lines were established from in vivo- and in vitro-produced blastocyst- and morula-stage embryos (Table 1). Cell colony formation was observed approximately 3 to 7 days after initiation of culture (Fig. 1a). An embryonic cell line was considered established when a homogenous population of cells could be maintained for several generations. Embryonic cell lines were established from all types of embryos tested. Each cell line maintained a low cytoplasmic to nuclear ratio, prominent nucleoli in the nucleus, and lipid vesicles in the cytoplasm. Some cell lines were allowed to proliferate, maintaining proper morphology for over 50 passages (over 12 mo of in vitro culture). Furthermore, cell lines from each of the four types of embryos formed embryoid bodies when colonies became overcrowded in vitro (Fig. 1d). These structures were considered embryoid bodies because of their resemblance to blastocyst-stage embryos and the differentiation of cells within the structure (muscle, red blood cells; S.L. Stice, personal observations). In general, there were no morphologically distinguishable differences among embryonic cell lines derived from various stages (blastocyst or morula) and types (in vitro or in vivo derived) of donor embryos (Table 1).

Besides forming embryoid bodies, the embryonic cell lines also formed differentiated cell types in vitro. Large, loosely attached, highly refractory, and irregularly shaped endoderm-like cells (not shown) were present as were trophectoderm-like cells (Fig. 1b). Trophectoderm-like cells were often present in the primary culture and later removed and discarded. These cells had distinguishing features that included a larger cytoplasmic/nuclear volume ratio than the embryonic cell lines and had numerous cytoplasmic vacuoles. When dissociated, trophectoderm-like cells were not round in shape and were obviously larger in diameter than

TABLE 1. Derivation of embryonic cell lines derived from different stages and sources of embryos.

| Embryo stage | Source of embryo | No. of embryos placed in culture | No. of established cell lines* | % Established | Formed embryoid bodies |
|---|---|---|---|---|---|
| Morula | In vitro | 12 | 8 | 67% | Yes |
| Morula | In vivo | 11 | 6 | 55% | Yes |
| Blastocyst | In vitro | 15 | 7 | 47% | Yes |
| Blastocyst | In vivo | 27 | 15 | 55% | Yes |

*Numbers of established embryonic cell lines were not different among embryo stages and sources.

the embryonic cell line cells (Fig. 1c). Disaggregated trophoblast cells obtained directly from a blastocyst-stage embryo had similar trophectoderm-like characteristics.

*NT*

*Experiment I: Time of activation.* Previously it was reported that temporal relationship between activation and fusion affected the developmental rate of bovine 32-cell-stage blastomere-derived NT embryos [15, 18, 19]. Therefore, developmental rates were determined for NT embryos in which the donor cells (blastomeres or embryonic cell line cells) were fused with the enucleated oocyte either before, simultaneously with, or after oocyte activation (Table 2). The temporal relation between activation and fusion did affect developmental rates, but embryonic cell line nuclei

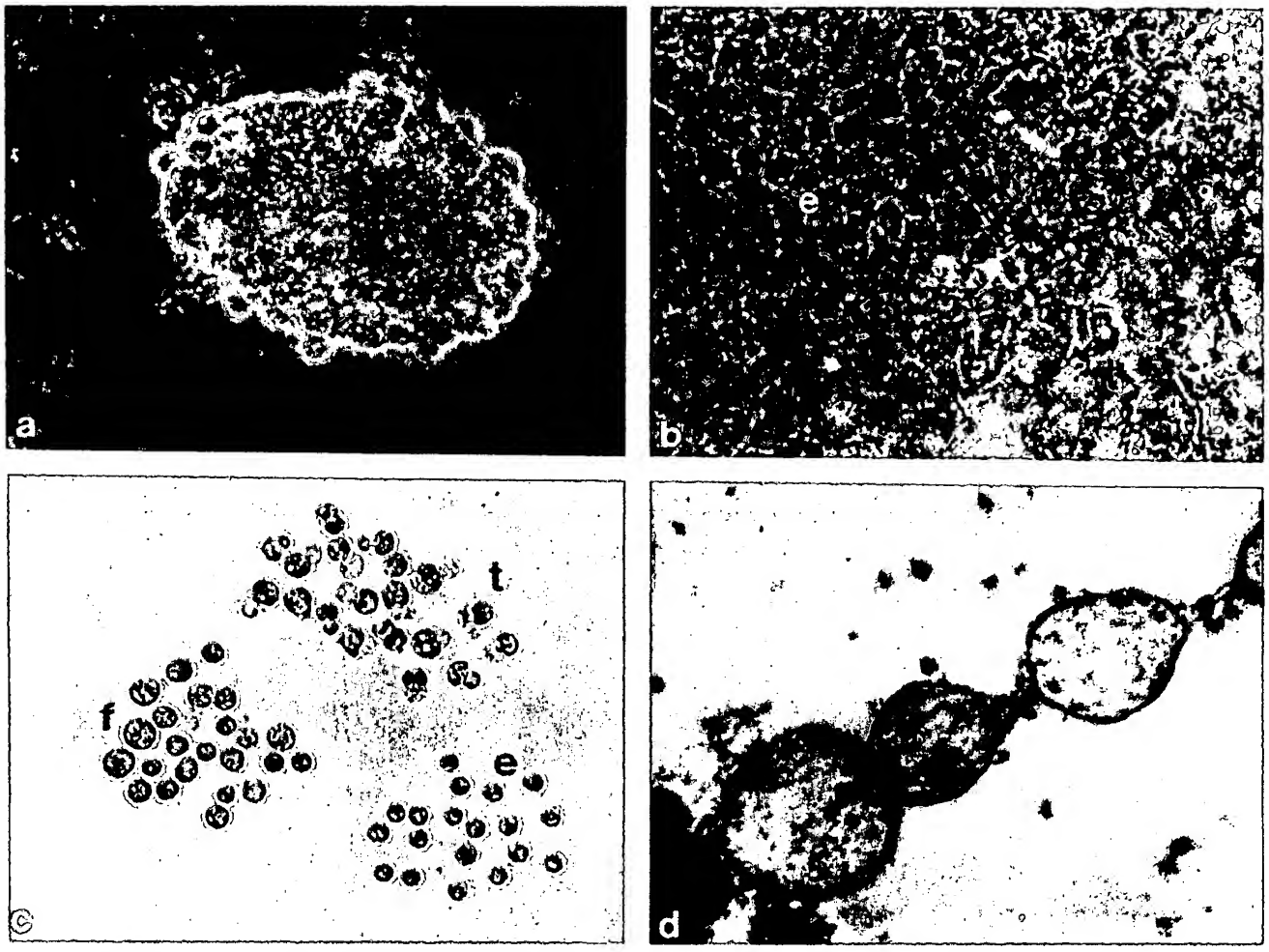


FIG. 1. a) A typical cell colony from morula- and blastocyst-stage embryos 4–7 days after being seeded on top of a feeder layer. b) An embryonic cell line (e) colony exhibiting a high nuclear-to-cytoplasmic ratio and some vesicles in the cytoplasm. An outgrowth of trophoblast cells (t) developing around the perimeter of a colony. c) Disaggregated cells, mouse embryonic fibroblast cells (f), trophoblast cells (t), and embryonic cell line cells (e). d) Simple embryoid body or vesicle formation after overcrowding of cell colonies in culture. a–c, ×186, original ×200; d, ×93, original ×100.

TABLE 2. The effect of time of activation in relation to time of fusion on development to blastocyst and establishment of pregnancies in NT embryos derived from either blastomere or embryonic cell line nuclei.

| Type of donor nuclei | Time of fusion* | No. of donor cell lines or embryos | No. NTs produced | No. NTs to blastocysts (%) | No. NTs transferred to recipients | No. pregnant (%)[c] | | |
|---|---|---|---|---|---|---|---|---|
| | | | | | | > 30 Days | > 40 Days | > 50 Days |
| 32-cell blastomere | 20 h | 4 | 74 | 0[a] (0) | — | — | — | — |
| Embryonic cell line | 20 h | 3 | 1045 | 103[b] (10) | 45 | 6 (13) | 1 (2) | 0 |
| 32-cell stage blastomere | 24 h | 4 | 105 | 7[b] (7) | 3 | 0 (0) | 0 | 0 |
| Embryonic cell line | 24 h | 3 | 1075 | 29[a] (3) | 19 | 1 (5) | 0 | 0 |
| 32-cell stage blastomere | 28 h | 15 | 475 | 62[b] (13) | 10 | 3 (30) | 3 (30) | 2 (20) |
| Embryonic cell line | 28 h | 7 | 2195 | 47[a] (2) | 41 | 3 (7) | 1 (2) | 0 |

*Time of fusion varied (20, 24 or 28 hpm), but time of activation remained constant (24 hpm).
[a,b]Number developing to the blastocyst stage without a common superscript differed ($p < 0.05$).
[c]Too few of the NT embryos were transferred to determine differences in pregnancy rates.

responded differently than did the blastomere nuclei. As expected, developmental rates were highest for blastomere-derived NT embryos when the blastomeres were fused (28 hpm) with previously activated oocytes (13%; $p < 0.05$). The embryonic cell line NT embryos' highest developmental rates to blastocyst stage (10%) were obtained when the NT embryo was activated 4 h after the cell fusion procedure (20 hpm). Although the fusion pulse might have induced partial activation of NT embryos, complete activation was accomplished only after the activation stimulus was given 4 h later. NT embryos not receiving the activation stimulus after fusion underwent premature chromatic condensation and did not cleave. These nonactivated NT embryos were also used to determine fusion rate. Fusion rates did not differ among experimental groups in this study (data not presented). In this initial experiment, a limited number of NT blastocysts were transferred to recipient females. Only the blastomere NT embryos developed past 50 days of pregnancy and eventually to full term (Table 2). Although all of the embryonic cell line NT pregnancies eventually aborted, the pregnancies had clearly been established as determined by ultrasound.

*Experiment II: Donor cell size.* The relative size of mouse ES cells used to produce chimeric embryos has been shown to be correlated with resulting percentage of germline chimeras [20]. Smaller-diameter mouse ES cells resulted in a higher percentage of germ-line chimeras. Therefore, the effect of cell diameter on developmental rates to the blastocyst stage after NT was monitored. Following disaggregation, individual cells were categorized into three different groups: large, medium, and small cells with approximate diameters of 21 μm, 18 μm, and 15 μm, respectively. Cells from each group were used in the NT procedure. The fusion pulse (20 hpm) was applied 4 h prior to the activation stimulus. Developmental rates were affected by the size of the donor cell (Table 3), with small cells having significantly higher developmental rates to the blastocyst stage than medium or large cells ($p < 0.005$). Only 19 NT embryos derived from these cell groups were transferred to recipient animals, and those that were transferred failed to maintain the pregnancy beyond 39 days of gestation (Table 3).

*Experiment III: Individual cell lines.* Embryonic cell lines derived from various sources of embryos were used as donor nuclei in the NT procedures. The NT parameters that yielded the highest developmental rates to the blastocyst stage in experiments I and II (i.e., fusion prior to activation and small cells) were used in this experiment. Developmental rates to the blastocyst stage as well as pregnancy rates were monitored (Fig. 2a). Of the sexed cell lines, the male line had a lower developmental rate to the blastocyst stage than did the female lines ($p < 0.001$). Conversely, NT blastocysts derived from the male line (0761) had a higher proportion of established pregnancies developing past 40 days (6 of 39, 15%) than did those from the female lines (pooled results, 0734 and 0713; 9 of 177, 5%; $p < 0.05$). Two conceptuses reached greater than 50 days of gestation before the heartbeats were no longer detected during ultrasound examination.

Five conceptuses ranging from 35 to 55 days of gestation were recovered after their heartbeat was no longer detected by ultrasound. A 55-day fetus showed no gross abnormalities when recovered (Fig. 2b). Similarly, the other four conceptuses exhibited no overt abnormalities. Two of the five fetuses were prepared for histological analysis and DNA marker analysis. DNA marker identification confirmed that these fetuses were derived from the embryonic cell line

TABLE 3. The development of NT using donor nuclei from embryonic cell line cells of various sizes derived from blastocyst-stage embryos with activation occurring 4 h after fusion.

| Embryonic cell line cell diameter | No. NTs produced | No. NTs to blastocyst (%) | No. NTs transferred to recipients | No. pregnant | |
|---|---|---|---|---|---|
| | | | | > 30 Days | > 40 Days |
| 15 μm | 592 | 117[a] (20) | 11 | 0 | — |
| 18 μm | 703 | 88[b] (13) | 4 | 1 | 0 |
| 21 μm | 643 | 77[b] (10) | 4 | 0 | — |

[a,b]Numbers developing to the blastocyst stage without a common superscript differ ($p < .0005$).

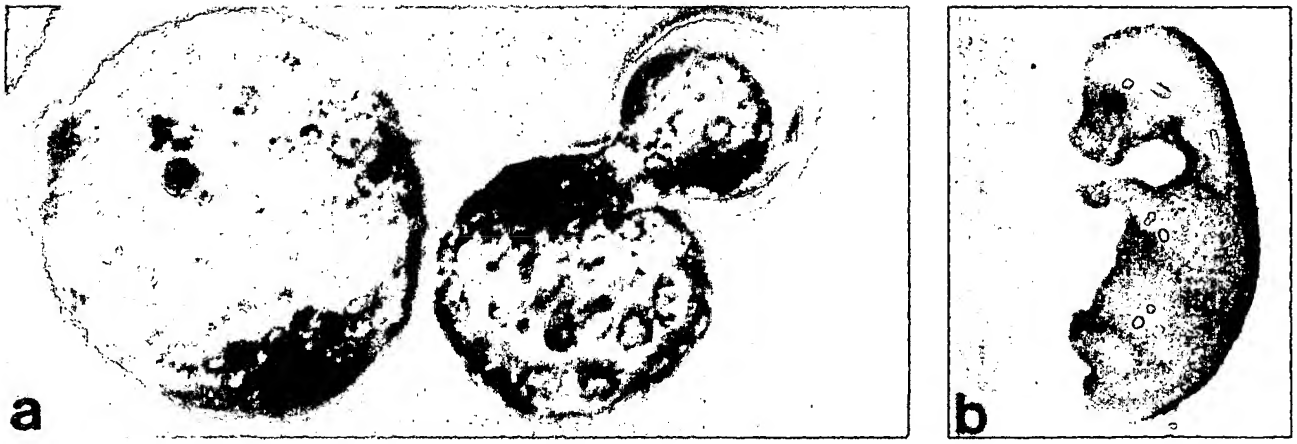


FIG. 2. a) Day 8 blastocyst-stage embryos derived from embryonic cell lines (×200). b) A Day 55 fetus derived from an embryonic cell line NT embryo (shown actual size).

FIG. 3. A sagittal section of a Day 40 fetus derived from an embryonic cell line NT embryo (×4).

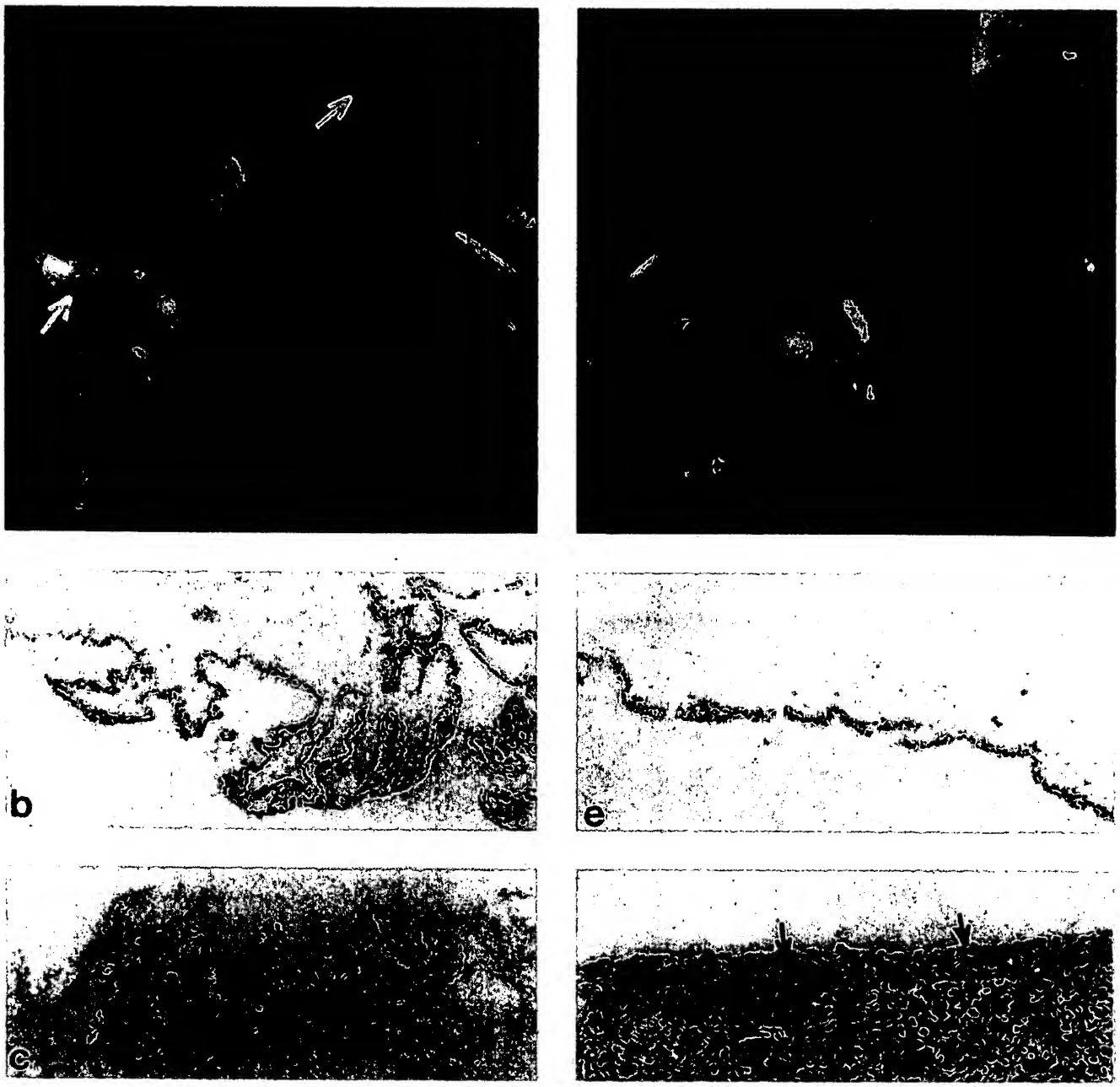


FIG. 4. a-c) Day 38 conceptus derived from an in vitro-produced embryo where multiple cotyledons were observed (white arrows). The placentomes were developmentally normal with cotyledons (b) and caruncles (c) forming villi and crypts, respectively, at this time point. d-f) Day 38 conceptus derived from an embryonic cell line NT embryo. Note the absence of cotyledonary structures (d), an absence of villi in the placental tissue (e), and caruncles (f) void of crypts. The caruncular tissue also had large areas containing erythrocytes near the surface epithelium (black arrows). a and d, shown actual size; b,c,e,f, ×100.

0734. Sagittal sections from these fetuses were not informative as to the cause of death in these pregnancies (Fig. 3). However, gross examination of the placental tissue of the NT conceptuses showed that cotyledonary tissue was obviously absent (Fig. 4, d and e). Binucleate cells were present in the placental membranes of the NT pregnancies. However, whether these cells were physiologically normal

FIG. 5. a) An 85-day chimeric conceptus (shown at 95% of actual size) derived from an embryonic cell line NT embryo (50% contribution) aggregated with a fertilized embryo (50% contribution). This placenta was largely deficient of cotyledons; however, a few rudimentary structures were observed (arrows). b) The fetus from the same conceptus appeared normal (×1.4).

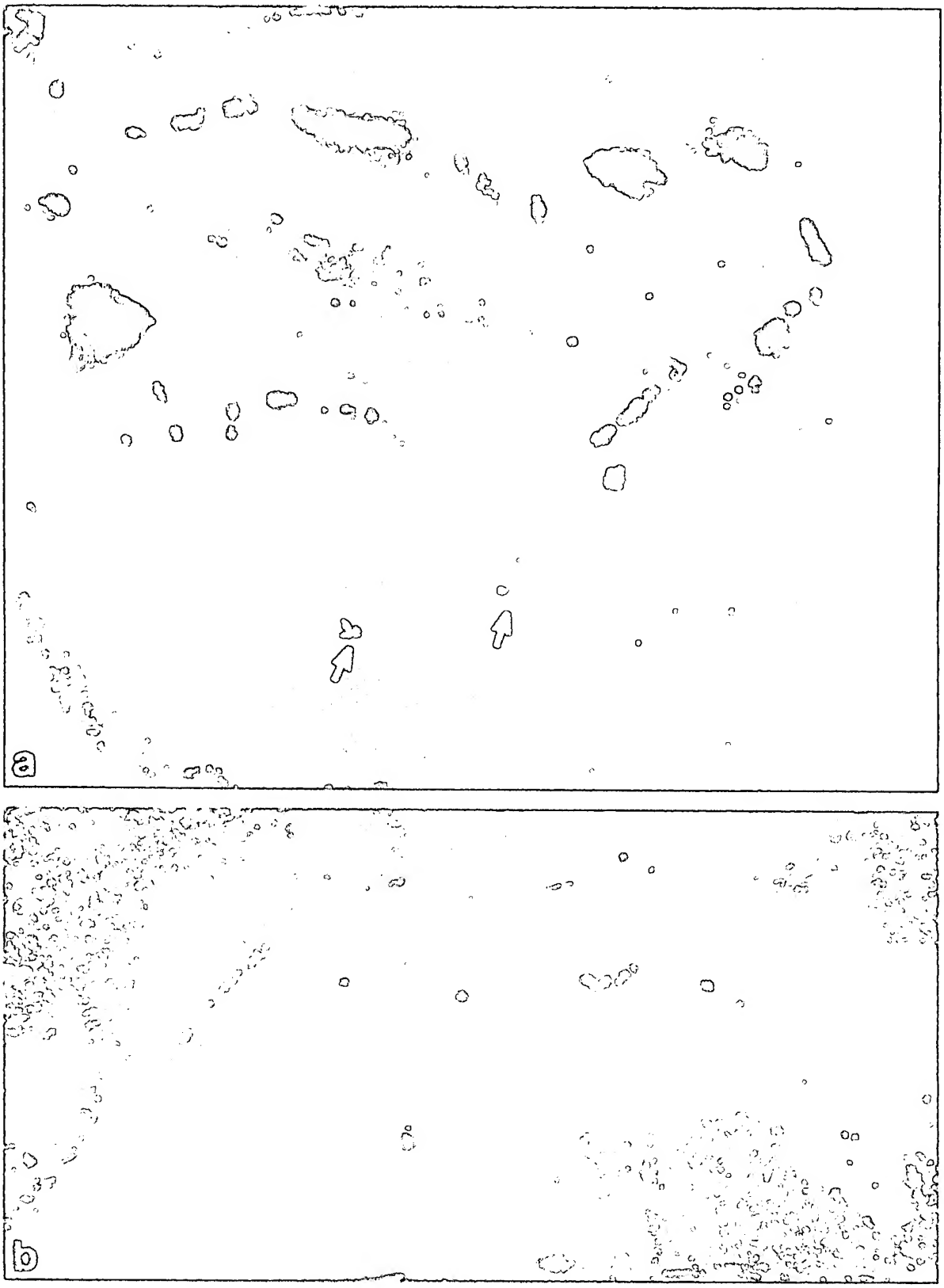

TABLE 4. The development of NT using donor nuclei from embryonic cell lines derived from morula- or blastocyst-stage embryos using 15-μm donor cell and activation 4 h after fusion.

| Embryonic cell line ID | Stage | Source | Sex | No. NTs produced | No. blastocysts (%) | No. blastocysts transferred to recipients | No. pregnant (%) | | |
|---|---|---|---|---|---|---|---|---|---|
| | | | | | | | > 30 Days | > 40 Days | > 50 Days |
| 0734 | Blastocyst | In vivo | F | 1047 | 246[a] (23) | 164 | 27 (16) | 9[d] (5) | 1 (1) |
| 0761 | Blastocyst | In vivo | M | 498 | 58[b] (12) | 39 | 8 (21) | 6[e] (15) | 1 (3) |
| 0713 | Blastocyst | In vitro | F | 863 | 314[c] (36) | 13 | 4 (31) | 0[d] | 0 |
| 0870 | Morula | In vivo | — | 84 | 34[c] (40) | 15 | 2 (13) | 0 | 0 |
| 0677 | Morula | In vitro | — | 704 | 250[c] (36) | 20 | 6 (30) | 1 (5) | 0 |

*Pregnancy rates did not differ at 30 days.

[a,b,c]Numbers developing to the blastocyst stage without a common superscript differ ($p < 0.001$).

[d,e]Numbers pregnant past 40 days without a common superscript did differ among the blastocyst-derived cell lines when results within the same sex were pooled ($p < 0.05$).

remains unknown. Four conceptuses derived from in vitro-produced embryos taken at similar times (30–55 days of gestation) possessed cotyledonary tissue. Furthermore, the caruncular tissue from the NT pregnancies did not develop crypts and had a hemorrhagic response at the surface of the caruncles (Fig. 4f). In all cases, NT embryo placentation was abnormal for that stage of gestation.

*Experiment IV: Aggregation chimeras.* In an attempt to rescue the NT pregnancies, aggregate chimeras were produced by combining the 8-cell-stage blastomeres from NT embryos with two blastomeres from in vitro-produced embryos of a similar stage (Fig. 1b). Aggregate embryos (n = 53) were transferred to recipient females. Initially, eight pregnancies were established past 60 days of gestation. Three pregnancies were lost between 60 and 90 days of gestation, and five pregnancies were carried to term. One of the pregnancies that aborted at 85 days was recovered (Fig. 5). DNA microsatellite markers were used to establish parental origin and percentage of embryonic cell line contribution to the chimeras. Tissue from the placenta, skin, muscle, and heart showed approximately a 50/50 contribution from the two embryos used to make the aggregate chimeras. Again, no abnormalities were observed in the fetus, but abnormally fewer and smaller cotyledons were present on the placenta than expected for that stage of gestation (Fig. 5). There was no detection of embryonic cell line contribution to the blood and ear punch samples obtained from the offspring. Sensitivity of the DNA marker assay should allow the detection of an embryonic cell line contribution of 10% or greater in any tissue.

## DISCUSSION

Established bovine embryonic cell lines directed embryonic development through organogenesis when used as donor nuclei in NT procedures. In order to make conclusive genetic identification of fetuses and offspring using DNA markers, the marker genotype of either the maternal and paternal source or, as in the present study, the embryonic cells themselves must be analyzed. DNA marker results confirmed that embryonic cell lines did contribute to NT fetuses and multiple tissue types in an 85-day NT chimeric fetus. Marker analysis of offspring indicated that there was little or no genetic contribution from the embryonic cell lines to blood or ear tissues samples.

The exact cause(s) of pregnancy loss for both NT embryos and chimeras is unknown. However, placental developmental failure should be considered a contributing factor. Normally, cotyledon formation occurs by Days 25–30 of gestation in cattle [21, 22]. It has been reported that until approximately Day 40, it is possible for the bovine conceptus to survive on "uterine milk" [21]. However, after this time point, fetal-maternal exchange of nutrients and gases must occur through functioning placentomes in order to maintain the pregnancy. The timing of pregnancy losses in the present study coincides with timing of placentome formation in normal conceptuses. The hemorrhaging in the caruncles of NT pregnancies indicated that there was a maternal response to the presence of the conceptus but that proper placentome formation did not ensue. There was also a marked reduction in the number and size of cotyledons in the chimeric pregnancy, indicating that the contribution of the in vitro-produced embryo could prolong the pregnancy but not totally rescue it. Future chimera experiments in which the placental contribution from the NT embryo is minimized might extend these pregnancies past 85 days of gestation.

The timing of fusion in relation to activation and the size of the donor cell had a significant effect on NT embryo development rates to the blastocyst stage. Fusion (20 hpm) at 4 h prior to activation (24 hpm) was most beneficial for embryonic cell line NT embryos, whereas for blastomere NT embryos, the developmental rates were higher when fusion (28 hpm) occurred at least 4 h after activation (24 hpm). In previous studies [15, 18, 19], the fusion pulse has been used to activate aged oocytes (> 30 hpm). Thus, it is possible that the fusion pulse might have also induced oocyte activation in the present study. However, NT embryos were not activated when given a fusion pulse alone (20 hpm), suggesting that fusion pulse-induced activation was negligible in this study. The data for blastomere NT embryos were in agreement with results from previous bovine studies in which developmental rates were improved when the recipient oocytes

were activated prior to blastomere fusion [15, 18, 19]. The cell cycle stage of the donor blastomere has also been shown to affect bovine NT embryo developmental rates. The optimal developmental rates occurred when 32-cell-stage bovine blastomeres (10–15 h after M phase) were fused with a previously activated oocyte [23]. The cell cycle of blastomeres differs greatly from that of the embryonic cell lines. Approximately 80% of cleavage-stage bovine blastomeres are in the S phase [18], whereas 40–60% of embryonic cell line cells are in G1 phase at any given time (S.L. Stice and N.S. Strelchenko, unpublished results from flow cytometry analysis). Dissimilarities in the cell cycle characteristics might account for differences in developmental rates observed between these two types of donor nuclei. In the rabbit, a blastomere in G1 phase had a higher developmental rate to the blastocyst stage when placed in a nonactivated M-phase oocyte [24]. As most of the embryonic cell line nuclei in the present study resided in G1 phase, resulting NT embryos had a higher development capacity when these nuclei were fused with a nonactivated oocyte.

In a study in the mouse, the percentage of offspring that were chimeric increased when smaller (7–9 μm) rather than larger (9–18 μm) ES cells were injected into the blastocoele cavity of the host blastocysts [21]. Similarly to mouse ES cell chimera experiments, the present studies showed that individual bovine embryonic cells with a smaller cell diameter (15 μm) had a higher developmental capacity than larger cells (18 or 21 μm). Perhaps smaller cells have divided more recently and therefore were earlier in the cell cycle (G1) than the larger cells. Alternatively, the larger cells might have been polyploid and thus less likely to develop to the blastocyst stage when used as donor nuclei in the NT procedure. A proportion of cells within bovine embryonic cell lines have been shown to possess an abnormal karyotype [25]. In any case, the status of the cell cycle and the cell's ploidy are important factors to consider when one attempts to improve the efficiency of NT procedures.

Similarities in the pluripotent properties between the bovine embryonic cell lines in the present study and mouse ES cells in other studies were observed. NT embryos derived from mouse ES cells [10] and NT embryos derived from the bovine embryonic cell line developed to the blastocyst stage, but in both cases the resulting pregnancies were either reabsorbed (mouse) or lost early in gestation (bovine). Furthermore, tetraploid cells aggregated with mouse ES cells resulted in conceptuses with placental tissue almost exclusively derived from the tetraploid cells [11], indicating a failure of the ES cells to make a major contribution to the placenta. Likewise, the bovine embryonic cells were not able to direct normal placentome formation. While chimerism prolonged development of the conceptus to 85 days, the in vitro-produced embryo contribution to the placenta was only 50%. Perhaps a higher contribution from these cells would extend pregnancies further. Bovine tetraploid embryos did not develop beyond the 8-cell-stage in our laboratory (data not presented), thus prohibiting the use of tetraploid embryos as helper cells in placentation for bovine NT embryos.

From the male and female bovine embryonic cell lines studied (Table 4), sex- or cell line-dependent differences appear to exist. The male line (0761) derived from a blastocyst-stage embryo had a higher proportion of resulting NT embryos developing past 40 days of gestation than did similar lines derived from female embryos (0734 and 0713). Male mouse ES cell lines are more easily obtained, and they maintain a more stable karyotype than female lines [26]. Bovine embryonic cell lines do undergo karyotypic changes over time, and female lines have an increase in X-inactivation over 15 passages [25]. Subtle differences in genomic stability might explain developmental differences observed among embryonic cell lines used in this study. Additional experiments are needed to determine whether or not these differences are related to the sex of a particular cell line.

Differences in pluripotent properties between morula- and blastocyst-stage-derived embryonic cell lines were not observed in the current study. Pluripotent mouse ES cells have been produced from mouse morula-stage embryos but have not been tested for germ-line contribution [27]. Mink embryonic cell lines derived from morula-stage embryos give rise to more diverse differentiated tissue types than cell lines derived from early blastocysts [28]. However, the techniques used to determine the potency of the cell lines differed greatly among these studies. Species-specific differences may also explain these observed differences.

Previous bovine NT investigations using blastomeres as donor nuclei also showed a high incidence of pregnancy loss and placental abnormalities. The greatest number of established pregnancies were lost between Days 30 and 90 of gestation [29]. In addition, multiple generational cloning leads to a higher incidence of pregnancy losses ([30]; K. Bondioli, personal communications). In fact, all pregnancies produced from greater than three generations of recloning have aborted prior to 60 days of gestation (S.L. Stice, unpublished results). A higher incidence of hydrops or hydrallantois, an abnormal accumulation of fluid in the allantoic cavity, has been observed with blastomere NT pregnancies [29]. Therefore, blastomere NT embryos also appear to have placental development deficiencies, albeit not to the extent observed with embryonic cell line NT embryos.

In summary, bovine embryonic cell lines derived from either morula- or blastocyst-stage embryos exhibit in vivo pluripotential properties. Pluripotency was demonstrated through NT procedures resulting in NT embryos that developed through early organogenesis. Developmental capacity of NT embryos could be extended out to 85 days when they were aggregated with cleavage-stage in vitro-derived embryos. Pregnancies should be extended even further when placental deficiencies observed in both the NT and chimera are reduced or eliminated.

## ACKNOWLEDGMENTS

The authors wish to thank Mr. Jeff Betthauser, Mr. Paul Golueke, Ms. Gail Jurgella, Ms. Ann Marie Paprocki, and Mr. Brett Scott for their technical assistance and Ms. Rita Wells for help in preparing this manuscript. In addition, we appreciate the technical assistance in DNA marker analysis from Mr. Victor David and Dr. Jim Jackson of W.R. Grace.

## REFERENCES

1. Saito S, Strelchenko N, Niemann H. Bovine embryonic stem cell-like cell lines cultured over several passages. Roux's Arch Dev Biol 1992; 201:134–141.
2. Notarianni E, Laurie S, Moor RM, Evans MJ. Maintenance and differentiation in culture of pluripotential embryonic cell lines from pig blastocysts. J Reprod Fertil Suppl 1990; 41:51–56.
3. Piedrahita JA, Anderson GB, BonDurant RH. On the isolation of embryonic stem cells: comparative behavior of murine, porcine and ovine embryos. Theriogenology 1990; 34:879–901.
4. Strojek RM, Reed MA, Hoover JL, Wagner TE. A method for cultivating morphologically undifferentiated embryonic stem cells from porcine blastocysts. Theriogenology 1990; 33:901–913.
5. Wheeler MB. Development and validation of swine embryonic stem cells: a review. Reprod Fertil Dev 1994 6:563–568.
6. Iannaccone PM, Taborn GU, Garton RL, Caplice MD, Brenin DR. Pluripotent embryonic stem cells from the rat are capable of producing chimeras. Dev Biol 1994; 163:288–292.
7. Keefer CL, Stice SL, Matthews DL. Bovine inner cell mass cells as donor nuclei in the production of nuclear transfer embryos and calves. Biol Reprod 1994; 50:935–939.
8. Collas P, Barnes FL. Nuclear transplantation by microinjection of inner cell mass and granulosa cell nuclei. Mol Reprod Dev 1994; 38:264–267.
9. Sims M, First NL. Production of calves by nuclear transfer of nuclei from cultured inner cell mass cells. Proc Natl Acad Sci USA 1993; 91:6143–6147.
10. Tsunoda Y, Kato Y. Nuclear transplantation of embryonic stem cells in mice. J Reprod Fertil 1993; 98:537–540.
11. Nagy A, Rossant J, Nagy R, Abramow-Newerly W, Roder JC. Derivation of completely cell culture-derived mice from early-passage embryonic stem cells. Proc Natl Acad Sci USA 1993; 90:8424–8428.
12. Keefer CL, Stice, SL, Dobrinsky J. Effect of FSH and LH during bovine in vitro maturation on development following in vitro fertilization and nuclear transfer. Mol Reprod Dev 1993; 36:469–474.
13. Seshagiri PB, Bavister BD. Phosphate is required for inhibition by glucose of development of hamster 8-cell embryos in vitro. Biol Reprod 1989; 40:607–614.
14. Prather RS, Barnes FL, Sims MM, Robl JM, Eyestone W, First NL. Nuclear transfer in the bovine embryo: assessment of donor nuclei and recipient oocyte. Biol Reprod 1987; 37:859–866.
15. Stice SL, Keefer CL, Matthews L. Bovine nuclear transfer embryos: oocyte activation prior to blastomere fusion. Mol Reprod Dev 1994; 38:61–68.
16. Susko-Parrish JL, Leibfried-Rutledge ML, Northey DL, Shutzkus V, First NL. Inhibition of protein kinases after an induced calcium transient causes transition of bovine oocytes to embryonic cycles without meiotic completion. Dev Biol 1995; 729–739.
17. Rosenkrans CF, First NL. Culture of bovine zygotes to the blastocyst stage: effects of amino acids and vitamins. Theriogenology 1991; 35:Abstract 266.
18. Barnes FL, Collas P, Powell R, King WA, Westhusin M, Shepherd D. Influence of recipient oocyte cell cycle stage on DNA synthesis nuclear envelope breakdown, chromosome constitution, and development in nuclear transfer bovine embryos. Mol Reprod Dev 1993; 36:33–41.
19. Kono T, Sotomaru Y, Aono F, Takahasi T, Ogiwara I, Sekizawa F, Arai T, Nakahara T. Effect of ooplast activation on the development of oocytes following nucleus transfer in cattle. Theriogenology 1994; 41:1463–1471.
20. Brown DG, Willington I, Findley I, Muggleton-Harris AL. Criteria that optimize the potential of murine embryonic stem cells for in vitro and in vivo developmental studies. In Vitro Cell Dev Biol 1992; 28A:773–778.
21. Melton AA, Berry RO, Butler OD. The interval between the time of ovulation and attachment of the bovine embryo. J Anim Sci 1951; 10:993–1005.
22. King GJ, Atkinson BA, Robertson HA. Development of the placentome from days 20 to 29 of gestation. J Reprod Fertil 1980; 59:95–100.
23. Stice SL, Keefer CL, Maki-Laurila M, Matthews L. Donor blastomere cell cycle stage affects developmental competence of bovine nuclear transfer embryos. Theriogenology 1993; 39:Abstract 318.
24. Collas P, Balise JJ, Robl JM. Influence of cell cycle stage of donor nucleus on development of nuclear transplant rabbit embryos. Biol Reprod 1992; 46:492–500.
25. Strelchenko N, Miltipova M, Stice SL. Further characterization of bovine pluripotent stem cells. Theriogenology 1995; 43:Abstract 327.
26. Robertson EJ, Kaufman MH, Bradley A, Evans MJ. Isolation, properties and karyotype analysis of pluripotent (EK) cell lines from normal and parthenogenetic embryos. In: Silver LM, Martin GR, Strickland S (eds.), Teratocarcinoma Stem Cells. Cold Spring Harbor Conference on Cell Proliferation. New York: Cold Spring Harbor Laboratory; 1983: 10:647–663.
27. Eistetter HR. Pluripotent embryonal stem cells lines can be established from disaggregated mouse morulae. Dev Growth Differ 1989; 31:275–282.
28. Sukoyan MA, Vatolin SY, Golubitsa AN, Zehelezova AI, Semenova LA, Serov OL. Embryonic stem cells derived from morulae, inner cell mass, and blastocyst of mink: comparisons of their pluripotencies. Mol Reprod Dev 1993; 36:148–158.
29. Willadsen SM, Janzen RE, McAlister RJ, Shea BF, Hamilton G, McDermand D. The viability of late morulae and blastocysts produced by nuclear transplantation in cattle. Theriogenology 1991; 35:161–170.
30. Stice SL, Keefer CL. Multiple generational bovine embryo cloning. Biol Reprod 1993; 48:715–719.

*Proc. Natl. Acad. Sci. USA*
Vol. 92, pp. 7844–7848, August 1995
Developmental Biology

# Isolation of a primate embryonic stem cell line

JAMES A. THOMSON*†, JENNIFER KALISHMAN*, THADDEUS G. GOLOS*, MAUREEN DURNING*, CHARLES P. HARRIS‡, ROBERT A. BECKER*, AND JOHN P. HEARN*§

*The Wisconsin Regional Primate Research Center, §Department of Physiology, School of Medicine, and ‡Cytogenetics Laboratory, State Hygiene Laboratory, University of Wisconsin, 1223 Capitol Court, Madison, WI 53715-1299

*Communicated by Neal L. First, University of Wisconsin, Madison, WI, May 4, 1995 (received for review January 23, 1995)*

**ABSTRACT** **Embryonic stem cells have the ability to remain undifferentiated and proliferate indefinitely *in vitro* while maintaining the potential to differentiate into derivatives of all three embryonic germ layers. Here we report the derivation of a cloned cell line (R278.5) from a rhesus monkey blastocyst that remains undifferentiated in continuous passage for >1 year, maintains a normal XY karyotype, and expresses the cell surface markers (alkaline phosphatase, stage-specific embryonic antigen 3, stage-specific embryonic antigen 4, TRA-1-60, and TRA-1-81) that are characteristic of human embryonal carcinoma cells. R278.5 cells remain undifferentiated when grown on mouse embryonic fibroblast feeder layers but differentiate or die in the absence of fibroblasts, despite the presence of recombinant human leukemia inhibitory factor. R278.5 cells allowed to differentiate *in vitro* secrete bioactive chorionic gonadotropin into the medium, express chorionic gonadotropin α- and β-subunit mRNAs, and express α-fetoprotein mRNA, indicating trophoblast and endoderm differentiation. When injected into severe combined immunodeficient mice, R278.5 cells consistently differentiate into derivatives of all three embryonic germ layers. These results define R278.5 cells as an embryonic stem cell line, to our knowledge, the first to be derived from any primate species.**

Embryonic stem (ES) cells, derived from preimplantation embryos (1, 2), and embryonic germ (EG) cells, derived from fetal germ cells (3, 4), are undifferentiated, immortal cells capable of differentiating into derivatives of all three embryonic germ layers. Well-characterized ES and EG cells have been derived only from rodents (1, 2, 5, 6). Pluripotent cell lines have been derived from preimplantation embryos of several non-rodent species (7–10), but the developmental potentials of these cell lines remain poorly characterized. Mouse ES cells remain undifferentiated through serial passages when cultured in the presence of leukemia inhibitory factor (LIF) and differentiate in the absence of LIF (11). Mouse ES cells injected into syngeneic mice form teratocarcinomas that exhibit disorganized differentiation, with representatives of all three embryonic germ layers. Mouse ES cells combined with normal preimplantation embryos as chimeras and returned to the uterus participate in normal development (12). Because mouse ES cells can contribute to functional germ cells in chimeras, specific genetic changes can be introduced into the mouse germ line through the use of ES cell chimeras (13).

The mechanisms controlling differentiation of specific lineages can be studied with mouse ES cells grown *in vitro*; however, significant differences between early human and mouse development suggest that human development will be more accurately represented by primate ES cells. For example, human and mouse embryos differ in the timing of embryonic genome expression (14), in the structure and function of the fetal membranes and placenta (15), and in formation of an embryonic disc instead of an egg cylinder. Human embryonal carcinoma (EC) cells, which are pluripotent, immortal stem cells from teratocarcinomas, provide an important *in vitro* model for understanding human differentiation (16). Some EC cell lines can be induced to differentiate in culture (17), which results in the loss of specific cell surface markers [stage-specific embryonic antigen 3 (SSEA-3), SSEA-4, TRA-1-60, and TRA-1-81] and the appearance of new markers (16). When pluripotent human EC cells are injected into immunocompromised mice, they form teratocarcinomas, some with derivatives of all three embryonic germ layers. However, there are limitations to the use of human EC cells in the study of development. (*i*) The range of differentiation obtained from human EC cell lines is more limited than that obtained from mouse ES cells and varies widely between cell lines (18). (*ii*) All pluripotent human EC cell lines derived to date are aneuploid (19), suggesting EC cells may not provide a completely accurate representation of normal differentiation. (*iii*) Ethical considerations severely restrict the study of human embryos, often making it impossible to verify that *in vitro* results have significance in the intact embryo. None of these limitations would be present with nonhuman primate ES cell lines.

Here we report the isolation of an ES cell line (R278.5) from a rhesus monkey blastocyst. This cloned cell line remains undifferentiated and continues to proliferate for >1 year in culture, maintains a normal XY karyotype, and maintains the potential to differentiate into trophoblast and to derivatives of embryonic endoderm, mesoderm, and ectoderm. The morphology, cell surface markers, and growth factor requirements of these cells differ significantly from mouse ES cells but closely resemble human EC cells.

## MATERIALS AND METHODS

**Cell Line Isolation.** Six days after ovulation, an azonal blastocyst was recovered by a nonsurgical uterine flush technique from a 15-year-old rhesus monkey (20). The trophectoderm was removed by immunosurgery (21) using a rabbit anti-rhesus spleen cell antiserum followed by exposure to guinea pig complement. The intact inner cell mass (ICM) was separated from lysed trophectoderm cells and plated on mouse embryonic fibroblasts [previously exposed to 3000 rads (1 rad = 0.01 Gy) γ-radiation] in medium consisting of 80% Dulbecco's modified Eagle medium (4500 mg of glucose per liter, with L-glutamine, without sodium pyruvate; GIBCO) with 20% fetal bovine serum (HyClone), 0.1 mM 2-mercaptoethanol (Sigma), 1% nonessential amino acid stock (GIBCO) (22), and 1000 units of cloned human LIF per ml (GIBCO). After 16 days of culture, a central mass of cells was removed from

The publication costs of this article were defrayed in part by page charge payment. This article must therefore be hereby marked "*advertisement*" in accordance with 18 U.S.C. §1734 solely to indicate this fact.

Abbreviations: CG, chorionic gonadotropin; ES, embryonic stem; EC, embryonal carcinoma; G3PDH, glyceraldehyde-3-phosphate dehydrogenase; ICM, inner cell mass; LIF, leukemia inhibitory factor; RT-PCR, reverse transcription polymerase chain reaction; SCID, severe combined immunodeficiency; SSEA, stage-specific embryonic antigen.

†To whom reprint requests should be addressed.

epithelial outgrowths, exposed for 3 min to 0.05% trypsin-EDTA (GIBCO), gently dissociated by pipetting through a micropipette, and replated on mouse embryonic fibroblasts. After 3 weeks of growth, colonies with a morphology resembling human EC cells were selected and expanded. At five passages, individual cells were selected by micropipette and plated in individual wells of a 96-well plate (Falcon) with mouse embryonic fibroblast feeder layers. One clone with a normal karyotype (R278.5) was expanded for further analysis.

**Cell Surface Markers.** R278.5 cells grown on a layer of mouse embryonic fibroblasts were used to examine the expression of cell surface markers. Alkaline phosphatase was detected histochemically following fixation of cells with 100% ethanol using "Vector red" (Vector Laboratories) as a substrate, as described by the manufacturer. The SSEA-1, SSEA-3, SSEA-4, TRA-1-60, and TRA-1-81 antigens were detected by immunocytochemistry with specific primary monoclonal antibodies (gifts of Peter Andrews, University of Sheffield, U.K.) (16, 23–25) and localized with a biotinylated secondary antibody and then an avidin/biotinylated horseradish peroxidase complex (Vectastain ABC system, Vector Laboratories).

***In Vitro* Differentiation.** R278.5 cells were plated at low density (≈5000 cells/cm$^2$ of surface area) in the absence of fibroblasts on gelatin-treated four-well tissue culture plates (Nunc) in the same medium as that used for initial cell line isolation, but with 0–10$^4$ units of added human LIF per ml (GIBCO). The resulting differentiated cells were photographed 8 days after plating.

A mouse Leydig cell bioassay (26) was used to measure luteinizing hormone/chorionic gonadotropin (CG) activity in medium conditioned for 2 days either by undifferentiated R278.5 cells (at 80% confluence on fibroblast feeder layers) or by spontaneously differentiated R278.5 cells (cultured for 2 weeks after achieving confluence on fibroblast feeders). The relative levels of the mRNAs for α-fetoprotein and the α- and β-subunits of CG relative to glyceraldehyde-3-phosphate dehydrogenase (G3PDH) were determined by semi-quantitative reverse transcription polymerase chain reaction (RT-PCR) (27) using RNA from the same undifferentiated and differentiated cells. The PCR primers for human G3PDH (Clontech) do not amplify mouse G3PDH mRNA. Primers for human α-fetoprotein mRNA flank the seventh intron (5′ primer, 5′-GCTGGATTGTCTGCAGGATGGGGAA; 3′ primer, 5′-TCCCCTGAAGAAAATTGGTTAAAAT) and amplify a cDNA of 216 bp. Primers for the β-subunit of human CG flank the second intron (5′ primer, 5′-*ggatc*CACCGTCAACACCACCATCTGTGC; 3′ primer, 5′-*ggatc*CACAGGTCAAAGGGTGGTCCTTGGG) (nucleotides added to the CGβ sequence to facilitate subcloning are shown in italics) and amplify a cDNA of 262 bp. The primers for the CGα subunit were based on sequences of the first and fourth exon of the rhesus gene (28) (5′ primer, 5′-*gggaattc*GCAGTTACTGAGAACTCACAAG; 3′ primer, 5′-*gggaattc*GAAGCATGTCAAAGTGGTATGG) and amplify a cDNA of 556 bp. The identity of all cDNAs was verified by sequencing (not shown).

For RT-PCR, 1–5 μl of total R278.5 RNA was reverse transcribed, and 1–20 μl of reverse transcription reaction was subjected to the PCR in the presence of 2.5 μCi of deoxycytidine 5′-[α-$^{32}$P]triphosphate (1 Ci = 37 GBq; DuPont). The number of amplification rounds that produced linear increases in target cDNAs and the relation between input RNA and amount of PCR product were empirically determined. Following agarose gel electrophoresis, DNA bands of interest were cut out and radioactivity was determined by liquid scintillation spectroscopy. The ratio of cpm in a specific PCR product relative to cpm of G3PDH PCR product was used to estimate the relative levels of mRNAs among differentiated and undifferentiated cells.

**Tumor Formation in Severe Combined Immunodeficient (SCID) Mice.** In the passage immediately prior to SCID mouse injection (7 months after initial derivation of R278), karyotypes of R278.5 were confirmed as euploid. Approximately 5 × 10$^5$ R278.5 cells were injected either into the rear leg muscles (seven mice) or into the testis (two mice) of 8- to 12-week-old male SCID mice. The resulting tumors were fixed in 4% paraformaldehyde and examined histologically after paraffin embedding at 8–15 weeks of development.

## RESULTS

The morphology and cell surface markers of R278.5 cells (Fig. 1*A*) more closely resembled human EC cells than mouse ES cells. R278.5 cells had a high nucleus/cytoplasm ratio and prominent nucleoli, but rather than forming compact, piled-up colonies with indistinct cell borders similar to mouse ES cells, R278.5 cells formed flatter colonies with individual, distinct cells. R278.5 cells expressed alkaline phosphatase activity and the cell surface antigens SSEA-3, SSEA-4, TRA-1-60, and TRA-1-81 (Fig. 2), cell surface markers characteristic of human EC cell lines (16). Although cloned human LIF was present in the medium at cell line derivation and for initial passages, R278.5 cells grown on mouse embryonic fibroblasts without exogenous LIF remained undifferentiated and continued to proliferate. R278.5 cells plated on gelatin-treated tissue culture plates without fibroblasts differentiated to multiple cell types or failed to attach and died, regardless of the presence or absence of exogenously added human LIF (Fig. 1*B*).

The mRNA for α-fetoprotein, a marker for endoderm, increased substantially with *in vitro* differentiation (Fig. 3). α-Fetoprotein is expressed by extra-embryonic (yolk sac) and embryonic (fetal liver and intestines) endoderm. Epithelial cells resembling extraembryonic endoderm were present in cells differentiated *in vitro* from R278.5 cells (Fig. 1*B*).

Luteinizing hormone activity, an indication of CG secretion and trophoblast differentiation, was present in culture medium collected from differentiated cells [3.89 milli-international units (mIU)/ml] but not in medium collected from undiffer-

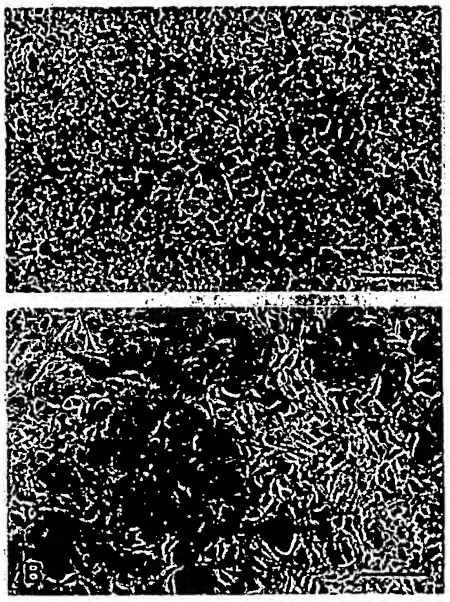

FIG. 1. Colony morphology and *in vitro* differentiation of cell line R278.5. (*A*) Undifferentiated R278.5 cells. Note the distinct cell borders, high nucleus to cytoplasm ratio, and prominent nucleoli. (Bar = 100 μm.) (*B*) Differentiated cells 8 days after plating R278.5 cells on gelatin-treated tissue culture plastic, with 10$^3$ units of added human LIF per ml. (Bar = 100 μm.)

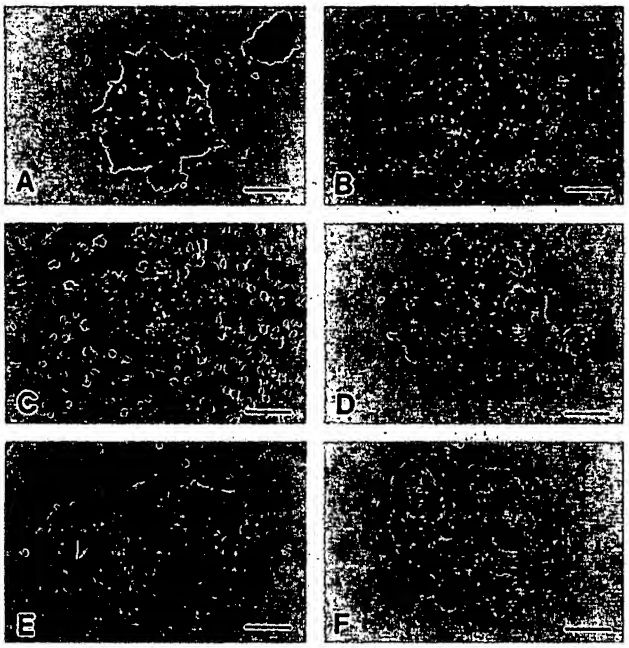


FIG. 2. Expression of cell surface markers by undifferentiated R278.5 cells. (*A*) Alkaline phosphatase. (*B*) SSEA-1. (*C*) SSEA-3. (*D*) SSEA-4. (*E*) TRA-1-60. (*F*) TRA-1-81. (Bars = 100 μm.) SSEA-3 staining of R278.5 cells was consistently weaker than the other positive antigens, and cell staining intensity varied within and between colonies.

entiated cells (<0.03 mIU/ml). The mRNAs for the CG subunits were readily detectable in the differentiated cells, although the relative level of the CGβ subunit mRNA was considerably lower than that for the CGα subunit (Fig. 4). The relative level of the CGα mRNA was quite low in undifferentiated cells, but the relative level was increased 23.9-fold after differentiation. The levels of the CGβ mRNA, on the other hand, increased only about 2-fold after differentiation for 2 weeks. Minor subpopulations of R278.5 cells differentiated even in the presence of fibroblasts, and the low level of α-fetoprotein, CGα, and CGβ mRNA present prior to the removal from fibroblasts could have been from these cells.

All SCID mice injected with R278.5 cells in either intramuscular or intratesticular sites formed tumors, and tumors in both sites demonstrated a similar range of differentiation. The

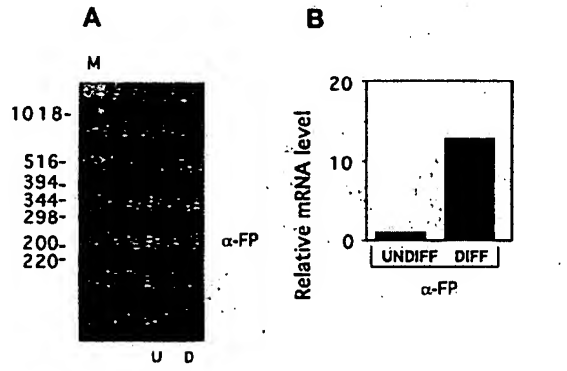


FIG. 3. Expression of α-fetoprotein mRNA. (*A*) PCR amplification of α-fetoprotein (αFP) cDNA from reverse-transcribed total RNA from undifferentiated (U) and differentiated (D) R278.5 cells. The DNA size markers (M) are indicated in bp. (*B*) The α-fetoprotein mRNA levels are expressed relative to the levels of the mRNA for G3PDH in each sample (not shown) as described in the text. Similar results were obtained in a second independent differentiation experiment.

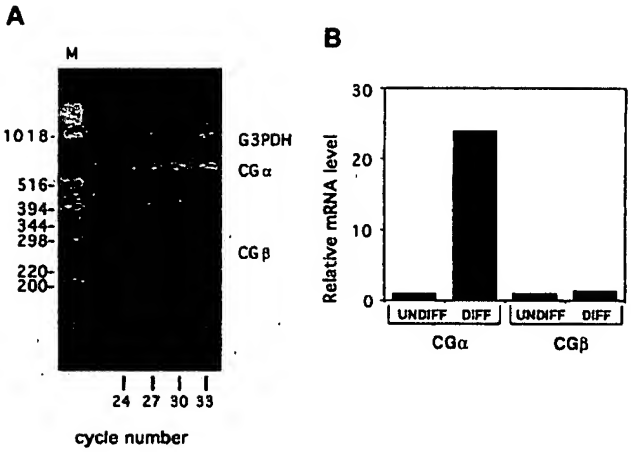


FIG. 4. Expression of CG subunit mRNA. (*A*) PCR amplification of cDNAs for G3PDH, CGα, and CGβ subunits from reverse-transcribed total RNA from differentiated R278.5 cells. The DNA size markers (M) are indicated in bp. (*B*) Relative levels of CGα and CGβ mRNAs in undifferentiated and differentiated R278.5 cells. Total RNA from cultured cells was analyzed for CG mRNA levels by RT-PCR and expressed relative to the levels of G3PDH mRNA. Similar results were obtained in a second independent differentiation experiment.

oldest tumors examined (15 weeks) had the most advanced differentiation, and all had abundant, unambiguous derivatives of all three embryonic germ layers, including ciliated columnar epithelium and nonciliated columnar epithelium (probable respiratory and gut epithelium; endoderm); bone, cartilage, smooth muscle, striated muscle (mesoderm); ganglia, other neural tissue, and stratified squamous epithelium (ectoderm), and other unidentified cell types (Fig. 5). Neural tissue included stratified cellular structures with remarkable resemblance to developing neural tube (Fig. 5*D*). Gut-like structures were often encircled by multiple layers of smooth muscle and were sometimes lined by villi with columnar epithelium interspersed with scattered mucus-secreting goblet cells (Fig. 5 *A* and *F*). Stratified squamous epithelium often contained well-differentiated hair follicles with hair shafts (Fig. 5*C*).

## DISCUSSION

To our knowledge, there have been no previous reports of the isolation of a primate ES cell line. The characteristics that define R278.5 cells as ES cells include indefinite (>1 year) undifferentiated proliferation *in vitro*, maintenance of a normal karyotype, and potential to differentiate to derivatives of trophectoderm and all three embryonic germ layers. The development of complex structures in tumors in SCID mice with remarkable resemblance to normal hair follicles, neural tube, and gut demonstrates the ability of R278.5 cells to participate in complex developmental processes requiring coordinated interactions between multiple cell types. In the mouse embryo, the last cells capable of contributing to derivatives of trophectoderm and ICM are early ICM cells of the expanding blastocyst (29). The timing of commitment to ICM or trophectoderm has not been established for any primate species, but the potential of R278.5 cells to contribute to derivatives of both suggests that they most closely resemble early totipotent embryonic cells. The very limited ability of mouse ES cells to contribute to trophoblast in chimeras (30) suggests that the R278.5 cells represent an earlier developmental stage than mouse ES cells or that the ability of ICM cells to form trophectoderm persists longer in primates. Human EC cells share the ability of R278.5 cells to differentiate to trophoblast *in vitro* (16) and this potential may be a general distinguishing property of primate ES cell lines.

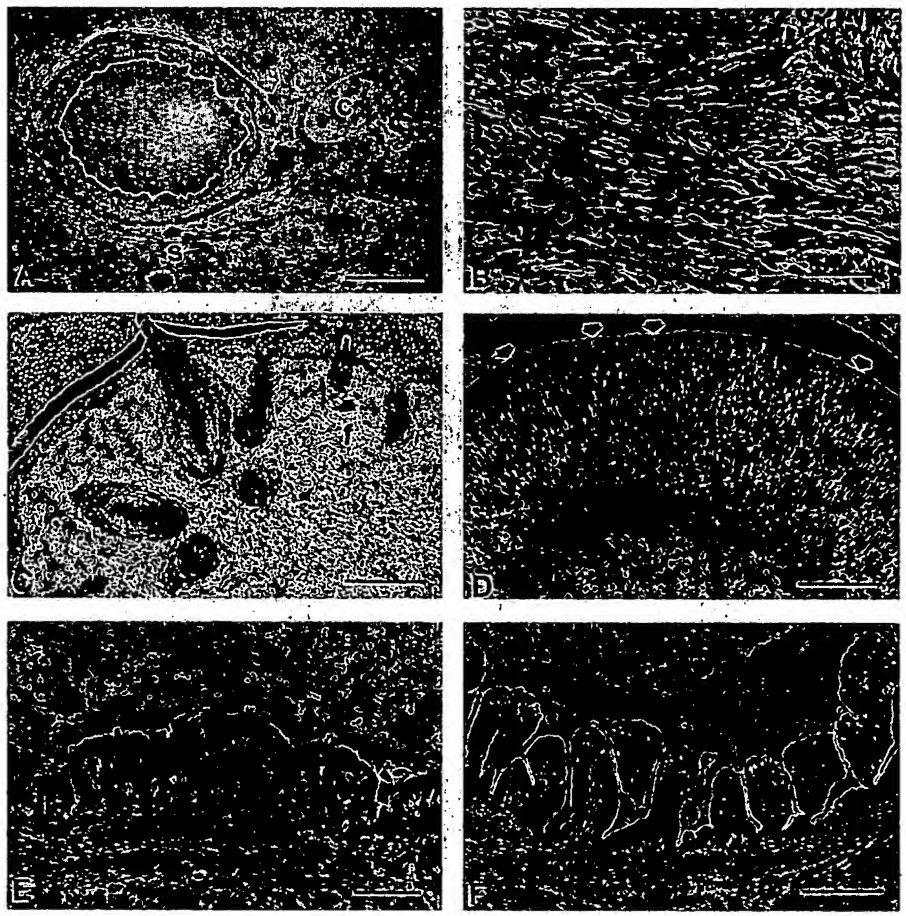


FIG. 5. Tumors formed by R278.5 cells injected into SCID mice and examined at 15 weeks. (*A*) Low-power field demonstrating disorganized differentiation of multiple cell types. A gut-like structure is encircled by smooth muscle (s), and elsewhere foci of cartilage (c) are present. (Bar = 400 μm.) (*B*) Striated muscle. (Bar = 40 μm.). (*C*) Stratified squamous epithelium with several hair follicles. The labeled hair follicle (f) has a visible hair shaft. (Bar = 200 μm.). (*D*) Stratified layers of neural cells in the pattern of a developing neural tube. An upper "ventricular" layer, containing numerous mitotic figures (arrows), overlies a lower "mantle" layer. (Bar = 100 μm.) (*E*) Ciliated columnar epithelium. (Bar = 40 μm.) (*F*) Villi covered with columnar epithelium with interspersed mucus-secreting goblet cells. (Bar = 200 μm.)

The only cells known to express the combination of markers alkaline phosphatase, SSEA-3, SSEA-4, TRA-1-60, and TRA-1-81 other than R278.5 cells are human EC cells (16, 25, 31). This expression pattern contrasts with undifferentiated mouse ES and EC cells, which instead express SSEA-1 and do not express SSEA-3, SSEA-4, TRA-1-60, or TRA-1-81 (23, 24). Differentiation of human EC cells such as NTERA2 cl.D1 (17) results in the loss of SSEA-3, SSEA-4, TRA-1-60, and TRA-1-81 expression and an increased SSEA-1 expression (16). These antigens have yet to be studied in early human or nonhuman primate embryos, and their functions are unknown, but their shared expression by R278.5 cells and human EC cells suggests a close embryological similarity.

In the absence of fibroblast feeder layers, soluble LIF fails to prevent the differentiation of R278.5 cells or of feeder-dependent human EC cells (19). The factors that fibroblasts produce that prevent the differentiation of R278.5 cells or feeder-dependent human EC cells are unknown. Other factors that fail to support the growth of feeder-dependent human EC cells in the absence of feeder layers include oncostatin M and ciliary neurotrophic factor (19), both of which can substitute for LIF in preventing the differentiation of mouse ES cells (32, 33). A trypsin-sensitive factor from a human yolk sac carcinoma cell line (GCT 44) supports the growth of feeder-dependent human EC cells in the absence of fibroblasts, but the factor has not yet been purified (19).

Although exogenous LIF was added during the initial derivation of R278.5 cells, the cell line is now routinely passaged without added LIF. We have also recently derived two additional cell lines (R366 and R367) from four additional rhesus blastocysts, using the same techniques as described for R278.5 cells, but without added LIF (data not shown). R366 and R367 cells have normal karyotypes and continue to proliferate *in vitro* for at least 3 months. R366 and R367 cell lines have not yet been tested for tumor formation in SCID mice, but they are indistinguishable from R278.5 cells in undifferentiated morphology, growth characteristics, and *in vitro* differentiation in the absence of feeder layers.

The differentiation of R278.5 cells to trophoblast was demonstrated by the expression of CGα and CGβ subunit mRNAs and the secretion of bioactive CG into the culture medium by differentiated ES cells. We were surprised to note that while the relative levels of the CGα subunit were increased >20 times in differentiated cells, the relative levels of the CGβ subunit only changed about 2-fold. The fact that CG secretion increased substantially with differentiation may mean that under our *in vitro* culture conditions, expression of the CGα subunit is limiting for CG secretion. CGβ subunit mRNA is detectable in human preimplantation embryos as early as the eight-cell stage, which is before trophectoderm differentiation (34), consistent with a low level of CGβ mRNA expression in undifferentiated R278.5 cells. Although there may be some coordinate mechanisms regulating CGα and CGβ gene transcription in the placenta (35), it is clear that there is differential regulation of these genes *in vitro* and *in vivo* (36). Since the expression of the CGβ subunit is also divergent among villous

and extravillous trophoblasts (37), further studies are needed to determine the phenotype of the trophoblasts derived from R278.5 cells.

Primate ES cells will be particularly useful for *in vitro* developmental studies of lineages that differ substantially between humans and mice. However, the most accurate *in vitro* model of the differentiation of human tissues would be provided by human ES cells. In one published report, ICM-derived cells from spare *in vitro* fertilized human embryos were cultured with LIF in the absence of feeder layers, and, although alkaline phosphatase positive cells proliferated, they failed to survive beyond two passages (38). These results suggest that soluble LIF alone will not prevent the differentiation of human ES cells, just as it fails to prevent the differentiation of rhesus ES cells. The growth of rhesus monkey ES cells in culture conditions that support feeder-dependent human EC cells suggests that similar conditions may support human ES cells.

Human ES cells would offer exciting new possibilities for transplantation medicine. Because ES cells have the developmental potential to give rise to all adult cell types, any disease resulting from the failure of specific cell types would be potentially treatable through the transplantation of differentiated cells derived from ES cells. Because ES cells are immortal cell lines, they could be genetically manipulated prior to differentiation either to reduce immunogenicity or to give them new properties to combat specific diseases. Rhesus monkey ES cells and rhesus monkeys will be invaluable for testing the safety and efficacy of the transplantation of specific cell types for the treatment of specific diseases. Because of the range of diseases potentially treatable by this approach, elucidating the basic mechanisms controlling the differentiation of primate ES cells has dramatic clinical significance.

We thank Steve Eisele and Scott Kudia for performing the embryo recovery, Fritz Wegner and Dan Wittwer for performing the luteinizing hormone assays, and the animal care staff at the Wisconsin Regional Primate Research Center. We thank Dr. Peter Andrews for helpful comments on the manuscript and for providing us with monoclonal antibodies to SSEA-1, -3, and -4, TRA-1-60, and TRA-1-81, and the cell line NTERA2 cl.D1. This work was supported by U.S. Public Health Service, National Institutes of Health Grant RR-00167, with a supplement (to J.P.H.) from the National Institutes of Health Women's Health Initiative, and by National Institutes of Health Grant HD26458 to T.G.G. This is Wisconsin Regional Primate Research Center publication no. 34-032.

1. Martin, G. (1981) *Proc. Natl. Acad. Sci. USA* **78**, 7634–7638.
2. Evans, M. & Kaufman, M. (1981) *Nature (London)* **292**, 154–156.
3. Matsui, Y., Zsebo, K. & Hogan, B. L. M. (1992) *Cell* **70**, 841–847.
4. Resnick, J. L., Bixler, L. S., Cheng, L. & Donovan, P. J. (1992) *Nature (London)* **359**, 550–551.
5. Doetschman, T., Williams, P. & Maeda, N. (1988) *Dev. Biol.* **127**, 224–227.
6. Iannaccone, P. M., Taborn, G. U., Garton, R. L., Caplice, M. D. & Brenin, D. R. (1994) *Dev. Biol.* **163**, 288–292.
7. Evans, M., Notaranni, E., Laurie, S. & Moor, R. (1990) *Theriogenology* **33**, 125–128.
8. Graves, K. H. & Moreadith, R. W. (1993) *Mol. Reprod. Dev.* **36**, 424–433.
9. Notarianni, E., Galli, C., Laurie, S., Moore, R. M. & Evans, M. J. (1991) *J. Reprod. Fertil. Suppl.* **43**, 255–260.
10. Sukoyan, M. A., Golubitsa, A. N., Zhelezova, A. I., Shilov, A. G., Vatolin, S. Y., Maximovsky, L. P., Andreeva, L. E., McWhir, J., Pack, S. D., Bayborodin, S. I., Kerkis, A. Y., Kizilova, H. I. & Serov, O. L. (1992) *Mol. Reprod. Dev.* **33**, 418–431.
11. Williams, R., Hilton, D., Pease, S., Wilson, T., Stewart, C., Gearing, D., Wagner, E., Metcalf, D., Nicola, N. & Gough, N. (1988) *Nature (London)* **336**, 684–687.
12. Bradley, A., Evans, M., Kaufman, M. & Robertson, E. (1984) *Nature (London)* **309**, 255–256.
13. Ramirez Solis, R., Davis, A. C. & Bradley, A. (1993) *Methods Enzymol.* **225**, 855–878.
14. Braude, P., Bolton, V. & Moore, S. (1988) *Nature (London)* **332**, 459–461.
15. Benirschke, K. & Kaufmann, P. (1990) *Pathology of the Human Placenta* (Springer, New York).
16. Andrews, P., Oosterhuis, J. & Damjanov, I. (1987) in *Teratocarcinomas and Embryonic Stem Cells: A Practical Approach*, ed. Robertson, E. (IRL, Oxford), pp. 207–246.
17. Andrews, P., Damjanov, I., Simon, D., Banting, G., Carlin, C., Dracopoli, N. & Fogh, J. (1984) *Lab. Invest.* **50**, 147–162.
18. Pera, M. F., Blasco Lafita, M. J. & Mills, J. (1987) *Int. J. Cancer* **40**, 334–343.
19. Roach, S., Cooper, S., Bennett, W. & Pera, M. F. (1993) *Eur. Urol.* **23**, 82–88.
20. Seshagiri, P. B., Bridson, W. E., Dierschke, D. J., Eisele, S. G. & Hearn, J. P. (1993) *Am. J. Primatol.* **29**, 81–91.
21. Solter, D. & Knowles, B. (1975) *Proc. Natl. Acad. Sci. USA* **72**, 5099–5102.
22. Robertson, E. J. (1987) in *Teratocarcinomas and Embryonic Stem Cells: A Practical Approach*. ed. Robertson, E. J. (IRL, Oxford), pp. 71–112.
23. Solter, D. & Knowles, B. B. (1978) *Proc. Natl. Acad. Sci. USA* **75**, 5565–5569.
24. Kannagi, R., Cochran, N. A., Ishigami, F., Hakomori, S., Andrews, P. W., Knowles, B. B. & Solter, D. (1983) *EMBO J.* **2**, 2355–2361.
25. Andrews, P. W., Banting, G., Damjanov, I., Arnaud, D. & Avner, P. (1984) *Hybridoma* **3**, 347–361.
26. Terasawa, E., Bridson, W. E., Nass, T. E., Noonan, J. J. & Dierschke, D. J. (1984) *Endocrinology* **115**, 2233–2240.
27. Golos, T. G., Durning, M., Fisher, J. M. & Fowler, P. D. (1993) *Endocrinology* **133**, 1744–1752.
28. Golos, T. G., Durning, M. & Fisher, J. M. (1991) *DNA Cell Biol.* **10**, 367–379.
29. Winkel, G. K. & Pedersen, R. A. (1988) *Dev. Biol.* **127**, 143–156.
30. Beddington, R. S. P. & Robertson, E. J. (1989) *Development (Cambridge, U.K.)* **105**, 733–737.
31. Wenk, J., Andrews, P. W., Casper, J., Hata, J., Pera, M. F., von Keitz, A., Damjanov, I. & Fenderson, B. A. (1994) *Int. J. Cancer* **58**, 108–115.
32. Wolf, E., Kramer, R., Polejaeva, I., Thoenen, H. & Brem, G. (1994) *Transgenic Res.* **3**, 152–158.
33. Rose, T. M., Wieford, D. M., Gunderson, N. L. & Bruce, A. G. (1994) *Cytokine* **6**, 48–54.
34. Bonduelle, M. L., Dodd, R., Liebaers, I., Van Steirteghem, A., Williamson, R. & Akhurst, R. (1988) *Hum. Reprod.* **3**, 909–914.
35. Steger, D. J., Buscher, M., Hecht, J. H. & Mellon, P. L. (1993) *Mol. Endocrinol.* **7**, 1579–1588.
36. Jameson, J. L. & Hollenberg, A. N. (1993) *Endocr. Rev.* **14**, 203–221.
37. Babury, R. A. & Moscovic, E. A. (1993) *Histol. Histopathol.* **8**, 323–328.
38. Bongso, A., Fong, C. Y., Ng, S. C. & Ratnam, S. (1994) *Hum. Reprod.* **9**, 2110–2117.

BIOLOGY OF REPRODUCTION 55, 254–259 (1996)

# Pluripotent Cell Lines Derived from Common Marmoset (*Callithrix jacchus*) Blastocysts[1]

James A. Thomson,[2,3] Jennifer Kalishman,[3] Thaddeus G. Golos,[3,4] Maureen Durning,[3] Charles P. Harris,[6] and John P. Hearn[3,5]

*The Wisconsin Regional Primate Research Center,[3] Departments of Obstetrics and Gynecology[4] and Physiology,[5] School of Medicine, and Cytogenetics Laboratory,[6] State Hygiene Laboratory, University of Wisconsin, Madison, Wisconsin 53715–1299*

## ABSTRACT

**We report the derivation of eight pluripotent cell lines from common marmoset (*Callithrix jacchus*) blastocysts. These cell lines are positive for a series of markers (alkaline phosphatase, SSEA-3, SSEA-4, TRA-1–60, and TRA-1–81) that characterize undifferentiated human embryonal carcinoma cells and rhesus embryonic stem cells. All eight cell lines had a modal chromosome number of 46; seven cell lines were XX and one was XY. Two cell lines (Cj11 and Cj62) were cultured continuously for over a year and remained undifferentiated and euploid. In the absence of fibroblast feeder layers, these cell lines differentiated to multiple cell types, even in the presence of leukemia inhibiting factor. Differentiated cells secreted bioactive CG into the culture medium and expressed α-CG, β-CG, and α -fetoprotein mRNA, indicating trophoblast and endoderm differentiation. Bioactive CG secretion in differentiating cells was increased substantially in the presence of GnRH agonist D-Trp⁶-Pro⁹-NHEt. When grown at high densities, these cells formed embryoid bodies with a close resemblance to early postimplantation embryos, including the formation of a yolk sac, amnion, and an embryonic disc with an early primitive streak. These results make these pluripotent cells strong candidates for marmoset embryonic stem cells.**

## INTRODUCTION

Embryonic stem (ES) cells are pluripotent cell lines capable of contributing to derivatives of all three embryonic germ layers even after prolonged culture [1–3]. Mouse ES cells in chimeras sometimes contribute to germ cells, thus providing a vehicle for introducing genetic changes into the germ line [4]. Because homologous recombination allows the alteration of specific loci of the genome, mouse ES cells allow the production of very specific models of human genetic diseases [5]. However, because of the differences between human and mouse development, anatomy, and physiology, transgenic mice can provide only a limited understanding of some human diseases. In addition, the testing of new therapies in transgenic mice is limited by mouse size, life span, and physiology. Transgenic primate models would increase our understanding of the pathogenesis of specific diseases and allow the testing of new therapies. In transgenic primates, therapeutic efficacy for treating degenerative neural diseases, such as Alzheimer's disease, could be assessed not only by morphological and biochemical changes in the brain, but by changes in complex behaviors.

We have recently reported the isolation of ES cells from the rhesus monkey that are immortal, have a stable normal karyotype, and have the potential to differentiate to derivatives of trophectoderm and all three embryonic germ layers [6]. Rhesus monkey ES cells provide a powerful new in vitro model for understanding the differentiation of human tissues, but the reproductive biology of rhesus monkeys makes testing the ability of these cells to contribute to the germ line in chimeras impractical. The rhesus monkey, which is an Old World primate species, has single young, reaches sexual maturity at 4–5 yr, and has an ovarian cycle that cannot be routinely synchronized. The common marmoset, a New World primate species, has more favorable reproductive characteristics for experimental primate embryology, including the natural birth of twins or triplets, an early age at sexual maturity (about 18 mo), and an ovarian cycle that can be synchronized with prostaglandins, thus allowing efficient embryo collection and transfer [7–9].

Here we report the derivation of eight pluripotent cell lines from common marmoset blastocysts that closely resemble rhesus ES cells and human embryonal carcinoma (EC) cells in morphology, growth characteristics, cell surface markers, and in vitro differentiation. Because of the reproductive characteristics of the common marmoset, it will be possible to define the developmental potential of these pluripotent cell lines in chimeras with normal embryos in vivo, initiating exciting advances in experimental primate embryology.

## MATERIALS AND METHODS

### *Embryo Recovery and Cell Line Isolation*

For embryo donors, female marmosets greater than 2 yr of age and demonstrating regular ovarian cycles were maintained in groups with a fertile male and up to five progeny. Ovarian cycles were controlled by i.m. injection of 0.75 μg of the prostaglandin $F_{2\alpha}$ analog cloprostenol (Estrumate; Mobay Corp., Shawnee, KS) during the middle to late luteal phase [7]. Blood samples (0.2 ml) were collected in heparinized syringes on Day 0 (immediately before cloprostenol injection), and on Days 3, 7, 9, 11, and 13. Plasma progesterone concentrations were determined by ELISA [10]. The day of ovulation was taken as the day preceding a plasma progesterone concentration of 10 ng/ml or more [8]. Eight days after ovulation, marmosets were lightly anesthetized by the i.m. injection of alphaxalone and alphadolone (Saffan; Glaxovet, Ltd., Uxbridge, UK), and blastocysts were recovered by a nonsurgical uterine flush procedure [9].

Blastocysts were incubated in 0.5% pronase-Dulbecco's

Accepted March 22, 1996.
Received December 28, 1995.
[1]This work was supported by USPHS, NIH grant RR00167, with a supplement (to J.P.H.) from the NIH Women's Health Initiative, and by NIH grant HD26458 to T.G.G. This is Wisconsin Regional Primate Research Center publication no. 36–005.
[2]Correspondence: James Thomson, The Wisconsin Regional Primate Research Center, University of Wisconsin, 1223 Capitol Court, Madison, WI 53715–1299. FAX: (608) 263–3524.

Modified Eagle Medium (DMEM) while observed under a binocular microscope. Immediately after zona pellucida dissolution, the blastocysts were washed through two changes of DMEM. To remove the trophectoderm by immunosurgery [11], the blastocysts were exposed to a 1:50 dilution of rabbit anti-marmoset spleen cell antiserum in DMEM for 30 min, washed three times in DMEM, and then incubated in a 1:10 dilution of guinea pig complement (Gibco Labs., Grand Island, NY) for 30 min. After two further washes in DMEM, lysed trophectoderm cells were removed from the intact inner cell mass (ICM) by gentle pipetting, and the ICM was plated on inactivated (3500 rads gamma irradiation) mouse embryonic fibroblasts. Unless otherwise noted, culture medium consisted of 80% Dulbecco's Modified Eagle's Medium (DMEM; no pyruvate, high-glucose formulation, Gibco BRL), with 20% fetal bovine serum (Hyclone Labs., Logan, UT), 0.1 mM β-mercaptoethanol (Sigma Chemical Company, St. Louis, MO), and 1% nonessential amino acid stock (Gibco BRL) [12]. After 7–10 days, ICM-derived masses were removed from endoderm outgrowths, exposed to 0.05% Trypsin-EDTA (Gibco BRL) for 3–5 min, and gently dissociated by gentle pipetting through a micropipette. Dissociated cells were replated on embryonic feeder layers in fresh medium and observed for colony formation. Colonies composed of closely packed cells with high nuclear/cytoplasmic ratios were individually selected, split again, and cultured in the same DMEM-supplemented medium. Early passage cells were frozen and stored in liquid nitrogen [12]. Cell lines were karyotyped with a standard G-banding technique and compared to published karyotypes for the common marmoset [13].

### *Cell Surface Markers*

Cell lines Cj11 and Cj62 cultured on a layer of mouse embryonic fibroblasts were used to examine the expression of cell surface markers. Alkaline phosphatase was detected histochemically after fixation of cells with 100% ethanol, with "Vector Blue" (Vector Labs., Burlingame, CA) used as a substrate, as described by the manufacturer. The SSEA-1, SSEA-3, SSEA-4, TRA-1–60, and TRA-1–81 antigens were detected by immunocytochemistry with specific primary monoclonal antibodies (gifts of Peter Andrews, University of Sheffield, Sheffield, UK) and were localized with a biotinylated secondary antibody and then an avidin/biotinylated horseradish peroxidase complex (Vectastain ABC system, Vector Labs.) [14–16]. NTERA2 cl.D1, a pluripotent human EC cell line (gift of Peter Andrews, University of Sheffield), was used as a negative control for SSEA-1, and as a positive control for SSEA-3, SSEA-4, TRA-1–60, and TRA-1–81 [17, 18]. Mouse ES cells (ES-jt3) were used as a positive control for SSEA-1, and as a negative control for SSEA-3, SSEA-4, TRA-1–60, and TRA-1–81.

### *Differentiation*

Embryo-derived marmoset cells were plated at low density in the absence of fibroblasts on gelatin-treated four-well tissue culture plates (Nunc, Roskilde, Denmark) in the same medium used for initial cell line isolation, but with either 0 or 1000 U/ml of added human leukemia inhibitory factor (LIF; Gibco). The resulting differentiated cells were photographed 8 days after plating.

RNA was prepared by guanidine isothiocyanate-phenol/chloroform extraction [19] from cultures of Cj11 and Cj62 cells grown on embryonic fibroblasts and allowed to differentiate spontaneously for 2 wk after achieving confluence. The mRNAs for α-fetoprotein (αFP), the α- and ß-subunits of CG (CGα and CGβ), and GnRH were detected by reverse transcriptase-polymerase chain reaction (RT-PCR). Primers for the αFP, CGα, and CGβ mRNAs were as previously reported [6]. Primers for GnRH were based on human sequences of the second and fourth exons (5′ primer = (5′) *ggg*tc*g*ac*TCCAGCCAGCACTGGTCCTATGG*; 3′ primer = (5′) *ggg*tc*g*ac*CTGCCCAGTTTCCTCTTCAATCAG*) and amplify a cDNA of 219 bp (lower-case italics indicate nucleotides added to facilitate subcloning) [20]. The identities of the αFP, CGα, CGβ, and GnRH cDNAs were verified by subcloning and sequencing (not shown). Homology of all marmoset cDNAs with the human sequences was > 90%.

To measure the response of CG secretion to a GnRH agonist, Cj62 cells were plated on two four-well plates (Nunc) and allowed to grow to confluence. At confluence, the medium of one plate was supplemented with the GnRH agonist D-Trp$^6$-Pro$^9$-NHEt [21] at 0.30 nM; a second control plate was left unsupplemented. Medium was changed every other day for 2 wk, and fresh agonist was prepared from frozen 100-strength stocks at each medium change. Medium from each individual well was assayed for LH/CG activity by a mouse Leydig cell bioassay [22].

For embryoid body formation, Cj62 cells were grown beyond confluence on fibroblast feeder layers and allowed to spontaneously differentiate for 4 wk. One embryoid body was sectioned at 1 μm, rinsed twice with 0.1 M cacodylate buffer, pH 7.0, fixed with Karnovsky's fixative, post-fixed with osmium, and embedded in epoxy. One-micrometer sections were stained with toluidine blue dye and examined under a light microscope; selected ultrathin sections were stained with lead citrate and uranyl acetate, and examined on a Phillips 410 transmission electron microscope.

## RESULTS

Eight pluripotent cell lines were derived from marmoset blastocysts, two of which, Cj11 and Cj62, were cultured continuously for over 12 mo; the others were frozen at 3–8 mo of culture for later analysis. These cells had a high nucleus:cytoplasm ratio, prominent nucleoli, and a compact colony morphology (Fig. 1A) similar to, but distinguishable from, that of human EC cells. Cj11 and Cj62 cells expressed a series of cell surface markers (alkaline phosphatase, SSEA-3, SSEA-4, TRA-1–60, and TRA-1–81) that characterize undifferentiated human EC cells and rhesus ES cells (Fig. 2) [6, 16, 18, 23]. Immunostaining for SSEA-3 and TRA-1–81 was weaker than that for SSEA-4 and TRA-1–60, and the intensity varied both between and within colonies. Each of the marmoset cell lines had a modal chromosome number of 46; seven were XX and one was XY (Table 1).

When each of the eight pluripotent marmoset lines was

TABLE 1. Karyotypes of pluripotent marmoset cell lines.

| Cell line | Chromosome number | Sex |
|---|---|---|
| Cj11.2 | 46* | XX |
| Cj25.1 | 46* | XX |
| Cj28 | 46 | XY |
| Cj33 | 46* | XX |
| Cj35 | 46* | XX |
| Cj36 | 46* | XX |
| Cj39 | 46 | XX |
| Cj62 | 46* | XX |

* Some rare cells with abnormal karyotypes were observed, including fused chromosomes, marker chromosomes, and extra chromosomes.

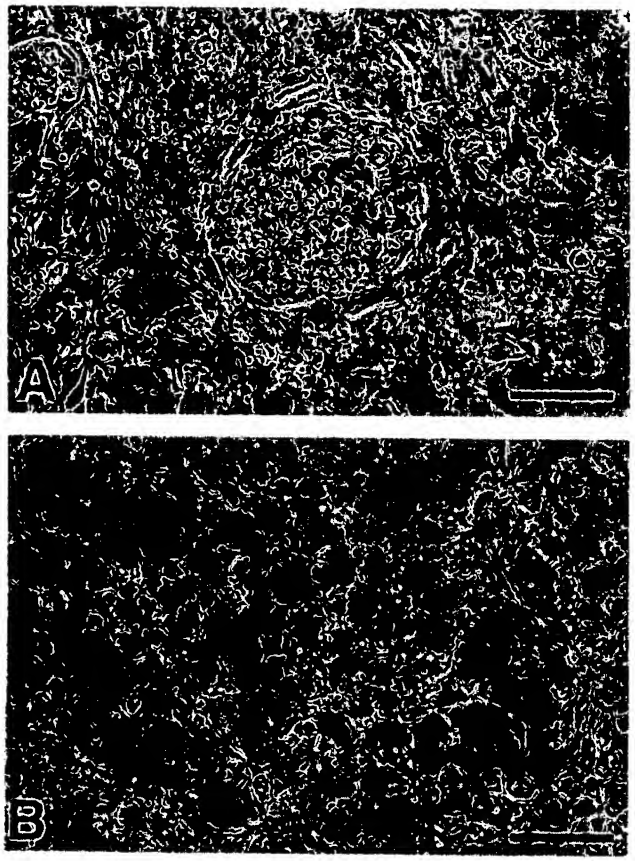


FIG. 1. Colony morphology and in vitro differentiation of cell line Cj62. A) Undifferentiated Cj62 cells on a background of embryonic fibroblasts. Note the distinct colony border, high nucleus:cytoplasm ratio, and prominent nucleoli (bar = 100 μM). B) Differentiated cells 8 days after Cj62 cells were plated on gelatin-treated tissue culture plastic, with $10^3$ U/ml added human LIF (bar = 100 μM).

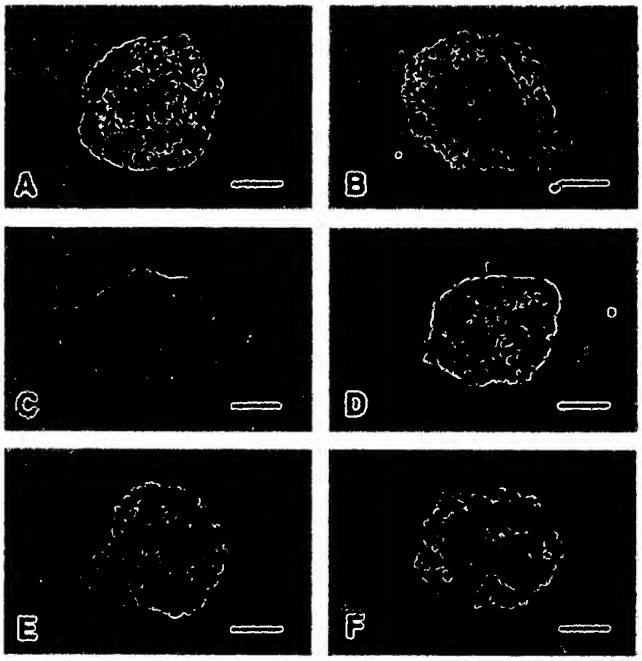


FIG. 2. Expression of cell surface markers by undifferentiated Cj62 cells (bar = 100 μM). A) Alkaline phosphatase (Vector Blue substrate). Because no counterstain was used, the fibroblast feeder layer is not visible. B) SSEA-1. C) SSEA-3. D) SSEA-4. E) TRA-1-60. F) TRA-1-81. For panels B-F, detection was with horseradish peroxidase/diaminobenzadine, and positive cells are brown. Counterstaining was with hematoxylin. Although consistently positive, SSEA-3 and TRA-1-81 staining of Cj62 cells was weaker than SSEA-4 and TRA-1-61 staining, and cell-staining intensity varied within and between colonies.

removed from fibroblast feeders, they differentiated into cells of several distinct morphologies, even in the presence of human LIF (Fig. 1B). The cells also differentiated when allowed to grow beyond confluence on fibroblast feeder layers. Among the differentiated cells derived from Cj11 and Cj62, trophectoderm was indicated by the expression of the CGα and CGβ mRNAs detected by RT-PCR (Fig. 3), and by the secretion of bioactive CG into the culture medium (Fig. 4). Differentiated cells also expressed mRNA for GnRH (Fig. 3), and the secretion of bioactive CG increased substantially when differentiating cells were exposed to GnRH agonist (Fig. 4). Endoderm differentiation (probable extra-embryonic endoderm) was indicated by the presence of αFP mRNA, detected by RT-PCR (Fig. 3).

When each of the eight pluripotent marmoset cell lines was grown at high density, over a period of 1–2 wk epithelial cells differentiated and covered the culture dish; the remaining groups of undifferentiated cells contracted into compact balls and then formed embryoid bodies. Over 3–4 wk, some of the embryoid bodies formed a bilaterally symmetric pyriform embryonic disc, an amnion, a yolk sac, and a mesoblast outgrowth attaching the caudal pole of the amnion to the culture dish. Histological and ultrastructural examination of one of these embryoid bodies (formed from a cell line, Cj62, that had been passaged continuously for 6 mo) revealed a close resemblance to an early primitive

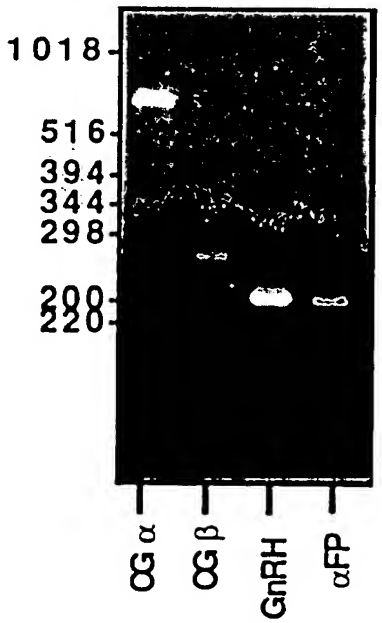


FIG. 3. RT-PCR amplification of mRNAs for CGα, CGβ, GnRH, and αFP from total RNA from pluripotent marmoset cells allowed to differentiate in vitro. Identities of all cDNAs were confirmed by subcloning and sequencing. Negative controls, which contained no template DNA, produced no bands (not shown).

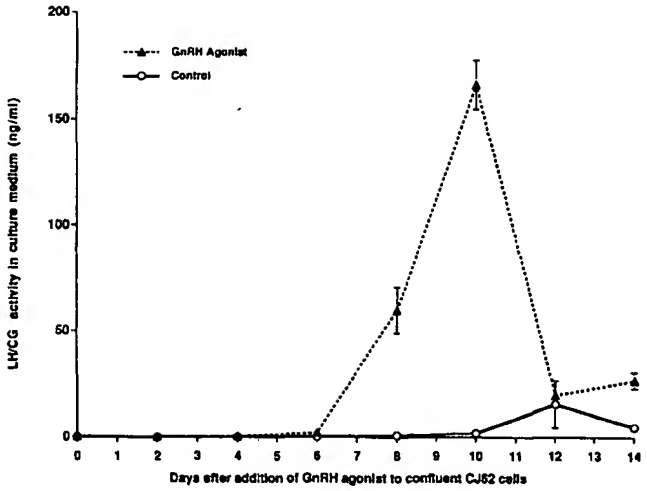


FIG. 4. GnRH agonist D-Trp$^6$-Pro$^9$-NHEt responsiveness of CG secretion in differentiating Cj62 cells. LH/CG bioactivity was measured by Leydig cell bioassay in culture medium conditioned by differentiating Cj62 cells. GnRH agonist was added to undifferentiated Cj62 cells at confluence (Day 0); medium was changed every 2 days and supplemented with fresh agonist. Bars represent SEM.

streak-stage embryo (Fig. 5). The embryonic disc was composed of a polarized, columnar epithelial epiblast (primitive ectoderm) layer separated from a hypoblast (primitive endoderm) layer. Electron microscopy of the epiblast revealed apical junctional complexes, apical microvilli, subapical intermediate filaments, and a basement membrane separating the epiblast from underlying endoderm—all features of the normal embryonic disc. In the caudal third of the embryonic disc, there was a midline groove, disruption of the basement membrane, and mixing of epiblast cells with underlying endoderm cells (early primitive streak; Fig. 5). An amnion was composed of an inner squamous (ectoderm) layer continuous with the epiblast, and an outer mesoderm layer.

## DISCUSSION

Our criteria for ES cells are as follows: derivation from the preimplantation embryo, immortality, a normal karyotype, and the maintained ability to differentiate to derivatives of all three embryonic germ layers. Contribution to the germ line in chimeras is also a property of some mouse ES cell lines, but originally the term was introduced to distinguish the origin of pluripotent mouse cell lines derived from preimplantation embryos (ES cells) from those derived from teratocarcinomas (EC cells) [3]. Although mouse ES and EC cells are very similar, ES cells generally have a greater developmental potential, a difference thought to be related to the selective pressures of the teratocarcinoma environment that are avoided by the in vitro derivation of ES cells [3].

Several characteristics of the pluripotent marmoset cell lines we have isolated make them strong candidates for ES cells. First, the pluripotent marmoset cells continue to proliferate rapidly for at least 18 mo in continuous culture, and at least some maintain a normal karyotype. Although spontaneously immortal cell lines have been derived from primary cultures of mouse cells, this occurs rarely, if ever,

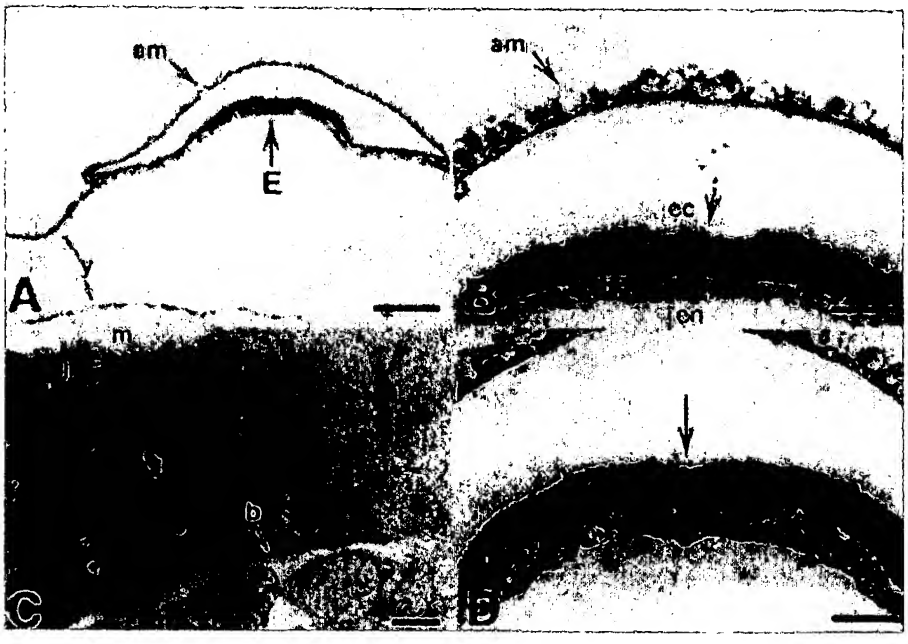


FIG. 5. Embryoid body formed from cell line Cj62 after 6 mo of undifferentiated culture. Cj62 cells were grown to confluence and then were allowed to spontaneously differentiate for 4 wk. A) Structures with morphological characteristic of yolk sac (y), amnion (am), and bilayered embryonic disc (E). The yolk sac was spherical, but collapsed during embedding, and the portion of the yolk sac to the right of the photograph was trimmed so the block would fit the diamond knife for sectioning. The embryonic disc was pyriform-shaped with a central groove in its caudal (narrow) aspect, and was connected to the tissue culture plate at its caudal pole by a stalk of mesenchymal cells. (Bar = 200 μM, toluidine blue stain). B) Section in cranial 1/3 of embryonic disc. Note that the primitive ectoderm (ec) forms a distinct cell layer from the underlying primitive endoderm (en), with no mixing of cell layers. Note also that the amnion (am) is composed of two distinct layers; the inner layer is continuous with the primitive ectoderm at the margins. (Bar = 50 μM, toluidine blue stain). C) Electron micrograph of embryonic disc. Apical microvilli (m) and apical junctional complexes (j) are present in the ectoderm layer, and the basement membrane (b) separates the ectoderm from the underlying endoderm. (Bar = 5 μM, lead citrate and uranyl acetate). D) Section in caudal 1/3 of embryonic disc. Note the central groove (arrow) and the mixing of primitive ectoderm and endoderm. This is the approximate level of early primitive streak formation in the normal primate embryo. (Bar = 50 μM, toluidine blue stain).

from primary cultures of somatic cells of primates, which consistently undergo crisis after a characteristic number of cell divisions [24]. Our success in isolating multiple immortal cell lines from both rhesus monkey and marmoset ICMs suggests that, unlike adult somatic cells, the undifferentiated, totipotent cells of the early embryo are immortal; that is, they are capable of unlimited proliferation. A second characteristic of the pluripotent marmoset cells is the expression of SSEA-3, SSEA-4, TRA-1-60, TRA-1-81, and alkaline phosphatase—a combination of cell surface markers previously described only for rhesus monkey ES cells and human EC cells [6, 14–16, 18]. The differentiation of human EC cells results in the loss of SSEA-3, SSEA-4, TRA-1-60, and TRA-1-81 expression, and the earliest lineages to differentiate from the ICM in the human embryo, extra-embryonic endoderm and trophoblast, lack this combination of markers [18]. A third important characteristic of the pluripotent marmoset cells is the potential to differentiate to both endoderm and trophoblast, as the last cells in the mammalian embryo capable of contributing progeny to both these lineages are the totipotent early ICM cells [25]. And finally, the pluripotent marmoset cells differentiate to embryoid bodies with a remarkable resemblance to postimplantation early primitive streak-stage embryos [26].

Pluripotent marmoset cells offer an important new in vitro model for studying the differentiation and function of tissues that differ significantly between mice and primates. For example, the structure and the function of the trophoblast, which forms the outer layer of the placenta, differs dramatically between primates and rodents. Trophoblast secretion of CG in primates, including humans, is central to the maternal recognition of pregnancy. The mouse placenta does not express a CG, and mouse ES cells fail to differentiate to trophoblast or do so infrequently [27]. If the primate corpus luteum is exposed to CG, progesterone secretion is continued and pregnancy is maintained; in the absence of CG, the corpus luteum regresses, progesterone secretion declines, and a new ovarian cycle is initiated. GnRH is expressed in the placenta and has been proposed to have a local regulatory role in CG secretion [28]. The increase in CG secretion we observed in differentiating pluripotent marmoset cells in the presence of GnRH agonist supports a role in CG expression. Further, the dramatic effects observed suggest that GnRH may not only act *on* differentiated trophoblasts but might also be directly involved in the differentiation *of* trophoblasts. GnRH has been shown to be expressed and have biological effects in extrapituitary tissues other than the placenta [29–31], and this may point to a wider role for this regulatory peptide in differentiation and development. Because these pluripotent marmoset cells can be grown indefinitely, prior to differentiation it will be possible to use homologous recombination to modify trophoblast-specific genes, such as CG, GnRH, or their receptors, to help elucidate their function and regulation during and after differentiation.

The pluripotent marmoset cells initiate the formation of all three germ layers in embryoid bodies. If culture conditions can be established that allow efficient, synchronous development of organized embryoid bodies, then it will be possible to use these pluripotent marmoset cells to genetically dissect in vitro the mechanisms controlling early primitive streak formation in primates. We are not aware of primitive streak formation occurring in mouse embryoid bodies, which exhibit a more disorganized development [32]. With our present culture conditions, however, embryoid body formation is asynchronous, and many embryoid bodies develop into simple multilayered vesicular structures without the well-organized structure represented in Figure 5. To date, we have not observed development of embryoid bodies beyond the initiation of primitive streak formation, which is also the approximate stage where intact marmoset embryos degenerate in our culture conditions. To rigorously test the developmental potential of these pluripotent marmoset cells, it will be necessary to provide them with a normal embryonic environment, in chimeras with intact embryos.

## ACKNOWLEDGMENTS

The authors thank Guenther Scheffler for performing the progesterone assays, and the animal care and Molecular Biology Core staff at the Wisconsin Regional Primate Research Center. We thank Dr. Peter Andrews for providing us with monoclonal antibodies to SSEA-1, 3, 4, TRA-1-60, and TRA-1-81, and the cell line NTERA2 cl.D1. GnRH agonist D-Trp$^6$-Pro$^9$-NHEt was synthesized at the Salk Institute (La Jolla, CA; under Contract NO1-HD-02906 with NIH) and made available by the Contraceptive Development Branch, Center for Population Research, NICHD.

## REFERENCES

1. Martin G. Isolation of a pluripotent cell line from early mouse embryos cultured in medium conditioned by teratocarcinoma stem cells. Proc Natl Acad Sci USA 1981; 78:7634–7638.
2. Evans M, Kaufman M. Establishment in culture of pluripotential cells from mouse embryos. Nature 1981; 292:154–156.
3. Rossant J, Papaioannou V. The relationship between embryonic, embryonal carcinoma and embryo-derived stem cells. Cell Differ 1984; 15:155–161.
4. Bradley A, Evans M, Kaufman M, Robertson E. Formation of germline chimaeras from embryo-derived teratocarcinoma cell lines. Nature 1984; 309:255–256.
5. Rossant J, Bernelot Moens C, Nagy A. Genome manipulation in embryonic stem cells. Philos Trans R Soc Lond Biol 1993; 339:207–215.
6. Thomson JA, Kalishman J, Golos TG, Durning M, Harris CP, Becker RA, Hearn JP. Isolation of a primate embryonic stem cell line. Proc Natl Acad Sci USA 1995; 92:7844–7848.
7. Summers PM, Wennink CJ, Hodges JK. Cloprostenol-induced luteolysis in the marmoset monkey (*Callithrix jacchus*). J Reprod Fertil 1985; 73:133–138.
8. Lopata A, Summers P, Hearn J. Births following the transfer of cultured embryos obtained by *in vitro* and *in vivo* fertilization in the marmoset monkey (*Callithrix jacchus*). Fertil Steril 1988; 50:503–509.
9. Thomson JA, Kalishman J, Hearn JP. Non-surgical uterine stage preimplantation embryo collection from the common marmoset. J Med Primatol 1994; 23:333–336.
10. Saltzman W, Schultz-Darken NJ, Scheffler G, Wegner FH, Abbott DH. Social and reproductive influences on plasma cortisol in female marmoset monkeys. Physiol Behav 1994; 56:801–810.
11. Solter D, Knowles B. Immunosurgery of mouse blastocysts. Proc Natl Acad Sci USA 1975; 72:5099–5102.
12. Robertson EJ. Embryo-derived stem cell lines. In: Robertson EJ (ed.), Teratocarcinomas and Embryonic Stem Cells: A Practical Approach. Washington, DC: IRL Press; 1987: 71–112.
13. Hsu T, Benirschke K. An Atlas of Mammalian Chromosomes. New York: Springer-Verlag; 1970.
14. Solter D, Knowles BB. Monoclonal antibody defining a stage-specific mouse embryonic antigen (SSEA-1). Proc Natl Acad Sci USA 1978; 75:5565–5569.
15. Kannagi R, Cochran NA, Ishigami F, Hakomori S, Andrews PW, Knowles BB, Solter D. Stage-specific embryonic antigens (SSEA-3 and -4) are epitopes of a unique globo-series ganglioside isolated from human teratocarcinoma cells. EMBO J 1983; 2:2355–2361.
16. Andrews PW, Banting G, Damjanov I, Arnaud D, Avner P. Three monoclonal antibodies defining distinct differentiation antigens associated with different high molecular weight polypeptides on the surface of human embryonal carcinoma cells. Hybridoma 1984; 3:347–361.
17. Andrews P, Damjanov I, Simon D, Banting G, Carlin C, Dracopoli

N, Fogh J. Pluripotent embryonal carcinoma clones derived from the human teratocarcinoma cell line Tera-2. Lab Invest 1984; 50:147–162.
18. Andrews P, Oosterhuis J, Damjanov I. Cell lines from human germ cell tumors. In: Robertson E (ed.), Teratocarcinomas and Embryonic Stem Cells: A Practical Approach. Oxford: IRL Press; 1987: 207–246.
19. Golos TG, Durning M, Fisher JM, Fowler PD. Cloning of four growth hormone/chorionic somatomammotropin-related complementary deoxyribonucleic acids differentially expressed during pregnancy in rhesus monkey placenta. Endocrinology 1993; 133:1744–1752.
20. Adelman JP, Mason AJ, Hayflick JS, Seeburg PH. Isolation of the gene and hypothalamic cDNA for the common precursor of gonadotropin-releasing hormone and prolactin release-inhibiting factor in human and rat. Proc Natl Acad Sci USA 1986; 83:179–183.
21. Vale W, Rivier C, Brown M, Leppaluoto J, Monahan M, Rivier J. Pharmacology of hypothalamic regulatory peptides. Clin Endocrinol 1976; 5:261.
22. Terasawa E, Bridson WE, Nass TE, Noonan JJ, Dierschke DJ. Developmental changes in the luteinizing hormone secretory pattern in peripubertal female rhesus monkeys: comparisons between gonadally intact and ovariectomized animals. Endocrinology 1984; 115:2233–2240.
23. Andrews PW. Human teratocarcinomas. Biochim Biophys Acta 1988; 948:17–36.
24. Shay JW, Wright WE, Werbin H. Defining the molecular mechanisms of human cell immortalization. Biochim Biophys Acta 1991; 1072: 1–7.
25. Winkel GK, Pedersen RA. Fate of the inner cell mass in mouse embryos as studied by microinjection of lineage tracers. Dev Biol 1988; 127:143–156.
26. Lopata A, Berka J, Simula A, Norman R, Otani T. Differential distribution of mRNA for the α- and ß-subunits of chorionic gonadotropin in the implantation stage blastocyst of the marmoset monkey. Placenta 1995; 16:335–346.
27. Beddington RSP, Robertson EJ. An assessment of the developmental potential of embryonic stem cells in the midgestation mouse embryo. Development 1989; 105:733–737.
28. Siler-Khodr TM, Khodr GS. Luteinizing hormone releasing factor content of the human placenta. Am J Obstet Gynecol 1978; 130:216–219.
29. Peng C, Fan NC, Ligier M, Vaananen J, Leung PCK. Expression and regulation of gonadotropin-releasing hormone (GnRH) and GnRH receptor messenger ribonucleic acids in human granulosa-luteal cells. Endocrinology 1994; 135:1740–1746.
30. Whitelaw PF, Eidne KA, Sellar R, Smyth CD, Hillier SG. Gonadotropin-releasing hormone receptor messenger ribonucleic acid expression in rat ovary. Endocrinology 1995; 136:172–178.
31. Olofsson JI, Conti CC, Leung PCK. Homologous and heterologous regulation of gonadotropin-releasing hormone receptor gene expression in preovulatory rat granulosa cells. Endocrinology 1995; 136: 974–980.
32. Doetschman T, Eistetter H, Katz M, Schmidt W, Kemler R. The *in vitro* development of blastocyst-derived embryonic stem cell lines: formation of visceral yolk sac, blood islands and myocardium. J Embryol Exp Morphol 1985; 87:27–45.

gradients close to the air–water interface, where veils develop within a few minutes. A suspension of latex beads (1 or 0.5 μm) was then added with a capillary pipette. Preparations were recorded with dark-field illumination using a CCD camera (Sony) attached to the microscope and a video recorder. Afterwards, positions of individual latex beads were recorded frame by frame (at 0.04-s intervals). Only trajectories that were almost parallel to the plane of observation were included.

**Oxygen gradients.** Oxygen microelectrodes (with a 5–10-μm tip)[3] connected to a picoammeter were mounted in a micromanipulator. The surface of the *Thiovulum* veil and the electrode tip were observed through a dissection microscope tilted at an angle of 45°; this made it possible to map the $O_2$ isopleths inside and above the veil. Microelectrodes penetrating from above tend to deform the $O_2$ diffusion gradients above the sediment[14], but this should not affect the relative position of $O_2$ isopleths in different areas of the veil. The fact that $O_2$ was measured in a vertical convective flow is also likely to minimize this effect.

Received 27 January; accepted 8 May 1998.


1. Purcell, E. M. Life at low Reynolds number. *Am. J. Phys.* **45**, 3–11 (1977).
2. Revsbech, N. P., Jørgensen, B. B. & Blackburn, T. H. Oxygen in the sea bottom measured with a microelectrode. *Science* **207**, 1355–1356 (1980).
3. Revsbech, N. P. & Jørgensen, B. B. Microelectrodes: their use in microbial ecology. *Adv. Microbiol. Ecol.* **9**, 293–352 (1986).
4. Wirsen, C. O. & Jannasch, H. W. Physiological and morphological observations on *Thiovulum* sp. *J. Bacteriol.* **136**, 765–774 (1978).
5. Garcia-Pichel, F. Rapid bacterial swimming measured in swarming cells of *Thiovulum majus*. *J. Bacteriol.* **171**, 3560–3563 (1989).
6. Fenchel, T. Motility and chemosensory behaviour of the sulphur bacterium *Thiovulum majus*. *Microbiology* **140**, 3109–3116 (1994).
7. Jørgensen, B. B. & Revsbech, N. P. Colorless sulfur bacteria, *Beggiatoa* spp. and *Thiovulum* spp. in $O_2$ and $H_2S$ microgradients. *Appl. Environ. Microbiol.* **45**, 1261–1270 (1983).
8. Lighthill, J. Flagellar hydrodynamics. *Soc. Indust. Appl. Math. Rev.* **18**, 161–230 (1976).
9. Vogel, S. *Life in moving fluids* (Grant, Boston, 1981).
10. Fenchel, T. & Bernard, C. Mats of colourless sulphur bacteria. I Major microbial processes. *Mar. Ecol. Prog. Ser.* **128**, 161–170 (1995).
11. Aller, R. C. & Yingst, J. Y. Effects of marine deposit-feeders *Heteromastus filiformis* (Polychaeta), *Macoma balthica* (Bivalvia), and *Tellina texana* (Bivalvia) on averaged solute transport, reaction rates, and microbial distributions. *J. Mar. Res.* **41**, 299–322 (1985).
12. Dando, P. R. *et al.* The effects of methane seepage at an intertidal/shallow subtidal site on the shore of Kattegat, Vendsyssel. *Bull. Geol. Soc. Denmark* **41**, 65–79 (1994).
13. Gundersen, J. K., Jørgensen, B. B., Larsen, E. & Jannasch, H. W. Mats of giant sulphur bacteria on deep-sea sediments due to fluctuating hydrothermal flow. *Nature* **360**, 454–455 (1992).
14. Glud, R. N., Gundersen, J. K., Revsbech, N. P. & Jørgensen, B. B. Effects on the benthic diffusive boundary layer imposed by microelectrodes. *Limnol. Oceanogr.* **39**, 462–467 (1994).


Acknowledgements. We thank J. Johansen for technical assistance. This study was supported by grants from the Danish Natural Science Research Council.

Correspondence and requests for materials should be addressed to T.F. (e-mail: mbltf@inet.uni2.dk).

# Full-term development of mice from enucleated oocytes injected with cumulus cell nuclei

**T. Wakayama*†, A. C. F. Perry*‡, M. Zuccotti*§, K. R. Johnson‖ & R. Yanagimachi***

* *Department of Anatomy and Reproductive Biology, John A. Burns School of Medicine, University of Hawaii, Honolulu, Hawaii 96822, USA*
† *Department of Veterinary Anatomy, Faculty of Agriculture, University of Tokyo, Bunkyo-ku, Tokyo 113, Japan*
‡ *Department of Signalling, Babraham Institute, Cambridge CB2 4AT, UK*
§ *Dipartimento Biologia Animale, Laboratorio Biologia dello Sviluppo, University of Pavia, Piazza Botta 10, 27100, Pavia, Italy*
‖ *Jackson Laboratory, 600 Main Street, Bar Harbor, Maine 04609, USA*

**Until recently, fertilization was the only way to produce viable mammalian offspring, a process implicitly involving male and female gametes. However, techniques involving fusion of embryonic or fetal somatic cells with enucleated oocytes have become steadily more successful in generating cloned young[1–3]. Dolly the sheep[4] was produced by electrofusion of sheep mammary-derived cells with enucleated sheep oocytes. Here we investigate the factors governing embryonic development by introducing nuclei from somatic cells (Sertoli, neuronal and cumulus cells) taken from adult mice into enucleated mouse oocytes. We found that some enucleated oocytes receiving Sertoli or neuronal nuclei developed *in vitro* and implanted following transfer, but none developed beyond 8.5 days post coitum; however, a high percentage of enucleated oocytes receiving cumulus nuclei developed *in vitro*. Once transferred, many of these embryos implanted and, although most were subsequently resorbed, a significant proportion (2 to 2.8%) developed to term. These experiments show that for mammals, nuclei from terminally differentiated, adult somatic cells of known phenotype introduced into enucleated oocytes are capable of supporting full development.**

Previous studies have suggested that embryonic development is enhanced when donor nuclei are in the G0 or G1 phase of the cell cycle[1,3,4], and Dolly the sheep developed from an enucleated oocyte electrofused with a mammary-derived cell presumed to be in G0 following culture in serum-deficient medium for 5 days[4]. We have investigated the developmental potential of oocytes injected with the nuclei of non-cultured cells known to be at G0. We selected

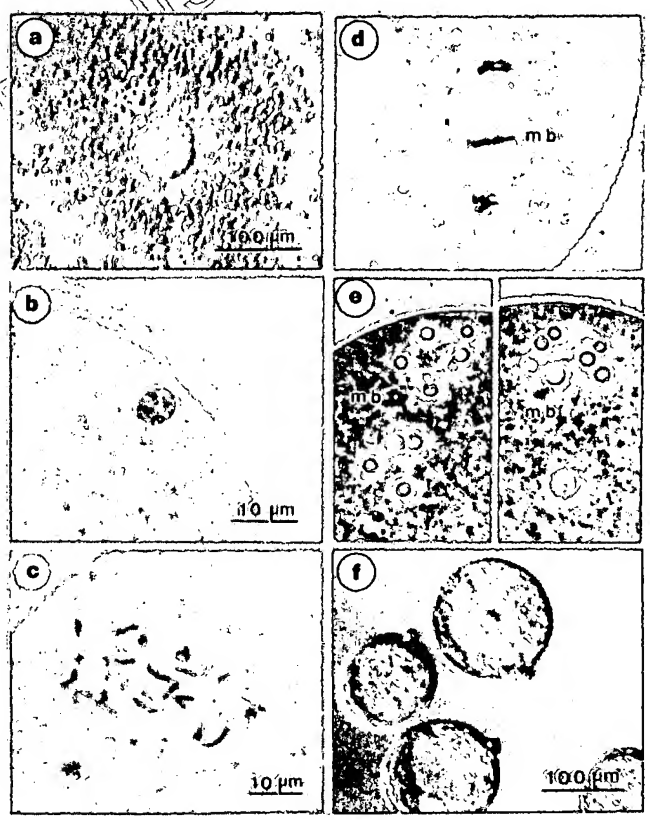


**Figure 1** *In vitro* development of enucleated oocytes following injection of cumulus cell nuclei. **a**, Live oocyte surrounded by cumulus cells. The egg coat (the zona pellucida) appears in this micrograph as a relatively clear zone around the oocyte. **b–e**, Behaviour of cumulus cell nuclei following injection into enucleated oocytes, photographed after fixation and staining. **b**, A cumulus cell nucleus within 10 min of injection. **c**, Transformation of the nucleus into disarrayed chromosomes 3 h after injection. The disorder reflects an unusual situation in which single, condensed chromatids are each attached to a single pole of the spindle and are therefore not aligned on a metaphase plate. **d**, 1 h after $Sr^{2+}$ activation, chromosomes are segregated into two groups (mb, midbody). **e**, 5 h after $Sr^{2+}$ activation, two pseudo-pronuclei (left and right panels) with a varying number of distinct nucleolus-like structures are discernible in each egg. The size and number of pseudo-pronuclei varied, suggesting that segregation of chromosomes was random after oocyte activation. **f**, Live blastocysts produced following injection of enucleated oocytes with cumulus cell nuclei.

**Table 1 Preimplantation of enucleated eggs injected with cumulus cell nuclei**

| Time of oocyte activation | Total no. of oocytes used | No. of enucleated oocytes | No. of surviving oocytes after injection | No. (%) of activated oocytes | No. (%, mean ± s.d.) of embryos developed from oocytes at 72 h after activation | | |
|---|---|---|---|---|---|---|---|
| | | | | | 1-cell and abnormal | 2-8-cell | Morula/blastocyst* |
| Simultaneously with injection | 233 | 230 | 182 | 153 (84.1) | 17 | 75 | 61 (39.9 ± 16.6) |
| 1-3 h after injection | 573 | 565 | 508 | 474 (93.3) | 20 | 177 | 277 (58.4 ± 12.6) |
| 3-6 h after injection | 195 | 191 | 182 | 151 (83.0) | 9 | 41 | 101 (66.9 ± 14.4) |

* There is a significant different ($P < 0.005$) between the top result and the bottom two. Data were analysed using the $\chi^2$ test.

Sertoli, neuronal and cumulus from adult mice as representatives of this class; Sertoli cells and neurons do not normally divide in adults but remain at G0, and more than 90% of cumulus cells surrounding recently ovulated oocytes (Fig. 1a) are in the G0/G1 phase of the cell cycle[5]. These somatic cell types have very distinctive morphologies, making them easy to identify with confidence. All cells were used immediately (that is, without *in vitro* culturing) following the removal of tissue from freshly killed mice.

Enucleated mouse oocytes were each injected with a single nucleus from one of the three somatic cell types and left for 0 to 6 hours before activation. Examination of enucleated oocytes injected with cumulus nuclei revealed that chromosome condensation had occurred within 1 hour of injection (Fig. 1b, c). When, after 1 to 6 hours incubation, oocytes were activated in culture medium containing $Sr^{2+}$ and cytochalasin B, their cumulus-derived chromosomes segregated (Fig. 1d) to form structures resembling the pronuclei that are formed after normal fertilization (referred to here as pseudo-pronuclei). Examination of 47 such oocytes after fixation and staining showed that 64% had two pseudo-pronuclei (Fig. 1e) and 36% had three or more. Oocytes with distinct pseudo-pronuclei were considered to be activated. Owing to the cytokinesis-blocking effect of cytochalasin B, no polar body was formed and therefore all chromosomes were retained within the oocyte, regardless of the number of pseudo-pronuclei. Chromosome analysis of 13 such oocytes fixed before the first cleavage (data not shown) revealed that 85% had a normal total chromosome number ($2n = 40$). The time interval between nucleus injection and oocyte activation appeared to affect the rate of oocyte development (Table 1). Activation immediately after nucleus injection led to

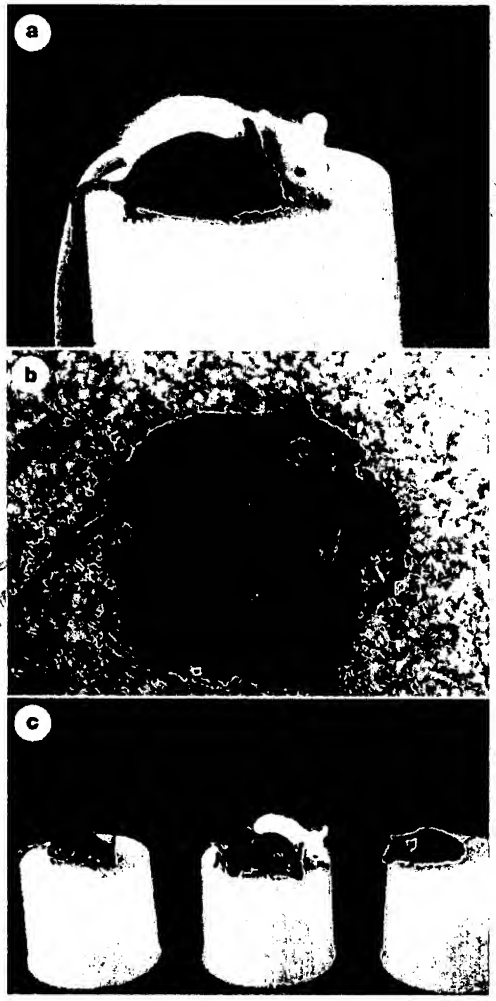


**Figure 2** Cloned mice. **a**, The first surviving cloned mouse, Cumulina (born 3 October 1997) at four weeks (foreground) with her foster mother. **b**, Cumulina at 2.5 months with the pups she produced following mating with a CD-1 (albino) male. **c**, Two B6C3F1-derived, cloned, agouti young (centre) in front of their albino foster mother (CD-1), and a B6D2F1 oocyte donor (black, right). The two agouti offspring in the centre are clones (identical 'twin' sisters) of the agouti B6C3F1 cumulus donor shown on the left, and are two of the offspring described in series C (see text) and Table 2.

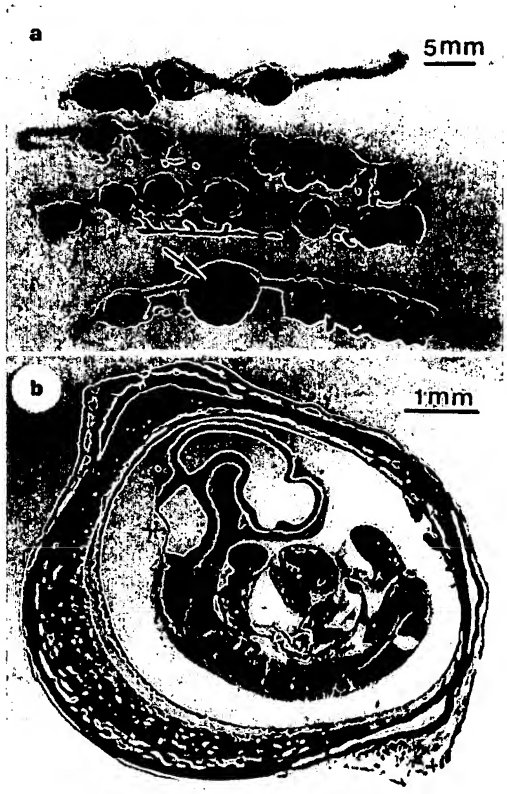


**Figure 3** Development following uterine transfer of embryos produced after injection of Sertoli cell nuclei into enucleated oocytes. **a**, Uteri of recipient females 8.5 d.p.c., fixed with Bouin's fluid, dehydrated and cleared with benzyl benzoate. All uterine implantation sites failed to develop except for one (arrow), in which an embryo (**b**) appeared to be normal and was at the ~12-somite stage.

**Table 2 Development of enucleated eggs injected with Sertoli or brain-cell nuclei***

| Cell type injected | No. of surviving oocytes injected | No. (%) of oocytes activated | Total no. (%) of morulae/blastocysts developed† | No. of transferred embryos (recipients) | No. (%) of implantation sites | No. (%) of fetuses |
|---|---|---|---|---|---|---|
| Sertoli | 159 | 159 (100) | 63 (39.6) | 59 (8) | 41 (69.5) | 1 (1.7) |
| Brain | 228 | 223 (97.8) | 50 (22.4) | 46 (5) | 25 (54.3) | 1 (2.2)‡ |

* All recipients were killed at 8.5 d.p.c.
† There is a significant difference ($P < 0.005$) between the top and bottom result.
‡ Died at about 6–7 d.p.c.

significantly poorer development to morulae/blastocysts *in vitro* (Fig. 1f) than was achieved when activation followed a delay of 1 to 6 hours.

On the basis of this information, we injected Sertoli and neuronal nuclei into enucleated oocytes and delayed activation for 1 to 6 hours: about 40% of enucleated oocytes that had been injected with Sertoli cell nuclei, and 22% of those injected with neuronal nuclei, developed into morulae/blastocysts *in vitro* (Table 2). As these values were less than those achieved after cumulus nucleus injection (58–67%; Table 1), we concentrated on the potential of cumulus cell nuclei to support embryonic development *in vivo*.

In the first series of experiments (series A in Table 3), a total of 142 developing embryos (at the 2-cell to blastocyst stage) were transferred to 16 recipient females. When these females were examined at 8.5 and 11.5 d.p.c., 5 live and 5 dead fetuses were seen *in uteri*. In the second series (series B in Table 3), a total of 800 embryos were transferred into 54 foster mothers, and caesarean sections at 18.5–19.5 d.p.c. revealed 17 live fetuses. Of these, six died soon after delivery, one died approximately 7 days after delivery, but the remaining ten females survived and are apparently healthy. All of these, including the first-born survivor (born on 3 October 1997 and named 'Cumulina'; Fig. 2a), have been mated and have delivered and raised normal offspring (Fig. 2b). Several of these offspring have, in turn, now developed into fertile adults.

In the third series of experiments (series C in Table 3), B6C3F1 mice carry a copy of the *agouti* (A) gene, and are consequently agouti; offspring from this experiment should therefore have an agouti coat colour, rather than the black of the B6D2F1 oocyte donors. A total of 298 embryos derived from B6C3F1 cumulus cell nuclei were transferred to 18 foster mothers. Caesarean sections at 19.5 d.p.c. revealed six live fetuses whose placentas were used in DNA-typing analysis. Although one died a day after birth, the five extant females are healthy and have the agouti coat phenotype. Figure 2c shows two such agouti pups with their albino foster mother (CD-1).

We did additional experiments (series D in Table 3) to investigate whether clones could be more efficiently cloned in subsequent rounds of recloning. We therefore collected cumulus cells from B6C3F1 (agouti) clones generated in series C and injected their nuclei into enucleated B6D2F1 oocytes to generate embryos that were transferred as described for series B and C. A total of 287 embryos derived from cloned B6C3F1 cumulus-cell nuclei were transferred to 18 foster mothers. When caesarean sections were done at 19.5 d.p.c. eight live fetuses were recovered. Although one died soon after birth, the seven surviving females are healthy and have the predicted agouti coat phenotype. These results indicate that clones (series B and C) and cloned clones (series D) are produced with comparable efficiency. This argues that successive generations of clones do not undergo changes (either positive or negative) that influence the outcome of the cloning process.

We also monitored the developmental potential *in vivo* of morulae/blastocysts generated following the injection of either Sertoli-cell or neuronal nuclei into enucleated oocytes (all cells from non-clones) (Table 2). Embryos produced by Sertoli-nucleus injection resulted in a single live fetus (Fig. 3) in the uterus of a foster mother killed 8.5 d.p.c. (Table 2). We failed to detect *in vivo* development of embryos derived following injection of neuronal nuclei beyond 6–7 d.p.c.

We believe that all of the live offspring reported here represent clones derived from cumulus-cell nuclei in the absence of genetic

**Table 3 Postimplantation development of enucleated eggs injected with cumulus cell nuclei**

| Experiment series* | Time of oocyte activation | No. of injected oocytes | No. of transferred embryos (recipients) | No. (%) of implantations from transferred embryos† | No. of fetuses developed from transferred embryos | | | | | No. (%) of newborn from transferred embryos |
|---|---|---|---|---|---|---|---|---|---|---|
| | | | | | Total (%)† | 8.5 d.p.c. | | 11.5 d.p.c. | | |
| | | | | | | Live | Dead | Live | Dead | |
| A | Simultaneously with injection | 82 | 34 (4) | 8 (23.5) | 0 | | | | | – |
| | 1–3 h after injection | 136 | 45 (5) | 32 (71.1) | 7 (15.6) | 3 | 2‡ | 2 | 0 | – |
| | 3–6 h after injection | 124 | 63 (7) | 36 (57.1) | 3 (4.8) | 0 | 2§ | 0 | 1‖ | – |
| B | 1–3 h after injection | 1345 | 760 (49) | – | – | – | – | – | – | 16 (2.1) |
| | 3–6 h after injection | 62 | 40 (5) | – | – | – | – | – | – | 1 (2.5) |
| C | 1–3 h after injection | 458 | 298 (18) | – | – | – | – | – | – | 6 (2.0) |
| D | 1–3 h after injection | 603 | 287 (18) | – | – | – | – | – | – | 8 (2.8) |

* Series A, caesarean sections were done at 8.5 or 11.5 d.p.c.; series B and C, caesarean sections were done at 18.5–19.5 d.p.c. In series A and B, each donor nucleus is from a B6D2F1 cumulus cells; in series C, each donor nucleus is from a B6C3F1 cumulus cell; in series D, each donor nucleus is from a B6C3F1 clones mouse from series C.
† There is a significant difference between the top result and the bottom two: implantation ($P < 0.005$); fetal development ($P < 0.05$). Data were analysed by $\chi^2$ tests.
‡ Died 6–7 d.p.c.
§ Died 7–8 d.p.c.
‖ Died 10 d.p.c.

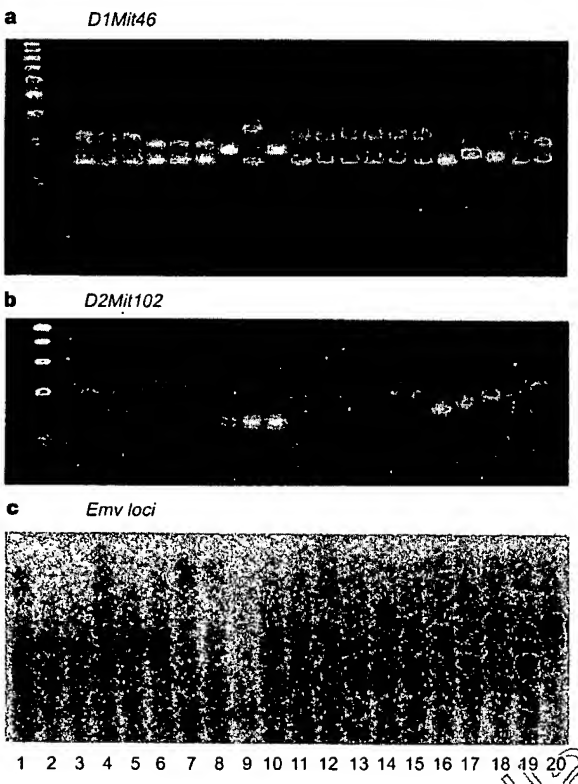


**Figure 4** DNA typing of donors and offspring in series C corroborates the genetic identify of the cloned offspring to cumulus cell donors, and non-identity to oocyte donors and host foster females. **a**, PCR typing using the strain-specific marker *D1Mit46*. **b**, PCR-amplified DNA (**a**, **b**) from $F_1$ hybrid mice gives an additional gel band not seen in the DNA from inbred parental strains (lanes 16–20); this extra band corresponds to a heteroduplex derived from the two parental products, whose conformation results in anomolous gel migration. **c**, Southern blot typing of strain-specific *Emv* loci (*Emv1*, *Emv2* and *Emv3*). Placental DNA from the six cloned series C offspring (lanes 10–15) was compared with DNA from the three cumulus cell donor females (lanes 1–3), the three oocyte recipient females (lanes 4–6), and the three host females (lanes 7–9). Control DNA was from C57BL/6 (lane 16), C3H (lane 17), DBA/2 (lane 18), B6C3F1 (lane 19) or B6D2F1 (lane 20). 100-bp DNA size-marker ladders are shown on the left of **a** and **b**.

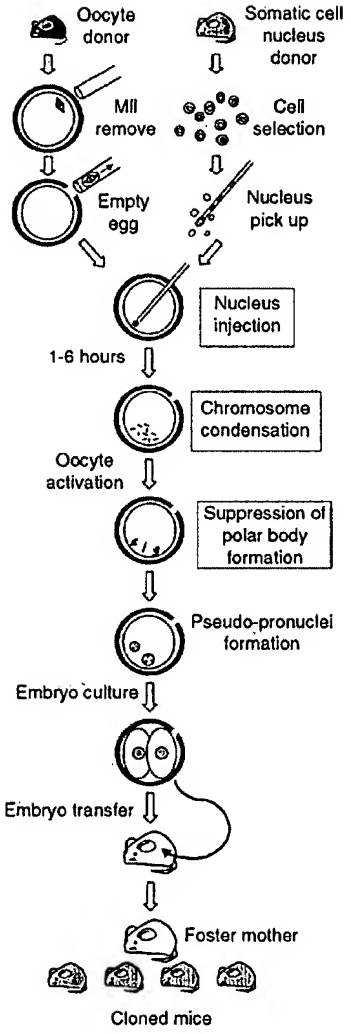


**Figure 5** The cloning procedure developed here, as described in the text and Methods section.

contamination, for the following reasons. (1) Oocytes/eggs were not exposed to spermatozoa *in vitro*. (2) Foster mothers (CD-1, albino) were mated with vasectomized males (CD-1, albino) of established infertility. In the unlikely event of fertilization by such a vasectomized male, the offspring would be albino. We transferred 2- to 8-cell embryos/blastocysts into the oviducts/uteri of foster mothers; it is well established that 2- to 8-cell mouse embryos/blastocysts cannot be fertilized by spermatozoa[6]. (3) All full-term animals were born with black eyes; the surviving ten from series B have black coats and the surviving five in series C have agouti coats. This pattern of coat colour inheritance exactly matches that predicted by the genotype of the nucleus donor in each case. As B6D2F1 mice lack the *agouti* gene, the agouti mice in series C must have inherited their agouti coat colour from a non-B6D2F1 nucleus. (4) Where possible, all putative clones have been sexed, and all were found to be females, consistent with their genetic progenitors invariably being female. (5) DNA typing of highly variable alleles diagnostic of the B6, C3, D2 and CD-1 strains used here (Fig. 4) demonstrates beyond reasonable doubt that the six cloned offspring in series C (which includes one that died soon after birth) are isogenic with the three cumulus cell donor females used (B6C3F1) and do not contain DNA derived from either the oocyte donors (B6D2F1) or host foster mothers (CD-1). (6) Following enucleation, we suppressed extrusion of chromosomes into polar bodies using cytochalasin B. Thus, even if enucleation of the oocytes had been either totally unsuccessful or only partly successful, all resulting zygotes would be hyperploid; such embryos are inviable and cannot develop into normal offspring[7]. Moreover, in mock experiments, we enucleated 204 oocytes and examined them after fixation and staining[8]: no chromosomes were apparent, suggesting that the efficiency of chromosome removal exceeded 99.99%.

In general, nuclei have previously been transferred either into enucleated, one-cell embryos[9], or into unfertilized, enucleated oocytes[10,11] which were then immediately activated, thereby preventing chromosome condensation[12]. Mouse embryonic stem[13] or primordial germ[14] cell nuclei transferred into enucleated oocytes that were then immediately activated produced embryos capable of developing to blastocysts, with a minority of these implanting. In contrast, activation that was delayed for 30 to 60 minutes after the introduction of thymocyte nuclei into enucleated oocytes[15] often resulted in the extrusion of a pseudo-polar body, with a consequently high incidence of hypoaneuploidy (78%) and with none of the embryos developing beyond the 4-cell stage.

We have shown that a relatively high proportion of enucleated oocytes can develop to morulae/blastocysts and beyond when they are activated after a prolonged delay following injection of adult-

derived, somatic cell nuclei. Indeed, the inclusion of a prolonged interval between nuclear injection and oocyte activation (and suppression of cytokinesis) was apparently beneficial for both pre- and post-implantation development (Tables 1, 3). Although this seems paradoxical after earlier work, prolonged exposure of incoming nuclei to a cytoplasm rich in metaphase promoting factor causes persistent chromosome condensation (in the absence of DNA synthesis) and may facilitate the nuclear changes that are essential for development. We are studying the molecular events attending this latent period with respect to potential epigenetic 'reprogramming' and chromatin repair, *inter alia*. Also, the use of a piezo-impact pipette drive unit[16,17] may have contributed to a high rate of embryonic development by enabling oocyte and donor nucleus manipulation to be quick and efficient, thereby reducing the trauma to both in comparison with methods using electrofusion, Sendai virus or polyethylene glycol. Furthermore, we minimized the amount of somatic cell cytoplasm introduced into enucleated oocytes, which might otherwise have interfered with the onset of development.

It is unclear why Sertoli and neuronal cell nuclei failed to produce full-term embryos. Although our study does not preclude the possibility that these nuclei (and nuclei from other cell types) may be able to support full-term development, this finding suggests that the G0 status of donor nuclei is not sufficient *per se* to ensure embryonic development. We did not use mural granulosa cells, which differ functionally and in their subsequent fate from cumulus cells[18], and the question is open as to whether their nuclei might prime embryonic development to term. The contrastingly high implantation rate (57–71%) and low fetal (5–16%) and full-term (2–3%) developmental rates (Table 3) indicate that several regulatory morphogenic factors and checkpoints may be involved in the development of post-implantation embryos/fetuses.

Our results suggest that, contrary to previous opinion[9], mammals can be reproducibly cloned from adult somatic cells. Furthermore, we believe that the success of these experiments in the mouse provides an amenable model with which to evaluate the molecular mechanisms that regulate the reprogramming of somatic cell genomes, genomic imprinting, embryonic genome activation and cell differentiation. □

## Methods

The cloning procedure is summarized in Fig. 5.

**Isolation of cumulus cells.** Female B6D2F1 (C57BL/6 × DBA/2 used in series A and B), B6C3F1 (C57BL/6 × C3H/He used in series C) or B6C3F1 clones produced in series C were induced to superovulate by consecutive injection of eCG and hCG. 13 h after hCG injection, cumulus–oocyte complexes were collected from oviducts and treated in HEPES–CZB medium[19] supplemented with bovine testicular hyaluronidase (0.1% (w/v), 300 U $mg^{-1}$) to disperse cumulus cells. We selected cumulus cells of modal (>70%) diameter (10–12 μm) for injection. From preliminary experiments, nuclei from cells with smaller or larger diameters (8–9 or 13–15 μm, respectively) seldom supported development of injected eggs beyond the 8-cell stage (data not shown). Following dispersal, cells were transferred to HEPES–CZB containing 10% (w/v) polyvinylpyrrolidone (average $M_r$, 360,000) and kept at room temperature for up to 3 h before injection.

**Isolation of Sertoli cells and neurons.** Sertoli cells were isolated from the testes of 6-month-old B6D2F1 males as described[20], except that HEPES–Ham F-12 medium was used. Manipulation of individual Sertoli cells was done by using a large injection pipette (inner diameter ~10 μm). Neuronal cells were isolated from the cerebral cortex of adult B6D2F1 females. Brain tissue was removed with sterile scissors, quickly washed in erythrocyte-lysing buffer and gently hand-homogenized for several seconds in nucleus isolation medium[21] at room temperature. Nuclei (7–8 μm in diameter) harbouring a conspicuous nucleolus were individually collected from the resulting suspension using the injection pipette before delivery into a recipient enucleated oocyte.

**Enucleation of metaphase II oocytes and donor cell nucleus injection.** B6D2F1 oocytes (obtained 13 h after hCG injection of eCG-primed females) were freed from the cumulus oophorous and held in CZB medium at 37.5 °C under 5% (v/v) $CO_2$ in air until required. Groups of oocytes (usually 10–15) were transferred into a droplet of HEPES–CZB containing 5 μg $ml^{-1}$ cytochalasin B, which had previously been placed in the operation chamber on the microscope stage. Oocytes undergoing microsurgery were held with a holding pipette and the zona pellucida 'cored' following the application of several piezo-pulses to an enucleation pipette. The metaphase II chromosome–spindle complex (identifiable as a translucent region) was aspirated into the pipette with a minimal volume of oocyte cytoplasm[22]. After enucleation of all oocytes in one group (~10 min), they were transferred into cytochalasin B-free CZB and held there for up to 2 h at 37.5 °C, then returned to the microscope stage immediately before further manipulation. Nuclei were removed from their respective somatic cells and gently aspirated in and out of the injection pipette (~7 μm inner diameter) until their nuclei were largely devoid of visible cytoplasmic material. Each nucleus was injected into a separate enucleated oocyte within 5 min of its isolation as described[17].

**Oocyte activation.** Following somatic-cell nucleus injection, some groups of oocytes were placed immediately in $Ca^{2+}$-free CZB containing both 10 mM $Sr^{2+}$ and 5 μg $ml^{-1}$ cytochalasin B for 6 h. Additional groups of enucleated oocytes injected with cumulus cell nuclei were left in CZB medium at 37.5 °C under 5% (v/v) $CO_2$ in air for 1–6 h before activation by $Sr^{2+}$ in the presence of 5 μg $ml^{-1}$ cytochalasin B. $Sr^{2+}$ treatment activated the oocytes[23], whereas cytochalasin B prevented subsequent polar-body formation and therefore chromosome expulsion. Following activation, all resulting embryos were transferred to $Sr^{2+}$-free, cytochalasin B-free CZB medium and incubation was continued at 37.5 °C under 5% (v/v) $CO_2$ in air.

**Embryo transfer.** Where appropriate, 2- to 8-cell embryos or morulae/blastocysts were respectively transferred into oviducts or uteri of foster mothers (CD-1, albino) that had been mated with vasectomized CD-1 males 1 or 3 days previously. Following caesarean section of recipient females at 18.5–19.5 d.p.c., live young were raised by lactating CD-1 foster mothers.

**DNA typing.** DNA from the following control strains and hybrids was obtained from spleen tissue: C57BL/6J (B6), C3H/HeJ (C3), DBA/2J (D2), B6C3F1 and B6D2F1. DNA from the three cumulus cell donor females (B6C3F1), the three oocyte recipient females (B6D2F1) and the three foster females (CD-1) was prepared from tail-tip biopsies. DNA from the six B6C3F1-derived, cloned offspring was prepared from their associated placentas. For the microsatellite markers *D1Mit46*, *D2Mit102* and *D3Mit49*, primer pairs (MapPairs) were purchased from Research Genetics and typed as described[24], except that PCR was carried out for 30 cycles and products were separated by 3% agarose gels (Metaphor) and visualized by ethidium bromide staining. Endogenous ecotropic murine leukaemia provirus DNA sequences (*Emv* loci) were identified following hybridization of *Pvu*II-digested genomic DNA to the diagnostic probe, pEc-B4 (ref. 25). Probe labelling, Southern blotting and hybridization procedures have been described[26].

Received 23 December 1997; accepted 19 June 1998.


1. Campbell, K. H. S., Loi, P., Otaegui, P. J. & Wilmut, I. Cell cycle co-ordination in embryo cloning by nuclear transfer. *Rev. Reprod.* **1**, 40–45 (1996).
2. Kono, T. Nuclear transfer and reprogramming. *Rev. Reprod.* **2**, 74–80 (1997).
3. Campbell, K. H. S., McWhir, J., Ritchie, W. A. & Wilmut, I. Sheep cloned by nuclear transfer from a cultured cell line. *Nature* **380**, 64–66 (1996).
4. Wilmut, I., Schnieke, A. E., McWhir, J., Kind, A. J. & Campbell, K. H. S. Viable offspring derived from fetal and adult mammalian cells. *Nature* **385**, 810–813 (1997).
5. Schuetz, A. W., Whittingham, D. G. & Snowden, R. Alterations in the cell cycle of mouse cumulus granulosa cells during expansion and mucification *in vivo* and *in vitro*. *Reprod. Fertil. Dev.* **8**, 935–943 (1996).
6. Wassarman, P. The biology and chemistry of fertilization. *Science* **235**, 553–560 (1987).
7. Epstein, C. J. *The Consequences of Chromosome Imbalance* (Cambridge University Press, 1986).
8. Yanagida, K., Yanagimachi, R., Perreault, S. D. & Kleinfeld, R. G. Thermostability of sperm nuclei assessed by microinjection into hamster oocytes. *Biol. Reprod.* **44**, 440–447 (1991).
9. McGrath, J. & Solter, D. Inability of mouse blastmere nuclei transferred to enucleated zygotes to support development *in vitro*. *Science* **226**, 1317–1319 (1984).
10. Willadsen, S. M. Nuclear transplantation in sheep embryos. *Nature* **320**, 63–65 (1986).
11. Collas, P. & Barnes, F. L. Nuclear transplantation by microinjection of inner cell mass and granulosa cell nuclei. *Mol. Reprod. Dev.* **38**, 264–267 (1994).
12. Czolowska, R., Modlinski, J. A. & Tarkowski, A. K. Behavior of thymocyte nuclei in non-activated and activated mouse oocytes. *J. Cell Sci.* **69**, 19–34 (1984).
13. Tsunoda, T. & Kato, Y. Nuclear transplantation of embryonic stem cells in mice. *J. Reprod. Fertil.* **98**, 537–540 (1993).
14. Tsunoda, T., Tokunaga, T., Imai, I. & Uchida, T. Nuclear transplantation of male primordial germ cells in the mouse. *Development* **107**, 407–411 (1989).
15. Kono, T., Ogawa, M. & Nakahara, T. Thymocyte transfer to enucleated oocytes in the mouse. *J. Reprod. Dev.* **39**, 301–307 (1993).
16. Kimura, Y. & Yanagimachi, R. Intracytoplasmic sperm injection in the mouse. *Biol. Reprod.* **52**, 709–720 (1995).

17. Kimura, Y. & Yanagimachi, R. Mouse oocytes injected with testicular spermatozoa or round spermatids can develop into normal offspring. *Development* **121**, 2397–2405 (1995).
18. Eppig, J., Wigglesworth, K., Pendola, F. & Hirao, Y. Murine oocytes suppress expression of luteinizing hormone receptor messenger ribonucleic acid by granulosa cells. *Biol. Reprod.* **56**, 976–984 (1997).
19. Chatot, C. L., Lewis, J. L., Torres, I. & Ziomek, C. A. Development of 1-cell embryos from different strains of mice in CZB medium. *Biol. Reprod.* **42**, 432–440 (1990).
20. Erickson, R. P., Zwigman, T. & Ao, A. Gene expression, X-inactivation, and methylation during spermatogenesis: the case of *Zfa*, *Zfx* and *Zfy* in mice. *Mol. Reprod. Dev.* **35**, 114–120 (1993).
21. Kuretake, S., Kimura, Y., Hoshi, K. & Yanagimachi, R. Fertilization and development of mouse oocytes injected with isolated sperm heads. *Biol. Reprod.* **55**, 789–795 (1996).
22. Kono, T., Sotomaru, Y., Sato, Y. & Nakahara, T. Development of androgenetic mouse embryos produced by *in vitro* fertilization of enucleated oocytes. *Mol. Reprod. Dev.* **34**, 43–46 (1993).
23. Bos-Mikich, A., Whittingham, D. G. & Kones, K. T. Meiotic and Mitotic $Ca^{2+}$ oscillations affect cell composition in resulting blastocysts. *Dev. Biol.* **182**, 172–179 (1997).
24. Dietrich, W. *et al.* A genetic map of the mouse suitable for typing intraspecific crosses. *Genetics* **131**, 423–447 (1992).
25. Taylor, B. A. & Rowe, L. A mouse linkage testing stock possessing multiple copies of the endogenous ecotropic murine leukemia virus genome. *Genomics* **5**, 221–232 (1989).
26. Johnson, K. R., Cook, S. A. & Davisson, M. T. Chromosomal localization of the murine gene and two related sequences encoding high-mobility-group 1 and Y proteins. *Genomics* **12**, 503–509 (1992).

**Acknowledgements.** This study was supported in part by grants from the National Institutes of Health, ProBio America Inc., and fellowships from the Japanese Society for the Promotion of Science (T.W.) and European Molecular Biology Organization (A.C.F.P.). We thank H. Tateno for chromosome analysis, Y. Nakamura for help with DNA fingerprinting, H. Kishikawa, T. Kasai and R. Kleinfeld for assistance in preparing this manuscript, and J. Eppig for help and advice.

Correspondence and requests for materials should be addressed to R.Y.

# Defects in somite formation in *lunatic fringe*-deficient mice

**Nian Zhang & Thomas Gridley**

*The Jackson Laboratory, 600 Main Street, Bar Harbor, Maine 04609-1500, USA*

**Segmentation in vertebrates first arises when the unsegmented paraxial mesoderm subdivides to form paired epithelial spheres called somites[1,2]. The Notch signalling pathway is important in regulating the formation and anterior–posterior patterning of the vertebrate somite[3–7]. One component of the Notch signalling pathway in *Drosophila* is the *fringe* gene, which encodes a secreted signalling molecule required for activation of Notch during specification of the wing margin[8–11]. Here we show that mice homozygous for a targeted mutation of the *lunatic fringe* (*Lfng*) gene, one of the mouse homologues[12,13] of *fringe*, have defects in somite formation and anterior–posterior patterning of the somites. Somites in the mutant embryos are irregular in size and shape, and their anterior–posterior patterning is disturbed. Marker analysis revealed that in the presomitic mesoderm of the mutant embryos, sharply demarcated domains of expression of several components of the Notch signalling pathway are replaced by even gradients of gene expression. These results indicate that *Lfng* encodes an essential component of the Notch signalling pathway during somitogenesis in mice.**

The *Lfng* gene is expressed during somitogenesis in mice in a dynamic pattern that suggests a possible role for *Lfng* in regulating somite formation and establishing somite borders[12,13]. To analyse the role of the *Lfng* gene during embryogenesis, we constructed a targeting vector that deleted 0.7 kilobases (kb) of genomic sequence encoding the putative signal peptide and proprotein region of the Lfng protein, and replaced the deleted sequence with the *lacZ* gene of *Escherichia coli* (Fig. 1a, b). Mice heterozygous for the $Lfng^{LacZ}$ mutant allele were viable and fertile. The pattern of RNA expression from the $Lfng^{LacZ}$ mutant allele was identical to that of *Lfng* RNA expression, but expression of β-galactosidase protein from the $Lfng^{LacZ}$ mutant allele was not useful as a marker for visualizing the normal pattern of *Lfng* expression during somitogenesis owing to the perdurance of the β-galactosidase protein and the dynamic nature of the *Lfng* expression pattern (Fig. 1c–e).

At birth, $Lfng^{LacZ}$ homozygous neonates had a shortened trunk with a rudimentary tail (Fig. 2a). Some $Lfng^{LacZ}$ homozygous neonates died within a few hours of birth, apparently from respiratory difficulties due to malformed rib cages (see below), but other, less severely affected, $Lfng^{LacZ}$ homozygotes could survive to adulthood. Analysis of stained skeletal preparations revealed substantial defects in formation of the vertebral column and ribs in the $Lfng^{LacZ}$ homozygotes (Fig. 2b, c). The regular metameric pattern of the vertebrae was disrupted along the entire longitudinal axis. The ribs of the $Lfng^{LacZ}$ homozygotes were bifurcated and fused, and some ribs were detached from the vertebral column (Fig. 2c).

$Lfng^{LacZ}$ homozygous mutant embryos could be distinguished

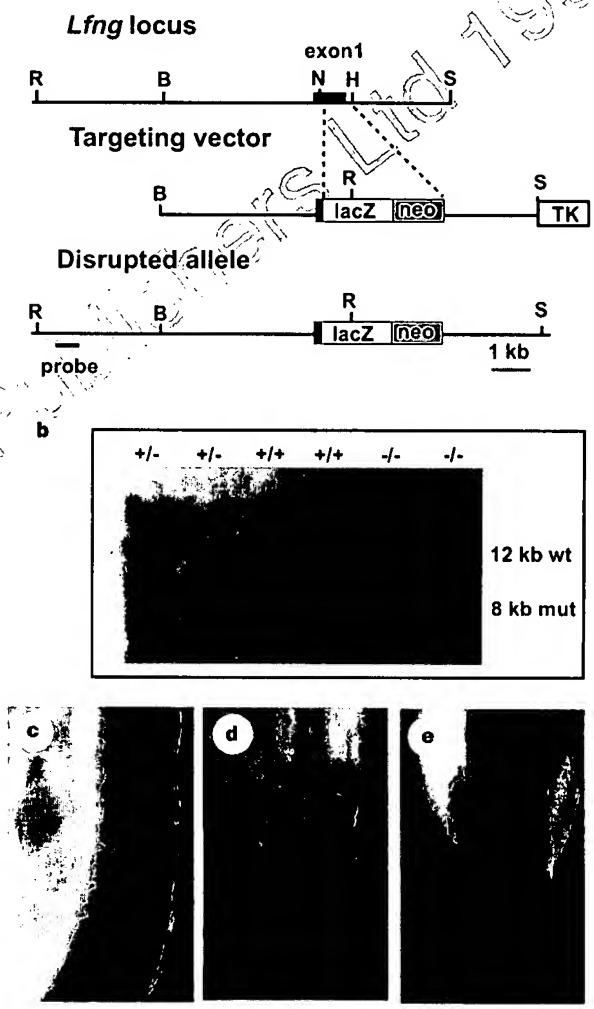


**Figure 1** Targeted disruption of the *Lfng* gene. **a**, Targeting scheme. The top line shows the genomic organization of a portion of the *Lfng* gene; the middle line shows the structure of the targeting vector. A 0.7-kb deletion was created which removes most of exon 1, replacing it with the *lacZ* gene and a *neo* cassette. At the bottom is the predicted structure of the *Lfng* locus following homologous recombination of the targeting vector. The probe used for Southern blot analysis in **b** is indicated. Restriction enzymes: B, *Bam*HI; H, *Hin*dIII; N, *Not*I; R, *Eco*RV; S, *Sal*I. **b**, DNA isolated from embryos of the intercross of $Lfng^{LacZ}$/+ heterozygous mice was digested with *Eco*RV, blotted, and hybridized with the indicated probe. Genotypes of progeny are indicated at the top of each lane. **c**, β-Galactosidase expression in $Lfng^{LacZ}$/+ heterozygous embryos revealed that, unlike *Lfng* RNA, β-galactosidase protein was expressed throughout the rostral presomitic mesoderm and the most recently formed somites. **d**, *In situ* hybridization of a $Lfng^{LacZ}$/+ heterozygous embryo with a *lacZ* probe revealed the same banding pattern in the presomitic mesoderm as is observed with a *Lfng* probe, demonstrating that the constitutive expression observed in **c** is due to perdurance of β-galactosidase. **e**, *In situ* hybridization of a $Lfng^{LacZ}$ homozygous mutant embryo with a *lacZ* probe revealed that the stripe of *lacZ* RNA expression is expanded and is more diffuse than in $Lfng^{LacZ}$/+ heterozygous embryos. In **c**–**e**, posterior is at the bottom. **c**, Sagittal view; **d**, **e**, dorsal views.

BIOLOGY OF REPRODUCTION 57, 385–393 (1997)

# Production of Cloned Lambs from an Established Embryonic Cell Line: A Comparison between In Vivo- and In Vitro-Matured Cytoplasts[1]

**David N. Wells,[2,3] Pavla M. Misica,[3] (Tony) A.M. Day,[4] and H. Robin Tervit[3]**

*AgResearch,[3] Ruakura Research Centre, Hamilton, New Zealand*
*Tony Day Veterinarian Ltd.,[4] c/o Ruakura Research Centre, Hamilton, New Zealand*

## ABSTRACT

**Nuclear transfer procedures were used to determine the in vivo developmental potential of an ovine embryonic cell line isolated from the inner cell mass of a Day 8 blastocyst-stage embryo. This cell line possessed a differentiated epithelial-like cell morphology. In this study, a comparison was made between in vivo- and in vitro-derived oocytes used as recipient cytoplasts in the nuclear transfer procedure. Cultured cells were induced to quiesce and enter presumptive G0 before being used as donor karyoplasts between passages 8 and 16 of culture. After cell fusion, reconstructed embryos were cultured for 6 days in vitro in embryo culture medium. Blastocyst-stage embryos were subsequently transferred to synchronized recipient ewes (n = 37), and development was allowed to proceed to term. There was a significant effect of source of recipient cytoplast, with development being consistently greater with in vivo compared to in vitro cytoplasts in terms of, respectively, blastocysts produced (24.2 ± 3.8% vs. 17.1 ± 2.3%; $p = 0.1$), Day 35 pregnancy rate (40.0% vs. 9.1%; $p < 0.05$), and Day 35 embryo survival (19.4% vs. 4.5%; $p < 0.05$). A high proportion of fetuses died during late gestation (5 of 8). The major abnormalities were associated with the urogenital tract. However, three lambs were delivered alive following cesarean section on Day 147. One lamb, derived from an in vitro-matured oocyte, died after 10 min, while the remaining two from in vivo-ovulated oocytes are apparently normal and healthy. DNA microsatellite markers conclusively show that the three lambs are genetically identical and were derived from the embryonic cell line. In conclusion, some cells from this blastocyst-derived embryonic cell line are totipotent by nuclear transfer and can produce viable offspring.**

## INTRODUCTION

Over the past decade, considerable research effort has been spent attempting to establish embryonic stem (ES) cell lines from farm animal species. The prime reason for isolating these undifferentiated, pluripotent cells has been to provide a means of generating transgenic livestock other than by pronuclear injection of DNA. With use of conventional cell genetic techniques, precise genetic modifications could be made while the cells are in culture, and after selection, the altered stem cells could be used to contribute to the germline following the production of a chimeric animal. In the mouse, the ES cell and gene targeting technologies have become routine procedures to introduce desired genetic change into the genome [1].

In recent years there have been numerous claims of cell lines possessing "ES-like" characteristics in a number of species, including the pig [2], cow [3], sheep [4], rabbit [5], hamster [6], mink [7], rat [8], and primate [9]. While some cultured cell populations have contributed to somatic chimeras in the pig [2], rabbit [10], and rat [8], and furthermore with evidence of cultured cells contributing to primordial germ cells and/or gonadal tissue in pigs [11] and cattle [12], as yet there are no reports of germline transmission of cultured cells in any species other than the mouse. Germline chimeras in farm animals, even once they are generated, will be problematic with the considerably longer generation intervals involved as compared to those for mice. This, coupled with the undoubtedly low frequency of germline transmission, will result in substantial animal costs, probably necessitating the screening of stem cell-derived sperm or oocytes from chimeras.

An alternative strategy has been to consider using ES cells for nuclear transfer and to produce an animal derived entirely from a cultured cell, thus bypassing the chimeric step. The possibility of this approach in farm animals originated from the work of Smith and Wilmut [13] whereby they produced a lamb that developed to term following fusion of an enucleated metaphase II oocyte to a sheep inner cell mass cell—a cell lineage that potentially could be maintained as ES cells. This work was later repeated with bovine inner cell mass cells [14, 15]. In subsequent studies, lambs were produced from primary cell cultures derived from an ovine Day 9 embryonic disk up to passage 3 [16], but not from later-passage cells, following the transfer of unsynchronized donor nuclei to in vivo-matured preactivated cytoplasts [17]. Similar investigations on the totipotency of bovine ES-like cell lines have been conducted by Stice and colleagues [3]. However, using in vitro-matured cytoplasts, pregnancies have not been maintained beyond Day 55, and despite apparently normal fetal development, the pregnancies appear to fail because of a deficiency in placentome development [3].

The eventual production of lambs from cells of an established embryonic cell line was achieved by inducing the cells to exit the normal cell division cycle and enter a quiescent or G0 state [17]. This result was all the more extraordinary because the cultured cells used were not ES cells but a more differentiated epithelial cell type (denoted "TNT," or totipotent for nuclear transfer). This raises the possibility that nuclei from other cell types can be similarly reprogrammed and yield offspring. Nuclear transfer has previously been utilized to determine the developmental potential of embryonic nuclei and to establish when they become restricted and no longer totipotent, especially in amphibians (see [18]) and to a more limited extent in mammals [13, 15, 19–21]. Now, with the prospect of synchronizing cells in G0, the totipotency of the cell nucleus in a range of differentiated cell types may be restored.

In this study we have examined the in vivo developmental potential of one of our established ovine embryonic cell lines by nuclear transfer and demonstrate the production of viable lambs. This report also details the effects of

Accepted April 1, 1997.
Received February 27, 1997.
[1]This research was supported by the Foundation for Research Science and Technology, New Zealand (contract number C10 402).
[2]Correspondence: David N. Wells, AgResearch, Ruakura Research Centre, PB 3123, Hamilton, New Zealand. FAX: 64-7-8385536; e-mail: wellsd@agresearch.cri.nz

in vivo- or in vitro-produced cytoplasts on subsequent blastocyst and fetal development following a period of in vitro culture.

## MATERIALS AND METHODS

### *Isolation of the Embryonic Cell Line*

The cell line used in this study was isolated from the inner cell mass of a Day 8 in vivo-produced embryo, obtained from a superovulated Romney ewe inseminated with frozen/thawed East Friesian semen (Silverstream East Friesian Ltd., Dunedin, New Zealand). Cell culture was initiated on a feeder cell layer of mitotically inactivated mouse STO fibroblasts [22] in 20-μl drops of medium under paraffin oil (Squibb, Princeton, NJ) on 5-cm tissue culture plates (Falcon; Becton Dickinson Labware, Lincoln Park, NJ). Medium consisted of Dulbecco's Minimum Eagle's medium/Ham's F12 (DMEM/F12) supplemented with 15% fetal calf serum (FCS; Life Technologies, Auckland, New Zealand), 0.1 mM 2-mercaptoethanol (Sigma Chemical Co., St. Louis, MO), and 10 ng/ml human leukemia inhibitory factor (Amrad, Uppsala, Sweden). After 8 days of culture, an expanding putative ES cell-like colony comprising several thousand cells was disaggregated into many small aggregates after incubation in a 0.25% (w:v) trypsin (porcine pancreas; Life Technologies) and 0.04% (w:v) EGTA (Sigma) solution for 7 min at 37°C. The cells were passaged onto a fresh feeder cell layer prepared in a well of a four-well plate (Nunc, Roskilde, The Netherlands). During passage 1, cell colonies began to differentiate into more flattened, epithelial-like cells. This cell morphology was stable, and colonies were expanded at each subsequent passage after brief incubation in the trypsin solution described above. The cell line was routinely maintained on gelatin-coated 5-cm tissue culture plates (Falcon) from passage 5 onward, up to at least passage 30. Aliquots of early-passage cells were frozen in 10% dimethyl sulfoxide (BDH, Poole, Dorset, England) and stored in liquid nitrogen. This (male) embryo-derived epithelial cell line has been designated REF38b (Romney × East Friesian), and the cell morphology is illustrated in Figure 1A.

### *Karyotyping REF38b*

Chromosome counts were determined at passages 12 and 24 of culture following the preparation of metaphase spreads essentially as described elsewhere [23]. Cells were arrested in metaphase by addition of 0.02 μg/ml of colcemid (Sigma) to the culture medium for 4 h. The cells were then trypsinized and resuspended in 0.075 M KCl for 20 min at 37°C. Cells were pelleted and fixed in three changes of ice-cold acetic methanol (1:3, v:v) before drops of cell suspension were applied to clean microscope slides. Chromosomes were stained in a 3% (v:v) solution of Gurr's Giemsa stain (BDH) in PBS for 10 min.

### *In Vivo Oocyte Production*

In vivo-ovulated metaphase-arrested (MII) oocytes were recovered from mature superovulated Romney or Romney-cross ewes. The estrous cycles of ewes were synchronized with two sequentially administered, controlled intravaginal progesterone-releasing devices (CIDR, Type G; InterAg, Hamilton, New Zealand); the first device was inserted for 10 days and the second was inserted immediately after removal of the first and left in place for another 4 days. On the morning of the second CIDR insertion, 300 IU eCG (Folligon; Intervet, Boxmeer, The Netherlands) was administered concurrently with the first of eight equal injections of Ovagen (Immuno-Chemical Products [ICP], Auckland, New Zealand) administered twice daily. On the morning of the seventh injection of Ovagen, the CIDR was removed and the ewes were exposed to vasectomized teaser rams. Fifteen hours after CIDR withdrawal, a GnRH analogue (Fertagyl, 150 μg/ewe; Intervet) was administered (at approximately the time of estrus onset). Mature oocytes were recovered 33–34 h after GnRH injection by flushing the oviducts of each ewe, under surgical conditions, with Hepes-buffered Synthetic Oviduct Fluid (HSOF) supplemented with 0.3% (w:v) BSA (fraction V BSA; Sigma) [24].

### *In Vitro Oocyte Production*

Slaughterhouse ovaries were collected from mature ewes, placed in saline (30°C), and transported within 2 h to the laboratory. Cumulus-oocyte complexes (COCs) were recovered by aspiration of 1- to 5-mm follicles using a 20-gauge needle and negative pressure (40 mm Hg) delivered through a vacuum pump. COCs were collected into Hepes-buffered Tissue Culture Medium 199 (H199; Life Technologies) supplemented with 10 μg/ml heparin (Sigma) and 0.4% (w:v) BSA (ICP). Before in vitro maturation, COCs were assessed morphologically, and only those that possessed a compact, nonatretic cumulus oophorus-corona radiata and a homogenous ooplasm were selected. All selected COCs were washed thoroughly in H199 medium supplemented with 10% FCS (Life Technologies) before being washed once in bicarbonate-buffered Tissue Culture Medium 199 and 10% FCS. Ten COCs were transferred in 10 μl of this medium and placed into a 40-μl drop of maturation medium in 5-cm Petri dishes (Falcon) overlaid with paraffin oil (Squibb). The maturation medium comprised Tissue Culture Medium 199 supplemented with 10% FCS, 10 μg/ml ovine FSH (Ovagen; ICP), 10 μg/ml ovine LH (ICP), 1 μg/ml estradiol (Sigma), and 0.1 mM cysteamine (Sigma) [25]. Microdrop plates were cultured at 39°C in a humidified 5% $CO_2$ in air atmosphere for 24 h. After maturation, the cumulus-corona was totally removed by vortexing COCs in 0.1% hyaluronidase (from bovine testis; Sigma) in HSOF for 1 min, followed by three washes in H199 plus 10% FCS.

### *Nuclear Transfer*

*a) Enucleation.* Mature oocytes were enucleated by aspirating the first polar body and the metaphase II plate in a small amount of surrounding cytoplasm with a 30-μm (outer diameter) glass pipette. The oocytes had been previously stained in H199 medium containing 10% FCS, 5 μg/ml Hoechst 33342 (Sigma), and 7.5 μg/ml cytochalasin B (Sigma) for 20 min. Confirmation of successful enucleation was achieved by visualizing the karyoplast, while still inside the pipette, under ultraviolet light. In this manner, the oocyte was not exposed to ultraviolet light. After enucleation, the resulting cytoplasts were washed extensively in H199 supplemented with 10% FCS and held in this medium until injection of donor cells.

*b) Preparation of cells.* The donor cells used for nuclear transfer were synchronized in presumptive G0 by serum deprivation [17]. One day after routine passage, the culture medium was aspirated and the cells were washed three times with fresh changes of PBS before 5 ml of fresh medium containing only 0.5% FCS was added. The cells were returned to culture for a further 9–12 days before use.

Immediately prior to injection, a single cell suspension of the donor cells was prepared by standard trypsinization. The cells were pelleted and resuspended in H199 supplemented with 0.5% FCS, and they remained in this medium until injection.

Cells used for nuclear transfer in these experiments were between passages 8 and 16 of culture.

*c) Microinjection.* Recipient cytoplasts were dehydrated in H199 containing 10% FCS and 5% sucrose. This medium was also utilized as the micromanipulation medium. After trypsinization, cells were graded into small, medium, and large sizes with approximate diameters of 12 μm, 15 μm, and 20 μm, respectively. All cells were injected using the same 30-μm pipette. The pipette was introduced through the same slit in the zona pellucida as made during enucleation, and the cell was wedged between the zona and the cytoplast membrane to facilitate close membrane contact for subsequent fusion.

After injection, the reconstructed embryos were rehydrated in two steps: they were held in H199 containing 10% FCS and 2.5% sucrose for 5 min and then in H199 containing 10% FCS prior to fusion.

*d) Fusion/activation.* Reconstructed embryos were washed in fusion buffer for 5 min prior to electrofusion. The buffer comprised 0.3 M mannitol, 0.05 mM calcium, 0.1 mM magnesium, 0.5 mM Hepes, and 0.05% fatty acid-free (FAF) BSA (Sigma). Fusion was performed at room temperature, in a chamber with two stainless steel electrodes 500 μm apart overlaid with fusion buffer. The reconstructed embryos were manually aligned with a fine, mouth-controlled Pasteur pipette so that the contact surface between the cytoplast and the donor cell was parallel to the electrodes. Cell fusion was induced with two DC pulses of 2.0 kV/cm for 75 μsec each, delivered by a BTX Electrocell Manipulator 200 (BTX, San Diego, CA). This pulse was also utilized to simultaneously induce oocyte activation. Fusion and activation occurred between 27 and 30 h postmaturation for in vitro cytoplasts and between 38 and 40 h after GnRH injection for in vivo-derived cytoplasts. Following the fusion and activation pulse, the reconstructed embryos were washed in H199 and 10% FCS. They were then cultured for a period of 1 h in H199 supplemented with 10% FCS and 7.5 μg/ml cytochalasin B. Fusion was then determined by microscopic examination prior to in vitro culture.

### *In Vitro Culture of Nuclear Transfer Embryos*

Embryo culture was performed in 30-μl drops of SOFaaBSA (SOF supplemented with amino acids and 8 mg/ml FAF BSA [Sigma]) [26] overlaid with paraffin oil. Whenever possible, groups of 5–6 embryos were cultured together. Embryos were cultured in a humidified modular incubator chamber (ICN Biomedicals, Aurora, OH) at 39°C in a 5% $CO_2$:7% $O_2$:88% $N_2$ gas mix. On Day 3, embryos were transferred to fresh 30-μl drops of SOFaaBSA + 5% charcoal-stripped FCS (personal communication with JGE Thompson). On Day 6, the development of transferable-quality blastocysts was recorded.

### *Embryo Transfer*

Mature, multiparous Romney ewes were synchronized by a single 12-day CIDR treatment. Two days prior to CIDR withdrawal, each ewe received 200 IU eCG. After CIDR withdrawal, ewes were placed with vasectomized rams, and estrus onset was recorded during thrice-daily observations. Surgical embryo transfer was performed on Day 6 after estrus (estrus: Day 0). This corresponded to Day 6 of embryo culture (or Day 7 of embryo development; fusion: Day 1). Thus, blastocyst-stage embryos were transferred to a recipient uterus that was assessed to be 1 day less advanced. Typically, each ewe received two embryos, transferred into the uterine lumen ipsilateral to the preferred corpus luteum. However, depending upon the availability of embryos and recipients on a given day, some ewes received either one or three embryos. All ewes received a CIDR device, immediately following embryo transfer, that remained in place for approximately 14 days.

### *Pregnancy Assessment*

Blood samples were taken by jugular venipuncture on the day after withdrawal of the posttransfer CIDR (i.e., on approximately Day 21 of pregnancy), and plasma was extracted and frozen (−20°C) until assayed for progesterone by RIA (performed by the Dairying Research Corporation, Hamilton, New Zealand). Ewes were considered "biochemically pregnant" if plasma progesterone concentration was above 1.0 ng/ml [27].

All ewes were further assessed for pregnancy by ultrasonography at approximately Day 28 (Aloka 500, 5-MHz transducer; Aloka Co., Tokyo, Japan). Pregnant ewes were monitored by ultrasonography at weekly intervals thereafter, until at least Day 70.

Commencing approximately 2 wk before expected full term, ewes were monitored closely and fetal heartbeats confirmed by stethoscopic examination. Late-gestation deaths and abortions were recorded, and fetuses were recovered for examination of gross anatomy and histology by veterinary pathologists.

### *Lambing*

The initial intention was to allow parturition to commence naturally. However, during the course of the experiment it became apparent that intervention was necessary, and cesarean sections were performed on Day 147 of gestation, either with or without an injection of dexamethasone (5 mg Dexadreson; Intervet) administered 40 h earlier.

### *Health Tests of Lambs*

Blood samples were taken by jugular venipuncture for biochemical and hematological analyses 6 days after birth and at approximately fortnightly intervals thereafter.

### *Microsatellite Analyses*

Genomic DNA was extracted from tissues of nuclear transfer-derived fetuses (muscle) and liveborn lambs (white blood cells) utilizing DNAzol reagent (Life Technologies) and a guanidine hydrochloride method [28], respectively. In addition, DNAzol reagent was also used to isolate DNA from the REF38b tissue culture cell line. The polymerase chain reaction was utilized to amplify microsatellite markers (OarHH64, OarHH41, OarAE25, BM8125, and JMP29; generous gifts from Dr. Grant Montgomery, AgResearch Molecular Biology Unit, University of Otago, New Zealand) as described elsewhere [29], with the exception that [$\gamma$-$^{33}$P]ATP (Amersham Life Science, Buckinghamshire, England) end-labeled primer was used. Nuclear transfer-derived fetal and lamb DNA microsatellite results were compared with the DNA marker profile of the embryonic cell line used to produce the animals, as well as that of the

TABLE 1. Effect of cytoplast source on the percentage of reconstructed nuclear transfer embryos that fused and the percentage of fused embryos developing to the blastocyst stage following in vitro culture (mean ± SEM).

| Cytoplast | NT* | Replicates | % Fused | % Blastocytes |
|---|---|---|---|---|
| In vivo | 258 | 3 | 64.0 ± 3.4 | 24.2 ± 3.8 |
| In vitro | 407 | 9 | 63.4 ± 2.4 | 17.1 ± 2.3 |

* NT, number of reconstructed nuclear transfer embryos.

East Friesian sire used to generate the original embryo from which the cell line was derived. These DNA profiles were contrasted with those of the recipient ewes that carried the respective pregnancies. As negative controls, DNA was obtained from five random Romney-cross male lambs (Limestone Downs Station, Port Waikato, New Zealand) sired by the same East Friesian ram used to generate the cell line in this study.

### *Animal Ethics*

This project was approved by both the AgResearch Ruakura Animal Ethics Committee and the AgResearch Ruakura Biosafety Committee.

### *Statistical Analyses*

The embryo development results were analyzed as binomial data using a log linear procedure in the GENSTAT 5 statistical package (Lawes Agricultural Trust, Rothamsted, UK). Pregnancy and embryo survival rates were analyzed by Fisher's exact probability test within the GENSTAT program.

## RESULTS

### *Karyotype of the REF38b Cell Line*

Of 120 metaphase spreads examined at passage 12, 50 (42%) possessed a normal 54 chromosome count, including 6 metacentric chromosomes and a Y chromosome. An additional 32 spreads (27%) were hypodiploid and may have been artifacts of preparation. However, a substantial 27% of the population were tetraploid, and 4% of spreads possessed a small seventh metacentric chromosome. Karyotypically, the cell line was largely stable: by passage 24, among the 103 spreads examined, the proportions of normal diploid cells and tetraploid cells had not altered significantly (41% and 29%, respectively). However, the proportion of cells containing the seventh metacentric chromosome had risen to 13% ($p < 0.05$).

### *Embryo Development*

The development of embryos reconstructed by nuclear transfer using quiescent REF38b cells and in vivo- or in vitro-derived MII cytoplasts is summarized in Table 1. All 12 replicates of this experiment yielded blastocysts following in vitro culture (Fig. 1B). Fusion rate was not affected by oocyte source or size of cell. Development to blastocyst from those reconstructed embryos that fused tended to be greater with in vivo-derived cytoplasts than with in vitro-matured cytoplasts (31 of 128 vs. 44 of 258; $p = 0.1$). The overall efficiency of blastocyst production from the total number of reconstructed embryos for in vivo and in vitro cytoplasts was not significantly different at 15.5 ± 2.6% and 10.8 ± 1.5%, respectively. No significant difference was observed in the frequency of blastocyst development with passage number (between 8 and 16) or size of donor cell.

### *Pregnancy Rate and Embryo Survival*

The proportion of recipient ewes classified as biochemically pregnant on Day 21 was 20 of 37 (54%, Table 2) and did not differ with source of cytoplast. From ultrasonography on Day 35, more pregnancies were lost with in vitro cytoplasts (9 of 11 biochemically pregnant) than in vivo cytoplasts (only 3 of 9). One more in vivo cytoplast pregnancy was lost by Day 70, and the remaining 7 single-bearing pregnancies were maintained until near full term. There was no effect of cell size on pregnancy rate.

Four of the seven pregnancies were lost late in gestation: one was lost on each of Days 134 and 141, and two fetuses died in utero on Day 154. Of these two, one was subsequently aborted and the other was recovered after the recipient ewe was killed. All four fetuses had significant abnormalities (see below). Three were derived from large-sized cells at either passage 10 or 14, while the fourth was from a small-sized cell at passage 8.

Three lambs were delivered alive by cesarean section on Day 147 of gestation. One lamb (L68) was produced from an in vitro-matured oocyte reconstructed with a medium-sized cell at passage 8. This animal breathed for 10 min before dying of respiratory failure. The other two lambs were delivered on November 28, 1996, following an induction with dexamethasone; these were derived from in vivo-ovulated cytoplasts receiving either one medium-sized or one small-sized cell, at passage 9. These two lambs (L5 and L35) are apparently normal (Fig. 1C) and have been shown to be physiologically healthy and thriving with excellent daily live weight gains (see below).

The birth weight of two of the liveborn lambs was 6.8 kg, while that of the third (L35) was only 3.0 kg. The placenta from L35 had a substantial amount of necrosing tissue that may have compromised fetal growth.

### *Microsatellite Analyses*

All seven cloned lambs or late fetuses produced were phenotypically male—the same sex as REF38b cells. DNA analyses using microsatellite markers conclusively demonstrated the lambs to have originated from the REF38b cell line (Fig. 1D). Lane 1 is from the East Friesian sire (B75) used to produce the original embryo from which the REF38b cell line was derived, shown in lane 2. Lanes 3–6 represent the fetuses lost on Days 134, 141, 154, and 154, respectively. The three liveborn lambs (L68, L5, and L35) are shown in lanes 7, 8, and 9, respectively. All the fetuses and lambs showed a pattern identical to that of the cell line, with the two alleles indicated by arrows. Lanes 10–15 show the recipient ewes that carried the respective pregnancies (DNA from the ewe that carried the aborted fetus in lane 3 is missing), with both alleles distinctly different from those of the cloned animals except for the uppermost allele in lane 15. In this case, subsequent analysis with the microsatellite marker JMP29 showed the ewe to be genetically unrelated to the cloned lamb. Finally, lanes 16–20 show the genotype of five random Romney × East Friesian ram lambs sired by B75, none of which showed a pattern identical to that of the nuclear transfer group. DNA samples from the nuclear transfer-derived animals were examined at four other microsatellite loci (OarHH41, OarAE25, BM8125, and JMP29) and provided unequivocal confir-

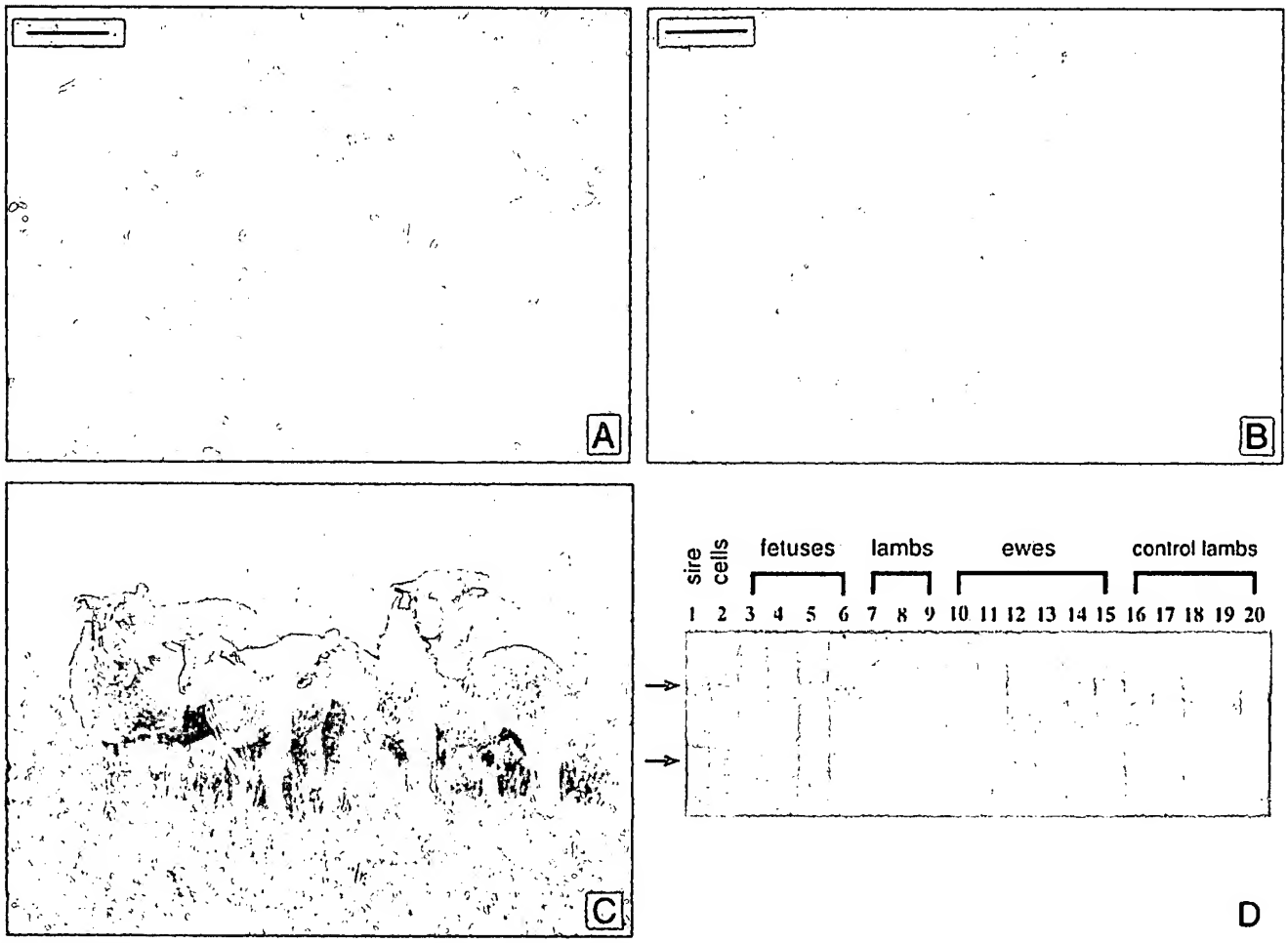


FIG. 1. Demonstration of the totipotency of the REF38b cell line. A) Morphology of REF38b cells at passage 12. B) A hatching blastocyst in SOFaaBSA medium 6 days after fusion of an REF38b cell to an in vivo cytoplast. A, B) Bar = 50 μm. C) Two lambs (at 7 wk of age) produced by nuclear transfer with cells from the established embryonic cell line REF38b. D) Autoradiogram demonstrating the genetic origin of both the cloned lambs and the aborted fetuses with the microsatellite OarHH64 (refer to text).

mation that the cloned fetuses and lambs were all genetically identical.

### *Fetal Abnormalities*

The four aborted fetuses all exhibited underdevelopment for their respective ages (based primarily on wool development), varying degrees of edema and hydronephrosis, and testicular hypoplasia. Three fetuses each had a unique abnormality not observed in another animal, including an interventricular septal defect, a cleft palate, and an undershot jaw. There were few overt indications of readiness for parturition in the recipients of the aborted pregnancies. Similarly, in the ewes that produced the three liveborn lambs, development of the mammary gland had begun prior to Day 147 but still appeared to be substantially less than expected from multiparous ewes carrying nonmanipulated fetuses at a similar stage of pregnancy.

Dissection of the lamb (L68) that died after 10 min revealed a considerable amount of unexplained "froth" in the airways of the lungs. Lung histology was normal, and plasma cortisol, as determined after cardiac puncture, was considered high (87 ng/ml). Necropsy and histology of other organs showed the only other abnormality to be moderate bilateral hydronephrosis. However, there was considered to be sufficient kidney tissue present for normal function, and there was no edema.

### *Lamb Health and Growth Rate*

Blood biochemistry results taken 6 days after birth showed that serum urea and electrolyte levels were within the normal range in both L5 and L35, indicating normal

TABLE 2. Pregnancy rate and embryo survival of nuclear transfer-produced blastocysts.

| | Pregnancy rate (%) | | Embryo survival (%) | |
|---|---|---|---|---|
| Source of cytoplast | In vivo | In vitro | In vivo | In vitro |
| Number | 15* | 22* | 31** | 44** |
| Day 21 (biochemical) | 9 (60.0) | 11 (50.0) | — | — |
| Day 35 (scanning) | 6 (40.0)[a] | 2 (9.1)[b] | 6 (19.4)[c] | 2 (4.5)[d] |
| Day 70 (scanning) | 5 (33.3) | 2 (9.1) | 5 (16.1) | 2 (4.5) |
| Late abortions | 3† | 1†† | 3† | 1†† |
| Live lambs | 2 (13.3) | 1 (4.5) | 2 (6.5) | 1 (2.3) |

* Recipient ewes.
** Embryos transferred.
† Fetuses lost on Days 134, 154, 154.
†† Fetus lost on Day 141.
[a–d] $p < 0.05$ for ab and cd.

kidney function. This was confirmed with subsequent animal health tests at 3 and 6 wk of age. However, initial tests showed that red and white blood cell counts were slightly lower in one lamb (L35), and a vitamin and amino acid supplement (Hemo 15; Sanofi Animal Health, Victoriaville, PQ, Canada) was given. Subsequent tests revealed both lambs to be mildly anemic, probably as a consequence of an associated *Eperythrozoon ovis* infection. Anemia was remedied by dosing daily with 5 ml Collovet Animal Tonic (Young's Animal Health, Upper Hutt, New Zealand) for 2 wk.

Colostral transfer from the ewes to the lambs following the induction of parturition was poor (as is often the case [30]), so a supplementary clostridial vaccination was administered (Vaxall; Arthur Webster Ltd., Castle Hill, New South Wales, Australia). Additionally, it became clear that L5 was not receiving sufficient milk from the dam, and supplementary feeding with Anlamb powdered milk replacer (Anchor, Auckland, New Zealand) was initiated.

The mean daily live weight gain of the two lambs reared outdoors, between birth and weaning at 12 wk of age, was not significantly different and averaged 313 ± 8 g/day.

## DISCUSSION

In this study we demonstrate the totipotency of one of our established ovine embryonic cell lines following nuclear transfer. Three liveborn cloned lambs were delivered, and currently two are apparently normal and healthy (at 12 wk of age). This result is significant in that full-term development was achieved in a cloned lamb derived from a cultured cell using an entirely in vitro embryo production system. This is an advance on the first study of cloned lambs from cultured cell lines, in which in vivo-derived oocytes and in vivo culture, in a ligated sheep oviduct, were utilized [17]. In fact, the majority of cloning studies in sheep, with preimplantation embryo cells, have utilized in vivo-ovulated oocytes as cytoplasts [13, 31, 32]. Although the use of in vitro-matured oocytes is commonplace in cattle embryo cloning [33–35], to our knowledge there is only one previous instance of cloned lambs having been produced from in vitro cytoplasts (using embryo blastomeres) (Anne Pugh, personal communication), while other pregnancies have been lost around Day 60 of gestation [36].

This study, along with an earlier investigation [17], is a significant advance toward the production of transgenic livestock. We have demonstrated the successful reprogramming of nuclei from a differentiated epithelial cell line and produced live lambs. Extensive research has focused on the isolation of ES cells from farm animals. These undifferentiated cells, isolated from the inner cell mass or primordial germ cells, are potential candidate cell lines for genetic manipulation. They could then be utilized to generate germline chimeras or, indeed, nuclear transfer-derived animals. However, there have been difficulties in both the establishment of stem cells in culture and the generation of animals from them [2, 3, 37]. With refined nuclear transfer technology [17], it appears that nuclear reprogramming may occur in many different cell types, thus negating the originally perceived requirement for ES cells. We have additional pregnancies from an embryonic fibroblast cell line (unpublished results), and others have successfully reprogrammed nuclei from fetal and adult cells and produced lambs (Dr. Ian Wilmut, personal communication). Collectively, these results do not exclude continued interest in stem cell isolation, as presumably nuclear reprogramming will be easier with less differentiated cells and thus improved efficiencies might be expected.

There has been previous interest in utilizing cloning from embryonic blastomeres to multiply animals of high genetic merit [38]. If efficiencies can be improved, consideration could be given to cloning from primary cell cultures from individual elite embryos and thus having access to several hundreds or thousands of cells. Utilizing early-passage cells in this way may make it possible to avoid many of the developmental problems associated with some established cell lines. This may be a better approach to generating large numbers of genetically identical animals than the serial recloning of embryos [39].

The cell line used in these studies is derived from a Day 8 inner cell mass and is established in culture, having been stably maintained for 30 passages and frozen and thawed during this time. This relates to at least 75 cell doublings, so it is not known whether the cells are truly immortal. The cells express cytokeratin-18 indicative of early epithelial cell differentiation [40] and grow as a monolayer. We consider there to be sufficient growth potential in this cell line to allow time for selection following genetic modification. The average cell doubling time is 24 h. This is considerably slower than that of many (but not all) mouse ES cell lines. This has implications for procedures such as homologous recombination, as the more slowly cells grow the less efficient gene targeting becomes [41].

The efficiency of producing cloned lambs from cultured cells achieved here is at least equal to that reported by Campbell and colleagues [17]. They showed that with in vivo cytoplasts, and after a period of in vivo culture, 14% of reconstructed embryos developed to morula/blastocyst. We achieved 16% blastocysts with in vivo cytoplasts after in vitro culture, and with incorporation of in vitro maturation, the blastocyst rate was reduced slightly to 11%. Only blastocyst development is expressed here in our work, as morulae present after 6 days of in vitro culture would be expected to survive poorly following embryo transfer [42]. The overall efficiency of viable lambs from total reconstructed oocytes with in vivo cytoplasts (1.0%) is also similar to that reported previously (0.8%) [17].

It appears that modifying the donor karyoplast, by inducing the cells into a quiescent G0 cell-cycle state, is a critical event for nuclear totipotency. Cells used for nuclear transfer were synchronized in presumptive G0 by culture in media containing low serum, as described previously [17], for 9–12 days. Specific markers demonstrating exit from the normal cell cycle and induction of G0 were not used here. However, after 4 days of culture in low-serum media, the cells had reached confluence and remained essentially quiescent during the remainder of culture. There was also evidence of nuclear remodeling, with fewer nucleoli present in the presumptive G0 cells as compared to mitotic cultures. The chromatin of quiescent nuclei has been reported to undergo modification, along with decreases in the levels of transcription [43]. As a consequence, the introduced G0 nucleus from a differentiated cell may be more readily reprogrammed following reconstruction, so that it behaves as if it were a zygotic nucleus.

After nuclear transfer, the reprogramming of the donor nucleus most probably involves oocyte factors stored in the maternal recipient cytoplast and the exchange of these factors with the introduced nucleus [44]. The quality of the recipient cytoplast affects gene expression during nuclear reprogramming in the mouse [45], and the lower rates of blastocyst production and fetal survival from the in vitro-

matured cytoplasts reported here most probably relate to the poorer quality of the ooplasm. Improving in vitro oocyte quality, particularly cytoplasmic maturation, is an important area of future research that will also benefit nuclear transfer.

Fusion rates (64%) were not affected by cytoplast source, in contrast to findings reported earlier [36]. We consider the rate satisfactory, especially given the small relative size of the cultured cells, which posed technical difficulties in the accurate alignment of the reconstructed embryo within the fusion chamber. It might be possible to increase cell fusion rates following the generation of isofusion contours [46] in order to optimize the electrofusion parameters for each particular cell line under investigation.

There was no significant effect of size of donor cell on subsequent blastocyst development or embryo survival. Differences in cell size might relate simply to the availability of space in the culture dish or to differences in ploidy. Although cells greater than 20 μm in diameter were present in the population, they were not used for nuclear transfer. It is noteworthy that of the four abnormal fetuses lost near full term, three were derived from large-sized cells, whereas the three liveborn lambs were produced from small- and medium-sized cells. Unfortunately, due to autolysis, we were unable to karyotype any of the aborted fetuses. However, data from a preliminary slaughter trial showed that fetuses derived from cells classified as small or medium can possess an abnormal seventh metacentric chromosome (present in 4% of cells). This is thought to have arisen from chromosomal duplication and fusion to an existing acrocentric chromosome. Clearly there are karyotypically abnormal cells in the parental REF38b cell line; and although the developmental problems encountered in the near-term fetuses might not necessarily relate to these chromosomal abnormalities, overall efficiencies would be expected to increase if clonal sub-lines were established. This emphasizes the importance of using a karyotypically normal cell line for nuclear transfer and, furthermore, one that is stable with increasing passage number.

The in vitro culture system utilized here was a development on the previously reported SOFaaBSA system [26]. After 3 days of culture the medium was changed to SOFaaBSA supplemented with 5% charcoal-stripped FCS. This has been shown to increase the rates of blastocyst formation and also to result in a relatively high percentage of embryos surviving to term in cattle (JGE Thompson, personal communication). This system is also noted for the absence of high birth weight calves (JGE Thompson, personal communication). Its effect, however, on sheep in vitro embryo production, subsequent embryo survival, and birth weight has not been examined before this study.

The ability of the blastocyst-stage embryo to elongate, produce interferon τ, and initiate organogenesis, in conjunction with attachment to the endometrium, is the most critical time for the developing conceptus. Generally, most embryonic loss occurs before Day 35 in sheep [47]. However, embryo cloning is typified by higher-than-normal instances of late-gestation fetal loss [34, 35]. The finding here that 46% of recipient ewes had low progesterone on Day 21 suggests that the cloned embryos either failed to continue to develop in utero or that the elongating trophectoderm may not have produced sufficient interferon τ to maintain corpus luteum function and establish pregnancy [48]. This is in contrast to what occurs with in vitro-produced sheep embryos, where only 24% of pregnancies fail by Day 15 with only a small loss to Day 60 [27]. More nuclear transfer pregnancies were lost between Days 21 and 35 with in vitro compared to in vivo cytoplasts, culminating in lower embryo survival. Morphological assessment showed embryo quality to be poorer with in vitro cytoplasts (although no cell counts were performed). While there may have been sufficient trophoblast to initiate some nuclear transfer pregnancies, failure beyond Day 21 was possibly a consequence of poor inner cell mass formation in the initial blastocyst. Alternatively, it may be that cytoplasmic maturation of the in vitro-matured oocytes was inadequate to completely reprogram the donor nucleus and that inappropriate gene expression subsequently compromised inner cell mass differentiation and the embryo eventually died. The poor embryo survival with in vitro-matured cytoplasts was disappointing, as 58% (30 of 59) of grade 1 and 2 in vitro-produced sheep blastocysts cultured in SOFaaBSA have recently survived to full term (unpublished results) as compared to the present observation of only 2.3% survival following nuclear transfer.

The general deformities are similar between the aborted fetuses reported here and the first lambs produced by Campbell and colleagues [17], particularly the kidney abnormalities [49], perhaps suggesting a problem with the nuclear transfer procedure. The developmental abnormalities may relate to (epi)genetic defects associated with the particular cell line used in these studies, either intrinsic or acquired as a consequence of the manipulation procedures. Possible disruptions to the regulation of (imprinted) genes resulting from the culture of the cell line, or after nuclear transfer, could lead to perturbations in embryo and fetal development [50]. These effects may become more predominant with later-passage cultures, as the only liveborn lambs produced here were from cells at passages 8 and 9, the two youngest passages used for cloning.

Two of the cloned lambs born did have Day 147 birth weights considerably higher than the average expected with in vitro-produced sheep embryos [27, 42]. Large offspring, perinatal deaths, and poor adaptation to extrauterine life have been reported previously and may relate to the nuclear transfer procedure and/or some aspect of the in vitro culture systems used [50–52]. However, in the SOF-based culture system used here, supplementation with BSA or charcoal-stripped FCS rather than human serum prevents the incidence of prolonged gestation and large birth weights ([27] and JGE Thompson, personal communication). Thus, the large lambs are more likely a consequence of the cloning procedures than the in vitro culture system.

In some of the nuclear transfer pregnancies, there appeared to be problems with either the fetal hypothalamic-anterior pituitary-adrenal axis and/or the transduction of the resulting rise in fetal cortisol to the ewe near the time of birth [53]. At some point in this cascade, there appeared to be a breakdown in communication between the fetus and the ewe, and the appropriate signaling in preparation for birth did not occur. In the present study this phenomenon was particularly apparent in the two abnormal fetuses that went 7 days over their expected due date before dying in utero. Similar problems with fetal-maternal signaling may have also been associated with the three pregnancies that yielded the liveborn lambs, as evidenced by inadequate mammary gland development in the recipient ewes. Nevertheless, one of these three lambs was bled shortly after its death (L68) and had elevated plasma cortisol levels, suggesting fetal maturity, adequate pulmonary surfactant production, and thus preparation for birth [54].

This report confirms the original findings of Campbell

and colleagues [17] that it is possible to produce animals that are entirely derived from a single cell from a cultured cell line by nuclear transfer. Although it is clear that the current efficiencies are very low (1%) and a high proportion of the animals are abnormal and not viable, future research should eliminate these problems. With this achieved, this technology could have tremendous applications in basic research, animal breeding, and particularly biotechnology. The ability to use powerful genetic techniques to modify cells while they are in culture will provide enormous benefits in producing transgenic livestock compared to current pronuclear injection procedures [55].

## ACKNOWLEDGMENTS

We wish to thank the staff of the Reproductive Technologies Group, AgResearch Ruakura, for their support and assistance throughout this project. Special thanks go to John Lange for his care of the experimental animals, Robyn Wells for surgical assistance, Lindsay McGowan for pregnancy scanning, and Lydia Weilert and Helen Davey for assisting with DNA analyses. Finally, we gratefully acknowledge the help of staff from the Ruakura Animal Health Laboratory for the hematological and serum biochemistry analyses and particularly Angus Black and Alan Julian for the postmortem examinations.

## REFERENCES

1. Hooper ML. Embryonal Stem Cells: Introducing Planned Changes into the Animal Germline. Chur, Switzerland: Harwood Academic; 1992.
2. Wheeler MB. Development and validation of swine embryonic stem cells: a review. Reprod Fertil Dev 1994; 6:563–568.
3. Stice SL, Strelchenko NS, Keefer CL, Matthews L. Pluripotent bovine embryonic cell lines direct embryonic development following nuclear transfer. Biol Reprod 1996; 54:100–110.
4. Notarianni E, Galli C, Laurie S, Moor RM, Evans MJ. Derivation of pluripotent, embryonic cell lines from the pig and sheep. J Reprod Fertil Suppl 1991; 43:255–260.
5. Graves KH, Moreadith RW. Derivation and characterization of putative pluripotential embryonic stem cells from preimplantation rabbit embryos. Mol Reprod Dev 1993; 36:424–433.
6. Doetschman T, Williams P, Maeda N. Establishment of hamster blastocyst-derived embryonic stem (ES) cells. Dev Biol 1988; 127:224–227.
7. Sukoyan MA, Golubitsa AN, Zhelezova AI, Shilov AG, Vatolin SY, Maximovsky LP, Andreeva LE, McWhir J, Pack SD, Bayborodin SI, Kerkis AY, Kizilova HI, Serov OL. Isolation and cultivation of blastocyst-derived stem cell lines from American Mink (*Mustela vison*). Mol Reprod Dev 1992; 33:418–431.
8. Iannaccone PM, Taborn GU, Garton RL, Caplice MD, Brenin DR. Pluripotent embryonic stem cells from the rat are capable of producing chimaeras. Dev Biol 1994; 163:288–292.
9. Thomson JA, Kalishman J, Golos TG, Durning M, Harris CP, Hearn JP. Pluripotent cell lines derived from common Marmoset (*Callithrix jacchus*) blastocysts. Biol Reprod 1996; 55:254–259.
10. Schoonjans L, Albright GM, Li J-L, Collen D, Moreadith RW. Pluripotential rabbit embryonic stem (ES) cells are capable of forming overt coat color chimeras following injection into blastocysts. Mol Reprod Dev 1996; 45:439–443.
11. Shim H, Gutiérrez-Adán A, Chen LR, BonDurant RH, Anderson GB. Isolation of pluripotent stem cells from cultured porcine primordial germ cells. Theriogenology 1997; 47:245 (abstract).
12. Cibelli JB, Stice SL, Kane JJ, Golueke PG, Jerry J, Dickinson ES, Gao XY, Ponce de León A, Robl JM. Production of germline chimeric bovine fetuses from transgenic embryonic stem cells. Theriogenology 1997; 47:241 (abstract).
13. Smith LC, Wilmut I. Influence of nuclear and cytoplasmic activity on the development in vivo of sheep embryos after nuclear transplantation. Biol Reprod 1989; 40:1027–1035.
14. Keefer CL, Stice SL, Matthews DL. Bovine inner cell mass cells as donor nuclei in the production of nuclear transfer embryos and calves. Biol Reprod 1994; 50:935–939.
15. Collas P, Barnes FL. Nuclear transplantation by microinjection of inner cell mass and granulosa cell nuclei. Mol Reprod Dev 1994; 38: 264–267.
16. Campbell K, McWhir J, Ritchie B, Wilmut I. Production of live lambs following nuclear transfer of cultured embryonic disc cells. Theriogenology 1995; 43:181 (abstract).
17. Campbell KHS, McWhir J, Ritchie WA, Wilmut I. Sheep cloned by nuclear transfer from a cultured cell line. Nature 1996; 380:64–66.
18. DiBerardino MA. Genomic potential of differentiated cells analyzed by nuclear transplantation. Am Zool 1987; 27:623–644.
19. Collas P, Robl JM. Development of rabbit nuclear transplant embryos from morula and blastocyst stage donor nuclei. Theriogenology 1991; 35:190 (abstract).
20. Kono T, Kwon OY, Ogawa M, Nakahra T. Development of mouse oocytes receiving embryonic nuclei and thymocytes. Theriogenology 1991; 35:227 (abstract).
21. Moens A, Chesne P, Delhaise F, Delval A, Ectors F-J, Dessey F, Renard J-P, Heyman Y. Assessment of nuclear totipotency of fetal bovine diploid germ cells by nuclear transfer. Theriogenology 1996; 46:871–880.
22. Martin GR, Evans MJ. Differentiation of clonal lines of teratocarcinoma cells: formation of embryoid bodies in vitro. Proc Natl Acad Sci USA 1975; 72:1441–1445.
23. Freshney RI. Culture of Animal Cells: A Manual of Basic Technique, 3rd ed. New York: Wiley-Liss; 1994: 197–217.
24. Thompson JGE, Simpson AC, Pugh PA, Donnelly PE, Tervit HR. The effect of oxygen concentration on the in vitro development of preimplantation sheep and cattle embryos. J Reprod Fertil 1990; 89: 573–578.
25. de Matos DG, Furnus CC, Moses DF, Baldassarre H. Effect of cysteamine on glutathione level and developmental capacity of bovine oocyte matured in vitro. Mol Reprod Dev 1995; 42:432–436.
26. Gardner DK, Lane M, Spitzer A, Batt P. Enhanced rates of cleavage and development for sheep zygotes cultured to the blastocyst stage in vitro in the absence of serum and somatic cells: amino acids, vitamins and culturing embryos in groups stimulate development. Biol Reprod 1994; 50:390–400.
27. Thompson JG, Gardner DK, Pugh PA, McMillan WH, Tervit HR. Lamb birth weight is affected by culture system utilized during in vitro pre-elongation development of ovine embryos. Biol Reprod 1995; 53:1385–1391.
28. Montgomery GW, Sise JA. Extraction of DNA from sheep white blood cells. NZ J Agric Res 1990; 33:437–441.
29. Montgomery GW, Crawford AM, Penty JM, Dodds KG, Ede AJ, Henry HM, Pierson CA, Lord EA, Galloway SM, Schmack AE, Sise JA, Swarbrick PA, Hanrahan V, Buchanan FC, Hill DF. The ovine Booroola fecundity gene (FecB) is linked to markers from a region of human chromosome 4q. Nature Genet 1993; 4:410–414.
30. Dawe ST, Husband AJ, Langford CM. Effects of induction of parturition in ewes with dexamethasone or oestrogen on concentration of immunoglobulins in colostrum and absorption of immunoglobulins by lambs. Aust J Biol Sci 1982; 35:223–229.
31. Willadsen SM. Nuclear transplantation in sheep embryos. Nature 1986; 320:63–65.
32. McLaughlin KJ, Davies L, Seamark RF. In vitro embryo culture in the production of identical Merino lambs by nuclear transplantation. Reprod Fertil Dev 1990; 2:619–622.
33. Barnes F, Endebrock, Looney C, Powell R, Westhusin M, Bondioloi K. Embryo cloning in cattle: the use of in vitro matured oocytes. J Reprod Fertil 1993; 97:317–320.
34. Heyman Y, Chesne P, Lebourhis D, Peynot N, Renard JP. Developmental ability of bovine embryos after nuclear transfer based on the nuclear source: in vivo versus in vitro. Theriogenology 1994; 42:695–702.
35. Yang X, Jiang S, Farrell P, Foote RH, McGrath AB. Nuclear transfer in cattle: effect of nuclear donor cells, cytoplast age, co-culture, and embryo transfer. Mol Reprod Dev 1993; 35:29–36.
36. Holm P, Nagashima H, Sun F-J, Seamark RF. In vitro and in vivo development of cloned ovine embryos using in vitro and in vivo matured oocytes. Reprod Domest Anim 1995; 30:125–128.
37. Piedrahita JA, Anderson GB, BonDurant RH. On the isolation of embryonic stem cells: comparative behavior of murine, porcine and ovine embryos. Theriogenology 1990; 34:879–901.
38. Baker RL, Shannon P, Garrick DJ, Blair HT, Wickham BW. The future impact of new opportunities in reproductive physiology and molecular biology on genetic improvement programmes. Proc NZ Soc Anim Prod 1990; 50:197–210.
39. Stice SL, Keefer CL. Multiple generational bovine embryo cloning. Biol Reprod 1993; 48:715–719.

40. Galli C, Lazzari G, Flechon JE, Moor RM. Embryonic stem cells in farm animals. Zygote 1994; 2:385–389.
41. Udy GB, Parkes BD, Wells DN. ES cell cycle rates affect gene targeting frequencies. Exp Cell Res 1997; 231:(in press).
42. Holm P, Walker SK, Seamark RF. Embryo viability, duration of gestation and birth weight in sheep after transfer of *in vitro* matured and *in vitro* fertilized zygotes cultured *in vitro* or *in vivo*. J Reprod Fertil 1996; 107:175–181.
43. Whitfield JF, Boynton AL, Rixon RH, Youdale T. The control of cell proliferation by calcium, $Ca^{2+}$-calmodulin, and cyclic AMP. In: Boynton AL, Leffert HL (eds.), Control of Animal Cell Proliferation, Vol. 1. London: Academic Press; 1985: 331–365.
44. Prather RS, First NL. Cloning embryos by nuclear transfer. J Reprod Fertil Suppl 1990; 41:125–134.
45. Chastant S, Christians E, Campion E, Renard J-P. Quantitative control of gene expression by nucleocytoplasmic interactions in early mouse embryos: consequences for reprogrammation by nuclear transfer. Mol Reprod Dev 1996; 44:423–432.
46. Tatham BG, Giliam KJ, Trounson AO. Electrofusion parameters for nuclear transfer predicted using isofusion contours produced with bovine embryonic cells. Mol Reprod Dev 1996; 43:306–312.
47. Bolet G. Timing and extent of embryonic mortality in pigs, sheep and goats: genetic variability. In: Sreenan JM, Diskin MG (eds.), Embryonic Mortality in Farm Animals. Dordrecht, The Netherlands: Martinus Nijhoff Publishers; 1986: 12–43.
48. Bazer FW. Mediators of maternal recognition of pregnancy in mammals. Proc Soc Exp Biol Med 1992; 199:373–384.
49. Wilmut I, McWhir J, Campbell K. Nuclear transfer from cultured cells: a new opportunity in animal breeding? In: Welch RAS, Burns DB, Davis SR, Popay AI, Prosser CG (eds.), Milk Composition, Production and Biotechnology. Oxfordshire, UK: CAB International; 1997: (in press).
50. Walker SK, Hartwich KM, Seamark RF. The production of unusually large offspring following embryo manipulation: concepts and challenges. Theriogenology 1996; 45:111–120.
51. Wilson JM, Williams JD, Bondioli KR, Looney CR, Westhusin ME, McCalla DF. Comparison of birth weight and growth characteristics of bovine calves produced by nuclear transfer (cloning), embryo transfer and natural mating. Anim Reprod Sci 1995; 38:73–83.
52. Garry FB, Adams R, McCann JP, Odde KG. Postnatal characteristics of calves produced by nuclear transfer cloning. Theriogenology 1996; 45:141–152.
53. Nathanielsz PW. The timing of birth. Am Sci 1996; 84:562–569.
54. Kitterman JA, Liggins GC, Campos GA, Clements JA, Forster CS, Lee CH, Creasy RK. Prepartum maturation of the lung in fetal sheep: relation to cortisol. J Appl Physiol 1981; 51:384–390.
55. Wilmut I, Clark AJ. Basic techniques for transgenesis. J Reprod Fertil Suppl 1991; 43:265–275.

ELSEVIER

# TRANSGENIC TECHNOLOGY AND APPLICATIONS IN SWINE

M. B. Wheeler and E. M. Walters

Department of Animal Sciences
University of Illinois
Urbana, IL 61801, U.S.A.

Received for publication: July 9, 2001
Accepted: September 21, 2001

## ABSTRACT

The introduction of foreign DNA into the genome of livestock and its stable integration into the germ line has been a major technical advance in agriculture. Production of transgenic livestock provides a method to rapidly introduce "new" genes into cattle, swine, sheep and goats without crossbreeding. It is a more extreme methodology, but in essence, not really different from crossbreeding or genetic selection in its result. Several recent developments will profoundly impact the use of transgenic technology in livestock production. These developments are: 1) the ability to isolate and maintain in vitro embryonic stem (ES) cells from preimplantation embryos, embryonic germ (EG) and somatic cells from fetuses; and somatic cells from adults, and 2) the ability to use these embryonic and somatic cells as nuclei donors in nuclear transfer or "cloning" strategies. Cell based (ES, EG, and somatic cells) strategies have several distinct advantages for use in the production of transgenic livestock that cannot be attained using pronuclear injection of DNA. There are many potential applications of transgenic methodology to develop new and improved strains of livestock. Practical applications of transgenesis in livestock production include enhanced prolificacy and reproductive performance, increased feed utilization and growth rate, improved carcass composition, improved milk production and/or composition and increased disease resistance. Development of transgenic farm animals will allow more flexibility in direct genetic manipulation of livestock.



Key words: transgenics, embryonic stem cells, microinjection, nuclear transfer, pigs

Acknowledgments

The authors wish to thank Dr. Sherrie Clark for critical comments during preparation of this manuscript. The authors would also like to thank their colleagues who have contributed to the work described G.T. Bleck, L.A. Rund, S.J. Choi, B.R. White, R.W. Gerfen, M. Izard-Hentges , L. Grum, J. Barnes, M. Ellis, D. Bidner, and S. Hughes. The authors would like to dedicate this paper to Raymond W. Gerfen .



0093-691X/01/$–see front matter
PII: S0093-691X(01)00635-5

## INTRODUCTION

Gene transfer is a beneficial way of modifying the genome of domestic livestock. The use of this methodology will have a great impact toward improving the efficiency of animal agriculture. Transgenic animals are routinely produced by pronuclear injection of foreign DNA into fertilized ova (9, 12, 21, 42, 49, 91, 146, 145). This allows the DNA to integrate randomly into chromosomes and subsequently be expressed in somatic and germ tissues of the individual. Application of an alternative strategy, previously developed in mice (8, 27), may greatly increase the efficiency of transgenic livestock production. This strategy involves the use of pluripotent or totipotent embryonic cells. The ability of the embryonic cells to differentiate into a wide variety of cell types has led to their designation as embryonic stem (ES) cells.

Recently, new methods have been reported which allow for the production of genetically identical individuals from embryonic (14, 156) and adult somatic (156) cells via nuclear transfer. The development of ES/EG cells from livestock provides an additional source of embryonic nuclei that can be used in nuclear transfer protocols. The combination of ES/EG cell and nuclear transfer methodologies may allow the rapid development of genetically identical animals with a targeted gene insertion.

The obvious question is "Why Make Transgenic Animals?" The answer is not so simple; however, some of the reasons are 1) to gain new knowledge, 2) to decipher the genetic code, 3) to study the genetic control of physiological systems, 4) to build genetic disease models, 5) to improve animal production traits, and 6) to produce new animal products.

## PIG EMBRYO MANIPULATION METHODOLOGY

### Production of Transgenic Animals

The objective of transgenic technology is to produce animals that have stable incorporation of foreign DNA in their germ line. Such individuals are able to act as 'founder' stock to produce many offspring that carry a desirable gene or genes. The first animals to carry experimentally inserted genes were mice produced by injecting retroviral Simian virus 40 (SV40) DNA into the cavity of blastocysts (59). These mice however, did not incorporate the SV40 DNA into their germ cells. Germ line incorporation was later shown by exposing mouse embryos to an infectious strain of Moloney leukemia virus, which resulted in the first strain of transgenic mice (57, 58). In addition to DNA transfer by retroviruses, transgenic animals have been produced by a number of other technologies including: 1) microinjection of genes into pronuclei of ova; 2) injection of ES and /or EG cells, previously exposed to foreign DNA, into the cavity of blastocysts; 3) sperm-mediated exogenous DNA transfer during in vitro fertilization; and 4) nuclear transfer with somatic, ES or EG cells.

Retroviral Gene Transfer Methods

Retroviruses are viruses that insert a DNA copy of their genetic material, produced from RNA as a template, into the host cell DNA following infection. The retrovirus acts as a naturally occurring delivery system to transfer DNA into various types of mammalian cells (142). Both inherent and genetically engineered retroviruses can be used to infect cells of mammalian embryos. Genetically engineered retroviruses are produced by deleting the viral gene sequences, replacing them with the gene(s) of interest and packaging them into infectious viral particles.

Retroviruses incorporate into the DNA of host cells by specific mechanisms (142), which are beyond the scope of this paper. DNA is introduced at a random chromosomal site and is usually limited to a single copy of the viral genome. Preimplantation embryos or oocytes (16, 56) can be exposed in vitro to concentrated virus solutions or incubated over a single layer of virus-producing cells (Figure 1) or have the virus injected into the perivitelline space under the zona pellucida of the oocyte (Figure 2). Following microinjection, the oocytes are then fertilized in vitro to produce embryos. Following exposure to viruses, in vitro infected embryos are transferred to recipient females to complete gestation. This method is called 'transgametic gene transfer' (16).

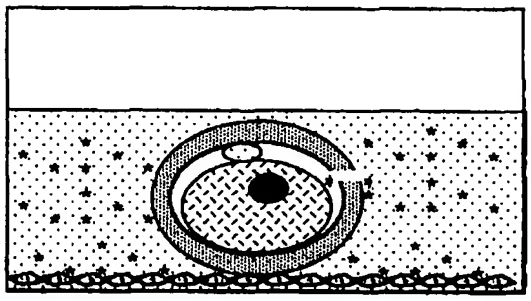

Figure 1. Retroviral infection of DNA into oocytes, zygotes, or embryos. The virus (*) enters the perivitelline space through a slit in the zona pellucida in order to "infect" the cell(s).

The main advantage of retroviral-mediated gene transfer into animals is the technical ease of presenting a virus to embryos at various developmental stages. There are, however, disadvantages with the use of retroviruses to produce transgenic animals. These disadvantages include: 1) the sequence of DNA transferred is limited by size, 2) the inserted gene is not always expressed in the second generation, and 3) many founders are mosaic, with potentially multiple insertion sites. Breeding experiments are usually required to sort out the mosaicism and multiple insertion site problems. The goal of such breeding studies is to produce a "true" founder animal, one with a single insertion site in all its cells, that can pass the gene via Mendelian inheritance. This may be more practical in pigs than in other livestock species, but it is not as easy as has been shown in mice.

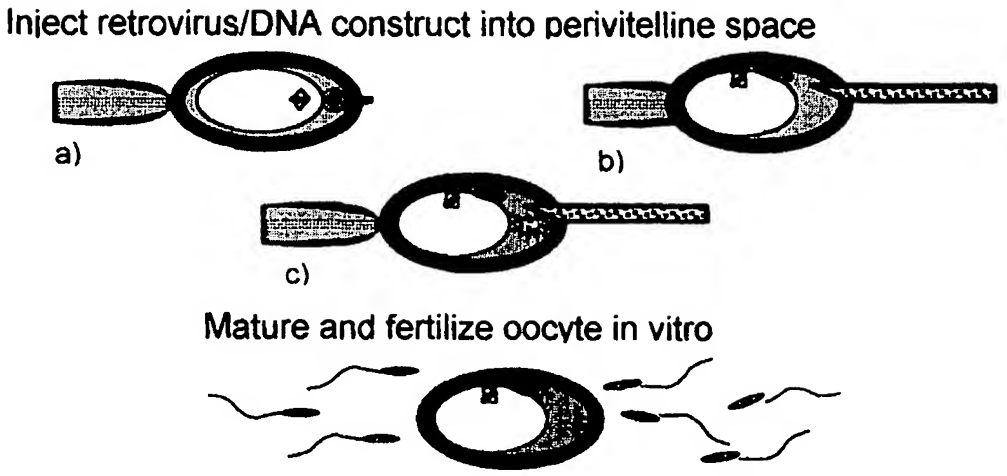


Figure 2. Transgametic gene transfer is a technique utilizing the injection of a recombinant retrovirus under the zona pellucida of the oocyte with subsequent in vitro maturation and fertilization. Panel (a) shows a oocyte being held in place with a finely drawn glass pipette. Panel (b) demonstrates the injection of the micropipette tip through the zona pellucida prior to injection. Panel (c) shows the injection of the retrovirus into the perivitelline space.

Gene Transfer by Pronuclear Injection

Another method for introducing foreign genes into animals is by pronuclear injection. Microinjection of cloned DNA into the pronucleus of an ovum has been the most widely used and most successful method for producing transgenic mice and livestock (12, 21, 42, 146, 145). The first step is to remove the recently fertilized ova from the animal. The fertilized ova are then visualized with a specialized microscope equipped with micromanipulators which is required for this method of gene transfer. The micromanipulators enable the retention and manipulation of the fertilized ova, which are individually grasped and immobilized on one side by a finely drawn-out glass pipette (Figure 3). On the opposite side, a second finely drawn injection pipette loaded with the foreign DNA is inserted into the pronucleus of the fertilized ova. The needle tip is brought to rest just inside the pronucleus where the DNA solution is injected. Following injection, the fertilized ova are transferred back into appropriately prepared recipient females. After transfer, pregnant recipients will undergo normal gestation and deliver term young.

The primary advantage to microinjection of cloned DNA into pronuclei is the relatively higher efficiency compared with other methods for the generation of transgenic animal lines (96). The success rate is approximately 30% in mice and 1 to 10% in domestic livestock species. The disadvantages of this technique are: 1) the method cannot be used with embryos of later (>4 cells) developmental stages, 2) screening of the insertion site in the host chromosome is difficult because the DNA integrates as multiple copies, which are configured in a tandem head-to-tail

manner or array, and 3) livestock species have a much lower frequency of integration of foreign DNA into their chromosomes, which makes production expensive.

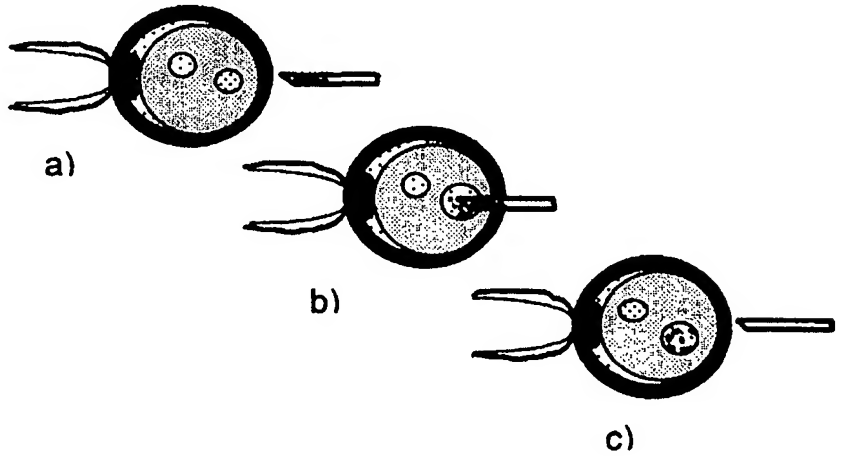


Figure 3. Pronuclear injection of DNA into a fertilized ovum. Panel (a) demonstrates a fertilizated ovum being held in position by a holding pipette prior to microinjection. Panel(b) illustrates the injection of a gene construct into to one pronucleus. Panel (c) shows the gene construct in the pronucleus prior to DNA replication.

Gene Transfer by Embryonic Stem/Embryonic Germ Cells

Embryonic stem cells and embryonic germ cells (87, 111) provide yet another to produce transgenic offspring. This gene transfer method involves injection of embryonic cells into expanded blastocysts to produce 'chimeric' embryos composed of two or more distinct cell lines (100). The ES cell lines are derived from the inner cell mass of blastocysts (8, 22, 27, 71) (Figure 4). These cells are able to produce all tissues of an individual. The isolation of ES cells has been developed from the pioneering studies performed with embryonal carcinoma (EC) cell lines (119). Once isolated, ES cells can be grown in vitro indefinitely, resulting in an unlimited number of identical cells each of which has the potential to differentiate into various tissue types (157).

Embryonic stem cells may also be transformed genetically with exogenous DNA before being used to produce chimeric embryos. When these transformed cells form the gonads and participate in the formation of sperm and oogonia, the offspring that are produced by these chimeric individuals will be transgenic. It is not the individual that results originally from the chimeric embryo that is purely transgenic, but it is the next generation of offspring. This is an important distinction in that the chimeric individual can act as 'founder' stock to produce many

offspring which carry the desired gene(s). Results have shown that this method is effective for the production of transgenic mice.

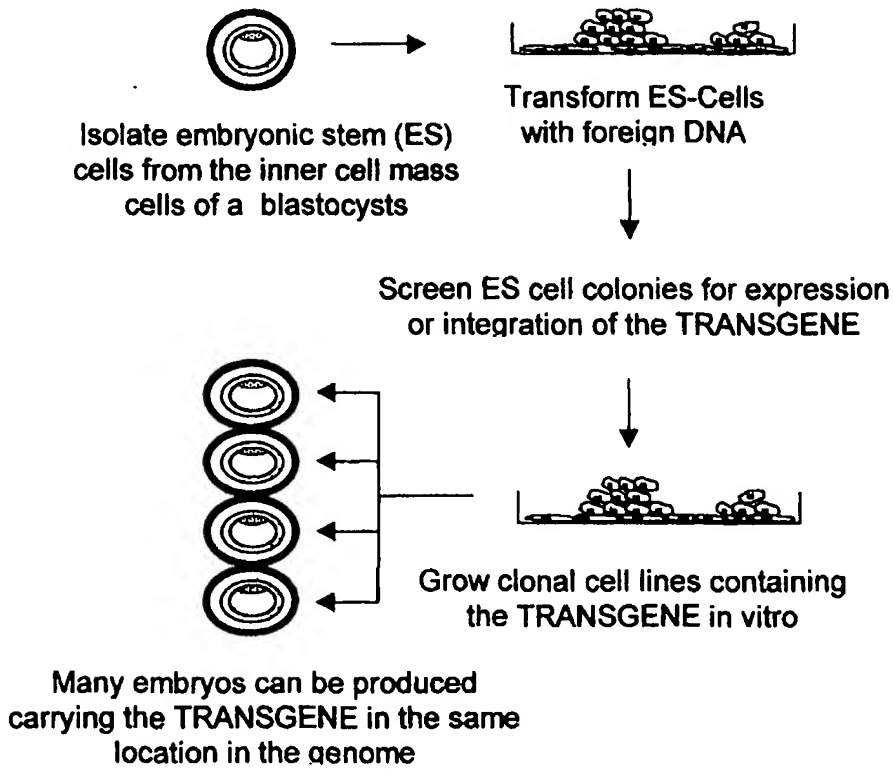


Figure 4. Schematic representation of the derivation and genetic transformation of embryonic stem cells from of a mammalian blastocyst.

Embryonic stem cells have a number of distinct advantages for the production of transgenic animals (15, 76, 97, 98, 99). These advantages include: 1) ES cells may be grown in vitro for many generations to produce unlimited numbers of identical cells, 2) ES cells can be transformed in vitro with foreign DNA (15, 99, 133), 3) ES cell lines can be isolated and derived from a single cell (97, 98, 99), 4) transformed ES cells can be screened and selected for incorporation of the foreign DNA before being used to produce chimeric or cloned embryos (43, 133), 5) all tissues of the chimeric offspring that arise from the ES cells carry the transgene in an identical site in the genome, 6) DNA-transformed, individually derived and screened embryonic cell lines would allow large numbers of genetically identical animals to be established, 7) the efficiency of transgenic animal production may be increased (43, 96), 8) it may be possible to screen for the tissue specific expression of the inserted gene prior to insertion of the ES cells into the blastocyst (15, 33, 99), and 9) it may eventually be possible to replace existing livestock genes

with genetically altered genes, via homologous recombination (133). Similar statements can be made for the advantage and use of EG cells. In this article, however, we will focus on ES cells.

The establishment of ES cells from a wide variety of species will allow more flexibility in direct genetic manipulation of livestock as well as gene regulation and developmental biology research. Studies involving the isolation of ES cells have recently been accelerated in non-murine species. Isolation of embryo-derived cell lines has been reported from Syrian golden hamster (23), rat (55), rabbit (24, 39, 40, 44, 77, 108), mink (126, 127), pig (17, 28, 37, 79, 80, 82, 83, 85, 86, 125, 130), cow (31, 105, 113, 121, 122, 123, 124, 131, 141), sheep (14, 32, 50, 85, 132, 137, 149, 156), primate (135, 136), and human (5, 134) preimplantation embryos. However, the production of a chimeric livestock species (swine and cattle) produced from ES cells has only been recently reported (19, 150, 153). Furthermore, validation of the totipotency of these embryo-derived ES cell lines awaits confirmation.

Due to the potential use of ES cells for genetic modification in livestock, our laboratory has been involved in studies to examine the feasibility of producing ES cell lines from swine (38, 46, 104, 150, 153). The overall efficiency for production of ES cell lines from porcine blastocysts has been low. In one study, a total of 1628 blastocysts was collected and cultured (Figure 5). Only 1219 (75%) of 1628 embryos attached to the culture vessel. However, of the 1219 embryos that attached to the culture vessel, the number of embryos surviving to passage 1 was 597 (37% overall survival). The number of embryos surviving to passage 1 was not directly correlated to the ability of the embryo to survive to passages 4 to 6 (178 survived, 30% of embryos passaged, 11% overall). Twenty-one percent (22/178, 1.3% overall) of the presumptive ES cell lines that reached passage 4 retained morphological and growth characteristics of pig ES cells. Porcine ES cells are small (8-15 μm diameter), rounded and dark, yet translucent. The porcine ES cell exhibits a high nuclear/cytoplasmic ratio and contains several prominent nucleoli (Figure 6). The ES cells usually grow in colonies with colony diameters ranging from 0.08 to 1.5 mm 4 days after plating as a single cell suspension. The average doubling time of the pig ES cells is 18 to 36 h after passages 5 to 7 and is relatively constant thereafter.

The ability of the isolated ES cells to participate in development of porcine chimeras was tested by Duroc morula, blastocyst and expanded blastocyst stage embryos injected with Meishan ES cells (153). In this study, a high percentage (86%, 64/74) of recipient embryos that received male ES cells survived micromanipulation. Three offspring were born after transfer of 64 micromanipulated embryos. A single female piglet exhibited coat color chimerism at birth. A combination of Meishan ES cells and Duroc blastocyst cells provided easy visual detection of chimeric animals. The resulting individuals have patches of different color skin and hair derived from each embryonic cell lineage with different genotypes. Similar coat color patterns have been reported previously for chimeric mice (74). Deoxyribonucleic acid was isolated from blood and/or tissue of the three potentially chimeric piglets. At the cellular level, chimerism was analyzed and confirmed by polymerase chain reaction amplification of a Meishan-specific 120 bp SW16 microsatellite allele. Tissues from the chimeric piglet positive for the Meishan allele included ear, skin from black spots, and blood (153). These samples were also positive for a Y-chromosome specific sequence (30), although this animal is a phenotypic female.

In another study, 29 piglets were born and 15 of these were DNA chimeras. Performance testing showed growth rates, measured by average daily gain (ADG), of the chimeras to be intermediate between the Duroc (embryo donor) and the Meishan (ES cell line donor) age-matched control pigs. The ADG of the chimeras was different ($P<0.05$) from both the Duroc and Meishan control pigs. The chimera growth rate was about 90% of the Duroc pigs and higher ($P<0.01$) than that of Meishan pigs (M.E. Ellis and M.B. Wheeler, unpublished data). Results of these studies have shown the feasibility of isolating ES cells from swine embryos. Development of efficient methods to utilize the ES cells in transgenic programs should facilitate the generation of useful transgenic pigs.

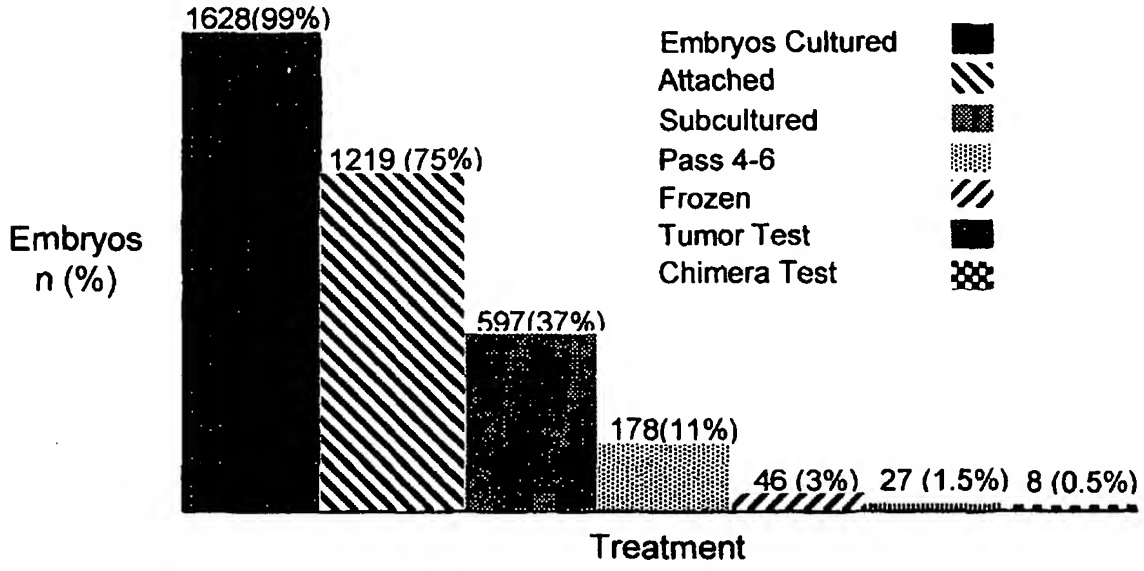


Figure 5. Efficiency of derivation of embryonic stem cells from porcine embryos.

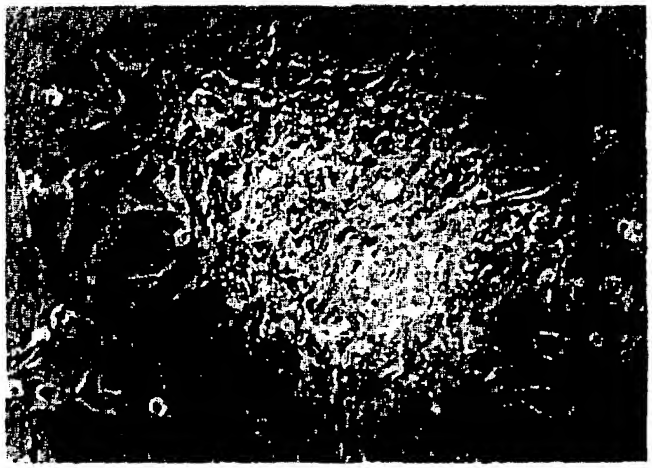

Figure 6. A representative porcine ES cell colony growing on STO feeder cells (x 200).

Along with ES cells, another type of pluripotent embryonic cells, EG cells, have been derived from the primordial germ cells (PGC), which are progenitor cells of the sperm and oogonia in the adult animal. The EG cells share common characteristics with ES cells both in vivo and in vitro. Embryonic germ cell lines have been established in mouse (72, 95), pig (86, 111) and human (110). The potential for gene transfer using EG cells has been described above in the section on ES cells.

Gene Transfer By Sperm-Mediated Gene Transfer

Another method for introducing exogenous DNA into animals for the purpose of producing transgenic animals is sperm-mediated gene transfer. Sperm of many species have been shown to bind naked DNA (54, 65, 117) as well as DNA-liposome complexes (1, 101). In general, sperm are collected at ejaculation or from the epididymis and incubated for varying lengths of time at 37 to 39°C in fertilization medium. During the last 30 min to 1 h, DNA solution is added to the sperm suspension to give a final DNA concentration of 1 to 25 μg/mL (65, 70, 114). The transformed sperm cells have been be used for in vitro fertilization (65, 70, 117) or artificial insemination (36, 106, 117); however, the majority of studies have focused on in vitro fertilization. In order to use sperm cells as vectors for gene transfer, transportation of exogenous DNA into the oocyte at fertilization must occur. Numerous studies have analyzed and shown this form of gene transfer at various stages of development, including two-cell embryo, blastocysts, and adult animals. Successful sperm-mediated gene transfer has been reported in the mouse (1, 53, 65, 70), rabbit (7, 63), pig (35, 117), chicken (29), Xenopus (61) and cattle (85, 106, 117).

The major advantage to this method for producing transgenic animals is its simplicity; however, the disadvantage of this technique is the decreased ability of the host's genome to incorporate DNA presented in such a fashion. Although transgenic animals have been produced by sperm-mediated DNA transfer, the results are not very reproducible. Most studies have been successful in binding DNA to sperm and delivering the sperm to the oocyte. Fewer studies have actually documented the production of transgenic embryos, and even fewer studies have produced transgenic animals.

Gene Transfer by Nuclear Transfer with Embryonic and Somatic Cells

Since the famous cloned sheep "Dolly" was born (156), nuclear transfer technology has become another methodology available for the production of transgenic animals. The birth (March 5, 2000) of the world's first cloned piglets using adult somatic cells has been reported (88). This opens the door for the use of nuclear transfer technology in swine. The nuclear transfer procedure utilizes either in vitro or in vivo oocytes as the cytoplasm donor (cytoplast). The genetic material of the cytoplast is removed (enucleation) leaving only the cytoplasm (Figure 7). Following the enucleation of the oocyte, a donor nucleus (karyoplast) is injected into the perivitelline space of the enucleated oocyte or injected into the cytoplasm of the oocyte (81). The enucleated oocyte and donor cell are fused by electrofusion. Electrofusion of the cytoplast and the karyoplast is highly species-dependent for the duration, amplitude of the pulse fusion medium, and equilibration to the fusion medium. After fusion of the donor nuclei and the enucleated oocyte, the

oocyte is activated by either chemical or mechanical stimulation. Successful activation initiates development to the blastocyst stage, followed by transfer to suitable recipient.

Prior to the birth of "Dolly," investigations were conducted on assessments of cytoplast and karyoplast. Prather et al. (90) investigated the use of pig activated ova as the cytoplast in pig nuclear transfer. There are several advantages to using the activated ova as the cytoplast, one of, which is the decreased level of maturation promoting factor (MPF). Another advantage is that the activated cytoplast is ready for subsequent development to the various stages of embryonic development. However, there are disadvantages to the use of activated ova as cytoplast donors. The major disadvantage is the need to remove large portions of the cytoplasm. The first successful cloned pig, however, was produced using the activated Metaphase II oocyte as the cytoplast (90).

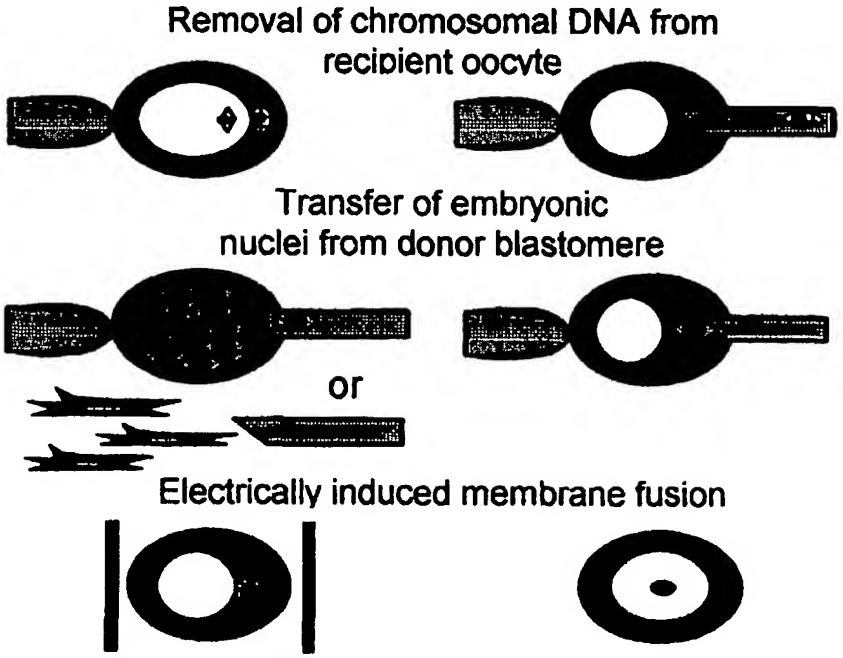


Figure 7. Nuclear transfer with a karyoplast of a derived from blastomere from a preimplantation embryo or an adult somatic cell.

Before 1997, nuclear transfer was limited only to karyoplasts from embryonic origin (4, 89, 90, 101, 114, 120, 139, 140, 155). The karyoplast of choice was from blastomeres or the inner cell mass from preimplantation stage embryos. The birth of the cloned sheep "Dolly" showed that adult somatic cells can also be used as donor nuclei in nuclear transfer. After the successful production of "Dolly," various cell types have been investigated for the production the cloned animals, including trophectodermal (140), cumulus and oviductal (60, 147), and fetal fibroblast cells (20, 81, 107, 156).

Cultured ES and ES-like cells have also been used as karyoplasts for nuclear transfer (14, 75, 138). The potential for nuclear transfer to be used in the production of transgenic animals depends greatly on the transfection of somatic, ES and/or EG cells. The combination of transformed ES cells and nuclear transfer methodologies should provide the tools necessary for the production of large numbers of genetically identical transgenic livestock. Embryonic stem cell and nuclear transfer technologies are still experimental, and a considerable number of variables need to be examined. Furthermore, few laboratories are proficient at these procedures, and the projected cost of a cloned, transgenic porcine embryo remains unknown. Commercialization of this technology will enable selection pressure to be exerted upon females, which is similar to that currently exerted on the male through artificial insemination (151).

## APPLICATIONS OF TRANSGENIC ANIMALS

### Biological, Biomedical and Genetic Research

The production of transgenic organisms has been a major technical advance in the study of biology. It is an important method for changing the genetic makeup of an animal providing a directed, sudden, induced mutation and species crossing technology. Transgenic animals have been instrumental in providing new insights into the study of the mechanisms of gene regulation and developmental biology. Additional areas where transgenic technology has provided significant advances and offers exciting future possibilities are 1) the action of genes implicated with having a role in the development of cancer (oncogenes) and oncogenic viruses; 2) the mechanisms of regulation and cell interaction in the immune system; 3) as models for human genetic diseases; 4) the mechanisms and control of growth and 5) the basic mechanisms of biology and genetics.

Every non-gametic cell of an individual has all the required information to synthesize the proteins that are characteristic of each and every tissue. However, only a distinct subset of the information present is utilized by any particular cell. The fate of the animal depends on regulation of gene expression to the appropriate cell types and the orchestration of the expression into the proper pattern during the development from an embryo to an adult. The utility of transgenic mice in examining regulation of developmentally controlled and tissue-specific gene expression has been elegantly illustrated in studies with the α-fetoprotein (AFP) gene (41, 48, 62). Alpha-fetoprotein is a predominant blood serum protein in the developing mouse fetus that is linked to a related protein, albumin. These two genes are activated harmonically in the liver, gut and kidney of the developing mouse fetus. The AFP gene is inactivated shortly after birth, yet the albumin gene continues to be expressed in the livers of adult animals. Transgenic mice produced by pronuclear injection have been used to map the regulatory sequences in the AFP gene, which are essential for its appropriate expression. The particular DNA sequences of interest were those that restrict AFP expression to a few tissues and initiate its regression after birth. Additional areas of developmental biology utilizing transgenic animals include nucleus-cytoplasm interactions in cells and the effect of gene location in the chromosome on its expression.

## Livestock Production

There are numerous potential applications of transgenic methodology to develop new or altered strains of agriculturally important livestock. Practical applications of transgenesis in livestock production include improved milk production and composition, increased growth rate, improved feed utilization, improved carcass composition, increased disease resistance, enhanced reproductive performance, increased prolificacy, and altered cell and tissue characteristics for biomedical research (152). The production of transgenic swine with growth hormone serves as an excellent example of the potential value of this technology (9, 49). Transgenic alteration of milk composition has the potential to enhance the production of certain proteins and/or growth factors deficient in milk (10). The improvement of the nutrient or therapeutic value of milk may have a profound impact on survival and growth of newborns in both humans and animals. Genes coding for proteins with pharmaceutical value such as human blood clotting factor IX, which is genetically deficient in hemophiliacs, may be incorporated into the mammary gland of transgenic cows, sheep, or goats. This protein could be harvested from the milk, purified and provided therapeutically to hemophiliacs. The use of ES/EG cells and/or nuclear transfer will facilitate the introduction of these genes in a directed manner via homologous recombination.

## Modification of Milk

Advances in recombinant DNA technology have provided the opportunity to change the composition of milk, increase milk volume (3) and to produce entirely novel proteins in milk. These changes may add value to, as well as increase the potential uses of milk.

The improvement of livestock growth or survivability through the modification of milk composition requires production of transgenic animals that: 1) produce a greater quantity of milk; 2) produce milk of higher nutrient content; or 3) produce milk that contains a beneficial "nutriceutical" protein. The major nutrients in milk are protein, fat and lactose. By elevating any of these components we can impact growth and health of the developing offspring. In many production species such as cattle, sheep and goats, the nutrients available to the young may not be limiting. However, milk production in the sow limits piglet growth and therefore pig production (51). In swine, 44% of the growth rate of the developing piglets can be attributed to yield and composition of the sow's milk (67). Methods that increase the growth of piglets during suckling result in an increase in weaning weights, and a decrease in the number of days required to reach market.

Transgenic pigs containing the bovine alpha lactalbumin (α-LA) gene allow us to study α-LA's ability to improve milk production and composition in swine. Alpha lactalbumin is a component of the lactose synthesis complex and is involved in the synthesis of lactose in milk. Milk produced by bovine α–LA transgenic sows contained 0.4 to 0.9 g of bovine α-LA per liter (3). The concentration of bovine α-LA was directly correlated with the concentration of endogenous porcine milk proteins throughout the 21 days of lactation. The addition of bovine α-LA increased the concentration of total (bovine + porcine) α-LA found in milk by 50%. The concentration of bovine α-LA was highest on day 0 and day 5 of lactation and decreased as lactation progressed. The ratio of bovine to porcine α-LA changed during the sow's lactation.

This ratio was 4.3 to 1 on day 0 of lactation, but by day 20 of lactation the ratio was 0.43 to 1. This suggested that the bovine transgene and the endogenous porcine gene are under slightly different control mechanisms. The higher level of total α-LA present on day 0 of lactation was correlated with higher lactose percentage on day 0 in transgenic sows (3.8 %) as compared with controls (2.6 %) ($P < 0.01$). Although there was also a trend for higher lactose percentage in transgenic sows on 5 d and 10 d of lactation, no significant differences were observed. These data suggest that α-LA is limited early in lactation of swine. Furthermore, higher concentrations of α-LA early in lactation boost milk output and piglet growth (3). In fact, piglet growth is higher ($P< 0.05$) when the piglets are suckling sows containing the α-LA transgene (78).

A second mechanism by which the alteration of milk composition may affect animal growth is the addition or supplementation of beneficial hormones, growth factors or bioactive factors to the milk through the use of transgenic animals. It has been suggested that bioactive substances (IGF-I, EGF, TGF-α and lactoferrin) in milk possess important functions in the neonate. These proteins influence growth, as well as the development and maturation of the gut, the immune system and the endocrine organs (45). The overexpression of a number of these proteins in milk through the use of transgenic animals may improve growth, development, health and survivability of the developing offspring.

Other properties of milk that merit consideration for modification are those which affect human and animal health. It has been shown that preformed specific antibodies can be produced in transgenic animals (122). It should be possible to produce antibodies in the mammary gland that are capable of preventing a mastitis infection in cattle, sheep and goats and MMA (mastitis-metritis-agalactia) in pigs, and/or antibodies that aid in the prevention of domestic animal or human diseases (93). Another example is to increase proteins that have physiological roles within the mammary gland itself such as lysozyme (69) or other anti-microbial peptides.

By using transgenics and recombinant DNA technology it is feasible to add virtually any protein from any animal, plant or bacterial species to milk (10). For example, it is possible to express additional milk proteins and other proteins of pharmaceutical value in the milk of mice, rabbits, pigs, goats, and sheep (13, 25, 112, 148, 158). Advantages of the mammary synthesis of proteins include the ability of the mammary secretory cells to properly modify the protein so it is biologically active and then secrete the protein in milk in large quantities. This has resulted in the development of a new segment of the pharmaceutical industry which has become known as "bio-pharming".

Modification of Growth and Carcass Composition

The production of transgenic livestock has been instrumental in providing new insights into the mechanisms of gene action implicated in the control of growth (9, 49, 90, 108, 144, 154). Transgenic mice, sheep and pigs have been used to examine postnatal growth of mammals. Growth hormone and insulin-like growth factor genes have been incorporated and expressed at various levels in transgenic animals (109). This type of work enabled the study of chronic expression of these hormones on mammalian growth (109). Results from the study have shown that an increase in human GH leads to enhancement of growth and feed efficiency in pigs yet is

accompanied by side effects such as an increased incidence of arthritis and bone thickening (91). Similar increases in growth have been shown with the porcine growth hormone (pGH) gene, but without increased arthritis and abnormal skeletal growth (144). Several other genes have also been introduced into transgenic pigs in an effort to alter growth. An alternative approach was performed by introduction of the chicken 'ski' oncogene, which was previously shown to cause hypertrophy of numerous muscles while reducing body fat (128). This strategy, however, has resulted in limited success although muscle hypertrophy has been observed in some transgenic pigs (92) and transgenic cattle (6).

Other specific loci which may affect growth patterns are the ryanodine receptor (formerly the halothane sensitivity gene locus, Hal; 34), the myo-D (52, 116), the callipyge (115) and the myostatin (growth/differentiation factor-8, GDF-8; 73) genes. Based on a recent report in the mouse (73), the myostatin gene is an exceptionally intriguing potential locus for "knock-out" using ES cells in meat producing species. The loss of the myostatin protein results in an increase in lean muscle mass. Mice lacking this gene have enlarged shoulders and hips. The increased skeletal muscle mass is widespread throughout the carcass and appears grossly normal. Individual muscle groups from homozygous knockouts have 2 to 3 times the weight of control animals. Fat content was comparable in both the wild-type and mutant genotypes (73). Researchers concluded that a large part of the observed increase in skeletal muscle mass was due to muscle cell hyperplasia. Certainly, there are numerous potential genes related to growth, including growth factors, receptors or modulators which have not been used, but may be of practical importance in producing transgenic livestock with increased growth rates and/or feed efficiencies.

Modification of Disease Resistance

A very interesting aspect of agricultural transgenics is the potential to increase disease resistance by introducing specific genes into livestock. Identification of single genes in the major histocompatibility complex (MHC), which influence the immune response, was instrumental in the recognition of the genetic basis of disease resistance or susceptibility (2). It has only been realized recently that there are many aspects of disease resistance or susceptibility in livestock that are genetically determined (66). Embryonic stem cells and/or nuclear transfer (NT) will be very useful for manipulation of genes or large clusters of genes from the MHC. The use of ES/EG cells or NT will allow transfer and integration of much larger (>100 kb) DNA fragments than previously possible with pronuclear injection. Large yeast artificial chromosome (*YAC*) vectors containing extremely large genes (>400 kb) have been transfected into ES cells and produced germline transgenics (18, 64). Manipulation of the MHC in farm animals through ES cells or NT transgenesis could have a major beneficial effect on disease resistance for livestock producers.

One specific example where transgenesis has been applied to disease resistance in livestock is the production of pigs that are resistant to influenza. Mice and mouse fibroblast cell lines that contain the Mx+ protein were shown to be resistant to infection with influenza virus (47, 118). The Mx cDNA has been introduced into porcine fertilized ova, producing pigs that are resistant to influenza infection (11). This manipulation is an excellent example of how transgenesis may be used to increase disease resistance in livestock. The application of ES/EG cells or NT technology will enable the augmentation of beneficial alleles and/or the removal (via gene 'knock-

out') of undesirable alleles associated with disease resistance or susceptibility. An example is "knocking-out" the intestinal receptor for the E. coli K88 antigen. The absence of the antigen has been shown to confer resistance to both experimentally and naturally induced infection with K88-positive E. coli (26). Potential areas of investigation include resistance to: 1) parasitic organisms such as trypanosomes and nematodes, 2) viral or bacterial organisms such as bovine leukemia virus, pseudorabies virus, hoof and mouth disease virus, clostridium and streptococcus, and 3) genetic diseases. This is only a partial list of organisms or genetic diseases that decrease production efficiency and may also be targets for manipulation via ES/EG cells or NT methodologies.

Modification of Reproductive Performance and Prolificacy

Several potential genes have recently been identified which may profoundly affect reproductive performance and prolificacy. One of these is the estrogen receptor (*ESR*) gene. Rothschild et. al. (102) have reported an association of a polymorphism in the estrogen receptor (*ESR*) gene with litter size in pigs. They found a difference of 1.4 more pigs born per litter between the two homozygous genotypes. Introduction of a mutated or polymorphic *ESR* gene could increase litter size in a number of diverse breeds of pigs.

Modification of Cell and Tissue Characteristics

A unique application of ES/EG cells or NT technologies in transgenic livestock is the production of cells, tissues or organs that contain human antigens or proteins for xenotransplantation and other biomedical uses. Examples using swine include development of: pancreatic β cells for insulin therapy; dopaminergic cells for Parkinson's therapy; human hemoglobin and protein C for artificial blood (129, 143); hepatocytes for artificial livers; hematopoietic stem cells for leukemia or anemia; and hearts, lungs, kidneys, livers and corneas for organ transplants (68). Additionally, specific cell lines derived from ES/EG cell or NT-produced transgenic animals may be useful for other biomedical production or manufacturing applications.

## DISCUSSION

The overall goals of producing transgenic animals are to increase our knowledge of biology and biomedical science, and to increase our ability to efficiently produce milk, meat and fiber. To successfully obtain these improvements, we will test our ability to quantify desirable traits, identify genes responsible for these traits, and to introduce those genes into laboratory animals as well as production livestock. We must select and/or "re-design" populations of superior individuals which can be propagated. The incorporation of cell based (ES, EG, and somatic cells), nuclear transfer and recombinant DNA technologies into these strategies will continue to be an important aspect of future advances. However, we must remember that the production capability of genetically selected and/or genetically engineered animals will only be realized when their true genetic potential is attained through appropriate environmental and management considerations.

The ultimate utility and value of transgenic technology will be limited by our ability to 1) identify genes and appropriate regulatory sequences for the production of traits we wish to study, improve or include in development of transgenic animals and 2) incorporate these desired genes in an appropriately expressed and regulated manner into our domestic livestock.

The establishment of ES cells, EG cells and nuclear transfer methods in livestock will be useful for the production of transgenic livestock as well as for studies of cell differentiation, development and gene regulation in farm animals. In spite of this tremendous potential, there is some concern that the use of genetically modified adult somatic cells plus nuclear transfer may make the ES or EG cell strategies in livestock less useful in the future. While the use of adult or other somatic cells is becoming a viable strategy, the use of stem cell populations will continue to have a place in the genetic modification of domestic livestock. The major advantage of stem cells is that they provide an essentially unlimited supply of undifferentiated, genetically identical cells for manipulation with few of the barriers seen with primary cell cultures. The use of ES/EG cell-mediated gene transfer has not been employed in domestic livestock mainly due to the lack of established, stable ES/EG cell lines. There are two barriers to overcome to produce transgenic livestock with this technology: 1) establishment of undifferentiated ES/EG cell lines and 2) the successful transformation of the ES/EG cells with the 'foreign' gene(s). Great progress has been made toward overcoming the first of these barriers (38, 87, 104, 111, 153), that is, the isolation of undifferentiated porcine ES or EG cell lines. However, a significant amount of work still remains to enable the routine production of transgenic livestock from ES or EG cells.

## REFERENCES

1. Bachiller D, Schellander K, Peli K, Ruther U. Liposome-mediated DNA uptake by sperm cells. Mol Reprod Dev 1991;30:194-200.
2. Benacerraf B, McDevitt HO. Histocompatibility linked immune response genes. A new class of genes that controls the formation of species immune response has been identified. Science 1972;175:273-279.
3. Bleck GT, White BR, Miller DJ, Wheeler MB. Production of bovine α–lactalbumin in the milk of transgenic pigs. J Anim Sci 1998;76:3072-3078.
4. Bondioli KR, Westhusin ME, Looney CR. Production of identical bovine offspring by nuclear transfer. Theriogenology 1990;33:165-174.
5. Bongso A, Fong C-Y, Ng S-C, Ratnam S. Isolation and culture of inner cell mass from human blastocyst. Hum Reprod 1994;9:2110-2117.
6. Bowen RA, Reed M, Schnieke A, Seidel GE, Stacey A, Thomas WK, Kaijkawa O. Transgenic cattle resulting from biopsied embryos: Expression of c-ski in a transgenic calf. Biol Reprod 1994;50:664-668.
7. Brackett BG, Boranska W, Sawicki W, Koprowski H. Uptake of heterologous genome by mammalian spermatozoa and its transfer to ova through fertilization. Proc Natl Acad Sci USA 1971;68:353-357.
8. Bradley A, Evans M, Kaufman MH, Robertson E. Formation of germ-line chimaeras from embryo-derived teratocarcinoma cell lines. Nature 1984;309:255-256.

9. Brem G, Brenig B, Goodman HM, Selden RC, Graf F, Kruff B, Springman K, Hondele J, Meyer J, Winnacker E-L, Kraublich H. Production of transgenic mice, rabbits and pigs by microinjection into pronuclei. Zuchthygiene 1985;20:241-245.
10. Bremel RD, Yom H-C, Bleck GT. Alteration of milk composition using molecular genetics. J Dairy Sci 1989;72:2826-2833.
11. Brenig B, Muller M, Brem G. Gene transfer in pigs. Proc 4th World Cong Genet Applied to Livestock Prod. , 1990;12:41-48.
12. Brinster RL, Chen HY, Trumbauer ME, Senear AW, Warren R, Palmiter, RD. Somatic expression of herpes thymidine kinase in mice following injection of a foreign gene into eggs. Cell 1981;27:223-231.
13. Buehler TA, Bruyere T, Went DF, Stranzinger G, Buerki K. Rabbit β-casein promoter directs secretion of human interleukin-2 into the milk of transgenic rabbits. Bio/Technology 1990;8:140-143.
14. Campbell KHS, McWhir J, Ritchie WA, Wilmut I. Sheep cloned by nuclear transfer from a cultured cell line. Nature 1996;380:64-66.
15. Capecchi MR. Altering the genome by homologous recombination. Science 1989;244:1288-1292.
16. Chan AWS, Homan EJ, Ballou LU, Burns JC, Bremel RD. Transgenic cattle produced by reverse-transcribed gene transfer in oocytes. Proc Natl Acad Sci USA 1998;95:14028-14033.
17. Chen LR, Wu MC. Establishment of porcine-blastocyst-derived embryonic stem cells and production of chimeras by blastocyst injection. J Reprod Fertil 1993;48(Suppl):94 abstr
18. Choi TK, Hollenbach PW, Pearson BE, Udea RM, Weddell GN, Kurahara CG, Woodhouse CS, Kay RM, Loring J. Transgenic mice containing a human heavy chain immunoglobulin gene fragment cloned in a yeast artificial chromosome. Nat Genet 1993;4:117-123.
19. Cibelli JB, Stice SL, Golueke PJ, Kane JJ, Jerry J, Blackwell C, Ponce deLeon FA, Robl JM. Transgenic bovine chimeric offspring produced from somatic cell-derived stem-like cells. Nat Biotechnol 1998a;16:642-646.
20. Cibelli JB, Stice SL, Golueke PJ, Kane JJ, Jerry J, Blackwell C, Ponce de Leon FA, Robl JM. Cloned transgenic calves produced from nonquiescent fetal fibroblasts. Science 1998b;280:1256-1258.
21. Costantini F, Lacy E. Introduction of a rabbit β–globin gene into the mouse germ line. Nature 1981;294:92-94.
22. Doetschman TC, Eistetter H, Katz M, Schmidt W, Kemler R. The in vitro development of blastocyst-derived embryonic stem cell lines: formation of visceral yolk sac, blood islands and myocardium. J Embryol Exp Morph 1985;87:27-45.
23. Doetschman T, Williams P, Maeda N. Establishment of hamster blastocyst-derived embryonic stem (ES) cells. Dev Biol 1988;127:224-227.
24. Du F, Giles JR, Foote RH, Graves KH, Yang X, Moreadith RW. Nuclear transfer of putative rabbit stem cells leads to normal blastocyst development. J Reprod Fertil 1995;104:219-223.

25. Ebert KM, Selgrath JP, Ditullio P, Denman J, Smith TE, Memon MA, Schindler JE, Monastersky GM, Vitale JA, Gordon K. Transgenic production of a variant of human tissue-type plasminogen activator in goat milk: Generation of transgenic goats and analysis of expression. Bio/Technology 1991;9:835-840.
26. Edfors-Lilia I, Petersson H, Gahne B. Performance of pigs with or without the intestinal receptor for Escherichia Coli K88. Anim Prod 1986;42:381-387.
27. Evans MJ, Kaufman MH. Establishment in culture of pluripotent cells from mouse embryos. Nature 1981;292:154-156.
28. Evans MJ, Notarianni E, Laurie S, Moor RM. Derivation and preliminary characterization of pluripotent cell lines from porcine and bovine blastocysts. Theriogenology 1990;33:125-128.
29. Fainsold A, Frumpkin A, Rangini Z, Revel E, Yarus S, Ben-Yehuda A, Gruembaum Y. Chicken homeogenes expressed during gastrulation and the generation of transgenic chicken. In: EMBO-EMBL Symp, Mol Biol Vertebrate Dev. 1990;31.
30. Fajfar-Whetstone CJ, Rayburn III AL, Schook LB, Wheeler MB. Sex determination of porcine preimplantation embryos via Y-chromosome specific DNA sequences. Anim Biotechol 1993;4:183-193.
31. First NL, Simms MM, Park SP, Kent-First MJ. Systems for production of calves from cultured bovine embryonic stem cells. Reprod Fertil Dev 1994;6:553-562.
32. Flechon JE, Notarianni E, Galli C, Laurie S, Moor RM, Evans MJ. Characterization of ovine and porcine embryonic stem cells. J Reprod Fertil 1990;Abstr Series 6:25 abstr.
33. Foley GL, Rund LA, Wheeler MB. Factors affecting murine embryonic stem cell teratoma development. Biol Reprod 1994;50(Suppl 1):291 abstr.
34. Fujii J, Otsu K, Zorzto F, De Leon S, Khanna VK, Weiler JE, O'Brian PJ, MacLennan DH. Identification of a mutation in the porcine ryanodine receptor associated with malignant hyperthermia. Science 1991;253:448-451.
35. Gandolfi F, Lavitrano M, Camaioni A, Spadafora C, Siracusa G, Lauria A. The use of sperm-mediated gene transfer for the generation of transgenic pigs. J Reprod Fertil 1989;Abstr Ser 4:10 abstr.
36. Gandolfi F, Terqui M, Modina S, Brevini TAL, Ajmone-Marsan P, Foulon-Gauze F, Courot M. Failure to produce transgenic offspring by intra-tubal insemination of gilts with DNA treated sperm. Reprod Fertil Dev 1996;8:1055-1060.
37. Gerfen RW, Fajfar-Whetstone CJ, Wheeler MB. Isolation of embryonic cell lines from porcine blastocysts. In: Serono Symp Preimplant Embryo Dev. Boston, MA, 1991:16 abstr.
38. Gerfen RW, Wheeler MB. Isolation of pluripotent embryonic cell lines from porcine blastocysts. Anim Biotechol 1995;6:1-14.
39. Giles JR, Foote RH, Mark W. Development of embryo stem cell technology for production of chimeric rabbits. Biol Reprod 1991;44(Suppl 1):57 abstr.
40. Giles JR, Yang X, Mark W, Foote RH. Pluripotency of cultured rabbit inner cell mass cells detected by isozyme analysis and eye pigmentation of fetuses following injection into blastocysts or morulae. Mol Reprod Dev 1993;36:130-138.
41. Godbout R, Ingram R, Tilghman SM. Multiple regulatory elements in the intergenic region between the α–fetoprotein and albumin genes. Mol Cell Biol 1986;6:477-487.

42. Gordon MF, Scangos GA, Plotkin DJ, Barbosa JA, Ruddle FH. Genetic transformation of mouse embryos by microinjection of purified DNA. Proc Natl Acad Sci USA 1980;77:7380-7384.
43. Gossler A, Doetschman T, Korn R, Serfling E, Kemler R. Transgenesis by means of blastocyst-derived embryonic stem cell lines. Proc Natl Acad Sci USA 1986;83:9065-9069.
44. Graves KH, Moreadith RW. Derivation and characterization of putative pluripotential embryonic stem cells from preimplantation rabbit embryos. Mol Reprod Dev 1993;36:424-433.
45. Grosvenor CE, Picciano MF, Baumrucker CR. Hormones and growth factors in milk. Endocrinol Rev 1993;14:6:710-728.
46. Grum LR, White BR, Rund LA, Bleck GT, Wheeler MB. Attachment capability of swine blastocysts cultured from Duroc, Yorkshire, Landrace X Yorkshire pigs and Meishan. J Anim Sci 1994;72(Suppl 1):1091 abstr.
47. Haller O, Arnheiter H, Gresser I, Lindenmann J. Virus-specific interferon action/protection of newborn Mx carries against lethal infection with influenza virus. J Exp Med 1981;154:199-203.
48. Hammer RE, Krumlauf R, Camper SA, Brinster RL, Tilghman SM. Diversity of alpha fetoprotein gene expression in mice is generated by a combination of separate enhancer elements. Science 1987;235:53-58.
49. Hammer RE, Pursel VG, Rexroad Jr. CE, Wall RJ, Bolt DJ, Ebert KM, Palmiter RD, Brinster RL. Production of transgenic rabbits, sheep and pigs by microinjection. Nature 1985;315:680-683.
50. Handyside A, Hooper ML, Kaufman MH, Wilmut I. Towards the isolation of embryonal stem cell lines from sheep. Roux's Arch Dev Biol 1987;196:185-190.
51. Hartmann PE, McCauley I, Gooneratne AD, Whitely JL. Inadequacies of sow lactation: survival of the fittest. In: Symp Zool Soc. London, 1984;51: 301-326.
52. Harvey RP. Widespread expression of MyoD genes in Xenopus embryos is amplified in presumptive muscle as a delayed response to mesoderm induction. Proc Natl Acad Sci USA 1991;88:9198-9202.
53. Hochi S, Ninomiya T, Mizuna A, Honma M, Yuki A. Fate of exogenous DNA carried into mouse eggs by spermatozoa. Anim Biotechnol 1990;1:25-30.
54. Horan R, Powell R, McQuaid S, Gannon F, Houghton JA. Association of foreign DNA with porcine spermatozoa. Arch Androl 1991;26:83-92.
55. Iannaccone PM, Taborn GU, Garton RL, Caplice MD, Brenin DR. Pluripotent embryonic stem cells from the rat are capable of producing chimeras. Dev Biol 1994;163:288-292.
56. Jaenisch R, Fan H, Croker B. Infection of preimplantation mouse embryos and of newborn mice with leukaemia virus: Tissue distribution of viral DNA and RNA leukemogenesis in adult animal. Proc Natl Acad Sci USA 1975;72:4008-4012.
57. Jaenisch R, Hrabers K, Schmieke A, Loehler J, Chumakov I, Jaehner D, Grotkopp D, Hoffman E. Germline integration of moloney murine leukemia virus at the movB locus leads to recessive lethal mutation and early embryonic death. Cell 1983;32:209-216.
58. Jaenisch R, Jaehner D, Nobis P, Simon I, Loehler J, Harbers K, Grotokopp D. Chromosomal position and activation of retroviral genomes inserted into the germ line of mice. Cell 1981;24:519-529.

59. Jaenisch R, Mintz A. Simian virus 40 DNA sequences in DNA of healthy adult mice derived from preimplantation blastocysts injected with viral DNA. Proc Natl Acad Sci USA 1974;71:1250-1254.
60. Kato Y, Tani T, Sotomaru Y, Kurokawa K, Kato J, Doguchi H, Yasue H, Tsunoda Y. Eight calves cloned from somatic cells of a single adult. Science 1998;282:2095-2098.
61. Kroll K, Amaya E. Transgenic Xenopus embryos from sperm nuclear transplantation reveal FGF signaling requirements during gastrulation. Development 1996;122:3173-3183.
62. Krumlauf R, Hammer RE, Tilghman SM, Brinster RL. Developmental regulation of α–fetoprotein genes in transgenic mice. Mol Cell Biol 1985;5:1639-1648.
63. Kuznetsov AV, Kuznetsov IV. The binding of exogenous DNA pRK3lacZ by rabbit spermatozoa, its transfer to oocytes and expression in preimplantation embryos. Ontogenez 1995;26:300-309.
64. Lamb BT, Sisodia SS, Lawler AM, Slunt HH, Kitt CA, Kearns WG, Pearson PL, Price DL, Gearhart JD. Introduction and expression of the 400 kilobase precursor amyloid protein gene in transgenic mice. Nat Genet 1993;5:22-30.
65. Lavitrano M, Camaioni A, Fazio VM, Dolci S, Farace MG, Spadafora C. Sperm cells as vectors for introducing foreign DNA into eggs: Genetic transformation of mice. Cell 1989;57:717-723.
66. Lewin HA. Disease resistance and immune response genes in cattle: strategies for their detection and evidence of their existence. J Dairy Sci 1989;72:1334-1348.
67. Lewis AJ, Speer VC, Haught DG. Relationship between yield and composition of sow's milk and weight gains of nursing pigs. J Anim Sci 1978; 47:634-638.
68. Lin SS, Platt JL. Immunological advances towards clinical xenotransplantation. In: Tumbleson ME, Schook LB (eds), Advances in Swine in Biomedical Research. New York: Plenum Press, 1996;147-162.
69. Maga EA, Anderson GB, Murray JD. The effect of mammary gland expression of human lysozyme on the properties of milk from transgenic mice. J Dairy Sci 1995;78:2645-2652.
70. Maione B, Lavitrano M, Spadafora C, Kiessling A. Sperm-mediated gene transfer in mice. Mol Repod Dev 1998;50:406-409.
71. Martin GR. Isolation of a pluripotent cell line from early mouse embryos cultured in medium conditioned by teratocarcinoma stem cells. Proc Natl Acad Sci USA 1981;78:7634-7638.
72. Matsui Y, Zsebo K, Hogan BLM. Derivation of pluripotent embryonic stem cells from murine primordial germ cells in culture. Cell 1992;70:841-847.
73. McPherron AC, Lawler AM, Le S-J. Regulation of skeletal muscle mass in mice by a new TGF-beta superfamily member. Nature 1997;387:83-90.
74. Mintz B. Genetic mosaicism in adult mice of quadriparental lineage. Science 1965; 148:1232-1233.
75. Modlinski JA, Gerhauser D, Lioi B, Winking H, Illmensee K. Nuclear transfer from teratocarcinoma cells into mouse oocytes and eggs. Development 1990;108:337-348.
76. Murray JD, Nancarrow CD, Ward KA. Controlled production of sheep growth hormone in transgenic mice and sheep. Proc. 11th Intl Cong Anim Reprod & Artificial Insemination. Dublin, Ireland, 1988;5:20-27.

77. Niemann H, Strelchenko N. Isolation and maintenance of rabbit embryonic stem (ES) cell like cells. Theriogenology 1994;41:265 abstr.
78. Noble MS, Bleck GT, Rodrequez-Zas S, Cook JB, Hurley WL, Wheeler MB. Lactational performance of first parity transgenic gilts expressing bovine α-lactalbumin in their milk: Milk production results and piglet growth rate. J Anim Sci (accepted).
79. Notarianni E, Galli C, Laurie S, Moor RM, Evans MJ. Derivation of pluripotent embryonic cell lines from the pig and sheep. J Reprod Fertil 1991;Suppl 43:255-260.
80. Notarianni E, Laurie S, Moor RM, Evans MJ. Maintenance and differentiation in culture of pluripotent embryonic cell lines from pig blastocysts. J Reprod Fertil 1990;Suppl 41:51-56.
81. Onishi A, Iwamoto M, Akita T, Mikawa S, Takeda K, Awata T, Hanada H, Perry ACF Pig cloning by microinjection of fetal fibroblast nuclei. Science. 2000;289:1188-1190.
82. Onishi A, Youngs CR. Comparison of immunosurgery with calcium ionophore treatment for isolation of inner cell masses of porcine blastocysts. Theriogenology 1993a;39:274 abstr.
83. Onishi A, Youngs CR. Isolation of inner cell mass (ICM) derived cell colonies from intact porcine blastocysts. J Anim Sci 1993b;71(Suppl 1):74 abstr.
84. Perez A, Solano R, Castro R, Lleonart R, de Armas R, Martinez R, Aguilar A, Herrera L, de la Fuente J. Sperm cells mediated gene transfer in cattle. Biotechnol Aplicada 1991;8:90- 94.
85. Piedrahita JA, Anderson GB, BonDurant RH. On the isolation of embryonic stem cells: comparative behavior of murine, porcine, and ovine embryos. Theriogenology 1990a;34:879-901.
86. Piedrahita JA, Anderson GB, BonDurant RH. Influence of feeder layer type on the efficiency of isolation of porcine embryo-derived cell lines. Theriogenology 1990b;34:865-877.
87. Piedrahita JA, Moore K, Oetama B, Lee CK, Scales N, Ramsoondar J, Bazer FW, Ott T. Generation of transgenic porcine chimera using primordial germ cell-derived colonies. Biol Reprod 1998;58:1321-1329.
88. Polejaeva IA, Chen SH, Vaught TD, Page RL, Mullins, J, Ball S, Dai Y, Boone J, Walker S, Ayares D, Coleman A, Campbell KH. Cloned pigs produced by nuclear transfer from adult somatic cells. Nature. 2000;407:505-509.
89. Prather RS, Barnes FL, Sims MM, Robl JM, Eyestone WH, First NL. Nuclear transplantation in the bovine embryo: assessment of donor nuclei and recipient oocyte. Biol Reprod 1987;37:859-866.
90. Prather R, Sims M, First N. Nuclear transplantation in early pig embryos. Biol Reprod 1989;41:414-418.
91. Pursel VG, Hammer RE, Bolt DJ, Palmiter RD, Brinster RL. Integration, expression and germ-line transmission of growth-related genes in pigs. J Reprod Fertil 1990;Suppl 41:77-87.
92. Pursel VG, Pinkert CA, Miller KF, Bolt DJ, Cambell RG, Palmiter RD, Brinster RL, Hammer, R.E. Genetic engineering of livestock. Science 1989;244:1281-1288.
93. Pursel VG, Rexroad CE. Status of research with transgenic farm animals. J Anim Sci 1993;71(Suppl 3):10-19.

94. Pursel VG, Sutrave P, Wall RJ, Kelly AM, Hughes SH. Transfer of c-ski gene into swine to enhance muscle development. Theriogenology 1992;37:278 abstr.
95. Resnick JL, Bixler LS, Cheng L, Donovan PJ. Long-term proliferation of mouse primordial germ cells in culture. Nature 1992;359:550-551.
96. Rexroad CE Jr, Pursel VG. Status of gene transfer in domestic animals. Proc 11th Int Con Anim Reprod & Artificial Insemination. Dublin, Ieland, 1988;5:29-35.
97. Robertson EJ. Pluripotent stem cell lines as a route into the mouse germ line. Trends Genet 1987a;2:9-13.
98. Robertson EJ. Embryo-derived stem cell lines. In: Robertson EJ (ed), Teratocarcinomas and Embryonic Stem Cells: A practical approach. Oxford-Washington DC: IRL Press Limited, 1987b;71-122.
99. Robertson EJ. Using embryonic stem cells to introduce mutations into the mouse germ line. Biol Reprod 1991;44:238-245.
100. Robertson E, Bradley A, Kuehn M, Evans M. Germ-line transmission of genes introduced into cultured pluripotential cells by retroviral vector. Nature 1986;323:445-448.
101. Robl JM, Prather R, Barnes F, Eyestone W, Northey, D, Gilligan B, First NL. Nuclear transplantation in bovine embryos. J Anim Sci 1987;64:642-647.
102. Rothschild MF, Jacobson C, Vaske DA, Tuggle CK, Short TH, Sasaki S, Eckardt GR, McLaren DG. A major gene for litter size in pigs. Proc 5th World Cong Genet Applied to Livestock Prod. Guelph, Canada, 1994;21:225-228.
103. Rottmann OJ, Antes R, Hoefer P, Maierhofer G. Liposome mediated gene transfer via spermatazoa into avian egg cells. J Anim Breed Genet 1992;109:64-70.
104. Rund LA, Bleck GT, Izard MM, Grum LR, Gerfen RW, White BR, Wheeler MB. Development of swine embryonic stem (ES) cells. In: Tumbleson ME, Schook LB (eds), Advances in Swine in Biomedical Research. New York: Plenum Press, 1996;207-222.
105. Saito S, Strelchenko N, Niemann H. Bovine embryonic stem cell-like cells lines cultured over several passages. Roux's Arch Dev Biol 1992;201:134-141.
106. Schellander K, Peli J, Schmall F, Brem G. Artificial insemination in cattle with DNA-treated sperm. Anim Biotechnol 1995;6:41-50.
107. Schnieke AE, Kind AJ, Ritchie WA, Mycock K, Scott AR, Rithie M, Wilmut I, Coleman A, Campbell KH. Human factor IX transgenic sheep produced by transfer of nuclei from transfected fetal fibroblasts.Science 1997;278:2130-2133.
108. Schoonjans L, Albright GM, Li J-L, Collen D, Moreadith RW. Pluripotential rabbit embryonic stem (ES) cells are capable of forming overt coat color chimeras following injection into blastocysts. Mol Reprod Dev 1996;45:439-443.
109. Seamark RE. Potential of transgenic pigs and related technology for the pig industry. In: Barnett JL, Batterham ES, Cronin GM, Hansen C, Hemsworth PH, Hennessy DP, Hughes PE, Johnston NE, King RH (eds), Manipulating Pig Production. Australia: VIP Printing Pty Ltd, 1987;165-170.
110. Shamblott MJ, Axelman J, Wang S, Bugg EM, Littlefield JW, Donovan PJ, Blumenthal PD, Huggins GR, Gearhart JD. Derivation of pluripotent stem cells from cultured human primordial germ cells. Proc Natl Acad Sci USA 1998;95:13726-13731.
111. Shim H, Gutierrez-Adan A, Chen LR, BonDurant RH, Behboodi E, Anderson GB. Isolation of pluripotent stem cells from cultured porcine primordial germ cells. Biol Reprod 1997;57:1089-1095.

112. Simons JP, McClenaghan M, Clark AJ. Alteration of the quality of milk by expression of sheep beta-lactoglobulin in transgenic mice. Nature 1987;328:530-532.
113. Sims MM, First NL. Production of fetuses from totipotent cultured bovine inner cell mass cells. Proc Natl Acad Sci USA 1993;90:6143-6147.
114. Smith LC, Wilmut I. Influence of nuclear and cytoplasmic activity on the development in vivo of sheep embryos after nuclear transplantation. Biol Reprod 1989;40:1027-1035.
115. Snowder GD, Busboom JR, Cockett NE, Hendrix F, Mendenhall VT. Effect of the Callipyge gene on lamb growth and carcass characteristics. Proc 5th World Cong Genet Applied to Livestock Prod. Guelph, Canada, 1994;18:51-54.
116. Sorrentino V, Pepperkok R, Davis RL, Ansorge W, Phillipson L. Cell proliferation inhibited by myoD1 independently of myogenic differentiation. Nature 1990;345:813-814.
117. Sperandio S, Lulli V, Bacci ML, Forni M, Maidone B, Spadafora C, Lavitrano M. Sperm-mediated DNA transfer in bovine and swine species. Anim Biotechnol 1996;7:59-77.
118. Staeheli P, Haller O, Boll W, Lindemann NJ, Weismann C. Mx protein: Constitutive expression in 3T3 cells transformed with cloned MxcDNA confers selective resistance to influenza virus. Cell 1986;44:147-158.
119. Stevens LC. The development of transplantable teratocarcinomas from intratesticular grafts of pre- and postimplantation mouse embryos. Dev Biol 1970;21:364-382.
120. Stice SL, Robl JM. Nuclear reprogramming in nuclear transplant rabbit embryos. Biol Reprod 1988;39:657-664.
121. Stice SL, Strelchenko NS, Keefer CL, Matthews L. Pluripotent bovine embryonic cell lines direct embryonic development following nuclear transfer. Mol Reprod Dev1996; 54:100-110.
122. Storb U. Transgenic mice with immunoglobin genes. Annu Rev Immunol 1987;5:151-174.
123. Strelchenko N, Saito S, Niemann H. Towards the establishment of bovine embryonic stem cells. Theriogenology 1991;35:274 abstr.
124. Stringfellow DA, Gray BW, Toivio-Kinnucan M, Galik P, Riddell KP, Brock KV, Kemppainen RJ. A continuous cell line established from a preimplantation bovine embryo. Theriogenology 1991;35:275 abstr.
125. Strojek RM, Reed MA, Hoover JL, Wagner TE. A method for cultivating morphologically undifferentiated embryonic stem cells from porcine blastocysts.Theriogenology 1990;33:901-913.
126. Sukoyan MA, Golubitsa AN, Zhelezova AI, Shilov SY, Vatolin SY, Maximovsky LP, Andreeva LE, McWhir J, Pack SD, Bayborodin SI, Kerkis AY, Kizilova HI, Serov OL. Isolation and cultivation of blastocyst-derived stem cell lines from american mink (Mustela vison). Mol Reprod Dev 1992;33:418-431.
127. Sukoyan MA, Vatolin SY, Golubitsa AN, Zhelezova AI, Semenova LA, Serov OL. Embryonic stem cells derived from morula, inner cell mass, and blastocysts of mink: Comparisons of their pluripotencies. Mol Reprod Dev 1993;36: 148-158.
128. Sutrave P, Kelly AM, Hughes SH. ski can cause selective growth of skeletal muscle in transgenic mice. Genes Dev 1990;4:1462-1472.

129. Swanson ME, Martin MJ, O'Donnell JK, Hoover K, Lago W, Huntress V, Parsons CT, Pinkert CA, Pilder S, Logan JS. Production of functional human hemoglobin in transgenic swine. Bio/Technology 1992;10:557-559.
130. Talbot NC, Powell AM, Nel ND, Pursel VG, Rexroad Jr CE. Culturing the epiblast cells of the pig blastocyst. In Vitro Cell Dev Biol 1993a;29:543-554.
131. Talbot NC, Powell AM, Rexroad Jr CE. In vitro pluripotency of epiblasts derived from bovine blastocyst. Mol Reprod Dev 1995;42:35-52.
132. Talbot NC, Rexroad Jr CE, Pursel VG, Powell AM. Alkaline phosphatase staining of pig and sheep epiblast cells in culture. Mol Reprod Dev 1993;36:139-147.
133. Thomas KR, Capecchi MR. Site-directed mutagenesis by gene targeting in mouse embryo-derived stem cells. Cell 1987;51:503-512.
134. Thompson JA, Itskovitz-Eldor J, Shapiro SS, Waknitz MA, Swiergiel JJ, Marshall VS, Jones JM. Embryonic stem cell lines derived from human blastocysts. Science 1998;282:1145-1147.
135. Thomson JA, Kalishman J, Golos TG, Durning M, Harris CP, Becker RA, Hearn JP. Isolation of a primate embryonic stem cell line. Proc Natl Acad Sci USA 1995;92:7844-7848.
136. Thomson JA, Kalishman J, Golos TG, Durning M, Harris CP, Hearn JP. Pluripotent cell lines derived from common marmoset (Callithrix jacchus) blastocysts. Biol Reprod 1996;55:254-259.
137. Tsuchiya Y, Raasch GA, Brandes TL, Mizoshita K, Youngs CR. Isolation of ICM-derived cell colonies from sheep blastocysts. Theriogenology 1994;41:321.
138. Tsunoda, Y. and Y. Kato. Nuclear transplantation of embryonic stem cells in mice. J Reprod Fertil 1993;98:537 abstr.
139. Tsunoda Y, Kato Y. Full-term development after transfer of nuclei from 4-cell and compacted morula stage embryos to enucleated oocytes in the mouse. Exp Zool 1997;278:250-254.
140. Tsunoda Y, Kato Y. Not only inner cell mass cell nuclei but also trophectoderm nuclei of mouse blastocysts have a developmental totipotency. J Reprod Fertil 1998;113:181-184.
141. Van Stekelenburg-Hamers AEP, Van Achterberg TAE, Rebel HG, Flechon JE, Campbell KHS, Weima SM, Mummery CL. Isolation and characterization of permanent cell lines from inner cell mass cells of bovine blastocysts. Mol Reprod Dev 1995;40:444-454.
142. Varmus H. Retroviruses. Science 1998;240:1427-1435.
143. Velander WH, Johnson JL, Page RL, Russell CG, Subramanian A, Wilkins TD, Gwazdauskas FC, Pittius C, Drohan WN. High-level of expression of a heterologous protein in the milk of transgenic swine using the cDNA encoding human protein C. Proc Natl Acad Sci USA 1992;89:12003-12007.
144. Vise PD, Michalska AE, Ashuman R, Lloyd B, Stone AB, Quinn P, Wells JRE, Seamark RR. Introduction of a porcine growth hormone fusion gene into transgenic pigs promotes growth. J Cell Sci 1988;90:295-300.
145. Wagner EF, Stewart TA, Mintz B. The human α–globin gene and a functional thymidine kinase gene in developing mice. Proc Natl Acad Sci USA 1981a;78:5016-5020.
146. Wagner TE, Hoppe PC, Jollick, JD, Scholl DR, Hondinka RL, Gault JB. Microinjection of a rabbit β–globin gene in zygotes and its subsequent expression in adult mice and their offspring. Proc Natl Acad Sci USA 1981b;78:6376-6380.

147. Wakayama T, Perry ACF, Zuccotti M, Johnson KR, Yanagimachi R. Full-term development of mice from enucleatd oocytes injected with cumulus cell nuclei. Nature 1998;394:369-373.
148. Wall RJ, Pursel VG, Shamay A, McKnight RA, Pittius CW, Henninhausen L. High-level synthesis of a heterologous milk protein in the mammary glands of transgenic swine. Proc Natl Acad Sci USA 1991;88:1696-1700.
149. Wells DN, Driessen CA, Udy GB, Tervit HR. Putative ovine embryonic stem cells grow in media containing different levels of energy substrates. Theriogenology 1995; 43:349 abstr.
150. Wheeler MB. Development and validation of swine embryonic stem cells: a review.Reprod Fertil Dev 1994;6:563-568.
151. Wheeler MB, Campion DR. Animal production--a longstanding biotechnological success. Am J Clin Nutr 1993;Suppl 58:276S-281S.
152. Wheeler MB, Choi SJ. Embryonic stem cells and transgenics: Recent advances. Arch Fac Vet UFRGS 1997;25:64-83.
153. Wheeler MB, Rund LA, Bleck GT, Izard MM, Grum LR, Davis AM, Hunt ED, White BR, Barnes J. Production of chimeric swine by embryonic stem (ES) cells. Biol Reprod 1995;52(Suppl 1):319 abstr.
154. Wieghart M, Hoover JL, McGrane MM, Hanson RW, Rottman FM, Holtzman SH,Wagner TE, Pinkert CA. Production of transgenic pigs harbouring a rat phosphoenolpyruvate carboxykinase-bovine growth hormone fusion gene. J Reprod Fertil 1990;Suppl 41:89-96.
155. Willadsen SM. Nuclear transplantation in sheep embryos. Nature 1986;320:63-65.
156. Wilmut I, Schneieke AE, McWhir JM, Kind AJ, Campbell KHS. Viable offspring from fetal and adult mammalian cells. Nature 1997;385:810-813.
157. Wobus AM, Holzhausen H, Jakel P, Schoneich J. Characterization of a pluripotent stem cell line derived from a mouse embryo. Exp Cell Res 1984;152:212-219.
158. Wright G, Carver A, Cottom D, Reeves D, Scott A, Simons P, Wilmut I, Garner I, Coleman A. High level of expression of active alpha-1-antitrypsin in the milk of transgenic sheep. Bio/Technology 1991;9:830-834.

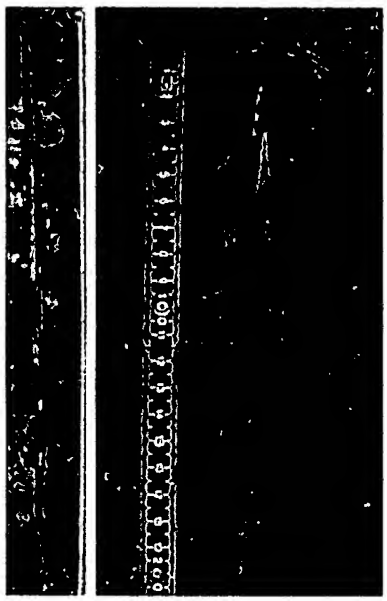

**Figure 5** Spear II, which is 2.30 m long. The spear is shown to the left of an incomplete pelvis of a horse, and the base has been broken off. Inset shows a detail of the tip of spear II. Scale in cm.

isotope stage 7, and are at least of stage 9. Correlations of the Schöningen sequence to other areas[12,14] suggest that they were deposited during the fourth-last interglacial, probably at the end of stage 11. Judging from the mammalian fauna, the Reinsdorf assemblage is younger than the Lower Palaeolithic site of Boxgrove (West Sussex, UK)[19,20].

Before our discovery, the oldest complete 'spear' known was discovered in Eemian deposits at Lehringen (Lower Saxony, Germany) in 1948 (ref. 2). Thought to be about 125 kyr old (oxygen-isotope substage 5e), this thrusting spear was recovered from between the ribs of a straight-tusked elephant, and was made from yew (*Taxus*). The Schöningen spears are probably three full interglacial/glacial cycles older than the Lehringen lance (Fig. 2).

The discovery of spears designed for throwing means that theories of the development of hunting capacities and subsistence strategies of Middle Pleistocene hominids must be revised, as well-balanced, sophisticated hunting weapons were common from an early period of the Middle Pleistocene onwards. Accordingly, meat from hunting may have provided a larger dietary contribution than has previously been acknowledged[21,22]. The Schöningen evidence also illustrates how little is known about the 'organic' component of early hominid material culture. □

Received 27 September; accepted 23 December 1996.


1. Oakley, K. P., Andrews, P., Keeley, L. H. & Clark, J. D. A reappraisal of the Clacton spearpoint. *Proc. Prehist. Soc.* **43**, 13–30 (1977).
2. Thieme, H. & Veil, S. Neue Untersuchungen zum eemzeitlichen Elefanten-Jagdplatz Lehringen, Ldkr. Verden. *Die Kunde N.F.* **36**, 11–58 (1985).
3. Thieme, H., Maier, R. & Urban, B. Archäologische Schwerpunktuntersuchungen im Helmstedter Braunkohlerevier (ASHB). –Zum Stand der Arbeiten 1983–1986. *Archäol. Korrespondenzbl.* **17**, 445–462 (1987).
4. Thieme, H., Maier, R. & Urban, B. Neue Erkenntnisse zum urgeschichtlichen Siedlungsgeschehen. *Archäol. Deutsch.* **8**(2), 26–30 (1992).
5. Urban, B., Thieme, H. & Elsner, H. Biostratigraphische, quartärgeologische und urgeschichtliche Befunde aus dem Tagebau 'Schöningen', Ldkr. Helmstedt. *Z. Deutsch. Geol. Ges.* **139**, 123–154 (1988).
6. Urban, B., Elsner, H., Hölzer, A., Mania, D. & Albrecht, B. Eine eem- und frühweichselzeitliche Abfolge im Tagebau Schöningen, Landkreis Helmstedt. *Eiszeit. Gegenw.* **41**, 85–99 (1991).
7. Urban, B., Lenhard, R., Mania, D. & Albrecht, B. Mittelpleistozän im Tagebau Schöningen, Ldkr. Helmstedt. *Z. Deutsch. Geol. Ges.* **142**, 351–372 (1991).
8. Thieme, H. & Maier, R. *Archäologische Ausgrabungen im Braunkohlentagebau Schöningen, Landkreis Helmstedt.* (Hahnsche, Hannover, 1995).
9. Thieme, H. & Mania, D. 'Schöningen 12'—ein mittelpleistozänes Interglazialvorkommen im Nordharzvorland mit paläolithischen Funden. *Ethnogr.-Archäol. Z.* **34**, 610–619 (1993).
10. Urban, B. Mittelpleistozäne Interglaziale im Tagebau Schöningen. *Ethnogr.-Archäol. Z.* **34**, 620–622 (1993).
11. Urban, B. in *Archäologische Ausgrabungen im Braunkohlentagebau Schöningen, Landkreis Helmstedt* (eds Thieme, H. & Maier, R.) 44–56 (Hahnsche, Hannover, 1995).
12. Mania, D. Die Terrassen-Travertin-Sequenz von Bilzingsleben. Ein Beitrag zur Stratigraphie des Mittel- und Jungpleistozäns im Elbe-Saale-Gebiet. *Ethnogr.-Archäol. Z.* **34**, 554–575 (1993).
13. Mania, D. in *Archäologische Ausgrabungen im Braunkohlentagebau Schöningen, Landkreis Helmstedt* (eds Thieme, H. & Maier, R.) 33–43 (Hahnsche, Hannover, 1995).
14. Mania, D. in *The Earliest Occupation of Europe* (eds Roebroeks, W. & van Kolfschoten, T.) 85–101 (University of Leiden, 1995).
15. Thieme, H., Mania, D., Urban, B. & van Kolfschoten, T. Schöningen (Nordharzvorland). Eine altpaläolithische Fundstelle aus dem mittleren Eiszeitalter. *Archäol. Korrespondenzbl.* **23**, 147–163 (1993).
16. van Kolfschoten, T. Die Vertebraten des Interglazials von Schöningen 12. *Ethnogr.-Archäol. Z.* **34**, 623–628 (1993).
17. van Kolfschoten, T. in *Archäologische Ausgrabungen im Braunkohlentagebau Schöningen, Landkreis Helmstedt* (eds Thieme, H. & Maier, R.) 85–94 (Hahnsche, Hannover, 1995).
18. Schoch, W. H. in *Archäologische Ausgrabungen im Braunkohlentagebau Schöningen, Landkreis Helmstedt* (eds Thieme, H. & Maier, R.) 73–84 (Hahnsche, Hannover, 1995).
19. Roberts, M. B., Stringer, C. B. & Parfitt, S. A. *Nature* **369**, 311–313 (1994).
20. Roebroeks, W. & van Kolfschoten, T. in *The Earliest Occupation of Europe* (eds Roebroeks, W. & van Kolfschoten, T.) 297–315 (University of Leiden, 1995).
21. Nitecki, M. H. in *The Evolution of Human Hunting* (eds Nitecki, M. H. & Nitecki, D. V.) 1–9 (Plenum, New York, 1987).
22. Gamble, C. in *The Pleistocene Old World. Regional Perspectives* (ed. Soffer, O.) 81–98 (Plenum, New York, 1987).


**Acknowledgements.** We thank the Braunschweigische Kohlen-Bergwerke AG for the technical and organizational support of the archaeological excavations in the Schöningen mine; W. H. Schoch for identifying the wood; D. Mania for the drawings in Figs 1 and 2; P. Pfarr and C. S. Fuchs for the photographs in Figs 3–5; and M. Roberts, W. Roebroeks and T. van Kolfschoten for translating and reviewing the original German manuscript. The excavation of the spear site was supported by the Deutsche Stiftung Denkmalschutz.

Correspondence and requests for materials should be addressed to the author.

# Viable offspring derived from fetal and adult mammalian cells

**I. Wilmut, A. E. Schnieke*, J. McWhir, A. J. Kind* & K. H. S. Campbell**

*Roslin Institute (Edinburgh), Roslin, Midlothian EH25 9PS, UK*
** PPL Therapeutics, Roslin, Midlothian EH25 9PP, UK*

**Fertilization of mammalian eggs is followed by successive cell divisions and progressive differentiation, first into the early embryo and subsequently into all of the cell types that make up the adult animal. Transfer of a single nucleus at a specific stage of development, to an enucleated unfertilized egg, provided an opportunity to investigate whether cellular differentiation to that stage involved irreversible genetic modification. The first offspring to develop from a differentiated cell were born after nuclear transfer from an embryo-derived cell line that had been induced to become quiescent[1]. Using the same procedure, we now report the birth of live lambs from three new cell populations established from adult mammary gland, fetus and embryo. The fact that a lamb was derived from an adult cell confirms that differentiation of that cell did not involve the irreversible modification of genetic material required for development to term. The birth of lambs from differentiated fetal and adult cells also reinforces previous speculation[1,2] that by inducing donor cells to become quiescent it will be possible to obtain normal development from a wide variety of differentiated cells.**

It has long been known that in amphibians, nuclei transferred from adult keratinocytes established in culture support development to the juvenile, tadpole stage[3]. Although this involves differentiation into complex tissues and organs, no development to the adult stage was reported, leaving open the question of whether a differentiated adult nucleus can be fully reprogrammed. Previously we reported the birth of live lambs after nuclear transfer from cultured embryonic cells that had been induced into quiescence. We suggested that inducing the donor cell to exit the growth phase

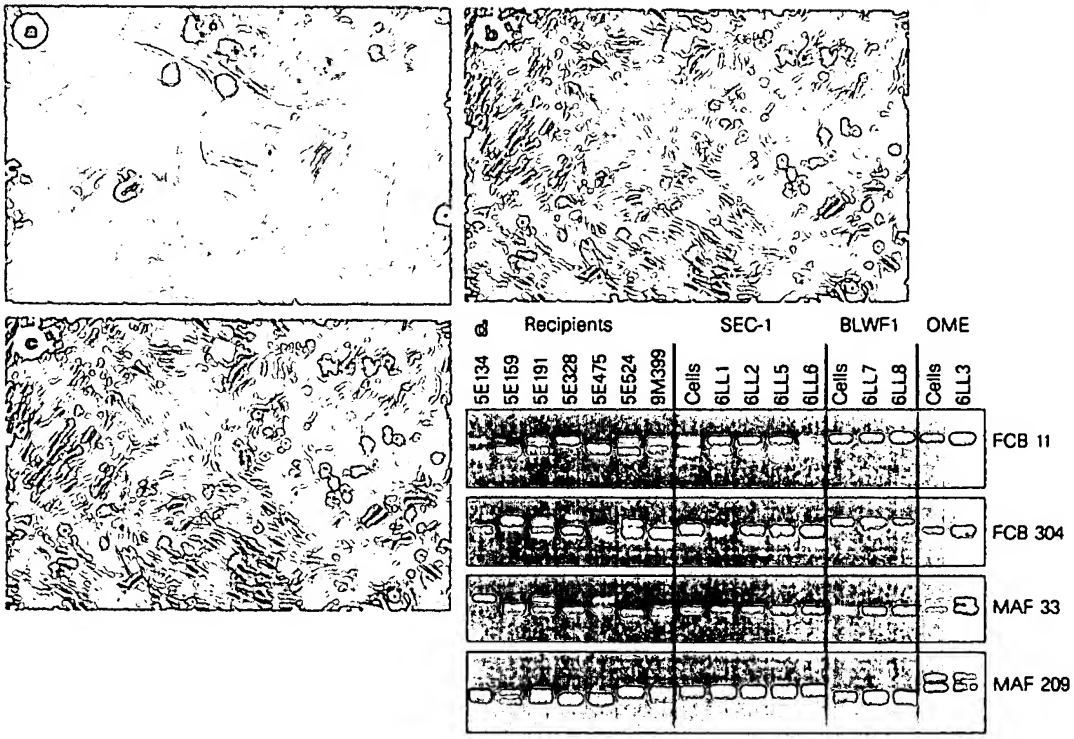


**Figure 1** Phase-contrast photomicrograph of donor-cell populations: **a**, Embryo-derived cells (SEC1); **b**, fetal fibroblasts (BLWF1); **c**, mammary-derived cells (OME). **d**, Microsatellite analysis of recipient ewes, nuclear donor cells and lambs using four polymorphic ovine markers[22]. The ewes are arranged from left to right in the same order as the lambs. Cell populations are embryo-derived (SEC1), fetal-derived (BLW1), and mammary-derived (OME), respectively. Lambs have the same genotype as the donor cells and differ from their recipient mothers.

causes changes in chromatin structure that facilitate reprogramming of gene expression and that development would be normal if nuclei are used from a variety of differentiated donor cells in similar regimes. Here we investigate whether normal development to term is possible when donor cells derived from fetal or adult tissue are induced to exit the growth cycle and enter the G0 phase of the cell cycle before nuclear transfer.

Three new populations of cells were derived from (1) a day-9 embryo, (2) a day-26 fetus and (3) mammary gland of a 6-year-old ewe in the last trimester of pregnancy. Morphology of the embryo-derived cells (Fig. 1) is unlike both mouse embryonic stem (ES) cells and the embryo-derived cells used in our previous study. Nuclear transfer was carried out according to one of our established protocols[1] and reconstructed embryos transferred into recipient ewes. Ultrasound scanning detected 21 single fetuses on day 50–60 after oestrus (Table 1). On subsequent scanning at ~14-day intervals, fewer fetuses were observed, suggesting either mis-diagnosis or fetal loss. In total, 62% of fetuses were lost, a significantly greater proportion than the estimate of 6% after natural mating[4]. Increased prenatal loss has been reported after embryo manipulation or culture of unreconstructed embryos[5]. At about day 110 of pregnancy, four fetuses were dead, all from embryo-derived cells, and post-mortem analysis was possible after killing the ewes. Two fetuses had abnormal liver development, but no other abnormalities were detected and there was no evidence of infection.

Eight ewes gave birth to live lambs (Table 1, Fig. 2). All three cell populations were represented. One weak lamb, derived from the fetal fibroblasts, weighed 3.1 kg and died within a few minutes of birth, although post-mortem analysis failed to find any abnormality or infection. At 12.5%, perinatal loss was not dissimilar to that occurring in a large study of commercial sheep, when 8% of lambs died within 24 h of birth[6]. In all cases the lambs displayed the morphological characteristics of the breed used to derive the nucleus donors and not that of the oocyte donor (Table 2). This

**Table 1 Development of embryos reconstructed with three different cell types**

| Cell type | No. of fused couplets (%)* | No. recovered from oviduct (%) | No. cultured | No. of morula/ blastocyst (%) | No. of morula or blastocysts transferred† | No. of pregnancies/ no. of recipients (%) | No. of live lambs (%)‡ |
|---|---|---|---|---|---|---|---|
| Mammary epithelium | 277 (63.8)[a] | 247 (89.2) | - | 29 (11.7)[a] | 29 | 1/13 (7.7) | 1 (3.4%) |
| Fetal fibroblast | 172 (84.7)[b] | 124 (86.7) | - | 34 (27.4)[b] | 34 | 4/10 (40.0) | 2 (5.9%) |
| | | | 24 | 13 (54.2)[b] | 6 | 1/6 (16.6) | 1 (16.6%)§ |
| Embryo-derived | 385 (82.8)[b] | 231 (85.3) | - | 90 (39.0)[b] | 72 | 14/27 (51.8) | 4 (5.6%) |
| | | | 92 | 36 (39.0)[b] | 15 | 1/5 (20.0) | 0 |

* As assessed 1 h after fusion by examination on a dissecting microscope. Superscripts a or b within a column indicate a significant difference between donor cell types in the efficiency of fusion ($P < 0.001$) or the proportion of embryos that developed to morula or blastocyst ($P < 0.001$).
† It was not practicable to transfer all morulae/blastocysts.
‡ As a proportion of morulae or blastocysts transferred. Not all recipients were perfectly synchronized.
§ This lamb died within a few minutes of birth.

**Figure 2** Lamb number 6LL3 derived from the mammary gland of a Finn Dorset ewe with the Scottish Blackface ewe which was the recipient.

**Table 2 Delivery of lambs developing from embryos derived by nuclear transfer from three different donor cells types, showing gestation length and birth weight**

| Cell type | Breed of lamb | Lamb identity | Duration of pregnancy (days)* | Birth weight (kg) |
|---|---|---|---|---|
| Mammary epithelium | Finn Dorset | 6LL3 | 148 | 6.6 |
| Fetal fibroblast | Black Welsh | 6LL7 | 152 | 5.6 |
| | Black Welsh | 6LL8 | 149 | 2.8 |
| | Black Welsh | 6LL9† | 156 | 3.1 |
| Embryo-derived | Poll Dorset | 6LL1 | 149 | 6.5 |
| | Poll Dorset | 6LL2‡ | 152 | 6.2 |
| | Poll Dorset | 6LL5 | 148 | 4.2 |
| | Poll Dorset | 6LL6‡ | 152 | 5.3 |

* Breed averages are 143, 147 and 145 days, respectively for the three genotypes Finn Dorset, Black Welsh Mountain and Poll Dorset.
† This lamb died within a few minutes of birth.
‡These lambs were delivered by caesarian section. Overall the nature of the assistance provided by the veterinary surgeon was similar to that expected in a commercial flock.

alone indicates that the lambs could not have been born after inadvertent mating of either the oocyte donor or recipient ewes. In addition, DNA microsatellite analysis of the cell populations and the lambs at four polymorphic loci confirmed that each lamb was derived from the cell population used as nuclear donor (Fig. 1). Duration of gestation is determined by fetal genotype[7], and in all cases gestation was longer than the breed mean (Table 2). By contrast, birth weight is influenced by both maternal and fetal genotype[8]. The birth weight of all lambs was within the range for single lambs born to Blackface ewes on our farm (up to 6.6 kg) and in most cases was within the range for the breed of the nuclear donor. There are no strict control observations for birth weight after embryo transfer between breeds, but the range in weight of lambs born to their own breed on our farms is 1.2–5.0 kg, 2–4.9 kg and 3–9 kg for the Finn Dorset, Welsh Mountain and Poll Dorset genotypes, respectively. The attainment of sexual maturity in the lambs is being monitored.

Development of embryos produced by nuclear transfer depends upon the maintenance of normal ploidy and creating the conditions for developmental regulation of gene expression. These responses are both influenced by the cell-cycle stage of donor and recipient cells and the interaction between them (reviewed in ref. 9). A comparison of development of mouse and cattle embryos produced by nuclear transfer to oocytes[10,11] or enucleated zygotes[12,13] suggests that a greater proportion develop if the recipient is an oocyte. This may be because factors that bring about reprogramming of gene expression in a transferred nucleus are required for early development and are taken up by the pronuclei during development of the zygote.

If the recipient cytoplasm is prepared by enucleation of an oocyte at metaphase II, it is only possible to avoid chromosomal damage and maintain normal ploidy by transfer of diploid nuclei[14,15], but further experiments are required to define the optimum cell-cycle stage. Our studies with cultured cells suggest that there is an advantage if cells are quiescent (ref. 1, and this work). In earlier studies, donor cells were embryonic blastomeres that had not been induced into quiescence. Comparisons of the phases of the growth cycle showed that development was greater if donor cells were in mitosis[16] or in the G1 (ref. 10) phase of the cycle, rather than in S or G2 phases. Increased development using donor cells in G0, G1 or mitosis may reflect greater access for reprogramming factors present in the oocyte cycoplasm, but a direct comparison of these phases in the same cell population is required for a clearer understanding of the underlying mechanisms.

Together these results indicate that nuclei from a wide range of cell types should prove to be totipotent after enhancing opportunities for reprogramming by using appropriate combinations of these cell-cycle stages. In turn, the dissemination of the genetic improvement obtained within elite selection herds will be enhanced by limited replication of animals with proven performance by nuclear transfer from cells derived from adult animals. In addition, gene targeting in livestock should now be feasible by nuclear transfer from modified cell populations and will offer new opportunities in biotechnology. The techniques described also offer an opportunity to study the possible persistence and impact of epigenetic changes, such as imprinting and telomere shortening, which are known to occur in somatic cells during development and senescence, respectively.

The lamb born after nuclear transfer from a mammary gland cell is, to our knowledge, the first mammal to develop from a cell derived from an adult tissue. The phenotype of the donor cell is unknown. The primary culture contains mainly mammary epithelial (over 90%) as well as other differentiated cell types, including myoepithelial cells and fibroblasts. We cannot exclude the possibility that there is a small proportion of relatively undifferentiated stem cells able to support regeneration of the mammary gland during pregnancy. Birth of the lamb shows that during the development of that mammary cell there was no irreversible modification of genetic information required for development to term. This is consistent with the generally accepted view that mammalian differentiation is almost all achieved by systematic, sequential changes in gene expression brought about by interactions between the nucleus and the changing cytoplasmic environment[17]. □

### Methods

Embryo-derived cells were obtained from embryonic disc of a day-9 embryo from a Poll Dorset ewe cultured as described[1], with the following modifications. Stem-cell medium was supplemented with bovine DIA/LIF. After 8 days, the explanted disc was disaggregated by enzymatic digestion and cells replated onto fresh feeders. After a further 7 days, a single colony of large flattened cells was isolated and grown further in the absence of feeder cells. At passage 8, the modal chromosome number was 54. These cells were used as nuclear donors at passages 7–9. Fetal-derived cells were obtained from an eviscerated Black Welsh Mountain fetus recovered at autopsy on day 26 of pregnancy. The head was removed before tissues were cut into small pieces and the cells dispersed by exposure to trypsin. Culture was in BHK 21 (Glasgow MEM; Gibco Life Sciences) supplemented with L-glutamine (2 mM), sodium pyruvate (1 mM) and 10% fetal calf serum. At 90% confluency, the cells were passaged with a 1 : 2

division. At passage 4, these fibroblast-like cells (Fig. 1) had modal chromosome number of 54. Fetal cells were used as nuclear donors at passages 4–6. Cells from mammary gland were obtained from a 6-year-old Finn Dorset ewe in the last trimester of pregnancy[18]. At passages 3 and 6, the modal chromosome number was 54 and these cells were used as nuclear donors at passage numbers 3–6.

Nuclear transfer was done according to a previous protocol[1]. Oocytes were recovered from Scottish Blackface ewes between 28 and 33 h after injection of gonadotropin-releasing hormone (GnRH), and enucleated as soon as possible. They were recovered in calcium- and magnesium-free PBS containing 1% FCS and transferred to calcium-free M2 medium[19] containing 10% FCS at 37 °C. Quiescent, diploid donor cells were produced by reducing the concentration of serum in the medium from 10 to 0.5% for 5 days, causing the cells to exit the growth cycle and arrest in G0. Confirmation that cells had left the cycle was obtained by staining with antiPCNA/cyclin antibody (Immuno Concepts), revealed by a second antibody conjugated with rhodamine (Dakopatts).

Fusion of the donor cell to the enucleated oocyte and activation of the oocyte were induced by the same electrical pulses, between 34 and 36 h after GnRH injection to donor ewes. The majority of reconstructed embryos were cultured in ligated oviducts of sheep as before, but some embryos produced by transfer from embryo-derived cells or fetal fibroblasts were cultured in a chemically defined medium[20]. Most embryos that developed to morula or blastocyst after 6 days of culture were transferred to recipients and allowed to develop to term (Table 1). One, two or three embryos were transferred to each ewe depending upon the availability of embryos. The effect of cell type upon fusion and development to morula or blastocyst was analysed using the marginal model of Breslow and Clayton[21]. No comparison was possible of development to term as it was not practicable to transfer all embryos developing to a suitable stage for transfer. When too many embryos were available, those having better morphology were selected.

Ultrasound scan was used for pregnancy diagnosis at around day 60 after oestrus and to monitor fetal development thereafter at 2-week intervals. Pregnant recipient ewes were monitored for nutritional status, body condition and signs of EAE, Q fever, border disease, louping ill and toxoplasmosis. As lambing approached, they were under constant observation and a veterinary surgeon called at the onset of parturition. Microsatellite analysis was carried out on DNA from the lambs and recipient ewes using four polymorphic ovine markers[22].

Received 25 November 1996; accepted 10 January 1997.


1. Campbell, K. H. S., McWhir, J., Ritchie, W. A. & Wilmut, I. Sheep cloned by nuclear transfer from a cultured cell line. *Nature* 380, 64–66 (1996).
2. Solter, D. Lambing by nuclear transfer. *Nature* 380, 24–25 (1996).
3. Gurdon, J. B., Laskey, R. A. & Reeves, O. R. The developmental capacity of nuclei transplanted from keratinized skin cells of adult frogs. *J. Embryol. Exp. Morph.* 34, 93–112 (1975).
4. Quinlivan, T. D., Martin, C. A., Taylor, W. B. & Cairney, I. M. Pre- and perinatal mortality in those ewes that conceived to one service. *J. Reprod. Fert.* 11, 379–390 (1966).
5. Walker, S. K., Heard, T. M. & Seamark, R. F. *In vitro* culture of sheep embryos without co-culture: successes and perspectives. *Therio* 37, 111–126 (1992).
6. Nash, M. L., Hungerford, L. L., Nash, T. G. & Zinn, G. M. Risk factors for perinatal and postnatal mortality in lambs. *Vet. Rec.* 139, 64–67 (1996).
7. Bradford, G. E., Hart, R., Quirke, J. F. & Land, R. B. Genetic control of the duration of gestation in sheep. *J. Reprod. Fert.* 30, 459–463 (1972).
8. Walton, A. & Hammond, J. The maternal effects on growth and conformation in Shire horse–Shetland pony crosses. *Proc. R. Soc. B* 125, 311–335 (1938).
9. Campbell, K. H. S., Loi, P., Otaegui, P. J. & Wilmut, I. Cell cycle co-ordination in embryo cloning by nuclear transfer. *Rev. Reprod.* 1, 40–46 (1996).
10. Cheong, H.-T., Takahashi, Y. & Kanagawa, H. Birth of mice after transplantation of early-cell-cycle-stage embryonic nuclei into enucleated oocytes. *Biol. Reprod.* 48, 958–963 (1993).
11. Prather, R. S. *et al.* Nuclear transplantation in the bovine embryo. Assessment of donor nuclei and recipient oocyte. *Biol. Reprod.* 37, 859–866 (1987).
12. McGrath, J. & Solter, D. Inability of mouse blastomere nuclei transferred to enucleated zygotes to support development *in vitro*. *Science* 226, 1317–1318 (1984).
13. Robl, J. M. *et al.* Nuclear transplantation in bovine embryos. *J. Anim. Sci.* 64, 642–647 (1987).
14. Campbell, K. H. S., Ritchie, W. A. & Wilmut, I. Nuclear-cytoplasmic interactions during the first cell cycle of nuclear transfer reconstructed bovine embryos: Implications for deoxyribonucleic acid replication and development. *Biol. Reprod.* 49, 933–942 (1993).
15. Barnes, F. L. *et al.* Influence of recipient oocyte cell cycle stage on DNA synthesis, nuclear envelope breakdown, chromosome constitution, and development in nuclear transplant bovine embryos. *Mol. Reprod. Dev.* 36, 33–41 (1993).
16. Kwon, O. Y. & Kono, T. Production of identical sextuplet mice by transferring metaphase nuclei from 4-cell embryos. *J. Reprod. Fert.* Abst. Ser. 17, 30 (1996).
17. Gurdon, J. B. The control of gene expression in animal development (Oxford University Press, Oxford, 1974).
18. Finch, L. M. B. *et al.* Primary culture of ovine mammary epithelial cells. *Biochem. Soc. Trans.* 24, 369S (1996).
19. Whitten, W. K. & Biggers, J. D. Complete development *in vitro* of the preimplantation stages of the mouse in a simple chemically defined medium. *J. Reprod. Fertil.* 17, 399–401 (1968).
20. Gardner, D. K., Lane, M., Spitzer, A. & Batt, P. A. Enhanced rates of cleavage and development for sheep zygotes cultured to the blastocyst stage in vitro in the absence of serum and somatic cells. Amino acids, vitamins, and culturing embryos in groups stimulate development. *Biol. Reprod.* 50, 390–400 (1994).
21. Breslow, N. E. & Clayton, D. G. Approximate inference in generalized linear mixed models. *J. Am. Stat. Assoc.* 88, 9–25 (1993).
22. Buchanan, F. C., Littlejohn, R. P., Galloway, S. M. & Crawford, A. L. Microsatellites and associated repetitive elements in the sheep genome. *Mammal. Gen.* 4, 258–264 (1993).


**Acknowledgements.** We thank A. Colman for his involvement throughout this experiment and for guidance during the preparation of this manuscript; C. Wilde for mammary-derived cells; M. Ritchie, J. Bracken, M. Malcolm-Smith, W. A. Ritchie, P. Ferrier and K. Mycock for technical assistance; D. Waddington for statistical analysis; and H. Bowran and his colleagues for care of the animals. This research was supported in part by the Ministry of Agriculture, Fisheries and Food. The experiments were conducted under the Animals (Scientific Procedures) Act 1986 and with the approval of the Roslin Institute Animal Welfare and Experiments Committee.

Correspondence should be addressed to I.W. (e-mail Ian.Wilmut@bbsrc.ac.uk).

# Evidence against a dedicated system for word learning in children

**Lori Markson & Paul Bloom**

*Department of Psychology, University of Arizona, Tucson, Arizona 85721, USA*

**Children can learn aspects of the meaning of a new word on the basis of only a few incidental exposures and can retain this knowledge for a long period—a process dubbed 'fast mapping'[1–8]. It is often maintained that fast mapping is the result of a dedicated language mechanism, but it is possible that this same capacity might apply in domains other than language learning. Here we present two experiments in which three- and four-year-old children and adults were taught a novel name and a novel fact about an object, and were tested on their retention immediately, after a 1-week delay or after a 1-month delay. Our findings show that fast mapping is not limited to word learning, suggesting that the capacity to learn and retain new words is the result of learning and memory abilities that are not specific to language.**

In two experiments (study 1 and study 2), 48 three-year-old children (mean age, 3 yr 7 months), 47 four-year-old children (mean age, 4 yr 5 months) and 48 undergraduate students first participated in a training phase that lasted for about twenty minutes. This phase involved the manipulation of ten kinds of objects, four of them familiar (for example, pennies) and six of them novel (see Methods). Subjects were asked to use some of the objects to measure other objects: for instance, they were asked to use pennies to measure the circumference of a plastic disc. Children were told it was a game, and adults were told it was a game designed to teach young children how to measure.

In the course of the training phase, subjects in both study 1 and study 2 were exposed to a new word—'koba'—used to refer to one of the six unfamiliar kinds of objects. Subjects in study 1 were also taught a new fact about one or more objects belonging to anotheer kind. They were told that the object or objects was given to the experimenter by her uncle. Subjects in study 2 were given information about an unfamiliar object, presented visually. They watched as a sticker was placed on one of the unfamiliar objects, and were told that was where the sticker should go (see Methods).

In each of the studies, one-third of the subjects from each age group were tested for comprehension immediately after the training phase, one-third were tested after a 1-week delay (6–8 days), and one-third after a 1-month delay (28–30 days). Subjects were presented with the original array of ten items and asked to recall which object was the koba. Subjects in study 1 were also asked to recall which object was given to the experimenter by her uncle. Subjects in study 2 were handed a small sticker and instructed to put it where it should go (see Methods).